SHORT-CIRCUIT ANALYSIS OF UNBALANCED DISTRIBUTION SYSTEMS

Ph.D. THESIS

by

AKHILESH MATHUR

DEPARTMENT OF ELECTRICAL ENGINEERING
INDIAN INSTITUTE OF TECHNOLOGY ROORKEE
ROORKEE – 247667 (INDIA)
MAY, 2018

SHORT-CIRCUIT ANALYSIS OF UNBALANCED DISTRIBUTION SYSTEMS

A THESIS

Submitted in partial fulfilment of the requirements for the award of the degree

of

DOCTOR OF PHILOSOPHY

in

ELECTRICAL ENGINEERING

by

AKHILESH MATHUR

DEPARTMENT OF ELECTRICAL ENGINEERING
INDIAN INSTITUTE OF TECHNOLOGY ROORKEE
ROORKEE – 247667 (INDIA)
MAY, 2018

INDIAN INSTITUTE OF TECHNOLOGY ROORKEE
ROORKEE

CANDIDATE'S DECLARATION

I hereby certify that the work which is being presented in the thesis entitled **"SHORT-CIRCUIT ANALYSIS OF UNBALANCED DISTRIBUTION SYSTEMS"** in partial fulfilment of the requirements for the award of the Degree of Doctor of Philosophy and submitted in the **Department of Electrical Engineering** of the **Indian Institute of Technology Roorkee, Roorkee** is an authentic record of my own work carried out during a period from January, 2013 to May, 2018 under the supervision of **Dr. Vinay Pant**, Assistant Professor, Department of Electrical Engineering, Indian Institute of Technology Roorkee, Roorkee.

The matter presented in this thesis has not been submitted by me for the award of any other degree of this or any other Institution.

(AKHILESH MATHUR)

This is to certify that the above statement made by the candidate is correct to the best of my knowledge.

(Vinay Pant)
Supervisor

Dated:

Abstract

To improve the reliability and efficiency of the distribution system, an important tool is required, named as Distribution automation (DA). It includes many applications such as distribution network reconfiguration, network optimization, state-estimation, reactive power management, short-circuit analysis etc. In this thesis, one of the application of DA, namely, short-circuit analysis of distribution network, is explored. Short-circuit analysis is an important tool for analyzing the system behavior (system voltage profile and currents) under the short-circuit conditions. Modernize distribution systems have some inherent features, such as radial as well as weakly meshed configurations with several thousands of nodes, untransposed lines, multiphase line sections, unbalanced loads, integrated various types of Distributed Generations (DGs) at any locations etc. Therefore, it becomes necessary to develop the short-circuit analysis algorithm for the distribution network which considers all these special features of the system in the short-circuit study.

The information provided by the short circuit studies can be used for real-time applications, such as distribution adaptive relay coordination and settings when feeder reconfiguration is performed automatically and identification of fault locations. The results of short-circuit studies can also be used for the selection of ratings of the protective equipments. It can also be used for the selection of appropriate size of the fault current limiters (required in the network to limit the fault current to a safer value).

Nowadays, the distribution systems are changing from one source supplying structure into multi-source supplying structure with participations of distributed generations (DGs). Both conventional and renewable energy resources can energize the DG units. Technologies, based on conventional energy resources, include internal-combustion engines, reciprocating engines, gas turbines, fuel cells, micro-turbines and batteries, while renewable energy technologies included photovoltaic energy conversion system (solar PVs), wind energy conversion systems, small hydro systems, biomass systems, solar-thermal electric systems and geothermal systems. There are so many advantages of the integration of DGs into the distribution network. DG provides an alternative for satisfying the increasing load demand in the network without the need of expansion of distribution system. DG improves the system efficiency by enhancing the system voltage profile and minimizing the number of required voltage regulators and capacitors and reducing feeder

power losses.

However, the integration of a large number of DGs into the network introduces so many challenges. One of the problem mentioned in the literature is the violation of original settings of the protective equipments during the short-circuit conditions because of the introduction of additional DG fault current into the network. Generally, the protective devices are designed based on the fault current analysis of the original system without DGs. When DGs are added to the system, they also contribute to the fault current in addition to the grid current. Therefore, the fault current sensed by the protective devices is greater than the original fault current from the grid. It might be possible that the protective devices can get damaged due to this excessive fault current. Even if the increase in fault current does not exceed the rating of installed devices, coordination of the primary and secondary protective devices may be disturbed due to excessive DG fault currents. Therefore, the appropriate short-circuit analysis algorithm is required for the analysis of unbalanced distribution network considering DGs under the fault conditions.

In the literature, initially the classical symmetrical component based approach was used for the short-circuit analysis of distribution system. In this approach the phase quantities of the voltage, current and impedances in the distribution system are first converted into their respective positive, negative and zero sequence components and then the short-circuit calculations are performed on these components separately. This approach is advantageous only when all the three sequence components are decoupled from each other. But in case of distribution system, this condition is not true as the mutual impedances between the phases of distribution lines are not equal (since the distribution lines are untransposed). Therefore, the results obtained by this approach are erroneous. To overcome this problem, the phase component based approach was introduced in the literature. In this approach, the short-circuit calculations are directly performed on phase components. Some of the phase component based short-circuit analysis methods are based on the concepts of Thevenin equivalent impedance and bus admittance matrices of the systems, while some are based on $[\mathbf{BIBC}]$ (Bus injection to branch current) and $[\mathbf{BCBV}]$ (branch current to bus voltage) matrices of the system. In most of these methods, it has been assumed that the load currents are negligible as compared to the fault currents. Therefore, the load currents have been ignored in the calculations of short-circuit currents.

Also, the short-circuit analysis methods for the unbalanced distribution system considering

the effect of DGs are also available in the literature. In these methods, the contribution of DGs into the fault current have been considered during the short-circuit calculations. Generally, the inverter based DG models have been considered in these studies. The appropriate inverter control strategies have been applied to the IBDGs during the faults. Most of these methods are based on $dq-0$ sequence component based approach and have carried out only the time domain simulation studies for the analysis of short-circuit faults. However, sequence component based fault analysis methods are not suitable for unbalanced distribution network with single and two phase lines and for distribution lines with unequal mutual impedances. Also, the available short-circuit analysis methods for the unbalanced distribution system with IBDGs have not considered the loads during short-circuit calculations. Hence, the accurate and the efficient short-circuit analysis algorithm is required for the unbalanced distribution system which also includes the effect of loads in the short-circuit calculations.

Initially, the short-circuit analysis method, for the unbalanced radial as well weakly meshed distribution system has been developed which considers the effect of loads during short-circuit calculations. The proposed method is based on bus admittance matrix of the system. It is a single iteration method and hence is a less time consuming. This method can also be applicable for the analysis of multiple faults in the distribution system. To demonstrates the accuracy and the effectiveness of the proposed method, it has been tested on modified IEEE 123-bus radial and weakly meshed test distribution system. Subsequently, the proposed method has been extended for the short-circuit analysis of unbalanced distribution system considering IBDGs. Since, with the inclusions of IBDGs in the distribution system, the KCL equations of the network become non-linear. Hence, to solve these set of non-linear equations, the Newton-Raphson based numerical method has been applied. In this method, initially the current control strategy of the inverters has been applied to the IBDGs and perform the short-circuit calculations to obtain the values of bus voltages, branch currents and inverter currents under the fault conditions. Next, on the basis of obtained values of inverter bus voltages magnitudes, appropriate voltage control strategy has also been applied to the IBDGs and recalculate the voltages and currents under the short-circuit conditions. To validate the proposed method, various short-circuit faults have been simulated on modified IEEE 123-bus test system. Analysis of multiple faults has also been performed on the same test system using the proposed method.

Further, a novel load flow analysis method for the unbalanced distribution system considering various three-phase transformer models and IBDGs is proposed in this work. The nodal admittance matrix based transformer models (p.u.) have been considered in this approach. This method is based on $[\mathbf{BIBC}]$ and $[\mathbf{BCBV}]$ matrices of the distribution network. Two modes of operation of IBDGs, namely "Constant active power mode" and "Power and voltage control mode", have been considered in this approach. The proposed method is applicable for the radial as well as weakly meshed distribution systems. The singularity problem for particular types of transformer connections such as, star-grounded/delta ($Yg-\Delta$), star/delta ($Y-\Delta$), delta/star ($\Delta-Y$), delta/delta ($\Delta-\Delta$) connections etc., has also been addressed in this method. Next, the short-circuit analysis method has been developed for the distribution system considering three-phase transformer models and IBDGs. It is also a Newton-Raphson based approach. The proposed method has been tested on modified IEEE 123-bus test system and the obtained results have been compared with the results obtained by the PSCAD/EMTDC simulink software. A case of multiple faults has also been simulated on the same test system using the proposed method.

Furthermore, the method for the load flow analysis of unbalanced three-phase four wire multigrounded radial distribution system has been proposed in this thesis. This method is also based on $[\mathbf{BIBC}]$ and $[\mathbf{BCBV}]$ matrices of the network. Separate $[\mathbf{BIBC}]$ and $[\mathbf{BCBV}]$ matrices have been developed for phase, neutral and ground currents and bus voltages. Well established Carson's formula has been used for the calculation of line impedances of three-phase four wire multigrounded distribution system. A case of isolated neutral has also been simulated using the proposed method. The proposed method has been tested on two different systems, modified three-phase four wire multigrounded IEEE 34-bus and IEEE 123-bus distribution systems. Subsequently, two different short-circuit analysis methods have been proposed for three-phase four wire multigrounded distribution system. One of the proposed method is based on $[\mathbf{BIBC}]$ and $[\mathbf{BCBV}]$ matrices of the system, while the other one is based on bus admittance matrix $[\mathbf{Y_{bus}}]$ of the system. Both of these methods have also considered the effect of loads during the short-circuit calculations. The results obtained by these methods show their accuracy and effectiveness.

Finally, the load flow and short-circuit analysis methods have been developed for the three-phase four wire multigrounded distribution system considering three-phase transformer models and IBDGs. These methods have been developed separately for two different configurations of

transformer models, first one is Delta/Star-grounded (Δ-Y_g) and the second one is Star-grounded/Star-grounded (Y_g-Y_g). First, the load flow analysis method, based on $[\mathbf{BIBC}]$ and $[\mathbf{BCBV}]$ matrices, has been developed for the two different transformer configurations. Next, two different short-circuit analysis methods (one is $[\mathbf{BIBC}]$ and $[\mathbf{BCBV}]$ matrices based, while the other one is bus admittance matrix $[\mathbf{Y_{bus}}]$ based method) for both the transformer models have been developed. Again, the current control mode of operation of IBDGs has been considered during the short-circuit analysis. Both of the proposed short-circuit analysis methods uses the Newton-Raphson based technique. The results obtained by the proposed methods have been compared with the results obtained by PSCAD/EMTDC simulink software which show the accuracy of the proposed methods.

Acknowledgements

In the name of God, the infinitely Good, the All Merciful

All praise is due to God, Lord of the Universe.

I take this opportunity to express my sincere gratitude toward my guide: Dr. Vinay Pant, Department of Electrical Engineering, Indian Institute of Technology Roorkee. I have been very fortunate to receive his continued academic advice, constant encouragement, endless patience, and priceless guidance and support throughout this work. He has been training me the skill and art to identify attractive and important research problems and to propose effective solutions to them.

I would like to especially thank Prof. Biswarup Das, Head of the Department of Electrical Engineering, who has been my second guide throughout the Ph.D. course. I would like to thank Dr. Ganesh Kumbhar, Department of Electrical Engineering and Prof. R. C. Mittal, Department of Mathematics for their constant suggestions and advices. Further, I would like to thank Prof. R. Prasad, Chairman DRC, Prof. Narayan Prasad Padhy, Dean, Academic Affairs, Indian Institute of Technology Roorkee, Prof. Pramod Agrawal, former Dean, Academic Affairs and Prof. S. P. Srivastava, former Head of the Department of Electrical Engineering for their continued support. In addition, I would like to thank Prof. G. K. Singh, Dr. Mukesh Kumar Pathak and Dr. Premalata Jena for their valuable suggestions. Also, officers in the department office, Mr. Mohan Singh and Rishabh Verma in particular, have been continuously helping me in all possible steps. Also, the technician at the Power System Simulation Laboratory, Mr. Ravindar and his colleagues, deserve my highest appreciation.

I have been blessed with many friends during this course, including: Pushkar Triphati, Mahamad Nabab Alam, Haresh Shabhadia, Hari Krishna Muda, Afroz Alam, Kanhaiya Kumar, Arun Balodi, Shuklal Sisodiya, Yogesh Makwana, Kunal Bhatt, Sandeep Kaur, Soumetri Jena, Vishal Gaur and many more. I am very fortunate to be blessed with a very especial friend Novalio Daratha from Indonesia. He was my senior and graduate his Ph.D. course last year. He has been a constant source of guidance and support throughout his stay at this Institute and I have learned many things from him. In additions, I have been blessed with many friends from the Institute including: Dr. Afzal Sikander, Dr. Anurag Chauhan, Ankit Bhatt and many more. All have been a great source of happiness throughout my stay at the Institute.

My Ph.D. is dedicated to my father (late) Madan Lal Mathur. He was recalled by the Almighty on 26 November 2011. He has been the real source of love, help, inspiration, guidance and everything to me. He always tried his best to fulfill all my dreams. He has been a great father and I am proud of his being the only son. In fact, he has been and will always remain everything to me.

Further, I especially thank all of my family members, including my grand mother Mrs. Shubhkanwar Mathur, my mother Mrs. Rajdulari Mathur and my sister Dr. Mohita Mathur for making me, feel free to get the best possible education since my childhood. Their patience and support are priceless. I especially would like to thank my brother in law, Er. Akhil Mathur for his best support in my time period of Ph.D. I would also like to thank my nephew, Rishit for the infinite love to me.

My special, sincere, heartfelt gratitude and indebtedness are due to my father in law Er. Rakesh Mathur and my mother in law Mrs. Sudha Mathur for their sincere prayers, constant encouragement and blessings. My sincere regards are also due to my sister in law Dr. Rinki Mathur and my brother in laws Er. Sushant Mathur and Er. Ankit Mathur. I cherish deeply the love of my niece, Swara.

Above all, I am lucky to get such a nice wife Chinki Mathur. My heartiest regards and love for shouldering the responsibilities, which makes me, concentrate on my research work. Her loving, caring and sacrificing attitude has been the inspiring and driving force in this endeavor.

Finally, I would like to thank the Ministry of Human Resource Development, Government of India, for providing fellowship throughout this course and Indian Institute of Technology Roorkee for giving me the opportunity to start my research career as a Ph.D. student.

Akhilesh Mathur

Roorkee, February 2018

Contents

Abstract i

Acknowledgements vi

List of Tables xv

List of Figures xxi

List of Abbreviations xxxi

List of Symbols xxxiii

1 Introduction 1

1.1 Overview 1

1.2 Literature review 3

1.2.1 Short-circuit analysis of three-phase three wire distribution system 3

1.2.2 Short-circuit analysis of three-phase three wire distribution system with inverter based Distributed Generations (IBDGs) and three-phase transformer models 6

1.2.3 Load flow and short-circuit analysis of three-phase four wire multigrounded distribution system 9

1.3 Motivation 11

1.4 Contribution of the author 12

1.5 Thesis organization 13

2 Short-circuit analysis of unbalanced Distribution system considering loads 15

2.1 Introduction 15

2.2 Short-circuit analysis of unbalanced distribution system considering loads 16

2.2.1 System modeling 16

2.2.2 Single line-to-ground fault (SLG) 20

2.2.3 Double and three line-to-ground faults (LLG and LLLG) 20

2.2.4 Line-to-line fault (LL) . . . 22
2.3 Test results and discussions . . . 23
2.3.1 Results of IEEE 123-bus (modified) system (radial system) . . . 23
2.3.2 Results of IEEE 123-bus (modified) system (meshed system) . . . 27
2.4 Conclusion . . . 33

3 Short-circuit analysis of unbalanced radial and meshed distribution system with inverter based Distributed Generation (IBDG) 35
3.1 Introduction . . . 35
3.2 Short-circuit analysis of unbalanced distribution system with IBDG . . . 36
3.2.1 System modeling with IBDG . . . 36
3.2.2 Short-circuit calculations . . . 38
3.2.2.1 Steps of algorithm for proposed short circuit analysis method of a distribution system with IBDG . . . 44
3.3 Test results and discussions . . . 46
3.3.1 Results of modified IEEE 123-bus unbalanced radial distribution system . 48
3.3.2 Results of modified IEEE 123-bus unbalanced weakly meshed distribution system . . . 54
3.3.3 Results of multiple fault analysis of modified IEEE 123-bus unbalanced distribution system . . . 59
3.3.4 General discussion of the results . . . 61
3.4 Conclusion . . . 62

4 Load flow and short-circuit analysis of unbalanced distribution system with three phase transformer models and inverter based Distributed Generations 65
4.1 Introduction . . . 65
4.2 Load flow analysis of an unbalanced distribution system with transformer model and IBDG . . . 66
4.2.1 Radial distribution system . . . 66
4.2.1.1 Algorithm for generation of $[\mathbf{BIBC_{Sm}}]$ and $[\mathbf{TIBC_{Tm}}]$ matrices for radial distribution system . . . 72

4.2.1.2 Algorithm for generation of $[\mathbf{BCBV_{Tm}}]$ and $[\mathbf{C}]$ matrices for radial distribution system . . . 73
4.2.2 Meshed distribution system . . . 74
4.2.2.1 Algorithm for generation of $[\mathbf{BIBC^{mesh}_{Sm}}]$ and $[\mathbf{TIBC^{mesh}_{Tm}}]$ matrices for meshed distribution system . . . 77
4.2.2.2 Algorithm for generation of $[\mathbf{BCBV^{mesh}_{Tm}}]$ and $[\mathbf{C^{mesh}_{new}}]$ matrices for meshed distribution system . . . 78
4.2.3 Singularity problem and its solution . . . 79
4.2.4 IBDG model for the load flow . . . 80
4.3 Short-circuit analysis of an unbalanced distribution system with transformer modeling . . . 82
4.4 Test results and discussions . . . 83
4.4.1 Results for radial test distribution system . . . 85
4.4.1.1 Results of load flow studies . . . 85
4.4.1.2 Results of short-circuit studies . . . 86
4.4.2 Results for weakly meshed test distribution system . . . 92
4.4.2.1 Results of load flow studies . . . 93
4.4.2.2 Results of short-circuit studies . . . 94
4.5 Conclusion . . . 100

5 Load flow and short-circuit analysis of unbalanced three phase four wire multigrounded radial distribution system 101
5.1 Introduction . . . 101
5.2 Load flow analysis of unbalanced three phase four wire multigrounded radial distribution system . . . 102
5.2.1 Formulation of $[\mathbf{BIBC}]$ matrix . . . 105
5.2.1.1 Formulation of $[\mathbf{BIBC}]$ matrix for phase currents $\left[\mathbf{B_p}\right]$ . . . 105
5.2.1.2 Formulation of $[\mathbf{BIBC}]$ matrix for neutral currents $\left[\mathbf{B_n}\right]$ . . . 107
5.2.1.3 Formulation of $[\mathbf{BIBC}]$ matrix for ground currents $\left[\mathbf{B_g}\right]$ . . . 110
5.2.2 Formulation of $[\mathbf{BCBV}]$ matrix . . . 110

5.2.2.1 Formulation of $[\mathbf{BCBV}]$ matrices for the voltages of phase buses $\left[\mathbf{V_p}\right]$ . . . 110
5.2.2.2 Formulation of $[\mathbf{BCBV}]$ matrices for neutral bus voltages $\left[\mathbf{V_n}\right]$ 115
5.2.2.3 Formulation of $[\mathbf{BCBV}]$ matrices for ground bus voltages $\left[\mathbf{V_g}\right]$ 118
5.3 Short-circuit analysis of unbalanced three phase four wire multigrounded radial distribution system . . . 126
5.3.1 Method 1: $\left[\mathbf{BIBC}\right]$ matrix based short-circuit analysis method . . . 126
5.3.2 Method 2: $\left[\mathbf{Y_{bus}}\right]$ matrix based short-circuit analysis method . . . 141
5.4 Test results and discussions . . . 151
5.4.1 Results of modified three phase four wire multigrounded IEEE 34-bus test system . . . 153
5.4.1.1 Results of load flow studies . . . 153
5.4.1.2 Results of short-circuit studies . . . 160
5.4.2 Results of modified three phase four wire multigrounded IEEE 123-bus test system . . . 164
5.4.2.1 Results of load flow studies . . . 164
5.4.2.2 Results of short-circuit studies . . . 169
5.5 Conclusion . . . 173

6 Load flow and short-circuit analysis of unbalanced three phase four wire multigrounded radial distribution system incorporating IBDG and transformer models 175

6.1 Introduction . . . 175
6.2 Three phase four wire multigrounded radial distribution system in the presence of IBDG and Δ-Y_g IBDG transformer . . . 176
6.2.1 Load flow analysis with Delta/Star-grounded (Δ-Y_g) IBDG transformer for the connection of IBDG . . . 178
6.2.1.1 Formulation of [BIBC] matrix . . . 178
6.2.1.2 Formulation of [BCBV] matrix . . . 180

6.2.2 Short-circuit analysis of unbalanced three phase four wire multigrounded radial distribution system in the presence of IBDG and Δ-Y_g IBDG transformer . . . 183
6.2.2.1 Method 1: $\left[\mathbf{BIBC}\right]$ matrix based method . . . 183
6.2.2.2 Method 2: $\left[\mathbf{Y_{bus}}\right]$ matrix based method . . . 201
6.3 Three phase four wire multigrounded radial distribution system with IBDG and Y_g-Y_g IBDG transformer . . . 205
6.3.1 Load flow analysis with Star-grounded/Star-grounded (Y_g-Y_g) IBDG transformer for the connection of IBDG . . . 208
6.3.1.1 Formulation of $[\mathbf{BIBC}]$ matrices . . . 208
6.3.2 Short-circuit analysis of unbalanced three phase four wire multigrounded radial distribution system with IBDG and Y_g-Y_g IBDG transformer . . . 211
6.3.2.1 Method 1: $\left[\mathbf{BIBC}\right]$ matrix based method . . . 212
6.3.2.2 Method 2: $\left[\mathbf{Y_{bus}}\right]$ matrix based method . . . 221
6.4 Test results and discussions . . . 223
6.4.1 Results of test systems with IBDGs and Δ-Y_g IBDG transformers . . . 223
6.4.1.1 Results of modified three phase four wire multigrounded IEEE 34-bus test system in the presence of IBDGs and Δ-Y_g IBDG transformers . . . 223
6.4.1.2 Results of modified three phase four wire multigrounded IEEE 123-bus test system in the presence of IBDGs and Δ-Y_g IBDG transformers . . . 234
6.4.2 Results of test systems with IBDGs and Y_g-Y_g IBDG transformers . . . 245
6.4.2.1 Results of modified three phase four wire multigrounded IEEE 34-bus test system in the presence of IBDGs and Y_g-Y_g IBDGs transformers . . . 245
6.4.2.2 Results of modified three phase four wire multigrounded IEEE 123-bus test system in the presence of IBDGs and Y_g-Y_g IBDG transformers . . . 256
6.5 Conclusion . . . 265

7 Conclusions and scope of further works **267**

7.1 Conclusions 267

7.2 Scope of further Works 268

Publications from the research work **271**

Bibliography **272**

A Modified IEEE 34-Bus three-phase four wire multigrounded Distribution System **289**

B Modified IEEE 123-Bus three-phase four wire multigrounded Distribution System **291**

List of Tables

1.1 Case study to observe the effect of load currents in fault analysis 12

2.1 Error Analysis of proposed technique and [**BIBC**] matrix based technique with respect to PSCAD/EMTDC simulation study for IEEE 123-bus (modified) radial system 26

2.2 List of loop branches added in IEEE 123-bus (modified) radial system 27

2.3 Error Analysis of proposed technique and [**BIBC**] matrix based technique with respect to PSCAD/EMTDC simulation study for IEEE 123-bus (modified) meshed system 31

2.4 Error Analysis of proposed technique and [BIBC] matrix based technique with respect to PSCAD/EMTDC simulation study for multiple faults for IEEE 123-bus system 34

3.1 Details of the IBDGs installed in the modified IEEE 123-bus unbalanced distribution system 48

3.2 Results for SLG(a-g) fault in modified IEEE 123-bus radial distribution system with IBDGs for scenario 1 49

3.3 Error analysis of proposed technique (scenario 1) with respect to PSCAD/EMTDC simulations 50

3.4 Comparison between Gauss-Seidel and Proposed method 51

3.5 Intermediate and final post-fault inverter bus voltages and injected power by IBDGs for SLG(a-g) fault at bus 105, with $\bar{z}_f$ = 0.001+0.000i p.u., in scenario 2 . . . 53

3.6 Results for different unsymmetrical short-circuit faults at bus 105, with $\bar{z}_f$ = 0.001+0.000i p.u., using proposed technique (scenario 2) and PSCAD/EMTDC simulation 54

3.7 Intermediate and final post-fault inverter bus voltages and injected power by IBDGs for SLG(a-g) fault at bus 27, with $\bar{z}_f$ = 0.5+0.0i p.u., in scenario 2 55

3.8 Results for different unsymmetrical short-circuit faults at bus 27, with $\bar{z}_f$ = 0.5+0.0i p.u., using proposed technique (scenario 2) and PSCAD/EMTDC simulation 55

3.9 List of loop branches in IEEE 123 bus (modified) meshed distribution system . . . 56

3.10 Results for SLG(a-g) fault in modified IEEE 123 bus meshed distribution system with IBDGs for scenario 1 56

3.11 Error analysis of proposed technique (scenario 1) with respect to PSCAD/EMTDC simulations for different unsymmetrical short-circuit faults at bus 105 in modified IEEE 123 bus meshed distribution system 56

3.12 Intermediate and final post fault inverter bus voltages and injected power by IBDGs for SLG(a-g) fault at bus 27, with $\bar{z}_f$ = 0.5+0.0i p.u., in scenario 2 in modified IEEE 123-bus meshed distribution system 59

3.13 Results for different unsymmetrical short-circuit faults at bus 27, with $\bar{z}_f$ = 0.5+0.0i p.u., using proposed technique (scenario 2) and PSCAD/EMTDC simulation in modified IEEE 123-bus meshed distribution system 60

3.14 Error analysis of Proposed technique (scenario 1) with respect to PSCAD/EMTDC simulations for multiple faults in modified IEEE 123-bus distribution system 60

3.15 Error analysis of Proposed technique (scenario 2) with respect to PSCAD/EMTDC simulations for multiple faults in modified IEEE 123-bus distribution system 61

3.16 Maximum % deviation, with respect to 'no IBDG' case 62

4.1 Details of the IBDGs installed in the IEEE 123-bus modified test system 85

4.2 Injected power by the IBDGs and Inverter currents of phase a in Mode 1 and Mode 2 operation of IBDGs, for case 1 and case 2, of radial test distribution system under normal operating conditions 86

4.3 Results for SLG(a-g) fault in modified IEEE 123-bus radial distribution system with IBDGs and ΔY_g-1 IBDG transformers (Case 1) for scenario 1 88

4.4 Results for SLG(a-g) fault in modified IEEE 123-bus radial distribution system with IBDGs and Y_gY_g-0 IBDG transformers (Case 2) for scenario 1 89

4.5 Intermediate (after scenario 1) and final (after scenario 2) inverter bus voltages and injected power by IBDGs for SLG(a-g) fault at bus 105, with $\bar{z}_f$ = 0.001+0.000i p.u., for Case 1 89

4.6 Intermediate (after scenario 1) and final (after scenario 2) inverter bus voltages and injected power by IBDGs for SLG(a-g) fault at bus 105, with $\bar{z}_f$ = 0.001+0.000i p.u., for Case 2 90

4.7 Error analysis of proposed method with respect to PSCAD/EMTDC simulation studies for various short-circuit faults at bus 105 (in scenario 1) in radial test system with ΔY_g-1 IBDG transformers (Case 1) 91

4.8 Error analysis of proposed method with respect to PSCAD/EMTDC simulation studies for various short-circuit faults at bus 105 (in scenario 1) in radial test system with Y_gY_g-0 IBDG transformers (Case 2) 91

4.9 Results for different short-circuit faults at bus 105, with $\bar{z}_f$ = 0.001+0.000i p.u., using proposed technique (scenario 2) and PSCAD/EMTDC simulation for Case 1 92

4.10 Results for different short-circuit faults at bus 105, with $\bar{z}_f$ = 0.001+0.000i p.u., using proposed technique (scenario 2) and PSCAD/EMTDC simulation for Case 2 93

4.11 Injected power by the IBDGs and Inverter currents of phase a in Mode 1 and Mode 2 operation of IBDGs, for case 1 and case 2, of weakly meshed test distribution system 94

4.12 Results for SLG(a-g) fault in modified IEEE 123-bus meshed distribution system with IBDGs and ΔY_g-1 IBDG transformers (Case 1) for scenario 1 96

4.13 Results for SLG(a-g) fault in modified IEEE 123-bus meshed distribution system with IBDGs and Y_gY_g-0 IBDG transformers (Case 2) for scenario 1 96

4.14 Intermediate (after scenario 1) and final (after scenario 2) inverter bus voltages and injected power by IBDGs for SLG(a-g) fault at bus 105, with $\bar{z}_f$ = 0.001+0.000i p.u., for Case 1 of meshed system 97

4.15 Intermediate (after scenario 1) and final (after scenario 2) inverter bus voltages and injected power by IBDGs for SLG(a-g) fault at bus 105, with $\bar{z}_f$ = 0.001+0.000i p.u., for Case 2 of meshed system 97

4.16 Error analysis of proposed method with respect to PSCAD/EMTDC simulations for various short-circuit faults at bus 105 (in scenario 1) in meshed test system with ΔY_g-1 IBDG transformers (Case 1) 98

4.17 Error analysis of proposed method with respect to PSCAD/EMTDC simulations for various short-circuit faults at bus 105 (in scenario 1) in meshed test system with Y_gY_g-0 IBDG transformers (Case 2) 98

4.18 Results for different unsymmetrical short-circuit faults at bus 105, with $\bar{z}_f$ = 0.001+0.000i p.u., using proposed technique (scenario 2) and PSCAD/EMTDC simulation for Case 1 of meshed system 99

4.19 Results for different unsymmetrical short-circuit faults at bus 105, with $\bar{z}_f$ = 0.001+0.000i p.u., using proposed technique (scenario 2) and PSCAD/EMTDC simulation for Case 2 of meshed system 99

4.20 Error analysis of proposed technique with respect to PSCAD/EMTDC simulations for multiple faults (in scenario 1) in test distribution system with IBDGs and ΔY_g-1 IBDG transformer 100

5.1 Sizes of various $[\mathbf{BIBC}]$ and $[\mathbf{BCBV}]$ matrices of the unbalanced three-phase four wire multigrounded distribution system 125

5.2 Error Analysis of proposed $[\mathbf{BIBC}]$ matrix based technique and $[\mathbf{Y_{bus}}]$ matrix based technique with respect to PSCAD/EMTDC simulation study for modified three phase four wire multigrounded IEEE 34-bus radial test system 161

5.3 Results of the proposed short-circuit analysis methods for modified three phase four wire multigrounded IEEE 123-bus radial test system 171

6.1 Details of the IBDGs installed in the modified IEEE 34-bus test system 224

6.2 Inverter currents of modified IEEE 34-bus test system in the presence of IBDGs and Δ-Y_g IBDG transformers under normal operating conditions 228

6.3 Inverter bus voltages of modified IEEE 34-bus test system in the presence of IBDGs and Δ-Y_g IBDG transformers under normal operating conditions 228

6.4 Results for SLG(a-g) fault at bus 28 in modified three phase four wire multigrounded IEEE 34-bus radial test system in the presence of IBDGs and Δ-Y_g IBDG transformers using proposed $[\mathbf{BIBC}]$ method 231

6.5 Results for SLG(a-g) fault at bus 28 in modified three phase four wire multigrounded IEEE 34-bus radial test system in the presence of IBDGs and Δ-Y_g IBDG transformers using proposed $[\mathbf{Y_{bus}}]$ method 231

6.6 Error Analysis of proposed $[\mathbf{BIBC}]$ matrix based technique and $[\mathbf{Y_{bus}}]$ matrix based technique with respect to PSCAD/EMTDC simulation study for modified three phase four wire multigrounded IEEE 34-bus radial test system in the presence of IBDGs and Δ-Y_g IBDG transformers 232

6.7 Details of the IBDGs installed in the modified IEEE 123-bus distribution system . . 234

6.8 Inverter currents of modified IEEE 123-bus test system in the presence of IBDGs and Δ-Y_g IBDG transformers under normal operating conditions 240

6.9 Inverter bus voltages of modified IEEE 123-bus test system in the presence of IBDGs and Δ-Y_g IBDG transformers under normal operating conditions 240

6.10 Results for SLG(a-g) fault at bus 105 in modified three phase four wire multigrounded IEEE 123-bus radial test system in the presence of IBDGs and Δ-Y_g IBDG transformers using proposed $[\mathbf{BIBC}]$ method 242

6.11 Results for SLG(a-g) fault at bus 105 in modified three phase four wire multigrounded IEEE 123-bus radial test system in the presence of IBDGs and Δ-Y_g IBDG transformers using proposed $[\mathbf{Y_{bus}}]$ method 242

6.12 Results of the proposed short-circuit analysis methods for modified three phase four wire multigrounded IEEE 123-bus radial test system in the presence of IBDGs and Δ-Y_g IBDG transformers 243

6.13 Inverter currents of modified IEEE 34-bus test system in the presence of IBDG and Y_g-Y_g IBDG transformers under normal operating conditions 250

6.14 Inverter bus voltages of modified IEEE 34-bus test system in the presence of IBDG and Y_g-Y_g IBDG transformers under normal operating conditions 250

6.15 Results for SLG(a-g) fault at bus 28 in modified three phase four wire multigrounded IEEE 34-bus radial test system in the presence of IBDGs and Y_g-Y_g IBDG transformers using proposed $[\mathbf{BIBC}]$ method 253

6.16 Results for SLG(a-g) fault at bus 28 in modified three phase four wire multigrounded IEEE 34-bus radial test system in the presence of IBDGs and Y_g-Y_g IBDG transformers using proposed $[\mathbf{Y_{bus}}]$ method 253
6.17 Error Analysis of proposed $[\mathbf{BIBC}]$ matrix based technique and $[\mathbf{Y_{bus}}]$ matrix based technique with respect to PSCAD/EMTDC simulation study for modified three phase four wire multigrounded IEEE 34-bus radial test system in the presence of IBDGs and Y_g-Y_g IBDG transformers 254
6.18 Inverter currents of modified IEEE 123-bus test system in the presence of IBDGs and Y_g-Y_g IBDG transformers under normal operating conditions 260
6.19 Inverter bus voltages of modified IEEE 123-bus test system in the presence of IBDGs and Y_g-Y_g IBDG transformers under normal operating conditions 261
6.20 Results for SLG(a-g) fault at bus 105 in modified three phase four wire multigrounded IEEE 123-bus radial test system in the presence of IBDGs and Y_g-Y_g IBDG transformers using proposed $[\mathbf{BIBC}]$ method 261
6.21 Results for SLG(a-g) fault at bus 105 in modified three phase four wire multigrounded IEEE 123-bus radial test system in the presence of IBDGs and Y_g-Y_g IBDG transformers using proposed $[\mathbf{Y_{bus}}]$ method 263
6.22 Results of proposed short-circuit analysis methods for modified three phase four wire multigrounded IEEE 123-bus radial test system in the presence of IBDGs and Y_g-Y_g IBDG transformers 263

A.1 Line Data 289
A.2 Load Data 290
A.3 Overhead Line Configurations 290

B.1 Line Data 291
B.2 Load Data 294
B.3 Overhead Line Configurations 296

List of Figures

2.1 An n bus unbalanced radial distribution system 17

2.2 Unsymmetrical Short-circuit faults, (a) SLG fault, (b) LLG fault, (c) LLLG fault, (d) LL fault 21

2.3 The IEEE 123-bus (modified) system 24

2.4 Source current during various type of faults for IEEE 123-bus (modified) radial system using PSCAD/EMTDC, proposed technique and $[\mathbf{BIBC}]$ matrix based technique 25

2.5 Maximum difference in branch current (between loaded and unloaded condition) at different fault locations in IEEE 123-bus (modified) radial system for SLG $(a-g)$ fault 27

2.6 Voltage profiles of IEEE 123-bus (modified) radial system under loaded condition, (a) $\bar{z}_f$ = $0.001 + 0.000i$ p.u., (b) $\bar{z}_f$ = $0.1 + 0.0i$ p.u. 28

2.7 Branch currents of IEEE 123-bus (modified) radial system under loaded condition, (a) $\bar{z}_f$ = $0.001 + 0.000i$ p.u., (b) $\bar{z}_f$ = $0.1 + 0.0i$ p.u. 29

2.8 Maximum difference in branch current (between loaded and unloaded condition) in IEEE 123-bus (modified) radial system with load increment factor for SLG $(a-g)$ fault at bus 8 30

2.9 Source current during various type of faults for IEEE 123-bus (modified) meshed system using PSCAD/EMTDC, proposed technique and $[\mathbf{BIBC}]$ matrix based technique 30

2.10 Maximum difference in branch current (between loaded and unloaded condition) at different fault locations in IEEE 123-bus (modified) meshed system for SLG $(a-g)$ fault 31

2.11 Voltage profiles of IEEE 123-bus (modified) meshed system under loaded condition, (a) $\bar{z}_f = 0.001 + 0.000i$ p.u., (b) $\bar{z}_f = 0.1 + 0.0i$ p.u. 32

2.12 Branch currents of IEEE 123-bus (modified) meshed system under loaded condition, (a) $\bar{z}_f = 0.001 + 0.000i$ p.u., (b) $\bar{z}_f = 0.1 + 0.0i$ p.u. 33

2.13 Maximum difference in branch current (between loaded and unloaded condition) in IEEE 123-bus (modified) meshed system with load increment factor for SLG $(a-g)$ fault at bus 8 34

3.1 An unbalanced distribution system with inverter based DG (IBDG) 37

3.2 Flow-chart of the proposed fault analysis method 47

3.3 Voltage profile for different unsymmetrical short-circuit faults in scenario 1 51

3.4 Voltage profile for SLG and LL faults using proposed method (scenario 1) and PSCAD/EMTDC simulation 52

3.5 (a) Fault current (I_f) (b) Source current (I_s) for different fault cases in modified IEEE 123 bus radial distribution system with IBDGs and with voltage dependent loads using proposed method (scenario 1) and PSCAD/EMTDC simulation 52

3.6 Voltage profile of phase a for modified IEEE 123-bus meshed distribution system for different unsymmetrical short-circuit faults in scenario 1 57

3.7 Voltage profile of phase a for modified IEEE 123 bus meshed distribution system for SLG and LL fault using proposed technique (scenario 1) and PSCAD/EMTDC simulation 58

3.8 (a) Fault current (I_f) (b) Source current (I_s) for different fault cases in modified IEEE 123 bus meshed distribution system with IBDGs and with voltage dependent loads using proposed method (scenario 1) and PSCAD/EMTDC simulation 59

4.1 An unbalanced distribution system with transformers and IBDG 67

4.2 Voltage profile of phase a for radial test system with (a) ΔY_g-1 (Case 1) and (b) Y_gY_g-0 (Case 2) IBDG transformers under normal operating conditions 87

4.3 Voltage profile of phase a for radial test system with (a) ΔY_g-1 (Case 1) and (b) Y_gY_g-0 (Case 2) IBDG transformers, using proposed technique and PSCAD/EMTDC simulation under normal operating conditions 87

4.4 Voltage profile of phase a for meshed test system with (a) ΔY_g-1 (Case 1) and (b) Y_gY_g-0 (Case 2) IBDG transformers under normal operating conditions 94

4.5 Voltage profile of phase a for meshed test system with (a) ΔY_g-1 (Case 1) and (b) Y_gY_g-0 (Case 2) IBDG transformers, using proposed technique and PSCAD/EMTDC simulation under normal operating conditions 95

5.1 An unbalanced three phase four wire multigrounded radial distribution system . . . 103

5.2 Unsymmetrical short-circuit faults, (a) SLG fault, (b) LLG fault, (c) LLLG fault, (d) LL fault 127

5.3 Flow-chart of the proposed $[\mathbf{BIBC}]$ matrix based short-circuit analysis method . . 142

5.4 Voltage profile of phase a of modified IEEE 34-bus test system using proposed $[\mathbf{BIBC}]$ technique, $[\mathbf{Y_{bus}}]$ technique and PSCAD/EMTDC simulation under the normal operating conditions 155

5.5 Voltage profile of neutral bus of modified IEEE 34-bus test system using proposed $[\mathbf{BIBC}]$ technique, $[\mathbf{Y_{bus}}]$ technique and PSCAD/EMTDC simulation under normal operating conditions 155

5.6 Voltage profile of ground bus of modified IEEE 34-bus test system using proposed $[\mathbf{BIBC}]$ technique, $[\mathbf{Y_{bus}}]$ technique and PSCAD/EMTDC simulation under normal operating conditions 156

5.7 Branch current of phase a of modified IEEE 34-bus test system using proposed $[\mathbf{BIBC}]$ technique, $[\mathbf{Y_{bus}}]$ technique and PSCAD/EMTDC simulation under normal operating conditions 156

5.8 Neutral current of modified IEEE 34-bus test system using proposed $[\mathbf{BIBC}]$ technique, $[\mathbf{Y_{bus}}]$ technique and PSCAD/EMTDC simulation under normal operating conditions 157

5.9 Ground current of modified IEEE 34-bus test system using proposed $[\mathbf{BIBC}]$ technique, $[\mathbf{Y_{bus}}]$ technique and PSCAD/EMTDC simulation under normal operating conditions 157

5.10 Currents distribution between neutral and ground wires of branch nos. 8, 9, 10, 11 and 12 of modified IEEE 34-bus test system under normal operating conditions . . 158

5.11 (a) Neutral bus voltage profile, (b) Neutral current of modified IEEE 34-bus test system in "isolated neutral" and "grounded neutral" cases under normal operating conditions 159

5.12 (a) Maximum ground bus voltage, (b) Maximum ground current, in modified IEEE 34-bus test system for various grounding resistance under normal operating condition 160

5.13 Voltage profile of phase a, for an SLG fault (a-g) at bus 28, of modified IEEE 34-bus test system using proposed $\left[\mathbf{BIBC}\right]$ technique, $\left[\mathbf{Y_{bus}}\right]$ technique and PSCAD/EMTDC simulation 162

5.14 Voltage profile of neutral bus, for an SLG fault (a-g) at bus 28, of modified IEEE 34-bus test system using proposed $\left[\mathbf{BIBC}\right]$ technique, $\left[\mathbf{Y_{bus}}\right]$ technique and PSCAD/EMTDC simulation 162

5.15 Voltage profile of ground bus, for an SLG fault (a-g) at bus 28, of modified IEEE 34-bus test system using proposed $\left[\mathbf{BIBC}\right]$ technique, $\left[\mathbf{Y_{bus}}\right]$ technique and PSCAD/EMTDC simulation 163

5.16 (a) Voltage profile of ground bus, (b) Ground current, for various ground faults at bus 28, of modified IEEE 34-bus test system 164

5.17 Path of the fault current for an SLG fault ($a - g$) at bus 28 in IEEE 34-bus test system 165

5.18 Maximum ground bus voltage and Maximum ground current in modified IEEE 34-bus test system for various grounding resistance under SLG fault ((a) and (b)), LLG fault ((c) and (d)) and LLLG fault ((e) and (f)) 166

5.19 Voltage profile of phase a of modified IEEE 123-bus test system using proposed $\left[\mathbf{BIBC}\right]$ technique and $\left[\mathbf{Y_{bus}}\right]$ technique under normal operating conditions . . . 167

5.20 Voltage profile of neutral bus of modified IEEE 123-bus test system using proposed $\left[\mathbf{BIBC}\right]$ technique and $\left[\mathbf{Y_{bus}}\right]$ technique under normal operating conditions . . . 167

5.21 Voltage profile of ground bus of modified IEEE 123-bus test system using proposed $\left[\mathbf{BIBC}\right]$ technique and $\left[\mathbf{Y_{bus}}\right]$ technique under normal operating conditions . . . 168

5.22 Branch current of phase a of modified IEEE 123-bus test system using proposed $\left[\mathbf{BIBC}\right]$ technique and $\left[\mathbf{Y_{bus}}\right]$ technique under normal operating conditions . . . 168

5.23 Neutral current of modified IEEE 123-bus test system using proposed $\left[\mathbf{BIBC}\right]$ technique and $\left[\mathbf{Y_{bus}}\right]$ technique under normal operating conditions 169

5.24 Ground current of modified IEEE 123 bus-test system using proposed $\left[\mathbf{BIBC}\right]$ technique and $\left[\mathbf{Y_{bus}}\right]$ technique under normal operating conditions 169

5.25 (*a*) Neutral bus voltage profile, (*b*) Neutral current of modified IEEE 123-bus test system in "isolated neutral" and "grounded neutral" cases under the normal operating conditions 170

5.26 Voltage profile of phase a, for an SLG fault (a-g) at bus 105, of modified IEEE 123-bus test system using proposed $\left[\mathbf{BIBC}\right]$ technique and $\left[\mathbf{Y_{bus}}\right]$ technique . . . 172

5.27 Voltage profile of neutral bus, for an SLG fault (a-g) at bus 105, of modified IEEE 123-bus test system using proposed $\left[\mathbf{BIBC}\right]$ technique and $\left[\mathbf{Y_{bus}}\right]$ technique . . . 172

5.28 Voltage profile of ground bus, for an SLG fault (a-g) at bus 105, of modified IEEE 123-bus test system using proposed $\left[\mathbf{BIBC}\right]$ technique and $\left[\mathbf{Y_{bus}}\right]$ technique . . . 173

5.29 (*a*) Voltage profile of ground bus, (*b*) Ground current, for various ground faults at bus 105, of modified IEEE 123-bus test system 174

6.1 An unbalanced three phase four wire multigrounded radial distribution system with IBDG and Δ-Y_g IBDG transformer 177

6.2 Unsymmetrical short-circuit faults, (a) SLG fault, (b) LLG fault, (c) LLLG fault, (d) LL fault 184

6.3 Flow-chart of the proposed $\left[\mathbf{BIBC}\right]$ matrix based short-circuit analysis method in the presence of IBDG and Δ-Y_g IBDG transformer 202

6.4 An unbalanced three phase four wire multigrounded radial distribution system with IBDG and Y_g-Y_g IBDG transformer 206

6.5 Flow-chart of the proposed $\left[\mathbf{BIBC}\right]$ matrix based short-circuit analysis method with IBDG and Y_g-Y_g IBDG transformer 221

6.6 Voltage profile of phase a of modified IEEE 34-bus test system in the presence of IBDG and Δ-Y_g IBDG transformer using proposed $\left[\mathbf{BIBC}\right]$ technique, $\left[\mathbf{Y_{bus}}\right]$ technique and PSCAD/EMTDC simulation under normal operating conditions . . . 225

6.7 Voltage profile of neutral bus of modified IEEE 34-bus test system in the presence of IBDG and Δ-Y_g IBDG transformer using proposed $\left[\mathbf{BIBC}\right]$ technique, $\left[\mathbf{Y_{bus}}\right]$ technique and PSCAD/EMTDC simulation under normal operating conditions . . . 225

6.8 Voltage profile of ground bus of modified IEEE 34-bus test system in the presence of IBDG and Δ-Y_g IBDG transformer using proposed $\left[\mathbf{BIBC}\right]$ technique, $\left[\mathbf{Y_{bus}}\right]$ technique and PSCAD/EMTDC simulation under normal operating conditions . . . 226

6.9 Branch current of phase a of modified IEEE 34-bus test system in the presence of IBDG and Δ-Y_g IBDG transformer using proposed $\left[\mathbf{BIBC}\right]$ technique, $\left[\mathbf{Y_{bus}}\right]$ technique and PSCAD/EMTDC simulation under normal operating conditions . . . 226

6.10 Neutral current of modified IEEE 34-bus test system in the presence of IBDG and Δ-Y_g IBDG transformer using proposed $\left[\mathbf{BIBC}\right]$ technique, $\left[\mathbf{Y_{bus}}\right]$ technique and PSCAD/EMTDC simulation under normal operating conditions 227

6.11 Ground current of modified IEEE 34-bus test system in the presence of IBDG and Δ-Y_g IBDG transformer using proposed $\left[\mathbf{BIBC}\right]$ technique, $\left[\mathbf{Y_{bus}}\right]$ technique and PSCAD/EMTDC simulation under normal operating conditions 227

6.12 (a) Neutral bus voltage profile, (b) Neutral current of modified IEEE 34-bus test system in the presence of IBDG and Δ-Y_g IBDG transformer in "isolated neutral" and "grounded neutral" cases under normal operating conditions 229

6.13 (a) Maximum ground bus voltage, (b) Maximum ground current, in modified IEEE 34-bus test system in the presence of IBDG and Δ-Y_g IBDG transformer for various grounding resistance under normal operating condition 230

6.14 Voltage profile of phase a, for an SLG fault (a-g) at bus 28, of modified IEEE 34-bus test system in the presence of IBDG and Δ-Y_g IBDG transformer using proposed $\left[\mathbf{BIBC}\right]$ technique, $\left[\mathbf{Y_{bus}}\right]$ technique and PSCAD/EMTDC simulation . 232

6.15 Voltage profile of neutral bus, for an SLG fault (a-g) at bus 28, of modified IEEE 34-bus test system in the presence of IBDG and Δ-Y_g IBDG transformer using proposed $\left[\mathbf{BIBC}\right]$ technique, $\left[\mathbf{Y_{bus}}\right]$ technique and PSCAD/EMTDC simulation . 233

6.16 Voltage profile of ground bus, for an SLG fault (a-g) at bus 28, of modified IEEE 34-bus test system in the presence of IBDG and Δ-Y_g IBDG transformer using proposed $\left[\mathbf{BIBC}\right]$ technique, $\left[\mathbf{Y_{bus}}\right]$ technique and PSCAD/EMTDC simulation . 233

6.17 (a) Voltage profile of ground bus, (b) Ground current, for various ground faults at bus 28, of modified IEEE 34-bus test system in the presence of IBDG and Δ-Y_g IBDG transformer 235

6.18 Ground bus voltage and ground current at fault point in modified IEEE 34-bus test system in the presence of IBDG and Δ-Y_g IBDG transformer for various grounding resistance under SLG fault (a) and (b), LLG fault (c) and (d) and LLLG fault (e) and (f) 236

6.19 Voltage profile of phase a of modified IEEE 123-bus test system in the presence of IBDG and Δ-Y_g IBDG transformer using proposed $\left[\mathbf{BIBC}\right]$ technique and $\left[\mathbf{Y_{bus}}\right]$ technique under normal operating conditions 237

6.20 Voltage profile of neutral bus of modified IEEE 123-bus test system in the presence of IBDG and Δ-Y_g IBDG transformer using proposed $\left[\mathbf{BIBC}\right]$ technique and $\left[\mathbf{Y_{bus}}\right]$ technique under normal operating conditions 237

6.21 Voltage profile of ground bus of modified IEEE 123-bus test system in the presence of IBDG and Δ-Y_g IBDG transformer using proposed $\left[\mathbf{BIBC}\right]$ technique and $\left[\mathbf{Y_{bus}}\right]$ technique under normal operating conditions 238

6.22 Branch current of phase a of modified IEEE 123-bus test system in the presence of IBDG and Δ-Y_g IBDG transformer using proposed $\left[\mathbf{BIBC}\right]$ technique and $\left[\mathbf{Y_{bus}}\right]$ technique under normal operating conditions 238

6.23 Neutral current of modified IEEE 123-bus test system in the presence of IBDG and Δ-Y_g IBDG transformer using proposed $\left[\mathbf{BIBC}\right]$ technique and $\left[\mathbf{Y_{bus}}\right]$ technique under normal operating conditions 239

6.24 Ground current of modified IEEE 123 bus-test system in the presence of IBDG and Δ-Y_g IBDG transformer using proposed $\left[\mathbf{BIBC}\right]$ technique and $\left[\mathbf{Y_{bus}}\right]$ technique under normal operating conditions 239

6.25 (a) Neutral bus voltage profile, (b) Neutral current of modified IEEE 123-bus test system in the presence of IBDG and Δ-Y_g IBDG transformer in "isolated neutral" and "grounded neutral" cases under normal operating conditions 241

6.26 Voltage profile of phase a, for an SLG fault (a-g) at bus 105, of modified IEEE 123-bus test system in the presence of IBDG and Δ-Y_g IBDG transformer using proposed $\left[\mathbf{BIBC}\right]$ technique and $\left[\mathbf{Y_{bus}}\right]$ technique 243
6.27 Voltage profile of neutral bus, for an SLG fault (a-g) at bus 105, of modified IEEE 123-bus test system in the presence of IBDG and Δ-Y_g IBDG transformer using proposed $\left[\mathbf{BIBC}\right]$ technique and $\left[\mathbf{Y_{bus}}\right]$ technique 244
6.28 Voltage profile of ground bus, for an SLG fault (a-g) at bus 105, of modified IEEE 123-bus test system in the presence of IBDG and Δ-Y_g IBDG transformer using proposed $\left[\mathbf{BIBC}\right]$ technique and $\left[\mathbf{Y_{bus}}\right]$ technique 244
6.29 (a) Voltage profile of ground bus, (b) Ground current, for various ground faults at bus 105, of modified IEEE 123-bus test system in the presence of IBDG and Δ-Y_g IBDG transformer 246
6.30 Voltage profile of phase a of modified IEEE 34-bus test system in the presence of IBDG and Y_g-Y_g IBDG transformer using proposed $\left[\mathbf{BIBC}\right]$ technique, $\left[\mathbf{Y_{bus}}\right]$ technique and PSCAD/EMTDC simulation under normal operating conditions . . . 247
6.31 Voltage profile of neutral bus of modified IEEE 34-bus test system in the presence of IBDG and Y_g-Y_g IBDG transformer using proposed $\left[\mathbf{BIBC}\right]$ technique, $\left[\mathbf{Y_{bus}}\right]$ technique and PSCAD/EMTDC simulation under normal operating conditions . . . 247
6.32 Voltage profile of ground bus of modified IEEE 34-bus test system in the presence of IBDG and Y_g-Y_g IBDG transformer using proposed $\left[\mathbf{BIBC}\right]$ technique, $\left[\mathbf{Y_{bus}}\right]$ technique and PSCAD/EMTDC simulation under normal operating conditions . . . 248
6.33 Branch current of phase a of modified IEEE 34-bus test system in the presence of IBDG and Y_g-Y_g IBDG transformer using proposed $\left[\mathbf{BIBC}\right]$ technique, $\left[\mathbf{Y_{bus}}\right]$ technique and PSCAD/EMTDC simulation under normal operating conditions . . . 248
6.34 Neutral current of modified IEEE 34-bus test system in the presence of IBDG and Y_g-Y_g IBDG transformer using proposed $\left[\mathbf{BIBC}\right]$ technique, $\left[\mathbf{Y_{bus}}\right]$ technique and PSCAD/EMTDC simulation under normal operating conditions 249
6.35 Ground current of modified IEEE 34-bus test system in the presence of IBDG and Y_g-Y_g IBDG transformer using proposed $\left[\mathbf{BIBC}\right]$ technique, $\left[\mathbf{Y_{bus}}\right]$ technique and PSCAD/EMTDC simulation under normal operating conditions 249

6.36 (a) Neutral bus voltage profile, (b) Neutral current of modified IEEE 34-bus test system in the presence of IBDG and Y_g-Y_g IBDG transformer in "isolated neutral" and "grounded neutral" cases under normal operating conditions 251
6.37 (a) Maximum ground bus voltage, (b) Maximum ground current, in modified IEEE 34-bus test system in the presence of IBDG and Y_g-Y_g IBDG transformer for various grounding resistance under normal operating condition 252
6.38 Voltage profile of phase a, for an SLG fault (a-g) at bus 28, of modified IEEE 34-bus test system in the presence of IBDG and Y_g-Y_g IBDG transformer using proposed $\left[\mathbf{BIBC}\right]$ technique, $\left[\mathbf{Y_{bus}}\right]$ technique and PSCAD/EMTDC simulation . 254
6.39 Voltage profile of neutral bus, for an SLG fault (a-g) at bus 28, of modified IEEE 34-bus test system in the presence of IBDG and Y_g-Y_g IBDG transformer using proposed $\left[\mathbf{BIBC}\right]$ technique, $\left[\mathbf{Y_{bus}}\right]$ technique and PSCAD/EMTDC simulation . 255
6.40 Voltage profile of ground bus, for an SLG fault (a-g) at bus 28, of modified IEEE 34-bus test system in the presence of IBDG and Y_g-Y_g IBDG transformer using proposed $\left[\mathbf{BIBC}\right]$ technique, $\left[\mathbf{Y_{bus}}\right]$ technique and PSCAD/EMTDC simulation . 255
6.41 (a) Voltage profile of ground bus, (b) Ground current, for various ground faults at bus 28, of modified IEEE 34-bus test system in the presence of IBDG and Y_g-Y_g IBDG transformer 256
6.42 Voltage profile of phase a of modified IEEE 123-bus test system in the presence of IBDG and Y_g-Y_g IBDG transformer using proposed $\left[\mathbf{BIBC}\right]$ technique and $\left[\mathbf{Y_{bus}}\right]$ technique under normal operating conditions 257
6.43 Voltage profile of neutral bus of modified IEEE 123-bus test system in the presence of IBDG and Y_g-Y_g IBDG transformer using proposed $\left[\mathbf{BIBC}\right]$ technique and $\left[\mathbf{Y_{bus}}\right]$ technique under normal operating conditions 258
6.44 Voltage profile of ground bus of modified IEEE 123-bus test system in the presence of IBDG and Y_g-Y_g IBDG transformer using proposed $\left[\mathbf{BIBC}\right]$ technique and $\left[\mathbf{Y_{bus}}\right]$ technique under normal operating conditions 258
6.45 Branch current of phase a of modified IEEE 123-bus test system in the presence of IBDG and Y_g-Y_g IBDG transformer using proposed $\left[\mathbf{BIBC}\right]$ technique and $\left[\mathbf{Y_{bus}}\right]$ technique under normal operating conditions 259

6.46 Neutral current of modified IEEE 123-bus test system in the presence of IBDG and Y_g-Y_g IBDG transformer using proposed $\left[\mathbf{BIBC}\right]$ technique and $\left[\mathbf{Y_{bus}}\right]$ technique under normal operating conditions 259
6.47 Ground current of modified IEEE 123 bus-test system in the presence of IBDG and Y_g-Y_g IBDG transformer using proposed $\left[\mathbf{BIBC}\right]$ technique and $\left[\mathbf{Y_{bus}}\right]$ technique under normal operating conditions 260
6.48 (*a*) Neutral bus voltage profile, (*b*) Neutral current of modified IEEE 123-bus test system in the presence of IBDG and Y_g-Y_g IBDG transformer in "isolated neutral" and "grounded neutral" cases under normal operating conditions 262
6.49 Voltage profile of phase a, for an SLG fault (a-g) at bus 105, of modified IEEE 123-bus test system in the presence of IBDG and Y_g-Y_g IBDG transformer using proposed $\left[\mathbf{BIBC}\right]$ technique and $\left[\mathbf{Y_{bus}}\right]$ technique 264
6.50 Voltage profile of neutral bus, for an SLG fault (a-g) at bus 105, of modified IEEE 123-bus test system in the presence of IBDG and Y_g-Y_g IBDG transformer using proposed $\left[\mathbf{BIBC}\right]$ technique and $\left[\mathbf{Y_{bus}}\right]$ technique 264
6.51 Voltage profile of ground bus, for an SLG fault (a-g) at bus 105, of modified IEEE 123-bus test system in the presence of IBDG and Y_g-Y_g IBDG transformer using proposed $\left[\mathbf{BIBC}\right]$ technique and $\left[\mathbf{Y_{bus}}\right]$ technique 265
6.52 (*a*) Voltage profile of ground bus, (*b*) Ground current, for various ground faults at bus 105, of modified IEEE 123-bus test system in the presence of IBDG and Y_g-Y_g IBDG transformer 266

List of Abbreviations

Amp Ampere.

ANSI American National Standards Institute.

BIBC Bus Injection To Branch Current.

DFIG Doubly-Fed Induction Generator.

DG Distributed Generation.

DISCA Distribution Short Circuit Analysis.

DISFLO Distribution Power Flow.

DNER Distribution Network with Earth Return.

DSLF Distribution System Load Flow.

Eq. Equation.

Eqs. Equations.

Fig. Figure.

GMR Geometric Mean Radii.

GS Gauss Siedel.

i.e. that is to say.

IBDG Inverter Based Distributed Generation.

IEEE Institute of Electrical and Electronics Engineering.

kA kilo Ampere.

KCL Kirchhoff's Current Law.

kV kilo Volt.

kVA kilo Volt Ampere.

kVAR kilo Volt Ampere Reactive.

KVL Kirchhoff's Voltage Law.

kW kilo Watt.

LL Line To Line.

LLG Double Line To Ground.

LLLG Three Line To Ground.

LV Low Voltage.

MTG Micro-turbine Generation.

MV Medium Voltage.

No. Number.

NR Newton Raphson.

PSCAD/EMTDC Power Systems Computer Aided Design/Electro Magnetic Transient Design and Control.

PV Photo voltaic.

SLG Single Line To Ground.

SPV Solar Photo Voltaic.

TIBC Transformer Inclusion To Branch Current.

ZIP Combination of constant-impedance (Z), constant-current (I) and constant power (P) loads.

List of Symbols

F_I	Coefficient of constant-current part of the real power of a ZIP load.
F_P	Coefficient of constant-power part of the real power of a ZIP load.
F_Z	Coefficient of constant-impedance part of the real power of a ZIP load.
$\angle$	Angle.
Ω	Ohm, unit of impedance.
$\Psi^p_{inv,f}$	Inverter current angle corresponding to phase p under the fault conditions.
$\theta^p_{dg,f}$	Voltage angle corresponding to phase p of DG bus (where an IBDG is connected) under the fault conditions.
$\theta^p_{n,f}$	Voltage angle corresponding to phase p of bus n under the fault conditions.
*	Complex conjugate operator.
^{T}	Transposition operator.
$F^{'}_I$	Coefficient of constant-current part of the reactive power of a ZIP load.
$F^{'}_P$	Coefficient of constant-power part of the reactive power of a ZIP load.
$F^{'}_Z$	Coefficient of constant-impedance part of the reactive power of a ZIP load.
nd	Number of Inverter based Distributed Generations (IBDGs).
$\%$	Percentage.
ϵ	Error.
π	A constant 'pi' which contains the value of 3.14159265359.
ρ	Ground resistivity.

f System frequency in Hz.

f_b fault bus (system bus where the fault occurs).

g_{f_b} ground bus at the location of fault bus.

g_i ground bus at the location of i^{th} system bus.

I_f Fault current.

I_s Source current.

m_b Total number of lines in a distribution network.

m_s Total number of meshes in a distribution network.

max Maximum value.

n_b Total number of buses in a distribution network.

n_i neutral bus at the location of i^{th} system bus.

nld Total number of loads in a distribution network.

nt Total number of transformers in a network.

$p.u.$ Per unit.

u Total number of three-phase buses in a distribution network.

v Total number of two-phase buses in a distribution network.

w Total number of single-phase buses in a distribution network.

z_f Fault impedance.

Chapter 1

Introduction

Abstract

Short-circuit analysis is an important tool for analyzing the behavior of power system under the fault conditions. The short-circuit studies provide the values of fault currents flowing in the system which helps in specifying the short time ratings of the system components and the design of required protective schemes. It is also used for estimating the size of fault current limiters, required in the system to limit the short-circuit currents to a safer value.

1.1 Overview

DURING normal operating conditions, the currents through the elements of a power system are well within their specified values. When a fault occurs in a system, the currents far in excess of normal values usually start flowing through network elements. These excessively high currents, if not interrupted or limited, can cause serious damage to the equipments [1]. The occurrence of fault affects reliability, security, and energy quality of the system.

According to ANSI/IEEE Std. 100-1992 [2], a ”fault” may be defined as, ”A physical condition that causes a device, a component, or an element to fail to perform in a required manner, for example, a short circuit or a broken wire. A fault almost always involves a short circuit between energized phase conductors or between phases and ground. A fault may be bolted connection or may have some impedance in the fault connection”.

The term ”fault” is often used synonymously with the term ”short-circuit” defined as (according to ANSI/IEEE Std. 100-1992 [2]), ”An abnormal connection (including an arc) of relatively low impedance, whether made accidentally or intentionally, between two points of different potential”.

An electric power system consists of generators, transformers, transmission lines, distribution lines, and consumer equipments (loads). The system must be protected against flow of heavy short-circuit currents by disconnecting the faulty section of the system by means of protective relays and

circuit breakers. The short-circuit current will be many times greater than the normal circuit current and if the circuit is not opened and the current is not interrupted quickly, then extensive damage can occur. To protect the power system from adverse affects of short-circuits, it is important to estimate or calculate the value of prospective current likely to occur under short circuit conditions and ensure that the protective devices provided to interrupt that current are properly rated to withstand the fault current and interrupt it timely. The severity of the fault depends on the location of short-circuit, the path taken by the fault current, fault impedance, system impedance and system voltage level [3]. In order to maintain the continuity of power supply to all customers which is the basic purpose of a power system, all faulted parts must be isolated from the system by the protection schemes [2].

Power system faults can be categorized as [1] -:

1. Symmetrical or balanced faults (all the phases are equally affected by the fault):

a) Three phase short-circuit fault (LLL), *b)* Three-phase to ground short-circuit fault (LLLG),

2. Unsymmetrical or unbalanced faults (balanced state of the network is disturbed):

a) Shunt type faults -: (i) Single-line-to-ground (SLG) fault, (ii) Line-to-Line (LL) fault, (iii) Double-line-to-ground (LLG) fault,

b) Series type faults -: (i) Open conductor fault.

Since, the distribution systems are unbalanced in nature (due to single and two phase lines, unbalanced loads and untransposed feeders) in normal operating conditions, all the type of faults are considered as unsymmetrical faults in case of distribution system.

The process of evaluating the system voltages and currents under different types of short-circuits is called short-circuit analysis [1]. The information provided by short-circuit analysis study can be used to specify the necessary safety measures and the design of the required protection system. The short-circuit analysis helps in the selection of appropriate type and size of protective equipments and coordinating their settings [2]. It can also be helpful in the estimation of the size of the protective reactors or fault current limiters which may be required to be inserted in the system to limit short-circuit currents to a safe value which is not beyond the withstand capability of the installed circuit-breakers.

Integration of Distributed Generation (DG) to the grid improves the system efficiency (by improving the system voltage profile) and reliability [4–21]. The DGs deliver electrical energy with

low carbon emission and also help to reduce the feeder loading and system losses [22–24]. Generally, Inverter Based Distributed Generations (IBDGs) such as, fuel cell, wind power, solar photovoltaic (SPV), micro-turbines etc. [25–30] are used in the distribution system. However, integration of a DG to a distribution system increases the fault level of the system as it contributes to the fault current during a fault [31–36]. A single small DG unit may not contribute much to the fault current, but the contributions of many small units may cause malfunctioning of protective devices due to increased fault current [37]. Hence, with the integration of DG, short-circuit currents may change from time to time due to the variation in generation of DG. Therefore, there is always a need for a suitable fault analysis method that can take the DG integration into account for estimating the short-circuit current.

1.2 Literature review

1.2.1 Short-circuit analysis of three-phase three wire distribution system

Two approaches are commonly used in the industry for analyzing short circuit faults in Distribution systems [38]

1. Classical symmetrical component based approach,
2. Phase variable approach,

1. Classical symmetrical component based approach -:

In symmetrical component method, the elements in the distribution system are represented by their positive, negative, and zero sequence equivalent circuits [39–41]. Fault analysis method using symmetrical components [39] uses a modeling approach for single and two phase lines in fault calculation based on symmetrical components. In this approach, single and two phase lines are presented as equivalent three phase lines by using dummy lines and dummy nodes for the purpose of the fault calculation. The voltage drop across dummy line is zero as there is no coupling between the dummy line and the other actual phases of the line, and the current injections at the dummy node is neglected. An error analysis of the symmetrical components based fault analysis methods has been performed for IEEE 13-bus, 34-bus, and 123-bus systems in [40]. Symmetrical component method takes the assumption that the mutual impedances between all the phases are equal. This assumption, which is not true in case of distribution system, introduces an error in the

values of fault currents in distribution systems. In this paper, all major type of faults, symmetrical and unsymmetrical, are considered at each bus and the results obtained from symmetrical component and three phase model approaches are compared. The maximum error obtained in all types of fault is 8.53%, which is substantial and cannot be neglected. It is also shown that these errors are independent of the size of the system, but are dependent on the degree of unbalance present in the system. A Fortescue short-circuit computation (SCC) method based on symmetrical components transformation of three-phase, two-phase and single-phase system has been proposed in [41]. It is based on Fortescue nodal admittance matrix of the network. The proposed method has resolved the problems occurred in symmetrical component based method due to unbalanced nature of distribution system and untransposed lines. In this method, first, the equivalent Fortescue Thevenin impedance matrix is obtained at the fault point (by deactivating all the active sources and injecting a unity current, one at a time, at each of the phases of Fortescue node) and next, the fault current is calculated with the help of current injection method. However, these methods [39–41] have not considered the effect of loads during the short-circuit calculations.

2. Phase variable approach -:

In phase variable method, the elements in the distribution system are represented in the phase domain by their corresponding three phase impedance or admittance matrices [42–56]. The method of triangular factorization of $[\mathbf{Y_{bus}}]$ matrix to simulate different faults is presented in [42]. Models of Co-generator (induction or synchronous generators) and three phase transformer are also included in the test system. The method has been applied to balanced, unbalanced, radial and meshed type distribution networks. A linear graph based network modeling approach to form the admittance matrix (that relates the bus voltages to the injected bus currents) has been proposed in [43]. In this approach, the fault analysis has been carried out in both time and frequency domain. A relatively smaller 16-bus meshed distribution system with one non-utility generator and one large induction machine load model has been used to demonstrate the steps of the proposed method. A hybrid compensation based short-circuit analysis method is proposed in [44]. In this method two algorithms namely, Distribution power flow (DISFLO) and Distribution short circuit analysis (DISCA) are utilized. DISFLO is used to solve the load flow for radial and weakly meshed distribution system in phase domain. DISCA is then used to simulate various types of faults, single

as well as simultaneous faults. Two different lateral and load equivalent compensation based approaches [45] have been proposed for the short circuit analysis of radial distribution networks. In this work, Initial Condition Boundary Matching (ICBM) method is used for the analysis of short circuit faults. The algorithm has been tested on two unbalanced (20-bus and 394-bus) distribution system.

A method that generalizes both backward-forward and short circuit hybrid compensation procedure for performing the short circuit analysis of four wire distribution network is proposed in [46]. It has been applied to a 29-bus real-life four-wire, three-phase LV (low-voltage) feeder and IEEE-34 bus four-wire, three-phase MV (medium-voltage) feeder. The short circuit analysis methods, based on two relationship matrices namely, $[\mathbf{BIBC}]$ and $[\mathbf{BCBV}]$, have been proposed for radial and meshed distribution systems in [47] and [48], respectively. The $[\mathbf{BIBC}]$ matrix represents the relationship between injected bus current and branch currents, while the $[\mathbf{BCBV}]$ matrix gives the relationship between branch current and bus voltages. Various short-circuit fault cases have been simulated on 11.4 kV test feeder of Taiwan Power Company using the proposed method. The short circuit analysis approach [47] has been extended in [49] to include the effect of Distributed Generation (DG) in the radial distribution system network. The DG model used in this work is similar to the synchronous generator model used in short-circuit studies [50]. The method has been extensively tested on different systems under different fault conditions. The effect of fault impedance on the unbalanced faulted distribution system has been described in the short-circuit analysis method given in [51]. This method is based on bus impedance matrix $[\mathbf{Z_{bus}}]$ of the network which includes the effect of fault impedances in the short-circuit calculations. Various short-circuit studies have been performed on IEEE 13-bus test feeder with different values of fault impedances to show its effect on system voltages and currents.

A fault analysis with hybrid compensation method, based on relationship matrices $[\mathbf{B_I}]$ (bus injection ot branch current) and $[\mathbf{Z}_{V-BC}]$ (branch current to bus voltage), has been proposed in [52]. Different short-circuit and open conductor fault cases have been simulated using this method for different test systems, with synchronous generator as DG model. A fault analysis algorithm, proposed in [53], includes the effect of fault resistance in the calculation of fault currents for both radial as well as weakly meshed distribution networks. In this method first the fault resistance is calculated and then the modified bus impedance matrix is obtained which includes the effect of

calculated fault resistance. A novel short-circuit analysis method has been presented in [54] to analyze different types of faults in the unbalanced distribution system. It is a hybrid compensation based method which includes the effects of microturbine generation (MTG) as a distributed generator (DG). In this paper, modeling of a MTG has been carried out in both islanded and grid-connected modes of operation. A 8-bus MG distribution system feeder is used as a test system which consists of a grid, a static switch, an MTG, a battery energy storage system (BESS), and photovoltaic arrays. A model-based fault diagnosis scheme has been designed in [55], which is capable of real time detection of all types of faults in the distribution network. In this paper a linear dynamical-fault dependent state space model of Single Machine Infinite BUS (SMIB) power system has been derived which is capable of capturing the dynamics of the complete system over full time scale and therefore is suitable for the fault studies of any kind of fault. A multiphase short-circuit analysis method based on the concept of selected inversion algorithm called Sellnv has been proposed in [56]. First, the Thevenin equivalent impedance has been obtained at the fault point with the help of augmented nodal admittance matrix. Next, the short-circuit currents are calculated with the help of obtained Thevenin equivalent impedance at fault bus.

However, most of these short-circuit analysis methods have not included the effect of loads during the short-circuit calculations, which may give less accurate results.

1.2.2 Short-circuit analysis of three-phase three wire distribution system with inverter based Distributed Generations (IBDGs) and three-phase transformer models

Integration of distributed generation (DG) to the grid improves the system efficiency and reliability. However, the integration of DG to a distribution system increases the fault level of the system as it contributes to the fault current during a fault. To overcome the above discussed problem, two schemes have been proposed in the literature. The first scheme recommends the disconnection of all the DGs present in the system during faults before the operation of protective devices [57], while the second scheme proposes to restrict the fault current contribution from DGs to a safer value, so that all the protective devices present in the system function properly [58–65]. This can be achieved by incorporating a control strategy in the inverter of the IBDGs to limit its current during fault conditions. First scheme has a drawback that for every sustained as well as temporary fault, all DGs will be first disconnected from the grid and subsequently would be synchronized

with the grid after fault clearance. Disconnection of DGs also causes a voltage dip in the system. Hence, the second scheme [58–65] is preferred nowadays.

In [58–65], for considering the IBDGs in fault analysis, an IBDG has been modeled in sequence component frame to represent the operation of the inverter in current control mode. The model of the current controlled inverter is based on dq-0 control schemes. In this scheme, the phase components of the inverter current from IBDG are first converted into dq-0 sequence components and a control scheme is provided for controlling these dq-0 components. The effectiveness of these control techniques have been demonstrated through time-domain simulation studies carried out on MATLAB/SIMULINK environment [66]. In [67], an experimental setup for fault analysis with dq-0 control scheme for inverter has been implemented. However, these dq-0 component based fault analysis methods have only been carried out in the time domain simulation studies and been tested only on the small size distribution systems.

In [68], a conventional fault analysis method, based on system admittance matrix, that also includes the inverter interfaced Distributed Generators (IIDGs), has been proposed. In this scheme, it is assumed that the IIDG is operating in its voltage control mode during the faults. The contribution of IIDGs during the sub transient and transient period of the fault has also been analyzed. In [54, 69] a short-circuit analysis method with micro turbine generation (MTG) system has been proposed, for both islanded and grid connected mode. This method is based on two matrices; $\mathbf{BIBC}$ (Bus injection to branch current) and $\mathbf{BCBV}$ (Branch current to bus voltage) [70]. A fault analysis method with multiple grid connected photovoltaic (PV) inverters has been developed in [71] which utilizes symmetrical component of impedances. In [72], a short-circuit calculations (SCC) method, based on superposition theorem, is developed which can incorporate different types of DG models (Synchronous DG, Induction DG, Double fed induction generator (DFIG) and IBDG) during the fault current calculations.

However, these analytical and dq-0 component based short-circuit analysis algorithms with DGs have also not considered the effect of loads during the calculations of fault current, branch currents and bus voltages under the short-circuit conditions.

In [54, 58–65, 67, 69, 71, 72], the short-circuit analysis has been performed for the distribution system with IBDGs only. While, in actual practice, the IBDGs are connected to the grid through a step down transformer [73,74]. Therefore, it becomes necessary to incorporate various three-phase

transformer models in load flow as well as short-circuit studies of distribution network [73, 74].

Different load flow analysis methods based on forward/backward sweep approach to incorporate three phase transformer models in the distribution network are available in the literature [73, 75–79]. In [73], the three-phase power flow approach, for integrated three wire and four wire multi-grounded LV distribution network with rooftop solar PV, has been developed. The proposed method has incorporated Delta/Star configuration of the transformer in the load flow analysis of LV distribution system. The method proposed in [75] has developed the models for various transformer configurations in terms of voltage and current based equations. But the drawback of this method is that for each transformer configuration of different vector group, separate current and voltage equations are formed, which is a lengthy procedure. In [76], only the model of an ungrounded star-delta transformer has been developed and incorporated in the proposed load flow analysis method. It uses the current and voltage equation based model of transformer (the equations are presented in a matrix form). Therefore, it also requires separate voltage and current equation based models for different vector groups of transformers.

In [77] and [78], nodal admittance matrix based transformer models have been used in the load flow analysis methods. Nodal admittance matrix models of various transformer configurations with different vector groups are given in [80]. These methods also resolve the singularity problem, occurring in backward/forward sweep algorithm based load flow method, for particular types of transformer connections such as, star-grounded/delta ($Yg - \Delta$), star/delta ($Y - \Delta$), delta/star ($\Delta - Y$), delta/delta ($\Delta - \Delta$) connections etc. In [77] actual nodal admittance matrix model is used, while in [78], the per unit nodal admittance matrix model is used. Modified augmented nodal analysis (MANA) based approach has been developed in [79]. In this method, a single matrix is formed which is used for both the backward and forward sweep operations. The $\mathbf{BIBC/BCBV}$ matrix based approach has been developed in [81] for the load flow solution of balanced distribution system with phase-shifting transformer model. The PI-equivalent model of the tap changing single-phase transformer has been used and incorporated in the load flow equations. But the drawback of this method is that it is only applicable to the balanced three-phase distribution systems.

Different short-circuit analysis methods of distribution system with transformer models are available in the literature [76, 82, 83]. In [76], the ungrounded star-delta configuration of transformer is used in short-circuit analysis method. This method is based on Thevenin equivalent

impedance matrix of the system. This method is only applicable to a particular type of transformer model. The short-circuit analysis method developed in [82] is based on admittance matrix based approach. The current and voltage equation based transformer models are used in [82]. In this method, first the connection matrices are formed for various transformer configurations and then these matrices are incorporated in the admittance matrix model of the network for carrying out short-circuit calculations. The admittance summation method, which is a sequence component based approach, is used for the short-circuit calculations with three-winding and two winding transformer models in [83]. Admittance summation matrix has been formed by the summation of sequence component of transformer admittances, load admittances and fault admittance.

However, most of these available load flow and short-circuit analysis methods of unbalanced distribution systems in the literature have not considered the IBDGs and three-phase transformer models simultaneously.

1.2.3 Load flow and short-circuit analysis of three-phase four wire multigrounded distribution system

For three-phase three wire unbalanced distribution systems, various load flow [70, 75–79, 84–120] and short-circuit analysis [39–49, 51–55, 58–65, 68, 76, 82, 83, 121–127] methods have been proposed. Most of the distribution systems are unbalanced in nature and are located in high density load areas, these systems can be highly meshed. Under these circumstances, the three-phase four wire multigrounded configuration has been largely adopted, due to smaller installation costs and better sensitivities for fault protection, when compared with three phase three wire configuration [128, 129]. In the literature, various load flow analysis methods have been developed for the three phase four wire multigrounded distribution systems [128–135].

A backward/forward technique based load flow analysis method for the three-phase four wire radial distribution system network has been proposed in [128]. Two different cases have been discussed in this work, namely, *i)* isolated neutral and *ii)* without neutral. The method has been implemented on two test systems; *i)* IEEE 34-bus MV (Medium Voltage) test feeder and *ii)* LV (Low Voltage)-29 bus test feeder. In [129, 130], the four conductor current injection method (FCIM) has been proposed for the load flow analysis of three-phase four wire distribution network. This method is based on Newton-Raphson technique in rectangular form to solve the set of non-linear

current injection equations. The proposed methodology has been tested on practical distribution feeder in Brazil as well as on IEEE 4 and 34-bus test feeders. In [131], the time domain studies have been performed for the analysis of multi-grounded three-phase four wire distribution system. A full-scale model of a multi-grounded four-wire unbalanced distribution system was developed using P-Spice. The effect of neutral and grounding has also been observed on the sample system in this work.

In [132], a backward/forward technique based power flow algorithm has been developed for the single wire and three wire distribution network with earth return (DNER). The method has been tested on IEEE 34-bus test feeder, with different types of load models. In [133], the backward/forward sweep approach based load flow analysis method for the three phase four wire distribution system with micro wind generation has been proposed. The modeled test network used in this work consists of a section of LV (urban) distribution network (Ireland) incorporating 74 domestic homes facilitated by 10 mini-pillar connections. In [134], the power flow method, based on backward/forward approach, for three-phase four wire distribution system with protective multiple earthing (PME), during an open neutral condition is developed. In addition to this, the return current flow is also modeled with the help of nodal analysis of the network formed by the open neutral wire, assumed earth wire and grounding electrodes. In [135], the asymmetrical three-phase (with neutral) power flow problem, based on correction current injection methodology, has been developed for unbalanced multiple-grounded 4 wire distribution systems. The proposed method is based on formulation of admittance matrix of the system. The proposed methodology has also incorporated voltage dependent load models and distributed generation models of micro wind generation and solar PV generation systems.

Various short-circuit analysis methods are also available in the literature for the three-phase four wire unbalanced distribution network [136, 137]. The current injection based short-circuit analysis method has been developed in [136] for the mutliphase electrical distribution system. The Newton-Raphson based technique has been used in the proposed method. A nodal admittance matrix based transformer model has also been considered in the short-circuit calculations. The proposed method has been tested on IEEE 4-bus, 13-bus and NEV (Neutral to earth voltages) test systems to demonstrate its efficiency. In [137], the short-circuit analysis method, for the computation of phase to earth currents for various short-circuit faults in unbalanced multi-wire radial

distribution model, has been developed. The proposed method is based on the analysis of unbalanced multi-wire line model using Kirchhoffs laws and linear equation solving techniques. It uses the tableau analysis technique to solve the set of linear KCL equations.

1.3 Motivation

In the literature, the loads are usually neglected in the calculation of fault currents, branch currents and bus voltages under the fault conditions. However, in [82, 83, 138] it has been indicated that the load model can be critical in short circuit analysis. To investigate the effect of loads on the short-circuit behavior of a distribution system, two types of fault cases (SLG and LLG) for different test systems have been simulated on PSCAD/EMTDC [139] platform. Table 1.1 shows the fault current supplied by source considering loads (I_{swl}) and neglecting loads (I_{swol}). It can be observed that, I_{swl} is always more than I_{swol}. Furthermore, the difference in the values increases with the system size. In general, as the real distribution systems are quite large as compared to the test systems considered, this difference can be quite substantial and influence the rating of the protective devices installed at the substation. Hence, it is important to consider the effect of loads in the short-circuit calculations.

Also in the literature, most of the fault analysis methods of distribution system with IBDGs are based on dq-0 sequence component approach and on time domain simulation studies. However, these methods have only considered the current control mode of operation of inverter under the short-circuit conditions. Most of the analytical methods available in the literature for short-circuit analysis of distribution system with IBDGs and three-phase transformer models (simultaneously) have not considered the loads during short-circuit calculations.

In the literature, different load flow analysis methods for three phase four wire distribution systems was developed. Most of the developed methods are based on backward/forward approach. The developed algorithms in these methods are only applicable to the following distribution systems; *i)* three-phase four wire Distribution system with isolated neutral (without ground conductor), *ii)* three-phase four wire Distribution system with ground return (without neutral conductor), and *iii)* three-phase four wire Distribution system with zero neutral to ground or grounding impedance (i.e. neutral at all the buses are short-circuited to their respective local ground). Therefore, these developed methods have not considered all the cases of three-phase four wire multi-

Table 1.1: Case study to observe the effect of load currents in fault analysis

System	Fault type	Fault at bus no.	Faulty phase	I_{swl} (kA)	I_{swol} (kA)	Error (%)
7-Bus [48]	SLG	5	*a*	1.9106	1.8657	2.35
	LLG		*a* and *b*	3.0552	3.0101	1.48
IEEE 13-Bus [140]	SLG	675	*a*	2.8126	2.6842	4.6
	LLG		*a* and *b*	4.3864	4.307	1.81
IEEE 37-Bus [140]	SLG	724	*a*	1.3045	1.2234	6.22
	LLG		*a* and *b*	1.4444	1.3687	5.24
IEEE 123-Bus [140]	SLG	95	*a*	1.7288	1.5537	10.12
	LLG		*a* and *b*	2.1468	1.9563	8.87

grounded distribution system. A case of three-phase four wire multigrounded distribution system through grounding resistance has not been discussed in the literature.

The available short-circuit analysis methods for three-phase four wire multigrounded distribution systems have not considered the IBDGs. The synchronous generator based DG model has only been used in the available short-circuit studies. Also, these methods have not considered the effect of loads in the short-circuit analysis of three-phase four wire distribution system with ground return.

1.4 Contribution of the author

Motivated by the above lacuna, the following studies have been carried out in this thesis,

- Development of a short-circuit analysis method for the unbalanced distribution system considering loads. The proposed method is based on admittance matrix $[\mathbf{Y_{bus}}]$ of the system.

- Formulation of a short-circuit analysis algorithm for the unbalanced radial as well as weakly meshed distribution network with inverter based Distributed Generation (IBDG) considering loads. The current control and voltage control modes of operation of the inverter have been considered during the short-circuit calculations.

- Development of load flow and short-circuit analysis methods for the unbalanced distribution network incorporating three-phase transformer models and IBDGs. First, the load flow analysis method, based on $[\mathbf{BIBC}]$ and $[\mathbf{BCBV}]$ matrices of the system, has been proposed which incorporates the three-phase transformer models and IBDGs. Next, the short-circuit

analysis method based on Newton-Raphson technique has been developed for the unbalanced distribution system with three-phase transformer models and IBDGs.

- Development of load flow and short-circuit analysis methods for the unbalanced three-phase four wire multigrounded radial distribution system. First, the load flow analysis method, based on $[\mathbf{BIBC}]$ and $[\mathbf{BCBV}]$ matrices of the system, has been developed. Next, two different short-circuit analysis methods, one based on $[\mathbf{BIBC}]$ and $[\mathbf{BCBV}]$ matrices of the system and the other one based on $[\mathbf{Y_{bus}}]$ matrix of the system, have been proposed.

- Development of load flow method (based on $[\mathbf{BIBC}]$ and $[\mathbf{BCBV}]$ matrices) and two different short-circuit analysis methods (one based on $[\mathbf{BIBC}]$ and $[\mathbf{BCBV}]$ matrices and next one based on $[\mathbf{Y_{bus}}]$ matrix) for the unbalanced three-phase four wire multigrounded radial distribution system which incorporate three-phase transformer models and IBDGs. Two different transformer configurations, namely Delta/Star-grounded (Δ-Y_g) and Star-grounded/Star-grounded (Y_g-Y_g), have been considered in both load flow and short-circuit studies.

1.5 Thesis organization

Apart from this chapter, there are six more chapters in this thesis. Chapter 2, describes the short-circuit analysis method for the unbalanced radial as well weakly meshed distribution system. In Chapter 3, short-circuit analysis method for the unbalanced distribution system with inverter based Distributed Generation (IBDG) is presented. Load flow and short-circuit analysis methods for the unbalanced distribution system considering three-phase transformer models and IBDGs are presented in Chapter 4. In Chapter 5, the load flow and short-circuit analysis methods for the unbalanced three-phase four wire multigrounded radial distribution system are presented. In Chapter 6, load flow and short-circuit analysis methods for the three-phase four wire multigrounded distribution system with two different three-phase transformer models (Delta/Star-grounded (Δ-Y_g) and Star-grounded/Star-grounded (Y_g-Y_g)) and IBDGs are presented. Lastly, Chapter 7 lists the major conclusions of this work as well as the future scope of work.

In this thesis all simulation studies have been carried out in PSCAD/EMTDC simulink software [139] and MATLAB 12a [66].

In the next chapter, a procedure for the short-circuit analysis of unbalanced radial and weakly meshed distribution system considering loads is described.

Chapter 2

Short-circuit analysis of unbalanced Distribution system considering loads

Abstract

This chapter proposes an efficient and accurate short-circuit fault analysis method for balanced and unbalanced distribution system considering the effect of loads. The proposed method is based on bus admittance matrix $[\mathbf{Y_{bus}}]$ *of the distribution system. This method is applicable to both radial as well as meshed distribution system. The developed method is implemented on modified IEEE 123-bus radial as well as meshed distribution system. Comparison of the test results obtained by the proposed method with those obtained by time-domain simulation studies using PSCAD/EMTDC software establishes the accuracy of the proposed method.*

2.1 Introduction

SHORT-circuit analysis is an essential tool for determining the short-circuit-current rating of the protective devices and different substation equipments to be installed in a distribution system as well as for co-ordination of the protective devices. Most of the available short-circuit analysis methods [42–49, 52, 54, 141–143] in the literature have assumed that the load currents are negligible as compared to the fault currents. Therefore, it is assumed that only the fault current is flowing in the system under the fault conditions, which is not the practical situation. However, in [82, 83, 138] it is indicated that the load model can be critical in short circuit analysis. In this chapter, a technique for short-circuit analysis is proposed which is based on bus admittance matrix $[\mathbf{Y_{bus}}]$ of the distribution network, considering the loads during short-circuit calculations.

This chapter is organized as follows. Section 2.2 describes the formulation of the proposed short-circuit analysis method for unbalanced radial as well as meshed distribution system. The main results of this chapter are presented in Section 2.3 and finally Section 2.4 highlights the main

conclusions of this chapter.

2.2 Short-circuit analysis of unbalanced distribution system considering loads

2.2.1 System modeling

Let us consider a three phase, unbalanced radial distribution system having n_b bus and m_b lines, as shown in Fig. 2.1. The system has $(m_b - 2)$ three phase lines, one two phase and one single phase line. Distribution line between buses i and g is a two phase line, while that between buses g and h is a single phase line. Bus 1 is the substation bus and $\bar{V}_s^a$,$\bar{V}_s^b$, and $\bar{V}_s^c$ are the voltages of phase a, b and c, respectively, of this bus. $\bar{z}_{ij}^{aa}$, $\bar{z}_{ij}^{bb}$, and $\bar{z}_{ij}^{cc}$ are the self impedances of phases a, b and c of line between buses i and j, respectively. $\bar{z}_{ij}^{ab}$, $\bar{z}_{ij}^{bc}$, and $\bar{z}_{ij}^{ac}$ are the mutual impedances between phases a and b, b and c, and a and c of line between buses i and j, respectively. The line impedance matrix between buses i and j is given as,

$$\bar{\mathbf{z}}_{\mathbf{ij}}^{\mathbf{abc}} = \begin{bmatrix} \bar{z}_{ij}^{aa} & \bar{z}_{ij}^{ab} & \bar{z}_{ij}^{ac} \\ \bar{z}_{ij}^{ba} & \bar{z}_{ij}^{bb} & \bar{z}_{ij}^{bc} \\ \bar{z}_{ij}^{ca} & \bar{z}_{ij}^{cb} & \bar{z}_{ij}^{cc} \end{bmatrix} \tag{2.1}$$

where, $\bar{z}_{ij}^{pq} = \bar{z}_{ij}^{qp};\ p, q = a, b, c;\ p \neq q$. The line admittance matrix between buses i and j can be calculated as,

$$\bar{\mathbf{y}}_{\mathbf{ij}}^{\mathbf{abc}} = \left[\bar{\mathbf{z}}_{\mathbf{ij}}^{\mathbf{abc}}\right]^{-\mathbf{1}} = \begin{bmatrix} \bar{y}_{ij}^{aa} & \bar{y}_{ij}^{ab} & \bar{y}_{ij}^{ac} \\ \bar{y}_{ij}^{ba} & \bar{y}_{ij}^{bb} & \bar{y}_{ij}^{bc} \\ \bar{y}_{ij}^{ca} & \bar{y}_{ij}^{cb} & \bar{y}_{ij}^{cc} \end{bmatrix} \tag{2.2}$$

The loads have been modelled as constant impedance obtained from pre-fault conditions. These load models can be easily included in the $[\mathbf{Y_{bus}}]$ matrix of the network. The load impedance and load admittance are given as,

$$\bar{z}_{id}^{p} = \frac{\bar{V}_i^p}{\bar{I}_i^p} \tag{2.3}$$

$$\bar{y}_{id}^{p} = \frac{1}{\bar{z}_{id}^{p}} \tag{2.4}$$

In eqs. (2.3) and (2.4), $\bar{z}_{id}^{p}$ and $\bar{y}_{id}^{p}$ are the equivalent load impedance and load admittance of phase p (p = a, b, c) of i^{th} bus respectively, $\bar{V}_i^p$ and $\bar{I}_i^p$ are the voltage and injected load current of phase

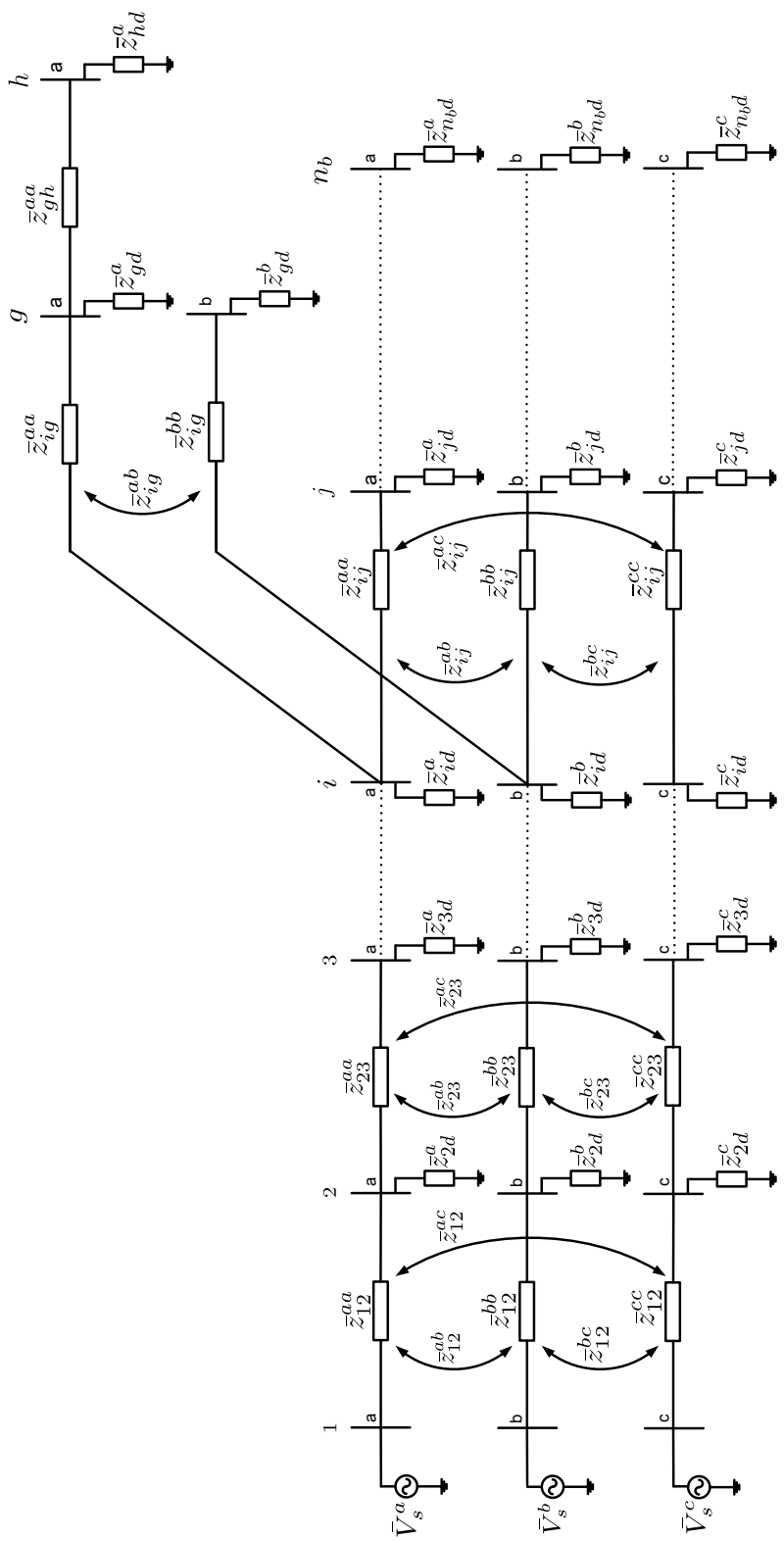

Figure 2.1: An n bus unbalanced radial distribution system

p (p = a, b, c) at i^{th} bus respectively, obtained from the load flow solution. The load admittance, calculated in eq. (2.4), is subsequently included in the $[\mathbf{Y_{bus}}]$ matrix of the distribution network to consider the effect of loads on short-circuit calculations. The load admittance matrix at bus i is given as,

$$\bar{\mathbf{y}}_{\mathbf{id}}^{\mathbf{abc}} = \begin{bmatrix} \bar{y}_{id}^{a} & 0 & 0 \\ 0 & \bar{y}_{id}^{b} & 0 \\ 0 & 0 & \bar{y}_{id}^{c} \end{bmatrix} \tag{2.5}$$

Applying Kirchhoff's Current Law (KCL) at bus 2 in Fig. 2.1, we get,

$$\bar{\mathbf{y}}_{\mathbf{12}}^{\mathbf{abc}}.(\bar{\mathbf{V}}_{\mathbf{2}}^{\mathbf{abc}} - \bar{\mathbf{V}}_{\mathbf{s}}^{\mathbf{abc}}) + \bar{\mathbf{y}}_{\mathbf{23}}^{\mathbf{abc}}.(\bar{\mathbf{V}}_{\mathbf{2}}^{\mathbf{abc}} - \bar{\mathbf{V}}_{\mathbf{3}}^{\mathbf{abc}}) + \bar{\mathbf{y}}_{\mathbf{2d}}^{\mathbf{abc}}.\bar{\mathbf{V}}_{\mathbf{2}}^{\mathbf{abc}} = \mathbf{0}$$

$$(\bar{\mathbf{y}}_{\mathbf{12}}^{\mathbf{abc}} + \bar{\mathbf{y}}_{\mathbf{23}}^{\mathbf{abc}} + \bar{\mathbf{y}}_{\mathbf{2d}}^{\mathbf{abc}}).\bar{\mathbf{V}}_{\mathbf{2}}^{\mathbf{abc}} - \bar{\mathbf{y}}_{\mathbf{23}}^{\mathbf{abc}}.\bar{\mathbf{V}}_{\mathbf{3}}^{\mathbf{abc}} = \bar{\mathbf{y}}_{\mathbf{12}}^{\mathbf{abc}}.\bar{\mathbf{V}}_{\mathbf{s}}^{\mathbf{abc}}$$

$$\bar{\mathbf{Y}}_{\mathbf{22}}^{\mathbf{abc}}.\bar{\mathbf{V}}_{\mathbf{2}}^{\mathbf{abc}} + \bar{\mathbf{Y}}_{\mathbf{23}}^{\mathbf{abc}}.\bar{\mathbf{V}}_{\mathbf{3}}^{\mathbf{abc}} = \bar{\mathbf{y}}_{\mathbf{12}}^{\mathbf{abc}}.\bar{\mathbf{V}}_{\mathbf{s}}^{\mathbf{abc}} \tag{2.6}$$

where $\bar{\mathbf{Y}}_{\mathbf{22}}^{\mathbf{abc}} = (\bar{\mathbf{y}}_{\mathbf{12}}^{\mathbf{abc}} + \bar{\mathbf{y}}_{\mathbf{23}}^{\mathbf{abc}} + \bar{\mathbf{y}}_{\mathbf{2d}}^{\mathbf{abc}})$; $\bar{\mathbf{Y}}_{\mathbf{23}}^{\mathbf{abc}} = -\bar{\mathbf{y}}_{\mathbf{23}}^{\mathbf{abc}}$.
$\bar{\mathbf{V}}_{\mathbf{s}}^{\mathbf{abc}} = \begin{bmatrix} \bar{V}_s^a & \bar{V}_s^b & \bar{V}_s^c \end{bmatrix}^{\mathbf{T}}$; $\bar{\mathbf{V}}_{\mathbf{r}}^{\mathbf{abc}} = \begin{bmatrix} \bar{V}_r^a & \bar{V}_r^b & \bar{V}_r^c \end{bmatrix}^{\mathbf{T}}$; where, $r = 2, 3$.
Next, applying KCL at bus i, we get,

$$\bar{\mathbf{Y}}_{\mathbf{i(i-1)}}^{\mathbf{abc}}.\bar{\mathbf{V}}_{\mathbf{(i-1)}}^{\mathbf{abc}} + \bar{\mathbf{Y}}_{\mathbf{ii}}^{\mathbf{abc}}.\bar{\mathbf{V}}_{\mathbf{i}}^{\mathbf{abc}} + \bar{\mathbf{Y}}_{\mathbf{ig}}^{\mathbf{ab}}.\bar{\mathbf{V}}_{\mathbf{g}}^{\mathbf{ab}} + \bar{\mathbf{Y}}_{\mathbf{ij}}^{\mathbf{abc}}.\bar{\mathbf{V}}_{\mathbf{j}}^{\mathbf{abc}} = \mathbf{0} \tag{2.7}$$

where $\bar{\mathbf{Y}}_{\mathbf{ig}}^{\mathbf{ab}} = -\begin{bmatrix} \bar{y}_{ig}^{aa} & \bar{y}_{ig}^{ab} \\ \bar{y}_{ig}^{ba} & \bar{y}_{ig}^{ba} \\ 0 & 0 \end{bmatrix} = \begin{bmatrix} \bar{\mathbf{Y}}_{\mathbf{gi}}^{\mathbf{ab}} \end{bmatrix}^{\mathbf{T}}$, and $\bar{\mathbf{V}}_{\mathbf{g}}^{\mathbf{ab}} = \begin{bmatrix} \bar{V}_g^a & \bar{V}_g^b \end{bmatrix}^{\mathbf{T}}$.
Similarly the KCL equations at bus g (two phase) and bus h (single phase) are given in eqs. (2.8) and (2.9), respectively as,

$$\bar{\mathbf{Y}}_{\mathbf{gi}}^{\mathbf{ab}}.\bar{\mathbf{V}}_{\mathbf{i}}^{\mathbf{abc}} + \bar{\mathbf{Y}}_{\mathbf{gg}}^{\mathbf{ab}}.\bar{\mathbf{V}}_{\mathbf{g}}^{\mathbf{ab}} + \bar{\mathbf{Y}}_{\mathbf{gh}}^{\mathbf{a}}.\bar{\mathbf{V}}_{\mathbf{h}}^{\mathbf{a}} = \mathbf{0} \tag{2.8}$$

$$\bar{\mathbf{Y}}_{\mathbf{hg}}^{\mathbf{a}}.\bar{\mathbf{V}}_{\mathbf{g}}^{\mathbf{ab}} + \bar{\mathbf{Y}}_{\mathbf{hh}}^{\mathbf{a}}.\bar{\mathbf{V}}_{\mathbf{h}}^{\mathbf{a}} = \mathbf{0} \tag{2.9}$$

where $\bar{\mathbf{Y}}_{\mathbf{gh}}^{\mathbf{a}} = -\begin{bmatrix} \bar{y}_{gh}^{aa} \\ 0 \end{bmatrix} = \begin{bmatrix} \bar{\mathbf{Y}}_{\mathbf{hg}}^{\mathbf{a}} \end{bmatrix}^{\mathbf{T}}$, and $\bar{\mathbf{V}}_{\mathbf{h}}^{\mathbf{a}} = \begin{bmatrix} \bar{V}_h^a \end{bmatrix}$.
Therefore, the KCL equations for an unbalanced distribution system (having u three phase, v two phase and w single phase buses) can be expressed in the matrix form as,

$$\begin{bmatrix} \mathbf{Y_{bus}} \end{bmatrix} \cdot \begin{bmatrix} \mathbf{V} \end{bmatrix} = \begin{bmatrix} \mathbf{I} \end{bmatrix} \tag{2.10}$$

where

$$[\mathbf{Y_{bus}}] = \begin{bmatrix}
\bar{\mathbf{Y}}^{\mathbf{abc}}_{\mathbf{22}} & \cdots & \bar{\mathbf{Y}}^{\mathbf{abc}}_{\mathbf{2u}} & \bar{\mathbf{Y}}^{\mathbf{pq}}_{\mathbf{2(u+1)}} & \cdots & \bar{\mathbf{Y}}^{\mathbf{pq}}_{\mathbf{2(u+v)}} & \bar{\mathbf{Y}}^{\mathbf{p}}_{\mathbf{2(u+v+1)}} & \cdots & \bar{\mathbf{Y}}^{\mathbf{p}}_{\mathbf{2(u+v+w)}} \\
\vdots & \ddots & \vdots & \vdots & \vdots & \vdots & \vdots & \vdots & \vdots \\
\bar{\mathbf{Y}}^{\mathbf{abc}}_{\mathbf{u2}} & \cdots & \bar{\mathbf{Y}}^{\mathbf{abc}}_{\mathbf{uu}} & \bar{\mathbf{Y}}^{\mathbf{pq}}_{\mathbf{u(u+1)}} & \cdots & \bar{\mathbf{Y}}^{\mathbf{pq}}_{\mathbf{u(u+v)}} & \bar{\mathbf{Y}}^{\mathbf{p}}_{\mathbf{u(u+v+1)}} & \cdots & \bar{\mathbf{Y}}^{\mathbf{p}}_{\mathbf{u(u+v+w)}} \\
\bar{\mathbf{Y}}^{\mathbf{pq}}_{\mathbf{(u+1)2}} & \cdots & \bar{\mathbf{Y}}^{\mathbf{pq}}_{\mathbf{(u+1)u}} & \bar{\mathbf{Y}}^{\mathbf{pq}}_{\mathbf{(u+1)(u+1)}} & \cdots & \bar{\mathbf{Y}}^{\mathbf{pq}}_{\mathbf{(u+1)(u+v)}} & \bar{\mathbf{Y}}^{\mathbf{p}}_{\mathbf{(u+1)(u+v+1)}} & \cdots & \bar{\mathbf{Y}}^{\mathbf{p}}_{\mathbf{(u+1)(u+v+w)}} \\
\vdots & \vdots & \vdots & \vdots & \ddots & \vdots & \vdots & \vdots & \vdots \\
\bar{\mathbf{Y}}^{\mathbf{pq}}_{\mathbf{(u+v)2}} & \cdots & \bar{\mathbf{Y}}^{\mathbf{pq}}_{\mathbf{(u+v)u}} & \bar{\mathbf{Y}}^{\mathbf{pq}}_{\mathbf{(u+v)(u+1)}} & \cdots & \bar{\mathbf{Y}}^{\mathbf{pq}}_{\mathbf{(u+v)(u+v)}} & \bar{\mathbf{Y}}^{\mathbf{p}}_{\mathbf{(u+v)(u+v+1)}} & \cdots & \bar{\mathbf{Y}}^{\mathbf{p}}_{\mathbf{(u+v)(u+v+w)}} \\
\bar{\mathbf{Y}}^{\mathbf{p}}_{\mathbf{(u+v+1)2}} & \cdots & \bar{\mathbf{Y}}^{\mathbf{p}}_{\mathbf{(u+v+1)u}} & \bar{\mathbf{Y}}^{\mathbf{p}}_{\mathbf{(u+v+1)(u+1)}} & \cdots & \bar{\mathbf{Y}}^{\mathbf{p}}_{\mathbf{(u+v+1)(u+v)}} & \bar{\mathbf{Y}}^{\mathbf{p}}_{\mathbf{(u+v+1)(u+v+1)}} & \cdots & \bar{\mathbf{Y}}^{\mathbf{p}}_{\mathbf{(u+v+1)(u+v+w)}} \\
\vdots & \vdots & \vdots & \vdots & \vdots & \vdots & \vdots & \ddots & \vdots \\
\bar{\mathbf{Y}}^{\mathbf{p}}_{\mathbf{(u+v+w)2}} & \cdots & \bar{\mathbf{Y}}^{\mathbf{p}}_{\mathbf{(u+v+w)u}} & \bar{\mathbf{Y}}^{\mathbf{p}}_{\mathbf{(u+v+w)(u+1)}} & \cdots & \bar{\mathbf{Y}}^{\mathbf{p}}_{\mathbf{(u+v+w)(u+v)}} & \bar{\mathbf{Y}}^{\mathbf{p}}_{\mathbf{(u+v+w)(u+v+1)}} & \cdots & \bar{\mathbf{Y}}^{\mathbf{p}}_{\mathbf{(u+v+w)(u+v+w)}}
\end{bmatrix}.$$

$$\begin{aligned}
[\mathbf{V}] &= \begin{bmatrix} \bar{\mathbf{V}}^{\mathbf{abc}}_{\mathbf{2}} & \cdots & \bar{\mathbf{V}}^{\mathbf{abc}}_{\mathbf{u}} & \bar{\mathbf{V}}^{\mathbf{pq}}_{\mathbf{(u+1)}} & \cdots & \bar{\mathbf{V}}^{\mathbf{pq}}_{\mathbf{(u+v)}} & \bar{\mathbf{V}}^{\mathbf{p}}_{\mathbf{(u+v+1)}} & \cdots & \bar{\mathbf{V}}^{\mathbf{p}}_{\mathbf{(u+v+w)}} \end{bmatrix}^T; \\
[\mathbf{I}] &= \begin{bmatrix} \bar{\mathbf{y}}^{\mathbf{abc}}_{\mathbf{12}}.\bar{\mathbf{V}}^{\mathbf{abc}}_{\mathbf{s}} & \mathbf{0} & \mathbf{0} & \cdots & \mathbf{0} & \mathbf{0} & \cdots & \mathbf{0} & \mathbf{0} \end{bmatrix}^T
\end{aligned}$$

The elements of the $[\mathbf{Y_{bus}}]$ matrix for the unbalanced distribution system (having u three phase, v two phase and w single phase buses) can be calculated as

$$\begin{aligned}
\bar{Y}^{pp}_{ii} &= \bar{y}^{pp}_{i1} + \bar{y}^{pp}_{i2} + \cdots + \bar{y}^{pp}_{iu} + \bar{y}^{pp}_{i(u+1)} + \cdots + \bar{y}^{pp}_{i(u+v)} + \bar{y}^{pp}_{i(u+v+1)} + \cdots + \bar{y}^{pp}_{i(u+v+w)} + \bar{y}^{p}_{id} \\
\bar{Y}^{pq}_{ii} &= \bar{y}^{pq}_{i1} + \bar{y}^{pq}_{i2} + \cdots + \bar{y}^{pq}_{iu} + \bar{y}^{pq}_{i(u+1)} + \cdots + \bar{y}^{pq}_{i(u+v)} \\
\bar{Y}^{pp}_{ij} &= -\bar{y}^{pp}_{ij} \\
\bar{Y}^{pq}_{ij} &= -\bar{y}^{pq}_{ij}. \qquad (2.11)
\end{aligned}$$

where i=2, ..., u; j=1, ..., u; $j \neq i$; p=a, b, c; q=a, b, c; $p \neq q$ for u three phase buses, i=(u+1), ..., ($u+v$); j=(u+1), ..., ($u+v$); $j \neq i$; p=(a, b) or (b, c) or (c, a); q=(a, b) or (b, c) or (c, a); $p \neq q$ for v two phase buses, i=($u+v$+1), ..., ($u+v+w$); j=($u+v$+1), ..., ($u+v+w$); $j \neq i$; p and q = (a or b or c), for w single phase buses.

Hence, the sizes of the $[\mathbf{Y_{bus}}]$ matrix, $[\mathbf{V}]$ and $[\mathbf{I}]$ vectors for an unbalanced distribution system having u three phase, v two phase and w single phase buses, are $((3u + 2v + w) - 3) \times ((3u + 2v + w) - 3)$, $((3u + 2v + w) - 3) \times 1$ and $((3u + 2v + w) - 3) \times 1$, respectively. Once the $[\mathbf{Y_{bus}}]$ matrix is formed for the given distribution network, the phase voltages at all the buses can easily be calculated by eq. (2.10). The branch current between bus i and j are then calculated using eq. (2.12) as,

$$\left[\bar{\mathbf{B}}^{\mathbf{abc}}_{\mathbf{ij}}\right] = \left[\bar{\mathbf{y}}^{\mathbf{abc}}_{\mathbf{ij}}\right] . \left[\bar{\mathbf{V}}^{\mathbf{abc}}_{\mathbf{i}} - \bar{\mathbf{V}}^{\mathbf{abc}}_{\mathbf{j}}\right] \qquad (2.12)$$

Now, most of the elements of $[\mathbf{Y_{bus}}]$ matrix are zero as there are a maximum of two or three connections at each bus. Hence the sparsity based technique has been used in this work for matrix operations. With the above modelling approach in place, we are now ready to discuss the method of short-circuit calculations for unsymmetrical faults.

2.2.2 Single line-to-ground fault (SLG)

Let us consider an SLG fault through fault impedance $\bar{z}_f$ on phase a of bus i, as shown in Fig. 2.2(a) [144]. In this figure, $\bar{I}^a_{id}$, $\bar{I}^b_{id}$ and $\bar{I}^c_{id}$ are the load currents of phases a, b, and c of bus i respectively. The fault current in the faulted phase a is given as,

$$\bar{I}^a_{if} = \frac{\bar{V}^a_i}{\bar{z}_f} = \bar{y}_f.\bar{V}^a_i \tag{2.13}$$

where $\bar{y}_f$=$\frac{1}{\bar{z}_f}$;
Applying KCL at phase a of bus i, we get

$$\begin{aligned}
&\bar{Y}^{aa}_{i2}.\bar{V}^a_2 + \bar{Y}^{ab}_{i2}.\bar{V}^b_2 + \cdots\cdots + \bar{Y}^{aa}_{ii}.\bar{V}^a_i + \cdots\cdots + \bar{Y}^{aa}_{i(u+v+w)}.\bar{V}^a_{i(u+v+w)} + \bar{y}_f.\bar{V}^a_i = 0 \\
&\bar{Y}^{aa}_{i2}.\bar{V}^a_2 + \bar{Y}^{ab}_{i2}.\bar{V}^b_2 + \cdots\cdots + (\bar{Y}^{aa}_{ii} + \bar{y}_f).\bar{V}^a_i + \cdots\cdots + \bar{Y}^{aa}_{i(u+v+w)}.\bar{V}^a_{i(u+v+w)} = 0
\end{aligned} \tag{2.14}$$

From eq. (2.14), it is evident that only the diagonal element of the i^{th} row of phase a of $[\mathbf{Y_{bus}}]$ matrix is modified. Hence, the modified element of the $[\mathbf{Y_{bus}}]$ matrix due to SLG fault is given as,

$$\bar{Y}^{aa}_{ii\_new} = \bar{Y}^{aa}_{ii} + \bar{y}_f \tag{2.15}$$

Once the elements of the $[\mathbf{Y_{bus}}]$ matrix are updated, the bus voltages for SLG fault are calculated using eq. (2.10) with the updated $[\mathbf{Y_{bus}}]$ matrix. The fault current and the branch currents under the fault condition are then calculated using eqs. (2.13) and (2.12) respectively.

2.2.3 Double and three line-to-ground faults (LLG and LLLG)

If an LLG fault occurs between phases a and b of bus i through a fault impedance $\bar{z}_f$, as shown in Fig. 2.2(b) [144], the fault currents in both the faulted phases are calculated as,

$$\bar{I}^a_{if} = \frac{\bar{V}^a_i}{\bar{z}_f} = \bar{y}_f.\bar{V}^a_i; \quad \bar{I}^b_{if} = \frac{\bar{V}^b_i}{\bar{z}_f} = \bar{y}_f.\bar{V}^b_i \tag{2.16}$$

The total fault current is then calculated as,

$$\bar{I}^{total}_f = \bar{I}^a_{if} + \bar{I}^b_{if} \tag{2.17}$$

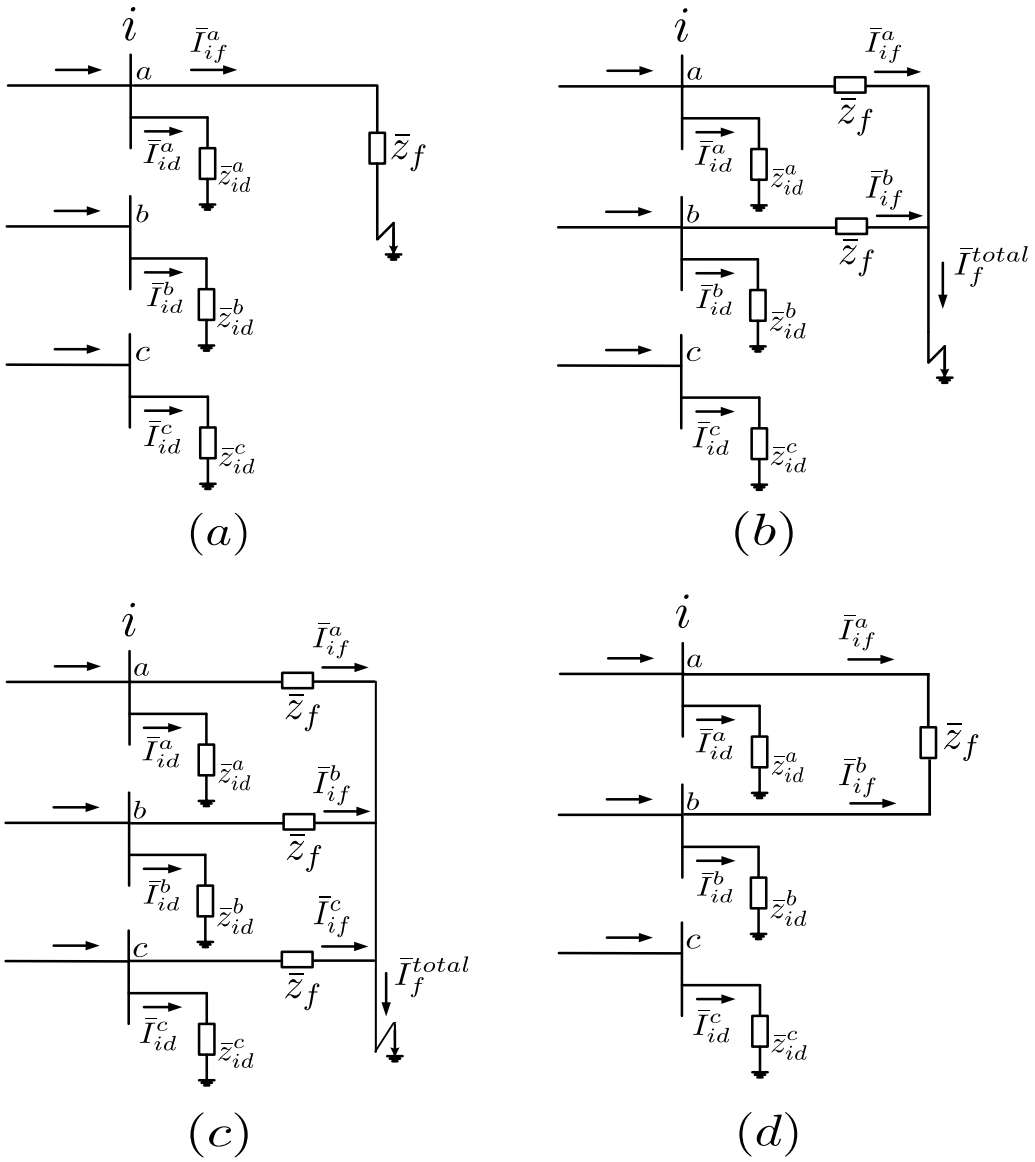

Figure 2.2: Unsymmetrical Short-circuit faults, (a) SLG fault, (b) LLG fault, (c) LLLG fault, (d) LL fault

The KCL equations at phases a and b of bus i are given in eqs. (2.18) and (2.19) respectively,

$$\bar{Y}^{aa}_{i2}.\bar{V}^a_2 + \bar{Y}^{ab}_{i2}.\bar{V}^b_2 + \cdots\cdots + (\bar{Y}^{aa}_{ii} + \bar{y}_f).\bar{V}^a_i + \cdots\cdots + \bar{Y}^{aa}_{i(u+v+w)}.\bar{V}^a_{i(u+v+w)} = 0 \tag{2.18}$$

$$\bar{Y}^{ba}_{i2}.\bar{V}^a_2 + \bar{Y}^{bb}_{i2}.\bar{V}^b_2 + \cdots\cdots + (\bar{Y}^{bb}_{ii} + \bar{y}_f).\bar{V}^b_i + \cdots\cdots + \bar{Y}^{bp}_{i(u+v)}.\bar{V}^p_{i(u+v)} = 0 \tag{2.19}$$

Hence, the modified elements of $[\mathbf{Y_{bus}}]$ matrix due to LLG fault are given as,

$$\bar{Y}^{aa}_{ii\_new} = \bar{Y}^{aa}_{ii} + \bar{y}_f \tag{2.20a}$$

$$\bar{Y}^{bb}_{ii\_new} = \bar{Y}^{bb}_{ii} + \bar{y}_f \tag{2.20b}$$

Similarly if an LLLG fault occurs on bus i through a fault impedance $\bar{z}_f$ (as shown in Fig. 2.2(c) [144]), the fault currents are then calculated as,

$$\bar{I}^a_{if} = \frac{\bar{V}^a_i}{\bar{z}_f} = \bar{y}_f.\bar{V}^a_i; \;\; \bar{I}^b_{if} = \frac{\bar{V}^b_i}{\bar{z}_f} = \bar{y}_f.\bar{V}^b_i; \;\; \bar{I}^c_{if} = \frac{\bar{V}^c_i}{\bar{z}_f} = \bar{y}_f.\bar{V}^c_i \tag{2.21}$$

The total fault current is therefore calculated as,

$$\bar{I}^{total}_f = \bar{I}^a_{if} + \bar{I}^b_{if} + \bar{I}^c_{if} \tag{2.22}$$

The modified elements of $[\mathbf{Y_{bus}}]$ matrix for LLLG fault are given as,

$$\bar{Y}^{aa}_{ii\_new} = \bar{Y}^{aa}_{ii} + \bar{y}_f \tag{2.23a}$$

$$\bar{Y}^{bb}_{ii\_new} = \bar{Y}^{bb}_{ii} + \bar{y}_f \tag{2.23b}$$

$$\bar{Y}^{cc}_{ii\_new} = \bar{Y}^{cc}_{ii} + \bar{y}_f \tag{2.23c}$$

2.2.4 Line-to-line fault (LL)

When an LL fault occurs between phases a and b of bus i through a fault impedance $\bar{z}_f$ (as shown in Fig. 2.2(d) [144]), the fault currents in both the faulted phases are calculated as,

$$\bar{I}^a_{if} = \frac{(\bar{V}^a_i - \bar{V}^b_i)}{\bar{z}_f} = \bar{y}_f.(\bar{V}^a_i - \bar{V}^b_i) = -\bar{I}^b_{if} \tag{2.24}$$

The KCL equations at phases a and b of bus i are given in eqs. (2.25) and (2.26) respectively,

$$\bar{Y}^{aa}_{i2}.\bar{V}^a_2 + \bar{Y}^{ab}_{i2}.\bar{V}^b_2 + \cdots\cdots + (\bar{Y}^{aa}_{ii} + \bar{y}_f).\bar{V}^a_i + (\bar{Y}^{ab}_{ii} - \bar{y}_f).\bar{V}^b_i + \cdots\cdots + \bar{Y}^{aa}_{i(u+v+w)}.\bar{V}^a_{i(u+v+w)} = 0 \tag{2.25}$$

$$\bar{Y}^{ba}_{i2}.\bar{V}^a_2 + \bar{Y}^{bb}_{i2}.\bar{V}^b_2 + \cdots\cdots + (\bar{Y}^{ba}_{ii} - \bar{y}_f).\bar{V}^a_i + (\bar{Y}^{bb}_{ii} + \bar{y}_f).\bar{V}^b_i + \cdots\cdots + \bar{Y}^{bp}_{i(u+v)}.\bar{V}^p_{i(u+v)} = 0 \tag{2.26}$$

Due to the LL fault, the following elements of the $[\mathbf{Y_{bus}}]$ matrix will be updated as,

$$\bar{Y}^{aa}_{ii\_new} = \bar{Y}^{aa}_{ii} + \bar{y}_f \tag{2.27a}$$

$$\bar{Y}^{ab}_{ii\_new} = \bar{Y}^{ab}_{ii} - \bar{y}_f \tag{2.27b}$$

$$\bar{Y}^{ba}_{ii\_new} = \bar{Y}^{ba}_{ii} - \bar{y}_f \tag{2.27c}$$

$$\bar{Y}^{bb}_{ii\_new} = \bar{Y}^{bb}_{ii} + \bar{y}_f \tag{2.27d}$$

The bus voltages for LL fault are calculated first using eq. (2.10) with the above modifications in $[\mathbf{Y_{bus}}]$ matrix, and then the fault currents and branch currents under the fault condition are calculated using eqs. (2.24) and (2.12), respectively.

Since the proposed method is based on bus admittance matrix $[\mathbf{Y_{bus}}]$ formulation, hence it can be easily applied to meshed distribution system also.

The following are the steps of the proposed method for simulating any type of fault:

1. Run base case load flow.
2. Calculate the equivalent load impedances at each bus using the load flow solutions.
3. Formulate the bus admittance matrix for the given network including the load impedances.
4. Modify the elements of bus admittance matrix corresponding to the type of fault occurring in the system as discussed above.
5. Calculate the fault currents, bus voltages and feeder currents under the fault condition for the given type of fault.

2.3 Test results and discussions

The IEEE 123-bus (modified) radial system, as shown in Fig. 2.3, has been used to validate the proposed short-circuit analysis method. In the original system, four buses have been used for connecting switches. These four switch buses have been omitted in the modified system. The proposed method has been implemented in MATLAB environment and the results have also been compared with those obtained by $[\mathbf{BIBC}]$ matrix based method [48] and time domain simulation studies carried out using PSCAD/EMTDC. The shunt capacitances in this system have also been neglected.

2.3.1 Results of IEEE 123-bus (modified) system (radial system)

The following cases have been simulated on the IEEE 123-bus (modified) system to demonstrate the validity of the proposed method:

Case 1. A single line-to-ground fault in phase a of bus 98 with a fault impedance $\bar{z}_f = 0.1 + 0.0i$ p.u.

Case 2. A double line-to-ground fault between phases a and b of bus 98 with a fault impedance $\bar{z}_f = 0.1 + 0.0i$ p.u.

Case 3. A three line-to-ground fault at bus 98 with a fault impedance $\bar{z}_f = 0.1 + 0.0i$ p.u.

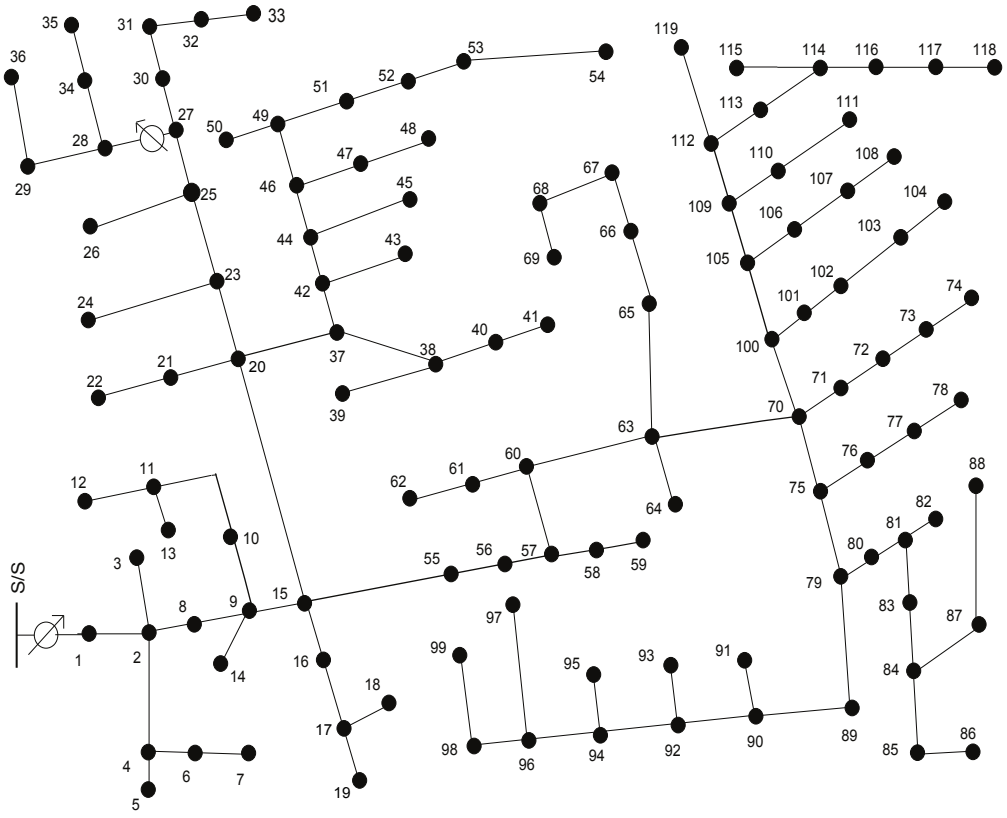

Figure 2.3: The IEEE 123-bus (modified) system

Case 4. A line-to-line fault between phases a and b of bus 98 with a fault impedance $\bar{z}_f = 0.1+0.0i$ p.u.

Fig. 2.4 shows the source current (I_s) of phase a for various type of faults at bus 98 obtained from PSCAD/EMTDC simulation study, proposed technique and $[\mathbf{BIBC}]$ matrix based technique [48]. It shows that the values of source current corresponding to the proposed method and PSCAD simulation are very close to each other, while the source current corresponding to $[\mathbf{BIBC}]$ matrix based technique are appreciably lower than these two values. Detailed results of all the above cases using proposed technique and PSCAD simulations are shown in Table 2.1. The results obtained using $[\mathbf{BIBC}]$ matrix based method have also been included in Table 2.1 for comparison with PSCAD/EMTDC simulation results. $[\mathbf{BIBC}]$ matrix based technique, however assumes that the load currents are negligible as compared to the fault current and can be neglected during short-circuit analysis. Further, the % error in the calculated values obtained by the proposed method and the $[\mathbf{BIBC}]$ matrix based method (with respect to the results obtained from PSCAD/EMTDC taken as benchmark) are also shown in Table 2.1. As can be seen in Table 2.1, maximum % error in both

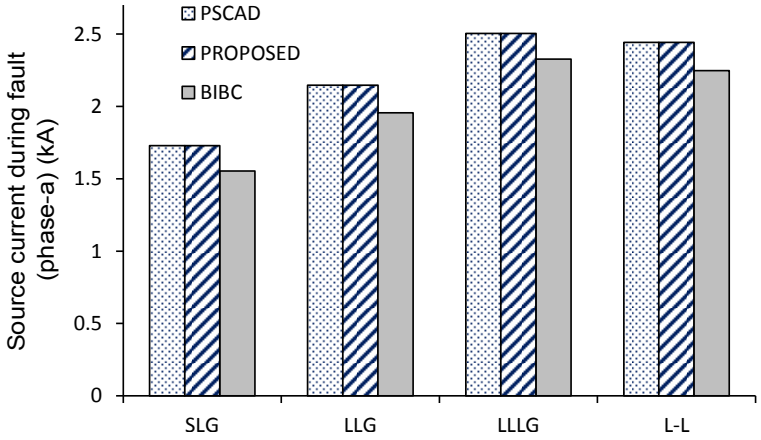

Figure 2.4: Source current during various type of faults for IEEE 123-bus (modified) radial system using PSCAD/EMTDC, proposed technique and $[\mathbf{BIBC}]$ matrix based technique

source and fault current calculation occurs in SLG fault, which is the type of fault most frequently occurring in distribution systems. In Table 2.1, the maximum error in the fault current (I_f) at fault point is 1.814% and 0.0036% in the $[\mathbf{BIBC}]$ matrix based technique and in proposed technique respectively, while the maximum error in source current (I_s) calculation during fault is 10.12% and 0.0035% in the $[\mathbf{BIBC}]$ matrix technique and in proposed technique respectively. Also for LLG, LLLG and L-L faults, the error present in the source current (I_s) is greater than 5% in the $[\mathbf{BIBC}]$ matrix based technique, as shown in Table 2.1. This is due to non-considerations of loads during short-circuit calculations. The maximum error is highest in the fault current calculations of phase a as compared to other two phases for all kinds of faults. This can be attributed to the fact that phase a of the system is loaded more as compared to the other two phases. Table 2.1 thus shows that the proposed method gives much more accurate estimate of currents during fault than [BIBC] matrix based method which does not consider loads during faults.

Fig. 2.5 shows that for $\bar{z}_f = 0.001 + 0.000i$ p.u., the maximum difference in the branch fault current magnitude between the loaded and unloaded condition $\left(max|[\bar{\mathbf{B}}_{\mathbf{f}}^{\mathbf{load}} - \bar{\mathbf{B}}_{\mathbf{f}}^{\mathbf{noload}}]|\right)$ increases as the fault location shifts away from the supply point towards the far end for SLG $(a-g)$ fault. This is due to the increase in the number of connected loads in the fault path when the fault location moves towards the far end from the substation. For example, when an SLG $(a-g)$ fault occurs at bus 8 (which is near to the substation as shown in Fig. 2.3) with $\bar{z}_f = 0.001 + 0.000i$ p.u., the

Table 2.1: Error Analysis of proposed technique and [**BIBC**] matrix based technique with respect to PSCAD/EMTDC simulation study for IEEE 123-bus (modified) radial system

case	Fault type	phase	Fault current at fault point (I_f)			% Error in (I_f)		Current drawn from the supply (I_s)			% Error in (I_s)	
			PSCAD simulation (kA)	Proposed Technique (kA)	[BIBC] Technique [48](kA)	Proposed Technique (%)	[BIBC] Technique [48](%)	PSCAD simulation (kA)	Proposed Technique (kA)	[BIBC] Technique [48](kA)	Proposed Technique (%)	[BIBC] Technique [48](%)
1	SLG (a-g)	a	1.58245	1.58251	1.55374	0.00327	**1.81423**	1.72870	1.72871	1.55372	0.0032	**10.1206**
2	LLG (ab-g)	a	1.98333	1.98339	1.95631	0.00298	1.36218	2.14671	2.14680	1.95630	0.0029	8.8719
		b	2.2231	2.22316	2.21379	0.00327	0.41822	2.31211	2.31220	2.21370	0.0032	4.2542
3	LLLG (abc-g)	a	2.34810	2.34814	2.32713	0.00313	0.89145	2.50340	2.50350	2.32710	0.0031	7.0445
		b	2.33890	2.33892	2.32467	0.00308	0.60631	2.43850	2.43860	2.32460	0.0030	4.6703
		c	2.43336	2.43344	2.42075	0.00306	0.51846	2.56380	2.56390	2.42070	0.0030	5.5821
4	L-L (a-b)	a	2.26815	2.26824	2.24762	0.00326	0.90548	2.44250	2.44251	2.24760	0.0032	7.9791
		b	2.26815	2.26824	2.24762	**0.0036**	0.90514	2.31300	2.31310	2.24760	**0.0035**	2.8298

voltages (line to ground) at all the buses which are downstream to the bus 8 are almost equal to zero, as shown in Fig. 2.6(a). On the other hand, when an SLG $(a-g)$ fault occurs at bus 118 (which is at the far end of the system as shown in Fig. 2.3) with the same fault impedance, the voltages at all the buses which are upstream to bus 118 have considerable values (as shown in Fig. 2.6(a)), which will cause some load currents to flow at these buses. Because of these load currents, the maximum difference in the branch currents between the loaded and unloaded condition is more for far end faults as compared to near end faults, as shown in Fig. 2.5. The branch currents in all the lines for both the cases for $\bar{z}_f = 0.001 + 0.000i$ p.u. are shown in Fig. 2.7(a).

With a $\bar{z}_f = 0.1 + 0.0i$ p.u., the maximum error in branch currents occurs when the fault is at bus 8 instead of bus 118. It can be explained with the help of Fig. 2.6(b), which gives the voltage profiles for SLG $(a-g)$ fault occurring at bus 8 and bus 118 under the loaded condition, with $\bar{z}_f = 0.1 + 0.0i$ p.u. For an SLG $(a-g)$ fault at bus 8, due to high fault impedance the voltages at all the buses downstream to the bus 8 are approximately fixed at 1.86 kV (line to ground), while for the fault at bus 118, the voltages are decreasing from the substation end to the fault point as shown in Fig. 2.6(b). For near end faults, a higher voltage (equal to the voltage at the faulted bus) is maintained over the entire system downstream to the faulted bus (as shown in Fig. 2.6(b)). As a result higher load currents flow in the system even under faulted condition. This causes larger error in the branch current estimation for near end fault as compared to the far end fault. The branch currents for both the cases are shown in Fig. 2.7(b) with $\bar{z}_f = 0.1 + 0.0i$ p.u.

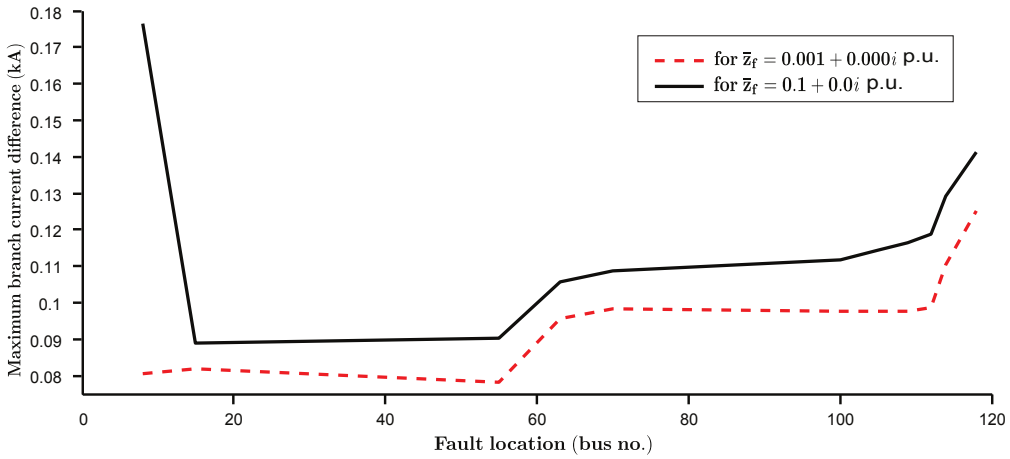

Figure 2.5: Maximum difference in branch current (between loaded and unloaded condition) at different fault locations in IEEE 123-bus (modified) radial system for SLG $(a-g)$ fault

Table 2.2: List of loop branches added in IEEE 123-bus (modified) radial system

From Bus	To Bus	Length (ft.)	type	Line impedance configuration
33	54	675	3-ϕ	1
37	69	700	3-ϕ	2

Fig. 2.8 shows the variation of the difference in branch currents between the loaded and unloaded condition with the load increment factor for different fault impedances for an SLG $(a-g)$ fault at bus 8. The difference in branch currents between the loaded and unloaded condition increases with the increase in loading conditions as shown in Fig. 2.8. Therefore, as the load grows in the future, the difference in branch currents between the loaded and unloaded condition will also increase, which may necessitate enhancing the rating of the components and protective equipments installed in the branches.

2.3.2 Results of IEEE 123-bus (modified) system (meshed system)

The IEEE 123-bus system shown in Fig. 2.3 has been modified to a meshed system by adding two loop branches in it. The details of these branches are given in Table 2.2 [140]. The four cases, as described in Subsection 2.3.1, have also been simulated on the modified meshed system

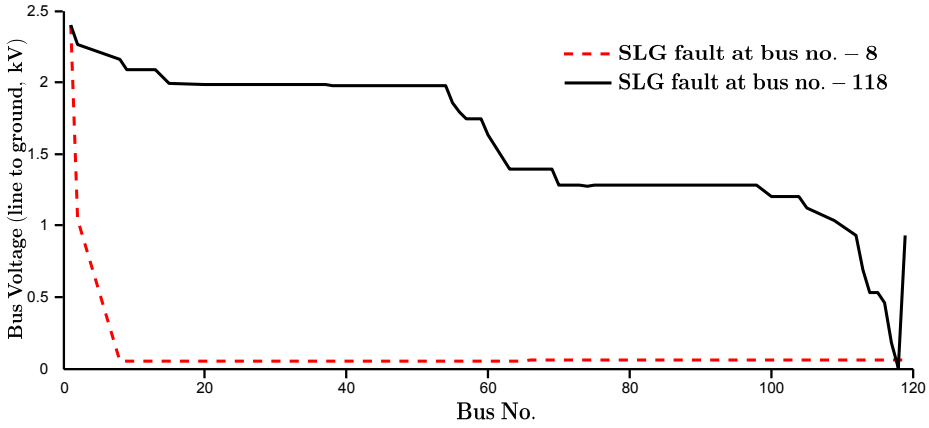

(a)

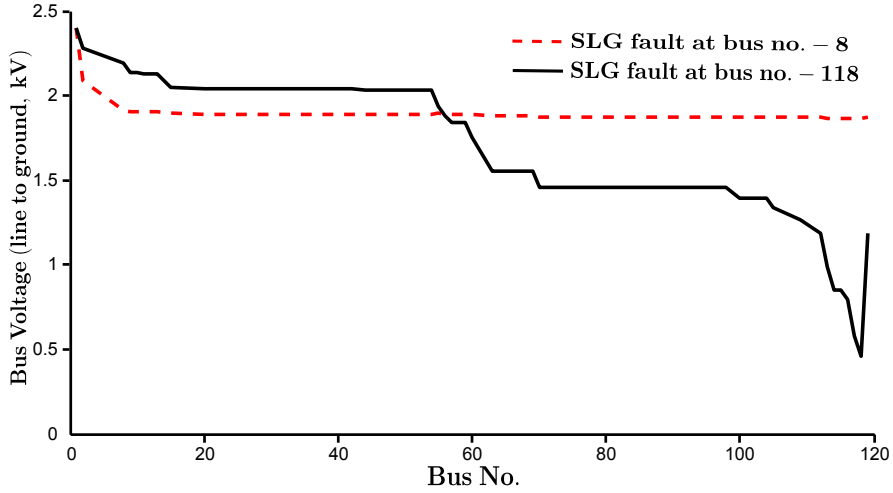

(b)

Figure 2.6: Voltage profiles of IEEE 123-bus (modified) radial system under loaded condition, (a) $\bar{z}_f = 0.001 + 0.000i$ p.u., (b) $\bar{z}_f = 0.1 + 0.0i$ p.u.

to demonstrate the validity of the proposed method for meshed network. In Fig. 2.9, the source current (I_s) of phase a during various type of faults at bus 98 using PSCAD/EMTDC simulation, proposed technique and $[\mathbf{BIBC}]$ matrix based technique are shown. Similar to the observations in radial system, the values of source current corresponding to the proposed method and PSCAD simulation are very close to each other, while the source current corresponding to $[\mathbf{BIBC}]$ matrix based technique are appreciably lower than these two values.

The results for PSCAD simulation and proposed technique are given in Table 2.3. The results obtained using $[\mathbf{BIBC}]$ matrix based technique have also been included in Table 2.3 for comparison with PSCAD/EMTDC simulation results. The maximum error in fault current (I_f) and source

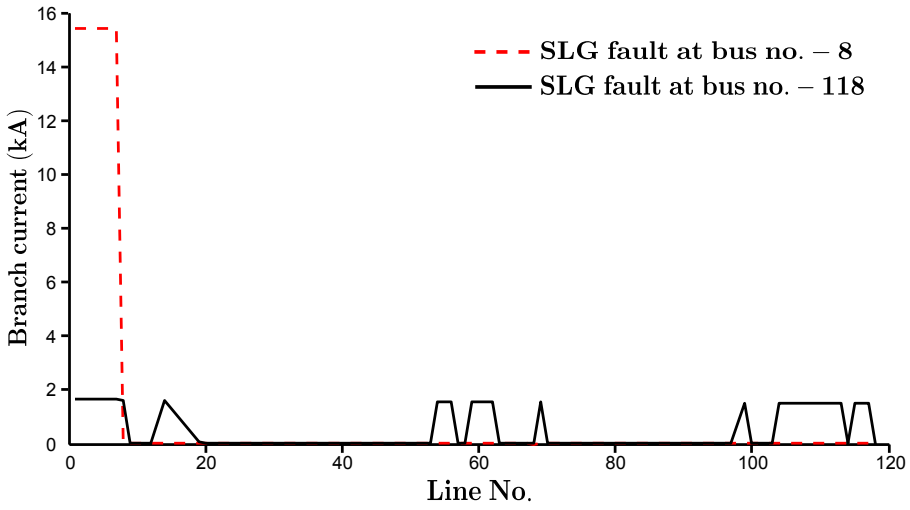

(a)

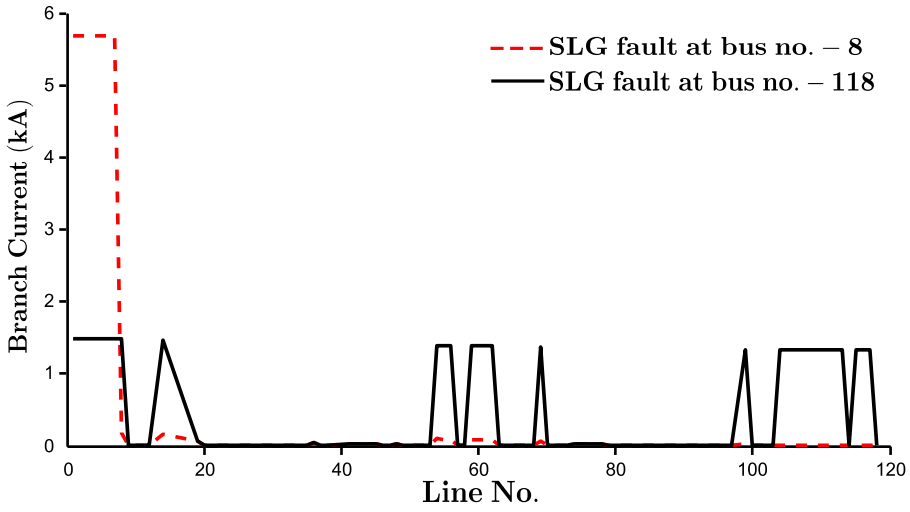

(b)

Figure 2.7: Branch currents of IEEE 123-bus (modified) radial system under loaded condition, (a) $\bar{z}_f$ = $0.001 + 0.000i$ p.u., (b) $\bar{z}_f$ = $0.1 + 0.0i$ p.u.

current (I_s) calculation using the proposed technique is 0.0034%, and 0.0037% respectively while those obtained using $[\mathbf{BIBC}]$ matrix based technique are 1.531% and 9.422% respectively. This shows the accuracy of the proposed method for meshed distribution network also.

Fig. 2.10 shows the variation of the difference in branch currents between the loaded and unloaded condition versus the fault locations, for SLG $(a-g)$ fault with different fault impedances. Similar to the radial system, this difference increases with the increase in fault distance from the source end for $\bar{z}_f = 0.001 + 0.000i$ p.u.. On the other hand, for $\bar{z}_f = 0.1 + 0.0i$ p.u., the maximum

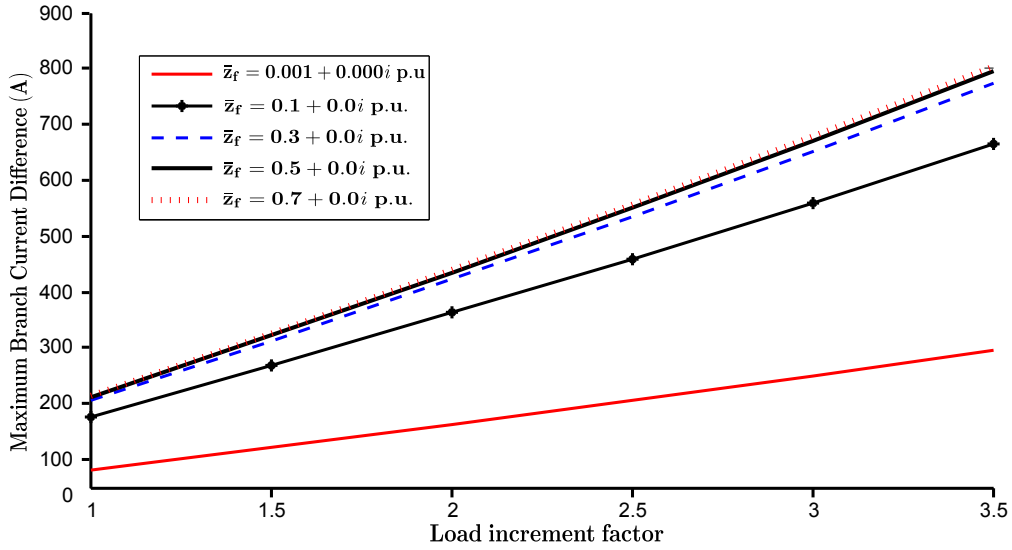

Figure 2.8: Maximum difference in branch current (between loaded and unloaded condition) in IEEE 123-bus (modified) radial system with load increment factor for SLG $(a-g)$ fault at bus 8

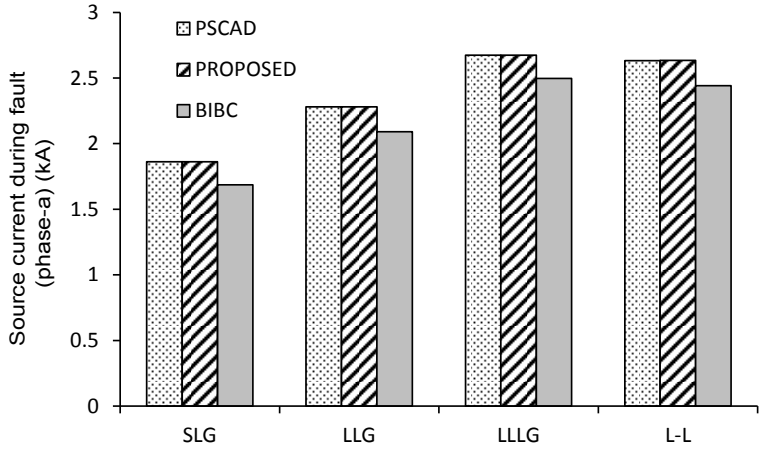

Figure 2.9: Source current during various type of faults for IEEE 123-bus (modified) meshed system using PSCAD/EMTDC, proposed technique and [**BIBC**] matrix based technique

difference in branch current (between the loaded and unloaded condition) was observed for the fault occurring near the substation end, which can be explained with the help of Fig. 2.11(a) and 2.11(b) (which show voltage profiles for SLG $(a-g)$ fault, with $\bar{z}_f = 0.001 + 0.000i$ p.u., at bus 8 and bus 118 under loaded condition), in the similar way as described in the previous subsection for the radial system.

Table 2.3: Error Analysis of proposed technique and [**BIBC**] matrix based technique with respect to PSCAD/EMTDC simulation study for IEEE 123-bus (modified) meshed system

case	Fault type	phase	Fault current at fault point (I_f)			% Error in (I_f)		Current drawn from the supply (I_s)			% Error in (I_s)	
			PSCAD simulation (kA)	Proposed Technique (kA)	[BIBC] Technique [48](kA)	Proposed Technique (%)	[BIBC] Technique [48](%)	PSCAD simulation (kA)	Proposed Technique (kA)	[BIBC] Technique [48](kA)	Proposed Technique (%)	[BIBC] Technique [48](%)
1	SLG (a-g)	a	1.71263	1.71268	1.68640	0.00335	**1.53148**	1.86182	1.86188	1.68640	0.00307	**9.42221**
2	LLG (ab-g)	a	2.11558	2.11565	2.09099	0.00298	1.16260	2.27984	2.27990	2.09099	0.00279	8.28357
		b	2.38578	2.38585	2.37736	0.00312	0.35279	2.47873	2.47882	2.37736	0.00347	4.08965
3	LLLG (abc-g)	a	2.51549	2.51557	2.49636	0.00306	0.76084	2.67420	2.67428	2.49636	0.00289	6.65032
		b	2.50127	2.50135	2.48911	0.00293	0.48606	2.60365	2.60373	2.48911	0.00328	4.39900
		c	2.58187	2.58194	2.57152	0.00274	0.40087	2.71661	2.71671	2.57152	0.00347	5.34103
4	L-L (a-b)	a	2.4606	2.46067	2.44163	0.00318	0.77082	2.63352	2.63360	2.44163	0.00303	7.28632
		b	2.46059	2.46067	2.44163	**0.00348**	0.77053	2.51049	2.51059	2.44163	**0.00375**	2.74310

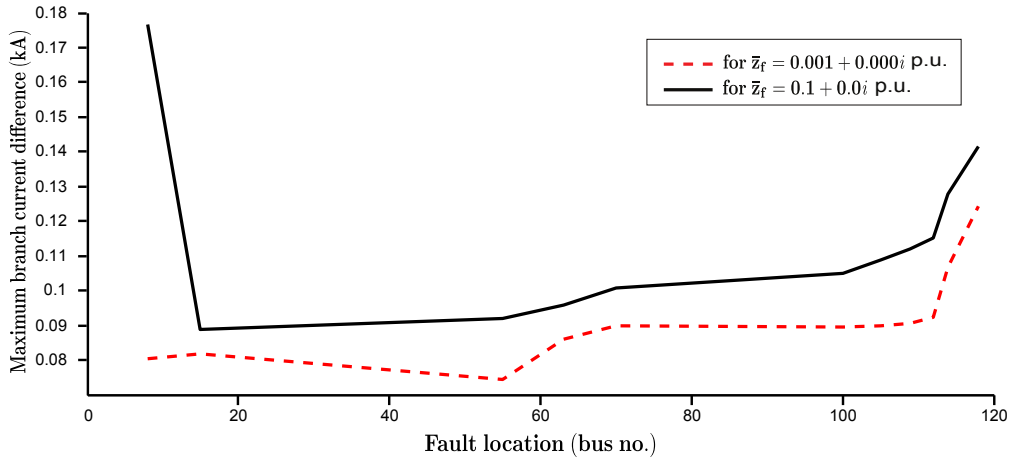

Figure 2.10: Maximum difference in branch current (between loaded and unloaded condition) at different fault locations in IEEE 123-bus (modified) meshed system for SLG $(a-g)$ fault

The branch currents for two different cases ((a) $\bar{z}_f = 0.001+0.000i$ p.u., and (b) $\bar{z}_f = 0.1+0.0i$ p.u.) for SLG fault $(a-g)$ at bus 8 and bus 118 under loaded condition are shown in Figs. 2.12(a) and 2.12(b) respectively. In Fig. 2.13, the maximum difference in the branch fault current magnitude between the loaded and unloaded condition $\left(max|[\bar{\mathbf{B}}_{\mathbf{f}}^{\mathbf{load}} - \bar{\mathbf{B}}_{\mathbf{f}}^{\mathbf{noload}}]|\right)$ has been plotted against load increment factor for SLG $(a-g)$ fault at bus 8 with different fault impedances. This shows that the error increases with increase in the loading conditions.

The proposed method has also been tested for simultaneous faults in the system. Two simul-

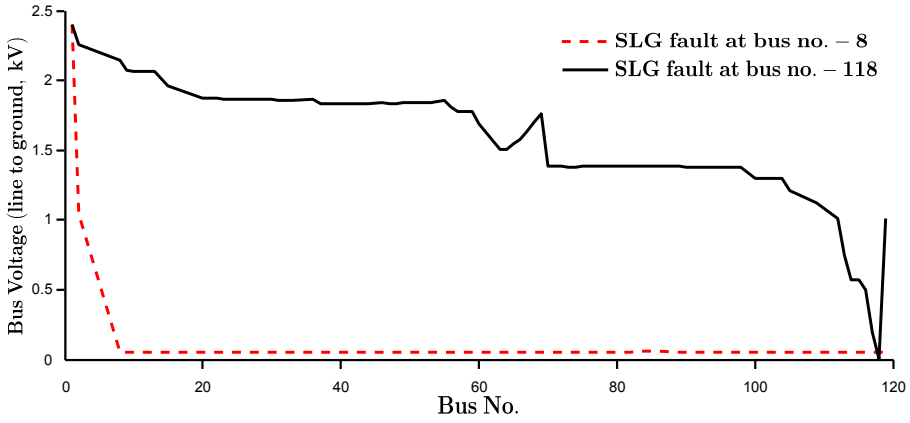

(a)

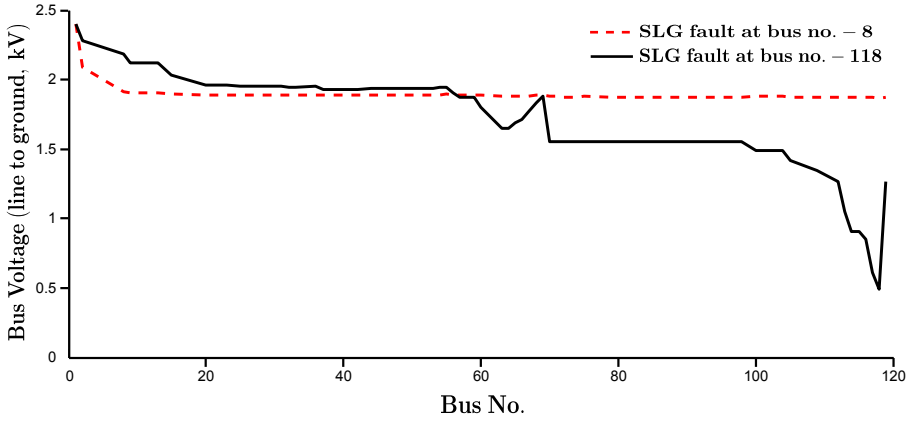

(b)

Figure 2.11: Voltage profiles of IEEE 123-bus (modified) meshed system under loaded condition, (a) $\bar{z}_f = 0.001 + 0.000i$ p.u., (b) $\bar{z}_f = 0.1 + 0.0i$ p.u.

taneous faults, namely, SLG $(a-g)$ and LLG $(ab-g)$ have been applied to the IEEE 123-bus (modified) system at bus 98 and bus 119 respectively. Simulation results using PSCAD/EMTDC, proposed method and $[\mathbf{BIBC}]$ matrix based technique are shown in Table 2.4. The maximum error present in the fault current (I_f) using proposed technique and $[\mathbf{BIBC}]$ matrix based technique with respect to PSCAD/EMTDC results are 0.00843% and 2.56546% respectively for radial system, and are 0.00849% and 2.21657% respectively for meshed system. Similarly, the maximum error in source current (I_s) are 0.00495% and 6.81383% for radial system, and 0.00491% and 5.26910% for meshed system.

The above results show the effectiveness of the proposed fault analysis method. The results presented show that for better accuracy in the results, the load currents should be considered dur-

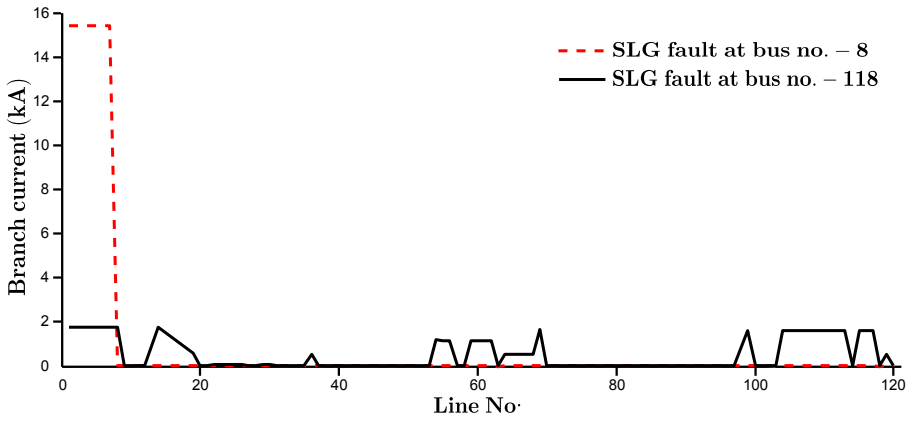

(a)

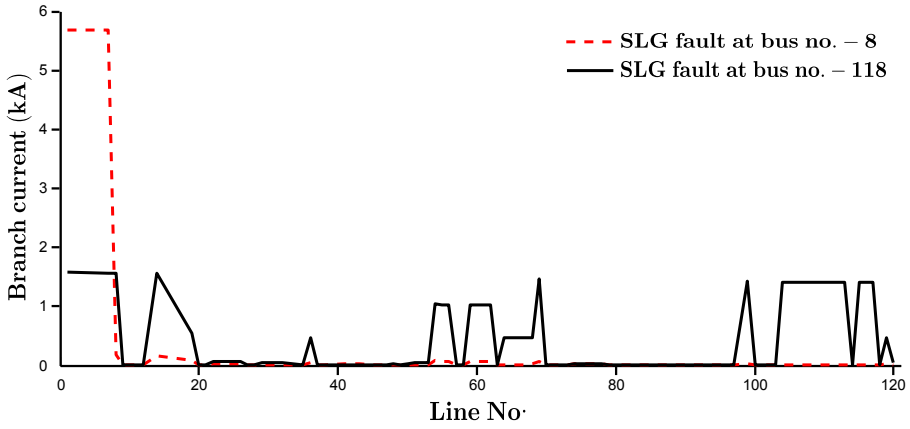

(b)

Figure 2.12: Branch currents of IEEE 123-bus (modified) meshed system under loaded condition, (a) $\bar{z}_f = 0.001 + 0.000i$ p.u., (b) $\bar{z}_f = 0.1 + 0.0i$ p.u.

ing short-circuit calculations. The maximum error present in the proposed technique for both radial as well as meshed system is less than the 0.004% for single faults and 0.0085% for multiple simultaneous faults (benchmarked against the PSCAD results). Thus, the given fault analysis technique is suitable for both radial as well as meshed distribution system.

2.4 Conclusion

In this chapter, an efficient and accurate short-circuit analysis method has been proposed for unbalanced radial and weakly meshed distribution systems. This method is also applicable for the analysis of multiple faults (simultaneous occurrence of more than one type of fault) in the distribution system. The proposed method has been tested on modified IEEE 123-bus radial as well as

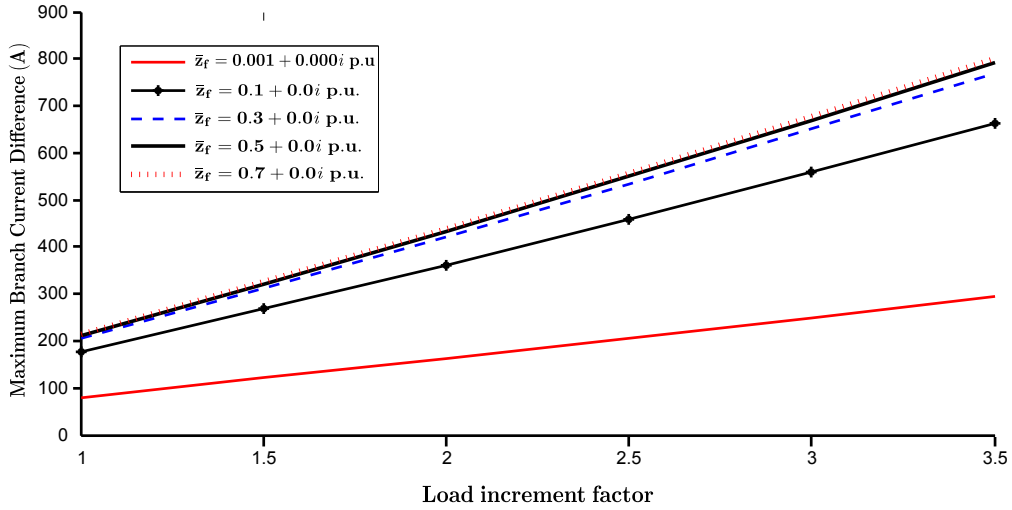

Figure 2.13: Maximum difference in branch current (between loaded and unloaded condition) in IEEE 123-bus (modified) meshed system with load increment factor for SLG $(a-g)$ fault at bus 8

Table 2.4: Error Analysis of proposed technique and [BIBC] matrix based technique with respect to PSCAD/EMTDC simulation study for multiple faults for IEEE 123-bus system

Topology	**Fault type**	**Fault bus**	**Phase**	**Fault current at fault point (I_f)**			**% Error in (I_f)**		**Current drawn from the supply (I_s)**			**% Error in (I_s)**	
				PSCAD simulation (kA)	**Proposed Technique (kA)**	**[BIBC] Technique [48](kA)**	**Proposed Technique (%)**	**[BIBC] Technique [48](%)**	**PSCAD simulation (kA)**	**Proposed Technique (kA)**	**[BIBC] Technique [48](kA)**	**Proposed Technique (%)**	**[BIBC] Technique [48](%)**
Radial	SLG (a-g)	98	a	1.15336	1.15337	1.12377	0.00127	2.56546	2.77414	2.77427	2.58511	0.00495	6.81383
	LLG (ab-g)	119	a	1.55736	1.55749	1.53028	0.00843	1.73898					
Meshed	SLG (a-g)	98	a	1.27526	1.27527	1.24699	0.00139	2.21657	3.04142	3.04143	2.85545	0.00491	5.26910
	LLG (ab-g)	119	a	1.70904	1.70918	1.68256	0.00849	1.54927					

meshed distribution test system. Test results of the proposed method have also been compared with the $[\mathbf{BIBC}]$ matrix based technique and PSCAD/EMTDC software results. Small values of errors show the accuracy and effectiveness of the proposed method. Further, the results of this work show that, with increase in the loading condition of the system, it may be necessary to upgrade the ratings of the components and protective equipments installed in the branches.

In the next chapter, an algorithm for the short-circuit analysis of unbalanced distribution system with Inverter based distribution generation (IBDG) is described considering different types of loads.

Chapter 3

Short-circuit analysis of unbalanced radial and meshed distribution system with inverter based Distributed Generation (IBDG)

Abstract

The fault current contribution of inverter based DGs (IBDGs) may affect the operation of protective devices present in the system. Hence, it is necessary to consider the presence of IBDGs in short-circuit analysis of distribution system. A short-circuit analysis method for unbalanced distribution system with IBDG, incorporating different voltage dependent control modes, is proposed in this chapter. The proposed method has been implemented on modified IEEE 123-bus radial as well as meshed distribution network and the obtained results have been compared with the results obtained by the time domain simulation studies carried out using PSCAD/EMTDC software. Comparison of the results shows the accuracy of the proposed technique.

3.1 Introduction

INITIALLY the distribution system were designed in such a way that power would always flow from the grid substation to the load end [145]. But the integration of distributed generation (DG) into the grid has changed this scenario. Nowadays, DGs are used in the distribution system to improve the system voltage profile and to reduce feeder loading [146]. Generally, the DGs used in the system are inverter based DGs. However, the integration of DG increases the fault level of the system as it contributes to the fault current during a fault. This may cause maloperation of protective equipments. Therefore, it becomes necessary to analyze the system with DG under the fault conditions. Different short-circuit analysis methods for distribution system with IBDGs are available in the literature [58–65]. These methods are based on the current control strategy of the inverter during short-circuit conditions. In this chapter, an analytical approach for the short-

circuit analysis of distribution system with IBDGs is proposed which also incorporates the inverter control strategy. In this control mode, the IBDGs operate at zero power factor (leading) under fault conditions to deliver reactive power to the system for supporting the bus voltages under fault conditions.

This chapter is organized as follows. Section 3.2 describes the formulation of the proposed short-circuit analysis method for unbalanced radial as well as meshed distribution system incorporating IBDGs during short-circuit calculations. The main results of this chapter are presented in Section 3.3 and finally Section 3.4 highlights the main conclusions of this chapter.

3.2 Short-circuit analysis of unbalanced distribution system with IBDG

3.2.1 System modeling with IBDG

In this work, it is assumed that the IBDGs are operating at unity power factor under normal operating conditions. Further, it is also assumed that the IBDGs operate in zero power factor (leading) under fault conditions [63, 65] to deliver reactive power to the system (to improve the system voltage profile during the fault). The short-circuit current contribution by the IBDG is limited to the short-circuit current capacity of the switching devices (I_{sc}^{inv}), by operating the inverter in a constant current mode [63, 65]. A three phase inverter, with separate control scheme for each phase, is used to integrate the DG with the grid through a step down transformer.

Let us consider an unbalanced distribution system with an IBDG connected to the n^{th} bus of the system through a step down transformer, as shown in Fig 3.1. The distribution system is assumed to have u three phase, v two phase and w single phase buses. It is assumed that the total no. of loads (balanced as well as unbalanced) connected to the system is nld. Two different types of loads have been considered in this work: constant power and voltage dependent loads. The polynomial voltage dependent load model (ZIP model) [147] is described by eqs. (3.1a) and (3.1b) as,

$$\frac{P(V)}{P_o} = F_Z\left(\frac{V}{V_o}\right)^2 + F_I\left(\frac{V}{V_o}\right) + F_P \tag{3.1a}$$

$$\frac{Q(V)}{Q_o} = F_Z^{'}\left(\frac{V}{V_o}\right)^2 + F_I^{'}\left(\frac{V}{V_o}\right) + F_P^{'} \tag{3.1b}$$

where P and Q are the active and reactive load power, respectively, and V is the magnitude of the terminal voltage. V_o, P_o and Q_o are the nominal values of voltage, active and reactive power, respectively. F and $F^{'}$ are the fractional constants, and the subscripts '$_Z$', '$_I$' and '$_P$' represent

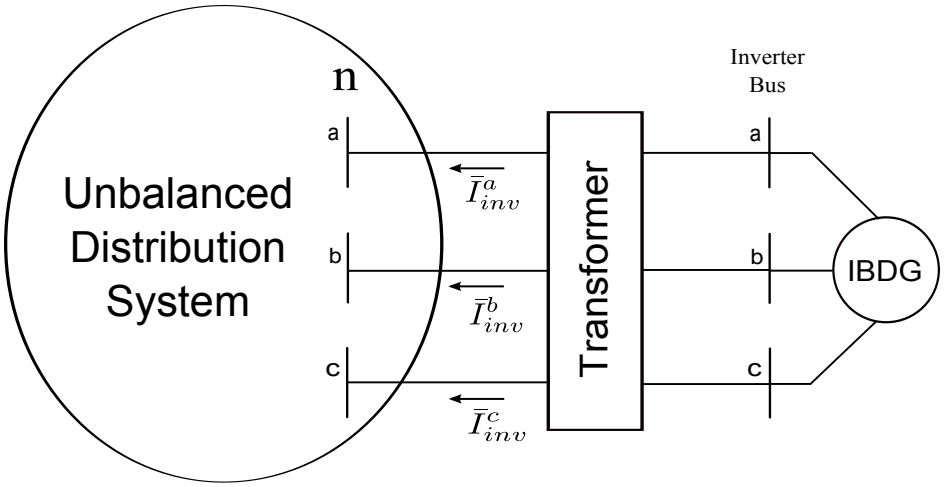

Figure 3.1: An unbalanced distribution system with inverter based DG (IBDG)

constant impedance, constant current and constant power loads, respectively. The pre-fault bus voltages of the unbalanced distribution network (shown in Fig 3.1) are calculated using distribution system load flow (DSLF) [70]. In DSLF, IBDG is considered to inject a complex power S^p_{dg} at each phase p ($p = a, b, c$) of the inverter bus under normal operating conditions where $S^p_{dg} = P^p_{dg} + j0.0$; P^p_{dg} denoting the real power injected by IBDG at phase p. In each iteration of DSLF, the load power consumed by the voltage dependent loads is updated using eq. (3.1). The pre-fault inverter current is then calculated using the values of bus voltages obtained from DSLF as,

$$\bar{\mathbf{I}}^{\mathbf{abc}}_{\mathbf{inv}} = \left[\bar{\mathbf{z}}^{\mathbf{abc}}_{\mathbf{t}}\right]^{-1} (\bar{\mathbf{V}}^{\mathbf{abc}}_{\mathbf{inv,st}} - \bar{\mathbf{V}}^{\mathbf{abc}}_{\mathbf{n}}) \tag{3.2}$$

where $\bar{\mathbf{I}}^{\mathbf{abc}}_{\mathbf{inv}} = \begin{bmatrix} \bar{I}^a_{inv} & \bar{I}^b_{inv} & \bar{I}^c_{inv} \end{bmatrix}^T$; $\left[\bar{\mathbf{z}}^{\mathbf{abc}}_{\mathbf{t}}\right] = \begin{bmatrix} \bar{z}^{aa}_t & \bar{z}^{ab}_t & \bar{z}^{ac}_t \\ \bar{z}^{ba}_t & \bar{z}^{bb}_t & \bar{z}^{bc}_t \\ \bar{z}^{ca}_t & \bar{z}^{cb}_t & \bar{z}^{cc}_t \end{bmatrix}$ is the transformer impedance matrix. $\bar{\mathbf{V}}^{\mathbf{abc}}_{\mathbf{inv,st}}$ and $\bar{\mathbf{V}}^{\mathbf{abc}}_{\mathbf{n}}$ are the three phase voltage vectors of the inverter bus and n^{th} bus, obtained from the load flow solutions, respectively. Next, all the loads are converted to constant impedance loads using pre-fault DSLF solution. Now, KCL equations are written for all the buses of the system except IBDG bus and substation bus. These KCL equations can then be expressed in the matrix form as,

$$\left[\mathbf{Y_{bus}}\right]\left[\mathbf{V}\right] = \left[\mathbf{I}\right] \tag{3.3}$$

The details of the bus admittance matrix $[\mathbf{Y_{bus}}]$, bus voltage vector $[\mathbf{V}]$ and current injection vector $[\mathbf{I}]$ are given in eq. (2.10) of Subsection 2.2.1 of Chapter 2. The sizes of the $[\mathbf{Y_{bus}}]$ matrix, $[\mathbf{V}]$

and $[\mathbf{I}]$ vectors for an unbalanced distribution system having u three phase, v two phase and w single phase buses, are $((3u+2v+w)-3) \times ((3u+2v+w)-3)$, $((3u+2v+w)-3) \times 1$ and $((3u+2v+w)-3) \times 1$, respectively (as described in Subsection 2.2.1 of Chapter 2). Now, if an IBDG is connected at n^{th} bus of the system, only the elements of $[\mathbf{Y_{bus}}]$ matrix corresponding to bus n (location of IBDG) will be modified as,

$$\bar{\mathbf{Y}}_{\mathbf{nn}}^{\mathbf{abc}} = \bar{\mathbf{Y}}_{\mathbf{nn}}^{\mathbf{abc}} + \bar{\mathbf{y}}_{\mathbf{t}}^{\mathbf{abc}} \tag{3.4}$$

where, $\bar{\mathbf{y}}_{\mathbf{t}}^{\mathbf{abc}}$ (transformer admittance matrix) $= \left[\bar{\mathbf{z}}_{\mathbf{t}}^{\mathbf{abc}}\right]^{-1}$ and $\bar{\mathbf{Y}}_{\mathbf{nn}}^{\mathbf{abc}}$ is the (3×3) sub-matrix (corresponding to bus n) of the $[\mathbf{Y_{bus}}]$ matrix. The vector $[\mathbf{I}]$ will also be modified to $[\mathbf{I_m}]$ (comprising of both the substation injected current and the current injected by the IBDGs) and is given as,

$$[\mathbf{I_m}] = \left[\bar{\mathbf{y}}_{\mathbf{12}}^{\mathbf{abc}}\bar{\mathbf{V}}_{\mathbf{s}}^{\mathbf{abc}} \quad \cdots \quad \bar{\mathbf{y}}_{\mathbf{t}}^{\mathbf{abc}}\bar{\mathbf{V}}_{\mathbf{inv,st}}^{\mathbf{abc}} \quad 0 \quad \cdots \quad 0 \quad 0\right]^{\mathbf{T}} \tag{3.5}$$

In eq. (3.5), it is to be noted that the term $(\bar{\mathbf{y}}_{\mathbf{t}}^{\mathbf{abc}}\bar{\mathbf{V}}_{\mathbf{inv,st}}^{\mathbf{abc}})$ occupies the position $(3(n-1)+1)$ to $(3(n-1)+3)$ in vector $[\mathbf{I_m}]$, corresponding to the IBDG location (n^{th} bus) in the distribution system. Also in eq. (3.5), $\bar{\mathbf{V}}_{\mathbf{s}}^{\mathbf{abc}} = \left[\bar{V}_s^a \quad \bar{V}_s^b \quad \bar{V}_s^c\right]^{\mathbf{T}}$ is the three phase sub-station bus voltage vector and $\bar{\mathbf{y}}_{\mathbf{12}}^{\mathbf{abc}}$ is the line admittance matrix between substation bus and bus 2 (which is directly connected to substation bus through a line impedance $\bar{\mathbf{z}}_{\mathbf{12}}^{\mathbf{abc}}$).

3.2.2 Short-circuit calculations

For the initial estimation of short-circuit currents, the fault analysis method, as discussed in Section 2.2 of Chapter 2, is used. In this method, the elements of the $[\mathbf{Y_{bus}}]$ matrix is modified corresponding to the type of fault occurring in the system. The details of the modified elements of the $[\mathbf{Y_{bus}}]$ matrix for different type of unsymmetrical faults in the distribution system are given in Subsections 2.2.2 to 2.2.4 of Chapter 2. The bus voltages under the fault conditions are then calculated using eq. (3.6) as,

$$\left[\mathbf{Y_{bus\_m}}\right]\left[\mathbf{V}\right] = \left[\mathbf{I_m}\right] \tag{3.6}$$

where $[\mathbf{Y_{bus\_m}}]$ is the modified bus admittance matrix which incorporates eq. (3.4) and modified elements of $[\mathbf{Y_{bus}}]$ matrix corresponding to the type of fault occurring in the system, and $[\mathbf{I_m}]$ is the modified source current injection vector given in eq. (3.5). It is to be noted that initially during fault analysis, the inverter is represented as a constant three phase voltage source (having a voltage

of $\bar{\mathbf{V}}^{\mathbf{abc}}_{\mathbf{inv,st}}$ behind a transformer impedance matrix $[\bar{\mathbf{z}}^{\mathbf{abc}}_{\mathbf{t}}]\big)$. Subsequently, the initial estimate of inverter current under the fault condition is calculated as,

$$\bar{\mathbf{I}}^{\mathbf{abc}}_{\mathbf{inv,f,est}} = \left[\bar{\mathbf{z}}^{\mathbf{abc}}_{\mathbf{t}}\right]^{-\mathbf{1}} (\bar{\mathbf{V}}^{\mathbf{abc}}_{\mathbf{inv,st}} - \bar{\mathbf{V}}^{\mathbf{abc}}_{\mathbf{n,f}}) \tag{3.7}$$

where $\bar{\mathbf{V}}^{\mathbf{abc}}_{\mathbf{n,f}}$ is the three phase voltage vector of the n^{th} bus under the fault condition. Depending upon the magnitude of $\bar{\mathbf{I}}^{\mathbf{abc}}_{\mathbf{inv,f,est}}$, there can be two possible cases of inverter operation during fault as discussed below:

Case 1: If $|\bar{I}^{p}_{inv,f,est}| \leq I^{inv}_{sc}$; ($p$ = a,b,c)

If the magnitude of estimated inverter current $|\bar{I}^{p}_{inv,f,est}|$ under the fault condition for each phase ($p = a, b, c$), calculated using eq. (3.7), is less than the short-circuit capacity of the inverter (I^{inv}_{sc}), then the bus voltages calculated using eq. (3.6) are the final values of the bus voltages of the system under the fault condition. Once the bus voltages are obtained, the fault currents and branch currents under the fault conditions are calculated using the fault analysis method given in Section 2.2 of Chapter 2.

Case 2: If $|\bar{I}^{p}_{inv,f,est}| > I^{inv}_{sc}$; ($p$=$a$, or b, or c)

In this case, the estimated inverter current magnitude of the inverter under the fault condition is restricted to its short-circuit capacity (I^{inv}_{sc}), by operating the inverter in constant current control mode [63, 65]. Hence the inverter current under the fault condition is given as,

$$\bar{I}^{p}_{inv,f} = |\bar{I}^{p}_{inv,f}|\angle\Psi^{p}_{inv,f} = I^{inv}_{sc}\angle\Psi^{p}_{inv,f}; p = a, b, c \tag{3.8}$$

where $\Psi^{p}_{inv,f}$ is the unknown inverter current angle corresponding to phase p under the fault condition. To solve for these unknown angles, it is assumed that, $\mathbf{\Psi}^{\mathbf{abc}}_{\mathbf{inv,f}} = \frac{\pi}{\mathbf{2}} + \theta^{\mathbf{abc}}_{\mathbf{n,f}}$ [63, 65], where $\theta^{\mathbf{abc}}_{\mathbf{n,f}} = \begin{bmatrix}\theta^{a}_{n,f} & \theta^{b}_{n,f} & \theta^{c}_{n,f}\end{bmatrix}^{T}$ is the three phase voltage angle vector of the n^{th} bus under the fault condition (where the IBDG is connected) and $\mathbf{\Psi}^{\mathbf{abc}}_{\mathbf{inv,f}} = \begin{bmatrix}\Psi^{a}_{inv,f} & \Psi^{b}_{inv,f} & \Psi^{c}_{inv,f}\end{bmatrix}^{\mathbf{T}}$.

The bus voltages along with the unknown current angles under the fault condition can be calculated by solving the KCL equations of the system (written at all buses and for all phases of the system, except the substation bus and inverter bus of IBDG).

Consider any bus k at which no IBDG is connected. Assume that the set of three phase buses directly connected to bus k is "T_{hk}", set of two phase buses directly connected to phase h of bus k is "T_{wk}" (two phase buses would always be connected to phase h and another phase r) and the

set of single phase buses directly connected to bus k and phase h is "S_{pk}". Hence, the real and imaginary parts of the KCL equation corresponding to phase h of bus k can be written as,

Real part

$$\begin{aligned}
&\sum_{p} |\bar{Y}_{kk}^{hp}||\bar{V}_{k}^{p}|cos(\theta_{k}^{p} + \phi_{kk}^{hp}) + \sum_{b\epsilon T_{hk}} \sum_{p} (|\bar{Y}_{kb}^{hp}||\bar{V}_{b}^{p}|cos(\theta_{b}^{p} + \phi_{kb}^{hp})) \\
&+ \sum_{b\epsilon T_{wk}} \sum_{r} |\bar{Y}_{kb}^{hr}||\bar{V}_{b}^{r}|cos(\theta_{b}^{r} + \phi_{kb}^{hr}) + \sum_{b\epsilon S_{pk}} |\bar{Y}_{kb}^{hh}||\bar{V}_{b}^{h}|cos(\theta_{b}^{h} + \phi_{kb}^{hh}) \\
&- \sum_{p} |\bar{y}_{ks}^{hp}||\bar{V}_{s}^{p}|cos(\theta_{s}^{p} + \phi_{ks}^{hp}) = 0 = f_{(k-1),re}^{h}(V, \theta)
\end{aligned} \tag{3.9a}$$

Imaginary part

$$\begin{aligned}
&\sum_{p} |\bar{Y}_{kk}^{hp}||\bar{V}_{k}^{p}|sin(\theta_{k}^{p} + \phi_{kk}^{hp}) + \sum_{b\epsilon T_{hk}} \sum_{p} (|\bar{Y}_{kb}^{hp}||\bar{V}_{b}^{p}|sin(\theta_{b}^{p} + \phi_{kb}^{hp})) \\
&+ \sum_{b\epsilon T_{wk}} \sum_{r} |\bar{Y}_{kb}^{hr}||\bar{V}_{b}^{r}|sin(\theta_{b}^{r} + \phi_{kb}^{hr}) + \sum_{b\epsilon S_{pk}} |\bar{Y}_{kb}^{hh}||\bar{V}_{b}^{h}|sin(\theta_{b}^{h} + \phi_{kb}^{hh}) \\
&- \sum_{p} |\bar{y}_{ks}^{hp}||\bar{V}_{s}^{p}|sin(\theta_{s}^{p} + \phi_{ks}^{hp}) = 0 = f_{(k-1),im}^{h}(V, \theta)
\end{aligned} \tag{3.9b}$$

where $k = 2, \cdots, \cdots, n_b$, ($n_b$ is the number of buses), $k \neq n$; $h = (a, b, c)$ for three phase buses; $h = (a$ and $b)$, or $(b$ and $c)$, or $(c$ and $a)$ for two phase buses; $h = (a$ or b or $c)$ for single phase buses; $p = (a, b, c)$; and $r = (a$ and $b)$, or $(b$ and $c)$, or $(c$ and $a)$. $\bar{y}_{ks}^{hp}$ is the element of line admittance matrix between bus k and substation bus s between phase h and p, and ϕ_{ks}^{hp} is the angle of $\bar{y}_{ks}^{hp}$.

Similarly, consider bus n at which an IBDG is connected through a transformer. Assume that the set of three phase buses directly connected to bus n is "T_{hn}", set of two phase buses directly connected to phase h of bus n is "T_{wn}" (two phase buses would always be connected to phase h and another phase r) and the set of single phase buses directly connected to bus n and phase h is "S_{pn}". Hence, the real and imaginary parts of the KCL equation corresponding to phase h of bus n can be written as,

Real part

$$\begin{aligned}
&\sum_{p}|\bar{Y}_{nn}^{hp}||\bar{V}_{n}^{p}|cos(\theta_{n}^{p}+\phi_{nn}^{hp})+\sum_{b\epsilon T_{hn}}\sum_{p}(|\bar{Y}_{nb}^{hp}||\bar{V}_{b}^{p}|cos(\theta_{b}^{p}+\phi_{nb}^{hp}))\\
&+\sum_{b\epsilon T_{wn}}\sum_{r}|\bar{Y}_{nb}^{hr}||\bar{V}_{b}^{r}|cos(\theta_{b}^{r}+\phi_{nb}^{hr})+\sum_{b\epsilon S_{pn}}|\bar{Y}_{nb}^{hh}||\bar{V}_{b}^{h}|cos(\theta_{b}^{h}+\phi_{nb}^{hh})\\
&-\sum_{p}|\bar{y}_{ns}^{hp}||\bar{V}_{s}^{p}|cos(\theta_{s}^{p}+\phi_{ns}^{hp})-I_{sc}^{inv}cos(90^{o}+\theta_{n}^{h})=0=f_{(n-1),re}^{h}(V,\theta)
\end{aligned}\tag{3.10a}$$

Imaginary part

$$\begin{aligned}
&\sum_{p}|\bar{Y}_{nn}^{hp}||\bar{V}_{n}^{p}|sin(\theta_{n}^{p}+\phi_{nn}^{hp})+\sum_{b\epsilon T_{hn}}\sum_{p}(|\bar{Y}_{nb}^{hp}||\bar{V}_{b}^{p}|sin(\theta_{b}^{p}+\phi_{nb}^{hp}))\\
&+\sum_{b\epsilon T_{wn}}\sum_{r}|\bar{Y}_{nb}^{hr}||\bar{V}_{b}^{r}|sin(\theta_{b}^{r}+\phi_{nb}^{hr})+\sum_{b\epsilon S_{pn}}|\bar{Y}_{nb}^{hh}||\bar{V}_{b}^{h}|sin(\theta_{b}^{h}+\phi_{nb}^{hh})\\
&-\sum_{p}|\bar{y}_{ns}^{hp}||\bar{V}_{s}^{p}|sin(\theta_{s}^{p}+\phi_{ns}^{hp})-I_{sc}^{inv}sin(90^{o}+\theta_{n}^{h})=0=f_{(n-1),im}^{h}(V,\theta)
\end{aligned}\tag{3.10b}$$

Hence, for an unbalanced distribution system having u three phase, v two phase and w single phase buses, there is a total of $2(3u+2v+w-3)$ non-linear equations. These equations are given in polar form. It is to be noted that the rectangluar form of these equations are also non-linear. To solve these non-linear equations, numerical method such as Gauss-Siedel or Newton-Raphson method, can be used. In this work, Newton-Raphson method has been used as Gauss-Siedel method [59] requires large execution time as shown later. The set of non-linear equations is given as,

$$\begin{aligned}
f_{1,re}^{a}(V_{2}^{a},V_{2}^{b},...,V_{n_b}^{\ell},\theta_{2}^{a},\theta_{2}^{b},...,\theta_{n_b}^{\ell}) &= 0\\
f_{1,re}^{b}(V_{2}^{a},V_{2}^{b},...,V_{n_b}^{\ell},\theta_{2}^{a},\theta_{2}^{b},...,\theta_{n_b}^{\ell}) &= 0\\
\vdots &\ \vdots\ \vdots\\
\vdots &\ \vdots\ \vdots\\
f_{(nb-1),re}^{\ell}(V_{2}^{a},V_{2}^{b},...,V_{n_b}^{\ell},\theta_{2}^{a},\theta_{2}^{b},...,\theta_{n_b}^{\ell}) &= 0\\
f_{1,im}^{a}(V_{2}^{a},V_{2}^{b},...,V_{n_b}^{\ell},\theta_{2}^{a},\theta_{2}^{b},...,\theta_{n_b}^{\ell}) &= 0\\
f_{1,im}^{b}(V_{2}^{a},V_{2}^{b},...,V_{n_b}^{\ell},\theta_{2}^{a},\theta_{2}^{b},...,\theta_{n_b}^{\ell}) &= 0\\
\vdots &\ \vdots\ \vdots\\
\vdots &\ \vdots\ \vdots\\
f_{(nb-1),im}^{\ell}(V_{2}^{a},V_{2}^{b},...,V_{n_b}^{\ell},\theta_{2}^{a},\theta_{2}^{b},...,\theta_{n_b}^{\ell}) &= 0
\end{aligned}\tag{3.11}$$

where $n_b = u + v + w$ and $\ell = a$, or b, or c. The above set of equations are solved using Newton-Raphson method as,

$$\begin{bmatrix} \mathbf{\Delta V} \\ \mathbf{\Delta \theta} \end{bmatrix} = \begin{bmatrix} \mathbf{J_1} & \mathbf{J_2} \\ \mathbf{J_3} & \mathbf{J_4} \end{bmatrix}^{-1} . \begin{bmatrix} \mathbf{\Delta f_{real}} \\ \mathbf{\Delta f_{imag}} \end{bmatrix} \tag{3.12}$$

where $\mathbf{\Delta V}$ and $\mathbf{\Delta}\theta$ are the correction vectors calculated at t^{th} iteration and hence given as,

$\mathbf{\Delta V} = \left[\Delta V_2^{a(t)}, \Delta V_2^{b(t)}, \cdots, \cdots, \Delta V_{n_b}^{\ell(t)}\right]^{\mathbf{T}}$;

$\mathbf{\Delta}\theta = \left[\Delta \theta_2^{a(t)}, \Delta \theta_2^{b(t)}, \cdots, \cdots, \Delta \theta_{n_b}^{\ell(t)}\right]^{T}$.

$\mathbf{\Delta f_{real}}$ and $\mathbf{\Delta f_{imag}}$ are the mismatch vectors calculated at t^{th} iteration and are given as,

$\mathbf{\Delta f_{real}} = \left[-f_{1,re}^{a(t)}, -f_{1,re}^{b(t)}, \cdots, \cdots, -f_{(n_b-1),re}^{\ell(t)}\right]^{\mathbf{T}}$;

$\mathbf{\Delta f_{imag}} = \left[-f_{1,im}^{a(t)}, -f_{1,im}^{b(t)}, \cdots, \cdots, -f_{(n_b-1),im}^{\ell(t)}\right]^{\mathbf{T}}$.

$\mathbf{J_1}$, $\mathbf{J_2}$, $\mathbf{J_3}$ and $\mathbf{J_4}$ are the sub-matrices of the Jacobian matrix [$\mathbf{J}$], and are given as,

$$\mathbf{J_1} = \frac{\partial \mathbf{f_{real}}}{\partial \mathbf{V}} = \begin{bmatrix} \frac{\partial f_{1,re}^a}{\partial V_2^a} & \frac{\partial f_{1,re}^a}{\partial V_2^b} & \cdots & \frac{\partial f_{1,re}^a}{\partial V_{n_b}^\ell} \\ \frac{\partial f_{1,re}^b}{\partial V_2^a} & \frac{\partial f_{1,re}^b}{\partial V_2^b} & \cdots & \frac{\partial f_{1,re}^b}{\partial V_{n_b}^\ell} \\ \vdots & \vdots & \ddots & \vdots \\ \frac{\partial f_{(n_b-1),re}^\ell}{\partial V_2^a} & \frac{\partial f_{(n_b-1),re}^\ell}{\partial V_2^b} & \cdots & \frac{\partial f_{(n_b-1),re}^\ell}{\partial V_{n_b}^\ell} \end{bmatrix};$$

$$\mathbf{J_2} = \frac{\partial \mathbf{f_{real}}}{\partial \theta} = \begin{bmatrix} \frac{\partial f_{1,re}^a}{\partial \theta_2^a} & \frac{\partial f_{1,re}^a}{\partial \theta_2^b} & \cdots & \frac{\partial f_{1,re}^a}{\partial \theta_{n_b}^\ell} \\ \frac{\partial f_{1,re}^b}{\partial \theta_2^a} & \frac{\partial f_{1,re}^b}{\partial \theta_2^b} & \cdots & \frac{\partial f_{1,re}^b}{\partial \theta_{n_b}^\ell} \\ \vdots & \vdots & \ddots & \vdots \\ \frac{\partial f_{(n_b-1),re}^\ell}{\partial \theta_2^a} & \frac{\partial f_{(n_b-1),re}^\ell}{\partial \theta_2^b} & \cdots & \frac{\partial f_{(n_b-1),re}^\ell}{\partial \theta_{n_b}^\ell} \end{bmatrix};$$

$$\mathbf{J_3} = \frac{\partial \mathbf{f_{imag}}}{\partial \mathbf{V}} = \begin{bmatrix} \frac{\partial f_{1,im}^a}{\partial V_2^a} & \frac{\partial f_{1,im}^a}{\partial V_2^b} & \cdots & \frac{\partial f_{1,im}^a}{\partial V_{n_b}^\ell} \\ \frac{\partial f_{1,im}^b}{\partial V_2^a} & \frac{\partial f_{1,im}^b}{\partial V_2^b} & \cdots & \frac{\partial f_{1,im}^b}{\partial V_{n_b}^\ell} \\ \vdots & \vdots & \ddots & \vdots \\ \frac{\partial f_{(n_b-1),im}^\ell}{\partial V_2^a} & \frac{\partial f_{(n_b-1),im}^\ell}{\partial V_2^b} & \cdots & \frac{\partial f_{(n_b-1),im}^\ell}{\partial V_{n_b}^\ell} \end{bmatrix};$$

$$\mathbf{J_4} = \frac{\partial \mathbf{f_{imag}}}{\partial \theta} = \begin{bmatrix} \frac{\partial f_{1,im}^a}{\partial \theta_2^a} & \frac{\partial f_{1,im}^a}{\partial \theta_2^b} & \cdots & \frac{\partial f_{1,im}^a}{\partial \theta_{n_b}^\ell} \\ \frac{\partial f_{1,im}^b}{\partial \theta_2^a} & \frac{\partial f_{1,im}^b}{\partial \theta_2^b} & \cdots & \frac{\partial f_{1,im}^b}{\partial \theta_{n_b}^\ell} \\ \vdots & \vdots & \ddots & \vdots \\ \frac{\partial f_{(n_b-1),im}^\ell}{\partial \theta_2^a} & \frac{\partial f_{(n_b-1),im}^\ell}{\partial \theta_2^b} & \cdots & \frac{\partial f_{(n_b-1),im}^\ell}{\partial \theta_{n_b}^\ell} \end{bmatrix}.$$

Elements of Jacobian matrix $[\mathbf{J}]$ (with no IBDG connected in the system) are calculated as,

$$\frac{\partial f^p_{i,re}}{\partial V^q_j} = Y^{pq}_{(i+1)j} cos(\theta^q_j + \phi^{pq}_{(i+1)j}) \tag{3.13a}$$

$$\frac{\partial f^p_{i,re}}{\partial \theta^q_j} = -Y^{pq}_{(i+1)j} V^q_j sin(\theta^q_j + \phi^{pq}_{(i+1)j}) \tag{3.13b}$$

$$\frac{\partial f^p_{i,im}}{\partial V^q_j} = Y^{pq}_{(i+1)j} sin(\theta^q_j + \phi^{pq}_{(i+1)j}) \tag{3.13c}$$

$$\frac{\partial f^p_{i,im}}{\partial \theta^q_j} = -Y^{pq}_{(i+1)j} V^q_j cos(\theta^q_j + \phi^{pq}_{(i+1)j}) \tag{3.13d}$$

where $i = 1, 2, ..., (n_b - 1)$; $j = 2, 3, ..., n_b$; $p, q = a$, or b or c. If an IBDG is connected at n^{th} bus of the distribution system, the following elements of the Jacobian matrix [$\mathbf{J}$] will be modified as,

$$\left.\frac{\partial f^p_{(n-1),re}}{\partial \theta^q_n}\right|_{new} = \frac{\partial f^p_{(n-1),re}}{\partial \theta^q_n} + I^{inv}_{sc} sin(90^o + \theta^q_n) \tag{3.14a}$$

$$\left.\frac{\partial f^p_{(n-1),im}}{\partial \theta^q_n}\right|_{new} = \frac{\partial f^p_{(n-1),im}}{\partial \theta^q_n} - I^{inv}_{sc} cos(90^o + \theta^q_n) \tag{3.14b}$$

where $p, q = a, b, c$.

In eq. (3.12), the dimension of all the four sub-matrices ($\mathbf{J_1}$, $\mathbf{J_2}$, $\mathbf{J_3}$, $\mathbf{J_4}$) for an unbalanced distribution system (having u three phase, v two phase and w single phase buses) is $(3u + 2v + w-3)\times(3u+2v+w-3)$ and that of the Jacobian matrix [$\mathbf{J}$] is $2(3u+2v+w-3)\times 2(3u+2v+w-3)$.

The elements of $[\mathbf{Y_{bus\_m}}]$ in eq. (3.6), corresponding to the voltage dependent load buses, are also modified at each iteration. The load admittances of the voltage dependent load buses are replaced with their new calculated values in each iteration. Hence, the modified elements of $[\mathbf{Y_{bus\_m}}]$, corresponding to the voltage dependent load buses, at t^{th} iteration are given as,

$$\bar{Y}^{pp(t)}_{vd,vd} = \bar{Y}^{pp(t)}_{vd,vd} + \bar{y}^{p(t)}_{vd} - \bar{y}^{p(t-1)}_{vd}; t > 1, p = a, b, c. \tag{3.15}$$

where vd is the voltage dependent load bus. $\bar{y}^{p(t)}_{vd}$ is the load admittance of phase p of vd^{th} bus calculated at t^{th} iteration, and is given as,

$$\bar{y}^{p(t)}_{vd} = \frac{\bar{I}^{p(t)}_{vd}}{\bar{V}^{p(t-1)}_{vd}}; \bar{I}^{p(t)}_{vd} = \left(\frac{\bar{P}^{p(t)}_{vd} + j\bar{Q}^{p(t)}_{vd}}{\bar{V}^{p(t-1)}_{vd}}\right)^* \tag{3.16}$$

where $\bar{P}^{p(t)}_{vd}$ and $\bar{Q}^{p(t)}_{vd}$ are the active and reactive load power calculated at phase p of vd^{th} bus using eq. (3.1) at t^{th} iteration, respectively and (*) stands for complex conjugate. $\bar{I}^{p(t)}_{vd}$ is the injected load current of phase p of vd^{th} bus, calculated at t^{th} iteration.

Initial guess for solving eq. (3.11) is taken as the solution of fault analysis method as obtained by solving eq. (3.6) with the inverter bus voltage set at $\bar{\mathbf{V}}^{\mathbf{abc}}_{\mathbf{inv,st}}$. Once the bus voltages under the fault condition are calculated by solving eq. (3.11), the fault current and branch currents under the fault condition are recalculated by the fault analysis method given in Section 2.2 of Chapter 2. Hence, the inverter bus voltage under the fault condition is calculated as,

$$\bar{\mathbf{V}}^{\mathbf{abc}}_{\mathbf{inv,f}} = \bar{\mathbf{V}}^{\mathbf{abc}}_{\mathbf{n,f}} + \bar{\mathbf{I}}^{\mathbf{abc}}_{\mathbf{inv,f}} \bar{\mathbf{z}}^{\mathbf{abc}}_{\mathbf{t}} \tag{3.17}$$

Similarly, if there are nd-no. of IBDGs with their short-circuit switching capacities as $I^{inv}_{sc,1}$, $I^{inv}_{sc,2}$, ..., $I^{inv}_{sc,nd}$, and connected at different buses $(DG_{bus,1}, DG_{bus,2}, ..., DG_{bus,nd})$ of the system, the following elements of the Jacobian matrix [**J**] will be modified as,

$$\left.\frac{\partial f^p_{(dg-1),re}}{\partial \theta^q_{dg}}\right|_{new} = \frac{\partial f^p_{(dg-1),re}}{\partial \theta^q_{dg}} + I^{inv}_{sc,ii} sin(90^o + \theta^q_{dg}) \tag{3.18a}$$

$$\left.\frac{\partial f^p_{(dg-1),im}}{\partial \theta^q_{dg}}\right|_{new} = \frac{\partial f^p_{(dg-1),im}}{\partial \theta^q_{dg}} - I^{inv}_{sc,ii} cos(90^o + \theta^q_{dg}) \tag{3.18b}$$

where dg = $(DG_{bus,1}, DG_{bus,2}, ..., DG_{bus,nd})$; ii = $1, 2, ..., nd$; $p = a, b, c$ and $q = p$.

3.2.2.1 Steps of algorithm for proposed short circuit analysis method of a distribution system with IBDG

In the literature, depending upon the terminal voltage, the IBDG is operated under different control modes [148, 149]. The steps for the proposed method for different control modes of inverter are given as,

1. Run base case DSLF with IBDG connected in the system and obtain pre-fault inverter bus voltage, $\bar{\mathbf{V}}^{\mathbf{abc}}_{\mathbf{inv,st}}$.

2. Convert all types of loads (constant PQ and voltage dependent loads) into constant impedance loads and form the $[\mathbf{Y_{bus}}]$ matrix of the system.

3. Modify the bus admittance matrix $[\mathbf{Y_{bus}}]$ to include the effect of transformer as in eq. (3.4) and further modify it corresponding to the type of fault occurring in the system (as given in Subsections 2.2.2 to 2.2.4 of Chapter 2) to obtain $[\mathbf{Y_{bus\_m}}]$ matrix. Also, the current injection vector $[\mathbf{I}]$ is modified to $[\mathbf{I_m}]$ using eq. (3.5).

4. Find the initial estimate of bus voltages under the fault condition by solving eq. (3.6) and estimate the inverter currents $\bar{I}^{p}_{inv,f,est}$, $(p = a, b, c)$ of all nd-no. of IBDGs present in the network from eq. (3.7).

5. Check whether $|\bar{I}^{p}_{inv,f,est}| \leq \bar{I}^{inv}_{sc}$, $(p = a, b, c)$ for all IBDGs in the system. The three possible cases are:

   Case (A): If $|\bar{I}^{p}_{inv,f,est}| \leq \bar{I}^{inv}_{sc}$, $(p = a, b, c)$ for all nd-no. of IBDGs, then go to step 6, else

   Case (B): If $|\bar{I}^{p}_{inv,f,est}|$, $(p = a, b, c)$ of all nd-no. of IBDGs are greater than their corresponding short-circuit current capacities, then solve the set of non-linear equations (eq. (3.11)) with $\bar{I}^{p}_{inv,f} = I^{inv}_{sc}\angle(\frac{\pi}{2} + \theta^{p}_{dg,f})$, $(p = a, b, c)$ for all IBDGs (Boost mode operation) using the proposed method and obtain the final values of bus voltages under the fault condition and go to step 6, else

   Case (C): If out of nd-no. of IBDGs, for kd-no. of IBDGs $|\bar{I}^{p}_{inv,f,est}| \leq I^{inv}_{sc}$, $(p = a, b, c)$ and for the remaining $(nd - kd)$-no. of IBDGs $|\bar{I}^{p}_{inv,f,est}| > I^{inv}_{sc}$, $(p = a, b, c)$, then set $\bar{I}^{p}_{inv,f} = I^{inv}_{sc}\angle(\frac{\pi}{2} + \theta^{p}_{dg,f})$, $(p = a, b, c)$, for $(nd - kd)$-no. of IBDGs, while for kd-no. of IBDGs set $\bar{\mathbf{I}}^{\mathbf{abc}}_{\mathbf{inv,f}} = \bar{\mathbf{I}}^{\mathbf{abc}}_{\mathbf{inv,f,est}}$, and carry out one iteration of solution of eq. (3.11), and obtain the bus voltages under the fault condition. Compute the $mismatch = max[|\mathbf{\Delta f_{real}}|, |\mathbf{\Delta f_{imag}}|]$. If $mismatch < \epsilon$ (tolerance), go to step 6, else estimate the inverter current $\bar{I}^{p}_{inv,f,est}$, $(p = a, b, c)$ using eq. (3.7) with new calculated bus voltages under the fault condition, for all IBDGs, and check the condition $|\bar{I}^{p}_{inv,f,est}| \leq I^{inv}_{sc}$, $(p = a, b, c)$ for these IBDGs and go to appropriate case of step 5.

6. Using the above obtained bus voltages under the fault condition, calculate the inverter bus voltages under the fault condition using eq. (3.17). Initialize the iteration count $k = 0$.

7. $k = k + 1$.

8. Depending upon the terminal voltage, the IBDG is operated under different modes as follows [148, 149]:

   (a) If $(min(|\mathbf{V}^{\mathbf{abc}}_{\mathbf{inv,f}}|) < 0.45\ p.u.)$ or $(max(|\mathbf{V}^{\mathbf{abc}}_{\mathbf{inv,f}}|) > 1.2\ p.u.)$, then IBDG will be disconnected ("Cut-off mode") and hence, the inverter current of IBDG is set as, $\bar{\mathbf{I}}^{\mathbf{abc}}_{\mathbf{inv,f}} =$

$0.0 + j0.0$.

(b) If $(0.45 \leq min(|\mathbf{V^{abc}_{inv,f}}|) < 0.88\ p.u.)$ and $(max(|\mathbf{V^{abc}_{inv,f}}|) \leq 1.0\ p.u.)$, then IBDG will operate in "Boost mode", and hence the inverter current of IBDG is set as, $\bar{I}^p_{inv,f} = I^{inv}_{sc}\angle(\theta^p_{dg,f} + \frac{\pi}{2})$, $(p = a, b, c)$.

(c) If $(min(|\mathbf{V^{abc}_{inv,f}}|) \geq 0.45\ p.u.)$ and $(max(|\mathbf{V^{abc}_{inv,f}}|) > 1.1\ p.u.)$, then IBDG will operate in "Absorb mode", and hence the inverter current of IBDG is set as, $\bar{I}^p_{inv,f} = I^{inv}_{sc}\angle(\theta^p_{dg,f} - \frac{\pi}{2})$, $(p = a, b, c)$.

(d) If $(0.45 \leq min(|\mathbf{V^{abc}_{inv,f}}|) < 0.88\ p.u.)$ and $(1.0 < max(|\mathbf{V^{abc}_{inv,f}}|) \leq 1.1\ p.u.)$, then IBDG will continue to operate in the same control mode as in the previous iteration. This hysteresis band is provided to prevent the IBDG from toggling frequently between "boost mode" and "absorb mode".

(e) If $(min(|\mathbf{V^{abc}_{inv,f}}|) \geq 0.88\ p.u.)$ and $(max(|\mathbf{V^{abc}_{inv,f}}|) \leq 1.1\ p.u.)$, then IBDG will operate in "Active-power injection mode" and hence, the inverter current of IBDG is set as, $\bar{I}^p_{inv,f} = \frac{P^p_{dg}}{\left(\bar{V}^{p(k-1)}_{inv,f}\right)^*}$; $(p = a, b, c)$, where $\bar{V}^{p(k-1)}_{inv,f}$ is the inverter bus voltage of p^{th} phase of IBDG, calculated in $(k-1)^{th}$ iteration.

9. Solve the set of non-linear equations (eq. (3.11)) with the above discussed voltage control strategies for all IBDGs for k^{th} iteration using the proposed method and obtain the bus voltages under the fault condition. Also compute the $mismatch$.

10. If $mismatch < \epsilon$ (tolerance), go to the next step, else calculate the new inverter bus voltages for all IBDGs under the fault condition using eq. (3.17) and go to step 7.

11. Using the above obtained bus voltages, calculate the fault current and branch currents under the fault condition following the procedure given in Section 2.2 of Chapter 2. Also calculate the inverter bus voltages under the fault condition using eq. (3.17).

The overall flow-chart of the proposed fault analysis method is shown in Fig 3.2.

3.3 Test results and discussions

The effectiveness of the developed method has been investigated on the modified IEEE 123-bus unbalanced distribution system in radial as well as weakly meshed configuration (as given in Section

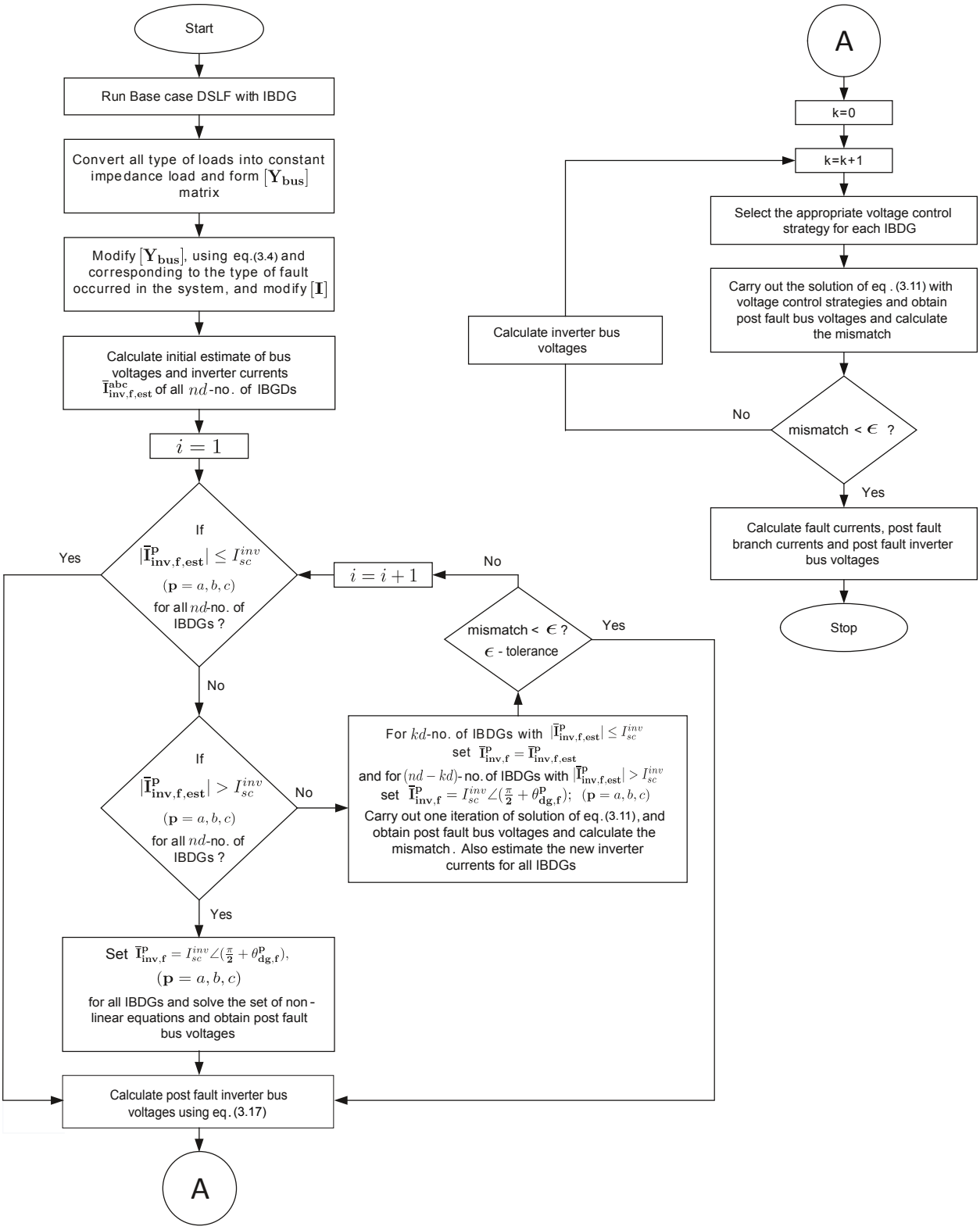

Figure 3.2: Flow-chart of the proposed fault analysis method

Table 3.1: Details of the IBDGs installed in the modified IEEE 123-bus unbalanced distribution system

IBDG No.	**IBDG location (Bus No.)**	**IBDG installed capacity, P_{dg} (per phase) (kW)**	**Short-circuit capacity, I_{sc}^{inv} (per phase) (Amp)**
1.	20	140	29.062
2.	25	105	21.796
3.	75	140	29.062
4.	98	175	36.327
5.	104	140	29.062

2.3 of Chapter 2). In this system, five different sized inverter based DGs have been assumed to be connected at different buses through three phase transformers (Yg-Yg), having an equivalent reactance of 0.2042 Ω/phase. The total installed capacity of IBDGs is taken as 20% of the total system load (active power load). Short-circuit current capacity of these inverter based DGs are assumed to be 150% of the rated inverter current. Detailed informations of these IBDGs are given in Table 3.1. The proposed method has been implemented in MATLAB environment [66] with a tolerance limit (ϵ) of 1.0×10^{-12}. For validating the developed method, the time-domain simulation study of the entire system has also been carried out using PSCAD/EMTDC software [139]. For verifying the correctness of the calculated values of inverter currents of IBDGs by the proposed method, these calculated currents have been represented as constant current sources in time domain simulation study.

3.3.1 Results of modified IEEE 123-bus unbalanced radial distribution system

In this work, two different scenarios have been considered as described below:

Scenario 1: For this scenario, it is assumed that the IBDG control scheme is not dependent on the terminal voltage (i.e. the algorithm terminates after Step-6). An SLG fault in phase a of bus 105, with a fault impedance $\bar{z}_f$ = 0.001+0.000i p.u. (the minimum value of fault impedance permissible in PSCAD/EMTDC software, used for comparison purpose), has been assumed in this case. In the first step, the inverter currents $\left(\bar{\mathbf{I}}^{\mathbf{abc}}_{\mathbf{inv,f,est}}\right)$ of all the five IBDGs have been calculated by assuming that the post fault inverter bus voltages ($\bar{\mathbf{V}}^{\mathbf{abc}}_{\mathbf{inv,f}}$) of all IBDGs are maintained at their pre-fault values ($\bar{\mathbf{V}}^{\mathbf{abc}}_{\mathbf{inv,st}}$). The calculated currents are given in Table 3.2. The table shows

Table 3.2: Results for SLG(a-g) fault in modified IEEE 123-bus radial distribution system with IBDGs for scenario 1

DG No.	Initial estimate of inverter current, $\bar{\mathbf{I}}^{\mathbf{p}}_{\mathbf{inv,f,est}}$, (Amp) when $\bar{\mathbf{V}}^{\mathbf{abc}}_{\mathbf{inv,f}} = \bar{\mathbf{V}}^{\mathbf{abc}}_{\mathbf{inv,st}}$			final value of inverter current, (Amp) $\bar{\mathbf{I}}^{\mathbf{abc}}_{\mathbf{inv,f}} = I^{inv}_{sc}\angle(\frac{\pi}{2} + \theta^{\mathbf{abc}}_{\mathbf{dg,f}})$,($\bar{\mathbf{I}}^{\mathbf{p}}_{\mathbf{inv,f}}$)			final value of injected DG power (capacitive reactive power) (kVAR)		
	Phase-a	**Phase-b**	**Phase-c**	**Phase-a**	**Phase-b**	**Phase-c**	**Phase-a**	**Phase-b**	**Phase-c**
1.	625.900∠-68.56^o	10.513∠-74.47^o	63.256∠121.46^o	29.062∠89.38^o	29.062∠-36.65^o	29.062∠214.26^o	144.865	227.206	222.112
2.	427.844∠-60.68^o	42.868∠108.97^o	106.964∠117.64^o	21.796∠89.33^o	21.796∠-36.65^o	21.796∠214.22^o	108.618	170.403	166.466
3.	4570.48∠-79.15^o	521.317∠-70.35^o	528.456∠-69.55^o	29.062∠88.10^o	29.062∠-45.12^o	29.062∠222.40^o	28.396	257.107	249.672
4.	1424.11∠-62.99^o	140.687∠103.40^o	272.567∠111.54^o	36.327∠88.16^o	36.327∠-45.40^o	36.327∠222.21^o	36.657	321.819	313.583
5.	2835.95∠-71.83^o	36.012∠9.06^o	60.464∠64.58^o	29.062∠85.69^o	29.062∠-45.95^o	29.062∠223.32^o	15.066	261.312	253.703

that, the magnitude of inverter currents $\left(|\bar{\mathbf{I}}^{\mathbf{abc}}_{\mathbf{inv,f,est}}|\right)$ of all the IBDGs are greater than their short-circuit current capacities, given in Table 3.1. Hence, according to [63, 65], the magnitudes of inverter currents of all the phases are to be maintained at their short-circuit current capacities $\left(|I^p_{inv,f}| = I^{inv}_{sc}, p = a, b, c\right)$ and their angles are maintained in such a way that all IBDGs will deliver reactive power to the system during the short-circuit condition ($\Psi^p_{inv,f} = \frac{\pi}{2} + \theta^p_{dg,f}, p = a, b, c$). With this strategy (Case (B) of Step-5), the bus voltages, branch currents, fault current and all the inverter currents under the fault conditions are recalculated using the proposed short-circuit analysis method. The calculated values of inverter currents ($\mathbf{I}^{\mathbf{abc}}_{\mathbf{inv,f}}$) and injected powers by all IBDGs under the fault condition are given in Table 3.2. The fault current (I_f) and source current (I_s) in phase a for this case using the proposed method and PSCAD/EMTDC simulation are given in Table 3.3. The rms values of I_f and I_s are measured with the help of "RMS Meter" in PSCAD/EMTDC software. The % error in the calculated values of I_f and I_s with respect to the values obtained by PSCAD/EMTDC simulation are 0.00369% and 0.00375%, respectively, as shown in Table 3.3. The above results show that the values of I_f and I_s calculated by the proposed method are very close to the values obtained by the PSCAD/EMTDC software, thereby validating the proposed method.

Different fault cases namely, LLG (ab-g), LLLG (abc-g), and LL (a-b) fault with $\bar{z}_f$ = 0.001+0.000i p.u., have also been simulated at bus 105 in the same system, using the proposed technique and PSCAD/EMTDC software. Detailed results of these cases are given in Table 3.3. The % error in I_f and I_s for all the fault cases, obtained by the proposed technique with respect to PSCAD/EMTDC simulation study are also given in Table 3.3. The maximum % error in the calculated fault current and the source current are 0.00496% and 0.00381%, respectively. These results again demonstrate

Table 3.3: Error analysis of proposed technique (scenario 1) with respect to PSCAD/EMTDC simulations

Fault type	**phase**	**Fault current at fault point (I_f)**		**% Error in I_f**	**Current drawn from the supply (I_s)**		**% Error in I_s**
		PSCAD simulation (kA)	**Proposed technique (kA)**		**PSCAD simulation (kA)**	**Proposed technique (kA)**	
SLG (a-g)	a	2.86046	2.86057	0.00369	2.80928	2.80939	0.00375
LLG (ab-g)	a	4.16862	4.16882	**0.00496**	4.15497	4.15499	0.00039
	b	4.30873	4.30889	0.00367	4.20519	4.20535	0.00369
LLLG (abc-g)	a	4.55136	4.55153	0.00367	4.49842	4.49859	0.00371
	b	4.84518	4.84536	0.00364	4.77608	4.77626	0.00368
	c	4.84245	4.84263	0.00368	4.77293	4.77311	0.00373
L-L (a-b)	a	4.06311	4.06325	0.00359	4.20943	4.20958	0.00363
	b	4.06311	4.06325	0.00359	3.95193	3.95208	**0.00381**

the accuracy of the proposed method. Table 3.3 also shows that, the fault current (I_f) is always greater than the current drawn from the supply (I_s) for all types of faults, except for the LL fault. This is due to the current contributions from the IBDGs to the fault current. For LL (a-b) fault, the source current is more than the fault current, as the voltage profile of faulty phase for LL fault is much better than the profile for other types of faults, as shown in Fig 3.3. Hence, the load currents are more in case of LL fault and therefore the current drawn from the source is higher as compared to the other fault cases. The voltage profiles for phase a, obtained by the proposed short-circuit analysis method and PSCAD/EMTDC simulation studies, for SLG and LL faults at bus-105 are shown in Fig 3.4. From this figure, it is observed that the voltage profiles obtained by these two methods are very close to each other which further validates the accuracy of the proposed method.

The above fault cases have also been simulated with voltage dependent loads. The polynomial load model (ZIP model) is used as voltage dependent load model, as given in eq. (3.1). It is assumed that the loads at bus 49 and 50 are 'residential ZIP load model', at bus 51 and 68 are 'commercial ZIP load model', and the load at bus 79 is 'industrial ZIP load model'. The fractional constants in eq. (3.1) for various load compositions are given in [147]. The rms values of I_f and I_s for various fault cases using the proposed method and PSCAD/EMTDC simulation are shown in Fig 3.5. A good agreement between the two results again establishes the accuracy of the proposed method.

Table 3.4 gives the comparison between the performance of Gauss-seidel (GS) [59] and the pro-

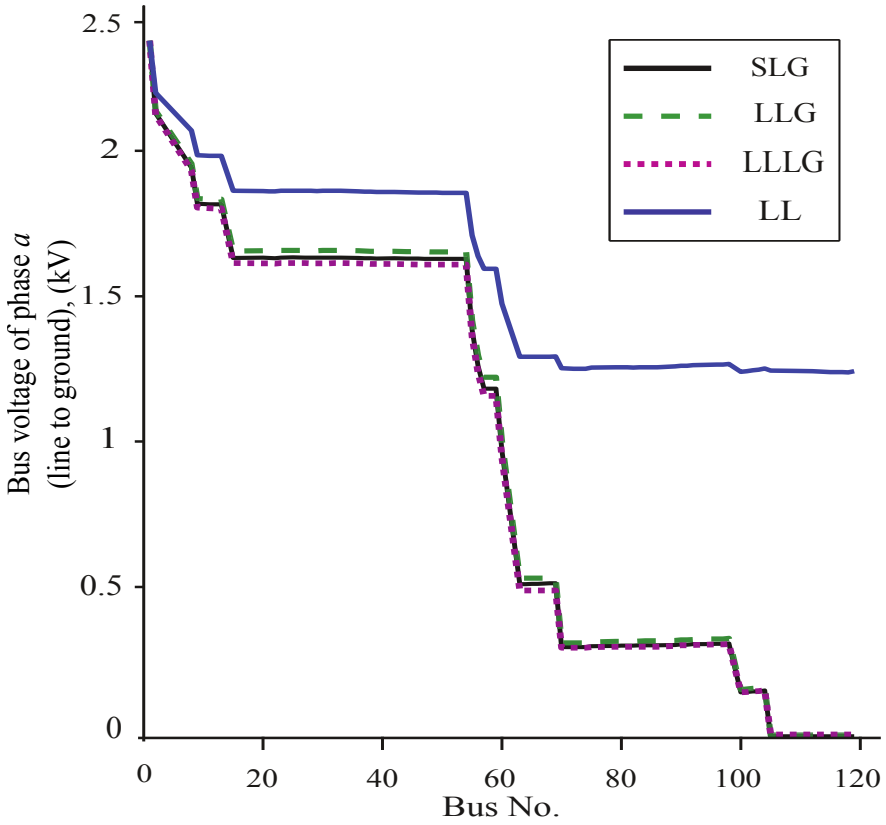

Figure 3.3: Voltage profile for different unsymmetrical short-circuit faults in scenario 1

Table 3.4: Comparison between Gauss-Seidel and Proposed method

Method	**SLG (a-g) Fault analysis**			
	I_f **(Amp)**	I_s **(Amp)**	**Iteration**	**Execution time (sec)**
Gauss-Siedel [59]	2860.58	2809.51	4769	37671.859
Proposed	2860.57	2809.39	6	1.253

posed Newton-Raphson (NR) method for analyzing an SLG-fault (a-g fault, with $\bar{z}_f$ = 0.001+0.000i p.u.) at bus 105, with the tolerance limit of 1.0×10^{-8}. From Table 3.4, it can be observed that the number of iterations and execution time taken by the GS method are much higher than those of proposed NR method. It is to be noted that in this study, the effect of terminal voltages on the IBDG control scheme has not been considered as the primary focus here is to compare the convergence rate of GS and NR methods.

Scenario 2: In all the above case studies, the voltage dependency of the IBDG control schemes

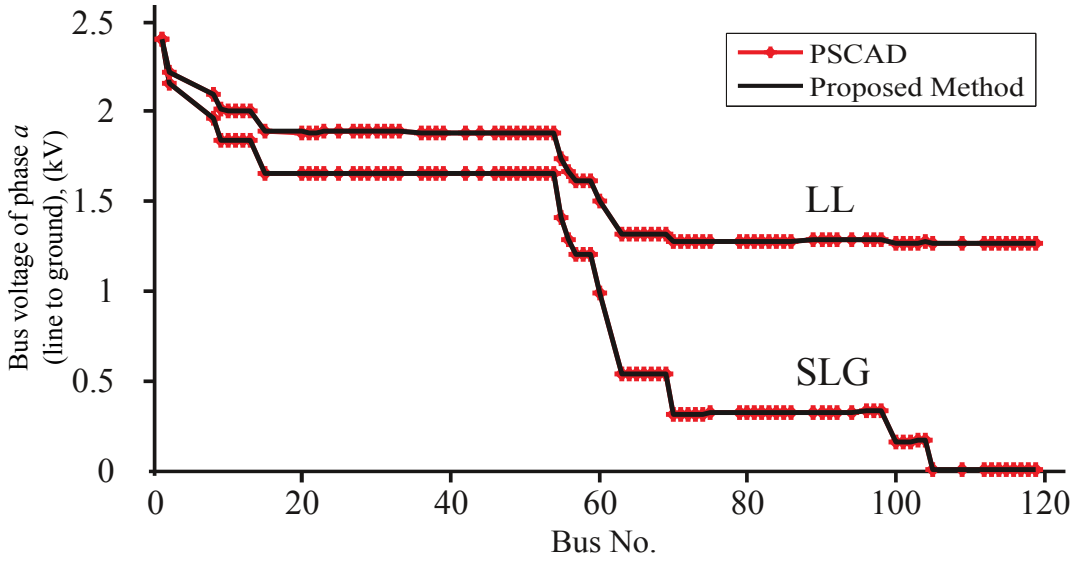

Figure 3.4: Voltage profile for SLG and LL faults using proposed method (scenario 1) and PSCAD/EMTDC simulation

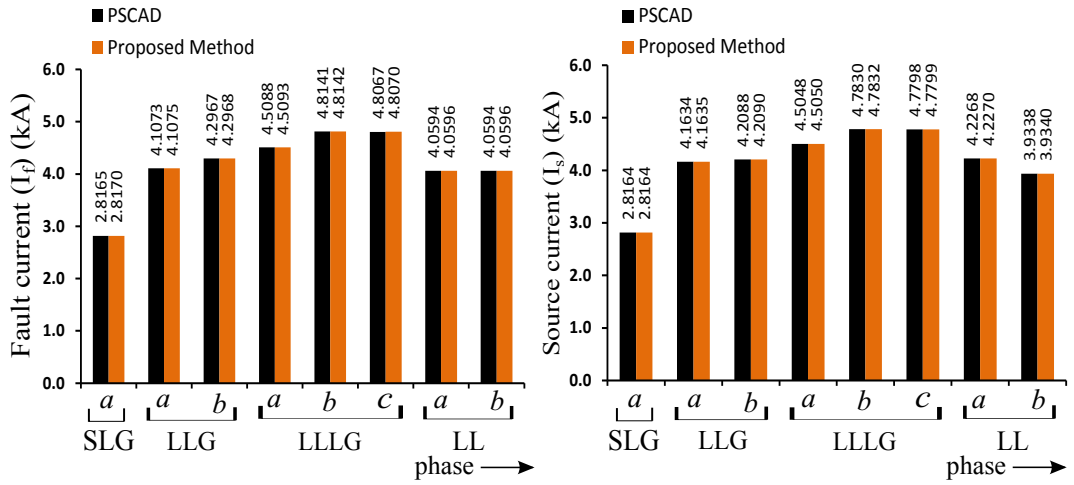

Figure 3.5: (a) Fault current (I_f) (b) Source current (I_s) for different fault cases in modified IEEE 123 bus radial distribution system with IBDGs and with voltage dependent loads using proposed method (scenario 1) and PSCAD/EMTDC simulation

has been neglected. For this scenario, it is now assumed that the control of IBDG is dependent on the terminal voltages (i.e. the algorithm (given in Subsection 3.2.2.1) follows all the 11 steps). An SLG fault in phase a of bus 105, with a fault impedance $\bar{z}_f$ = 0.001+0.000i p.u. has been

Table 3.5: Intermediate and final post-fault inverter bus voltages and injected power by IBDGs for SLG(a-g) fault at bus 105, with $\bar{z}_f$ = 0.001+0.000i p.u., in scenario 2

IBDG Location	**Intermediate post-fault inverter bus voltage magnitude (p.u.)**			**Intermediate post-fault injected power**	**Final post-fault inverter bus voltage magnitude (p.u.)**			**Control mode of operation**	**Final post-fault injected power**
(bus No.)	**Phase-a**	**Phase-b**	**Phase-c**	**by IBDG (kVA)**	**Phase-a**	**Phase-b**	**Phase-c**	**of IBDG**	**by IBDG (kVA)**
20	0.69181	1.08503	1.06071	0.0 + *j* 594.2	0.69148	1.07990	1.05196	Boost	0.0 + *j* 591.2
25	0.69161	1.08503	1.05995	0.0 + *j* 445.5	0.69128	1.07989	1.05121	Boost	0.0 + *j* 443.3
75	0.13561	1.22783	1.19232	0.0 + *j* 535.2	-			Cut-off	0.0 + *j* 0.0
98	0.14005	1.22949	1.19802	0.0 + *j* 672.1	-			Cut-off	0.0 + *j* 0.0
104	0.07195	1.24791	1.21157	0.0 + *j* 530.1	-			Cut-off	0.0 + *j* 0.0

assumed. The intermediate inverter bus voltage magnitude (obtained after Step 6 of the algorithm) for all IBDGs under the fault condition are shown in columns 2-4 of Table 3.5. The intermediate power injected by the IBDGs (again obtained after Step 6 of the algorithm) are shown in column 5 of Table 3.5. Following steps 8-10 of the algorithm, IBDGs at bus no. 20 and 25 are operated in "boost mode", while the remaining three IBDGs have been disconnected from the system. The final terminal voltages of the IBDGs and the reactive power exchanged by the IBDGs under the fault condition are shown in columns 6-8 and column 10 of Table 3.5, respectively. The final inverter bus voltages under the fault condition, corresponding to the IBDGs located at bus No. 75, 98 and 104, are not shown in columns 6-8 of Table 3.5, since, under fault condition, these IBDGs have been disconnected from the system.

Different fault cases at bus 105 with the fault impedance of $\bar{z}_f$ = 0.001+0.000i p.u., have also been simulated using the proposed method considering voltage dependency of IBDG control scheme (i.e. the algorithm follows all 11 steps). The values of I_f and I_s for various fault cases using the proposed method and PSCAD/EMTDC simulations are shown in Table 3.6. It can be observed from the table that the results obtained by proposed method match very well with the results obtained by the PSCAD/EMTDC simulation studies. Also, the control mode operation of the IBDGs for various fault cases are shown in column 5 of Table 3.6.

To further investigate the performance of the proposed method, another SLG fault at phase a of bus 27 has been considered with a fault impedance of $\bar{z}_f$ = 0.5+0.0 i p.u. The intermediate inverter bus voltages and reactive power supplied by IBDGs (obtained after Step 6) are shown in columns

Table 3.6: Results for different unsymmetrical short-circuit faults at bus 105, with $\bar{z}_f$ = 0.001+0.000i p.u., using proposed technique (scenario 2) and PSCAD/EMTDC simulation

Fault type	**phase**	**Fault current at faulty point (I_f)**		**Control mode operation of IBDG**	**Current drawn from the supply (I_s)**	
		PSCAD simulation (kA)	**Proposed technique (kA)**		**PSCAD simulation (kA)**	**Proposed technique (kA)**
SLG (a-g)	a	2.82626	2.82636	Boost-: IBDG No. 1,2 Cut-off-: IBDG No. 3,4,5	2.85887	2.85897
LLG (ab-g)	a	4.10159	4.10173	Boost-: IBDG No. 1,2	4.15671	4.15687
	b	4.24456	4.24472	Cut-off-: IBDG No. 3,4,5	4.23236	4.23252
LLLG (abc-g)	a	4.47645	4.47662	Boost-: IBDG No. 1,2	4.50819	4.50835
	b	4.77868	4.77886	Cut-off-: IBDG No. 3,4,5	4.78431	4.78448
	c	4.76778	4.76795		4.78114	4.78132
L-L (a-b)	a	4.06311	4.06325	Boost-: All IBDGs	4.20943	4.20958
	b	4.06311	4.06325		3.95193	3.95208

2-5 of Table 3.7. On following steps 8-10 of the proposed algorithm, it is observed that none of the IBDGs gets disconnected and all of them operate in different control modes, as depicted in column 9 of this table. The final inverter bus voltages and the complex power injection of the IBDGs are shown in columns 6-8 and column 10 of Table 3.7, respectively.

Other types of faults (SLG, LLG, LLLG and LL) at bus 27, with $\bar{z}_f$ = 0.5+0.0 i p.u. have also been considered for the validation of proposed method with voltage dependency of the IBDG control scheme (follow all 11 steps of the algorithm). The values of I_f and I_s for various fault cases obtained from the proposed method and PSCAD/EMTDC simulations are given in Table 3.8. The results show the accuracy of proposed method. The control mode operation of IBDGs in various fault cases are also given in column 5 of Table 3.8.

3.3.2 Results of modified IEEE 123-bus unbalanced weakly meshed distribution system

The proposed technique has also been applied to a modified IEEE 123-bus unbalanced meshed distribution system to validate its performance further. Two loop branches have been added in the modified IEEE 123-bus radial distribution system to convert it into a weakly meshed network. Details of these loop branches are given in Table 3.9 (as given in Table 2.2 of Chapter 2). For this case also, two scenarios, as described in Subsection 3.3.1, have been considered.

Table 3.7: Intermediate and final post-fault inverter bus voltages and injected power by IBDGs for SLG(a-g) fault at bus 27, with $\bar{z}_f$ = 0.5+0.0i p.u., in scenario 2

IBDG Location (bus No.)	Intermediate post-fault inverter bus voltage magnitude (p.u.)			Intermediate post-fault injected power by IBDG (kVA)	Final post-fault inverter bus voltage magnitude (p.u.)			Control mode of operation of IBDG	Final post-fault injected power by IBDG (kVA)
	Phase-a	Phase-b	Phase-c		Phase-a	Phase-b	Phase-c		
20	0.87261	1.09702	0.97237	0.0 + *j* 616.1	0.86910	1.08685	0.96325	Boost	0.0 + *j* 611.3
25	0.84564	1.11967	0.96230	0.0 + *j* 459.8	0.83767	1.10417	0.94826	Absorb	0.0 - *j* 453.9
75	0.91893	1.06472	0.98882	0.0 + *j* 622.4	0.90758	1.04623	0.97192	Active-Power	420.0 + *j* 0.0
98	0.92196	1.06762	0.99364	0.0 + *j* 780.9	0.90728	1.04522	0.97375	Active-Power	525.0 + *j* 0.0
104	0.92139	1.06737	0.99081	0.0 + *j* 623.9	0.90861	1.04726	0.97247	Active-Power	420.0 + *j* 0.0

Table 3.8: Results for different unsymmetrical short-circuit faults at bus 27, with $\bar{z}_f$ = 0.5+0.0i p.u., using proposed technique (scenario 2) and PSCAD/EMTDC simulation

Fault type	phase	Fault current at faulty point (I_f)		Control mode operation of IBDG	Current drawn from the supply (I_s)	
		PSCAD simulation (kA)	Proposed technique (kA)		PSCAD simulation (kA)	Proposed technique (kA)
SLG (a-g)	a	1.14819	1.14821	Boost-: IBDG No. 1 Absorb-: IBDG No. 2 Active Power-: IBDG No. 3,4,5	1.27429	1.27431
LLG (ab-g)	a	1.09574	1.09576	Boost-: IBDG No. 1,2	1.21054	1.21057
	b	1.30304	1.30306	Active Power-: IBDG No. 3,4,5	1.36701	1.36684
LLLG (abc-g)	a	1.22991	1.22993	Active Power-: All IBDGs	1.32318	1.32321
	b	1.25960	1.25962		1.28658	1.28660
	c	1.22359	1.22361		1.28351	1.28354
L-L (a-b)	a	1.91324	1.91328	Boost-: IBDG No. 1,2	2.01891	2.01895
	b	1.91324	1.91328	Active Power-: IBDG No. 3,4,5	1.95163	1.95167

Scenario 1: An SLG fault in phase a of bus 105, with a fault impedance $\bar{z}_f$ = 0.001+0.000i p.u., has been simulated in this weakly meshed distribution network. In this case, the effect of the terminal voltages on the IBDG control scheme has been neglected. The values of inverter currents $\left(\bar{\mathbf{I}}^{\mathbf{abc}}_{\mathbf{inv,f,est}}\right)$ for all IBDGs, with $\bar{\mathbf{V}}^{\mathbf{abc}}_{\mathbf{inv,f}} = \bar{\mathbf{V}}^{\mathbf{abc}}_{\mathbf{inv,st}}$, are given in Table 3.10. As can be seen from this table, the magnitude of inverter current of all IBDGs are greater than their respective short-circuit current capacities. Therefore, magnitudes of currents of all IBDGs for all phases are maintained at their short-circuit current capacities, i.e. $|\bar{I}^p_{inv,f}| = I^{inv}_{sc}$, $p = a, b, c$ and $\Psi^p_{inv,f} = \frac{\pi}{2} + \theta^p_{dg,f}$,

Table 3.9: List of loop branches in IEEE 123 bus (modified) meshed distribution system

From Bus	To Bus	Length (ft.)	type	Line impedance configuration
33	54	675	3-ϕ	1
37	69	700	3-ϕ	2

Table 3.10: Results for SLG(a-g) fault in modified IEEE 123 bus meshed distribution system with IBDGs for scenario 1

DG No.	Initial estimate of inverter current, $\bar{\mathbf{I}}^{\mathbf{p}}_{\mathbf{inv,f,est}}$, (Amp) when $\bar{\mathbf{V}}^{\mathbf{abc}}_{\mathbf{inv,f}} = \bar{\mathbf{V}}^{\mathbf{abc}}_{\mathbf{inv,st}}$			final value of inverter current, (Amp) $\bar{\mathbf{I}}^{\mathbf{abc}}_{\mathbf{inv,f}} = I^{inv}_{sc}\angle(\frac{\pi}{2} + \theta^{\mathbf{abc}}_{\mathbf{dg,f}})$,($\bar{\mathbf{I}}^{\mathbf{p}}_{\mathbf{inv,f}}$)			final value of injected DG power (capacitive reactive power) (kVAR)		
	Phase-a	**Phase-b**	**Phase-c**	**Phase-a**	**Phase-b**	**Phase-c**	**Phase-a**	**Phase-b**	**Phase-c**
1	1059.297∠-61.35^o	20.004∠-37.62^o	39.650∠84.11^o	29.062∠85.29^o	29.062∠-38.30^o	29.062∠217.14^o	118.319	237.120	225.328
2	770.959∠-54.52^o	72.738∠109.67^o	126.082∠110.66^o	21.796∠85.10^o	21.796∠-38.36^o	21.796∠217.17^o	88.129	177.951	168.937
3	4367.750∠-80.14^o	532.475∠-70.09^o	525.664∠-70.78^o	29.062∠90.81^o	29.062∠-44.70^o	29.062∠222.07^o	33.081	255.829	248.381
4	1357.327∠-63.98^o	126.706∠99.34^o	256.673∠110.70^o	36.327∠90.89^o	36.327∠-44.98^o	36.327∠221.88^o	42.546	320.200	311.984
5	2784.754∠-72.24^o	52.202∠-10.26^o	53.185∠49.30^o	29.062∠88.60^o	29.062∠-45.62^o	29.062∠223.19^o	17.454	260.773	252.748

Table 3.11: Error analysis of proposed technique (scenario 1) with respect to PSCAD/EMTDC simulations for different unsymmetrical short-circuit faults at bus 105 in modified IEEE 123 bus meshed distribution system

Fault type	phase	Fault current at faulty point (I_f)		% Error in I_f	Current drawn from the supply (I_s)		% Error in I_s
		PSCAD simulation (kA)	Proposed technique (kA)		PSCAD simulation (kA)	Proposed technique (kA)	
SLG (a-g)	a	3.34325	3.34321	0.00117	3.29116	3.29109	0.00207
LLG (ab-g)	a	4.85853	4.85863	0.00197	4.84181	4.84187	0.00141
	b	5.04491	5.04518	**0.00529**	4.94486	4.94509	0.00474
LLLG (abc-g)	a	5.30347	5.30368	0.00400	5.25076	5.25095	0.00356
	b	5.66491	5.66514	0.00404	5.59847	5.59866	0.00341
	c	5.56995	5.57020	0.00463	5.50492	5.50510	0.00335
L-L (a-b)	a	4.76031	4.76051	0.00418	4.90908	4.90921	0.00254
	b	4.76031	4.76051	0.00418	4.64714	4.64737	**0.00496**

$p = a, b, c$, during short-circuit calculations. The inverter current and DG injected power of all IBDGs under the fault condition are given in Table 3.10.

Different fault cases, as discussed in Subsection 3.3.1, have also been simulated on the modified

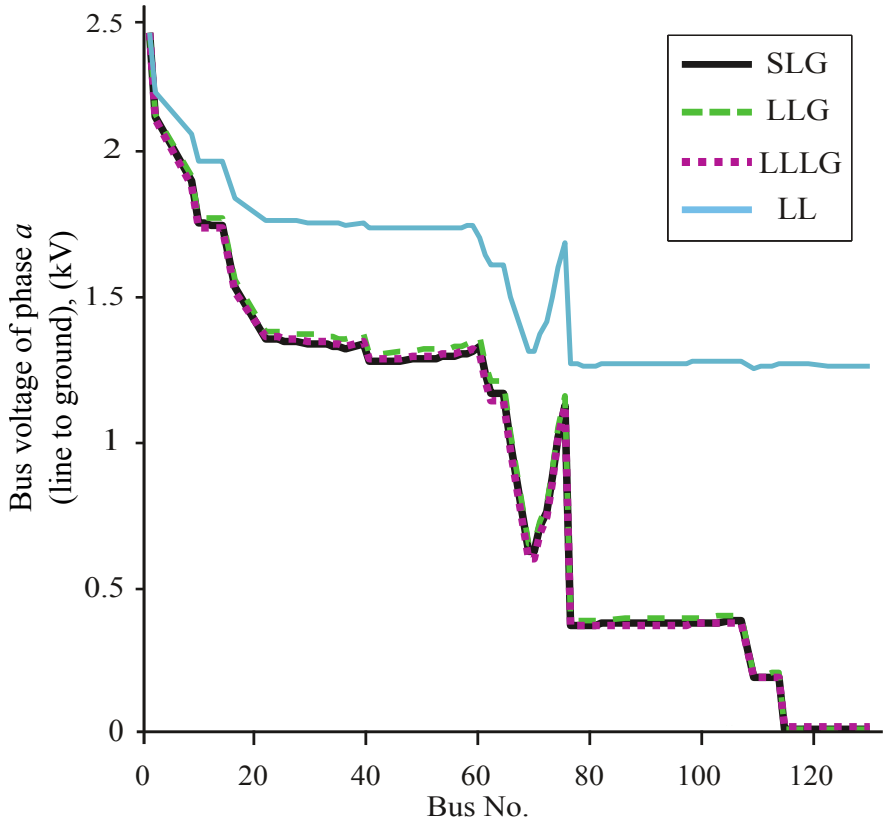

Figure 3.6: Voltage profile of phase a for modified IEEE 123-bus meshed distribution system for different unsymmetrical short-circuit faults in scenario 1

weakly meshed distribution network. Detailed results of theses cases obtained by the proposed technique and PSCAD/EMTDC simulation study are given in Table 3.11. The maximum % error obtained in calculated values of I_f and I_s are 0.00529% and 0.00496%, respectively, as shown in Table 3.11 in boldface. Except for the LL fault, the fault current at the fault point in all other fault cases are higher than the current drawn from the source due to the contribution of IBDGs to the fault current, as shown in Table 3.11. On the other hand, for LL fault, the voltage profile of faulty phase of the meshed distribution system is much better than the profile for the other fault cases, as shown in Fig 3.6. As a result, the load currents and hence the source current are larger, in case of LL fault, as compared to other fault cases. Fig 3.7 shows the voltage profile of phase a of the network for SLG(a-g) and LL(a-b) faults at bus 105 obtained by the proposed method and PSCAD/EMTDC simulation study.

To further validate the accuracy of the proposed method, various fault cases have also been simulated with voltage dependent loads. The results of I_f and I_s for these fault cases using the

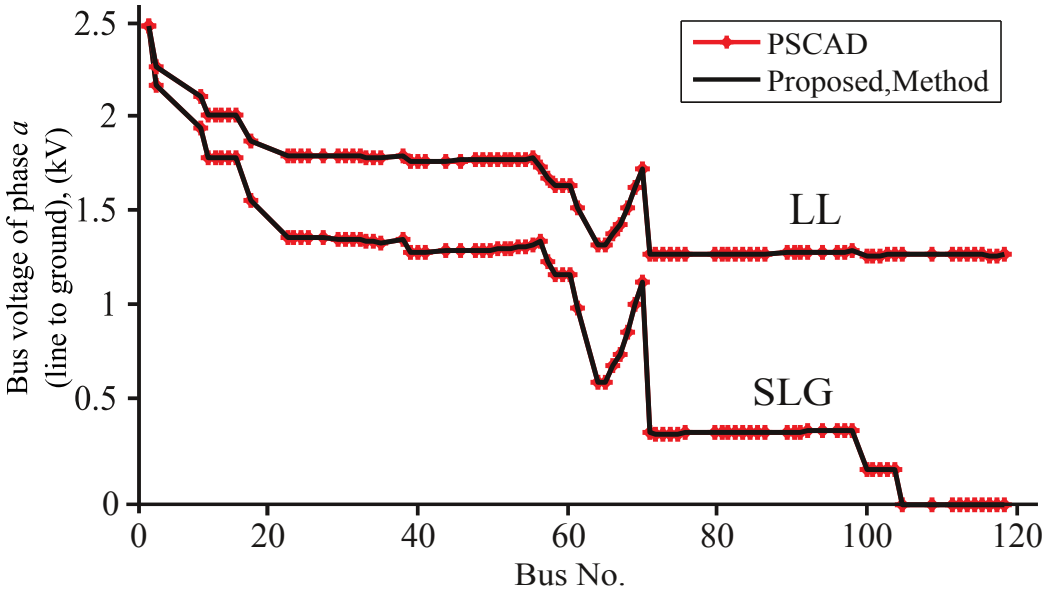

Figure 3.7: Voltage profile of phase a for modified IEEE 123 bus meshed distribution system for SLG and LL fault using proposed technique (scenario 1) and PSCAD/EMTDC simulation

proposed method and PSCAD/EMTDC simulation are given in Fig 3.8, which shows that the values of I_f and I_s for different faults calculated by the proposed method are very close to the values obtained by the PSCAD/EMTDC software.

Scenario 2: An SLG fault, with a fault impedance of $\bar{z}_f$ = 0.5+0.0 i p.u., at phase a of bus 27 has been assumed for the analysis of meshed distribution system as a representative case. The intermediate inverter bus voltages and reactive power supplied by IBDGs (obtained after Step 6) are shown in columns 2-5 of Table 3.12. Following steps 8-10 of the proposed algorithm, it is observed that none of the IBDGs gets disconnected and all of them operate in different control modes, as shown in column 9 of this table. The final inverter bus voltages and the complex power injections of the IBDGs are shown in columns 6-8 and column 10 of Table 3.12, respectively. Other types of short-circuit faults at bus 27, with $\bar{z}_f$ = 0.5+0.0 i p.u. have also been considered in this scenario and their results are shown in Table 3.13. Table 3.13 shows the values of I_f and I_s for various fault cases obtained from the proposed method (following all the 11 steps of the algorithm) and PSCAD/EMTDC simulations. The obtained results reaffirm the accuracy of proposed method. The control mode operation of IBDGs in various fault cases are also given in column 5 of Table 3.13.

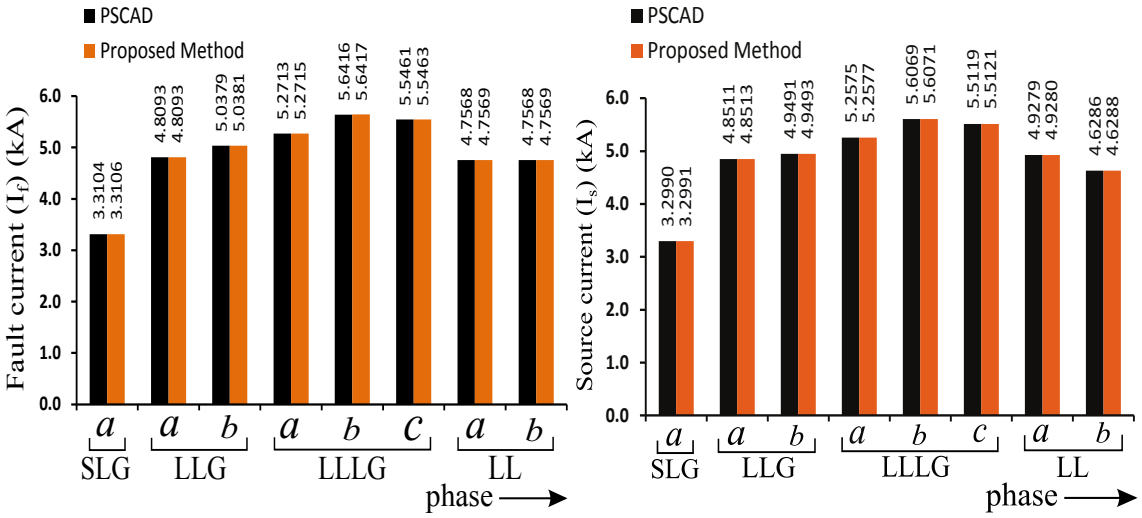

(a) (b)

Figure 3.8: (a) Fault current (I_f) (b) Source current (I_s) for different fault cases in modified IEEE 123 bus meshed distribution system with IBDGs and with voltage dependent loads using proposed method (scenario 1) and PSCAD/EMTDC simulation

Table 3.12: Intermediate and final post fault inverter bus voltages and injected power by IBDGs for SLG(a-g) fault at bus 27, with $\bar{z}_f$ = 0.5+0.0i p.u., in scenario 2 in modified IEEE 123-bus meshed distribution system

IBDG Location	**Intermediate post-fault inverter bus voltage magnitude (p.u.)**			**Intermediate post-fault injected power**	**Final post-fault inverter bus voltage magnitude (p.u.)**			**Control mode of operation**	**Final post-fault injected power**
(bus No.)	**Phase-a**	**Phase-b**	**Phase-c**	**by IBDG (kVA)**	**Phase-a**	**Phase-b**	**Phase-c**	**of IBDG**	**by IBDG (kVA)**
20	0.87901	1.09321	0.97496	0.0 + j 617.1	0.87519	1.08180	0.96503	Boost	0.0 + j 611.9
25	0.85633	1.11200	0.96599	0.0 + j 460.8	0.84806	1.09543	0.95124	Absorb	0.0 - j 454.6
75	0.91009	1.07760	0.97976	0.0 + j 621.4	0.90151	1.06050	0.96442	Active-Power	420.0 + j 0.0
98	0.91300	1.08058	0.98461	0.0 + j 779.5	0.90124	1.05942	0.96627	Active-Power	525.0 + j 0.0
104	0.91252	1.08033	0.98173	0.0 + j 622.9	0.90258	1.06153	0.96493	Active-Power	420.0 + j 0.0

3.3.3 Results of multiple fault analysis of modified IEEE 123-bus unbalanced distribution system

The proposed short-circuit analysis method is also applicable for the study of multiple faults in distribution systems. To illustrate this, two simultaneous faults– SLG (a-g) and LLG (bc-g) with a fault impedance of $\bar{z}_f$ = 0.001+0.000i p.u., have been considered in the modified IEEE-123 bus

Table 3.13: Results for different unsymmetrical short-circuit faults at bus 27, with $\bar{z}_f$ = 0.5+0.0i p.u., using proposed technique (scenario 2) and PSCAD/EMTDC simulation in modified IEEE 123-bus meshed distribution system

Fault type	**phase**	**Fault current at faulty point (I_f)**		**Control mode operation of IBDG**	**Current drawn from the supply (I_s)**	
		PSCAD simulation (kA)	**Proposed technique (kA)**		**PSCAD simulation (kA)**	**Proposed technique (kA)**
SLG (a-g)	a	1.16509	1.16514	Boost-: IBDG No. 1 Absorb-: IBDG No. 2 Active Power-: IBDG No. 3,4,5	1.28696	1.28686
LLG (ab-g)	a	1.11402	1.11406	Boost-: IBDG No. 1,2	1.22401	1.22391
	b	1.31017	1.31024	Active Power-: IBDG No. 3,4,5	1.37229	1.37217
LLLG (abc-g)	a	1.23525	1.23531	Active Power-: All IBDGs	1.32606	1.32592
	b	1.26726	1.26732		1.29159	1.29146
	c	1.23834	1.23844		1.29534	1.29521
L-L (a-b)	a	1.95338	1.95348	Boost-: All IBDGs	2.15022	2.15020
	b	1.95338	1.95348		1.98269	1.98261

Table 3.14: Error analysis of Proposed technique (scenario 1) with respect to PSCAD/EMTDC simulations for multiple faults in modified IEEE 123-bus distribution system

Topology	**Fault type**	**Fault Bus**	**phase**	**Fault current at fault point (I_f)**		**% Error in I_f**	**Current drawn from the supply (I_s)**		**% Error in I_s**
				PSCAD simulation (kA)	**Proposed technique (kA)**		**PSCAD simulation (kA)**	**Proposed technique (kA)**	
Radial	SLG (a-g)	42	a	4.56902	4.56873	**0.00638**	4.54249	4.54221	**0.00630**
	LLG (bc-g)	105	b	4.47217	4.47231	0.00630	4.45261	4.45275	0.00306
			c	4.55042	4.55058	0.00348	4.44856	4.44871	0.00346
Meshed	SLG (a-g)	42	a	5.62519	5.62492	**0.00480**	5.58930	5.58891	**0.00689**
	LLG (bc-g)	105	b	5.40171	5.40187	0.00285	5.38270	5.38281	0.00196
			c	5.24333	5.24355	0.00427	5.15016	5.15031	0.00303

radial as well as weakly meshed distribution system at bus 42 and bus 105 respectively and the obtained results are shown in Table 3.14. Again, in these cases, the voltage dependency of the IBDG control scheme has not been considered (scenario 1). The maximum % error in I_f and I_s, with respect to the values obtained by the PSCAD/EMTDC simulation study for this case (multiple fault) are 0.00638% and 0.00630% respectively for radial distribution system and 0.00480% and 0.00689% respectively, for meshed distribution system, as given in Table 3.14. Further, the above

Table 3.15: Error analysis of Proposed technique (scenario 2) with respect to PSCAD/EMTDC simulations for multiple faults in modified IEEE 123-bus distribution system

Topology	Fault type	Fault Bus	phase	Fault current at faulty point (I_f)		% Error in I_f	Current drawn from the supply (I_s)		% Error in I_s
				PSCAD simulation (kA)	Proposed technique (kA)		PSCAD simulation (kA)	Proposed technique (kA)	
Radial	SLG (a-g)	42	a	1.19156	1.19155	0.00083	1.33830	1.33831	0.00075
	LLG (bc-g)	105	b	1.09616	1.09618	**0.00182**	1.18194	1.18195	0.00085
			c	1.23046	1.23048	0.00163	1.35074	1.35076	**0.00148**
Meshed	SLG (a-g)	42	a	1.21777	1.21779	0.00164	1.36772	1.36767	0.00366
	LLG (bc-g)	105	b	1.15233	1.15236	**0.00260**	1.23818	1.23811	0.00565
			c	1.22933	1.22936	0.00244	1.34925	1.34912	**0.00963**

given multiple fault cases, with a fault impedance of $\bar{z}_f$ = 0.5+0.0i p.u., have also been simulated using the proposed method with voltage dependency of IBDG control scheme (scenario 2) and the results are shown in Table 3.15. In this control scheme, two IBDGs (located at bus 20 and 25) operate in "active-power mode", while the remaining three IBDGs (located at bus 75, 98 and 104) operate in "boost mode" in both radial and meshed distribution systems. The maximum % error in I_f and I_s, with respect to the values obtained by the PSCAD/EMTDC simulation study for this case are 0.00182% and 0.00260% respectively for radial distribution system and 0.00148% and 0.00963% respectively, for meshed distribution system, as shown in Table 3.15. These results also establish the accuracy of the proposed short-circuit analysis method for radial and weakly meshed distribution system in the presence of IBDGs.

3.3.4 General discussion of the results

From Tables 3.1, 3.2, 3.5, 3.7, 3.10 and 3.12, it is observed that the total three phase injected power supplied by i^{th} DG ($S_{DG_i}^{3phase}, i = 1, 2, \cdots, 5$) is more than its three phase power rating ($S_{DG_i}, i = 1, 2, \cdots, 5$) but less than $k \times S_{DG_i}$, where k is the factor at which the fault current from the inverter is limited, e.g. $k = 1.5$ in this work. Also, according to amended IEEE Standard 1547, the maximum fault clearing time in a distribution system can be up to 21 sec. [148]. Accordingly, from the intermediate post fault and final post fault injected power values (shown in Tables 3.1, 3.2, 3.5, 3.7, 3.10 and 3.12), it can be concluded that the inverters need to have a short-time rating of at least k times the normal steady state rating for a period of at least 21 sec.

Before concluding this chapter, it is worthwhile to note the importance of including IBDGs in

Table 3.16: Maximum % deviation, with respect to 'no IBDG' case

Fault bus	IBDGs penetration level			
	20% of total load power		40% of total load power	
	Maximum % deviation in I_f	Maximum % deviation in I_s	Maximum % deviation in I_f	Maximum % deviation in I_s
20	0.56 (LLLG)	1.60 (SLG)	1.10 (LLLG)	3.19 (SLG)
44	1.03 (LLLG)	2.55 (SLG)	2.27 (LLLG)	5.06 (SLG)
54	1.14 (LLLG)	4.33 (SLG)	2.28 (LLLG)	8.56 (SLG)
98	1.41 (LLG)	4.97 (SLG)	2.80 (LLG)	9.87 (SLG)
118	1.51 (SLG)	5.30 (SLG)	2.98 (SLG)	10.28 (SLG)

the short-circuit calculation. It is already mentioned in the literature that the presence of IBDGs in the system may cause malfunctioning of protective devices due to the contribution of IBDGs to the fault current [37].

The maximum percentage deviation in I_f and I_s, with respect to the case of 'no IBDGs' in the system, for different fault cases with different penetration level of IBDGs in modified IEEE 123-bus unbalanced radial distribution system for scenario 1, are shown in Table 3.16. From the table, it is observed that, as the penetration level of IBDGs increase, the percentage deviation in I_f and I_s also increases. Thus, it becomes necessary to include IBDGs in short-circuit calculation to ensure proper co-ordination of protective equipments.

Apart from protective device co-ordination, the values of steady state fault currents on each bus of the distribution system network are also required for probabilistic fault analysis and for optimum placement of fault current limiters. For these studies, repeated simulations are required by changing the fault locations. In PSCAD/EMTDC software, it takes a significant amount of time for carrying out repeated time domain simulation studies by changing the fault locations. Further, the fault studies of the large distribution system can not be performed using PSCAD/EMTDC software due to the node limitations in this software. However, in the proposed approach, such studies can be performed much more quickly.

3.4 Conclusion

An efficient and accurate analytical short-circuit analysis method for radial and meshed distribution system with IBDG, has been introduced in this chapter. Based on the detailed studies carried out in this work, following conclusions can be drawn:

- The developed methodology is general enough to consider any type of load including ZIP loads and is also quite accurate. It is also capable of including voltage dependent control modes of IBDGs.

- With increasing penetration of IBDG, the deviation in the source current and fault current increases, which may require recoordination of the existing protective schemes.

In the next chapter, the algorithms for the load flow and short-circuit analysis of unbalanced radial as well as meshed distribution system with various three phase transformer models and Inverter based distribution generations (IBDGs) are discussed.

Chapter 4

Load flow and short-circuit analysis of unbalanced distribution system with three phase transformer models and inverter based Distributed Generations

Abstract

Chapter 4 proposes a load flow and short-circuit analysis method for unbalanced distribution system incorporating three-phase transformer models and inverter based distributed generation (IBDG). Initially the load flow method of an unbalanced distribution system is developed which incorporates the mathematical model of a three phase transformer of any vector group and different modes of operation of IBDG. The fault analysis method with transformer models and IBDGs is also developed subsequently in this chapter. The results obtained from the proposed method have been compared with the time domain simulation studies carried out using PSCAD/EMTDC software to verify the accuracy of the proposed method.

4.1 Introduction

TRANSFORMERS are generally used in the distribution system to step down the voltage of the distribution system to the customer utility voltage level [75]. They are also used for connecting the inverter based distributed generations (IBDGs) to the grid [73]. Hence, it becomes necessary to incorporate various three phase distribution transformer models in the load flow and short-circuit studies of distribution system. Different load flow analysis methods based on forward/backward sweep approach to incorporate three phase transformer models in the distribution network are available in the literature [75–79]. In this chapter, a direct method of load flow analysis of distribution system [70] has been extended to incorporate three phase transformer models and different modes of operation of IBDGs. The singularity problem (in transformer nodal admittance matrix) encountered in certain transformer configurations has also been addressed in this chapter.

Subsequently, a method for short-circuit analysis of distribution system, considering three phase transformer models and IBDGs, has also been developed in this chapter.

This chapter is organized as follows. Section 4.2 describes the formulation of the proposed load-flow analysis method for unbalanced radial as well as meshed distribution system incorporating three phase transformer models and IBDGs. Section 4.3 describes the formulation of the proposed short-circuit analysis method for unbalanced radial as well as meshed distribution system incorporating IBDGs. The main results of this chapter are presented in Section 4.4 and finally Section 4.5 highlights the main conclusions of this chapter.

4.2 Load flow analysis of an unbalanced distribution system with transformer model and IBDG

In the proposed work, three-phase transformer model has been incorporated in the direct approach for the distribution system load flow analysis [70]. The phase component based nodal admittance matrix model (p.u.) for different distribution transformer configurations have been considered. The nodal admittance matrix based three phase distribution transformer model (p.u.) is given as [78],

$$\begin{bmatrix} \mathbf{I_p} \\ \mathbf{I_s} \end{bmatrix} = \begin{bmatrix} \mathbf{Y_{pp}} & \mathbf{Y_{ps}} \\ \mathbf{Y_{sp}} & \mathbf{Y_{ss}} \end{bmatrix} . \begin{bmatrix} \mathbf{V_p} \\ \mathbf{V_s} \end{bmatrix} = \begin{bmatrix} \mathbf{Y_T} \end{bmatrix} \begin{bmatrix} \mathbf{V_p} \\ \mathbf{V_s} \end{bmatrix} \tag{4.1}$$

where $\mathbf{Y_{pp}}$, $\mathbf{Y_{ps}}$, $\mathbf{Y_{sp}}$ and $\mathbf{Y_{ss}}$ are the sub-matrices, of size (3×3) each, of the transformer nodal admittance matrix $\mathbf{Y_T}$. $\mathbf{V_p}$ and $\mathbf{V_s}$ are the three-phase line to neutral voltage vectors, whereas $\mathbf{I_p}$ and $\mathbf{I_s}$ are the three-phase injection current vectors at the primary and secondary sides of the transformer, respectively. The direct approach for distribution system load flow analysis, with different models of transformer configurations, for radial as well as meshed distribution systems are given in the following sub-sections.

4.2.1 Radial distribution system

Let us consider an unbalanced radial distribution system, as shown in Fig 4.1. Let us assume that, two step down transformers T_1 and T_2, are connected between buses *i* and *j*, and buses *k* and *l* of the distribution network of Fig. 4.1, respectively.

The nodal equations for the transformers are given as

$$\begin{bmatrix} \mathbf{I^{abc}_{T_1,p}} \\ \mathbf{I^{abc}_{T_1,s}} \end{bmatrix} = \begin{bmatrix} \mathbf{Y_{T_1}} \end{bmatrix} . \begin{bmatrix} \mathbf{V^{abc}_i} \\ \mathbf{V^{abc}_j} \end{bmatrix} = \begin{bmatrix} \mathbf{Y^{abc}_{pp,T_1}} & \mathbf{Y^{abc}_{ps,T_1}} \\ \mathbf{Y^{abc}_{sp,T_1}} & \mathbf{Y^{abc}_{ss,T_1}} \end{bmatrix} . \begin{bmatrix} \mathbf{V^{abc}_i} \\ \mathbf{V^{abc}_j} \end{bmatrix} \tag{4.2}$$

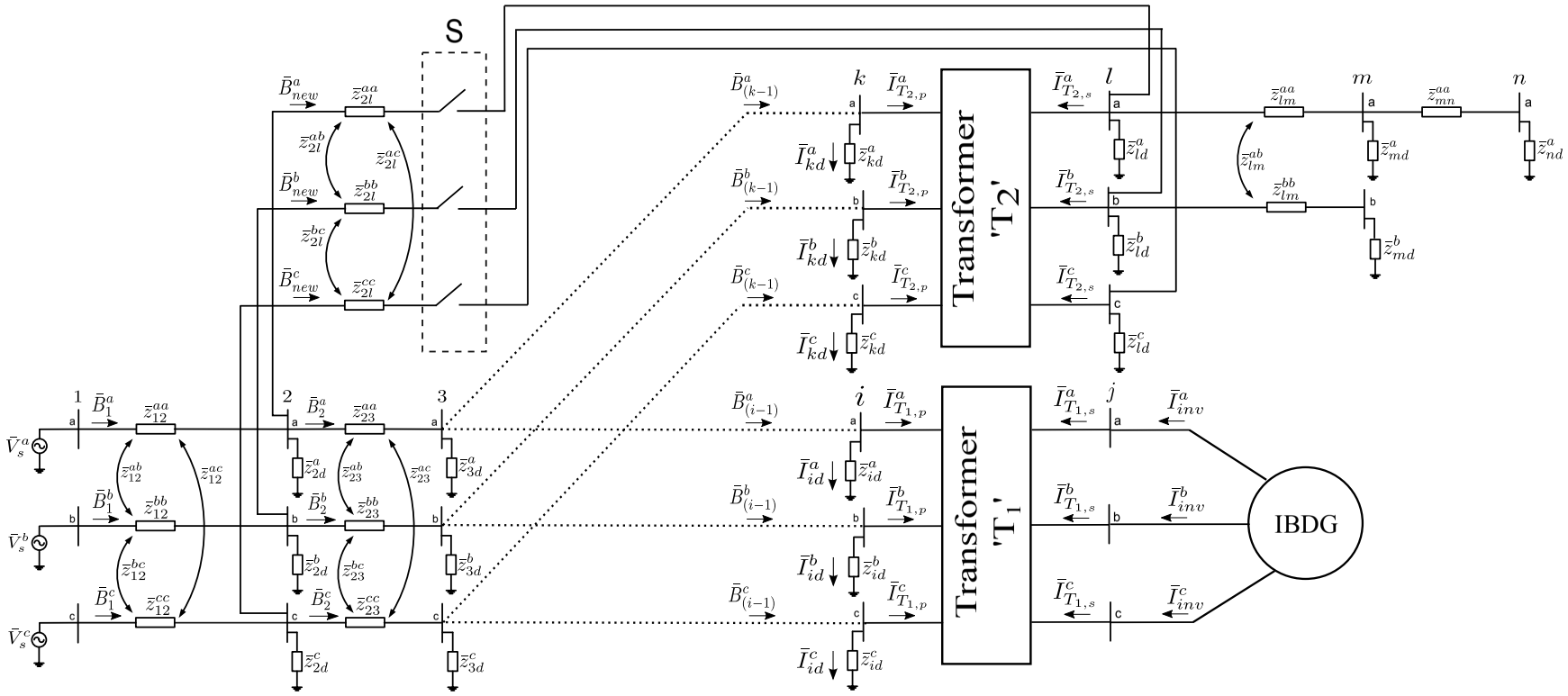

Figure 4.1: An unbalanced distribution system with transformers and IBDG

$$\begin{bmatrix} \mathbf{I}^{\mathbf{abc}}_{\mathbf{T_2,p}} \\ \mathbf{I}^{\mathbf{abc}}_{\mathbf{T_2,s}} \end{bmatrix} = \begin{bmatrix} \mathbf{Y}_{\mathbf{T_2}} \end{bmatrix} . \begin{bmatrix} \mathbf{V}^{\mathbf{abc}}_{\mathbf{k}} \\ \mathbf{V}^{\mathbf{abc}}_{\mathbf{l}} \end{bmatrix} = \begin{bmatrix} \mathbf{Y}^{\mathbf{abc}}_{\mathbf{pp,T_2}} & \mathbf{Y}^{\mathbf{abc}}_{\mathbf{ps,T_2}} \\ \mathbf{Y}^{\mathbf{abc}}_{\mathbf{sp,T_2}} & \mathbf{Y}^{\mathbf{abc}}_{\mathbf{ss,T_2}} \end{bmatrix} . \begin{bmatrix} \mathbf{V}^{\mathbf{abc}}_{\mathbf{k}} \\ \mathbf{V}^{\mathbf{abc}}_{\mathbf{l}} \end{bmatrix} \tag{4.3}$$

where, $\mathbf{I}^{\mathbf{abc}}_{\mathbf{T_1,p}}$ and $\mathbf{I}^{\mathbf{abc}}_{\mathbf{T_1,s}}$ are the three phase line current vectors on primary and secondary side of transformer T_1, respectively, whereas $\mathbf{I}^{\mathbf{abc}}_{\mathbf{T_2,p}}$ and $\mathbf{I}^{\mathbf{abc}}_{\mathbf{T_2,s}}$ are the three phase line current vectors on primary and secondary side of transformer T_2, respectively. $\mathbf{Y}_{\mathbf{T_1}}$ and $\mathbf{Y}_{\mathbf{T_2}}$ are the admittance matrices (corresponding to the type of the transformer connection) of size (6×6) of the transformers T_1 and T_2, respectively. $\mathbf{Y}^{\mathbf{abc}}_{\mathbf{pp,T_1}}$, $\mathbf{Y}^{\mathbf{abc}}_{\mathbf{ps,T_1}}$, $\mathbf{Y}^{\mathbf{abc}}_{\mathbf{sp,T_1}}$ and $\mathbf{Y}^{\mathbf{abc}}_{\mathbf{ss,T_1}}$ are the sub-matrices of size (3×3) of the admittance matrix $\mathbf{Y}_{\mathbf{T_1}}$ of transformer T_1. Similarly, $\mathbf{Y}^{\mathbf{abc}}_{\mathbf{pp,T_2}}$, $\mathbf{Y}^{\mathbf{abc}}_{\mathbf{ps,T_2}}$, $\mathbf{Y}^{\mathbf{abc}}_{\mathbf{sp,T_2}}$ and $\mathbf{Y}^{\mathbf{abc}}_{\mathbf{ss,T_2}}$ are the sub-matrices of size (3×3) of the admittance matrix $\mathbf{Y}_{\mathbf{T_2}}$ of transformer T_2. $\mathbf{V}^{\mathbf{abc}}_{\mathbf{i}}$, $\mathbf{V}^{\mathbf{abc}}_{\mathbf{j}}$, $\mathbf{V}^{\mathbf{abc}}_{\mathbf{k}}$ and $\mathbf{V}^{\mathbf{abc}}_{\mathbf{l}}$ are the three-phase voltage vectors of the buses i, j, k and l, respectively.

Now, the branch current vectors $\mathbf{B}^{\mathbf{abc}}_{\mathbf{1}}$, $\mathbf{B}^{\mathbf{abc}}_{\mathbf{2}}$, $\mathbf{B}^{\mathbf{abc}}_{\mathbf{i-1}}$ and $\mathbf{B}^{\mathbf{abc}}_{\mathbf{k-1}}$ of the system shown in Fig. 4.1 can be expressed in terms of equivalent bus injection current vectors as,

$$\begin{aligned} \mathbf{B}^{\mathbf{abc}}_{\mathbf{1}} &= \mathbf{I}^{\mathbf{abc}}_{\mathbf{2d}} + \mathbf{I}^{\mathbf{abc}}_{\mathbf{3d}} + \cdots + \mathbf{I}^{\mathbf{abc}}_{\mathbf{id}} + \mathbf{I}^{\mathbf{abc}}_{\mathbf{T_1,p}} + \cdots + \mathbf{I}^{\mathbf{abc}}_{\mathbf{kd}} + \mathbf{I}^{\mathbf{abc}}_{\mathbf{T_2,p}} \\ \mathbf{B}^{\mathbf{abc}}_{\mathbf{2}} &= \mathbf{I}^{\mathbf{abc}}_{\mathbf{3d}} + \cdots + \mathbf{I}^{\mathbf{abc}}_{\mathbf{id}} + \mathbf{I}^{\mathbf{abc}}_{\mathbf{T_1,p}} + \cdots + \mathbf{I}^{\mathbf{abc}}_{\mathbf{kd}} + \mathbf{I}^{\mathbf{abc}}_{\mathbf{T_2,p}} \\ \mathbf{B}^{\mathbf{abc}}_{\mathbf{i-1}} &= \mathbf{I}^{\mathbf{abc}}_{\mathbf{id}} + \mathbf{I}^{\mathbf{abc}}_{\mathbf{T_1,p}} \\ \mathbf{B}^{\mathbf{abc}}_{\mathbf{k-1}} &= \mathbf{I}^{\mathbf{abc}}_{\mathbf{kd}} + \mathbf{I}^{\mathbf{abc}}_{\mathbf{T_2,p}} \end{aligned} \tag{4.4}$$

where $\mathbf{I}^{\mathbf{abc}}_{\mathbf{2d}}$, $\mathbf{I}^{\mathbf{abc}}_{\mathbf{3d}}$, $\mathbf{I}^{\mathbf{abc}}_{\mathbf{id}}$ and $\mathbf{I}^{\mathbf{abc}}_{\mathbf{kd}}$ are the three phase equivalent bus injection current vectors at buses 2, 3, i and k, respectively. The equivalent bus injection current at any phase q ($q = a$ or b or c) of i^{th} bus $\left(\bar{I}^q_{id}\right)$ is calculated as [70],

$$\bar{I}^q_{id} = \left(\frac{\bar{S}^q_{id}}{\bar{V}^q_i}\right)^* = \left(\frac{\bar{P}^q_{id} + j\bar{Q}^q_{id}}{\bar{V}^q_i}\right)^* \tag{4.5}$$

where, $\bar{S}^q_{id}$ is the complex load power at phase q of i^{th} bus, $\bar{P}^q_{id}$ and $\bar{Q}^q_{id}$ are the active and reactive load power at phase q of i^{th} bus, respectively, $\bar{V}^q_i$ is the voltage at phase q of i^{th} bus and symbol $(^*)$ stands for complex conjugate operator.

Similarly, the currents in the secondary side of transformers T_1 and T_2 ($\mathbf{I}^{\mathbf{abc}}_{\mathbf{T_1,s}}$ and $\mathbf{I}^{\mathbf{abc}}_{\mathbf{T_2,s}}$), can be

expressed in terms of equivalent bus injection current vectors as,

$$\mathbf{I^{abc}_{T_{1},s}} = -\mathbf{I^{abc}_{jd}};\ \ where\ \mathbf{I^{abc}_{jd}} = -\mathbf{I^{abc}_{inv}} \tag{4.6a}$$

$$\mathbf{I^{abc}_{T_{2},s}} = \begin{bmatrix} \bar{I}^{a}_{T_2,s} \\ \bar{I}^{b}_{T_2,s} \\ \bar{I}^{c}_{T_2,s} \end{bmatrix} = - \begin{bmatrix} \bar{I}^{a}_{ld} \\ \bar{I}^{b}_{ld} \\ \bar{I}^{c}_{ld} \end{bmatrix} - \begin{bmatrix} \bar{I}^{a}_{md} \\ \bar{I}^{b}_{md} \\ 0 \end{bmatrix} - \begin{bmatrix} \bar{I}^{a}_{nd} \\ 0 \\ 0 \end{bmatrix} \tag{4.6b}$$

where I^{q}_{jd}, I^{q}_{ld}, I^{q}_{md} and I^{q}_{nd} are the equivalent bus injection currents at phase q ($q = a$ or b or c) of buses *j* (inverter bus), *l*, *m* and *n*, respectively; $\mathbf{I^{abc}_{inv}}$ is the three phase inverter current vector injected by the IBDG. Therefore, the branch current vectors of the system, shown in Fig. 4.1, can be expressed in terms of equivalent bus injection current vectors in the matrix form as,

$$\Big[\mathbf{B}\Big] = \Big[\mathbf{BIBC_{Sm}}\Big]\Big[\mathbf{I_{L}}\Big] + \Big[\mathbf{TIBC_{T_m}}\Big]\Big[\mathbf{I_{T_p}}\Big] \tag{4.7}$$

where,

$$\Big[\mathbf{BIBC_{Sm}}\Big] = \begin{bmatrix} \mathbf{I_{3\times3}} & \mathbf{I_{3\times3}} & \cdots & \mathbf{I_{3\times3}} & \mathbf{0_{3\times3}} & \cdots & \mathbf{I_{3\times3}} & \mathbf{0_{3\times3}} & \mathbf{0_{3\times2}} & \mathbf{0_{3\times1}} \\ \mathbf{0_{3\times3}} & \mathbf{I_{3\times3}} & \cdots & \mathbf{I_{3\times3}} & \mathbf{0_{3\times3}} & \cdots & \mathbf{I_{3\times3}} & \mathbf{0_{3\times3}} & \mathbf{0_{3\times2}} & \mathbf{0_{3\times1}} \\ \vdots & \vdots & \ddots & \vdots & \vdots & \vdots & \vdots & \vdots & \vdots & \vdots \\ \mathbf{0_{3\times3}} & \mathbf{0_{3\times3}} & \cdots & \mathbf{I_{3\times3}} & \mathbf{0_{3\times3}} & \cdots & \mathbf{0_{3\times3}} & \mathbf{0_{3\times3}} & \mathbf{0_{3\times2}} & \mathbf{0_{3\times1}} \\ \mathbf{0_{3\times3}} & \mathbf{0_{3\times3}} & \cdots & \mathbf{0_{3\times3}} & \mathbf{-I_{3\times3}} & \cdots & \mathbf{0_{3\times3}} & \mathbf{0_{3\times3}} & \mathbf{0_{3\times2}} & \mathbf{0_{3\times1}} \\ \vdots & \vdots & \vdots & \vdots & \vdots & \ddots & \vdots & \vdots & \vdots & \vdots \\ \mathbf{0_{3\times3}} & \mathbf{0_{3\times3}} & \cdots & \mathbf{0_{3\times3}} & \mathbf{0_{3\times3}} & \cdots & \mathbf{I_{3\times3}} & \mathbf{0_{3\times3}} & \mathbf{0_{3\times2}} & \mathbf{0_{3\times1}} \\ \mathbf{0_{3\times3}} & \mathbf{0_{3\times3}} & \cdots & \mathbf{0_{3\times3}} & \mathbf{0_{3\times3}} & \cdots & \mathbf{0_{3\times3}} & \mathbf{-I_{3\times3}} & \mathbf{-I_{3\times2}} & \mathbf{-I_{3\times1}} \\ \mathbf{0_{2\times3}} & \mathbf{0_{2\times3}} & \cdots & \mathbf{0_{2\times3}} & \mathbf{0_{2\times3}} & \cdots & \mathbf{0_{2\times3}} & \mathbf{0_{2\times3}} & \mathbf{I_{2\times2}} & \mathbf{I_{2\times1}} \\ \mathbf{0_{1\times3}} & \mathbf{0_{1\times3}} & \cdots & \mathbf{0_{1\times3}} & \mathbf{0_{1\times3}} & \cdots & \mathbf{0_{1\times3}} & \mathbf{0_{1\times3}} & \mathbf{0_{1\times2}} & \mathbf{I_{1\times1}} \end{bmatrix}$$

$$\Big[\mathbf{TIBC_{T_m}}\Big] = \begin{bmatrix} \mathbf{I_{3\times3}} & \mathbf{I_{3\times3}} & \cdots & \mathbf{I_{3\times3}} & \mathbf{0_{3\times3}} & \cdots & \mathbf{0_{3\times3}} & \mathbf{0_{3\times3}} & \mathbf{0_{3\times2}} & \mathbf{0_{3\times1}} \\ \mathbf{I_{3\times3}} & \mathbf{I_{3\times3}} & \cdots & \mathbf{0_{3\times3}} & \mathbf{0_{3\times3}} & \cdots & \mathbf{I_{3\times3}} & \mathbf{0_{3\times3}} & \mathbf{0_{3\times2}} & \mathbf{0_{3\times1}} \end{bmatrix}^{T}$$

$$\Big[\mathbf{B}\Big] = \Big[\mathbf{B^{abc}_{1}}\ \ \mathbf{B^{abc}_{2}}\ \ \cdots\ \ \mathbf{B^{abc}_{i-1}}\ \ \mathbf{I^{abc}_{T_{1},s}}\ \ \cdots\ \ \mathbf{B^{abc}_{k-1}}\ \ \mathbf{I^{abc}_{T_{2},s}}\ \ \mathbf{B^{ab}_{l}}\ \ \mathbf{B^{a}_{m}}\Big]^{T}$$

$$\Big[\mathbf{I_{L}}\Big] = \Big[\mathbf{I^{abc}_{2d}}\ \ \mathbf{I^{abc}_{3d}}\ \ \cdots\ \ \mathbf{I^{abc}_{id}}\ \ \mathbf{I^{abc}_{jd}}\ \ \cdots\ \ \mathbf{I^{abc}_{kd}}\ \ \mathbf{I^{abc}_{ld}}\ \ \mathbf{I^{ab}_{md}}\ \ \mathbf{I^{a}_{nd}}\Big]^{T}$$

$$\Big[\mathbf{I_{T_p}}\Big] = \Big[\mathbf{I^{abc}_{T_{1},p}}\ \ \mathbf{I^{abc}_{T_{2},p}}\Big]^{T}$$

where, $\mathbf{I_{n_r\times n_c}}$ denotes $(n_r \times n_c)$ identity matrix and $\mathbf{0_{n_r\times n_c}}$ denotes $(n_r \times n_c)$ null matrix. Here, $n_r = 3$ for 3-ϕ k^{th} branch current vector ($\mathbf{B^{abc}_{k}}$), $n_r = 2$ for 2-ϕ k^{th} branch current vector ($\mathbf{B^{ab}_{k}}$

or $\mathbf{B_k^{bc}}$ or $\mathbf{B_k^{ac}}$), $n_r = 1$ for 1-ϕ k^{th} branch current vector ($\mathbf{B_k^a}$ or $\mathbf{B_k^b}$ or $\mathbf{B_k^c}$). The value of n_c will depend on the number of phases of the branch connected at the receiving end of k^{th} branch. $n_c = 3$, if a three-phase branch is connected, $n_c = 2$, if a two-phase branch is connected and $n_c = 1$, if a single-phase branch is connected. $\left[\mathbf{BIBC_{Sm}}\right]$ is the "Bus injection to Branch current system matrix" and $\left[\mathbf{TIBC_{Tm}}\right]$ is the "Transformer inclusion to Branch current matrix". $\left[\mathbf{I_L}\right]$ is the equivalent bus injection current vector. $\left[\mathbf{I_{T_p}}\right]$ is the primary side current vector of all the transformers present in the system. Further, $[\mathbf{I_{T_p}}]$ in eq. (4.7), can be expressed in terms of bus voltages using eqs. (4.2) and (4.3) as,

$$\left[\mathbf{I_{T_p}}\right] = \left[\mathbf{Y_{trans}}\right]\left[\mathbf{V_{bus}}\right] \tag{4.8}$$

where,

$$\left[\mathbf{Y_{trans}}\right] = \begin{bmatrix} \mathbf{0_{3\times3}} & \mathbf{0_{3\times3}} & \cdots & \mathbf{Y_{pp,T_1}^{abc}} & \mathbf{Y_{ps,T_1}^{abc}} & \cdots & \mathbf{0_{3\times3}} & \mathbf{0_{3\times3}} & \mathbf{0_{3\times2}} & \mathbf{0_{3\times1}} \\ \mathbf{0_{3\times3}} & \mathbf{0_{3\times3}} & \cdots & \mathbf{0_{3\times3}} & \mathbf{0_{3\times3}} & \cdots & \mathbf{Y_{pp,T_2}^{abc}} & \mathbf{Y_{ps,T_2}^{abc}} & \mathbf{0_{3\times2}} & \mathbf{0_{3\times1}} \end{bmatrix}$$

$$\left[\mathbf{V_{bus}}\right] = \begin{bmatrix} \mathbf{V_2^{abc}} & \mathbf{V_3^{abc}} & \cdots & \mathbf{V_i^{abc}} & \mathbf{V_j^{abc}} & \cdots & \mathbf{V_k^{abc}} & \mathbf{V_l^{abc}} & \mathbf{V_m^{ab}} & \mathbf{V_n^{a}} \end{bmatrix}^T$$

Therefore, eq. (4.7) can be rewritten using eq. (4.8) as,

$$\left[\mathbf{B}\right] = \left[\mathbf{BIBC_{Sm}}\right]\left[\mathbf{I_L}\right] + \left[\mathbf{TIBC'_{Tm}}\right]\left[\mathbf{V_{bus}}\right] \tag{4.9}$$

where,

$$\left[\mathbf{TIBC'_{Tm}}\right] = \left[\mathbf{TIBC_{Tm}}\right]\left[\mathbf{Y_{trans}}\right]$$

Further, it is assumed that the generalized unbalanced radial distribution system considered has u three-phase, v two-phase, w single-phase buses and nt number of transformers. This generalized system will be considered throughout this chapter. The sizes of $[\mathbf{BIBC_{Sm}}]$, $[\mathbf{TIBC_{Tm}}]$, $[\mathbf{Y_{trans}}]$ and $[\mathbf{TIBC'_{Tm}}]$ matrices for this system will be $(3u+2v+w-3)\times(3u+2v+w-3)$, $(3u+2v+w-3)\times(3nt)$, $(3nt)\times(3u+2v+w-3)$ and $(3u+2v+w-3)\times(3u+2v+w-3)$, respectively.

The voltages at 3^{rd}, i^{th} and k^{th} buses can be described in terms of branch currents as,

$$\mathbf{V_3^{abc}} = \mathbf{V_1^{abc}} - \mathbf{z_{12}^{abc}B_1^{abc}} - \mathbf{z_{23}^{abc}B_2^{abc}} \tag{4.10}$$

$$\mathbf{V_i^{abc}} = \mathbf{V_1^{abc}} - \mathbf{z_{12}^{abc}B_1^{abc}} - \mathbf{z_{23}^{abc}B_2^{abc}} - \cdots - \mathbf{z_{(i-1)i}^{abc}B_{i-1}^{abc}} \tag{4.11}$$

$$\mathbf{V_k^{abc}} = \mathbf{V_1^{abc}} - \mathbf{z_{12}^{abc}B_1^{abc}} - \mathbf{z_{23}^{abc}B_2^{abc}} - \cdots - \mathbf{z_{(k-1)k}^{abc}B_{k-1}^{abc}} \tag{4.12}$$

where,$\mathbf{V_1^{abc}}$ is the three-phase voltage vector of the sub-station bus and $\mathbf{z_{12}^{abc}}, \mathbf{z_{23}^{abc}}, \mathbf{z_{(i-1)i}^{abc}}$ and $\mathbf{z_{(k-1)k}^{abc}}$ are the line impedance matrices of the lines between buses 1 and 2, buses 2 and 3, buses $(i-1)$ and i, and buses $(k-1)$ and k, respectively.

Similarly, the voltages at buses j and l (where the secondary windings of the transformers T_1 and T_2 are connected) can be obtained from eqs. (4.2) and (4.3) as,

$$\mathbf{V_j^{abc}} = \mathbf{Y_{ss,T_1}^{abc}}^{-1}(\mathbf{I_{T_1,s}^{abc}} - \mathbf{Y_{sp,T_1}^{abc}}\mathbf{V_i^{abc}}) \tag{4.13a}$$

$$\mathbf{V_l^{abc}} = \mathbf{Y_{ss,T_2}^{abc}}^{-1}(\mathbf{I_{T_2,s}^{abc}} - \mathbf{Y_{sp,T_2}^{abc}}\mathbf{V_k^{abc}}) \tag{4.13b}$$

Therefore, the bus voltages of the system, shown in Fig. 4.1, can be expressed in terms of branch currents in the matrix form as,

$$\left[\mathbf{V_{bus}}\right] = \left[\mathbf{C}\right]\left[\mathbf{V_s}\right] + \left[\mathbf{BCBV_{T_m}}\right]\left[\mathbf{B}\right] \tag{4.14}$$

where,

$$\left[\mathbf{BCBV_{T_m}}\right] =$$

$$\begin{bmatrix}
-\mathbf{z_{12}^{abc}} & \mathbf{0_{3\times3}} & \cdots & \mathbf{0_{3\times3}} & \mathbf{0_{3\times3}} & \cdots & \mathbf{0_{3\times3}} & \mathbf{0_{3\times3}} & \mathbf{0_{3\times2}} & \mathbf{0_{3\times1}} \\
-\mathbf{z_{12}^{abc}} & -\mathbf{z_{23}^{abc}} & \cdots & \mathbf{0_{3\times3}} & \mathbf{0_{3\times3}} & \cdots & \mathbf{0_{3\times3}} & \mathbf{0_{3\times3}} & \mathbf{0_{3\times2}} & \mathbf{0_{3\times1}} \\
\vdots & \vdots & \ddots & \vdots & \vdots & \vdots & \vdots & \vdots & \vdots & \vdots \\
-\mathbf{z_{12}^{abc}} & -\mathbf{z_{23}^{abc}} & \cdots & -\mathbf{z_{(i-1)i}^{abc}} & \mathbf{0_{3\times3}} & \cdots & \mathbf{0_{3\times3}} & \mathbf{0_{3\times3}} & \mathbf{0_{3\times2}} & \mathbf{0_{3\times1}} \\
-\mathbf{A_1 z_{12}^{abc}} & -\mathbf{A_1 z_{23}^{abc}} & \cdots & -\mathbf{A_1 z_{(i-1)i}^{abc}} & \mathbf{Y_{ss,T_1}^{abc}}^{-1} & \cdots & \mathbf{0_{3\times3}} & \mathbf{0_{3\times3}} & \mathbf{0_{3\times2}} & \mathbf{0_{3\times1}} \\
\vdots & \vdots & \vdots & \vdots & \vdots & \ddots & \vdots & \vdots & \vdots & \vdots \\
-\mathbf{z_{12}^{abc}} & -\mathbf{z_{23}^{abc}} & \cdots & \mathbf{0_{3\times3}} & \mathbf{0_{3\times3}} & \cdots & -\mathbf{z_{(k-1)k}^{abc}} & \mathbf{0_{3\times3}} & \mathbf{0_{3\times2}} & \mathbf{0_{3\times1}} \\
-\mathbf{A_2 z_{12}^{abc}} & -\mathbf{A_2 z_{23}^{abc}} & \cdots & \mathbf{0_{3\times3}} & \mathbf{0_{3\times3}} & \cdots & -\mathbf{A_2 z_{(k-1)k}^{abc}} & \mathbf{Y_{ss,T_2}^{abc}}^{-1} & \mathbf{0_{3\times2}} & \mathbf{0_{3\times1}} \\
-\mathbf{A_3 z_{12}^{ab}} & -\mathbf{A_3 z_{23}^{ab}} & \cdots & \mathbf{0_{3\times3}} & \mathbf{0_{3\times3}} & \cdots & -\mathbf{A_3 z_{(k-1)k}^{ab}} & \mathbf{Y_{ss,T_2}^{ab}}^{-1} & -\mathbf{z_{lm}^{ab}} & \mathbf{0_{3\times1}} \\
-\mathbf{A_4 z_{12}^{a}} & -\mathbf{A_4 z_{23}^{a}} & \cdots & \mathbf{0_{3\times3}} & \mathbf{0_{3\times3}} & \cdots & -\mathbf{A_4 z_{(k-1)k}^{a}} & \mathbf{Y_{ss,T_2}^{a}}^{-1} & -\mathbf{z_{lm}^{ab}} & -\mathbf{z_{mn}^{a}}
\end{bmatrix}$$

where,

$$\begin{aligned}
\mathbf{A_1} &= -\mathbf{Y_{ss,T_1}^{abc}}^{-1}\mathbf{Y_{sp,T_1}^{abc}}; \\
\mathbf{A_2} &= -\mathbf{Y_{ss,T_2}^{abc}}^{-1}\mathbf{Y_{sp,T_2}^{abc}}; \\
\mathbf{A_3} &= -\mathbf{Y_{ss,T_2}^{ab}}^{-1}\mathbf{Y_{sp,T_2}^{ab}}; \\
\mathbf{A_4} &= -\mathbf{Y_{ss,T_2}^{a}}^{-1}\mathbf{Y_{sp,T_2}^{a}}.
\end{aligned}$$

$$\Big[\mathbf{C}\Big] = \begin{bmatrix} \mathbf{I_{3\times 3}} \\ \mathbf{I_{3\times 3}} \\ \vdots \\ \mathbf{I_{3\times 3}} \\ -\mathbf{Y^{abc}_{ss,T_1}}^{-1}\mathbf{Y^{abc}_{sp,T_1}} \\ \vdots \\ \mathbf{I_{3\times 3}} \\ -\mathbf{Y^{abc}_{ss,T_2}}^{-1}\mathbf{Y^{abc}_{sp,T_2}} \\ -\mathbf{Y^{ab}_{ss,T_2}}^{-1}\mathbf{Y^{ab}_{sp,T_2}} \\ -\mathbf{Y^{a}_{ss,T_2}}^{-1}\mathbf{Y^{a}_{sp,T_2}} \end{bmatrix}; \Big[\mathbf{V_s}\Big] = [\mathbf{V_1^{abc}}] = \begin{bmatrix} V_1^a \\ V_1^b \\ V_1^c \end{bmatrix};$$

The size of $[\mathbf{BCBV_{Tm}}]$ ("Branch current to bus voltage matrix with transformer") and $[\mathbf{C}]$ matrices for the considered system will be $(3u+2v+w-3)\times(3u+2v+w-3)$ and $(3u+2v+w-3)\times(3)$, respectively.

Further, eq. (4.14) can be rewritten using eq. (4.9) as,

$$\Big[\mathbf{V_{bus}}\Big] = \Big[\mathbf{C}'\Big]\Big[\mathbf{V_s}\Big] + \Big[\mathbf{DLF}\Big]\Big[\mathbf{I_L}\Big] \tag{4.15}$$

where,

$$\begin{aligned} \Big[\mathbf{C}'\Big] &= \Big[\mathbf{I} - \Big[\mathbf{BCBV_{T_m}}\Big]\Big[\mathbf{TIBC'_{T_m}}\Big]\Big]^{-1}\Big[\mathbf{C}\Big]; \\ \Big[\mathbf{DLF}\Big] &= \Big\{\Big[\mathbf{I} - \Big[\mathbf{BCBV_{T_m}}\Big]\Big[\mathbf{TIBC'_{T_m}}\Big]\Big]^{-1}\Big[\Big[\mathbf{BCBV_{T_m}}\Big]\cdot\Big[\mathbf{BIBC_{S_m}}\Big]\Big]\Big\} \end{aligned}$$

where, $\Big[\mathbf{I}\Big]$ is an identity matrix of size $(3u+2v+w-3)\times(3u+2v+w-3)$.

In Fig. 4.1, z_{id}^q is the equivalent load impedance of phase q ($q = a$ or b or c) at bus i ($i = 1, 2, ..., n$), calculated using the results of the above discussed DSLF.

4.2.1.1 Algorithm for generation of $[\mathbf{BIBC_{Sm}}]$ and $[\mathbf{TIBC_{Tm}}]$ matrices for radial distribution system

Step 1. Initialize the $[\mathbf{BIBC_{Sm}}]$ and $[\mathbf{TIBC_{Tm}}]$ matrices as null matrices of size $(3u+2v+w-3)\times(3u+2v+w-3)$ and $(3u+2v+w-3)\times(3nt)$, respectively.

Step 2. If k^{th} line section ($\mathbf{L_k^p}$), having p phases, is connected between buses i and j, then

$$(i).\ \left[\mathbf{BIBC_{Sm}}(l_s,j)\right]_{(p\times p)} = \left[\mathbf{BIBC_{Sm}}(l_s,i)\right]_{(p\times p)};$$
$$(ii).\ \left[\mathbf{BIBC_{Sm}}(k,j)\right]_{(p\times p)} = \left[\mathbf{I}\right]_{(p\times p)}$$

where $l_s = 1, 2, \cdots, (k-1)$; $\left[\mathbf{I}\right]$ is an identity matrix of size $(p \times p)$ and $p = 3$ for 3-ϕ, $p = 2$ for 2-ϕ, $p = 1$ for 1-ϕ line section.

Step 3. If a three-phase transformer 't' is connected at the k^{th} line section between buses i and j, then

$$(i).\ \left[\mathbf{TIBC_{Tm}}(l_s,t)\right]_{(3\times 3)} = \left[\mathbf{BIBC_{Sm}}(l_s,i)\right]_{(3\times 3)};$$
$$(ii).\ \left[\mathbf{BIBC_{Sm}}(k,j)\right]_{(3\times 3)} = \left[\mathbf{I}\right]_{(3\times 3)}$$

where, $l_s = 1, 2, \cdots, (k-1)$, $t = 1$ or 2 or $\cdots$ nt, depending on the transformer number, and $\left[\mathbf{I}\right]$ is an identity matrix of size (3×3).

Step 4. Repeat Steps 2 and 3 until all line sections and the transformers are included in $[\mathbf{BIBC_{Sm}}]$ and $[\mathbf{TIBC_{Tm}}]$ matrices.

4.2.1.2 Algorithm for generation of $[\mathrm{BCBV_{Tm}}]$ and $[\mathrm{C}]$ matrices for radial distribution system

Step 1. Initialize $[\mathbf{BCBV_{Tm}}]$ matrix as a null matrix of size $(3u+2v+w-3) \times (3u+2v+w-3)$. Initialize $[\mathrm{C}]$ matrix as follows: (a) for three-phase bus, $\left[\mathbf{C}_i\right]^{abc}_{(3\times 3)} = \begin{bmatrix} 1 & 0 & 0 \\ 0 & 1 & 0 \\ 0 & 0 & 1 \end{bmatrix}$; ($b$) for two phase bus, $\left[\mathbf{C}_i\right]^{pq}_{(2\times 3)} = \begin{bmatrix} 1 & 0 & 0 \\ 0 & 1 & 0 \end{bmatrix}$, where pq = (a, b) or (b, c) or (c, a); (c) for single phase bus, $\left[\mathbf{C}_i\right]^{p}_{(1\times 3)} = \begin{bmatrix} 1 & 0 & 0 \end{bmatrix}$, where p = (a or b or c); i = bus number. The size of $[\mathrm{C}]$ matrix is $(3u + 2v + w - 3) \times 3$.

Step 2. If k^{th} line section ($\mathbf{L_k^p}$), having p phases, is connected between buses i and j, then

$$(i).\ \left[\mathbf{BCBV_{Tm}}(j,l_s)\right]_{(p\times p)} = \left[\mathbf{BCBV_{Tm}}(i,l_s)\right]_{(p\times p)};$$
$$(ii).\ \left[\mathbf{BCBV_{Tm}}(j,k)\right]_{(p\times p)} = \left[\mathbf{z_{ij}^{abc}}\right]_{(p\times p)};$$
$$(iii).\ \left[\mathbf{C}(j,l_s)\right]_{(p\times p)} = \left[\mathbf{C}(i,l_s)\right]_{(p\times p)}$$

where $l_s = 1, 2, \cdots, (k-1)$; $p = 3$ and $\left[\mathbf{z_{ij}^{abc}}\right]_{(3\times3)} = \begin{bmatrix} \bar{z}_{ij}^{aa} & \bar{z}_{ij}^{ab} & \bar{z}_{ij}^{ac} \\ \bar{z}_{ij}^{ba} & \bar{z}_{ij}^{bb} & \bar{z}_{ij}^{bc} \\ \bar{z}_{ij}^{ca} & \bar{z}_{ij}^{cb} & \bar{z}_{ij}^{cc} \end{bmatrix}$ for 3-ϕ; $p = 2$ and $\left[\mathbf{z_{ij}^{abc}}\right]_{(2\times2)} = \begin{bmatrix} \bar{z}_{ij}^{qq} & \bar{z}_{ij}^{qr} \\ \bar{z}_{ij}^{rq} & \bar{z}_{ij}^{rr} \end{bmatrix}$, where (q, r) = (a, b) or (b, c) or (c, a), for 2-ϕ; $p = 1$ and $\left[\mathbf{z_{ij}^{abc}}\right]_{(1\times1)} = \left[\bar{z}_{ij}^{qq}\right]$, where $q = a$ or b or c, for 1-ϕ line section.

Step 3. If a three-phase transformer $'t'$ is connected at the k^{th} line section between buses i and j, then

$$
\begin{aligned}
(i).\ \left[\mathbf{BCBV_{Tm}}(j, l_s)\right]_{(3\times3)} &= -\left[\mathbf{Y_{ss,t}^{abc^{-1}}}.\mathbf{Y_{sp,t}^{abc}}\right] * \left[\mathbf{BCBV_{Tm}}(i, l_s)\right]_{(3\times3)}; \\
(ii).\ \left[\mathbf{BCBV_{Tm}}(j, k)\right]_{(3\times3)} &= \left[\mathbf{Y_{ss,t}^{abc}}\right]^{-1}_{(3\times3)}; \\
(iii).\ \left[\mathbf{C}(j, l_s)\right]_{(3\times3)} &= -\left[\mathbf{Y_{ss,t}^{abc^{-1}}}.\mathbf{Y_{sp,t}^{abc}}\right] * \left[\mathbf{C}(i, l_s)\right]_{(3\times3)}
\end{aligned}
$$

where $l_s = 1, 2, \cdots, (k-1)$; $t = 1$ or 2 or $\cdots$ nt depending on the transformer number.

Step 4. Repeat Steps 2 and 3 until all line sections and the transformers are included in $[\mathbf{BCBV_{Tm}}]$ and $[\mathbf{C}]$ matrices.

4.2.2 Meshed distribution system

Let us consider a meshed distribution system with switch 'S' in close position in Fig. 4.1. A new branch is thus added between buses 2 and l and its branch current is denoted as $\mathbf{B_{new}^{abc}}$. The matrices $\left[\mathbf{BIBC_{Sm}}\right]$ and $\left[\mathbf{TIBC_{Tm}}\right]$ in eq. (4.7) will be modified with the addition of new mesh current $\mathbf{B_{new}^{abc}}$ [70] in the network. Hence, eq. (4.7) can be modified for the meshed distribution network as,

$$
\begin{bmatrix} \mathbf{B} \\ \mathbf{B_{new}^{abc}} \end{bmatrix} = \left[\mathbf{BIBC_{Sm}^{mesh}}\right] \begin{bmatrix} \mathbf{I_L} \\ \mathbf{B_{new}^{abc}} \end{bmatrix} + \left[\mathbf{TIBC_{T_m}^{mesh}}\right] \left[\mathbf{I_{T_p}}\right] \tag{4.16}
$$

where,

$$
\left[\mathbf{TIBC_{T_m}^{mesh}}\right] = \left[\begin{array}{cccccccccc|c} \mathbf{I_{3\times3}} & \mathbf{I_{3\times3}} & \cdots & \mathbf{I_{3\times3}} & \mathbf{0_{3\times3}} & \cdots & \mathbf{0_{3\times3}} & \mathbf{0_{3\times3}} & \mathbf{0_{3\times2}} & \mathbf{0_{3\times1}} & \mathbf{0_{3\times3}} \\ \mathbf{I_{3\times3}} & \mathbf{I_{3\times3}} & \cdots & \mathbf{0_{3\times3}} & \mathbf{0_{3\times3}} & \cdots & \mathbf{I_{3\times3}} & \mathbf{0_{3\times3}} & \mathbf{I_{3\times2}} & \mathbf{0_{3\times1}} & \mathbf{0_{3\times3}} \end{array}\right]^T
$$

$$\left[\mathbf{BIBC}^{\mathbf{mesh}}_{\mathbf{Sm}}\right] =$$

$$\left[\begin{array}{cccccccccc|c}
\mathbf{I_{3\times3}} & \mathbf{I_{3\times3}} & \cdots & \mathbf{I_{3\times3}} & \mathbf{0_{3\times3}} & \cdots & \mathbf{I_{3\times3}} & \mathbf{0_{3\times3}} & \mathbf{0_{3\times2}} & \mathbf{0_{3\times1}} & \mathbf{I_{3\times3}} \\
\mathbf{0_{3\times3}} & \mathbf{I_{3\times3}} & \cdots & \mathbf{I_{3\times3}} & \mathbf{0_{3\times3}} & \cdots & \mathbf{I_{3\times3}} & \mathbf{0_{3\times3}} & \mathbf{0_{3\times2}} & \mathbf{0_{3\times1}} & \mathbf{0_{3\times3}} \\
\vdots & \vdots & \ddots & \vdots & \vdots & \vdots & \vdots & \vdots & \vdots & \vdots & \vdots \\
\mathbf{0_{3\times3}} & \mathbf{0_{3\times3}} & \cdots & \mathbf{I_{3\times3}} & \mathbf{0_{3\times3}} & \cdots & \mathbf{0_{3\times3}} & \mathbf{0_{3\times3}} & \mathbf{0_{3\times2}} & \mathbf{0_{3\times1}} & \mathbf{0_{3\times3}} \\
\mathbf{0_{3\times3}} & \mathbf{0_{3\times3}} & \cdots & \mathbf{0_{3\times3}} & \mathbf{-I_{3\times3}} & \cdots & \mathbf{0_{3\times3}} & \mathbf{0_{3\times3}} & \mathbf{0_{3\times2}} & \mathbf{0_{3\times1}} & \mathbf{0_{3\times3}} \\
\vdots & \vdots & \vdots & \vdots & \vdots & \ddots & \vdots & \vdots & \vdots & \vdots & \vdots \\
\mathbf{0_{3\times3}} & \mathbf{0_{3\times3}} & \cdots & \mathbf{0_{3\times3}} & \mathbf{0_{3\times3}} & \cdots & \mathbf{I_{3\times3}} & \mathbf{0_{3\times3}} & \mathbf{0_{3\times2}} & \mathbf{0_{3\times1}} & \mathbf{0_{3\times3}} \\
\mathbf{0_{3\times3}} & \mathbf{0_{3\times3}} & \cdots & \mathbf{0_{3\times3}} & \mathbf{0_{3\times3}} & \cdots & \mathbf{0_{3\times3}} & \mathbf{-I_{3\times3}} & \mathbf{-I_{3\times2}} & \mathbf{-I_{3\times1}} & \mathbf{I_{3\times3}} \\
\mathbf{0_{2\times3}} & \mathbf{0_{2\times3}} & \cdots & \mathbf{0_{2\times3}} & \mathbf{0_{2\times3}} & \cdots & \mathbf{0_{2\times3}} & \mathbf{0_{2\times3}} & \mathbf{I_{2\times2}} & \mathbf{I_{2\times1}} & \mathbf{0_{2\times3}} \\
\mathbf{0_{1\times3}} & \mathbf{0_{1\times3}} & \cdots & \mathbf{0_{1\times3}} & \mathbf{0_{1\times3}} & \cdots & \mathbf{0_{1\times3}} & \mathbf{0_{1\times3}} & \mathbf{0_{1\times2}} & \mathbf{I_{1\times1}} & \mathbf{0_{1\times3}} \\
\hline
\mathbf{0_{3\times3}} & \mathbf{0_{3\times3}} & \cdots & \mathbf{0_{3\times3}} & \mathbf{0_{3\times3}} & \cdots & \mathbf{0_{3\times3}} & \mathbf{0_{3\times3}} & \mathbf{0_{3\times3}} & \mathbf{0_{3\times3}} & \mathbf{I_{3\times3}}
\end{array}\right]$$

Similarly, eq. (4.9) can also be modified for the meshed distribution network as,

$$\begin{bmatrix} \mathbf{B} \\ \mathbf{B^{abc}_{new}} \end{bmatrix} = \left[\mathbf{BIBC}^{\mathbf{mesh}}_{\mathbf{Sm}}\right] \begin{bmatrix} \mathbf{I_L} \\ \mathbf{B^{abc}_{new}} \end{bmatrix} + \left[\mathbf{TIBC}^{\mathbf{'mesh}}_{\mathbf{T_m}}\right] \begin{bmatrix} \mathbf{V_{bus}} \\ \mathbf{0} \end{bmatrix} \tag{4.17}$$

Now, applying KVL equation for the loop (with switch 'S' closed in Fig. 4.1), we have,

$$\mathbf{B^{abc}_2 Z^{abc}_{23}} + \cdots + \mathbf{B^{abc}_{(k-1)} Z^{abc}_{(k-1)k}} + \mathbf{V^{abc}_k} - \mathbf{V^{abc}_l} - \mathbf{B^{abc}_{new} Z^{abc}_{2l}} = \mathbf{0} \tag{4.18}$$

Hence, eq. (4.14) can be modified for the meshed distribution system with the inclusion of eq. (4.18) as,

$$\begin{bmatrix} \mathbf{V_{bus}} \\ \mathbf{0} \end{bmatrix} = \begin{bmatrix} \mathbf{C} \\ \mathbf{C^{mesh}} \end{bmatrix} \left[\mathbf{V_s}\right] + \left[\mathbf{BCBV}^{\mathbf{mesh}}_{\mathbf{T_m}}\right] \begin{bmatrix} \mathbf{B} \\ \mathbf{B^{abc}_{new}} \end{bmatrix} \tag{4.19}$$

where,

$$\left[\mathbf{BCBV}^{\mathbf{mesh}}_{\mathbf{T_m}}\right] =$$

$$\left[\begin{array}{cccccccccc|c}
\mathbf{-z^{abc}_{12}} & \mathbf{0_{3\times3}} & \cdots & \mathbf{0_{3\times3}} & \mathbf{0_{3\times3}} & \cdots & \mathbf{0_{3\times3}} & \mathbf{0_{3\times3}} & \mathbf{0_{3\times2}} & \mathbf{0_{3\times1}} & \mathbf{0_{3\times3}} \\
\mathbf{-z^{abc}_{12}} & \mathbf{-z^{abc}_{23}} & \cdots & \mathbf{0_{3\times3}} & \mathbf{0_{3\times3}} & \cdots & \mathbf{0_{3\times3}} & \mathbf{0_{3\times3}} & \mathbf{0_{3\times2}} & \mathbf{0_{3\times1}} & \mathbf{0_{3\times3}} \\
\vdots & \vdots & \ddots & \vdots & \vdots & \vdots & \vdots & \vdots & \vdots & \vdots & \vdots \\
\mathbf{-z^{abc}_{12}} & \mathbf{-z^{abc}_{23}} & \cdots & \mathbf{-z^{abc}_{(i-1)i}} & \mathbf{0_n} & \cdots & \mathbf{0_{3\times3}} & \mathbf{0_{3\times3}} & \mathbf{0_{3\times2}} & \mathbf{0_{3\times1}} & \mathbf{0_{3\times3}} \\
\mathbf{-A_1 z^{abc}_{12}} & \mathbf{-A_1 z^{abc}_{23}} & \cdots & \mathbf{-A_1 z^{abc}_{(i-1)i}} & \mathbf{Y^{abc}_{ss,T_1}}^{-1} & \cdots & \mathbf{0_{3\times3}} & \mathbf{0_{3\times3}} & \mathbf{0_{3\times2}} & \mathbf{0_{3\times1}} & \mathbf{0_{3\times3}} \\
\vdots & \vdots & \vdots & \vdots & \vdots & \ddots & \vdots & \vdots & \vdots & \vdots & \vdots \\
\mathbf{-z^{abc}_{12}} & \mathbf{-z^{abc}_{23}} & \cdots & \mathbf{0_{3\times3}} & \mathbf{0_{3\times3}} & \cdots & \mathbf{-z^{abc}_{(k-1)k}} & \mathbf{0_{3\times3}} & \mathbf{0_{3\times2}} & \mathbf{0_{3\times1}} & \mathbf{0_{3\times3}} \\
\mathbf{-A_2 z^{abc}_{12}} & \mathbf{-A_2 z^{abc}_{23}} & \cdots & \mathbf{0_{3\times3}} & \mathbf{0_{3\times3}} & \cdots & \mathbf{-A_2 z^{abc}_{(k-1)k}} & \mathbf{Y^{abc}_{ss,T_2}}^{-1} & \mathbf{0_{3\times2}} & \mathbf{0_{3\times1}} & \mathbf{0_{3\times3}} \\
\mathbf{-A_3 z^{ab}_{12}} & \mathbf{-A_3 z^{ab}_{23}} & \cdots & \mathbf{0_{2\times3}} & \mathbf{0_{2\times3}} & \cdots & \mathbf{-A_3 z^{ab}_{(k-1)k}} & \mathbf{Y^{ab}_{ss,T_2}}^{-1} & \mathbf{-z^{ab}_{lm}} & \mathbf{0_{2\times1}} & \mathbf{0_{2\times3}} \\
\mathbf{-A_4 z^{a}_{12}} & \mathbf{-A_4 z^{a}_{23}} & \cdots & \mathbf{0_{1\times3}} & \mathbf{0_{1\times3}} & \cdots & \mathbf{-A_4 z^{a}_{(k-1)k}} & \mathbf{Y^{a}_{ss,T_2}}^{-1} & \mathbf{-z^{ab}_{lm}} & \mathbf{-z^{a}_{mn}} & \mathbf{0_{1\times3}} \\
\hline
\mathbf{-A_5 z^{abc}_{12}} & \mathbf{-A_5 z^{abc}_{23}} & \cdots & \mathbf{0_{3\times3}} & \mathbf{0_{3\times3}} & \cdots & \mathbf{-A_5 z^{abc}_{(k-1)k}} & \mathbf{-Y^{abc}_{ss,T_2}}^{-1} & \mathbf{0_{3\times2}} & \mathbf{0_{3\times1}} & \mathbf{-z^{abc}_{2l}}
\end{array}\right]$$

$$\begin{bmatrix} \mathbf{C} \\ \mathbf{C^{mesh}} \end{bmatrix} = \begin{bmatrix} \mathbf{I_{3\times 3}} \\ \mathbf{I_{3\times 3}} \\ \vdots \\ \mathbf{I_{3\times 3}} \\ -\mathbf{Y^{abc}_{ss,T_1}}^{-1}\mathbf{Y^{abc}_{sp,T_1}} \\ \vdots \\ \mathbf{I_{3\times 3}} \\ -\mathbf{Y^{abc}_{ss,T_2}}^{-1}\mathbf{Y^{abc}_{sp,T_2}} \\ -\mathbf{Y^{ab}_{ss,T_2}}^{-1}\mathbf{Y^{ab}_{sp,T_2}} \\ -\mathbf{Y^{a}_{ss,T_2}}^{-1}\mathbf{Y^{a}_{sp,T_2}} \\ \hline \mathbf{1} + \mathbf{Y^{abc}_{ss,T_2}}^{-1}\mathbf{Y^{abc}_{sp,T_2}} \end{bmatrix} = \begin{bmatrix} \mathbf{C^{mesh}_{new}} \end{bmatrix};$$

where, $\mathbf{A_5} = (\mathbf{1} + \mathbf{Y^{abc}_{ss,T_2}}^{-1}\mathbf{Y^{abc}_{sp,T_2}})$.

Similarly, eq. (4.15) can also be modified for the meshed distribution network as,

$$\begin{bmatrix} \mathbf{V_{bus}} \\ \mathbf{0} \end{bmatrix} = \begin{bmatrix} \mathbf{C'} \\ \mathbf{C'^{mesh}} \end{bmatrix} \begin{bmatrix} \mathbf{V_s} \end{bmatrix} + \begin{bmatrix} \mathbf{DLF^{mesh}} \end{bmatrix} \begin{bmatrix} \mathbf{I_L} \\ \mathbf{B^{abc}_{new}} \end{bmatrix} \tag{4.20}$$

where,

$$\begin{bmatrix} \mathbf{C'} \\ \mathbf{C'^{mesh}} \end{bmatrix} = \left[\mathbf{I} - \left[\mathbf{BCBV^{mesh}_{T_m}}\right]\left[\mathbf{TIBC'^{mesh}_{T_m}}\right]\right]^{-1} \begin{bmatrix} \mathbf{C} \\ \mathbf{C^{mesh}} \end{bmatrix}$$

$$\left[\mathbf{DLF^{mesh}}\right] = \left\{\left[\mathbf{I} - \left[\mathbf{BCBV^{mesh}_{T_m}}\right]\left[\mathbf{TIBC'^{mesh}_{T_m}}\right]\right]^{-1}\left[\left[\mathbf{BCBV^{mesh}_{T_m}}\right] \cdot \left[\mathbf{BIBC^{mesh}_{S_m}}\right]\right]\right\}$$

Now, equation (4.20) can be further rewritten as,

$$\begin{bmatrix} \mathbf{V_{bus}} \\ \mathbf{0} \end{bmatrix} = \begin{bmatrix} \mathbf{C'} \\ \mathbf{C'^{mesh}} \end{bmatrix} \begin{bmatrix} \mathbf{V_s} \end{bmatrix} + \begin{bmatrix} \mathbf{M_1} & \mathbf{M_2}^T \\ \mathbf{M_2} & \mathbf{M_3} \end{bmatrix} \begin{bmatrix} \mathbf{I_L} \\ \mathbf{B^{abc}_{new}} \end{bmatrix} \tag{4.21}$$

Equation (4.21) can be further solved by Kron's reduction method to obtain the bus voltages of the meshed distribution network as,

$$\begin{aligned} \left[\mathbf{V_{bus}}\right] &= \left[\mathbf{C'} - \mathbf{M_2}^T\mathbf{M_3^{-1}}\mathbf{C'^{mesh}}\right]\left[\mathbf{V_s}\right] + \left[\mathbf{M_1} - \mathbf{M_2}^T\mathbf{M_3^{-1}}\mathbf{M_2}\right]\left[\mathbf{I_L}\right] \\ \left[\mathbf{V_{bus}}\right] &= \left[\mathbf{C'_{new}}\right]\left[\mathbf{V_s}\right] + \left[\mathbf{DLF_{new}}\right]\left[\mathbf{I_L}\right] \end{aligned} \tag{4.22}$$

where $[\mathbf{C'_{new}}] = \left[\mathbf{C'} - \mathbf{M_2}^T\mathbf{M_3^{-1}}\mathbf{C'^{mesh}}\right]$ and $[\mathbf{DLF_{new}}] = \left[\mathbf{M_1} - \mathbf{M_2}^T\mathbf{M_3^{-1}}\mathbf{M_2}\right]$.

The sizes of $[\mathbf{BIBC^{mesh}_{Sm}}]$, $[\mathbf{TIBC^{mesh}_{Tm}}]$, $[\mathbf{BCBV^{mesh}_{Tm}}]$ and $[\mathbf{C^{mesh}_{new}}]$ matrices for the considered system with m_s no. of meshes will be $(3u+2v+w-3+3m_s) \times (3u+2v+w-3+3m_s)$, $(3u+2v+w-3+3m_s) \times (3nt)$, $(3u+2v+w-3+3m_s) \times (3u+2v+w-3+3m_s)$ and $(3u+2v+w-3+3m_s) \times (3)$, respectively.

4.2.2.1 Algorithm for generation of $[\mathbf{BIBC^{mesh}_{Sm}}]$ and $[\mathbf{TIBC^{mesh}_{Tm}}]$ matrices for meshed distribution system

Step 1. Initialize the $[\mathbf{BIBC^{mesh}_{Sm}}]$ and $[\mathbf{TIBC^{mesh}_{Tm}}]$ matrices as null matrices of size $(3u+2v+w-3+3m_s) \times (3u+2v+w-3+3m_s)$ and $(3u+2v+w-3+3m_s) \times (3nt)$, respectively.

Step 2. If k^{th} line section ($\mathbf{L^p_k}$), having p phases, is connected between buses i and j, then

$$\begin{aligned} (i).\ \left[\mathbf{BIBC^{mesh}_{Sm}}(l_s,j)\right]_{(p\times p)} &= \left[\mathbf{BIBC^{mesh}_{Sm}}(l_s,i)\right]_{(p\times p)}; \\ (ii).\ \left[\mathbf{BIBC^{mesh}_{Sm}}(k,j)\right]_{(p\times p)} &= \left[\mathbf{I}\right]_{(p\times p)} \end{aligned}$$

where $l_s = 1, 2, \cdots, (k-1)$; $\left[\mathbf{I}\right]$ is an identity matrix of size $(p \times p)$ and $p = 3$ for 3-ϕ, $p = 2$ for 2-ϕ, $p = 1$ for 1-ϕ line section.

Step 3. If a three-phase transformer $'t'$ is connected at the k^{th} line section between buses i and j, then

$$\begin{aligned} (i).\ \left[\mathbf{TIBC^{mesh}_{Tm}}(l_s,t)\right]_{(3\times 3)} &= \left[\mathbf{BIBC^{mesh}_{Sm}}(l_s,i)\right]_{(3\times 3)}; \\ (ii).\ \left[\mathbf{BIBC^{mesh}_{Sm}}(k,j)\right]_{(3\times 3)} &= \left[\mathbf{I}\right]_{(3\times 3)} \end{aligned}$$

where, $l_s = 1, 2, \cdots, (k-1)$, $t = 1$ or 2 or $\cdots$ nt, depending on the transformer number, and $\left[\mathbf{I}\right]$ is an identity matrix of size (3×3).

Step 4. If a three-phase branch $\mathbf{L^{abc}_k}$, connected between buses i and j generates a mesh in the system, then

$$\begin{aligned} (i).\ \left[\mathbf{BIBC^{mesh}_{Sm}}(l_s,k)\right]_{(3\times 3)} &= \left[\mathbf{BIBC^{mesh}_{Sm}}(l_s,i)\right]_{(3\times 3)} - \left[\mathbf{BIBC^{mesh}_{Sm}}(l_s,j)\right]_{(3\times 3)} \\ (ii).\ \left[\mathbf{BIBC^{mesh}_{Sm}}(k,k)\right]_{(3\times 3)} &= \left[\mathbf{I}\right]_{(3\times 3)} \end{aligned}$$

where $l_s = 1, 2, \cdots, (k-1)$.

Step 5. Repeat Steps 2, 3 and 4 until all the line sections and the transformers are included in $[\mathbf{BIBC^{mesh}_{Sm}}]$ and $[\mathbf{TIBC^{mesh}_{Tm}}]$ matrices of the meshed distribution system.

4.2.2.2 Algorithm for generation of $[\mathbf{BCBV^{mesh}_{Tm}}]$ and $[\mathbf{C^{mesh}_{new}}]$ matrices for meshed distribution system

Step 1. Initialize $[\mathbf{BCBV^{mesh}_{Tm}}]$ matrix as a null matrix of size $(3u+2v+w-3+3m_s)\times(3u+2v+w-3+3m_s)$. Initialize $[\mathbf{C^{mesh}_{new}}]$ matrix as follows: (*a*) for three-phase bus, $\left[\mathbf{C^{mesh}_{new}}_i\right]^{abc}_{(3\times3)} = \begin{bmatrix}1&0&0\\0&1&0\\0&0&1\end{bmatrix}$; (*b*) for two phase bus, $\left[\mathbf{C^{mesh}_{new}}_i\right]^{pq}_{(2\times3)} = \begin{bmatrix}1&0&0\\0&1&0\end{bmatrix}$, where pq = (a,b) or (b,c) or (c,a); (*c*) for single phase bus, $\left[\mathbf{C^{mesh}_{new}}_i\right]^{p}_{(1\times3)} = \begin{bmatrix}1&0&0\end{bmatrix}$, where p = (a or b or c); i = bus number; (*d*) for m_s no. of meshes present in the system, $\left[\mathbf{C^{mesh}_{new}}_{,m_s}\right]^{abc}_{(3\times3)} = \begin{bmatrix}1&0&0\\0&1&0\\0&0&1\end{bmatrix}$. The size of $\left[\mathbf{C^{mesh}_{new}}\right]$ matrix is $(3u+2v+w-3+3m_s)\times3$.

Step 2. If k^{th} line section ($\mathbf{L^p_k}$), having p phases, is connected between buses i and j, then

$$
\begin{aligned}
(i).\ \left[\mathbf{BCBV^{mesh}_{Tm}}(j,l_s)\right]_{(p\times p)} &= \left[\mathbf{BCBV^{mesh}_{Tm}}(i,l_s)\right]_{(p\times p)};\\
(ii).\ \left[\mathbf{BCBV^{mesh}_{Tm}}(j,k)\right]_{(p\times p)} &= \left[\mathbf{z^{abc}_{ij}}\right]_{(p\times p)};\\
(iii).\ \left[\mathbf{C^{mesh}_{new}}(j,l_s)\right]_{(p\times p)} &= \left[\mathbf{C^{mesh}_{new}}(i,l_s)\right]_{(p\times p)}
\end{aligned}
$$

where $l_s = 1,2,\cdots,(k-1)$; $p=3$ and $\left[\mathbf{z^{abc}_{ij}}\right]_{(3\times3)} = \begin{bmatrix}\bar{z}^{aa}_{ij}&\bar{z}^{ab}_{ij}&\bar{z}^{ac}_{ij}\\\bar{z}^{ba}_{ij}&\bar{z}^{bb}_{ij}&\bar{z}^{bc}_{ij}\\\bar{z}^{ca}_{ij}&\bar{z}^{cb}_{ij}&\bar{z}^{cc}_{ij}\end{bmatrix}$ for 3-ϕ; $p=2$ and $\left[\mathbf{z^{abc}_{ij}}\right]_{(2\times2)} = \begin{bmatrix}\bar{z}^{qq}_{ij}&\bar{z}^{qr}_{ij}\\\bar{z}^{rq}_{ij}&\bar{z}^{rr}_{ij}\end{bmatrix}$, where (q,r) = (a,b) or (b,c) or (c,a), for 2-ϕ; $p=1$ and $\left[\mathbf{z^{abc}_{ij}}\right]_{(1\times1)} = \left[\bar{z}^{qq}_{ij}\right]$, where $q=a$ or b or c, for 1-ϕ line section.

Step 3. If a three-phase transformer $'t'$ is connected at the k^{th} line section between buses i and j, then

$$
\begin{aligned}
(i).\ \left[\mathbf{BCBV^{mesh}_{Tm}}(j,l_s)\right]_{(3\times3)} &= -\left[\mathbf{Y^{abc^{-1}}_{ss,t}}.\mathbf{Y^{abc}_{sp,t}}\right]*\left[\mathbf{BCBV^{mesh}_{Tm}}(i,l_s)\right]_{(3\times3)};\\
(ii).\ \left[\mathbf{BCBV^{mesh}_{Tm}}(j,k)\right]_{(3\times3)} &= \left[\mathbf{Y^{abc}_{ss,t}}\right]^{-1}_{(3\times3)};\\
(iii).\ \left[\mathbf{C^{mesh}_{new}}(j,l_s)\right]_{(3\times3)} &= -\left[\mathbf{Y^{abc^{-1}}_{ss,t}}.\mathbf{Y^{abc}_{sp,t}}\right]*\left[\mathbf{C^{mesh}_{new}}(i,l_s)\right]_{(3\times3)}
\end{aligned}
$$

where $l_s = 1, 2, \cdots, (k-1)$; $t = 1$ or 2 or $\cdots$ nt depending on the transformer number.

Step 4. If a three-phase branch $\mathbf{L_k^{abc}}$, connected between buses i and j generates a mesh in the system, then

$$
\begin{aligned}
(i).\ \left[\mathbf{BCBV_{Tm}^{mesh}}(k,l_s)\right]_{(3\times3)} &= \left[\mathbf{BCBV_{Tm}^{mesh}}(i,l_s)\right]_{(3\times3)} - \left[\mathbf{BCBV_{Tm}^{mesh}}(j,l_s)\right]_{(3\times3)};\\
(ii).\ \left[\mathbf{BCBV_{Tm}^{mesh}}(k,k)\right]_{(3\times3)} &= -\left[\mathbf{z_k^{abc}}\right]_{(3\times3)};\\
(iii).\ \left[\mathbf{C_{new}^{mesh}}(k,l_s)\right]_{(3\times3)} &= \left[\mathbf{C_{new}^{mesh}}(i,l_s)\right]_{(3\times3)} - \left[\mathbf{C_{new}^{mesh}}(j,l_s)\right]_{(3\times3)}
\end{aligned}
$$

Step 5. Repeat Steps 2, 3 and 4 until all line sections and transformers are included in $[\mathbf{BCBV_{Tm}^{mesh}}]$ and $[\mathbf{C_{new}^{mesh}}]$ matrices of the meshed distribution system.

4.2.3 Singularity problem and its solution

Let us assume that the transformer T_1, in Fig. 4.1, is a star grounded/delta (Y_gD-1) transformer. The nodal admittance matrix (p.u.) of this transformer is given as,

$$
\begin{aligned}
\mathbf{Y_T} &= y_t \left[\begin{array}{ccc|ccc}
1 & 0 & 0 & -\frac{1}{\sqrt{3}} & \frac{1}{\sqrt{3}} & 0\\
0 & 1 & 0 & 0 & -\frac{1}{\sqrt{3}} & \frac{1}{\sqrt{3}}\\
0 & 0 & 1 & \frac{1}{\sqrt{3}} & 0 & -\frac{1}{\sqrt{3}}\\
\hline
-\frac{1}{\sqrt{3}} & 0 & \frac{1}{\sqrt{3}} & \frac{2}{3} & -\frac{1}{3} & -\frac{1}{3}\\
\frac{1}{\sqrt{3}} & -\frac{1}{\sqrt{3}} & 0 & -\frac{1}{3} & \frac{2}{3} & -\frac{1}{3}\\
0 & \frac{1}{\sqrt{3}} & -\frac{1}{\sqrt{3}} & -\frac{1}{3} & -\frac{1}{3} & \frac{2}{3}
\end{array}\right]\\
&= \left[\begin{array}{c|c}
\mathbf{Y_{pp,T}^{abc}} & \mathbf{Y_{ps,T}^{abc}}\\
\hline
\mathbf{Y_{sp,T}^{abc}} & \mathbf{Y_{ss,T}^{abc}}
\end{array}\right]
\end{aligned}
\tag{4.23}
$$

where y_t is the per unit transformer leakage admittance. Now, to calculate transformer secondary side bus voltage $\mathbf{V_j^{abc}}$, using eq. (4.13), the inversion of sub-matrix $\mathbf{Y_{ss,T}^{abc}}$ is required. Eq. (4.23) shows that the sub-matrix $\mathbf{Y_{ss,T}^{abc}}$, for a (Y_gD-1) transformer, is a singular matrix. To overcome this singularity problem, the method given in [78] is followed. Initially, the sequence component voltage of transformer secondary side bus j ($\mathbf{V_j^{'abc}}$), that contains only the positive and negative sequence components, is calculated as,

$$
\mathbf{V_j^{'abc}} = \mathbf{V_j^{abc}} - \mathbf{V_j^{0abc}} \tag{4.24}
$$

where $\mathbf{V_j^{abc}}$ and $\mathbf{V_j^{0abc}}$ are the actual j^{th} bus voltage and zero sequence component of j^{th} bus voltage vector, respectively. Therefore, eq. (4.13) for the j^{th} bus voltage can be rewritten (using eq. (4.24)) as,

$$\mathbf{Y_{ss,T_1}^{abc}}(\mathbf{V_j^{'abc}} + \mathbf{V_j^{0abc}}) = (\mathbf{I_{T_1,s}^{abc}} - \mathbf{Y_{sp,T_1}^{abc}}\mathbf{V_i^{abc}}) \tag{4.25}$$

Since, $\mathbf{V_j^{0abc}}.\mathbf{Y_{ss,T_1}^{abc}} = \mathbf{0}$ [78], (for all transformers having singular $\mathbf{Y_{ss,T}^{abc}}$ matrix), eq. (4.25) can be rewritten as,

$$\mathbf{Y_{ss,T_1}^{abc}}\mathbf{V_j^{'abc}} = (\mathbf{I_{T_1,s}^{abc}} - \mathbf{Y_{sp,T_1}^{abc}}\mathbf{V_i^{abc}}) \tag{4.26}$$

Since $\mathbf{V_j^{'abc}}$ does not contain any zero sequence component,

$$\begin{bmatrix} 1 & 1 & 1 \end{bmatrix} \mathbf{V_j^{'abc}} = \mathbf{0} \tag{4.27}$$

Combined eqs. (4.26) and (4.27), we get,

$$\mathbf{Y_{ss,T_1}^{'abc}}\mathbf{V_j^{'abc}} = (\mathbf{I_{T_1,s}^{'abc}} - \mathbf{Y_{sp,T_1}^{'abc}}\mathbf{V_i^{abc}}) \tag{4.28}$$

where,

$\mathbf{Y_{ss,T_1}^{'abc}} = \frac{y_t}{3}\begin{bmatrix} 2 & -1 & -1 \\ -1 & 2 & -1 \\ 1 & 1 & 1 \end{bmatrix}$; $\mathbf{Y_{sp,T_1}^{'abc}} = \frac{y_t}{\sqrt{3}}\begin{bmatrix} -1 & 0 & 1 \\ 1 & -1 & 0 \\ 0 & 0 & 0 \end{bmatrix}$ and $\mathbf{I_{T_1,s}^{'abc}} = \begin{bmatrix} \bar{I}_{T_1,s}^{a} & \bar{I}_{T_1,s}^{b} & 0 \end{bmatrix}^T$.

Hence the sum of positive and negative sequence components of j^{th} bus voltage ($\mathbf{V_j^{'abc}}$) is calculated using eq. (4.28). The zero sequence component of the j^{th} bus voltage ($\mathbf{V_j^{0abc}}$) can be neglected [78], as in common practice, the single-phase to ground loads are connected to the ungrounded side of transformer in the distribution utility system [78] and therefore the zero sequence currents in transformer are very small as compared to the load currents. Hence, the actual voltage of transformer secondary side bus j ($\mathbf{V_j^{abc}}$) is obtained as the sum of positive and negative sequence component voltages at j^{th} bus.

4.2.4 IBDG model for the load flow

In general, the IBDGs are connected to the distribution system through a step-up distribution transformer. Hence, let us consider an IBDG is connected to bus j of the distribution system shown in Fig. 4.1. Two different modes of IBDG have been considered in the proposed distribution system load flow, as,

1. **Constant active power mode-** In this mode, IBDG operates in the constant active power injection mode (unity power factor mode). In this case, the IBDG directly feeds power to the grid irrespective of the voltage magnitude at its terminal. Hence the total injected complex power by the IBDG at inverter bus is, $\mathbf{S_{dg}^{abc}} = \mathbf{P_{dg}^{abc}} + j\mathbf{Q_{dg}^{abc}}$; where $\mathbf{P_{dg}^{abc}} = \begin{bmatrix} P_{dg}^{a} & P_{dg}^{b} & P_{dg}^{c} \end{bmatrix}^T$, $\mathbf{Q_{dg}^{abc}} = \begin{bmatrix} Q_{dg}^{a} & Q_{dg}^{b} & Q_{dg}^{c} \end{bmatrix}^T$. P_{dg}^{q} and Q_{dg}^{q} ($q = a$ or b or c) are the active and reactive power generated by the IBDG at phase q of inverter bus, respectively. In this mode, only the active power is injected by the IBDG, i.e. $\mathbf{Q_{dg}^{abc}} = \begin{bmatrix} 0 & 0 & 0 \end{bmatrix}^T$. Also, the inverter current in q^{th} phase ($\bar{I}_{inv}^{q}$) in this mode is calculated as,

$$\bar{I}_{inv}^{q} = \left(\frac{\bar{S}_{dg}^{q}}{\bar{V}_{inv}^{q}}\right)^{*} = \left(\frac{\bar{P}_{dg}^{q} + j\bar{Q}_{dg}^{q}}{\bar{V}_{inv}^{q}}\right)^{*} = \left(\frac{\bar{P}_{dg}^{q} + j0.0}{\bar{V}_{inv}^{q}}\right)^{*}; \quad (q = a, b, c) \tag{4.29}$$

where, $\bar{V}_{inv}^{q}$ is the q^{th} phase voltage of inverter bus.

2. **Power and voltage control (PV) mode-** In this mode, the inverter bus (where an IBDG is connected) is treated as a PV-bus. In this case, the IBDG also injects the required reactive power to the utility grid to maintain the inverter bus voltage magnitude at its pre-specified value. The calculation of required reactive power is performed by using the PV node sensitivity matrix based method, given in [90]. Hence the total complex power injected by the IBDG, at inverter bus, in this mode is, $\mathbf{S_{dg}^{abc}} = \mathbf{P_{dg}^{abc}} + j\mathbf{Q_{dg}^{abc}}$; where $\mathbf{Q_{dg}^{abc}} = \begin{bmatrix} Q_{dg}^{a} & Q_{dg}^{b} & Q_{dg}^{c} \end{bmatrix}^T$. Q_{dg}^{q} ($q = a$ or b or c) is the required reactive power injection by the IBDG at phase q to maintain the voltage magnitude of the q^{th} phase of inverter bus at its pre-specified value. In each iteration, $\mathbf{Q_{dg}^{abc}}$ is calculated for all IBDGs and the condition $Q_{dg}^{min} < Q_{dg}^{q} < Q_{dg}^{max}$ ($q = a, b, c$) is checked, where Q_{dg}^{min} and Q_{dg}^{max} are the minimum and maximum reactive power generation limits of the IBDG. For any IBDG, if $Q_{dg}^{q} < Q_{dg}^{min}$ at any iteration , then Q_{dg}^{q} ($q = a, b, c$) will be fixed at Q_{dg}^{min}, and if $Q_{dg}^{q} > Q_{dg}^{max}$, then Q_{dg}^{q} ($q = a, b, c$) will be fixed at Q_{dg}^{max}, and in both cases IBDG bus will be treated as a PQ bus in that particular iteration. Otherwise, if the condition $Q_{dg}^{min} < Q_{dg}^{q} < Q_{dg}^{max}$ ($q = a, b, c$) is true, then the IBDG will continue to operate in PV bus mode in the next iteration. The inverter current in q^{th} phase ($\bar{I}_{inv}^{q}$) in this mode is calculated as,

$$\bar{I}_{inv}^{q} = \left(\frac{\bar{S}_{dg}^{q}}{\bar{V}_{inv}^{q}}\right)^{*} = \left(\frac{\bar{P}_{dg}^{q} + j\bar{Q}_{dg}^{q}}{\bar{V}_{inv}^{q}}\right)^{*}; \quad (q = a, b, c) \tag{4.30}$$

4.3 Short-circuit analysis of an unbalanced distribution system with transformer modeling

With the help of the proposed DSLF, the injected load currents and the voltages at each bus of the distribution system are calculated. Subsequently, the equivalent load impedances at each bus can be calculated. For example, the equivalent load impedance at any phase q $(q = a, b, c)$ of bus i of the system, shown in Fig. 4.1, can be calculated as

$$\bar{z}_{id}^{q} = \left(\frac{\bar{V}_i^q}{\bar{I}_{id}^q}\right); \;\; q = (a, b, c) \tag{4.31}$$

where, $\bar{V}_i^q$ and $\bar{I}_{id}^q$ are the voltage and equivalent injection current at phase q of i^{th} bus, obtained from DSLF, respectively. Also, the inverter current of the IBDG, as shown in Fig. 4.1, is calculated using eq. (4.32) as

$$\mathbf{I_{inv}^{abc}} = \mathbf{I_{T_1,s}^{abc}} = (\mathbf{Y_{sp,T_1}^{abc}}\mathbf{V_i^{abc}} + \mathbf{Y_{ss,T_1}^{abc}}\mathbf{V_j^{abc}}) \tag{4.32}$$

Now, the KCL equations for all the buses of the system, except the inverter bus (j) (used for the connection of IBDG) and the substation bus, are written in the matrix form as (from eq. (2.10) of Subsection 2.2.1 of Chapter 2),

$$\Big[\mathbf{Y_{bus}}\Big]\Big[\mathbf{V}\Big] = \Big[\mathbf{I}\Big] \tag{4.33}$$

Details of the $[\mathbf{Y_{bus}}]$, $[\mathbf{V}]$ and $[\mathbf{I}]$ are given in eq. (2.10) of Subsection 2.2.1 of Chapter 2. If a transformer $'T_2'$, with its nodal admittance matrix model of eq. (4.3), is connected between bus k and bus l of the distribution system, as shown in Fig. 4.1, then the following elements of the $[\mathbf{Y_{bus}}]$ matrix will be modified as,

$$\mathbf{Y_{kk,new}^{abc}} = \mathbf{Y_{kk}^{abc}} + \mathbf{Y_{pp,T_2}^{abc}} \tag{4.34a}$$

$$\mathbf{Y_{kl,new}^{abc}} = \mathbf{Y_{kl}^{abc}} + \mathbf{Y_{ps,T_2}^{abc}} \tag{4.34b}$$

$$\mathbf{Y_{lk,new}^{abc}} = \mathbf{Y_{lk}^{abc}} + \mathbf{Y_{sp,T_2}^{abc}} \tag{4.34c}$$

$$\mathbf{Y_{ll,new}^{abc}} = \mathbf{Y_{ll}^{abc}} + \mathbf{Y_{ss,T_2}^{abc}} \tag{4.34d}$$

Similarly, if an IBDG transformer 'T_1' (used for the connection of IBDG to the grid) is connected between bus i and j (inverter bus) of the distribution system, as shown in Fig. 4.1, the following elements of the $[\mathbf{Y_{bus}}]$ matrix will be modified as,

$$\mathbf{Y_{ii}^{abc}} = \mathbf{Y_{ii}^{abc}} + \mathbf{Y_{pp,T_1}^{abc}} \tag{4.35}$$

Also, due to the connection of IBDG, the current vector $[\mathbf{I}]$ will be modified to $[\mathbf{I_m}]$ as explained in eq. (3.5) of Subsection 3.2.1 of Chapter 3, and is given as,

$$[\mathbf{I_m}] = \begin{bmatrix} \mathbf{y_{12}^{abc}V_s^{abc}} & \cdots & \mathbf{Y_{ps,T_1}^{abc}V_{inv,st}^{abc}} & 0 & \cdots & 0 & 0 \end{bmatrix}^{\mathbf{T}} \tag{4.36}$$

where $\mathbf{V_{inv,st}^{abc}}$ is the three-phase inverter bus voltage vector, obtained from the DSLF. In Fig 4.1, j^{th} bus of the system is treated as an inverter bus and hence $\mathbf{V_{inv,st}^{abc}} = \mathbf{V_{j,st}^{abc}}$; $\mathbf{V_{j,st}^{abc}}$ is the j^{th} bus voltage vector, obtained from DSLF.

Now, for the short-circuit calculations, the $[\mathbf{Y_{bus}}]$ matrix is further modified to $[\mathbf{Y_{bus\_m}}]$, corresponding to the type of fault occurring in the system (as described in eq. (3.6) of Subsection 3.2.2 of Chapter 3). Hence, the initial estimate of the bus voltages under the fault conditions are calculated as (as given in eq. (3.6) of Subsection 3.2.2 of Chapter 3),

$$\begin{bmatrix} \mathbf{Y_{bus\_m}} \end{bmatrix} \begin{bmatrix} \mathbf{V} \end{bmatrix} = \begin{bmatrix} \mathbf{I_m} \end{bmatrix} \tag{4.37}$$

Also, the initial estimate of inverter current under the fault condition is calculated as,

$$\mathbf{I_{inv,f,est}^{abc}} = \mathbf{I_{T_{1_f},s}^{abc}} = (\mathbf{Y_{sp,T_1}^{abc}V_{i,f}^{abc}} + \mathbf{Y_{ss,T_1}^{abc}V_{inv,st}^{abc}}) \tag{4.38}$$

where, $\mathbf{V_{i,f}^{abc}}$ is the estimated i^{th} bus three phase voltage vector and $\mathbf{I_{T_{1_f},s}^{abc}}$ is the estimated secondary side three phase current vector of transformer T_1 under the fault conditions.

Next compare the magnitude of estimated inverter current with its short-circuit capacity (I_{sc}^{inv}), and

(i) If $|\bar{I}_{inv,f,est}^{q}| \leq I_{sc}^{inv}$; $(q = a, b, c)$, then the bus voltages calculated using eq. (4.37) are the final values of the bus voltages under the fault conditions (as discussed in Subsection 3.2.2 of Chapter 3),

(ii) If $|\bar{I}_{inv,f,est}^{q}| > I_{sc}^{inv}$; ($q = a$, or b, or c), then the inverter will operate in constant current mode ($|\bar{I}_{inv,f,est}^{q}| = I_{sc}^{inv}; (q = a, b, c)$) and the fault currents, bus voltages and branch currents under the fault conditions will be obtained using the fault analysis method given in Subsection 3.2.2 of Chapter 3.

4.4 Test results and discussions

To validate the proposed load flow and short-circuit analysis methods, the IEEE 123-bus modified test system [146] has been used. Five different sized IBDGs have been considered in this system.

The detailed information of these IBDGs is given in Table 4.1. These IBDGs are connected at different buses of the test system, as shown in column 2 of Table 4.1. The total installed capacity of IBDGs is considered as 25% of the total active power load in the system. The short-circuit capacity of each IBDG is assumed to be 150% of the rated inverter current of individual IBDGs. The injected reactive power limits of the IBDGs are shown in column 5 of Table 4.1. In this study, it is assumed that all IBDGs are operating at unity power factor when they operate in the "constant power mode" and at 0.85 power factor leading when they operate in "PV bus mode", in the pre-fault conditions. These IBDGs are connected to the system grid through three-phase step down transformers, named as IBDG transformers, with their turns ratio assumed as 4.16/0.480 kV. It is also assumed that the primary side windings of the transformer are connected to the three phase bus of the grid, while the secondary side windings are connected to the IBDG. These transformers can be of different vector groups. In this study, Delta/Star-grounded ($\Delta - Y_g$) and Star-grounded/Star-grounded ($Y_g - Y_g$) types of step down transformers have been assumed [150, 151]. The nodal admittance matrix model (p.u.) of the ΔY_g-1 and $Y_g Y_g$-0 transformers are given as [80],

$$\mathbf{Y_{T}}_{(\Delta Y_g 1)} = y_t \begin{bmatrix} \frac{2}{3} & -\frac{1}{3} & -\frac{1}{3} & -\frac{1}{\sqrt{3}} & \frac{1}{\sqrt{3}} & 0 \\ -\frac{1}{3} & \frac{2}{3} & -\frac{1}{3} & 0 & -\frac{1}{\sqrt{3}} & \frac{1}{\sqrt{3}} \\ -\frac{1}{3} & -\frac{1}{3} & \frac{2}{3} & \frac{1}{\sqrt{3}} & 0 & -\frac{1}{\sqrt{3}} \\ -\frac{1}{\sqrt{3}} & 0 & \frac{1}{\sqrt{3}} & 1 & 0 & 0 \\ \frac{1}{\sqrt{3}} & -\frac{1}{\sqrt{3}} & 0 & 0 & 1 & 0 \\ 0 & \frac{1}{\sqrt{3}} & -\frac{1}{\sqrt{3}} & 0 & 0 & 1 \end{bmatrix} \tag{4.39}$$

$$\mathbf{Y_{T}}_{(Y_g Y_g 0)} = y_t \begin{bmatrix} 1 & 0 & 0 & -1 & 0 & 0 \\ 0 & 1 & 0 & 0 & -1 & 0 \\ 0 & 0 & 1 & 0 & 0 & -1 \\ -1 & 0 & 0 & 1 & 0 & 0 \\ 0 & -1 & 0 & 0 & 1 & 0 \\ 0 & 0 & -1 & 0 & 0 & 1 \end{bmatrix} \tag{4.40}$$

where y_t is an equivalent transformer leakage admittance in p.u.. In this paper, the value of y_t is assumed as $(0.000 - j16.952)$ p.u. [146]. MATLAB environment has been used to implement the proposed method with a tolerance limit (ϵ) of 1.0×10^{-12}. Further for checking the accuracy of the proposed method, the obtained results have been compared to the results obtained from time

Table 4.1: Details of the IBDGs installed in the IEEE 123-bus modified test system

IBDG No.	**IBDG location (Bus No.)**	**IBDG installed capacity, P_{dg} (per phase) (kW)**	**Short-circuit current capacity, I_{sc}^{inv} (per phase) (Amp)**	**IBDG Reactive power limits (per phase) (kVAR)**
1.	20	140	251.87	-86.52 $\leq Q_{dg,1} \leq$ 86.52
2.	25	105	188.90	-64.89 $\leq Q_{dg,2} \leq$ 64.89
3.	75	140	251.87	-86.52 $\leq Q_{dg,3} \leq$ 86.52
4.	98	175	314.84	-108.15 $\leq Q_{dg,4} \leq$ 108.15
5.	104	280	503.74	-173.03 $\leq Q_{dg,5} \leq$ 173.03

domain simulation studies carried out using PSCAD/EMTDC software [139]. All the IBDGs have been represented as a constant current source in the time domain simulation study using the current values calculated by the proposed method.

4.4.1 Results for radial test distribution system

In this study, following two cases have been simulated using the proposed load flow method :

Case 1: Delta/Star-grounded (ΔY_g-1) transformers are used with all five IBDGs (as given in Table 4.1)

Case 2: Star-grounded/Star-grounded ($Y_g Y_g$-0) transformers are used with all five IBDGs (as given in Table 4.1)

4.4.1.1 Results of load flow studies

Two modes of operation of IBDG has been considered in the above two given cases. In Mode 1, IBDG is operating in "Constant active power mode", while in Mode 2, IBDG is operating in "PV mode". The phase a calculated complex power injected by the IBDGs corresponding to Mode 1 and Mode 2 operations for both cases are shown in columns 2-3 and 6-7 of Table 4.2, respectively. This table shows that, in Mode-1 operation, only active power is injected by the IBDGs to the grid. On the other hand, in Mode-2 operation, to improve the system voltage profile, required amount of reactive power has also been injected (along with active power) by the IBDGs to the grid. The calculated inverter currents of all IBDGs (phase a) in Mode 1 and Mode 2 operations for both the cases are shown in columns 4-5 and 8-9 of Table 4.2, respectively. The magnitude of inverter

Table 4.2: Injected power by the IBDGs and Inverter currents of phase a in Mode 1 and Mode 2 operation of IBDGs, for case 1 and case 2, of radial test distribution system under normal operating conditions

IBDG No.	ΔY_g1- IBDG transformer configuration				Y_gY_g0- IBDG transformer configuration			
	Injected Power (kVA)		Inverter Current (Amp)		Injected Power (kVA)		Inverter Current (Amp)	
	Mode 1	Mode 2	Mode 1	Mode 2	Mode 1	Mode 2	Mode 1	Mode 2
1	140.00-j00.00	140.00-j86.52	169.40∠-30.00^o	198.16∠-61.93^o	140.00-j00.00	140.00-j86.52	170.05∠-0.17^o	198.97∠-32.11^o
2	105.00-j00.00	105.00-j64.89	127.08∠-30.02^o	148.66∠-61.96^o	105.00-j00.00	105.00-j64.89	127.56∠-0.21^o	149.25∠-32.15^o
3	140.00-j00.00	140.00-j86.52	170.18∠-29.89^o	198.31∠-61.91^o	140.00-j00.00	140.00-j86.52	170.83∠-0.07^o	199.10∠-32.11^o
4	175.00-j00.00	175.00-j104.83	212.63∠-29.77^o	245.25∠-61.03^o	175.00-j00.00	175.00-j104.76	213.67∠0.11^o	246.39∠-31.17^o
5	280.00-j00.00	280.00-j79.81	339.88∠-29.58^o	349.88∠-45.78^o	280.00-j00.00	280.00-j79.34	341.04∠0.26^o	350.96∠-15.89^o

currents in Mode 2 is greater than in Mode 1, due to the extra capacitive reactive power injection in Mode 2.

The voltage profiles of phase a of the test distribution system, obtained by the proposed load flow method for Mode 1 and Mode 2 operation of IBDGs, for the two given cases are shown in Figs. 4.2(a) and (b), respectively. These figures show that, as expected, the voltage profiles in Mode 2 operation of IBDGs are much better than in Mode 1 operation for both the cases, due to the injection of capacitive reactive power.

The voltage profiles of phase a in Mode 1 operation of the IBDGs for the two cases have also been obtained by the PSCAD/EMTDC simulation studies and are shown in Figs. 4.3(a) and (b), respectively, along with the voltage profiles obtained by the proposed method. These figures show that, the voltage profiles obtained by the proposed method in both the cases are very close to the voltage profiles obtained from the PSCAD/EMTDC simulation studies, which validates the accuracy of the proposed load flow method.

4.4.1.2 Results of short-circuit studies

In this work, again two different scenarios have been considered (as described in Subsection 3.3.1 of Chapter 3),

Scenario 1: In this scenario, it is assumed that the IBDG control scheme is not dependent on the inverter bus terminal voltage,

Scenario 2: In this scenario, it is assumed that the IBDG control scheme is dependent on the inverter bus terminal voltage.

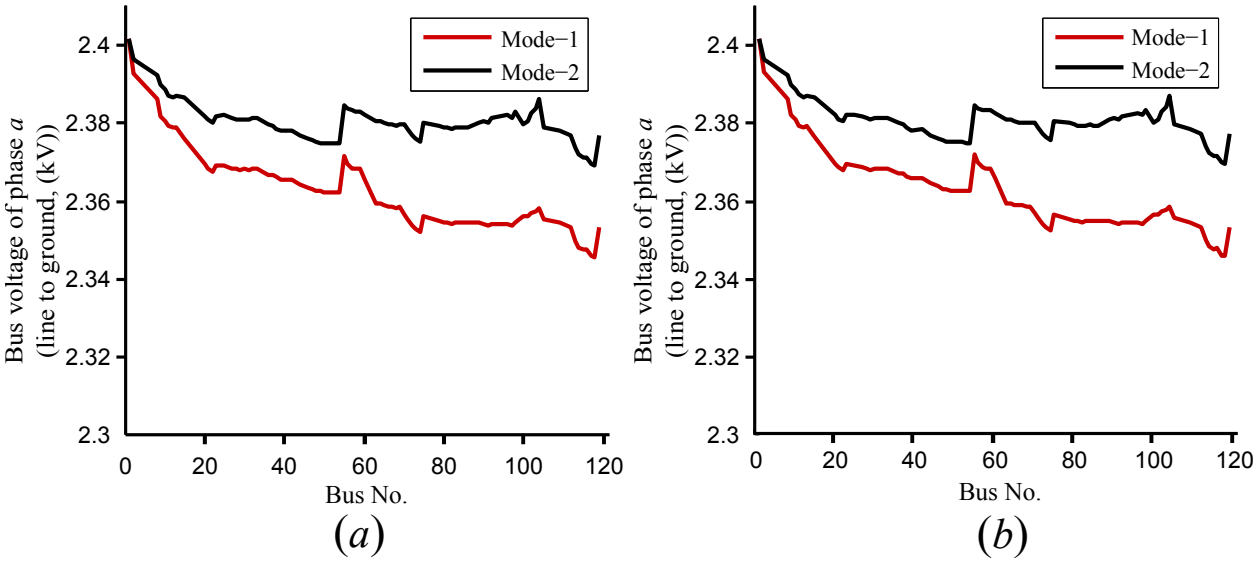

Figure 4.2: Voltage profile of phase a for radial test system with (a) ΔY_g-1 (Case 1) and (b) $Y_g Y_g$-0 (Case 2) IBDG transformers under normal operating conditions

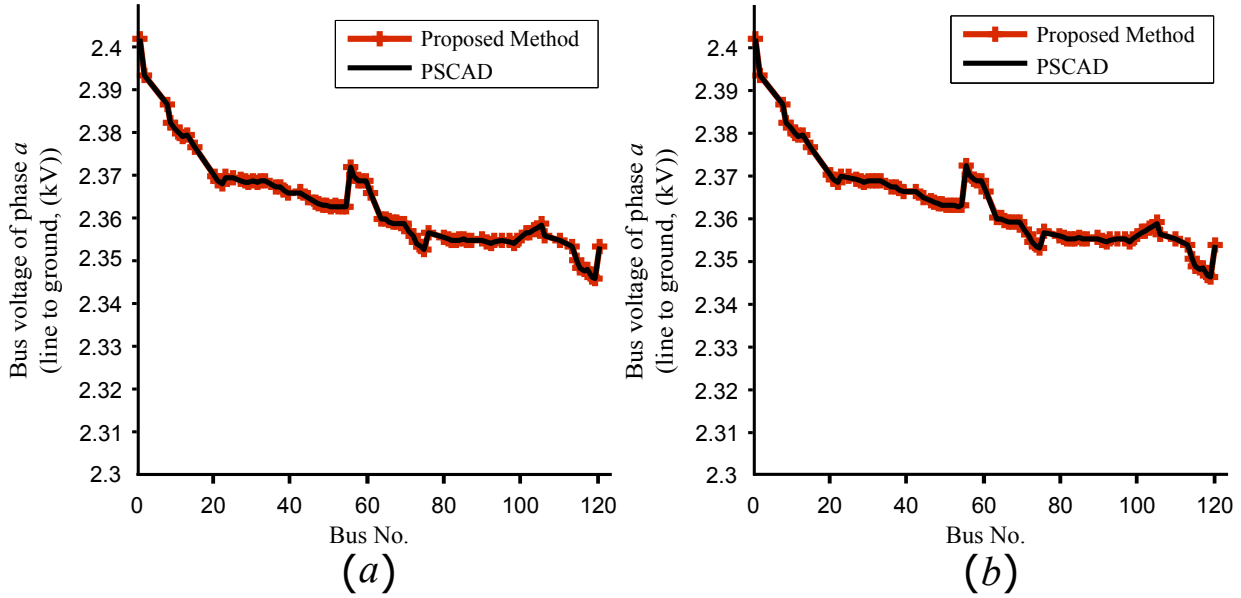

Figure 4.3: Voltage profile of phase a for radial test system with (a) ΔY_g-1 (Case 1) and (b) $Y_g Y_g$-0 (Case 2) IBDG transformers, using proposed technique and PSCAD/EMTDC simulation under normal operating conditions

An SLG fault in phase a of bus 105, with a fault impedance $\bar{z}_f$ = 0.001+0.000i p.u. has been assumed for the two given cases (Case 1 and 2). In the first step, the inverter currents $\left(\mathbf{I}^{\mathbf{abc}}_{\mathbf{inv,f,est}}\right)$ of

Table 4.3: Results for SLG(a-g) fault in modified IEEE 123-bus radial distribution system with IBDGs and ΔY_g-1 IBDG transformers (Case 1) for scenario 1

IBDG location (bus No.)	Initial estimate of inverter current, $\mathbf{I}^{\mathbf{abc}}_{\mathbf{inv,f,est}}$, (kA) when $\mathbf{V}^{\mathbf{abc}}_{\mathbf{inv,f}} = \mathbf{V}^{\mathbf{abc}}_{\mathbf{inv,st}}$			final value of inverter current, (kA) $\mathbf{I}^{\mathbf{abc}}_{\mathbf{inv,f}} = I^{inv}_{sc}\angle(\frac{\pi}{2} + \theta^{\mathbf{abc}}_{\mathbf{inv,f}})$			final value of injected IBDG power (kVAR)		
	Phase-a	**Phase-b**	**Phase-c**	**Phase-a**	**Phase-b**	**Phase-c**	**Phase-a**	**Phase-b**	**Phase-c**
20	1.504∠-60.52^o	1.134∠122.15^o	0.374∠111.43^o	0.252∠-124.64^o	0.252∠122.93^o	0.252∠-1.78^o	188.760	192.886	212.189
25	1.169∠-54.38^o	0.879∠128.78^o	0.294∠116.24^o	0.189∠-124.67^o	0.189∠122.91^o	0.189∠-1.82^o	141.493	144.626	159.121
75	7.424∠-75.12^o	7.184∠104.73^o	0.238∠109.06^o	0.252∠-133.84^o	0.252∠130.99^o	0.252∠-2.47^o	155.730	160.992	213.515
98	3.165∠-58.10^o	2.804∠122.97^o	0.363∠113.66^o	0.315∠-133.98^o	0.315∠130.73^o	0.315∠-2.64^o	195.703	202.120	267.824
104	5.345∠-66.42^o	4.942∠114.47^o	0.407∠102.72^o	0.504∠-135.16^o	0.504∠132.00^o	0.504∠-2.58^o	307.352	317.670	430.224

all the five IBDGs have been estimated (for scenario 1) by assuming that the inverter bus voltages under the fault condition ($\mathbf{V}^{\mathbf{abc}}_{\mathbf{inv,f}}$) of all IBDGs are maintained at their pre-fault values ($\mathbf{V}^{\mathbf{abc}}_{\mathbf{inv,st}}$). The calculated currents for the two cases are given in Tables 4.3 and 4.4, respectively. Both the tables show that, the magnitude of inverter currents $\left(|\mathbf{I}^{\mathbf{abc}}_{\mathbf{inv,f,est}}|\right)$ of all the IBDGs are greater than their short-circuit current capacities, given in Table 4.1. Hence, according to the inverter control strategy (as discussed in Case 2 of Subsection 3.2.2 of Chapter 3), the magnitudes of inverter currents of all the phases are to be limited to their short-circuit current capacities $\left(|\mathbf{I}^{\mathbf{p}}_{\mathbf{inv,f}}| = I^{inv}_{sc}, p = a, b, c\right)$ and their angles are maintained in such a way that all IBDGs will deliver reactive power to the system during the short-circuit condition ($\mathbf{\Psi}^{\mathbf{p}}_{\mathbf{inv,f}} = \frac{\pi}{2} + \theta^{\mathbf{p}}_{\mathbf{dg,f}}, p = a, b, c$). With this strategy, the inverter currents ($\mathbf{I}^{\mathbf{abc}}_{\mathbf{inv,f}}$) and the injected powers by all IBDGs under the fault conditions for both the cases are recalculated using the short-circuit analysis method (as given in Subsection 3.2.2 of Chapter 3) and their values for the two cases (for scenario 1) are given in Tables 4.3 and 4.4, respectively.

The results for SLG fault in phase a of bus 105, with a fault impedance $\bar{z}_f$ = 0.001+0.000i p.u., for the two given cases (for the scenarios 1 and 2) are shown in Tables 4.5 and 4.6, respectively. The intermediate inverter bus voltage magnitude, obtained in scenario 1, for all IBDGs under the fault condition for the two cases are shown in columns 2-4 of Tables 4.5 and 4.6, respectively. The intermediate power injected by the IBDGs, obtained in scenario 1, for the two cases are also shown in column 5 of Tables 4.5 and 4.6, respectively. Following the steps 7-11 of the algorithm described in Subsection 3.2.2.1 of Chapter 3, for case 1, the IBDGs at bus no. 20 and 25 are

Table 4.4: Results for SLG(a-g) fault in modified IEEE 123-bus radial distribution system with IBDGs and Y_gY_g-0 IBDG transformers (Case 2) for scenario 1

IBDG location (bus No.)	**Initial estimate of inverter current, $\mathbf{I}^{\mathbf{abc}}_{\mathbf{inv,f,est}}$, (kA) when $\mathbf{V}^{\mathbf{abc}}_{\mathbf{inv,f}} = \mathbf{V}^{\mathbf{abc}}_{\mathbf{inv,st}}$**			**final value of inverter current, (kA) $\mathbf{I}^{\mathbf{abc}}_{\mathbf{inv,f}} = I^{inv}_{sc}\angle(\frac{\pi}{2} + \theta^{\mathbf{abc}}_{\mathbf{inv,f}})$**			**final value of injected IBDG power (kVAR)**		
	Phase-a	**Phase-b**	**Phase-c**	**Phase-a**	**Phase-b**	**Phase-c**	**Phase-a**	**Phase-b**	**Phase-c**
20	5.435∠-68.35^o	0.091∠-74.26^o	0.548∠121.63^o	0.252∠-90.64^o	0.252∠143.24^o	0.252∠34.25^o	144.87	227.54	222.69
25	3.715∠-60.47^o	0.372∠109.18^o	0.928∠117.82^o	0.189∠-90.69^o	0.189∠143.23^o	0.189∠34.21^o	108.623	170.653	166.899
75	39.687∠-78.94^o	4.526∠-70.13^o	4.589∠-69.33^o	0.252∠-91.99^o	0.252∠134.62^o	0.252∠42.35^o	28.438	258.278	251.257
98	12.366∠-62.78^o	1.222∠103.59^o	2.366∠111.74^o	0.315∠-91.93^o	0.315∠134.34^o	0.315∠42.16^o	36.710	323.282	315.566
104	24.678∠-71.24^o	0.246∠-22.85^o	0.635∠77.57^o	0.504∠-95.45^o	0.504∠133.67^o	0.504∠43.23^o	32.137	527.681	513.274

Table 4.5: Intermediate (after scenario 1) and final (after scenario 2) inverter bus voltages and injected power by IBDGs for SLG(a-g) fault at bus 105, with $\bar{z}_f$ = 0.001+0.000i p.u., for Case 1

IBDG Location (bus No.)	**Intermediate inverter bus voltage magnitude (p.u.)**			**Intermediate injected power by IBDG (kVA)**	**Final inverter bus voltage magnitude (p.u.)**			**Control mode of operation of IBDG**	**Final injected power by IBDG (kVA)**
	Phase-a	**Phase-b**	**Phase-c**		**Phase-a**	**Phase-b**	**Phase-c**		
20	0.90143	0.92114	1.01332	0.0 + *j* 593.8	0.89609	0.91586	1.00702	Active-power	420.0 + *j* 0.0
25	0.90094	0.92089	1.01319	0.0 + *j* 445.3	0.89590	0.91583	1.00706	Active-power	315.0 + *j* 0.0
75	0.74370	0.76883	1.01966	0.0 + *j* 530.2	0.74220	0.76757	1.01741	Boost	0.0 + *j* 529.2
98	0.74767	0.77219	1.02321	0.0 + *j* 665.6	0.74617	0.77094	1.02096	Boost	0.0 + *j* 664.3
104	0.73389	0.75853	1.02728	0.0 + *j* 1055.2	0.73242	0.75728	1.02503	Boost	0.0 + *j* 1053.2

operated in "active power mode" in scenario 2, while the remaining three IBDGs are operated in "boost mode" (as shown in column 9 of Table 4.5). However, in case 2, the IBDGs at bus no. 20 and 25 are operated in "boost mode", while the remaining three IBDGs have been disconnected from the system (as shown in column 9 of Table 4.6). The final terminal voltages of the IBDGs and the reactive power exchanged by the IBDGs under the fault condition (in scenario 2) for the two given cases are shown in columns 6-8 and column 10 of Tables 4.5 and 4.6, respectively. The final inverter bus voltages under the fault condition in case 2, corresponding to the IBDGs located at bus No. 75, 98 and 104, are not shown in columns 6-8 of Table 4.6, since these IBDGs have been disconnected from the system.

Various short-circuit studies for two different scenarios have also been performed using the

Table 4.6: Intermediate (after scenario 1) and final (after scenario 2) inverter bus voltages and injected power by IBDGs for SLG(a-g) fault at bus 105, with $\bar{z}_f$ = 0.001+0.000i p.u., for Case 2

IBDG Location	**Intermediate inverter bus voltage magnitude (p.u.)**			**Intermediate injected power**	**Final inverter bus voltage magnitude (p.u.)**			**Control mode of operation**	**Final injected power by IBDG**
(bus No.)	**Phase-a**	**Phase-b**	**Phase-c**	**by IBDG (kVA)**	**Phase-a**	**Phase-b**	**Phase-c**	**of IBDG**	**(kVA)**
20	0.69185	1.08663	1.06347	0.0 + *j* 595.1	0.69150	1.07993	1.05198	Boost	0.0 + *j* 591.2
25	0.69165	1.08662	1.06272	0.0 + *j* 446.2	0.69130	1.07992	1.05123	Boost	0.0 + *j* 443.3
75	0.13581	1.23342	1.19989	0.0 + *j* 537.9	-			Cut-off	0.0 + *j* 0.0
98	0.14025	1.23508	1.20560	0.0 + *j* 675.6	-			Cut-off	0.0 + *j* 0.0
104	0.07674	1.25999	1.22558	0.0 + *j* 1073.1	-			Cut-off	0.0 + *j* 0.0

proposed short-circuit analysis method. The following unsymmetrical short-circuit faults have been simulated on the study system for the two given cases:

1. A single line-to-ground (SLG) fault in phase a of bus 105 with a fault impedance $z_f = 0.001 + 0.000i$ p.u.

2. A double line-to-ground (LLG) fault between phases a and b of bus 105 with a fault impedance $z_f = 0.001 + 0.000i$ p.u.

3. A three line-to-ground (LLLG) fault at bus 105 with a fault impedance $z_f = 0.001 + 0.000i$ p.u.

4. A line-to-line (LL) fault between phases a and b of bus 105 with a fault impedance $z_f = 0.001 + 0.000i$

The results for the above mentioned short-circuit studies in scenario 1 have been tabulated in Tables 4.7 and 4.8. The fault current (I_f) and the source current (I_s) values for various short-circuit faults obtained from the proposed method for case 1 are given in columns 4 and 7 of Table 4.7, respectively. The above fault cases have also been simulated using PSCAD/EMTDC time domain simulation software and the obtained fault current and the source current values are given in columns 3 and 6 of Table 4.7, respectively. The % error in calculated I_f and I_s by the proposed method with respect to the PSCAD/EMTDC results are given in columns 5 and 8 of Table 4.7, respectively. The maximum % errors in calculated I_f and I_s values are 0.00393% and 0.00370%,

Table 4.7: Error analysis of proposed method with respect to PSCAD/EMTDC simulation studies for various short-circuit faults at bus 105 (in scenario 1) in radial test system with ΔY_g-1 IBDG transformers (Case 1)

Fault type	**phase**	**Fault current at fault point (I_f)**		**% Error in I_f**	**Current drawn from the supply (I_s)**		**% Error in I_s**
		PSCAD simulation (kA)	**Proposed technique (kA)**		**PSCAD simulation (kA)**	**Proposed technique (kA)**	
SLG (a-g)	a	2.86610	2.86621	**0.00393**	2.82871	2.82881	0.00356
LLG (ab-g)	a	4.14499	4.14515	0.00379	4.16210	4.16225	0.00364
	b	4.29691	4.29707	0.00386	4.20435	4.20450	0.00369
LLLG (abc-g)	a	4.55015	4.55033	0.00387	4.49900	4.49916	0.00362
	b	4.85051	4.85069	0.00382	4.77458	4.77475	0.00359
	c	4.83822	4.83840	0.00387	4.77407	4.77424	0.00366
L-L (a-b)	a	4.09535	4.09550	0.00383	4.18227	4.18242	**0.00370**
	b	4.09535	4.09550	0.00383	3.96802	3.96816	0.00356

Table 4.8: Error analysis of proposed method with respect to PSCAD/EMTDC simulation studies for various short-circuit faults at bus 105 (in scenario 1) in radial test system with Y_gY_g-0 IBDG transformers (Case 2)

Fault type	**phase**	**Fault current at fault point (I_f)**		**% Error in I_f**	**Current drawn from the supply (I_s)**		**% Error in I_s**
		PSCAD simulation (kA)	**Proposed technique (kA)**		**PSCAD simulation (kA)**	**Proposed technique (kA)**	
SLG (a-g)	a	2.86046	2.86057	0.00387	2.80929	2.80939	0.00344
LLG (ab-g)	a	4.16867	4.16882	0.00381	4.15484	4.15499	0.00358
	b	4.30872	4.30889	**0.00396**	4.20520	4.20533	0.00363
LLLG (abc-g)	a	4.55135	4.55150	0.00389	4.49843	4.49853	0.00362
	b	4.84517	4.84532	0.00382	4.77608	4.77622	0.00361
	c	4.84244	4.84260	0.00391	4.77294	4.77318	0.00366
L-L (a-b)	a	4.06310	4.06321	0.00366	4.20942	4.20950	**0.00372**
	b	4.06310	4.06321	0.00366	3.95194	3.95203	0.00359

respectively. Similarly, the values of I_f and I_s for various short-circuit studies obtained by the proposed method and the PSCAD/EMTDC simulation study for case 2, are shown in Table 4.8. The maximum % errors in the estimated values of I_f and I_s, obtained from the proposed method, with respect to PSCAD/EMTDC software results are 0.00396% and 0.00372%, as shown in Table 4.8, respectively. These small values of errors establish that the proposed short circuit analysis method is quite accurate.

Table 4.9: Results for different short-circuit faults at bus 105, with $\bar{z}_f$ = 0.001+0.000i p.u., using proposed technique (scenario 2) and PSCAD/EMTDC simulation for Case 1

Fault type	**phase**	**Fault current at fault point (I_f)**		**Control mode operation of IBDG**	**Current drawn from the supply (I_s)**	
		PSCAD simulation (kA)	**Proposed technique (kA)**		**PSCAD simulation (kA)**	**Proposed technique (kA)**
SLG (a-g)	a	2.86197	2.86208	Active power-: IBDG No. 1,2 Boost-: IBDG No. 3,4,5	2.85252	2.85264
LLG (ab-g)	a	4.10039	4.10055	Boost-: IBDG No. 1,2	4.15976	4.15992
	b	4.24428	4.24445	Cut-off-: IBDG No. 3,4,5	4.23276	4.23292
LLLG (abc-g)	a	4.47628	4.47645	Boost-: IBDG No. 1,2	4.50857	4.50874
	b	4.77909	4.77928	Cut-off-: IBDG No. 3,4,5	4.78340	4.78358
	c	4.76754	4.76773		4.78172	4.78190
L-L (a-b)	a	4.04999	4.05014	Boost-: IBDG No. 1,2	4.16139	4.16155
	b	4.04999	4.05014	Cut-off-: IBDG No. 3,4,5	4.00209	4.00224

The above mentioned short-circuit studies have also been simulated for the two given cases in scenario 2 using the proposed method. The results for the two cases are shown in Tables 4.9 and 4.10, respectively. The results of the above short-circuit studies in scenario 2 for both the cases have also been obtained from the PSCAD/EMTDC simulation studies and are given in Tables 4.9 and 4.10, respectively. It can be observed from the tables, that the results obtained by proposed method match very well with the results obtained by the PSCAD/EMTDC simulation studies. Also, the control mode operation of the IBDGs for various fault studies for both the cases are shown in column 5 of Tables 4.9 and 4.10, respectively.

4.4.2 Results for weakly meshed test distribution system

To validate the performance of the proposed method for the meshed networks, the IEEE 123-bus modified meshed distribution system has been used [146]. In this work, again the following two cases have been considered :

Case 1: Delta/Star-grounded (ΔY_g-1) transformers used with all five IBDGs

Case 2: Star-grounded/Star-grounded ($Y_g Y_g$-0) transformers used with all five IBDGs.

Table 4.10: Results for different short-circuit faults at bus 105, with $\bar{z}_f$ = 0.001+0.000i p.u., using proposed technique (scenario 2) and PSCAD/EMTDC simulation for Case 2

Fault type	**phase**	**Fault current at fault point (I_f)**		**Control mode operation of IBDG**	**Current drawn from the supply (I_s)**	
		PSCAD simulation (kA)	**Proposed technique (kA)**		**PSCAD simulation (kA)**	**Proposed technique (kA)**
SLG (a-g)	a	2.82625	2.82636	Boost-: IBDG No. 1,2 Cut-off-: IBDG No. 3,4,5	2.85886	2.85897
LLG (ab-g)	a	4.10157	4.10173	Boost-: IBDG No. 1,2	4.15670	4.15686
	b	4.24454	4.24471	Cut-off-: IBDG No. 3,4,5	4.23235	4.23251
LLLG (abc-g)	a	4.47644	4.47661	Boost-: IBDG No. 1,2	4.50819	4.50835
	b	4.77867	4.77886	Cut-off-: IBDG No. 3,4,5	4.78430	4.78448
	c	4.76778	4.76795		4.78114	4.78132
L-L (a-b)	a	4.04969	4.04984	Boost-: All IBDGs	4.16413	4.16428
	b	4.04969	4.04984		4.00094	4.00108

4.4.2.1 Results of load flow studies

Two modes of operation of IBDG, as discussed in previous subsection, have also been considered in this study. The results of load flow for Mode 1 and Mode 2 operations of IBDGs for the two cases are shown in Table 4.11. In Mode 2 operation of IBDGs, the required capacitive reactive power is also injected (in conjunction with the active power) by the IBDGs, as shown in columns 3 and 7 of Table 4.11. This results in a higher magnitude of inverter currents in Mode 2 operation of IBDGs as compared to Mode 1 operation of IBDGs, as shown in columns 4-5 and 8-9 of Table 4.11.

The voltage profiles for phase a of the meshed distribution network, corresponding to Mode 1 and Mode 2 operation of IBDGs for the two given cases, are shown in Figs. 4.4(a) and (b), respectively. These figures show that the voltage profiles in Mode 2 operation are better than in Mode 1 operation of IBDGs. This is due to the injection of capacitive reactive power by the IBDG to the grid.

To validate the accuracy of the proposed method for the meshed network, the voltage profiles for phase a of the test system obtained by the proposed method in Mode 1 operation of IBDGs for both the cases have been plotted along with the voltage profiles obtained from the PSCAD/EMTDC

Table 4.11: Injected power by the IBDGs and Inverter currents of phase a in Mode 1 and Mode 2 operation of IBDGs, for case 1 and case 2, of weakly meshed test distribution system

IBDG No.	ΔY_g1- IBDG transformer configuration				Y_gY_g0- IBDG transformer configuration			
	Injected Power (kVA)		Inverter Current (Amp)		Injected Power (kVA)		Inverter Current (Amp)	
	Mode 1	Mode 2	Mode 1	Mode 2	Mode 1	Mode 2	Mode 1	Mode 2
1	140.00-j00.00	140.00-j86.52	169.56 ∠-29.99^o	198.27∠-61.92^o	140.00-j00.00	140.00-j86.52	170.13∠-0.17^o	199.00∠-32.10^o
2	105.00-j00.00	105.00-j64.89	127.24∠-30.02^o	148.78∠-61.95^o	105.00-j00.00	105.00-j64.89	127.66∠-0.22^o	149.32∠-32.15^o
3	140.00-j00.00	140.00-j86.51	169.76∠-29.90^o	198.23∠-61.91^o	140.00-j00.00	140.00-j86.52	170.61∠-0.08^o	199.19∠-32.09^o
4	175.00-j00.00	175.00-j91.80	212.11∠-29.78^o	237.53∠-57.77^o	175.00-j00.00	175.00-j91.78	213.40∠0.01^o	238.89∠-27.91^o
5	280.00-j00.00	280.00-j71.18	339.04∠-29.59^o	347.10∠-44.13^o	280.00-j00.00	280.00-j70.36	340.60∠0.25^o	348.39∠-14.15^o

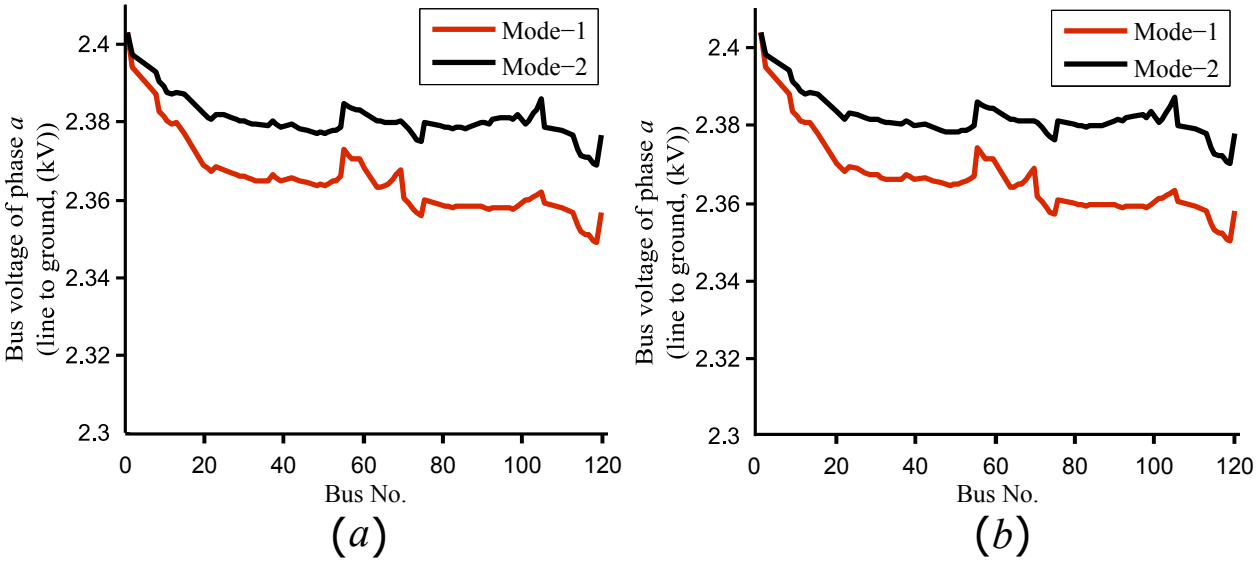

Figure 4.4: Voltage profile of phase a for meshed test system with (a) ΔY_g-1 (Case 1) and (b) Y_gY_g-0 (Case 2) IBDG transformers under normal operating conditions

simulation studies, as shown in Figs. 4.5(a) and (b), respectively. These figures show that the voltage profiles obtained from the proposed method and PSCAD/EMTDC simulation study are very close to each other.

4.4.2.2 Results of short-circuit studies

Again, for the meshed distribution test system, an SLG fault in phase a of bus 105, with a fault impedance $\bar{z}_f$ = 0.001+0.000i p.u. has been assumed. The SLG fault has been simulated using the

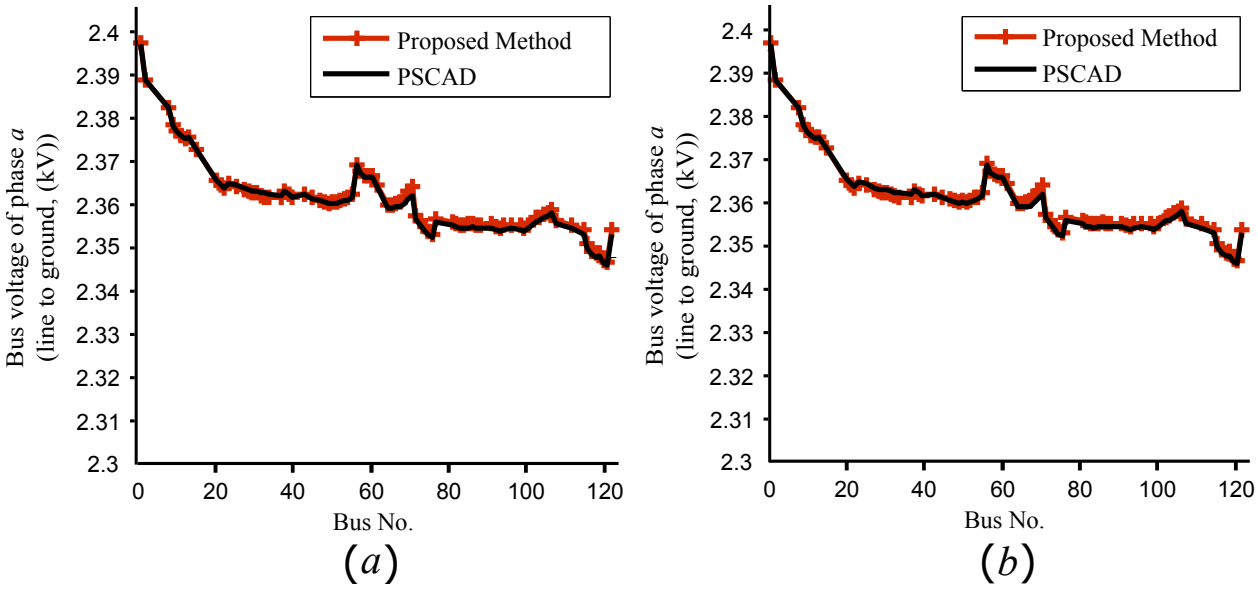

Figure 4.5: Voltage profile of phase a for meshed test system with (a) ΔY_g-1 (Case 1) and (b) $Y_g Y_g$-0 (Case 2) IBDG transformers, using proposed technique and PSCAD/EMTDC simulation under normal operating conditions

proposed short-circuit analysis method for the two given cases (Case 1 and 2). In the first step, the initial estimate of inverter currents $\left(\mathbf{I}^{\mathbf{abc}}_{\mathbf{inv,f,est}}\right)$ of all the five IBDGs has been obtained under the fault condition. The estimated values of inverter currents for the two cases are given in Tables 4.12 and 4.13, respectively. Both the tables show that, the magnitude of inverter currents $\left(|\mathbf{I}^{\mathbf{abc}}_{\mathbf{inv,f,est}}|\right)$ of all the IBDGs are greater than their short-circuit current capacities, given in Table 4.1. Hence, the inverter control strategy, as discussed in Case 2 of Subsection 3.2.2 of Chapter 3, has been applied and the inverter currents ($\mathbf{I}^{\mathbf{abc}}_{\mathbf{inv,f}}$) and the injected powers by all IBDGs under the fault conditions for both the cases are recalculated using the proposed short-circuit analysis method. The obtained values of inverter currents and the injected powers by the IBDGs for the two cases are given in Tables 4.12 and 4.13, respectively.

The results for SLG fault in phase a of bus 105, with a fault impedance $\bar{z}_f$ = 0.001+0.000i p.u., in two different scenarios for the two given cases are shown in Tables 4.14 and 4.15, respectively. The intermediate inverter bus voltage magnitude, obtained in scenario 1, for all IBDGs under the fault condition for the two cases are shown in columns 2-4 of Tables 4.14 and 4.15, respectively. The intermediate power injected by the IBDGs, obtained in scenario 1, for the two cases are also shown in column 5 of Tables 4.14 and 4.15, respectively. For case 1, all the IBDGs are operated in

Table 4.12: Results for SLG(a-g) fault in modified IEEE 123-bus meshed distribution system with IBDGs and ΔY_g-1 IBDG transformers (Case 1) for scenario 1

IBDG location (bus No.)	**Initial estimate of inverter current, $\mathbf{I}^{\mathbf{abc}}_{\mathbf{inv,f,est}}$, (kA) when $\mathbf{V}^{\mathbf{abc}}_{\mathbf{inv,f}} = \mathbf{V}^{\mathbf{abc}}_{\mathbf{inv,st}}$**			**final value of inverter current, (kA) $\mathbf{I}^{\mathbf{abc}}_{\mathbf{inv,f}} = I^{inv}_{sc}\angle(\frac{\pi}{2} + \theta^{\mathbf{abc}}_{\mathbf{inv,f}})$**			**final value of injected IBDG power (kVAR)**		
	Phase-a	**Phase-b**	**Phase-c**	**Phase-a**	**Phase-b**	**Phase-c**	**Phase-a**	**Phase-b**	**Phase-c**
20	2.450∠-56.21^o	2.132∠126.24^o	0.332∠107.94^o	0.252∠-126.93^o	0.252∠123.85^o	0.252∠-1.85 ^{o}	182.668	184.058	212.316
25	1.986∠-50.43^o	1.726∠131.76^o	0.268∠115.39^o	0.189∠-127.04^o	0.189∠123.85^o	0.189∠-1.89^o	136.768	137.767	159.170
75	7.824∠-75.39^o	7.564∠104.46^o	0.259∠109.22^o	0.252∠-133.17^o	0.252∠130.89^o	0.252∠-2.40^o	156.337	162.640	213.442
98	3.328∠-58.40^o	2.950∠122.53^o	0.381∠114.50^o	0.315∠-133.31^o	0.315∠130.64^o	0.315∠-2.57^o	196.462	204.184	267.733
104	5.761∠-66.35^o	5.349∠114.48^o	0.417∠103.03^o	0.504∠-134.75^o	0.504∠132.03^o	0.504∠-2.50^o	307.648	319.341	430.020

Table 4.13: Results for SLG(a-g) fault in modified IEEE 123-bus meshed distribution system with IBDGs and Y_gY_g-0 IBDG transformers (Case 2) for scenario 1

IBDG location (bus No.)	**Initial estimate of inverter current, $\mathbf{I}^{\mathbf{abc}}_{\mathbf{inv,f,est}}$, (kA) when $\mathbf{V}^{\mathbf{abc}}_{\mathbf{inv,f}} = \mathbf{V}^{\mathbf{abc}}_{\mathbf{inv,st}}$**			**final value of inverter current, (kA) $\mathbf{I}^{\mathbf{abc}}_{\mathbf{inv,f}} = I^{inv}_{sc}\angle(\frac{\pi}{2} + \theta^{\mathbf{abc}}_{\mathbf{inv,f}})$**			**final value of injected IBDG power (kVAR)**		
	Phase-a	**Phase-b**	**Phase-c**	**Phase-a**	**Phase-b**	**Phase-c**	**Phase-a**	**Phase-b**	**Phase-c**
20	9.189∠-61.17^o	0.183∠-36.87^o	0.324∠84.88^o	0.252∠-94.73^o	0.252∠141.59^o	0.252∠37.14^o	118.323	237.577	226.032
25	6.678∠-54.31^o	0.626∠108.27^o	1.076∠111.57^o	0.189∠-94.92^o	0.189∠141.52^o	0.189∠37.17^o	88.133	178.298	169.469
75	37.943∠-79.96^o	4.614∠-70.04^o	4.547∠-70.42^o	0.252∠-89.27^o	0.252∠135.08^o	0.252∠42.01^o	33.123	256.743	249.701
98	11.794∠-63.81^o	1.101∠99.76^o	2.236∠110.77^o	0.315∠-89.18^o	0.315∠134.80^o	0.315∠41.82^o	42.600	321.342	313.635
104	24.242∠-71.68^o	0.423∠-32.17^o	0.551∠67.00^o	0.504∠-92.26^o	0.504∠134.03^o	0.504∠43.09^o	36.948	526.037	510.840

"boost mode" (as shown in column 9 of Table 4.14). However, in case 2, the IBDGs at bus no. 20 and 25 are operated in "absorb mode", while the remaining three IBDGs have been disconnected from the system (as shown in column 9 of Table 4.15). The final terminal voltages of the IBDGs and the reactive power exchanged by the IBDGs under the fault condition (in scenario 2) for the two given cases are shown in columns 6-8 and column 10 of Tables 4.14 and 4.15, respectively. The final inverter bus voltages under the fault condition in case 2, corresponding to the IBDGs located at bus No. 75, 98 and 104, are not shown in columns 6-8 of Table 4.15, since these IBDGs have been disconnected from the system.

Various short-circuit studies, as given in the Subsection 4.4.1, have also been performed on meshed distribution network in scenario 1 using the proposed short-circuit analysis method. The results obtained in these studies for the two given cases are shown in Tables 4.16 and 4.17, respec-

Table 4.14: Intermediate (after scenario 1) and final (after scenario 2) inverter bus voltages and injected power by IBDGs for SLG(a-g) fault at bus 105, with $\bar{z}_f$ = 0.001+0.000i p.u., for Case 1 of meshed system

IBDG Location	**Intermediate inverter bus voltage magnitude (p.u.)**			**Intermediate injected power**	**Final inverter bus voltage magnitude (p.u.)**			**Control mode of operation**	**Final injected power by IBDG**
(bus No.)	**Phase-a**	**Phase-b**	**Phase-c**	**by IBDG (kVA)**	**Phase-a**	**Phase-b**	**Phase-c**	**of IBDG**	**(kVA)**
20	0.87234	0.87898	1.01393	0.0 + *j* 579.0	0.87234	0.87898	1.01393	Boost	0.0 + *j* 579.0
25	0.87085	0.87722	1.01350	0.0 + *j* 433.7	0.87085	0.87722	1.01350	Boost	0.0 + *j* 433.7
75	0.74659	0.77670	1.01930	0.0 + *j* 532.4	0.74659	0.77670	1.01930	Boost	0.0 + *j* 532.4
98	0.75057	0.78007	1.02286	0.0 + *j* 668.4	0.75057	0.78007	1.02286	Boost	0.0 + *j* 668.4
104	0.73459	0.76251	1.02679	0.0 + *j* 1057.0	0.73459	0.76251	1.02679	Boost	0.0 + *j* 1057.0

Table 4.15: Intermediate (after scenario 1) and final (after scenario 2) inverter bus voltages and injected power by IBDGs for SLG(a-g) fault at bus 105, with $\bar{z}_f$ = 0.001+0.000i p.u., for Case 2 of meshed system

IBDG Location	**Intermediate inverter bus voltage magnitude (p.u.)**			**Intermediate injected power**	**Final inverter bus voltage magnitude (p.u.)**			**Control mode of operation**	**Final injected power by IBDG**
(bus No.)	**Phase-a**	**Phase-b**	**Phase-c**	**by IBDG (kVA)**	**Phase-a**	**Phase-b**	**Phase-c**	**of IBDG**	**(kVA)**
20	0.56506	1.13456	1.07943	0.0 + *j* 581.9	0.55484	1.11034	1.04878	Absorb	0.0 - *j* 568.3
25	0.56118	1.13529	1.07908	0.0 + *j* 435.9	0.55143	1.11103	1.04845	Absorb	0.0 - *j* 425.7
75	0.15818	1.22609	1.19246	0.0 + *j* 539.6	-			Cut-off	0.0 + *j* 0.0
98	0.16275	1.22767	1.19822	0.0 + *j* 677.6	-			Cut-off	0.0 + *j* 0.0
104	0.08822	1.25606	1.21977	0.0 + *j* 1073.8	-			Cut-off	0.0 + *j* 0.0

tively. The results for these studies have also been obtained from the PSCAD/EMTDC simulation studies and are given in Tables 4.16 and 4.17. The maximum % errors in calculated values of I_f and I_s with respect to PSCAD/EMTDC results for case 1 are 0.00381% and 0.00365%, respectively, as shown in Table 4.16. Similarly, for case 2, the maximum % errors in calculated values of I_f and I_s with respect to PSCAD/EMTDC results are 0.00380% and 0.00361%, respectively, as shown in Table 4.17. These results again demonstrate the accuracy of the proposed method for the meshed distribution network.

The above mentioned short-circuit studies, as given in Subsection 4.4.1, have also been simulated for the two given cases in scenario 2 using the proposed method. The results for the two cases are shown in Tables 4.18 and 4.19, respectively. The results of the above short-circuit studies in

Table 4.16: Error analysis of proposed method with respect to PSCAD/EMTDC simulations for various short-circuit faults at bus 105 (in scenario 1) in meshed test system with ΔY_g-1 IBDG transformers (Case 1)

Fault type	**phase**	**Fault current at fault point (I_f)**		**% Error in I_f**	**Current drawn from the supply (I_s)**		**% Error in I_s**
		PSCAD simulation (kA)	**Proposed technique (kA)**		**PSCAD simulation (kA)**	**Proposed technique (kA)**	
SLG (a-g)	a	3.34798	3.34811	**0.00381**	3.31014	3.31026	0.00351
LLG (ab-g)	a	4.83345	4.83363	0.00368	4.84971	4.84988	0.00357
	b	5.03444	5.03462	0.00372	4.94387	4.94404	0.00350
LLLG (abc-g)	a	5.30245	5.30265	0.00375	5.25127	5.25145	0.00354
	b	5.67069	5.67090	0.00372	5.59680	5.59700	0.00352
	c	5.56508	5.56529	0.00378	5.50631	5.50651	0.00359
L-L (a-b)	a	4.79106	4.79124	0.00378	4.87704	4.87722	**0.00365**
	b	4.79106	4.79124	0.00378	4.66616	4.66632	0.00348

Table 4.17: Error analysis of proposed method with respect to PSCAD/EMTDC simulations for various short-circuit faults at bus 105 (in scenario 1) in meshed test system with Y_gY_g-0 IBDG transformers (Case 2)

Fault type	**phase**	**Fault current at fault point (I_f)**		**% Error in I_f**	**Current drawn from the supply (I_s)**		**% Error in I_s**
		PSCAD simulation (kA)	**Proposed technique (kA)**		**PSCAD simulation (kA)**	**Proposed technique (kA)**	
SLG (a-g)	a	3.34304	3.34317	**0.00380**	3.29092	3.29103	0.00341
LLG (ab-g)	a	4.85843	4.85861	0.00371	4.84168	4.84185	0.00349
	b	5.04501	5.04520	0.00380	4.94493	4.94510	0.00353
LLLG (abc-g)	a	5.30349	5.30369	0.00377	5.25076	5.25094	0.00352
	b	5.66494	5.66515	0.00371	5.59846	5.59866	0.00353
	c	5.57001	5.57022	0.00380	5.50490	5.50510	0.00358
L-L (a-b)	a	4.76035	4.76052	0.00358	4.90901	4.90919	**0.00361**
	b	4.76035	4.76052	0.00358	4.64722	4.64739	0.00354

scenario 2 for both the cases are also obtained from the PSCAD/EMTDC simulation studies and are given in Tables 4.18 and 4.19, respectively. It can be observed from the tables, that the results obtained by the proposed method match very well with the results obtained by the PSCAD/EMTDC simulation studies. Also, the control mode operation of the IBDGs for various fault studies for both the cases are shown in column 5 of Tables 4.18 and 4.19, respectively.

The proposed short-circuit analysis method is also suitable for the analysis of multiple faults in

Table 4.18: Results for different unsymmetrical short-circuit faults at bus 105, with $\bar{z}_f$ = 0.001+0.000i p.u., using proposed technique (scenario 2) and PSCAD/EMTDC simulation for Case 1 of meshed system

Fault type	**phase**	**Fault current at fault point (I_f)**		**Control mode operation of IBDG**	**Current drawn from the supply (I_s)**	
		PSCAD simulation (kA)	**Proposed technique (kA)**		**PSCAD simulation (kA)**	**Proposed technique (kA)**
SLG (a-g)	a	3.34798	3.34811	Boost-: IBDG No. 1-5	3.31013	3.31025
LLG (ab-g)	a	4.79077	4.79095	Boost-: IBDG No. 1,2	4.84791	4.84809
	b	4.98211	4.98229	Cut-off-: IBDG No. 3,4,5	4.97458	4.97476
LLLG (abc-g)	a	5.23038	5.23058	Boost-: IBDG No. 1,2	5.26281	5.26301
	b	5.60069	5.60090	Cut-off-: IBDG No. 3,4,5	5.60762	5.60782
	c	5.49611	5.49632		5.51536	5.51557
L-L (a-b)	a	4.74673	4.74691	Boost-: IBDG No. 1,2	4.85591	4.85609
	b	4.74673	4.74691	Cut-off-: IBDG No. 3,4,5	4.70357	4.70375

Table 4.19: Results for different unsymmetrical short-circuit faults at bus 105, with $\bar{z}_f$ = 0.001+0.000i p.u., using proposed technique (scenario 2) and PSCAD/EMTDC simulation for Case 2 of meshed system

Fault type	**phase**	**Fault current at fault point (I_f)**		**Control mode operation of IBDG**	**Current drawn from the supply (I_s)**	
		PSCAD simulation (kA)	**Proposed technique (kA)**		**PSCAD simulation (kA)**	**Proposed technique (kA)**
SLG (a-g)	a	3.28923	3.28936	Absorb-: IBDG No. 1,2 Cut-off-: IBDG No. 3,4,5	3.40710	3.40723
LLG (ab-g)	a	4.76009	4.76027	Absorb-: IBDG No. 1,2	4.88073	4.88091
	b	4.94979	4.94998	Cut-off-: IBDG No. 3,4,5	5.03674	5.03693
LLLG (abc-g)	a	5.23054	5.23073	Boost-: IBDG No. 1,2	5.26246	5.26266
	b	5.59998	5.60018	Cut-off-: IBDG No. 3,4,5	5.60855	5.60876
	c	5.49665	5.49686		5.51467	5.51488
L-L (a-b)	a	4.74585	4.74602	Boost-: All IBDGs	4.86168	4.86185
	b	4.74585	4.74602		4.70011	4.70028

radial as well as meshed distribution system. Two simultaneous faults, SLG (a-g) and LLG (bc-g) with a fault impedance $z_f = 0.001 + 0.000i$ p.u. have been simulated at bus 105 and 86, in radial as well as weakly meshed IEEE 123-bus distribution network for scenario 1, respectively. The results obtained from the proposed method and PSCAD/EMTDC simulation studies, are presented

Table 4.20: Error analysis of proposed technique with respect to PSCAD/EMTDC simulations for multiple faults (in scenario 1) in test distribution system with IBDGs and ΔY_g-1 IBDG transformer

Topology	Fault type	Fault Bus	phase	Fault current at fault point (I_f)		% Error in I_f	Current drawn from the supply (I_s)		% Error in I_s
				PSCAD simulation (kA)	Proposed technique (kA)		PSCAD simulation (kA)	Proposed technique (kA)	
Radial	SLG (a-g)	105	a	3.67374	3.67388	0.00381	3.63104	3.63117	0.00358
	LLG (bc-g)	86	b	3.07239	3.07251	**0.00390**	3.03567	3.03578	0.00362
			c	3.10273	3.10285	0.00386	3.04584	3.04595	**0.00361**
Meshed	SLG (a-g)	105	a	4.19367	4.19382	0.00357	4.15080	4.15094	0.00337
	LLG (bc-g)	86	b	3.37286	3.37299	**0.00385**	3.34201	3.34213	**0.00359**
			c	3.39329	3.39342	0.00383	3.33861	3.33872	0.00329

in Table 4.20. In this case, ΔY_g-1 transformers have been used with all the IBDGs. The maximum % errors in the value of I_f for radial and meshed distribution system are 0.00390% and 0.00385%, respectively, as shown in Table 4.20. Further, the maximum % errors in the value of I_s for radial and meshed distribution system are 0.00361% and 0.00359%, respectively, as shown in Table 4.20. Again, these small values of errors establish the accuracy of the proposed short-circuit analysis method.

4.5 Conclusion

In this chapter, accurate and efficient distribution system load flow and short-circuit analysis methods have been developed. The proposed methods are capable of incorporating various transformer models of different vector groups. These methods are also applicable to the analysis of multiple faults in radial as well as meshed distribution systems. The obtained results have been compared with the results of time domain simulation studies obtained using PSCAD/EMTDC simulation software. A good agreement in the results of the two methods establishes the accuracy of the proposed methods.

In the next chapter, the algorithms for the load flow and short-circuit analysis of the three phase four wire unbalanced radial distribution system with ground return are discussed.

Chapter 5

Load flow and short-circuit analysis of unbalanced three phase four wire multigrounded radial distribution system

Abstract

In this chapter, a new method for load flow and short-circuit analysis of an unbalanced three phase four wire multigrounded distribution system is proposed. Initially, a load flow method, based on $[\mathbf{BIBC}]$ *("Bus injection to branch current") and* $[\mathbf{BCBV}]$ *("Branch current to bus voltage") matrices of the system is proposed. Later on, in this chapter, two different short-circuit analysis methods, one based on* $\left[\mathbf{BIBC}\right]$ *and* $\left[\mathbf{BCBV}\right]$ *matrices of the system and the other one based on* $\left[\mathbf{Y_{bus}}\right]$ *matrix, are discussed. The proposed load flow and short-circuit methods have been tested on two test systems; i) modified unbalanced three phase four wire multigrounded IEEE 34-bus test system and ii) unbalanced three phase four wire multigrounded IEEE 123-bus test system. To validate the effectiveness of proposed methods, the results of modified IEEE 34-bus test system have been compared with the results of time domain simulation studies carried out using the PSCAD/EMTDC software.*

5.1 Introduction

THE three phase four wire distribution networks are commonly used in power distribution systems. It has been observed that a three phase four wire distribution system has more sensitivity towards the protection of various ground faults than a three phase three wire system [128]. The return current in neutral wire, under normal operating conditions, is mainly due to the unbalanced loads and unbalanced structure of distribution system. Sometimes, the neutral currents may be higher than the phase currents due to large unbalance in loads [128]. Also, the neutral in the distribution network plays an important role in safety and power quality problems [152–156]. It

is also a common practice to ground the neutral points directly or through a grounding impedance [128, 153, 157]. Hence, to calculate the neutral and ground currents in the system under normal operating conditions, load flow analysis of three phase four wire multigrounded distribution system is required. In the literature, most of the load flow analysis methods of three phase four wire multigrounded system are based on backward/forward approach [90, 128]. In this chapter, the direct approach of the load flow analysis of three phase three wire system has been modified for the analysis of three phase four wire multigrounded system. Further, in this chapter, two different short-circuit analysis methods for three phase four wire multigrounded distribution system are described.

This chapter is organized as follows. Section 5.2 describes the formulation of the proposed load flow analysis method for three phase four wire multigrounded distribution system. Section 5.3 describes the formulation of two proposed short-circuit analysis methods for three phase four wire multigrounded distribution system. The main results of this chapter are presented in Section 5.4 and finally Section 5.5 highlights the main conclusions of this chapter.

5.2 Load flow analysis of unbalanced three phase four wire multigrounded radial distribution system

Let us consider an unbalanced three phase four wire multigrounded radial distribution system having n_b bus and m_b lines, as shown in Fig. 5.1. The system has $(m_b - 2)$ three-phase lines, one two-phase line and one single-phase line. Each line section has its own neutral and fictitious ground (representing ground return) wires. The line section between buses l and m has two phases (phases a and b) while the line section between buses m and n_b has only one phase (phase a). Bus 1 represents the substation bus having its voltages as $\bar{V}_s^a$, $\bar{V}_s^b$ and $\bar{V}_s^c$ corresponding to the phases a, b and c, respectively. The impedance matrix of the three phase five wire line section between buses i and j $\left[\bar{\mathbf{z}}_{\mathbf{ij}}^{\mathbf{abcng}}\right]$, is given as,

$$\left[\bar{\mathbf{Z}}_{\mathbf{ij}}^{\mathbf{abcng}}\right] = \begin{bmatrix} \bar{z}_{ij}^{aa} & \bar{z}_{ij}^{ab} & \bar{z}_{ij}^{ac} & \bar{z}_{ij}^{an} & \bar{z}_{ij}^{ag} \\ \bar{z}_{ij}^{ba} & \bar{z}_{ij}^{bb} & \bar{z}_{ij}^{bc} & \bar{z}_{ij}^{bn} & \bar{z}_{ij}^{bg} \\ \bar{z}_{ij}^{ca} & \bar{z}_{ij}^{cb} & \bar{z}_{ij}^{cc} & \bar{z}_{ij}^{cn} & \bar{z}_{ij}^{cg} \\ \bar{z}_{ij}^{na} & \bar{z}_{ij}^{nb} & \bar{z}_{ij}^{nc} & \bar{z}_{ij}^{nn} & \bar{z}_{ij}^{ng} \\ \bar{z}_{ij}^{ga} & \bar{z}_{ij}^{gb} & \bar{z}_{ij}^{gc} & \bar{z}_{ij}^{gn} & \bar{z}_{ij}^{gg} \end{bmatrix}; \tag{5.1}$$

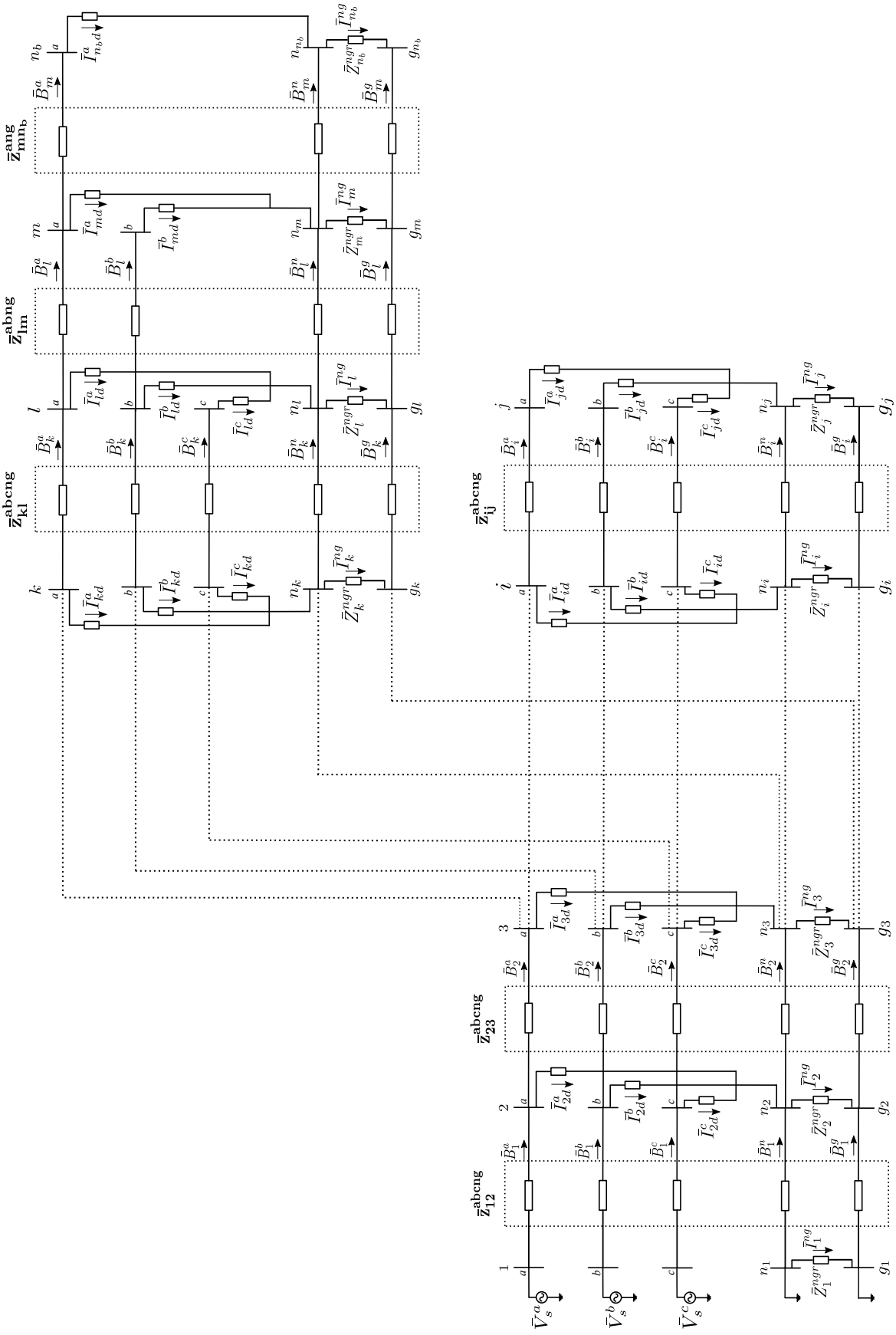

Figure 5.1: An unbalanced three phase four wire multigrounded radial distribution system

where $\bar{z}_{ij}^{pq} = \bar{z}_{ij}^{qp};\ p,q = a,b,c,n,g;\ p \neq q$; $\bar{z}_{ij}^{aa}$, $\bar{z}_{ij}^{bb}$ and $\bar{z}_{ij}^{cc}$ are the self impedances of phases a, b and c of the line section between buses i and j; $\bar{z}_{ij}^{nn}$ and $\bar{z}_{ij}^{gg}$ are the self impedances of neutral wire and ground wire of the line section between buses i and j, respectively. Similarly, $\bar{z}_{ij}^{ab}$, $\bar{z}_{ij}^{bc}$ and $\bar{z}_{ij}^{ac}$ are the mutual impedances between phases a and b, b and c, and a and c of the line section between buses i and j, respectively. Also, $\bar{z}_{ij}^{pn}$ is the mutual impedance between phase p ($p = a,b,c$) and neutral wire of the line section between buses i and j; $\bar{z}_{ij}^{pg}$ is the mutual impedance between phase p ($p = a,b,c$) and ground wire of the line section between buses i and j; $\bar{z}_{ij}^{ng}$ is the mutual impedances between neutral wire and ground wire of the line section between buses i and j. Similarly, the line impedance matrices of two phase line (having phases a and b) $\left[\bar{\mathbf{z}}_{\mathbf{lm}}^{\mathbf{abng}}\right]$ and single phase line (having phase a only) $\left[\bar{\mathbf{z}}_{\mathbf{mn_b}}^{\mathbf{ang}}\right]$ are given as,

$$\left[\bar{\mathbf{z}}_{\mathbf{lm}}^{\mathbf{abng}}\right] = \begin{bmatrix} \bar{z}_{lm}^{aa} & \bar{z}_{lm}^{ab} & \bar{z}_{lm}^{an} & \bar{z}_{lm}^{ag} \\ \bar{z}_{lm}^{ba} & \bar{z}_{lm}^{bb} & \bar{z}_{lm}^{bn} & \bar{z}_{lm}^{bg} \\ \bar{z}_{lm}^{na} & \bar{z}_{lm}^{nb} & \bar{z}_{lm}^{nn} & \bar{z}_{lm}^{ng} \\ \bar{z}_{lm}^{ga} & \bar{z}_{lm}^{gb} & \bar{z}_{lm}^{gn} & \bar{z}_{lm}^{gg} \end{bmatrix}; \left[\bar{\mathbf{z}}_{\mathbf{mn_b}}^{\mathbf{ang}}\right] = \begin{bmatrix} \bar{z}_{mn_b}^{aa} & \bar{z}_{mn_b}^{an} & \bar{z}_{mn_b}^{ag} \\ \bar{z}_{mn_b}^{na} & \bar{z}_{mn_b}^{nn} & \bar{z}_{mn_b}^{ng} \\ \bar{z}_{mn_b}^{ga} & \bar{z}_{mn_b}^{gn} & \bar{z}_{mn_b}^{gg} \end{bmatrix} \tag{5.2}$$

The complex injected load power S_{id}^{p} at any phase p of bus i (assuming that the load is connected between phase p ($p = a,b,c$) and neutral bus n_i at i^{th} bus location) is given as, $\bar{S}_{id}^{p} = \bar{P}_{id}^{p} + j\bar{Q}_{id}^{p}$. $\bar{P}_{id}^{p}$ and $\bar{Q}_{id}^{p}$ are the real and reactive load power injections at p^{th} phase of bus i. Therefore, the equivalent bus injection current $\bar{I}_{id}^{p}$ at any phase p of bus i is calculated as,

$$\bar{I}_{id}^{p} = \left(\frac{\bar{S}_{id}^{p}}{\bar{V}_{i}^{p} - \bar{V}_{i}^{n}}\right)^{*} = \left(\frac{\bar{P}_{id}^{p} + j\bar{Q}_{id}^{p}}{\bar{V}_{i}^{p} - \bar{V}_{i}^{n}}\right)^{*}; (p = a\ or\ b\ or\ c) \tag{5.3}$$

where, $\bar{V}_{i}^{p}$ and $\bar{V}_{i}^{n}$ are the voltages of phase p and neutral bus n_i at i^{th} bus location, respectively. The symbol (*) denotes the complex conjugate operator. In Fig. 5.1, $\bar{Z}_{i}^{ngr}$ is the neutral to ground impedance between neutral bus n_i and ground bus g_i (neutral grounding impedance) at i^{th} bus location and $\bar{I}_{i}^{ng}$ is the neutral to ground current at i^{th} bus location.

The proposed load flow analysis method is based on $[\mathbf{BIBC}]$ (bus injection to branch current) and [BCBV] (branch current to bus voltage) matrices of the system [70]. $[\mathbf{BIBC}]$ matrix gives the relationship between branch currents and the equivalent bus injection currents of the system, while $[\mathbf{BCBV}]$ matrix gives the relationship between branch currents and the bus voltages of the

system. The formulation of theses matrices for the load flow solution of a three phase four wire multigrounded distribution system (Fig. 5.1), is carried out in the following subsections.

5.2.1 Formulation of $[\mathrm{BIBC}]$ matrix

The $[\mathbf{BIBC}]$ matrix has been developed separately for the phase currents, neutral currents and ground currents of the system shown in Fig. 5.1. The detailed formulation of $[\mathbf{BIBC}]$ matrix for each current is as follows :

5.2.1.1 Formulation of $[\mathrm{BIBC}]$ matrix for phase currents $\left[\mathbf{B_p}\right]$

The phase branch currents of the distribution system can be obtained in terms of equivalent bus injection currents $\left[\mathbf{I_L}\right]$, by applying KCL equations at each phase (a, b, c) of all the buses in the system, except the substation bus. The branch currents of phases a, b and c of all the line sections in Fig. 5.1 can be expressed in terms of equivalent injection currents as,

$$
\begin{aligned}
\bar{B}_1^a &= \bar{I}_{2d}^a + \bar{I}_{3d}^a + \cdots + \bar{I}_{id}^a + \bar{I}_{jd}^a + \cdots + \bar{I}_{kd}^a + \bar{I}_{ld}^a + \bar{I}_{md}^a + \bar{I}_{n_bd}^a \\
\bar{B}_1^b &= \bar{I}_{2d}^b + \bar{I}_{3d}^b + \cdots + \bar{I}_{id}^b + \bar{I}_{jd}^b + \cdots + \bar{I}_{kd}^b + \bar{I}_{ld}^b + \bar{I}_{md}^b \\
\bar{B}_1^c &= \bar{I}_{2d}^c + \bar{I}_{3d}^c + \cdots + \bar{I}_{id}^c + \bar{I}_{jd}^c + \cdots + \bar{I}_{kd}^c + \bar{I}_{ld}^c \\
\bar{B}_2^a &= \bar{I}_{3d}^a + \cdots + \bar{I}_{id}^a + \bar{I}_{jd}^a + \cdots + \bar{I}_{kd}^a + \bar{I}_{ld}^a + \bar{I}_{md}^a + \bar{I}_{n_bd}^a \\
\bar{B}_2^b &= \bar{I}_{3d}^b + \cdots + \bar{I}_{id}^b + \bar{I}_{jd}^b + \cdots + \bar{I}_{kd}^b + \bar{I}_{ld}^b + \bar{I}_{md}^b \\
\bar{B}_2^c &= \bar{I}_{3d}^c + \cdots + \bar{I}_{id}^c + \bar{I}_{jd}^c + \cdots + \bar{I}_{kd}^c + \bar{I}_{ld}^c \\
\bar{B}_i^a &= \bar{I}_{jd}^a \\
\bar{B}_i^b &= \bar{I}_{jd}^b \\
\bar{B}_i^c &= \bar{I}_{jd}^c \\
\bar{B}_k^a &= \bar{I}_{ld}^a + \bar{I}_{md}^a + \bar{I}_{n_bd}^a \\
\bar{B}_k^b &= \bar{I}_{ld}^b + \bar{I}_{md}^b \\
\bar{B}_k^c &= \bar{I}_{ld}^c \\
\bar{B}_l^a &= \bar{I}_{md}^a + \bar{I}_{n_bd}^a \\
\bar{B}_l^b &= \bar{I}_{md}^b \\
\bar{B}_m^a &= \bar{I}_{n_bd}^a
\end{aligned}
\tag{5.4}
$$

Therefore, the phase branch currents can be expressed in the matrix form as,

$$\Big[\mathbf{B_p}\Big] = \Big[\mathbf{BIBC_p}\Big]\Big[\mathbf{I_L}\Big] \tag{5.5}$$

where

$$\Big[\mathbf{B_p}\Big] = \Big[\bar{B}_1^a \;\; \bar{B}_1^b \;\; \bar{B}_1^c \;\; \cdots \;\; \bar{B}_i^a \;\; \bar{B}_i^b \;\; \bar{B}_i^c \;\; \cdots \;\; \bar{B}_k^a \;\; \bar{B}_k^b \;\; \bar{B}_k^c \;\; \bar{B}_l^a \;\; \bar{B}_l^b \;\; \bar{B}_m^a\Big]^T;$$

$$\Big[\mathbf{I_L}\Big] = \Big[\bar{I}_{2d}^a \;\; \bar{I}_{2d}^b \;\; \bar{I}_{2d}^c \;\; \cdots \;\; \bar{I}_{jd}^a \;\; \bar{I}_{jd}^b \;\; \bar{I}_{jd}^c \;\; \cdots \;\; \bar{I}_{ld}^a \;\; \bar{I}_{ld}^b \;\; \bar{I}_{ld}^c \;\; \bar{I}_{md}^a \;\; \bar{I}_{md}^b \;\; \bar{I}_{n_b d}^a\Big]^T;$$

$$\Big[\mathbf{BIBC_p}\Big] = \begin{array}{c} \\ 1^a \\ 1^b \\ 1^c \\ \vdots \\ i^a \\ i^b \\ i^c \\ \vdots \\ k^a \\ k^b \\ k^c \\ l^a \\ l^b \\ m^a \end{array} \begin{array}{c} \begin{array}{cccccccccccccc} 2^a & 2^b & 2^c & \cdots & j^a & j^b & j^c & \cdots & l^a & l^b & l^c & m^a & m^b & {n_b}^a \end{array} \\ \left[\begin{array}{cccccccccccccc} 1 & 0 & 0 & \cdots & 1 & 0 & 0 & \cdots & 1 & 0 & 0 & 1 & 0 & 1 \\ 0 & 1 & 0 & \cdots & 0 & 1 & 0 & \cdots & 0 & 1 & 0 & 0 & 1 & 0 \\ 0 & 0 & 1 & \cdots & 0 & 0 & 1 & \cdots & 0 & 0 & 1 & 0 & 0 & 0 \\ \vdots & \vdots & \vdots & \ddots & \vdots & \vdots & \vdots & \cdots & \vdots & \vdots & \vdots & \vdots & \vdots & \vdots \\ 0 & 0 & 0 & \cdots & 1 & 0 & 0 & \cdots & 0 & 0 & 0 & 0 & 0 & 0 \\ 0 & 0 & 0 & \cdots & 0 & 1 & 0 & \cdots & 0 & 0 & 0 & 0 & 0 & 0 \\ 0 & 0 & 0 & \cdots & 0 & 0 & 1 & \cdots & 0 & 0 & 0 & 0 & 0 & 0 \\ \vdots & \vdots & \vdots & \cdots & \vdots & \vdots & \vdots & \ddots & \vdots & \vdots & \vdots & \vdots & \vdots & \vdots \\ 0 & 0 & 0 & \cdots & 0 & 0 & 0 & \cdots & 1 & 0 & 0 & 1 & 0 & 1 \\ 0 & 0 & 0 & \cdots & 0 & 0 & 0 & \cdots & 0 & 1 & 0 & 0 & 1 & 0 \\ 0 & 0 & 0 & \cdots & 0 & 0 & 0 & \cdots & 0 & 0 & 1 & 0 & 0 & 0 \\ 0 & 0 & 0 & \cdots & 0 & 0 & 0 & \cdots & 0 & 0 & 0 & 1 & 0 & 1 \\ 0 & 0 & 0 & \cdots & 0 & 0 & 0 & \cdots & 0 & 0 & 0 & 0 & 1 & 0 \\ 0 & 0 & 0 & \cdots & 0 & 0 & 0 & \cdots & 0 & 0 & 0 & 0 & 0 & 1 \end{array}\right] \end{array}$$

where $[\mathbf{B_p}]$ is the phase branch current vector, $[\mathbf{I_L}]$ is the equivalent bus injection current vector and $[\mathbf{BIBC_p}]$ is the bus injection to phase branch current matrix. In $[\mathbf{BIBC_p}]$ matrix, the row numbers $1^a, 1^b, \cdots, m^a$ correspond to the phase branches, while the column numbers $2^a, 2^b, \cdots, {n_b}^a$ correspond to the phase buses of the system. Further, it is assumed that the considered four wire multigrounded radial distribution system has u three-phase, v two-phase, w single-phase, $(u + v + w)$ neutral and $(u + v + w)$ ground buses. This generalized system will be considered throughout this chapter. The size of $[\mathbf{BIBC_p}]$ matrix for this system will therefore be

$(3u + 2v + w - 3) \times (3u + 2v + w - 3)$. Eq. (5.5) shows that, the $[\mathbf{BIBC_p}]$ matrix is an upper triangular matrix which contains zeros and ones only.

Development of algorithm for generation of $[\mathbf{BIBC_p}]$ ***matrix*** :

Step 1. Consider an unbalanced three phase four wire multigrounded distribution system, having u three-phase, v two phase and w single phase buses. Initialize the $[\mathbf{BIBC_p}]$ matrix as a null matrix of size $(3u + 2v + w - 3) \times (3u + 2v + w - 3)$.

Step 2. If a line section $\mathbf{L_k^{png}}$, having p phases, neutral n and ground g, is connected between buses i and j, then

$$\begin{aligned} (i). \quad \Big[\mathbf{BIBC_p}(l_s, j)\Big]_{(p\times p)} &= \Big[\mathbf{BIBC_p}(l_s, i)\Big]_{(p\times p)}; \\ (ii). \quad \Big[\mathbf{BIBC_p}(k, j)\Big]_{(p\times p)} &= \Big[\mathbf{I}\Big]_{(p\times p)} \end{aligned}$$

where $l_s = 1, 2, \cdots, (k-1)$; $\Big[\mathbf{I}\Big]$ is an identity matrix of size $(p \times p)$ and $p = 3$ for 3-ϕ, $p = 2$ for 2-ϕ, $p = 1$ for 1-ϕ line section.

Step 3. Repeat Step 2 until all the line sections are included in $[\mathbf{BIBC_p}]$ matrix.

5.2.1.2 Formulation of $[\mathrm{BIBC}]$ matrix for neutral currents $\left[\mathbf{B_n}\right]$

The neutral currents of the three phase four wire multigrounded distribution system can be expressed in terms of equivalent injection currents and the neutral to ground currents of the system, by applying KCL equations at all the neutral buses in the system, except the neutral bus at the substation location. For example, the neutral currents $\bar{B}_1^n$, $\bar{B}_2^n$, $\bar{B}_i^n$, $\bar{B}_k^n$, $\bar{B}_l^n$ and $\bar{B}_m^n$ of the system shown in Fig. 5.1 can be written as,

$$\begin{aligned} \bar{B}_1^n &= -\bar{I}_{2d}^a - \bar{I}_{2d}^b - \bar{I}_{2d}^c - \bar{I}_{3d}^a - \bar{I}_{3d}^b - \bar{I}_{3d}^c - \cdots - \bar{I}_{id}^a - \bar{I}_{id}^b - \bar{I}_{id}^c - \bar{I}_{jd}^a - \bar{I}_{jd}^b - \bar{I}_{jd}^c \\ &- \cdots - \bar{I}_{kd}^a - \bar{I}_{kd}^b - \bar{I}_{kd}^c - \bar{I}_{ld}^a - \bar{I}_{ld}^b - \bar{I}_{ld}^c - \bar{I}_{md}^a - \bar{I}_{md}^b - \bar{I}_{n_bd}^a + \bar{I}_2^{ng} + \bar{I}_3^{ng} + \cdots \\ &+ \bar{I}_i^{ng} + \bar{I}_j^{ng} + \cdots + \bar{I}_k^{ng} + \bar{I}_l^{ng} + \bar{I}_m^{ng} + \bar{I}_{n_b}^{ng} \\ \bar{B}_2^n &= -\bar{I}_{3d}^a - \bar{I}_{3d}^b - \bar{I}_{3d}^c - \cdots - \bar{I}_{id}^a - \bar{I}_{id}^b - \bar{I}_{id}^c - \bar{I}_{jd}^a - \bar{I}_{jd}^b - \bar{I}_{jd}^c - \cdots - \bar{I}_{kd}^a - \bar{I}_{kd}^b \\ &- \bar{I}_{kd}^c - \bar{I}_{ld}^a - \bar{I}_{ld}^b - \bar{I}_{ld}^c - \bar{I}_{md}^a - \bar{I}_{md}^b - \bar{I}_{n_bd}^a + \bar{I}_3^{ng} + \cdots + \bar{I}_i^{ng} + \bar{I}_j^{ng} + \cdots + \bar{I}_k^{ng} \\ &+ \bar{I}_l^{ng} + \bar{I}_m^{ng} + \bar{I}_{n_b}^{ng} \\ \bar{B}_i^n &= -\bar{I}_{jd}^a - \bar{I}_{jd}^b - \bar{I}_{jd}^c + \bar{I}_j^{ng} \end{aligned} \tag{5.6}$$

$$
\begin{aligned}
\bar{B}_k^n &= -\bar{I}_{ld}^a - \bar{I}_{ld}^b - \bar{I}_{ld}^c - \bar{I}_{md}^a - \bar{I}_{md}^b - \bar{I}_{n_b d}^a + \bar{I}_l^{ng} + \bar{I}_m^{ng} + \bar{I}_{n_b}^{ng} \\
\bar{B}_l^n &= -\bar{I}_{md}^a - \bar{I}_{md}^b - \bar{I}_{n_b d}^a + \bar{I}_m^{ng} + \bar{I}_{n_b}^{ng} \\
\bar{B}_m^n &= -\bar{I}_{n_b d}^a + \bar{I}_{n_b}^{ng}
\end{aligned} \tag{5.7}
$$

Therefore, the neutral currents of the system can be expressed in the matrix form as,

$$
\left[\mathbf{B_n}\right] = -\left[\mathbf{BIBC_{pn}}\right]\left[\mathbf{I_L}\right] + \left[\mathbf{BIBC_g}\right]\left[\mathbf{I_{ng}}\right] \tag{5.8}
$$

where

$$
\begin{aligned}
\left[\mathbf{B_n}\right] &= \begin{bmatrix} \bar{B}_1^n & \bar{B}_2^n & \cdots & \bar{B}_i^n & \cdots & \bar{B}_k^n & \bar{B}_l^n & \bar{B}_m^n \end{bmatrix}^T \\
\left[\mathbf{I_{ng}}\right] &= \begin{bmatrix} \bar{I}_2^{ng} & \bar{I}_3^{ng} & \cdots & \bar{I}_j^{ng} & \cdots & \bar{I}_l^{ng} & \bar{I}_m^{ng} & \bar{I}_{n_b}^{ng} \end{bmatrix}^T
\end{aligned}
$$

$$
\left[\mathbf{BIBC_{pn}}\right] = \begin{array}{c} \\ 1^n \\ 2^n \\ \vdots \\ i^n \\ \vdots \\ k^n \\ l^n \\ m^n \end{array} \begin{array}{c} \begin{array}{cccccccccccccc} 2^a & 2^b & 2^c & \cdots & j^a & j^b & j^c & \cdots & l^a & l^b & l^c & m^a & m^b & {n_b}^a \end{array} \\ \begin{bmatrix} -1 & -1 & -1 & \cdots & -1 & -1 & -1 & \cdots & -1 & -1 & -1 & -1 & -1 & -1 \\ 0 & 0 & 0 & \cdots & -1 & -1 & -1 & \cdots & -1 & -1 & -1 & -1 & -1 & -1 \\ \vdots & \vdots & \vdots & \cdots & \vdots & \vdots & \vdots & \cdots & \vdots & \vdots & \vdots & \vdots & \vdots & \vdots \\ 0 & 0 & 0 & \cdots & -1 & -1 & -1 & \cdots & 0 & 0 & 0 & 0 & 0 & 0 \\ \vdots & \vdots & \vdots & \cdots & \vdots & \vdots & \vdots & \cdots & \vdots & \vdots & \vdots & \vdots & \vdots & \vdots \\ 0 & 0 & 0 & \cdots & 0 & 0 & 0 & \cdots & -1 & -1 & -1 & -1 & -1 & -1 \\ 0 & 0 & 0 & \cdots & 0 & 0 & 0 & \cdots & 0 & 0 & 0 & -1 & -1 & -1 \\ 0 & 0 & 0 & \cdots & 0 & 0 & 0 & \cdots & 0 & 0 & 0 & 0 & 0 & -1 \end{bmatrix} \end{array}
$$

$$
\left[\mathbf{BIBC_g}\right] = \begin{array}{c} \\ 1^n \\ 2^n \\ \vdots \\ \bar{B}_i^n \\ \vdots \\ k^n \\ l^n \\ m^n \end{array} \begin{array}{c} \begin{array}{cccccccc} 2^{ng} & 3^{ng} & \cdots & j^{ng} & \cdots & l^{ng} & m^{ng} & {n_b}^{ng} \end{array} \\ \begin{bmatrix} 1 & 1 & \cdots & 1 & \cdots & 1 & 1 & 1 \\ 0 & 1 & \cdots & 1 & \cdots & 1 & 1 & 1 \\ \vdots & \vdots & \ddots & \vdots & \cdots & \vdots & \vdots & \vdots \\ 0 & 0 & \cdots & 1 & \cdots & 0 & 0 & 0 \\ \vdots & \vdots & \cdots & \vdots & \ddots & \vdots & \vdots & \vdots \\ 0 & 0 & \cdots & 0 & \cdots & 1 & 1 & 1 \\ 0 & 0 & \cdots & 0 & \cdots & 0 & 1 & 1 \\ 0 & 0 & \cdots & 0 & \cdots & 0 & 0 & 1 \end{bmatrix} \end{array}
$$

Here $[\mathbf{B_n}]$ is the neutral current vector and $[\mathbf{I_{ng}}]$ is the neutral to ground current vector. The $[\mathbf{BIBC_{pn}}]$ matrix gives the relationship between neutral currents and the equivalent bus injection currents of the system. In $[\mathbf{BIBC_{pn}}]$ matrix, the row numbers $1^n, 2^n, \cdots, m^n$ correspond to the neutral branches, while the column numbers $2^a, 2^b, \cdots, {n_b}^a$ correspond to the phase buses of the system. The $[\mathbf{BIBC_g}]$ matrix gives the relationship between neutral currents and neutral to ground currents of the system. In $[\mathbf{BIBC_g}]$ matrix, the row numbers $1^n, 2^n, \cdots, m^n$ correspond to the neutral branches, while the column numbers $2^{ng}, 3^{ng}, \cdots, {n_b}^{ng}$ correspond to the neutral to ground branches of the system. Hence, for the radial distribution system considered, the sizes of $[\mathbf{BIBC_{pn}}]$ and $[\mathbf{BIBC_g}]$ matrices will be $(u+v+w-1) \times (3u+2v+w-3)$ and $(u+v+w-1) \times (u+v+w-1)$, respectively.

Development of Algorithms for generation of $[\mathbf{BIBC_{pn}}]$ ***and*** $[\mathbf{BIBC_g}]$ ***matrices***:

Step 1. Initialize the $[\mathbf{BIBC_{pn}}]$ and $[\mathbf{BIBC_g}]$ matrices as null matrices of the sizes $(u+v+w-1) \times (3u+2v+w-3)$ and $(u+v+w-1) \times (u+v+w-1)$, respectively.

Step 2. (a). If k^{th} line section $\mathbf{L_k^{png}}$, having p phases, neutral n and ground g, is connected between buses i and j, then

$$\begin{aligned} (i).\ \left[\mathbf{BIBC_{pn}}(l_s, j)\right]_{(1\times p)} &= \left[\mathbf{BIBC_{pn}}(l_s, i)\right]_{(1\times p)}; \\ (ii).\ \left[\mathbf{BIBC_{pn}}(k, j)\right]_{(1\times p)} &= \left[\mathbf{I}\right]_{(1\times p)} \end{aligned}$$

where $l_s = 1, 2, \cdots, (k-1)$; $\left[\mathbf{I}\right]$ is an identity matrix of size $(1 \times p)$ and $p = 3$ for 3-ϕ, $p = 2$ for 2-ϕ, $p = 1$ for 1-ϕ line section.

(b). If k^{th} line section $\mathbf{L_k^{png}}$, having p phases, neutral n and ground g, is connected between buses i and j, then

$$\begin{aligned} (i).\ \left[\mathbf{BIBC_g}(l_s, j)\right] &= \left[\mathbf{BIBC_g}(l_s, i)\right]; \\ (ii).\ \left[\mathbf{BIBC_g}(k, j)\right] &= 1 \end{aligned}$$

where $l_s = 1, 2, \cdots, (k-1)$.

Step 3. Repeat Step 2 until all the line sections are included in $[\mathbf{BIBC_{pn}}]$ and $[\mathbf{BIBC_g}]$ matrices.

5.2.1.3 Formulation of $[\mathrm{BIBC}]$ matrix for ground currents $\left[\mathbf{B_g}\right]$

The ground currents of the three phase four wire multigrounded distribution system can be obtained in terms of neutral to ground currents ($\bar{I}_i^{ng}$, $i = 1, \cdots, n_b$), by applying KCL equations at all the ground buses of the system, except the ground bus at the substation location. For example, the ground currents $\bar{B}_1^g$, $\bar{B}_2^g$, $\bar{B}_i^g$, $\bar{B}_k^g$, $\bar{B}_l^g$ and $\bar{B}_m^g$ of the system shown in Fig. 5.1 can be expressed as,

$$\begin{aligned}
\bar{B}_1^g &= -\bar{I}_2^{ng} - \bar{I}_3^{ng} - \cdots - \bar{I}_i^{ng} - \bar{I}_j^{ng} - \cdots - \bar{I}_k^{ng} - \bar{I}_l^{ng} - \bar{I}_m^{ng} - \bar{I}_{n_b}^{ng} \\
\bar{B}_2^g &= -\bar{I}_3^{ng} - \cdots - \bar{I}_i^{ng} - \bar{I}_j^{ng} - \cdots - \bar{I}_k^{ng} - \bar{I}_l^{ng} - \bar{I}_m^{ng} - \bar{I}_{n_b}^{ng} \\
\bar{B}_i^g &= -\bar{I}_j^{ng} \\
\bar{B}_k^g &= -\bar{I}_l^{ng} - \bar{I}_m^{ng} - \bar{I}_{n_b}^{ng}; \quad \bar{B}_l^g = -\bar{I}_m^{ng} - \bar{I}_{n_b}^{ng}; \quad \bar{B}_m^g = -\bar{I}_{n_b}^{ng}
\end{aligned} \tag{5.9}$$

Hence, the ground currents of the system can be written in the matrix form as,

$$\left[\mathbf{B_g}\right] = -\left[\mathbf{BIBC_g}\right]\left[\mathbf{I_{ng}}\right] \tag{5.10}$$

5.2.2 Formulation of $[\mathrm{BCBV}]$ matrix

The $[\mathbf{BCBV}]$ matrix needs to be developed separately for the voltages of phase buses, neutral buses and ground buses of the distribution system shown in Fig. 5.1. The detailed formulations of these matrices are given as follows :

5.2.2.1 Formulation of $[\mathrm{BCBV}]$ matrices for the voltages of phase buses $\left[\mathbf{V_p}\right]$

The voltages of phase buses can be described in terms of phase branch currents, neutral currents and ground currents of the system, by applying KVL equations in the given system as,

$$\begin{aligned}
\bar{V}_2^a &= \bar{V}_s^a - \bar{B}_1^a \bar{z}_{12}^{aa} - \bar{B}_1^b \bar{z}_{12}^{ab} - \bar{B}_1^c \bar{z}_{12}^{ac} - \bar{B}_1^n \bar{z}_{12}^{an} - \bar{B}_1^g \bar{z}_{12}^{ag} \\
\bar{V}_2^b &= \bar{V}_s^b - \bar{B}_1^a \bar{z}_{12}^{ba} - \bar{B}_1^b \bar{z}_{12}^{bb} - \bar{B}_1^c \bar{z}_{12}^{bc} - \bar{B}_1^n \bar{z}_{12}^{bn} - \bar{B}_1^g \bar{z}_{12}^{bg} \\
\bar{V}_2^c &= \bar{V}_s^c - \bar{B}_1^a \bar{z}_{12}^{ca} - \bar{B}_1^b \bar{z}_{12}^{cb} - \bar{B}_1^c \bar{z}_{12}^{cc} - \bar{B}_1^n \bar{z}_{12}^{cn} - \bar{B}_1^g \bar{z}_{12}^{cg} \\
\bar{V}_3^a &= \bar{V}_s^a - \bar{B}_1^a \bar{z}_{12}^{aa} - \bar{B}_1^b \bar{z}_{12}^{ab} - \bar{B}_1^c \bar{z}_{12}^{ac} - \bar{B}_1^n \bar{z}_{12}^{an} - \bar{B}_1^g \bar{z}_{12}^{ag} - \bar{B}_2^a \bar{z}_{23}^{aa} - \bar{B}_2^b \bar{z}_{23}^{ab} - \bar{B}_2^c \bar{z}_{23}^{ac} \\
&\quad - \bar{B}_2^n \bar{z}_{23}^{an} - \bar{B}_2^g \bar{z}_{23}^{ag} \\
\bar{V}_3^b &= \bar{V}_s^b - \bar{B}_1^a \bar{z}_{12}^{ba} - \bar{B}_1^b \bar{z}_{12}^{bb} - \bar{B}_1^c \bar{z}_{12}^{bc} - \bar{B}_1^n \bar{z}_{12}^{bn} - \bar{B}_1^g \bar{z}_{12}^{bg} - \bar{B}_2^a \bar{z}_{23}^{ba} - \bar{B}_2^b \bar{z}_{23}^{bb} - \bar{B}_2^c \bar{z}_{23}^{bc} \\
&\quad - \bar{B}_2^n \bar{z}_{23}^{bn} - \bar{B}_2^g \bar{z}_{23}^{bg}
\end{aligned} \tag{5.11}$$

$$
\begin{aligned}
\bar{V}_3^c &= \bar{V}_s^c - \bar{B}_1^a \bar{z}_{12}^{ca} - \bar{B}_1^b \bar{z}_{12}^{cb} - \bar{B}_1^c \bar{z}_{12}^{cc} - \bar{B}_1^n \bar{z}_{12}^{cn} - \bar{B}_1^g \bar{z}_{12}^{cg} - \bar{B}_2^a \bar{z}_{23}^{ca} - \bar{B}_2^b \bar{z}_{23}^{cb} - \bar{B}_2^c \bar{z}_{23}^{cc} \\
&\quad - \bar{B}_2^n \bar{z}_{23}^{cn} - \bar{B}_2^g \bar{z}_{23}^{cg} \\
\bar{V}_j^a &= \bar{V}_s^a - \bar{B}_1^a \bar{z}_{12}^{aa} - \bar{B}_1^b \bar{z}_{12}^{ab} - \bar{B}_1^c \bar{z}_{12}^{ac} - \bar{B}_1^n \bar{z}_{12}^{an} - \bar{B}_1^g \bar{z}_{12}^{ag} - \bar{B}_2^a \bar{z}_{23}^{aa} - \bar{B}_2^b \bar{z}_{23}^{ab} - \bar{B}_2^c \bar{z}_{23}^{ac} \\
&\quad - \bar{B}_2^n \bar{z}_{23}^{an} - \bar{B}_2^g \bar{z}_{23}^{ag} - \cdots - \bar{B}_i^a \bar{z}_{ij}^{aa} - \bar{B}_i^b \bar{z}_{ij}^{ab} - \bar{B}_i^c \bar{z}_{ij}^{ac} - \bar{B}_i^n \bar{z}_{ij}^{an} - \bar{B}_i^g \bar{z}_{ij}^{ag} \\
\bar{V}_j^b &= \bar{V}_s^b - \bar{B}_1^a \bar{z}_{12}^{ba} - \bar{B}_1^b \bar{z}_{12}^{bb} - \bar{B}_1^c \bar{z}_{12}^{bc} - \bar{B}_1^n \bar{z}_{12}^{bn} - \bar{B}_1^g \bar{z}_{12}^{bg} - \bar{B}_2^a \bar{z}_{23}^{ba} - \bar{B}_2^b \bar{z}_{23}^{bb} - \bar{B}_2^c \bar{z}_{23}^{bc} \\
&\quad - \bar{B}_2^n \bar{z}_{23}^{bn} - \bar{B}_2^g \bar{z}_{23}^{bg} - \cdots - \bar{B}_i^a \bar{z}_{ij}^{ba} - \bar{B}_i^b \bar{z}_{ij}^{bb} - \bar{B}_i^c \bar{z}_{ij}^{bc} - \bar{B}_i^n \bar{z}_{ij}^{bn} - \bar{B}_i^g \bar{z}_{ij}^{bg} \\
\bar{V}_j^c &= \bar{V}_s^c - \bar{B}_1^a \bar{z}_{12}^{ca} - \bar{B}_1^b \bar{z}_{12}^{cb} - \bar{B}_1^c \bar{z}_{12}^{cc} - \bar{B}_1^n \bar{z}_{12}^{cn} - \bar{B}_1^g \bar{z}_{12}^{cg} - \bar{B}_2^a \bar{z}_{23}^{ca} - \bar{B}_2^b \bar{z}_{23}^{cb} - \bar{B}_2^c \bar{z}_{23}^{cc} \\
&\quad - \bar{B}_2^n \bar{z}_{23}^{cn} - \bar{B}_2^g \bar{z}_{23}^{cg} - \cdots - \bar{B}_i^a \bar{z}_{ij}^{ca} - \bar{B}_i^b \bar{z}_{ij}^{cb} - \bar{B}_i^c \bar{z}_{ij}^{cc} - \bar{B}_i^n \bar{z}_{ij}^{cn} - \bar{B}_i^g \bar{z}_{ij}^{cg} \\
\bar{V}_l^a &= \bar{V}_s^a - \bar{B}_1^a \bar{z}_{12}^{aa} - \bar{B}_1^b \bar{z}_{12}^{ab} - \bar{B}_1^c \bar{z}_{12}^{ac} - \bar{B}_1^n \bar{z}_{12}^{an} - \bar{B}_1^g \bar{z}_{12}^{ag} - \bar{B}_2^a \bar{z}_{23}^{aa} - \bar{B}_2^b \bar{z}_{23}^{ab} - \bar{B}_2^c \bar{z}_{23}^{ac} \\
&\quad - \bar{B}_2^n \bar{z}_{23}^{an} - \bar{B}_2^g \bar{z}_{23}^{ag} - \cdots - \bar{B}_k^a \bar{z}_{kl}^{aa} - \bar{B}_k^b \bar{z}_{kl}^{ab} - \bar{B}_k^c \bar{z}_{kl}^{ac} - \bar{B}_k^n \bar{z}_{kl}^{an} - \bar{B}_k^g \bar{z}_{kl}^{ag} \\
\bar{V}_l^b &= \bar{V}_s^b - \bar{B}_1^a \bar{z}_{12}^{ba} - \bar{B}_1^b \bar{z}_{12}^{bb} - \bar{B}_1^c \bar{z}_{12}^{bc} - \bar{B}_1^n \bar{z}_{12}^{bn} - \bar{B}_1^g \bar{z}_{12}^{bg} - \bar{B}_2^a \bar{z}_{23}^{ba} - \bar{B}_2^b \bar{z}_{23}^{bb} - \bar{B}_2^c \bar{z}_{23}^{bc} \\
&\quad - \bar{B}_2^n \bar{z}_{23}^{bn} - \bar{B}_2^g \bar{z}_{23}^{bg} - \cdots - \bar{B}_k^a \bar{z}_{kl}^{ba} - \bar{B}_k^b \bar{z}_{kl}^{bb} - \bar{B}_k^c \bar{z}_{kl}^{bc} - \bar{B}_k^n \bar{z}_{kl}^{bn} - \bar{B}_k^g \bar{z}_{kl}^{bg} \\
\bar{V}_l^c &= \bar{V}_s^c - \bar{B}_1^a \bar{z}_{12}^{ca} - \bar{B}_1^b \bar{z}_{12}^{cb} - \bar{B}_1^c \bar{z}_{12}^{cc} - \bar{B}_1^n \bar{z}_{12}^{cn} - \bar{B}_1^g \bar{z}_{12}^{cg} - \bar{B}_2^a \bar{z}_{23}^{ca} - \bar{B}_2^b \bar{z}_{23}^{cb} - \bar{B}_2^c \bar{z}_{23}^{cc} \\
&\quad - \bar{B}_2^n \bar{z}_{23}^{cn} - \bar{B}_2^g \bar{z}_{23}^{cg} - \cdots - \bar{B}_k^a \bar{z}_{kl}^{ca} - \bar{B}_k^b \bar{z}_{kl}^{cb} - \bar{B}_k^c \bar{z}_{kl}^{cc} - \bar{B}_k^n \bar{z}_{kl}^{cn} - \bar{B}_k^g \bar{z}_{kl}^{cg} \\
\bar{V}_m^a &= \bar{V}_s^a - \bar{B}_1^a \bar{z}_{12}^{aa} - \bar{B}_1^b \bar{z}_{12}^{ab} - \bar{B}_1^c \bar{z}_{12}^{ac} - \bar{B}_1^n \bar{z}_{12}^{an} - \bar{B}_1^g \bar{z}_{12}^{ag} - \bar{B}_2^a \bar{z}_{23}^{aa} - \bar{B}_2^b \bar{z}_{23}^{ab} - \bar{B}_2^c \bar{z}_{23}^{ac} \\
&\quad - \bar{B}_2^n \bar{z}_{23}^{an} - \bar{B}_2^g \bar{z}_{23}^{ag} - \cdots - \bar{B}_k^a \bar{z}_{kl}^{aa} - \bar{B}_k^b \bar{z}_{kl}^{ab} - \bar{B}_k^c \bar{z}_{kl}^{ac} - \bar{B}_k^n \bar{z}_{kl}^{an} - \bar{B}_k^g \bar{z}_{kl}^{ag} \\
&\quad - \bar{B}_l^a \bar{z}_{lm}^{aa} - \bar{B}_l^b \bar{z}_{lm}^{ab} - \bar{B}_l^n \bar{z}_{lm}^{an} - \bar{B}_l^g \bar{z}_{lm}^{ag} \\
\bar{V}_m^b &= \bar{V}_s^b - \bar{B}_1^a \bar{z}_{12}^{ba} - \bar{B}_1^b \bar{z}_{12}^{bb} - \bar{B}_1^c \bar{z}_{12}^{bc} - \bar{B}_1^n \bar{z}_{12}^{bn} - \bar{B}_1^g \bar{z}_{12}^{bg} - \bar{B}_2^a \bar{z}_{23}^{ba} - \bar{B}_2^b \bar{z}_{23}^{bb} - \bar{B}_2^c \bar{z}_{23}^{bc} \\
&\quad - \bar{B}_2^n \bar{z}_{23}^{bn} - \bar{B}_2^g \bar{z}_{23}^{bg} - \cdots - \bar{B}_k^a \bar{z}_{kl}^{ba} - \bar{B}_k^b \bar{z}_{kl}^{bb} - \bar{B}_k^c \bar{z}_{kl}^{bc} - \bar{B}_k^n \bar{z}_{kl}^{bn} - \bar{B}_k^g \bar{z}_{kl}^{bg} \\
&\quad - \bar{B}_l^a \bar{z}_{lm}^{ba} - \bar{B}_l^b \bar{z}_{lm}^{bb} - \bar{B}_l^n \bar{z}_{lm}^{bn} - \bar{B}_l^g \bar{z}_{lm}^{bg} \\
\bar{V}_{n_b}^a &= \bar{V}_s^a - \bar{B}_1^a \bar{z}_{12}^{aa} - \bar{B}_1^b \bar{z}_{12}^{ab} - \bar{B}_1^c \bar{z}_{12}^{ac} - \bar{B}_1^n \bar{z}_{12}^{an} - \bar{B}_1^g \bar{z}_{12}^{ag} - \bar{B}_2^a \bar{z}_{23}^{aa} - \bar{B}_2^b \bar{z}_{23}^{ab} - \bar{B}_2^c \bar{z}_{23}^{ac} \\
&\quad - \bar{B}_2^n \bar{z}_{23}^{an} - \bar{B}_2^g \bar{z}_{23}^{ag} - \cdots - \bar{B}_k^a \bar{z}_{kl}^{aa} - \bar{B}_k^b \bar{z}_{kl}^{ab} - \bar{B}_k^c \bar{z}_{kl}^{ac} - \bar{B}_k^n \bar{z}_{kl}^{an} - \bar{B}_k^g \bar{z}_{kl}^{ag} \\
&\quad - \bar{B}_l^a \bar{z}_{lm}^{aa} - \bar{B}_l^b \bar{z}_{lm}^{ab} - \bar{B}_l^n \bar{z}_{lm}^{an} - \bar{B}_l^g \bar{z}_{lm}^{ag} - \bar{B}_m^a \bar{z}_{mn_b}^{aa} - \bar{B}_m^n \bar{z}_{mn_b}^{an} - \bar{B}_m^g \bar{z}_{mn_b}^{ag}
\end{aligned} \tag{5.12}
$$

Therefore, the voltages of phase buses of the distribution system can be expressed in the matrix form as,

$$
\left[\mathbf{V_p}\right] = \left[\mathbf{V_{ss}}\right] - \left[\mathbf{BCBV_p}\right]\left[\mathbf{B_p}\right] - \left[\mathbf{BCBV_{pn}}\right]\left[\mathbf{B_n}\right] - \left[\mathbf{BCBV_{pg}}\right]\left[\mathbf{B_g}\right] \tag{5.13}
$$

where,

$$\left[\mathbf{BCBV_{pn}}\right] = \begin{bmatrix} \bar{z}_{12}^{an} & 0 & \cdots & 0 & \cdots & 0 & 0 & 0 \\ \bar{z}_{12}^{bn} & 0 & \cdots & 0 & \cdots & 0 & 0 & 0 \\ \bar{z}_{12}^{cn} & 0 & \cdots & 0 & \cdots & 0 & 0 & 0 \\ \vdots & \vdots & \cdots & \vdots & \cdots & \vdots & \vdots & \vdots \\ \bar{z}_{12}^{an} & \bar{z}_{23}^{an} & \cdots & \bar{z}_{ij}^{an} & \cdots & 0 & 0 & 0 \\ \bar{z}_{12}^{bn} & \bar{z}_{23}^{bn} & \cdots & \bar{z}_{ij}^{bn} & \cdots & 0 & 0 & 0 \\ \bar{z}_{12}^{cn} & \bar{z}_{23}^{cn} & \cdots & \bar{z}_{ij}^{cn} & \cdots & 0 & 0 & 0 \\ \vdots & \vdots & \cdots & \vdots & \cdots & \vdots & \vdots & \vdots \\ \bar{z}_{12}^{an} & \bar{z}_{23}^{an} & \cdots & 0 & \cdots & \bar{z}_{kl}^{an} & 0 & 0 \\ \bar{z}_{12}^{bn} & \bar{z}_{23}^{bn} & \cdots & 0 & \cdots & \bar{z}_{kl}^{bn} & 0 & 0 \\ \bar{z}_{12}^{cn} & \bar{z}_{23}^{cn} & \cdots & 0 & \cdots & \bar{z}_{kl}^{cn} & 0 & 0 \\ \bar{z}_{12}^{an} & \bar{z}_{23}^{an} & \cdots & 0 & \cdots & \bar{z}_{kl}^{an} & \bar{z}_{lm}^{an} & 0 \\ \bar{z}_{12}^{bn} & \bar{z}_{23}^{bn} & \cdots & 0 & \cdots & \bar{z}_{kl}^{bn} & \bar{z}_{lm}^{bn} & 0 \\ \bar{z}_{12}^{an} & \bar{z}_{23}^{an} & \cdots & 0 & \cdots & \bar{z}_{kl}^{an} & \bar{z}_{lm}^{an} & \bar{z}_{mn_b}^{an} \end{bmatrix}$$

$$\left[\mathbf{BCBV_{pg}}\right] = \begin{bmatrix} \bar{z}_{12}^{ag} & 0 & \cdots & 0 & \cdots & 0 & 0 & 0 \\ \bar{z}_{12}^{bg} & 0 & \cdots & 0 & \cdots & 0 & 0 & 0 \\ \bar{z}_{12}^{cg} & 0 & \cdots & 0 & \cdots & 0 & 0 & 0 \\ \vdots & \vdots & \cdots & \vdots & \cdots & \vdots & \vdots & \vdots \\ \bar{z}_{12}^{ag} & \bar{z}_{23}^{ag} & \cdots & \bar{z}_{ij}^{ag} & \cdots & 0 & 0 & 0 \\ \bar{z}_{12}^{bg} & \bar{z}_{23}^{bg} & \cdots & \bar{z}_{ij}^{bg} & \cdots & 0 & 0 & 0 \\ \bar{z}_{12}^{cg} & \bar{z}_{23}^{cg} & \cdots & \bar{z}_{ij}^{cg} & \cdots & 0 & 0 & 0 \\ \vdots & \vdots & \cdots & \vdots & \cdots & \vdots & \vdots & \vdots \\ \bar{z}_{12}^{ag} & \bar{z}_{23}^{ag} & \cdots & 0 & \cdots & \bar{z}_{kl}^{ag} & 0 & 0 \\ \bar{z}_{12}^{bg} & \bar{z}_{23}^{bg} & \cdots & 0 & \cdots & \bar{z}_{kl}^{bg} & 0 & 0 \\ \bar{z}_{12}^{cg} & \bar{z}_{23}^{cg} & \cdots & 0 & \cdots & \bar{z}_{kl}^{cg} & 0 & 0 \\ \bar{z}_{12}^{ag} & \bar{z}_{23}^{ag} & \cdots & 0 & \cdots & \bar{z}_{kl}^{ag} & \bar{z}_{lm}^{ag} & 0 \\ \bar{z}_{12}^{bg} & \bar{z}_{23}^{bg} & \cdots & 0 & \cdots & \bar{z}_{kl}^{bg} & \bar{z}_{lm}^{bg} & 0 \\ \bar{z}_{12}^{ag} & \bar{z}_{23}^{ag} & \cdots & 0 & \cdots & \bar{z}_{kl}^{ag} & \bar{z}_{lm}^{ag} & \bar{z}_{mn_b}^{ag} \end{bmatrix}$$

$$\left[\mathbf{BCBV_p}\right] = \begin{bmatrix}
\bar{z}_{12}^{aa} & \bar{z}_{12}^{ab} & \bar{z}_{12}^{ac} & \cdots & 0 & 0 & 0 & \cdots & 0 & 0 & 0 & 0 & 0 & 0 \\
\bar{z}_{12}^{ba} & \bar{z}_{12}^{bb} & \bar{z}_{12}^{bc} & \cdots & 0 & 0 & 0 & \cdots & 0 & 0 & 0 & 0 & 0 & 0 \\
\bar{z}_{12}^{ca} & \bar{z}_{12}^{cb} & \bar{z}_{12}^{cc} & \cdots & 0 & 0 & 0 & \cdots & 0 & 0 & 0 & 0 & 0 & 0 \\
\vdots & \vdots & \vdots & \ddots & \vdots & \vdots & \vdots & \cdots & \vdots & \vdots & \vdots & \vdots & \vdots & \vdots \\
\bar{z}_{12}^{aa} & \bar{z}_{12}^{ab} & \bar{z}_{12}^{ac} & \cdots & \bar{z}_{ij}^{aa} & \bar{z}_{ij}^{ab} & \bar{z}_{ij}^{ac} & \cdots & 0 & 0 & 0 & 0 & 0 & 0 \\
\bar{z}_{12}^{ba} & \bar{z}_{12}^{bb} & \bar{z}_{12}^{bc} & \cdots & \bar{z}_{ij}^{ba} & \bar{z}_{ij}^{bb} & \bar{z}_{ij}^{bc} & \cdots & 0 & 0 & 0 & 0 & 0 & 0 \\
\bar{z}_{12}^{ca} & \bar{z}_{12}^{cb} & \bar{z}_{12}^{cc} & \cdots & \bar{z}_{ij}^{ca} & \bar{z}_{ij}^{cb} & \bar{z}_{ij}^{cc} & \cdots & 0 & 0 & 0 & 0 & 0 & 0 \\
\vdots & \vdots & \vdots & \cdots & \vdots & \vdots & \vdots & \ddots & \vdots & \vdots & \vdots & \vdots & \vdots & \vdots \\
\bar{z}_{12}^{aa} & \bar{z}_{12}^{ab} & \bar{z}_{12}^{ac} & \cdots & 0 & 0 & 0 & \cdots & \bar{z}_{kl}^{aa} & \bar{z}_{kl}^{ab} & \bar{z}_{kl}^{ac} & 0 & 0 & 0 \\
\bar{z}_{12}^{ba} & \bar{z}_{12}^{bb} & \bar{z}_{12}^{bc} & \cdots & 0 & 0 & 0 & \cdots & \bar{z}_{kl}^{ba} & \bar{z}_{kl}^{bb} & \bar{z}_{kl}^{bc} & 0 & 0 & 0 \\
\bar{z}_{12}^{ca} & \bar{z}_{12}^{cb} & \bar{z}_{12}^{cc} & \cdots & 0 & 0 & 0 & \cdots & \bar{z}_{kl}^{ca} & \bar{z}_{kl}^{cb} & \bar{z}_{kl}^{cc} & 0 & 0 & 0 \\
\bar{z}_{12}^{aa} & \bar{z}_{12}^{ab} & \bar{z}_{12}^{ac} & \cdots & 0 & 0 & 0 & \cdots & \bar{z}_{kl}^{aa} & \bar{z}_{kl}^{ab} & \bar{z}_{kl}^{ac} & \bar{z}_{lm}^{aa} & \bar{z}_{lm}^{ab} & 0 \\
\bar{z}_{12}^{ba} & \bar{z}_{12}^{bb} & \bar{z}_{12}^{bc} & \cdots & 0 & 0 & 0 & \cdots & \bar{z}_{kl}^{ba} & \bar{z}_{kl}^{bb} & \bar{z}_{kl}^{bc} & \bar{z}_{lm}^{ba} & \bar{z}_{lm}^{bb} & 0 \\
\bar{z}_{12}^{aa} & \bar{z}_{12}^{ab} & \bar{z}_{12}^{ac} & \cdots & 0 & 0 & 0 & \cdots & \bar{z}_{kl}^{aa} & \bar{z}_{kl}^{ab} & \bar{z}_{kl}^{ac} & \bar{z}_{lm}^{aa} & \bar{z}_{lm}^{ab} & \bar{z}_{mn_b}^{aa}
\end{bmatrix}$$

$$[\mathbf{V_p}] = \begin{bmatrix} \bar{V}_2^a & \bar{V}_2^b & \bar{V}_2^c & \cdots & \bar{V}_j^a & \bar{V}_j^b & \bar{V}_j^c & \cdots & \bar{V}_l^a & \bar{V}_l^b & \bar{V}_l^c & \bar{V}_m^a & \bar{V}_m^b & \bar{V}_{n_b}^a \end{bmatrix}^T;$$

$$[\mathbf{V_{ss}}] = \begin{bmatrix} \bar{V}_s^a & \bar{V}_s^b & \bar{V}_s^c & \cdots & \bar{V}_s^a & \bar{V}_s^b & \bar{V}_s^c & \cdots & \bar{V}_s^a & \bar{V}_s^b & \bar{V}_s^c & \bar{V}_s^a & \bar{V}_s^b & \bar{V}_s^a \end{bmatrix}^T;$$

In the above, $[\mathbf{V_p}]$ is the voltage vector of phase buses and $[\mathbf{V_{ss}}]$ is the voltage vector of the substation bus. The substation phase voltages $\bar{V}_s^a$, $\bar{V}_s^b$ and $\bar{V}_s^c$ are assumed to be balanced. The $[\mathbf{BCBV_p}]$ matrix gives the relationship between the voltages of phase buses and the phase branch currents of the system, $[\mathbf{BCBV_{pn}}]$ matrix gives the relationship between the voltages of phase buses and neutral currents of the system while $[\mathbf{BCBV_{pg}}]$ matrix gives the relationship between the voltages of phase buses and ground currents of the system. Hence, for the considered unbalanced three phase four wire multigrounded radial distribution system, the sizes of the $[\mathbf{BCBV_p}]$, $[\mathbf{BCBV_{pn}}]$ and $[\mathbf{BCBV_{pg}}]$ matrices will be $(3u+2v+w-3)\times(3u+2v+w-3)$, $(3u+2v+w-3)\times(u+v+w-1)$ and $(3u+2v+w-3)\times(u+v+w-1)$, respectively.

Development of algorithms for generation of $[\mathbf{BCBV_p}]$***,*** $[\mathbf{BCBV_{pn}}]$ ***and*** $[\mathbf{BCBV_{pg}}]$ ***matrices***:

Step 1. Initialize the $[\mathbf{BCBV_p}]$, $[\mathbf{BCBV_{pn}}]$ and $[\mathbf{BCBV_{pg}}]$ matrices as null matrices of the sizes $(3u+2v+w-3)\times(3u+2v+w-3)$, $(3u+2v+w-3)\times(u+v+w-1)$ and $(3u+2v+w-3)\times(u+v+w-1)$, respectively.

Step 2. (a). If k^{th} line section $\mathbf{L_k^{png}}$, having p phases, neutral n and ground g, is connected between buses i and j, then

$$\begin{aligned}(i).\quad \left[\mathbf{BCBV_p}(j,l_s)\right]_{(p\times p)} &= \left[\mathbf{BCBV_p}(i,l_s)\right]_{(p\times p)};\\ (ii).\quad \left[\mathbf{BCBV_p}(j,k)\right]_{(p\times p)} &= \left[\mathbf{z_{ij}^{abc}}\right]_{(p\times p)}\end{aligned}$$

where $l_s=1,2,\cdots,(k-1)$; $p=3$ and $\left[\mathbf{z_{ij}^{abc}}\right]_{3\times3}$ = $\begin{bmatrix}\bar{z}_{ij}^{aa} & \bar{z}_{ij}^{ab} & \bar{z}_{ij}^{ac}\\ \bar{z}_{ij}^{ba} & \bar{z}_{ij}^{bb} & \bar{z}_{ij}^{bc}\\ \bar{z}_{ij}^{ca} & \bar{z}_{ij}^{cb} & \bar{z}_{ij}^{cc}\end{bmatrix}$ for 3-ϕ; $p=2$ and $\left[\mathbf{z_{ij}^{abc}}\right]_{2\times2}$ = $\begin{bmatrix}\bar{z}_{ij}^{qq} & \bar{z}_{ij}^{qr}\\ \bar{z}_{ij}^{rq} & \bar{z}_{ij}^{rr}\end{bmatrix}$, where, $(q,r)=(a,b)$ or (b,c) or (c,a) for 2-ϕ; $p=1$ and $\left[\mathbf{z_{ij}^{abc}}\right]_{1\times1}$ = $\left[\bar{z}_{ij}^{qq}\right]$, where, $q=(a$ or b or $c)$ for 1-ϕ line section.

(b). If k^{th} line section $\mathbf{L_k^{png}}$, having p phases, neutral n and ground g, is connected between buses i and j, then

$$\begin{aligned}(i).\quad \left[\mathbf{BCBV_{pn}}(j,l_s)\right]_{(p\times 1)} &= \left[\mathbf{BCBV_{pn}}(i,l_s)\right]_{(p\times 1)};\\ (ii).\quad \left[\mathbf{BCBV_{pn}}(j,k)\right]_{(p\times 1)} &= \left[\mathbf{z_{ij}^{qn}}\right]_{(p\times 1)}\end{aligned}$$

where $l_s=1,2,\cdots,(k-1)$; $p=3$ and $\left[\mathbf{z_{ij}^{qn}}\right]_{3\times1}$ = $\begin{bmatrix}\bar{z}_{ij}^{an}\\ \bar{z}_{ij}^{bn}\\ \bar{z}_{ij}^{cn}\end{bmatrix}$ for 3-ϕ; $p=2$ and $\left[\mathbf{z_{ij}^{qn}}\right]_{2\times2}$ = $\begin{bmatrix}\bar{z}_{ij}^{an}\\ \bar{z}_{ij}^{bn}\end{bmatrix}$ or $\begin{bmatrix}\bar{z}_{ij}^{bn}\\ \bar{z}_{ij}^{cn}\end{bmatrix}$ or $\begin{bmatrix}\bar{z}_{ij}^{an}\\ \bar{z}_{ij}^{cn}\end{bmatrix}$ for 2-ϕ; $p=1$ and $\left[\mathbf{z_{ij}^{qn}}\right]_{1\times1}$ = $\left[\bar{z}_{ij}^{an}\right]$ or $\left[\bar{z}_{ij}^{bn}\right]$ or $\left[\bar{z}_{ij}^{cn}\right]$ for 1-ϕ line section.

(c). If k^{th} line section $\mathbf{L_k^{png}}$, having p phases, neutral n and ground g, is connected between

buses i and j, then

$$
\begin{aligned}
(i).\quad \left[\mathbf{BCBV_{pg}}(j,l_s)\right]_{(p\times 1)} &= \left[\mathbf{BCBV_{pg}}(i,l_s)\right]_{(p\times 1)};\\
(ii).\quad \left[\mathbf{BCBV_{pg}}(j,k)\right]_{(p\times 1)} &= \left[\mathbf{z_{ij}^{qg}}\right]_{(p\times 1)}
\end{aligned}
$$

where $l_s = 1, 2, \cdots, (k-1)$; $p = 3$ and $\left[\mathbf{z_{ij}^{qg}}\right]_{3\times 1} = \begin{bmatrix} \bar{z}_{ij}^{ag} \\ \bar{z}_{ij}^{bg} \\ \bar{z}_{ij}^{cg} \end{bmatrix}$ for 3-ϕ; $p = 2$ and $\left[\mathbf{z_{ij}^{qg}}\right]_{2\times 2} = \begin{bmatrix} \bar{z}_{ij}^{ag} \\ \bar{z}_{ij}^{bg} \end{bmatrix}$ or $\begin{bmatrix} \bar{z}_{ij}^{bg} \\ \bar{z}_{ij}^{cg} \end{bmatrix}$ or $\begin{bmatrix} \bar{z}_{ij}^{ag} \\ \bar{z}_{ij}^{cg} \end{bmatrix}$ for 2-ϕ; $p = 1$ and $\left[\mathbf{z_{ij}^{qg}}\right]_{1\times 1} = \left[\bar{z}_{ij}^{ag}\right]$ or $\left[\bar{z}_{ij}^{bg}\right]$ or $\left[\bar{z}_{ij}^{cg}\right]$ for 1-ϕ line section.

Step 3. Repeat Step 2 until all the line sections are included in the $[\mathbf{BCBV_p}]$, $[\mathbf{BCBV_{pn}}]$ and $[\mathbf{BCBV_{pg}}]$ matrices.

5.2.2.2 Formulation of $[\mathrm{BCBV}]$ matrices for neutral bus voltages $\left[\mathbf{V_n}\right]$

The neutral bus voltages $\bar{V}_2^n$, $\bar{V}_3^n$, $\bar{V}_j^n$, $\bar{V}_l^n$, $\bar{V}_m^n$ and $\bar{V}_{n_b}^n$ of the system, shown in Fig. 5.1, can be obtained by applying KVL equations at the neutral branches of the system and are given as,

$$
\begin{aligned}
\bar{V}_2^n &= \bar{V}_s^n - \bar{B}_1^a \bar{z}_{12}^{na} - \bar{B}_1^b \bar{z}_{12}^{nb} - \bar{B}_1^c \bar{z}_{12}^{nc} - \bar{B}_1^n \bar{z}_{12}^{nn} - \bar{B}_1^g \bar{z}_{12}^{ng}\\
\bar{V}_3^n &= \bar{V}_s^n - \bar{B}_1^a \bar{z}_{12}^{na} - \bar{B}_1^b \bar{z}_{12}^{nb} - \bar{B}_1^c \bar{z}_{12}^{nc} - \bar{B}_1^n \bar{z}_{12}^{nn} - \bar{B}_1^g \bar{z}_{12}^{ng} - \bar{B}_2^a \bar{z}_{23}^{na} - \bar{B}_2^b \bar{z}_{23}^{nb} - \bar{B}_2^c \bar{z}_{23}^{nc}\\
&\quad - \bar{B}_2^n \bar{z}_{23}^{nn} - \bar{B}_2^g \bar{z}_{23}^{ng}\\
\bar{V}_j^n &= \bar{V}_s^n - \bar{B}_1^a \bar{z}_{12}^{na} - \bar{B}_1^b \bar{z}_{12}^{nb} - \bar{B}_1^c \bar{z}_{12}^{nc} - \bar{B}_1^n \bar{z}_{12}^{nn} - \bar{B}_1^g \bar{z}_{12}^{ng} - \bar{B}_2^a \bar{z}_{23}^{na} - \bar{B}_2^b \bar{z}_{23}^{nb} - \bar{B}_2^c \bar{z}_{23}^{nc}\\
&\quad - \bar{B}_2^n \bar{z}_{23}^{nn} - \bar{B}_2^g \bar{z}_{23}^{ng} - \cdots - \bar{B}_i^a \bar{z}_{ij}^{na} - \bar{B}_i^b \bar{z}_{ij}^{nb} - \bar{B}_i^c \bar{z}_{ij}^{nc} - \bar{B}_i^n \bar{z}_{ij}^{nn} - \bar{B}_i^g \bar{z}_{ij}^{ng}\\
\bar{V}_l^n &= \bar{V}_s^n - \bar{B}_1^a \bar{z}_{12}^{na} - \bar{B}_1^b \bar{z}_{12}^{nb} - \bar{B}_1^c \bar{z}_{12}^{nc} - \bar{B}_1^n \bar{z}_{12}^{nn} - \bar{B}_1^g \bar{z}_{12}^{ng} - \bar{B}_2^a \bar{z}_{23}^{na} - \bar{B}_2^b \bar{z}_{23}^{nb} - \bar{B}_2^c \bar{z}_{23}^{nc}\\
&\quad - \bar{B}_2^n \bar{z}_{23}^{nn} - \bar{B}_2^g \bar{z}_{23}^{ng} - \cdots - \bar{B}_k^a \bar{z}_{kl}^{na} - \bar{B}_k^b \bar{z}_{kl}^{nb} - \bar{B}_k^c \bar{z}_{kl}^{nc} - \bar{B}_k^n \bar{z}_{kl}^{nn} - \bar{B}_k^g \bar{z}_{kl}^{ng}\\
\bar{V}_m^n &= \bar{V}_s^n - \bar{B}_1^a \bar{z}_{12}^{na} - \bar{B}_1^b \bar{z}_{12}^{nb} - \bar{B}_1^c \bar{z}_{12}^{nc} - \bar{B}_1^n \bar{z}_{12}^{nn} - \bar{B}_1^g \bar{z}_{12}^{ng} - \bar{B}_2^a \bar{z}_{23}^{na} - \bar{B}_2^b \bar{z}_{23}^{nb} - \bar{B}_2^c \bar{z}_{23}^{nc}\\
&\quad - \bar{B}_2^n \bar{z}_{23}^{nn} - \bar{B}_2^g \bar{z}_{23}^{ng} - \cdots - \bar{B}_k^a \bar{z}_{kl}^{na} - \bar{B}_k^b \bar{z}_{kl}^{nb} - \bar{B}_k^c \bar{z}_{kl}^{nc} - \bar{B}_k^n \bar{z}_{kl}^{nn} - \bar{B}_k^g \bar{z}_{kl}^{ng} - \bar{B}_l^a \bar{z}_{lm}^{na}\\
&\quad - \bar{B}_l^b \bar{z}_{lm}^{nb} - \bar{B}_l^n \bar{z}_{lm}^{nn} - \bar{B}_l^g \bar{z}_{lm}^{ng}
\end{aligned}
$$

$$\begin{aligned}\bar{V}^n_{n_b} = \bar{V}^n_s &- \bar{B}^a_1\bar{z}^{na}_{12} - \bar{B}^b_1\bar{z}^{nb}_{12} - \bar{B}^c_1\bar{z}^{nc}_{12} - \bar{B}^n_1\bar{z}^{nn}_{12} - \bar{B}^g_1\bar{z}^{ng}_{12} - \bar{B}^a_2\bar{z}^{na}_{23} - \bar{B}^b_2\bar{z}^{nb}_{23} - \bar{B}^c_2\bar{z}^{nc}_{23} \\ &- \bar{B}^n_2\bar{z}^{nn}_{23} - \bar{B}^g_2\bar{z}^{ng}_{23} - \cdots - \bar{B}^a_k\bar{z}^{na}_{kl} - \bar{B}^b_k\bar{z}^{nb}_{kl} - \bar{B}^c_k\bar{z}^{nc}_{kl} - \bar{B}^n_k\bar{z}^{nn}_{kl} - \bar{B}^g_k\bar{z}^{ng}_{kl} - \bar{B}^a_l\bar{z}^{na}_{lm} \\ &- \bar{B}^b_l\bar{z}^{nb}_{lm} - \bar{B}^n_l\bar{z}^{nn}_{lm} - \bar{B}^g_l\bar{z}^{ng}_{lm} - \bar{B}^a_m\bar{z}^{na}_{mn_b} - \bar{B}^n_m\bar{z}^{nn}_{mn_b} - \bar{B}^g_m\bar{z}^{ng}_{mn_b}\end{aligned} \tag{5.14}$$

Hence, the neutral bus voltages of the distribution system can be expressed in the matrix form as,

$$\left[\mathbf{V_n}\right] = \left[\mathbf{V_{sn}}\right] - \left[\mathbf{BCBV_{np}}\right]\left[\mathbf{B_p}\right] - \left[\mathbf{BCBV_n}\right]\left[\mathbf{B_n}\right] - \left[\mathbf{BCBV_{ng}}\right]\left[\mathbf{B_g}\right] \tag{5.15}$$

where,

$$\left[\mathbf{BCBV_{np}}\right] = \begin{bmatrix}
\bar{z}^{na}_{12} & \bar{z}^{nb}_{12} & \bar{z}^{nc}_{12} & 0 & 0 & 0 & \cdots & 0 & 0 & 0 & \cdots & 0 & 0 & 0 & 0 & 0 & 0 \\
\bar{z}^{na}_{12} & \bar{z}^{nb}_{12} & \bar{z}^{nc}_{12} & \bar{z}^{na}_{23} & \bar{z}^{nb}_{23} & \bar{z}^{nc}_{23} & \cdots & 0 & 0 & 0 & \cdots & 0 & 0 & 0 & 0 & 0 & 0 \\
\vdots & \vdots & \vdots & \vdots & \vdots & \vdots & \cdots & \vdots & \vdots & \vdots & \cdots & \vdots & \vdots & \vdots & \vdots & \vdots & \vdots \\
\bar{z}^{na}_{12} & \bar{z}^{nb}_{12} & \bar{z}^{nc}_{12} & \bar{z}^{na}_{23} & \bar{z}^{nb}_{23} & \bar{z}^{nc}_{23} & \cdots & \bar{z}^{na}_{ij} & \bar{z}^{nb}_{ij} & \bar{z}^{nc}_{ij} & \cdots & 0 & 0 & 0 & 0 & 0 & 0 \\
\vdots & \vdots & \vdots & \vdots & \vdots & \vdots & \cdots & \vdots & \vdots & \vdots & \cdots & \vdots & \vdots & \vdots & \vdots & \vdots & \vdots \\
\bar{z}^{na}_{12} & \bar{z}^{nb}_{12} & \bar{z}^{nc}_{12} & \bar{z}^{na}_{23} & \bar{z}^{nb}_{23} & \bar{z}^{nc}_{23} & \cdots & 0 & 0 & 0 & \cdots & \bar{z}^{na}_{kl} & \bar{z}^{nb}_{kl} & \bar{z}^{nc}_{kl} & 0 & 0 & 0 \\
\bar{z}^{na}_{12} & \bar{z}^{nb}_{12} & \bar{z}^{nc}_{12} & \bar{z}^{na}_{23} & \bar{z}^{nb}_{23} & \bar{z}^{nc}_{23} & \cdots & 0 & 0 & 0 & \cdots & \bar{z}^{na}_{kl} & \bar{z}^{nb}_{kl} & \bar{z}^{nc}_{kl} & \bar{z}^{na}_{lm} & \bar{z}^{nb}_{lm} & 0 \\
\bar{z}^{na}_{12} & \bar{z}^{nb}_{12} & \bar{z}^{nc}_{12} & \bar{z}^{na}_{23} & \bar{z}^{nb}_{23} & \bar{z}^{nc}_{23} & \cdots & 0 & 0 & 0 & \cdots & \bar{z}^{na}_{kl} & \bar{z}^{nb}_{kl} & \bar{z}^{nc}_{kl} & \bar{z}^{na}_{lm} & \bar{z}^{nb}_{lm} & \bar{z}^{na}_{mn_b}
\end{bmatrix}$$

$$\left[\mathbf{BCBV_n}\right] = \begin{bmatrix}
\bar{z}^{nn}_{12} & 0 & \cdots & 0 & \cdots & 0 & 0 & 0 \\
\bar{z}^{nn}_{12} & \bar{z}^{nn}_{23} & \cdots & 0 & \cdots & 0 & 0 & 0 \\
\vdots & \vdots & \ddots & \vdots & \cdots & \vdots & \vdots & \vdots \\
\bar{z}^{nn}_{12} & \bar{z}^{nn}_{23} & \cdots & \bar{z}^{nn}_{ij} & \cdots & 0 & 0 & 0 \\
\vdots & \vdots & \cdots & \vdots & \ddots & \vdots & \vdots & \vdots \\
\bar{z}^{nn}_{12} & \bar{z}^{nn}_{23} & \cdots & 0 & \cdots & \bar{z}^{nn}_{kl} & 0 & 0 \\
\bar{z}^{nn}_{12} & \bar{z}^{nn}_{23} & \cdots & 0 & \cdots & \bar{z}^{nn}_{kl} & \bar{z}^{nn}_{lm} & 0 \\
\bar{z}^{nn}_{12} & \bar{z}^{nn}_{23} & \cdots & 0 & \cdots & \bar{z}^{nn}_{kl} & \bar{z}^{nn}_{lm} & \bar{z}^{nn}_{mn_b}
\end{bmatrix}; \quad \left[\mathbf{BCBV_{ng}}\right] = \begin{bmatrix}
\bar{z}^{ng}_{12} & 0 & \cdots & 0 & \cdots & 0 & 0 & 0 \\
\bar{z}^{ng}_{12} & \bar{z}^{ng}_{23} & \cdots & 0 & \cdots & 0 & 0 & 0 \\
\vdots & \vdots & \ddots & \vdots & \cdots & \vdots & \vdots & \vdots \\
\bar{z}^{ng}_{12} & \bar{z}^{ng}_{23} & \cdots & \bar{z}^{ng}_{ij} & \cdots & 0 & 0 & 0 \\
\vdots & \vdots & \cdots & \vdots & \ddots & \vdots & \vdots & \vdots \\
\bar{z}^{ng}_{12} & \bar{z}^{ng}_{23} & \cdots & 0 & \cdots & \bar{z}^{ng}_{kl} & 0 & 0 \\
\bar{z}^{ng}_{12} & \bar{z}^{ng}_{23} & \cdots & 0 & \cdots & \bar{z}^{ng}_{kl} & \bar{z}^{ng}_{lm} & 0 \\
\bar{z}^{ng}_{12} & \bar{z}^{ng}_{23} & \cdots & 0 & \cdots & \bar{z}^{ng}_{kl} & \bar{z}^{ng}_{lm} & \bar{z}^{ng}_{mn_b}
\end{bmatrix}$$

$$\begin{aligned}\left[\mathbf{V_n}\right] &= \begin{bmatrix}\bar{V}^n_2 & \bar{V}^n_3 & \cdots & \bar{V}^n_j & \cdots & \bar{V}^n_l & \bar{V}^n_m & \bar{V}^n_{n_b}\end{bmatrix}^T; \\ \left[\mathbf{V_{sn}}\right] &= \begin{bmatrix}\bar{V}^n_s & \bar{V}^n_s & \cdots & \bar{V}^n_s & \cdots & \bar{V}^n_s & \bar{V}^n_s & \bar{V}^n_s\end{bmatrix}^T.\end{aligned}$$

$[\mathbf{V_n}]$ is the neutral bus voltage vector and $[\mathbf{V_{sn}}]$ is a column vector that contains only the value of neutral bus voltage ($\bar{V}_s^n$) at the location of grid substation. In general, it is assumed that the neutral bus at substation end is perfectly grounded. Therefore, the value of $\bar{V}_s^n$ is assumed to be zero. The $[\mathbf{BCBV_{np}}]$ matrix gives the relationship between neutral bus voltages and phase branch currents, $[\mathbf{BCBV_n}]$ matrix gives the relationship between neutral bus voltages and neutral currents, and $[\mathbf{BCBV_{ng}}]$ matrix gives the relationship between neutral bus voltages and ground currents of the system. For the considered unbalanced three phase four wire multigrounded radial distribution system, the sizes of the $[\mathbf{BCBV_{np}}]$, $[\mathbf{BCBV_n}]$ and $[\mathbf{BCBV_{ng}}]$ matrices will be $(u+v+w-1)\times(3u+2v+w-3)$, $(u+v+w-1)\times(u+v+w-1)$ and $(u+v+w-1)\times(u+v+w-1)$, respectively.

Development of algorithms for generation of $[\mathbf{BCBV_{np}}]$***,*** $[\mathbf{BCBV_n}]$ ***and*** $[\mathbf{BCBV_{ng}}]$ ***matrices***:

Step 1. Consider an unbalanced three phase four wire multigrounded distribution system, having u three-phase, v two-phase, w single-phase, $(u+v+w)$ neutral and $(u+v+w)$ ground buses. Initialize the $[\mathbf{BCBV_{np}}]$, $[\mathbf{BCBV_n}]$ and $[\mathbf{BCBV_{ng}}]$ matrices as null matrices of the sizes $(u+v+w-1)\times(3u+2v+w-3)$, $(u+v+w-1)\times(u+v+w-1)$ and $(u+v+w-1)\times(u+v+w-1)$, respectively.

Step 2. (a). If k^{th} line section $\mathbf{L_k^{png}}$, having p phases, neutral n and ground g, is connected between buses i and j, then

$$\begin{aligned}(i).\quad \Big[\mathbf{BCBV_{np}}(j,l_s)\Big]_{(1\times p)} &= \Big[\mathbf{BCBV_{np}}(i,l_s)\Big]_{(1\times p)};\\ (ii).\quad \Big[\mathbf{BCBV_{np}}(j,k)\Big]_{(1\times p)} &= \Big[\mathbf{z_{ij}^{nq}}\Big]_{(1\times p)}\end{aligned}$$

where, $l_s = 1, 2, \cdots, (k-1)$; $p=3$ and $\Big[\mathbf{z_{ij}^{nq}}\Big]_{1\times 3}$ = $\begin{bmatrix}\bar{z}_{ij}^{na} & \bar{z}_{ij}^{nb} & \bar{z}_{ij}^{nc}\end{bmatrix}$ for 3-ϕ; $p=2$ and $\Big[\mathbf{z_{ij}^{nq}}\Big]_{1\times 2}$ = $\begin{bmatrix}\bar{z}_{ij}^{na} & \bar{z}_{ij}^{nb}\end{bmatrix}$ or $\begin{bmatrix}\bar{z}_{ij}^{nb} & \bar{z}_{ij}^{nc}\end{bmatrix}$ or $\begin{bmatrix}\bar{z}_{ij}^{na} & \bar{z}_{ij}^{nc}\end{bmatrix}$ for 2-ϕ; $p=1$ and $\Big[\mathbf{z_{ij}^{nq}}\Big]_{1\times 1}$ = $\begin{bmatrix}\bar{z}_{ij}^{na}\end{bmatrix}$ or $\begin{bmatrix}\bar{z}_{ij}^{nb}\end{bmatrix}$ or $\begin{bmatrix}\bar{z}_{ij}^{nc}\end{bmatrix}$ for 1-ϕ line section.

(b). If k^{th} line section $\mathbf{L_k^{png}}$, having p phases, neutral n and ground g, is connected between buses i and j, then

$$\begin{aligned}(i).\quad \Big[\mathbf{BCBV_n}(j,l_s)\Big] &= \Big[\mathbf{BCBV_n}(i,l_s)\Big];\\ (ii).\quad \Big[\mathbf{BCBV_n}(j,k)\Big] &= \bar{z}_{ij}^{nn}\end{aligned}$$

where $l_s = 1, 2, \cdots, (k-1)$;

(c). If k^{th} line section $\mathbf{L_k^{png}}$, having p phases, neutral n and ground g, is connected between buses i and j, then

$$\begin{aligned} (i). \quad \Big[\mathbf{BCBV_{ng}}(j, l_s)\Big] &= \Big[\mathbf{BCBV_{ng}}(i, l_s)\Big]; \\ (ii). \quad \Big[\mathbf{BCBV_{ng}}(j, k)\Big] &= \bar{z}_{ij}^{ng} \end{aligned}$$

where $l_s = 1, 2, \cdots, (k-1)$;

Step 3. Repeat Step 2 until all the line sections are included in the $[\mathbf{BCBV_{np}}]$,$[\mathbf{BCBV_n}]$ and $[\mathbf{BCBV_{ng}}]$ matrices.

5.2.2.3 Formulation of $[\mathrm{BCBV}]$ matrices for ground bus voltages $\left[\mathbf{V_g}\right]$

The ground bus voltages $\bar{V}_2^g$, $\bar{V}_3^g$, $\bar{V}_j^g$, $\bar{V}_l^g$, $\bar{V}_m^g$ and $\bar{V}_{n_b}^g$ of the system shown in Fig. 5.1 can be obtained by applying KVL equations at the fictitious ground branches of the system and are given as,

$$\begin{aligned}
\bar{V}_2^g &= \bar{V}_s^g - \bar{B}_1^a \bar{z}_{12}^{ga} - \bar{B}_1^b \bar{z}_{12}^{gb} - \bar{B}_1^c \bar{z}_{12}^{gc} - \bar{B}_1^n \bar{z}_{12}^{gn} - \bar{B}_1^g \bar{z}_{12}^{gg} \\
\bar{V}_3^g &= \bar{V}_s^g - \bar{B}_1^a \bar{z}_{12}^{ga} - \bar{B}_1^b \bar{z}_{12}^{gb} - \bar{B}_1^c \bar{z}_{12}^{gc} - \bar{B}_1^n \bar{z}_{12}^{gn} - \bar{B}_1^g \bar{z}_{12}^{gg} - \bar{B}_2^a \bar{z}_{23}^{ga} - \bar{B}_2^b \bar{z}_{23}^{gb} - \bar{B}_2^c \bar{z}_{23}^{gc} - \bar{B}_2^n \bar{z}_{23}^{gn} \\
&\quad - \bar{B}_2^g \bar{z}_{23}^{gg} \\
\bar{V}_j^g &= \bar{V}_s^g - \bar{B}_1^a \bar{z}_{12}^{ga} - \bar{B}_1^b \bar{z}_{12}^{gb} - \bar{B}_1^c \bar{z}_{12}^{gc} - \bar{B}_1^n \bar{z}_{12}^{gn} - \bar{B}_1^g \bar{z}_{12}^{gg} - \bar{B}_2^a \bar{z}_{23}^{ga} - \bar{B}_2^b \bar{z}_{23}^{gb} - \bar{B}_2^c \bar{z}_{23}^{gc} - \bar{B}_2^n \bar{z}_{23}^{gn} \\
&\quad - \bar{B}_2^g \bar{z}_{23}^{gg} - \cdots - \bar{B}_i^a \bar{z}_{ij}^{ga} - \bar{B}_i^b \bar{z}_{ij}^{gb} - \bar{B}_i^c \bar{z}_{ij}^{gc} - \bar{B}_i^n \bar{z}_{ij}^{gn} - \bar{B}_i^g \bar{z}_{ij}^{gg} \\
\bar{V}_l^g &= \bar{V}_s^g - \bar{B}_1^a \bar{z}_{12}^{ga} - \bar{B}_1^b \bar{z}_{12}^{gb} - \bar{B}_1^c \bar{z}_{12}^{gc} - \bar{B}_1^n \bar{z}_{12}^{gn} - \bar{B}_1^g \bar{z}_{12}^{gg} - \bar{B}_2^a \bar{z}_{23}^{ga} - \bar{B}_2^b \bar{z}_{23}^{gb} - \bar{B}_2^c \bar{z}_{23}^{gc} - \bar{B}_2^n \bar{z}_{23}^{gn} \\
&\quad - \bar{B}_2^g \bar{z}_{23}^{gg} - \cdots - \bar{B}_k^a \bar{z}_{kl}^{ga} - \bar{B}_k^b \bar{z}_{kl}^{gb} - \bar{B}_k^c \bar{z}_{kl}^{gc} - \bar{B}_k^n \bar{z}_{kl}^{gn} - \bar{B}_k^g \bar{z}_{kl}^{gg} \\
\bar{V}_m^g &= \bar{V}_s^g - \bar{B}_1^a \bar{z}_{12}^{ga} - \bar{B}_1^b \bar{z}_{12}^{gb} - \bar{B}_1^c \bar{z}_{12}^{gc} - \bar{B}_1^n \bar{z}_{12}^{gn} - \bar{B}_1^g \bar{z}_{12}^{gg} - \bar{B}_2^a \bar{z}_{23}^{ga} - \bar{B}_2^b \bar{z}_{23}^{gb} - \bar{B}_2^c \bar{z}_{23}^{gc} - \bar{B}_2^n \bar{z}_{23}^{gn} \\
&\quad - \bar{B}_2^g \bar{z}_{23}^{gg} - \cdots - \bar{B}_k^a \bar{z}_{kl}^{ga} - \bar{B}_k^b \bar{z}_{kl}^{gb} - \bar{B}_k^c \bar{z}_{kl}^{gc} - \bar{B}_k^n \bar{z}_{kl}^{gn} - \bar{B}_k^g \bar{z}_{kl}^{gg} - \bar{B}_l^a \bar{z}_{lm}^{ga} - \bar{B}_l^b \bar{z}_{lm}^{gb} \\
&\quad - \bar{B}_l^n \bar{z}_{lm}^{gn} - \bar{B}_l^g \bar{z}_{lm}^{gg} \\
\bar{V}_{n_b}^g &= \bar{V}_s^g - \bar{B}_1^a \bar{z}_{12}^{ga} - \bar{B}_1^b \bar{z}_{12}^{gb} - \bar{B}_1^c \bar{z}_{12}^{gc} - \bar{B}_1^n \bar{z}_{12}^{gn} - \bar{B}_1^g \bar{z}_{12}^{gg} - \bar{B}_2^a \bar{z}_{23}^{ga} - \bar{B}_2^b \bar{z}_{23}^{gb} - \bar{B}_2^c \bar{z}_{23}^{gc} - \bar{B}_2^n \bar{z}_{23}^{gn} \\
&\quad - \bar{B}_2^g \bar{z}_{23}^{gg} - \cdots - \bar{B}_k^a \bar{z}_{kl}^{ga} - \bar{B}_k^b \bar{z}_{kl}^{gb} - \bar{B}_k^c \bar{z}_{kl}^{gc} - \bar{B}_k^n \bar{z}_{kl}^{gn} - \bar{B}_k^g \bar{z}_{kl}^{gg} - \bar{B}_l^a \bar{z}_{lm}^{ga} - \bar{B}_l^b \bar{z}_{lm}^{gb} \\
&\quad - \bar{B}_l^n \bar{z}_{lm}^{gn} - \bar{B}_l^g \bar{z}_{lm}^{gg} - \bar{B}_m^a \bar{z}_{mn_b}^{ga} - \bar{B}_m^n \bar{z}_{mn_b}^{gn} - \bar{B}_m^g \bar{z}_{mn_b}^{gg}
\end{aligned} \tag{5.16}$$

Hence, the neutral bus voltages of the distribution system can be expressed in the matrix form as,

$$\Big[\mathbf{V_g}\Big] = \Big[\mathbf{V_{sg}}\Big] - \Big[\mathbf{BCBV_{gp}}\Big]\Big[\mathbf{B_p}\Big] - \Big[\mathbf{BCBV_{gn}}\Big]\Big[\mathbf{B_n}\Big] - \Big[\mathbf{BCBV_g}\Big]\Big[\mathbf{B_g}\Big] \tag{5.17}$$

where,

$$\Big[\mathbf{BCBV_{gp}}\Big] = \begin{bmatrix}
\bar{z}_{12}^{ga} & \bar{z}_{12}^{gb} & \bar{z}_{12}^{gc} & 0 & 0 & 0 & \cdots & 0 & 0 & 0 & \cdots & 0 & 0 & 0 & 0 & 0 & 0 \\
\bar{z}_{12}^{ga} & \bar{z}_{12}^{gb} & \bar{z}_{12}^{gc} & \bar{z}_{23}^{ga} & \bar{z}_{23}^{gb} & \bar{z}_{23}^{gc} & \cdots & 0 & 0 & 0 & \cdots & 0 & 0 & 0 & 0 & 0 & 0 \\
\vdots & \vdots & \vdots & \vdots & \vdots & \vdots & \cdots & \vdots & \vdots & \vdots & \cdots & \vdots & \vdots & \vdots & \vdots & \vdots & \vdots \\
\bar{z}_{12}^{ga} & \bar{z}_{12}^{gb} & \bar{z}_{12}^{gc} & \bar{z}_{23}^{ga} & \bar{z}_{23}^{gb} & \bar{z}_{23}^{gc} & \cdots & \bar{z}_{ij}^{ga} & \bar{z}_{ij}^{gb} & \bar{z}_{ij}^{gc} & \cdots & 0 & 0 & 0 & 0 & 0 & 0 \\
\vdots & \vdots & \vdots & \vdots & \vdots & \vdots & \cdots & \vdots & \vdots & \vdots & \cdots & \vdots & \vdots & \vdots & \vdots & \vdots & \vdots \\
\bar{z}_{12}^{ga} & \bar{z}_{12}^{gb} & \bar{z}_{12}^{gc} & \bar{z}_{23}^{ga} & \bar{z}_{23}^{gb} & \bar{z}_{23}^{gc} & \cdots & 0 & 0 & 0 & \cdots & \bar{z}_{kl}^{ga} & \bar{z}_{kl}^{gb} & \bar{z}_{kl}^{gc} & 0 & 0 & 0 \\
\bar{z}_{12}^{ga} & \bar{z}_{12}^{gb} & \bar{z}_{12}^{gc} & \bar{z}_{23}^{na} & \bar{z}_{23}^{gb} & \bar{z}_{23}^{gc} & \cdots & 0 & 0 & 0 & \cdots & \bar{z}_{kl}^{ga} & \bar{z}_{kl}^{gb} & \bar{z}_{kl}^{gc} & \bar{z}_{lm}^{ga} & \bar{z}_{lm}^{gb} & 0 \\
\bar{z}_{12}^{ga} & \bar{z}_{12}^{gb} & \bar{z}_{12}^{gc} & \bar{z}_{23}^{ga} & \bar{z}_{23}^{gb} & \bar{z}_{23}^{gc} & \cdots & 0 & 0 & 0 & \cdots & \bar{z}_{kl}^{ga} & \bar{z}_{kl}^{gb} & \bar{z}_{kl}^{gc} & \bar{z}_{lm}^{ga} & \bar{z}_{lm}^{gb} & \bar{z}_{mn_b}^{ga}
\end{bmatrix}$$

$$\Big[\mathbf{BCBV_{gn}}\Big] = \begin{bmatrix}
\bar{z}_{12}^{gn} & 0 & \cdots & 0 & \cdots & 0 & 0 & 0 \\
\bar{z}_{12}^{gn} & \bar{z}_{23}^{gn} & \cdots & 0 & \cdots & 0 & 0 & 0 \\
\vdots & \vdots & \ddots & \vdots & \cdots & \vdots & \vdots & \vdots \\
\bar{z}_{12}^{gn} & \bar{z}_{23}^{gn} & \cdots & \bar{z}_{ij}^{gn} & \cdots & 0 & 0 & 0 \\
\vdots & \vdots & \cdots & \vdots & \ddots & \vdots & \vdots & \vdots \\
\bar{z}_{12}^{gn} & \bar{z}_{23}^{gn} & \cdots & 0 & \cdots & \bar{z}_{kl}^{gn} & 0 & 0 \\
\bar{z}_{12}^{gn} & \bar{z}_{23}^{gn} & \cdots & 0 & \cdots & \bar{z}_{kl}^{gn} & \bar{z}_{lm}^{gn} & 0 \\
\bar{z}_{12}^{gn} & \bar{z}_{23}^{gn} & \cdots & 0 & \cdots & \bar{z}_{kl}^{gn} & \bar{z}_{lm}^{gn} & \bar{z}_{mn_b}^{gn}
\end{bmatrix}; \quad \Big[\mathbf{BCBV_g}\Big] = \begin{bmatrix}
\bar{z}_{12}^{gg} & 0 & \cdots & 0 & \cdots & 0 & 0 & 0 \\
\bar{z}_{12}^{gg} & \bar{z}_{23}^{gg} & \cdots & 0 & \cdots & 0 & 0 & 0 \\
\vdots & \vdots & \ddots & \vdots & \cdots & \vdots & \vdots & \vdots \\
\bar{z}_{12}^{gg} & \bar{z}_{23}^{gg} & \cdots & \bar{z}_{ij}^{gg} & \cdots & 0 & 0 & 0 \\
\vdots & \vdots & \cdots & \vdots & \ddots & \vdots & \vdots & \vdots \\
\bar{z}_{12}^{gg} & \bar{z}_{23}^{gg} & \cdots & 0 & \cdots & \bar{z}_{kl}^{gg} & 0 & 0 \\
\bar{z}_{12}^{gg} & \bar{z}_{23}^{gg} & \cdots & 0 & \cdots & \bar{z}_{kl}^{gg} & \bar{z}_{lm}^{gg} & 0 \\
\bar{z}_{12}^{gg} & \bar{z}_{23}^{gg} & \cdots & 0 & \cdots & \bar{z}_{kl}^{gg} & \bar{z}_{lm}^{gg} & \bar{z}_{mn_b}^{gg}
\end{bmatrix}$$

$$\begin{aligned}
[\mathbf{V_g}] &= \begin{bmatrix} \bar{V}_2^g & \bar{V}_3^g & \cdots & \bar{V}_j^g & \cdots & \bar{V}_l^g & \bar{V}_m^g & \bar{V}_{n_b}^g \end{bmatrix}^T; \\
[\mathbf{V_{sg}}] &= \begin{bmatrix} \bar{V}_s^g & \bar{V}_s^g & \cdots & \bar{V}_s^g & \cdots & \bar{V}_s^g & \bar{V}_s^g & \bar{V}_s^g \end{bmatrix}^T.
\end{aligned}$$

Here, $[\mathbf{V_g}]$ is the ground bus voltage vector and $[\mathbf{V_{sg}}]$ is a column vector that contains only the value of ground bus voltage ($\bar{V}_s^g$) at the location of grid substation. In general, it is assumed that

the potential of ground bus at substation end is zero. The $[\mathbf{BCBV_{gp}}]$ matrix gives the relationship between ground bus voltages and phase branch currents, $[\mathbf{BCBV_{gn}}]$ gives the relationship between ground bus voltages and neutral currents and $[\mathbf{BCBV_{g}}]$ matrix gives the relationship between ground bus voltages and ground currents of the system. For the considered three phase four wire multigrounded radial distribution system, the sizes of the $[\mathbf{BCBV_{gp}}]$, $[\mathbf{BCBV_{gn}}]$ and $[\mathbf{BCBV_{g}}]$ matrices will be $(u+v+w-1)\times(3u+2v+w-3)$, $(u+v+w-1)\times(u+v+w-1)$ and $(u+v+w-1)\times(u+v+w-1)$, respectively.

Development of Algorithms for generation of $[\mathbf{BCBV_{gp}}]$***,*** $[\mathbf{BCBV_{gn}}]$ ***and*** $[\mathbf{BCBV_{g}}]$ ***matrices***:

Step 1. Initialize the $[\mathbf{BCBV_{gp}}]$, $[\mathbf{BCBV_{gn}}]$ and $[\mathbf{BCBV_{g}}]$ matrices as null matrices of the sizes $(u+v+w-1)\times(3u+2v+w-3)$, $(u+v+w-1)\times(u+v+w-1)$ and $(u+v+w-1)\times(u+v+w-1)$, respectively.

Step 2. (a). If k^{th} line section $\mathbf{L_k^{png}}$, having p phases, neutral n and ground g, is connected between buses i and j, then

$$\begin{aligned}(i).\quad \Big[\mathbf{BCBV_{gp}}(j,l_s)\Big]_{(1\times p)} &= \Big[\mathbf{BCBV_{gp}}(i,l_s)\Big]_{(1\times p)};\\ (ii).\quad \Big[\mathbf{BCBV_{gp}}(j,k)\Big]_{(1\times p)} &= \Big[\mathbf{z_{ij}^{gq}}\Big]_{(1\times p)}\end{aligned}$$

where, $l_s = 1, 2, \cdots, (k-1)$; $p = 3$ and $\Big[\mathbf{z_{ij}^{gq}}\Big]_{1\times 3}$ = $\begin{bmatrix}\bar{z}_{ij}^{ga} & \bar{z}_{ij}^{gb} & \bar{z}_{ij}^{gc}\end{bmatrix}$ for 3-ϕ; $p = 2$ and $\Big[\mathbf{z_{ij}^{gq}}\Big]_{1\times 2}$ = $\begin{bmatrix}\bar{z}_{ij}^{ga} & \bar{z}_{ij}^{gb}\end{bmatrix}$ or $\begin{bmatrix}\bar{z}_{ij}^{gb} & \bar{z}_{ij}^{gc}\end{bmatrix}$ or $\begin{bmatrix}\bar{z}_{ij}^{ga} & \bar{z}_{ij}^{gc}\end{bmatrix}$ for 2-ϕ; $p = 1$ and $\Big[\mathbf{z_{ij}^{gq}}\Big]_{1\times 1}$ = $\begin{bmatrix}\bar{z}_{ij}^{ga}\end{bmatrix}$ or $\begin{bmatrix}\bar{z}_{ij}^{gb}\end{bmatrix}$ or $\begin{bmatrix}\bar{z}_{ij}^{gc}\end{bmatrix}$ for 1-ϕ line section.

(b). If k^{th} line section $\mathbf{L_k^{png}}$, having p phases, neutral n and ground g, is connected between buses i and j, then

$$\begin{aligned}(i).\quad \Big[\mathbf{BCBV_{gn}}(j,l_s)\Big] &= \Big[\mathbf{BCBV_{gn}}(i,l_s)\Big];\\ (ii).\quad \Big[\mathbf{BCBV_{gn}}(j,k)\Big] &= \bar{z}_{ij}^{gn}\end{aligned}$$

where $l_s = 1, 2, \cdots, (k-1)$;

(c). If k^{th} line section $\mathbf{L_k^{png}}$, having p phases, neutral n and ground g, is connected between buses

i and j, then

$$\begin{aligned}(i).\quad \left[\mathbf{BCBV_g}(j,l_s)\right] &= \left[\mathbf{BCBV_g}(i,l_s)\right];\\ (ii).\quad \left[\mathbf{BCBV_g}(j,k)\right] &= \bar{z}_{ij}^{gg}\end{aligned}$$

where $l_s = 1, 2, \cdots, (k-1)$;

Step 3. Repeat Step 2 until all the line sections are included in the $[\mathbf{BCBV_{gp}}]$,$[\mathbf{BCBV_{gn}}]$ and $[\mathbf{BCBV_g}]$ matrices.

The branch currents and the bus voltages of various phases, neutral and ground of the system can now be summarized as,

$$\left[\mathbf{B_p}\right] = \left[\mathbf{BIBC_p}\right]\left[\mathbf{I_L}\right] \tag{5.18}$$

$$\left[\mathbf{B_n}\right] = -\left[\mathbf{BIBC_{pn}}\right]\left[\mathbf{I_L}\right] + \left[\mathbf{BIBC_g}\right]\left[\mathbf{I_{ng}}\right] \tag{5.19}$$

$$\left[\mathbf{B_g}\right] = -\left[\mathbf{BIBC_g}\right]\left[\mathbf{I_{ng}}\right] \tag{5.20}$$

$$\left[\mathbf{V_p}\right] = \left[\mathbf{V_{ss}}\right] - \left[\mathbf{BCBV_p}\right]\left[\mathbf{B_p}\right] - \left[\mathbf{BCBV_{pn}}\right]\left[\mathbf{B_n}\right] - \left[\mathbf{BCBV_{pg}}\right]\left[\mathbf{B_g}\right] \tag{5.21}$$

$$\left[\mathbf{V_n}\right] = \left[\mathbf{V_{sn}}\right] - \left[\mathbf{BCBV_{np}}\right]\left[\mathbf{B_p}\right] - \left[\mathbf{BCBV_n}\right]\left[\mathbf{B_n}\right] - \left[\mathbf{BCBV_{ng}}\right]\left[\mathbf{B_g}\right] \tag{5.22}$$

$$\left[\mathbf{V_g}\right] = \left[\mathbf{V_{sg}}\right] - \left[\mathbf{BCBV_{gp}}\right]\left[\mathbf{B_p}\right] - \left[\mathbf{BCBV_{gn}}\right]\left[\mathbf{B_n}\right] - \left[\mathbf{BCBV_g}\right]\left[\mathbf{B_g}\right] \tag{5.23}$$

The voltages of phase buses of the three phase four wire multigrounded radial distribution system can be rewritten using eqs. (5.18)-(5.21) as,

$$\left[\mathbf{V_p}\right] = \left[\mathbf{V_{ss}}\right] - \left[\mathbf{DLF_1}\right]\left[\mathbf{I_L}\right] - \left[\mathbf{DLF_2}\right]\left[\mathbf{I_{ng}}\right] \tag{5.24}$$

where,

$$\left[\mathbf{DLF_1}\right] = \left[\mathbf{BCBV_p}\right]\left[\mathbf{BIBC_p}\right] - \left[\mathbf{BCBV_{pn}}\right]\left[\mathbf{BIBC_{pn}}\right]$$

$$\left[\mathbf{DLF_2}\right] = \left\{\left[\mathbf{BCBV_{pn}}\right] - \left[\mathbf{BCBV_{pg}}\right]\right\}\left[\mathbf{BIBC_g}\right]$$

Similarly, the neutral bus voltages of a three phase four wire multigrounded radial distribution system can be rewritten using eqs. (5.18)-(5.20) and (5.22) as,

$$\left[\mathbf{V_n}\right] = \left[\mathbf{V_{sn}}\right] - \left[\mathbf{DLF_3}\right]\left[\mathbf{I_L}\right] - \left[\mathbf{DLF_4}\right]\left[\mathbf{I_{ng}}\right] \tag{5.25}$$

where,

$$\left[\mathbf{DLF_3}\right] = \left[\mathbf{BCBV_{np}}\right]\left[\mathbf{BIBC_p}\right] - \left[\mathbf{BCBV_n}\right]\left[\mathbf{BIBC_{pn}}\right]$$

$$\left[\mathbf{DLF_4}\right] = \left\{\left[\mathbf{BCBV_n}\right] - \left[\mathbf{BCBV_{ng}}\right]\right\}\left[\mathbf{BIBC_g}\right]$$

Next, the ground bus voltages of a three phase four wire multigrounded radial distribution system can be rewritten using eqs. (5.18)-(5.20) and (5.23) as,

$$\left[\mathbf{V_g}\right] = \left[\mathbf{V_{sg}}\right] - \left[\mathbf{DLF_5}\right]\left[\mathbf{I_L}\right] - \left[\mathbf{DLF_6}\right]\left[\mathbf{I_{ng}}\right] \tag{5.26}$$

where,

$$\left[\mathbf{DLF_5}\right] = \left[\mathbf{BCBV_{gp}}\right]\left[\mathbf{BIBC_p}\right] - \left[\mathbf{BCBV_{gn}}\right]\left[\mathbf{BIBC_{pn}}\right]$$

$$\left[\mathbf{DLF_6}\right] = \left\{\left[\mathbf{BCBV_{gn}}\right] - \left[\mathbf{BCBV_g}\right]\right\}\left[\mathbf{BIBC_g}\right]$$

Now, the voltage drop between neutral bus voltages and ground bus voltages of the system can be expressed as,

$$\begin{aligned}
\bar{Z}_2^{ngr}\bar{I}_2^{ng} &= \bar{V}_2^n - \bar{V}_2^g \\
\bar{Z}_3^{ngr}\bar{I}_3^{ng} &= \bar{V}_3^n - \bar{V}_3^g \\
\bar{Z}_j^{ngr}\bar{I}_j^{ng} &= \bar{V}_j^n - \bar{V}_j^g \\
\bar{Z}_l^{ngr}\bar{I}_l^{ng} &= \bar{V}_l^n - \bar{V}_l^g \\
\bar{Z}_m^{ngr}\bar{I}_m^{ng} &= \bar{V}_m^n - \bar{V}_m^g \\
\bar{Z}_{n_b}^{ngr}\bar{I}_{n_b}^{ng} &= \bar{V}_{n_b}^n - \bar{V}_{n_b}^g
\end{aligned} \tag{5.27}$$

The voltage drops between neutral bus and ground bus can be written in the matrix form as,

$$\left[\mathbf{Z_{ngr}}\right]\left[\mathbf{I_{ng}}\right] = \left[\mathbf{V_n}\right] - \left[\mathbf{V_g}\right] \tag{5.28}$$

where, $[\mathbf{Z_{ngr}}]$ is a diagonal neutral to ground impedance matrix and is given as,

$$[\mathbf{Z_{ngr}}] = \begin{bmatrix} \bar{Z}_2^{ngr} & 0 & \cdots & 0 & \cdots & 0 & 0 & 0 \\ 0 & \bar{Z}_3^{ngr} & \cdots & 0 & \cdots & 0 & 0 & 0 \\ \vdots & \vdots & \ddots & \vdots & \cdots & \vdots & \vdots & \vdots \\ 0 & 0 & \cdots & \bar{Z}_j^{ngr} & \cdots & 0 & 0 & 0 \\ \vdots & \vdots & \cdots & \vdots & \ddots & \vdots & \vdots & \vdots \\ 0 & 0 & \cdots & 0 & \cdots & \bar{Z}_l^{ngr} & 0 & 0 \\ 0 & 0 & \cdots & 0 & \cdots & 0 & \bar{Z}_m^{ngr} & 0 \\ 0 & 0 & \cdots & 0 & \cdots & 0 & 0 & \bar{Z}_{n_b}^{ngr} \end{bmatrix}$$

The size of $[\mathbf{Z_{ngr}}]$, for the system considered, will be $(u+v+w-1) \times (u+v+w-1)$.

Now, from eqs. (5.25), (5.26) and (5.28),

$$\begin{aligned} \left[\mathbf{Z_{ngr}}\right]\left[\mathbf{I_{ng}}\right] &= \left\{\left[\mathbf{V_{sn}}\right] - \left[\mathbf{DLF_3}\right]\left[\mathbf{I_L}\right] - \left[\mathbf{DLF_4}\right]\left[\mathbf{I_{ng}}\right]\right\} - \left\{\left[\mathbf{V_{sg}}\right] - \left[\mathbf{DLF_5}\right]\left[\mathbf{I_L}\right]\right. \\ &- \left.\left[\mathbf{DLF_6}\right]\left[\mathbf{I_{ng}}\right]\right\} \end{aligned}$$

$$\left[\mathbf{I_{ng}}\right] = \left[\mathbf{Z_{FNG}}\right]^{-1}\left\{\left[\mathbf{V_{sn}}\right] - \left[\mathbf{V_{sg}}\right] + \left[\left[\mathbf{DLF_5}\right] - \left[\mathbf{DLF_3}\right]\right]\left[\mathbf{I_L}\right]\right\} \tag{5.29}$$

where,

$$\left[\mathbf{Z_{FNG}}\right] = \left[\mathbf{Z_{ngr}}\right] + \left[\mathbf{DLF_4}\right] - \left[\mathbf{DLF_6}\right]$$

Next, eliminating the neutral to ground currents $\left[\mathbf{I_{ng}}\right]$ from the expression of the voltages of phase bus (eq. (5.24)) by using eq. (5.29), we obtain,

$$\begin{aligned} \left[\mathbf{V_p}\right] &= \left[\mathbf{V_{ss}}\right] - \left[\mathbf{DLF_1}\right]\left[\mathbf{I_L}\right] - \left[\mathbf{DLF_2}\right]\left\{\left[\mathbf{Z_{FNG}}\right]^{-1}\left\{\left[\mathbf{V_{sn}}\right] - \left[\mathbf{V_{sg}}\right] + \left[\left[\mathbf{DLF_5}\right]\right.\right.\right. \\ &- \left.\left.\left.\left[\mathbf{DLF_3}\right]\right]\left[\mathbf{I_L}\right]\right\}\right\} \end{aligned}$$

$$\left[\mathbf{V_p}\right] = \left[\mathbf{V_{ss}}\right] - \left[\mathbf{F_{1ng}}\right]\left\{\left[\mathbf{V_{sn}}\right] - \left[\mathbf{V_{sg}}\right]\right\} - \left[\mathbf{F_{1PLD}}\right]\left[\mathbf{I_L}\right] \tag{5.30}$$

where,

$$\left[\mathbf{F_{1ng}}\right] = \left[\mathbf{DLF_2}\right]\left[\mathbf{Z_{FNG}}\right]^{-1}$$

$$\left[\mathbf{F_{1PLD}}\right] = \left[\mathbf{DLF_1}\right] + \left\{\left[\mathbf{DLF_2}\right]\left[\mathbf{Z_{FNG}}\right]^{-1}\left[\left[\mathbf{DLF_5}\right] - \left[\mathbf{DLF_3}\right]\right]\right\}$$

Also, eliminate the neutral to ground currents from the expression of neutral bus voltages (eq. (5.25)) by using eq. (5.29) as,

$$\begin{aligned}\left[\mathbf{V_n}\right] &= \left[\mathbf{V_{sn}}\right] - \left[\mathbf{DLF_3}\right]\left[\mathbf{I_L}\right] - \left[\mathbf{DLF_4}\right]\left\{\left[\mathbf{Z_{FNG}}\right]^{-1}\left\{\left[\mathbf{V_{sn}}\right] - \left[\mathbf{V_{sg}}\right] + \left[\left[\mathbf{DLF_5}\right]\right.\right.\right. \\ &- \left.\left.\left.\left[\mathbf{DLF_3}\right]\right]\left[\mathbf{I_L}\right]\right\}\right\}\end{aligned}$$

$$\left[\mathbf{V_n}\right] = \left[\mathbf{F_{2nn}}\right]\left[\mathbf{V_{sn}}\right] - \left[\mathbf{F_{2gg}}\right]\left[\mathbf{V_{sg}}\right] - \left[\mathbf{F_{2PLD}}\right]\left[\mathbf{I_L}\right] \tag{5.31}$$

where,

$$\left[\mathbf{F_{2nn}}\right] = \left[\mathbf{I}\right] - \left[\mathbf{DLF_4}\right]\left[\mathbf{Z_{FNG}}\right]^{-1}$$

$$\left[\mathbf{F_{2gg}}\right] = -\left[\mathbf{DLF_4}\right]\left[\mathbf{Z_{FNG}}\right]^{-1}$$

$$\left[\mathbf{F_{2PLD}}\right] = \left[\mathbf{DLF_3}\right] + \left\{\left[\mathbf{DLF_4}\right]\left[\mathbf{Z_{FNG}}\right]^{-1}\left[\left[\mathbf{DLF_5}\right] - \left[\mathbf{DLF_3}\right]\right]\right\}$$

where, $\left[\mathbf{I}\right]$ is an identity matrix of the size $(u+v+w-1)\times(u+v+w-1)$ for the system considered.

Next, eliminating the neutral to ground currents from the expression of ground bus voltages (eq. (5.26)) by using eq. (5.29), we obtain,

$$\begin{aligned}\left[\mathbf{V_g}\right] &= \left[\mathbf{V_{sg}}\right] - \left[\mathbf{DLF_5}\right]\left[\mathbf{I_L}\right] - \left[\mathbf{DLF_6}\right]\left\{\left[\mathbf{Z_{FNG}}\right]^{-1}\left\{\left[\mathbf{V_{sn}}\right] - \left[\mathbf{V_{sg}}\right] + \left[\left[\mathbf{DLF_5}\right]\right.\right.\right. \\ &- \left.\left.\left.\left[\mathbf{DLF_3}\right]\right]\left[\mathbf{I_L}\right]\right\}\right\}\end{aligned}$$

$$\left[\mathbf{V_g}\right] = \left[\mathbf{F_{3gg}}\right]\left[\mathbf{V_{sg}}\right] - \left[\mathbf{F_{3nn}}\right]\left[\mathbf{V_{sn}}\right] - \left[\mathbf{F_{3PLD}}\right]\left[\mathbf{I_L}\right] \tag{5.32}$$

where,

$$\left[\mathbf{F_{3gg}}\right] = \left[\mathbf{I}\right] + \left[\mathbf{DLF_6}\right]\left[\mathbf{Z_{FNG}}\right]^{-1}$$

$$\left[\mathbf{F_{3nn}}\right] = -\left[\mathbf{DLF_6}\right]\left[\mathbf{Z_{FNG}}\right]^{-1}$$

$$\left[\mathbf{F_{3PLD}}\right] = \left[\mathbf{DLF_5}\right] + \left\{\left[\mathbf{DLF_6}\right]\left[\mathbf{Z_{FNG}}\right]^{-1}\left[\left[\mathbf{DLF_5}\right] - \left[\mathbf{DLF_3}\right]\right]\right\}$$

where, $\left[\mathbf{I}\right]$ is an identity matrix of the size $(u+v+w-1)\times(u+v+w-1)$ for the system considered.

The sizes of various $[\mathbf{BIBC}]$ and $[\mathbf{BCBV}]$ matrices developed for the considered three phase four wire multigrounded radial distribution system are summarized in Table 5.1.

Table 5.1: Sizes of various $[\mathbf{BIBC}]$ and $[\mathbf{BCBV}]$ matrices of the unbalanced three-phase four wire multigrounded distribution system

Matrix	Size	Matrix	Size
$[\mathbf{BIBC_p}]$	$(3u+2v+w-3)\times(3u+2v+w-3)$	$[\mathbf{BIBC_{pn}}]$	$(u+v+w-1)\times(3u+2v+w-3)$
$[\mathbf{BIBC_g}]$	$(u+v+w-1)\times(3u+2v+w-3)$	$[\mathbf{BCBV_p}]$	$(u+v+w-1)\times(u+v+w-1)$
$[\mathbf{BCBV_{pn}}]$	$(u+v+w-1)\times(u+v+w-1)$	$[\mathbf{BCBV_{pg}}]$	$(u+v+w-1)\times(u+v+w-1)$
$[\mathbf{BCBV_{np}}]$	$(3u+2v+w-3)\times(3u+2v+w-3)$	$[\mathbf{BCBV_n}]$	$(u+v+w-1)\times(3u+2v+w-3)$
$[\mathbf{BCBV_{ng}}]$	$(3u+2v+w-3)\times(u+v+w-1)$	$[\mathbf{BCBV_{gp}}]$	$(u+v+w-1)\times(u+v+w-1)$
$[\mathbf{BCBV_{gn}}]$	$(3u+2v+w-3)\times(u+v+w-1)$	$[\mathbf{BCBV_g}]$	$(u+v+w-1)\times(u+v+w-1)$

Steps of algorithm for the load flow analysis of unbalanced three phase four wire multigrounded radial distribution system

1. Initialize the $\left[\mathbf{BIBC_p}\right]$, $\left[\mathbf{BIBC_{pn}}\right]$, $\left[\mathbf{BIBC_g}\right]$, $\left[\mathbf{BCBV_p}\right]$, $\left[\mathbf{BCBV_{pn}}\right]$, $\left[\mathbf{BCBV_{pg}}\right]$, $\left[\mathbf{BCBV_{np}}\right]$, $\left[\mathbf{BCBV_n}\right]$, $\left[\mathbf{BCBV_{ng}}\right]$, $\left[\mathbf{BCBV_{gp}}\right]$, $\left[\mathbf{BCBV_{gn}}\right]$ and $\left[\mathbf{BCBV_g}\right]$ matrices of the three phase four wire multigrounded distribution system as null matrices. The sizes of various matrices for the distribution system considered have been tabulated in Table 5.1.

2. Generate all these matrices as described in Subsections 5.2.1 and 5.2.2.

3. Set the iteration counter $k = 0$. Also, set the initial values of all phase a bus voltages at $1.0\underline{/0^o}$ p.u., phase b bus voltages at $1.0\underline{/-120^o}$ p.u., phase c bus voltages at $1.0\underline{/120^o}$ p.u. and all neutral and ground bus voltages at $(0.0 + j0.0)$ p.u. throughout the system.

4. Calculate the equivalent bus injection currents $\left[\mathbf{I_L}\right]^k$ at all the phase buses of the system using eq. (5.3).

5. $k = k + 1$.

6. Calculate the voltages of phase bus, neutral bus and ground bus $\left([\mathbf{V_p}]^k, [\mathbf{V_n}]^k \text{ and } [\mathbf{V_g}]^k\right)$ of the system using eqs. (5.30)-(5.32).

7. Calculate the error (ϵ),

$$\epsilon = max\left(\left|[\mathbf{V_p}]^k - [\mathbf{V_p}]^{k-1}\right|, \left|[\mathbf{V_n}]^k - [\mathbf{V_n}]^{k-1}\right|, \left|[\mathbf{V_g}]^k - [\mathbf{V_g}]^{k-1}\right|\right)$$

8. If $\epsilon \geq$ tolerance(1.0×10^{-12}), go to step 4, else go to the next step.

9. The obtained values of the voltages $[\mathbf{V_p}]$, $[\mathbf{V_n}]$ and $[\mathbf{V_g}]$ are the final values.

5.3 Short-circuit analysis of unbalanced three phase four wire multigrounded radial distribution system

In this work, two different methods are proposed for the short-circuit analysis of an unbalanced three phase four wire multigrounded distribution system. Relevant expressions have been derived for calculating the fault currents for various short-circuit faults, such as SLG, LLG, LLLG and LL. One of the proposed method is based on $\left[\mathbf{BIBC}\right]$ and $\left[\mathbf{BCBV}\right]$ matrices of the system, while the other one is based on $\left[\mathbf{Y_{bus}}\right]$ matrix of the system. Both the methods are discussed in details in the following sub-sections.

5.3.1 Method 1: $\left[\mathbf{BIBC}\right]$ matrix based short-circuit analysis method

Initially, the load flow analysis of the unbalanced three phase four wire multigrounded distribution system with ground return is performed, using the proposed load flow method to obtain the voltage and the equivalent bus injection current at each phase bus of the system. Next, all the loads are converted into equivalent load impedances using the pre-fault load flow results. For example, the equivalent load impedance at p^{th} phase of i^{th} bus can be calculated as,

$$\bar{z}_{id}^{p} = \frac{(\bar{V}_i^p - \bar{V}_i^n)}{\bar{I}_{id}^{p}}; \quad p = (a, b, c) \tag{5.33}$$

where, $\bar{V}_i^p$ and $\bar{V}_i^n$ are the p^{th} phase voltage and neutral bus voltage at i^{th} bus location obtained from the pre-fault load flow results, respectively. $\bar{I}_{id}^{p}$ is the equivalent injection current at p^{th} phase of i^{th} bus, estimated from the pre-fault load flow solution. Now, consider the different short-circuit faults as follows :

(a) Single line-to-ground (SLG) fault

Let us assume that an SLG fault occurs between phase a and the local ground g_j at j^{th} bus through a fault impedance $\bar{z}_f$, as shown in Fig. 5.2(a) [158], and the fault current $\bar{I}_f^a$ is flowing

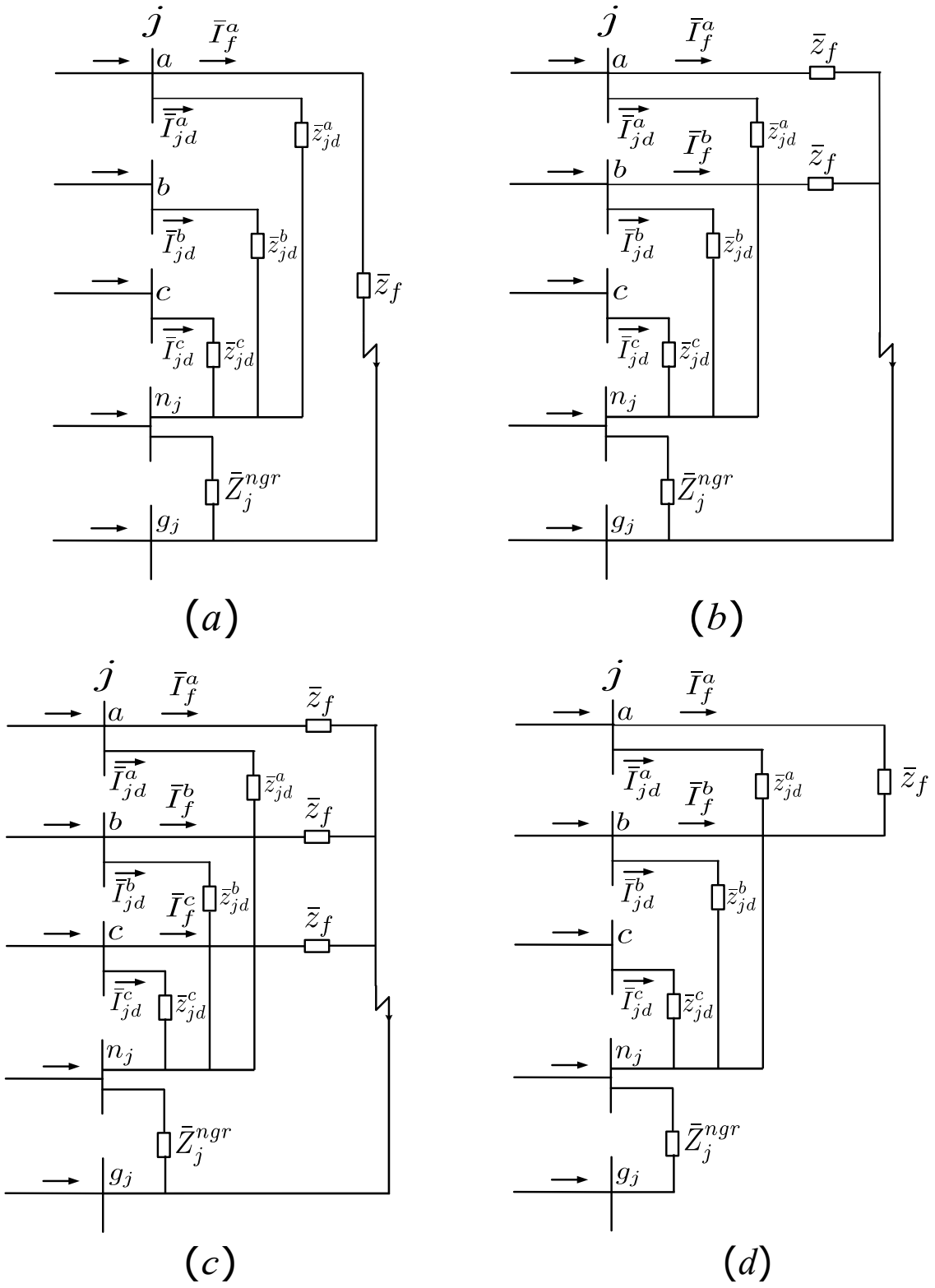

Figure 5.2: Unsymmetrical short-circuit faults, (a) SLG fault, (b) LLG fault, (c) LLLG fault, (d) LL fault

from phase a to the ground g_j. Therefore, only the phase and the ground currents of the system will get modified due to the SLG fault. The modified phase branch currents (only of the faulted phase i.e., phase a) can be written as,

$$\begin{aligned}
\bar{B}^a_{1,f} &= \bar{I}^a_{2d} + \bar{I}^a_{3d} + \cdots + \bar{I}^a_{id} + \bar{I}^a_{jd} + \cdots + \bar{I}^a_{kd} + \bar{I}^a_{ld} + \bar{I}^a_{md} + \bar{I}^a_{n_bd} + \bar{I}^a_f \\
\bar{B}^a_{2,f} &= \bar{I}^a_{3d} + \cdots + \bar{I}^a_{id} + \bar{I}^a_{jd} + \cdots + \bar{I}^a_{kd} + \bar{I}^a_{ld} + \bar{I}^a_{md} + \bar{I}^a_{n_bd} + \bar{I}^a_f \\
\bar{B}^a_{i,f} &= \bar{I}^a_{jd} + \bar{I}^a_f \\
\bar{B}^a_{k,f} &= \bar{I}^a_{ld} + \bar{I}^a_{md} + \bar{I}^a_{n_bd} \\
\bar{B}^a_{l,f} &= \bar{I}^a_{md} + \bar{I}^a_{n_bd} \\
\bar{B}^a_{m,f} &= \bar{I}^a_{n_bd}
\end{aligned} \tag{5.34}$$

Hence, the modified phase branch currents due to SLG fault can be expressed in the matrix form as,

$$\left[\mathbf{B_{p,f}}\right] = \left[\mathbf{BIBC_p}\right]\left[\mathbf{I_L}\right] + \left[\mathbf{BIBC_{fp}}\right]\left[\mathbf{I_f}\right] \tag{5.35}$$

where,

$$\left[\mathbf{BIBC_{fp}}\right] = \left[\mathbf{BIBC_p}(:, f_b^q)\right] = \begin{bmatrix} 1 & 0 & 0 & \cdots & 1 & 0 & 0 & \cdots & 0 & 0 & 0 & 0 & 0 & 0 \end{bmatrix}^T ; \left[\mathbf{I_f}\right] = \bar{I}^a_f$$

Here, $\left[\mathbf{BIBC_{fp}}\right]$ matrix for an SLG fault is a column vector of $\left[\mathbf{BIBC_p}\right]$ matrix corresponding to the faulted phase q (here, $q = a$) of the faulted bus f_b (here, $f_b = j$) and $\left[\mathbf{I_f}\right]$ is a fault current vector. The size of $\left[\mathbf{BIBC_{fp}}\right]$ matrix for SLG fault, for an unbalanced three phase four wire multigrounded distribution system considered, will be $(3u + 2v + w - 3) \times 1$.

Similarly, the modified ground currents due to SLG fault can be written as,

$$\begin{aligned}
\bar{B}^g_{1,f} &= -\bar{I}^{ng}_2 - \bar{I}^{ng}_3 - \cdots - \bar{I}^{ng}_i - \bar{I}^{ng}_j - \cdots - \bar{I}^{ng}_k - \bar{I}^{ng}_l - \bar{I}^{ng}_m - \bar{I}^{ng}_{n_b} - \bar{I}^a_f \\
\bar{B}^g_{2,f} &= -\bar{I}^{ng}_3 - \cdots - \bar{I}^{ng}_i - \bar{I}^{ng}_j - \cdots - \bar{I}^{ng}_k - \bar{I}^{ng}_l - \bar{I}^{ng}_m - \bar{I}^{ng}_{n_b} - \bar{I}^a_f \\
\bar{B}^g_{i,f} &= -\bar{I}^{ng}_j - \bar{I}^a_f \\
\bar{B}^g_{k,f} &= -\bar{I}^{ng}_l - \bar{I}^{ng}_m - \bar{I}^{ng}_{n_b} \\
\bar{B}^g_{l,f} &= -\bar{I}^{ng}_m - \bar{I}^{ng}_{n_b} \\
\bar{B}^g_{m,f} &= -\bar{I}^{ng}_{n_b}
\end{aligned} \tag{5.36}$$

Hence, the modified ground currents can be expressed in the matrix form as,

$$\left[\mathbf{B_{g,f}}\right] = -\left[\mathbf{BIBC_g}\right]\left[\mathbf{I_{ng}}\right] - \left[\mathbf{BIBC_{fg}}\right]\left[\mathbf{I_f}\right] \tag{5.37}$$

where,

$$\left[\mathbf{BIBC_{fg}}\right] = \left[\mathbf{BIBC_g}(:, f_b^{ng})\right] = \begin{bmatrix}1 & 1 & \cdots & 1 & \cdots & 0 & 0 & 0\end{bmatrix}^T$$

Here, $\left[\mathbf{BIBC_{fg}}\right]$ matrix for an SLG fault is a column vector of $\left[\mathbf{BIBC_g}\right]$ matrix corresponding to the neutral to ground connection (ng) of faulted bus (f_b). For a fault at j^{th} bus $(f_b = j)$, $\left[\mathbf{BIBC_{fg}}\right] = \left[\mathbf{BIBC_{fg}}(:, j^{ng})\right]$ as obtained from the definition of $\left[\mathbf{BIBC_g}\right]$ given in eq. (5.8). The size of $\left[\mathbf{BIBC_{fg}}\right]$ matrix will be $(u+v+w-1)\times 1$.

Rewriting the eqs. (5.21)-(5.23) for the voltages of phase buses, neutral buses and ground buses under the fault conditions (due to SLG fault), we obtain

$$\left[\mathbf{V_{p,f}}\right] = \left[\mathbf{V_{ss}}\right] - \left[\mathbf{BCBV_p}\right]\left[\mathbf{B_{p,f}}\right] - \left[\mathbf{BCBV_{pn}}\right]\left[\mathbf{B_n}\right] - \left[\mathbf{BCBV_{pg}}\right]\left[\mathbf{B_{g,f}}\right] \tag{5.38}$$

$$\left[\mathbf{V_{n,f}}\right] = \left[\mathbf{V_{sn}}\right] - \left[\mathbf{BCBV_{np}}\right]\left[\mathbf{B_{p,f}}\right] - \left[\mathbf{BCBV_n}\right]\left[\mathbf{B_n}\right] - \left[\mathbf{BCBV_{ng}}\right]\left[\mathbf{B_{g,f}}\right] \tag{5.39}$$

$$\left[\mathbf{V_{g,f}}\right] = \left[\mathbf{V_{sg}}\right] - \left[\mathbf{BCBV_{gp}}\right]\left[\mathbf{B_{p,f}}\right] - \left[\mathbf{BCBV_{gn}}\right]\left[\mathbf{B_n}\right] - \left[\mathbf{BCBV_g}\right]\left[\mathbf{B_{g,f}}\right] \tag{5.40}$$

Therefore, the expressions for voltages of phase buses, neutral buses and ground buses can be rewritten using eqs. (5.35), (5.37) and (5.38)-(5.40) as,

$$\left[\mathbf{V_{p,f}}\right] = \left[\mathbf{V_{ss}}\right] - \left[\mathbf{DLF_1}\right]\left[\mathbf{I_L}\right] - \left[\mathbf{DLF_2}\right]\left[\mathbf{I_{ng}}\right] - \left[\mathbf{DFF_1}\right]\left[\mathbf{I_f}\right] \tag{5.41}$$

$$\left[\mathbf{V_{n,f}}\right] = \left[\mathbf{V_{sn}}\right] - \left[\mathbf{DLF_3}\right]\left[\mathbf{I_L}\right] - \left[\mathbf{DLF_4}\right]\left[\mathbf{I_{ng}}\right] - \left[\mathbf{DFF_2}\right]\left[\mathbf{I_f}\right] \tag{5.42}$$

$$\left[\mathbf{V_{g,f}}\right] = \left[\mathbf{V_{sg}}\right] - \left[\mathbf{DLF_5}\right]\left[\mathbf{I_L}\right] - \left[\mathbf{DLF_6}\right]\left[\mathbf{I_{ng}}\right] - \left[\mathbf{DFF_3}\right]\left[\mathbf{I_f}\right] \tag{5.43}$$

where,

$$\begin{aligned}
\left[\mathbf{DFF_1}\right] &= \left[\mathbf{BCBV_p}\right]\left[\mathbf{BIBC_{fp}}\right] - \left[\mathbf{BCBV_{pg}}\right]\left[\mathbf{BIBC_{fg}}\right] \\
\left[\mathbf{DFF_2}\right] &= \left[\mathbf{BCBV_{np}}\right]\left[\mathbf{BIBC_{fp}}\right] - \left[\mathbf{BCBV_{ng}}\right]\left[\mathbf{BIBC_{fg}}\right] \\
\left[\mathbf{DFF_3}\right] &= \left[\mathbf{BCBV_{gp}}\right]\left[\mathbf{BIBC_{fp}}\right] - \left[\mathbf{BCBV_g}\right]\left[\mathbf{BIBC_{fg}}\right]
\end{aligned}$$

The neutral to ground currents under the fault conditions are then calculated using the neutral and ground bus voltages under fault conditions with the help of eqs. (5.28), (5.42) and (5.43) as,

$$\begin{aligned}
\left[\mathbf{Z_{ngr}}\right]\left[\mathbf{I_{ng}}\right] &= \left\{\left[\mathbf{V_{sn}}\right] - \left[\mathbf{DLF_3}\right]\left[\mathbf{I_L}\right] - \left[\mathbf{DLF_4}\right]\left[\mathbf{I_{ng}}\right] - \left[\mathbf{DFF_2}\right]\left[\mathbf{I_f}\right]\right\} \\
&- \left\{\left[\mathbf{V_{sg}}\right] - \left[\mathbf{DLF_5}\right]\left[\mathbf{I_L}\right] - \left[\mathbf{DLF_6}\right]\left[\mathbf{I_{ng}}\right] - \left[\mathbf{DFF_3}\right]\left[\mathbf{I_f}\right]\right\}
\end{aligned}$$

$$\begin{aligned}\left[\mathbf{I_{ng}}\right] &= \left[\mathbf{Z_{FNG}}\right]^{-1}\left\{\left[\mathbf{V_{sn}}\right]-\left[\mathbf{V_{sg}}\right]+\left[\left[\mathbf{DLF_5}\right]-\left[\mathbf{DLF_3}\right]\right]\left[\mathbf{I_L}\right]\right. \\ &+ \left.\left[\left[\mathbf{DFF_3}\right]-\left[\mathbf{DFF_2}\right]\right]\left[\mathbf{I_f}\right]\right\} \end{aligned} \tag{5.44}$$

where,

$$\left[\mathbf{Z_{FNG}}\right]=\left[\mathbf{Z_{ngr}}\right]+\left[\mathbf{DLF_4}\right]-\left[\mathbf{DLF_6}\right]$$

Again, the voltages of phase buses, neutral buses and ground buses are recalculated using eqs. (5.41)-(5.44) as,

$$\left[\mathbf{V_{p,f}}\right]=\left[\mathbf{V_{ss}}\right]-\left[\mathbf{F_{1ng}}\right]\left\{\left[\mathbf{V_{sn}}\right]-\left[\mathbf{V_{sg}}\right]\right\}-\left[\mathbf{F_{1PLD}}\right]\left[\mathbf{I_L}\right]-\left[\mathbf{DFF_{1n}}\right]\left[\mathbf{I_f}\right] \tag{5.45}$$

$$\left[\mathbf{V_{n,f}}\right]=\left[\mathbf{F_{2nn}}\right]\left[\mathbf{V_{sn}}\right]-\left[\mathbf{F_{2gg}}\right]\left[\mathbf{V_{sg}}\right]-\left[\mathbf{F_{2PLD}}\right]\left[\mathbf{I_L}\right]-\left[\mathbf{DFF_{2n}}\right]\left[\mathbf{I_f}\right] \tag{5.46}$$

$$\left[\mathbf{V_{g,f}}\right]=\left[\mathbf{F_{3gg}}\right]\left[\mathbf{V_{sg}}\right]-\left[\mathbf{F_{3nn}}\right]\left[\mathbf{V_{sn}}\right]-\left[\mathbf{F_{3PLD}}\right]\left[\mathbf{I_L}\right]-\left[\mathbf{DFF_{3n}}\right]\left[\mathbf{I_f}\right] \tag{5.47}$$

where, matrices $\left[\mathbf{F_{1ng}}\right]$, $\left[\mathbf{F_{1PLD}}\right]$, $\left[\mathbf{F_{2nn}}\right]$, $\left[\mathbf{F_{2gg}}\right]$, $\left[\mathbf{F_{2PLD}}\right]$, $\left[\mathbf{F_{3gg}}\right]$, $\left[\mathbf{F_{3nn}}\right]$ and $\left[\mathbf{F_{3PLD}}\right]$ have already been defined in eqs. (5.30)-(5.32) and

$$\left[\mathbf{DFF_{1n}}\right]=\left[\mathbf{DFF_1}\right]+\left[\mathbf{DLF_2}\right]\left[\mathbf{Z_{FNG}}\right]^{-1}\left\{\left[\mathbf{DFF_3}\right]-\left[\mathbf{DFF_2}\right]\right\}$$

$$\left[\mathbf{DFF_{2n}}\right]=\left[\mathbf{DFF_2}\right]+\left[\mathbf{DLF_4}\right]\left[\mathbf{Z_{FNG}}\right]^{-1}\left\{\left[\mathbf{DFF_3}\right]-\left[\mathbf{DFF_2}\right]\right\}$$

$$\left[\mathbf{DFF_{3n}}\right]=\left[\mathbf{DFF_3}\right]+\left[\mathbf{DLF_6}\right]\left[\mathbf{Z_{FNG}}\right]^{-1}\left\{\left[\mathbf{DFF_3}\right]-\left[\mathbf{DFF_2}\right]\right\}$$

For an SLG fault at phase a of j^{th} bus with a fault impedance $\bar{z}_f$, as shown in Fig. 5.2(a), the voltage equation at fault bus can be written as,

$$\bar{z}_f\bar{I}_f^a=\bar{V}_{j,f}^a-\bar{V}_{j,f}^g \tag{5.48}$$

where, $\bar{V}_{j,f}^a$ and $\bar{V}_{j,f}^g$ are the voltages of phase a and ground g_j at fault bus j under the fault conditions, respectively. Substituting the values of $\bar{V}_{j,f}^a$ and $\bar{V}_{j,f}^g$ from eqs. (5.45) and (5.47) into eq. (5.48), with an assumption that the neutral and ground buses at the substation end are perfectly grounded (i.e. at zero potential; $\bar{V}_s^n=0$, $\bar{V}_s^g=0$), and writing the resultant equation in a matrix form, we obtain

$$\begin{aligned}\left[\mathbf{Z_f}\right]\left[\mathbf{I_f}\right] &= \bar{V}_s^a-\left[\mathbf{F_{1PLD}}(f_b^q,:)\right]\left[\mathbf{I_L}\right]-\left[\mathbf{DFF_{1n}}(f_b^q,1)\right]\left[\mathbf{I_f}\right]+\left[\mathbf{F_{3PLD}}(g_{f_b},:)\right]\left[\mathbf{I_L}\right] \\ &+ \left[\mathbf{DFF_{3n}}(g_{f_b},1)\right]\left[\mathbf{I_f}\right] \end{aligned} \tag{5.49}$$

where, for SLG fault (at phase a of j^{th} bus), $\Big[\mathbf{Z_f}\Big] = \bar{z}_f$; $\Big[\mathbf{F_{1PLD}}(f_b^q, :)\Big]$ represents the row vector of matrix $\Big[\mathbf{F_{1PLD}}\Big]$ corresponding to the faulty phase q (here, $q = a$) of fault bus f_b (here, $f_b = j$); $\Big[\mathbf{DFF_{1n}}(f_b^q, 1)\Big]$ represents the row vector of matrix $\Big[\mathbf{DFF_{1n}}\Big]$ corresponding to the faulty phase q of fault bus f_b; $\Big[\mathbf{F_{3PLD}}(g_{f_b}, :)\Big]$ represents the row vector of matrix $\Big[\mathbf{F_{3PLD}}\Big]$ corresponding to the ground g_{f_b} at the location of fault bus f_b; $\Big[\mathbf{DFF_{3n}}(g_{f_b}, 1)\Big]$ represents the row vector of matrix $\Big[\mathbf{DFF_{3n}}\Big]$ corresponding to the ground g_{f_b} at the location of fault bus f_b.
Hence, the fault current $\Big[\mathbf{I_f}\Big]$ is obtained from eq. (5.49) as,

$$\Big[\mathbf{I_f}\Big] = \Big[\mathbf{Z_{F1}}\Big]^{-1} \bar{V}_s^a - \Big[\mathbf{F_{13PLD}^{flt}}\Big] \Big[\mathbf{I_L}\Big] \tag{5.50}$$

where,

$$\begin{aligned}
\Big[\mathbf{Z_{F1}}\Big] &= \Big[\mathbf{Z_f}\Big] + \Big[\mathbf{DFF_{1n}}(f_b^q, 1)\Big] - \Big[\mathbf{DFF_{3n}}(g_{f_b}, 1)\Big] \\
\Big[\mathbf{F_{13PLD}^{flt}}\Big] &= \Big[\mathbf{Z_{F1}}\Big]^{-1} \Big\{ \Big[\mathbf{F_{1PLD}}(f_b^q, :)\Big] - \Big[\mathbf{F_{3PLD}}(g_{f_b}, :)\Big] \Big\}
\end{aligned}$$

(b) Double line-to-ground (LLG) fault

Let us consider an LLG fault between phases a and b, and the local ground g_j at j^{th} bus location through a fault impedance $\bar{z}_f$, as shown in Fig. 5.2(b) [158]. The two fault currents $\bar{I}_f^a$ and $\bar{I}_f^b$ are flowing from phases a and b to the ground g_j at j^{th} bus, respectively. The modified phase branch currents (of faulty phases a and b) due to LLG fault in Fig. 5.2(b), can be written as,

$$\begin{aligned}
\bar{B}_{1,f}^a &= \bar{I}_{2d}^a + \bar{I}_{3d}^a + \cdots + \bar{I}_{id}^a + \bar{I}_{jd}^a + \cdots + \bar{I}_{kd}^a + \bar{I}_{ld}^a + \bar{I}_{md}^a + \bar{I}_{n_bd}^a + \bar{I}_f^a \\
\bar{B}_{1,f}^b &= \bar{I}_{2d}^b + \bar{I}_{3d}^b + \cdots + \bar{I}_{id}^b + \bar{I}_{jd}^b + \cdots + \bar{I}_{kd}^b + \bar{I}_{ld}^b + \bar{I}_{md}^b + \bar{I}_f^b \\
\bar{B}_{2,f}^a &= \bar{I}_{3d}^a + \cdots + \bar{I}_{id}^a + \bar{I}_{jd}^a + \cdots + \bar{I}_{kd}^a + \bar{I}_{ld}^a + \bar{I}_{md}^a + \bar{I}_{n_bd}^a + \bar{I}_f^a \\
\bar{B}_{2,f}^b &= \bar{I}_{3d}^b + \cdots + \bar{I}_{id}^b + \bar{I}_{jd}^b + \cdots + \bar{I}_{kd}^b + \bar{I}_{ld}^b + \bar{I}_{md}^b + \bar{I}_f^b \\
\bar{B}_{i,f}^a &= \bar{I}_{jd}^a + \bar{I}_f^a \\
\bar{B}_{i,f}^b &= \bar{I}_{jd}^b + \bar{I}_f^b \\
\bar{B}_{k,f}^a &= \bar{I}_{ld}^a + \bar{I}_{md}^a + \bar{I}_{n_bd}^a \\
\bar{B}_{k,f}^b &= \bar{I}_{ld}^b + \bar{I}_{md}^b \\
\bar{B}_{l,f}^a &= \bar{I}_{md}^a + \bar{I}_{n_bd}^a \\
\bar{B}_{l,f}^b &= \bar{I}_{md}^b \\
\bar{B}_{m,f}^a &= \bar{I}_{n_bd}^a
\end{aligned} \tag{5.51}$$

The phase branch currents under fault conditions can be written in a matrix form as,

$$\left[\mathbf{B_{p,f}}\right] = \left[\mathbf{BIBC_p}\right]\left[\mathbf{I_L}\right] + \left[\mathbf{BIBC_{fp}}\right]\left[\mathbf{I_f}\right] \tag{5.52}$$

where,

$$\begin{aligned}\left[\mathbf{BIBC_{fp}}\right] &= \begin{bmatrix}\mathbf{BIBC_p}(:, f_b^{q_1})\\ \mathbf{BIBC_p}(:, f_b^{q_2})\end{bmatrix}^T = \begin{bmatrix}1 & 0 & 0 & \cdots & 1 & 0 & 0 & \cdots & 0 & 0 & 0 & 0 & 0 & 0\\ 0 & 1 & 0 & \cdots & 0 & 1 & 0 & \cdots & 0 & 0 & 0 & 0 & 0 & 0\end{bmatrix}^T;\\ \left[\mathbf{I_f}\right] &= \begin{bmatrix}\bar{I}_f^a & \bar{I}_f^b\end{bmatrix}^T.\end{aligned}$$

Here, $\left[\mathbf{BIBC_{fp}}\right]$ matrix for a LLG fault contains column vectors of $\left[\mathbf{BIBC_p}\right]$ matrix corresponding to the faulty phases q_1 and q_2 (here, $q_1 = a, q_2 = b$) of the fault bus f_b (here, $f_b = j$). The size of $\left[\mathbf{BIBC_{fp}}\right]$ matrix for LLG fault will be $(3u + 2v + w - 3) \times 2$.

The modified ground currents due to LLG fault, as shown in Fig. 5.2(b), can be written as,

$$\begin{aligned}\bar{B}_{1,f}^g &= -\bar{I}_2^{ng} - \bar{I}_3^{ng} - \cdots - \bar{I}_i^{ng} - \bar{I}_j^{ng} - \cdots - \bar{I}_k^{ng} - \bar{I}_l^{ng} - \bar{I}_m^{ng} - \bar{I}_{n_b}^{ng} - \bar{I}_f^a - \bar{I}_f^b\\ \bar{B}_{2,f}^g &= -\bar{I}_3^{ng} - \cdots - \bar{I}_i^{ng} - \bar{I}_j^{ng} - \cdots - \bar{I}_k^{ng} - \bar{I}_l^{ng} - \bar{I}_m^{ng} - \bar{I}_{n_b}^{ng} - \bar{I}_f^a - \bar{I}_f^b\\ \bar{B}_{i,f}^g &= -\bar{I}_j^{ng} - \bar{I}_f^a - \bar{I}_f^b\\ \bar{B}_{k,f}^g &= -\bar{I}_l^{ng} - \bar{I}_m^{ng} - \bar{I}_{n_b}^{ng};\quad \bar{B}_{l,f}^g = -\bar{I}_m^{ng} - \bar{I}_{n_b}^{ng};\quad \bar{B}_{m,f}^g = -\bar{I}_{n_b}^{ng}\end{aligned} \tag{5.53}$$

Hence, the ground currents due to LLG fault can be expressed in a matrix form as,

$$\left[\mathbf{B_{g,f}}\right] = -\left[\mathbf{BIBC_g}\right]\left[\mathbf{I_{ng}}\right] - \left[\mathbf{BIBC_{fg}}\right]\left[\mathbf{I_f}\right] \tag{5.54}$$

where,

$$\left[\mathbf{BIBC_{fg}}\right] = \begin{bmatrix}\mathbf{BIBC_g}(:, g_{f_b})\\ \mathbf{BIBC_g}(:, g_{f_b})\end{bmatrix}^T = \begin{bmatrix}1 & 1 & \cdots & 1 & \cdots & 0 & 0 & 0\\ 1 & 1 & \cdots & 1 & \cdots & 0 & 0 & 0\end{bmatrix}^T$$

Here, $\left[\mathbf{BIBC_{fg}}\right]$ is a sub-matrix of $\left[\mathbf{BIBC_g}\right]$ matrix and contains two identical column vectors (due to LLG fault) corresponding to the ground bus g_{f_b} of fault bus f_b (here, $f_b = j$). The size of $\left[\mathbf{BIBC_{fg}}\right]$ matrix for LLG fault will be $(u+v+w-1)\times 2$. Once, the $\left[\mathbf{BIBC_{fp}}\right]$ and $\left[\mathbf{BIBC_{fg}}\right]$ matrices are formed for LLG fault, the voltages of phase buses, neutral buses and ground buses under the fault conditions are then calculated by using eqs. (5.45)-(5.47).

For an LLG fault at phases a and b of j^{th} bus through a fault impedance $\bar{z}_f$, as shown in Fig. 5.2(b), the voltage equations at the fault bus can be written as,

$$\begin{aligned} \bar{z}_f \bar{I}_f^a &= \bar{V}_{j,f}^a - \bar{V}_{j,f}^g \\ \bar{z}_f \bar{I}_f^b &= \bar{V}_{j,f}^b - \bar{V}_{j,f}^g \end{aligned} \tag{5.55}$$

where, $\bar{V}_{j,f}^a$ and $\bar{V}_{j,f}^b$ are the voltages of phase a and b of fault bus j under fault conditions, respectively; $\bar{V}_{j,f}^g$ is the ground bus voltage under fault conditions at fault location (bus j). Substituting the values of $\bar{V}_{j,f}^a$, $\bar{V}_{j,f}^b$ and $\bar{V}_{j,f}^g$ from eqs. (5.45) and (5.47) into eq. (5.55), with an assumption that the neutral and ground buses at the substation end are perfectly grounded (i.e. at zero potential; $\bar{V}_s^n = 0$, $\bar{V}_s^g = 0$), and writing it in the matrix form, we obtain,

$$\begin{aligned} \left[\mathbf{Z_f}\right]\left[\mathbf{I_f}\right] &= \begin{bmatrix} \bar{V}_s^a \\ \bar{V}_s^b \end{bmatrix} - \begin{bmatrix} \mathbf{F_{1PLD}}(f_b^{q_1},:) \\ \mathbf{F_{1PLD}}(f_b^{q_2},:) \end{bmatrix}\left[\mathbf{I_L}\right] - \begin{bmatrix} \mathbf{DFF_{1n}}(f_b^{q_1},:) \\ \mathbf{DFF_{1n}}(f_b^{q_2},:) \end{bmatrix}\left[\mathbf{I_f}\right] \\ &+ \begin{bmatrix} \mathbf{F_{3PLD}}(g_{f_b},:) \\ \mathbf{F_{3PLD}}(g_{f_b},:) \end{bmatrix}\left[\mathbf{I_L}\right] + \begin{bmatrix} \mathbf{DFF_{3n}}(g_{f_b},:) \\ \mathbf{DFF_{3n}}(g_{f_b},:) \end{bmatrix}\left[\mathbf{I_f}\right] \end{aligned} \tag{5.56}$$

where, for an LLG fault (at phases a and b of j^{th} bus), $\left[\mathbf{Z_f}\right] = \begin{bmatrix} \bar{z}_f & 0 \\ 0 & \bar{z}_f \end{bmatrix}$; $\left[\mathbf{F_{1PLD}}(f_b^{q_1},:)\right]$ and $\left[\mathbf{F_{1PLD}}(f_b^{q_2},:)\right]$ are the row vectors of matrix $\left[\mathbf{F_{1PLD}}\right]$ corresponding to the faulty phases q_1 and q_2 (here, $q_1 = a$, $q_2 = b$) of faulted bus f_b (here, $f_b = j$), respectively; $\left[\mathbf{DFF_{1n}}(f_b^{q_1},:)\right]$ and $\left[\mathbf{DFF_{1n}}(f_b^{q_2},:)\right]$ are the row vectors of matrix $\left[\mathbf{DFF_{1n}}\right]$ corresponding to the faulty phases q_1 and q_2 of faulted bus f_b, respectively; $\left[\mathbf{F_{3PLD}}(g_{f_b},:)\right]$ is the row vector of matrix $\left[\mathbf{F_{3PLD}}\right]$ corresponding to the ground g_{f_b} at the location of faulted bus f_b; $\left[\mathbf{DFF_{3n}}(g_{f_b},:)\right]$ is the row vector of matrix $\left[\mathbf{DFF_{3n}}\right]$ corresponding to the ground g_{f_b} at the location of faulted bus f_b. Hence, the fault current $\left[\mathbf{I_f}\right]$ for an LLG fault is obtained from eq. (5.56) as,

$$\left[\mathbf{I_f}\right] = \left[\mathbf{Z_{F1}}\right]^{-1}\begin{bmatrix} \bar{V}_s^a \\ \bar{V}_s^b \end{bmatrix} - \left[\mathbf{F}_{\mathbf{13PLD}}^{flt}\right]\left[\mathbf{I_L}\right] \tag{5.57}$$

where,

$$\left[\mathbf{Z_{F1}}\right] = \left[\mathbf{Z_f}\right] + \begin{bmatrix} \mathbf{DFF_{1n}}(f_b^{q_1},:) \\ \mathbf{DFF_{1n}}(f_b^{q_2},:) \end{bmatrix} - \begin{bmatrix} \mathbf{DFF_{3n}}(g_{f_b},:) \\ \mathbf{DFF_{3n}}(g_{f_b},:) \end{bmatrix}$$

$$\left[\mathbf{F}_{\mathbf{13PLD}}^{flt}\right] = \left[\mathbf{Z_{F1}}\right]^{-1} \left\{ \begin{bmatrix} \mathbf{F_{1PLD}}(f_b^{q_1},:) \\ \mathbf{F_{1PLD}}(f_b^{q_2},:) \end{bmatrix} - \begin{bmatrix} \mathbf{F_{3PLD}}(g_{f_b},:) \\ \mathbf{F_{3PLD}}(g_{f_b},:) \end{bmatrix} \right\}$$

(c) Triple line-to-ground (LLLG) fault

Let us now consider an LLLG fault between all the phases a, b and c, and the local ground g_j at j^{th} bus location through a fault impedance $\bar{z}_f$, as shown in Fig. 5.2(c) [158]. The fault currents $\bar{I}_f^a$, $\bar{I}_f^b$ and $\bar{I}_f^c$ are flowing from phases a, b and c to the ground g_j at j^{th} bus, respectively. The phase branch currents (of faulty phases a, b and c) due to LLLG fault in Fig. 5.2(c), can be written as,

$$\begin{aligned}
\bar{B}_{1,f}^a &= \bar{I}_{2d}^a + \bar{I}_{3d}^a + \cdots + \bar{I}_{id}^a + \bar{I}_{jd}^a + \cdots + \bar{I}_{kd}^a + \bar{I}_{ld}^a + \bar{I}_{md}^a + \bar{I}_{n_bd}^a + \bar{I}_f^a \\
\bar{B}_{1,f}^b &= \bar{I}_{2d}^b + \bar{I}_{3d}^b + \cdots + \bar{I}_{id}^b + \bar{I}_{jd}^b + \cdots + \bar{I}_{kd}^b + \bar{I}_{ld}^b + \bar{I}_{md}^b + \bar{I}_f^b \\
\bar{B}_{1,f}^c &= \bar{I}_{2d}^c + \bar{I}_{3d}^c + \cdots + \bar{I}_{id}^c + \bar{I}_{jd}^c + \cdots + \bar{I}_{kd}^c + \bar{I}_{ld}^c + \bar{I}_f^c \\
\bar{B}_{2,f}^a &= \bar{I}_{3d}^a + \cdots + \bar{I}_{id}^a + \bar{I}_{jd}^a + \cdots + \bar{I}_{kd}^a + \bar{I}_{ld}^a + \bar{I}_{md}^a + \bar{I}_{n_bd}^a + \bar{I}_f^a \\
\bar{B}_{2,f}^b &= \bar{I}_{3d}^b + \cdots + \bar{I}_{id}^b + \bar{I}_{jd}^b + \cdots + \bar{I}_{kd}^b + \bar{I}_{ld}^b + \bar{I}_{md}^b + \bar{I}_f^b \\
\bar{B}_{2,f}^c &= \bar{I}_{3d}^c + \cdots + \bar{I}_{id}^c + \bar{I}_{jd}^c + \cdots + \bar{I}_{kd}^c + \bar{I}_{ld}^c + \bar{I}_f^c \\
\bar{B}_{i,f}^a &= \bar{I}_{jd}^a + \bar{I}_f^a \\
\bar{B}_{i,f}^b &= \bar{I}_{jd}^b + \bar{I}_f^b \\
\bar{B}_{i,f}^c &= \bar{I}_{jd}^c + \bar{I}_f^c \\
\bar{B}_{k,f}^a &= \bar{I}_{ld}^a + \bar{I}_{md}^a + \bar{I}_{n_bd}^a \\
\bar{B}_{k,f}^b &= \bar{I}_{ld}^b + \bar{I}_{md}^b \\
\bar{B}_{k,f}^c &= \bar{I}_{ld}^c \\
\bar{B}_{l,f}^a &= \bar{I}_{md}^a + \bar{I}_{n_bd}^a \\
\bar{B}_{l,f}^b &= \bar{I}_{md}^b \\
\bar{B}_{m,f}^a &= \bar{I}_{n_bd}^a
\end{aligned} \tag{5.58}$$

The phase branch currents due to LLLG fault can be written in a matrix form as,

$$\left[\mathbf{B_{p,f}}\right] = \left[\mathbf{BIBC_p}\right]\left[\mathbf{I_L}\right] + \left[\mathbf{BIBC_{fp}}\right]\left[\mathbf{I_f}\right] \tag{5.59}$$

where,

$$\left[\mathbf{BIBC_{fp}}\right] = \begin{bmatrix}\mathbf{BIBC_p}(:, f_b^{q_1})\\ \mathbf{BIBC_p}(:, f_b^{q_2})\\ \mathbf{BIBC_p}(:, f_b^{q_3})\end{bmatrix}^T = \begin{bmatrix}1 & 0 & 0 & \cdots & 1 & 0 & 0 & \cdots & 0 & 0 & 0 & 0 & 0 & 0\\ 0 & 1 & 0 & \cdots & 0 & 1 & 0 & \cdots & 0 & 0 & 0 & 0 & 0 & 0\\ 0 & 0 & 1 & \cdots & 0 & 0 & 1 & \cdots & 0 & 0 & 0 & 0 & 0 & 0\end{bmatrix}^T ;$$

$$\left[\mathbf{I_f}\right] = \begin{bmatrix}\bar{I}_f^a & \bar{I}_f^b & \bar{I}_f^c\end{bmatrix}^T .$$

Here, $\left[\mathbf{BIBC_{fp}}\right]$ matrix for an LLLG fault contains column vectors of $\left[\mathbf{BIBC_p}\right]$ matrix corresponding to the faulty phases q_1, q_2 and q_3 (here, $q_1 = a, q_2 = b, q_3 = c$) of the faulted bus f_b (here, $f_b = j$). The size of the $\left[\mathbf{BIBC_{fp}}\right]$ matrix for a LLLG fault, will be $(3u + 2v + w - 3) \times 3$. The ground currents due to LLLG fault, as shown in Fig. 5.2(c), can be written as,

$$\begin{aligned}
\bar{B}_{1,f}^g &= -\bar{I}_2^{ng} - \bar{I}_3^{ng} - \cdots - \bar{I}_i^{ng} - \bar{I}_j^{ng} - \cdots - \bar{I}_k^{ng} - \bar{I}_l^{ng} - \bar{I}_m^{ng} - \bar{I}_{n_b}^{ng} - \bar{I}_f^a - \bar{I}_f^b - \bar{I}_f^c\\
\bar{B}_{2,f}^g &= -\bar{I}_3^{ng} - \cdots - \bar{I}_i^{ng} - \bar{I}_j^{ng} - \cdots - \bar{I}_k^{ng} - \bar{I}_l^{ng} - \bar{I}_m^{ng} - \bar{I}_{n_b}^{ng} - \bar{I}_f^a - \bar{I}_f^b - \bar{I}_f^c\\
\bar{B}_{i,f}^g &= -\bar{I}_j^{ng} - \bar{I}_f^a - \bar{I}_f^b - \bar{I}_f^c\\
\bar{B}_{k,f}^g &= -\bar{I}_l^{ng} - \bar{I}_m^{ng} - \bar{I}_{n_b}^{ng}\\
\bar{B}_{l,f}^g &= -\bar{I}_m^{ng} - \bar{I}_{n_b}^{ng}\\
\bar{B}_{m,f}^g &= -\bar{I}_{n_b}^{ng}
\end{aligned} \tag{5.60}$$

Hence, the modified ground currents due to LLLG fault can be expressed in the matrix form as,

$$\left[\mathbf{B_{g,f}}\right] = -\left[\mathbf{BIBC_g}\right]\left[\mathbf{I_{ng}}\right] - \left[\mathbf{BIBC_{fg}}\right]\left[\mathbf{I_f}\right] \tag{5.61}$$

where,

$$\left[\mathbf{BIBC_{fg}}\right] = \begin{bmatrix}\mathbf{BIBC_g}(:, g_{f_b})\\ \mathbf{BIBC_g}(:, g_{f_b})\\ \mathbf{BIBC_g}(:, g_{f_b})\end{bmatrix}^T = \begin{bmatrix}1 & 1 & \cdots & 1 & \cdots & 0 & 0 & 0\\ 1 & 1 & \cdots & 1 & \cdots & 0 & 0 & 0\\ 1 & 1 & \cdots & 1 & \cdots & 0 & 0 & 0\end{bmatrix}^T$$

Here, $\left[\mathbf{BIBC_{fg}}\right]$ is a sub-matrix of $\left[\mathbf{BIBC_g}\right]$ matrix and contains three identical column vectors (due to LLLG fault) corresponding to the ground bus g_{f_b} of faulted bus f_b (here, $f_b = j$). The size of $\left[\mathbf{BIBC_{fg}}\right]$ matrix for an LLLG fault, will be $(u + v + w - 1) \times 3$. Once, the $\left[\mathbf{BIBC_{fp}}\right]$ and $\left[\mathbf{BIBC_{fg}}\right]$ matrices are formed for LLLG fault, the voltages of phase buses, neutral buses and ground buses under the fault conditions are then calculated using eqs. (5.45)-(5.47).

For an LLLG fault at j^{th} bus through a fault impedance $\bar{z}_f$, as shown in Fig. 5.2(c), the voltage equations at fault bus can be written as,

$$\begin{aligned} \bar{z}_f \bar{I}_f^a &= \bar{V}_{j,f}^a - \bar{V}_{j,f}^g \\ \bar{z}_f \bar{I}_f^b &= \bar{V}_{j,f}^b - \bar{V}_{j,f}^g \\ \bar{z}_f \bar{I}_f^c &= \bar{V}_{j,f}^c - \bar{V}_{j,f}^g \end{aligned} \tag{5.62}$$

where, $\bar{V}_{j,f}^a$, $\bar{V}_{j,f}^b$ and $\bar{V}_{j,f}^c$ are the voltages of phases a, b and c of fault bus j under the fault conditions, respectively. $\bar{V}_{j,f}^g$ is the ground bus voltage at the fault location (bus j) under fault conditions. Substituting the values of $\bar{V}_{j,f}^a$, $\bar{V}_{j,f}^b$, $\bar{V}_{j,f}^c$ and $\bar{V}_{j,f}^g$ from eqs. (5.45) and (5.47) into eq. (5.62), with an assumption that the neutral and ground buses at the substation end are perfectly grounded (i.e at zero potential; $\bar{V}_s^n = 0$, $\bar{V}_s^g = 0$), and writing the resultant equation in the matrix form, we obtain,

$$\begin{aligned} \left[\mathbf{Z_f}\right]\left[\mathbf{I_f}\right] &= \begin{bmatrix} \bar{V}_s^a \\ \bar{V}_s^b \\ \bar{V}_s^c \end{bmatrix} - \begin{bmatrix} \mathbf{F_{1PLD}}(f_b^{q_1},:) \\ \mathbf{F_{1PLD}}(f_b^{q_2},:) \\ \mathbf{F_{1PLD}}(f_b^{q_3},:) \end{bmatrix}\left[\mathbf{I_L}\right] - \begin{bmatrix} \mathbf{DFF_{1n}}(f_b^{q_1},:) \\ \mathbf{DFF_{1n}}(f_b^{q_2},:) \\ \mathbf{DFF_{1n}}(f_b^{q_3},:) \end{bmatrix}\left[\mathbf{I_f}\right] \\ &+ \begin{bmatrix} \mathbf{F_{3PLD}}(g_{f_b},:) \\ \mathbf{F_{3PLD}}(g_{f_b},:) \\ \mathbf{F_{3PLD}}(g_{f_b},:) \end{bmatrix}\left[\mathbf{I_L}\right] + \begin{bmatrix} \mathbf{DFF_{3n}}(g_{f_b},:) \\ \mathbf{DFF_{3n}}(g_{f_b},:) \\ \mathbf{DFF_{3n}}(g_{f_b},:) \end{bmatrix}\left[\mathbf{I_f}\right] \end{aligned} \tag{5.63}$$

where, for an LLLG fault (at j^{th} bus), $\left[\mathbf{Z_f}\right] = \begin{bmatrix} \bar{z}_f & 0 & 0 \\ 0 & \bar{z}_f & 0 \\ 0 & 0 & \bar{z}_f \end{bmatrix}$; $\left[\mathbf{F_{1PLD}}(f_b^{q_1},:)\right]$, $\left[\mathbf{F_{1PLD}}(f_b^{q_2},:)\right]$ and $\left[\mathbf{F_{1PLD}}(f_b^{q_3},:)\right]$ are the row vectors of matrix $\left[\mathbf{F_{1PLD}}\right]$ corresponding to the faulty phases q_1, q_2 and q_3 (here, $q_1 = a$, $q_2 = b$, $q_2 = c$) of faulted bus f_b (here, $f_b = j$), respectively; $\left[\mathbf{DFF_{1n}}(f_b^{q_1},:)\right]$, $\left[\mathbf{DFF_{1n}}(f_b^{q_2},:)\right]$ and $\left[\mathbf{DFF_{1n}}(f_b^{q_3},:)\right]$ are the row vectors of matrix $\left[\mathbf{DFF_{1n}}\right]$ corresponding to the faulty phases q_1, q_2 and q_3 of faulted bus f_b, respectively; $\left[\mathbf{F_{3PLD}}(g_{f_b},:)\right]$ is the row vector of matrix $\left[\mathbf{F_{3PLD}}\right]$ corresponding to the ground g_{f_b} at the location of faulted bus f_b; $\left[\mathbf{DFF_{3n}}(g_{f_b},:)\right]$ is the row vector of matrix $\left[\mathbf{DFF_{3n}}\right]$ corresponding to the ground g_{f_b} at the location of faulted bus f_b. Hence, the fault current $\left[\mathbf{I_f}\right]$ for LLLG fault is obtained from eq. (5.63)

as,

$$\Big[\mathbf{I_f}\Big] = \Big[\mathbf{Z_{F1}}\Big]^{-1} \begin{bmatrix} \bar{V}_s^a \\ \bar{V}_s^b \\ \bar{V}_s^c \end{bmatrix} - \Big[\mathbf{F}_{\mathbf{13PLD}}^{flt}\Big] \Big[\mathbf{I_L}\Big] \tag{5.64}$$

where,

$$\begin{aligned} \Big[\mathbf{Z_{F1}}\Big] &= \Big[\mathbf{Z_f}\Big] + \begin{bmatrix} \mathbf{DFF_{1n}}(f_b^{q_1},:) \\ \mathbf{DFF_{1n}}(f_b^{q_2},:) \\ \mathbf{DFF_{1n}}(f_b^{q_3},:) \end{bmatrix} - \begin{bmatrix} \mathbf{DFF_{3n}}(g_{f_b},:) \\ \mathbf{DFF_{3n}}(g_{f_b},:) \\ \mathbf{DFF_{3n}}(g_{f_b},:) \end{bmatrix} \\ \Big[\mathbf{F}_{\mathbf{13PLD}}^{flt}\Big] &= \Big[\mathbf{Z_{F1}}\Big]^{-1} \left\{ \begin{bmatrix} \mathbf{F_{1PLD}}(f_b^{p_1},:) \\ \mathbf{F_{1PLD}}(f_b^{p_2},:) \\ \mathbf{F_{1PLD}}(f_b^{p_3},:) \end{bmatrix} - \begin{bmatrix} \mathbf{F_{3PLD}}(g_{f_b},:) \\ \mathbf{F_{3PLD}}(g_{f_b},:) \\ \mathbf{F_{3PLD}}(g_{f_b},:) \end{bmatrix} \right\} \end{aligned}$$

(d) Line-to-line (LL) fault

Let us consider an LL fault occurred between phases a and b of j^{th} bus through a fault impedance $\bar{z}_f$, as shown in Fig. 5.2(d) [158]. The fault current $\bar{I}_f^a$ is flowing from phase a to b at j^{th} bus. Hence, only the phase branch currents will be modified due to LL fault. The phase branch currents (of faulty phase a and b) due to LL fault, as shown in Fig. 5.2(d), can be written as,

$$\begin{aligned} \bar{B}_{1,f}^a &= \bar{I}_{2d}^a + \bar{I}_{3d}^a + \cdots + \bar{I}_{id}^a + \bar{I}_{jd}^a + \cdots + \bar{I}_{kd}^a + \bar{I}_{ld}^a + \bar{I}_{md}^a + \bar{I}_{n_bd}^a + \bar{I}_f^a \\ \bar{B}_{1,f}^b &= \bar{I}_{2d}^b + \bar{I}_{3d}^b + \cdots + \bar{I}_{id}^b + \bar{I}_{jd}^b + \cdots + \bar{I}_{kd}^b + \bar{I}_{ld}^b + \bar{I}_{md}^b - \bar{I}_f^a \\ \bar{B}_{2,f}^a &= \bar{I}_{3d}^a + \cdots + \bar{I}_{id}^a + \bar{I}_{jd}^a + \cdots + \bar{I}_{kd}^a + \bar{I}_{ld}^a + \bar{I}_{md}^a + \bar{I}_{n_bd}^a + \bar{I}_f^a \\ \bar{B}_{2,f}^b &= \bar{I}_{3d}^b + \cdots + \bar{I}_{id}^b + \bar{I}_{jd}^b + \cdots + \bar{I}_{kd}^b + \bar{I}_{ld}^b + \bar{I}_{md}^b - \bar{I}_f^a \\ \bar{B}_{i,f}^a &= \bar{I}_{jd}^a + \bar{I}_f^a \\ \bar{B}_{i,f}^b &= \bar{I}_{jd}^b - \bar{I}_f^a \\ \bar{B}_{k,f}^a &= \bar{I}_{ld}^a + \bar{I}_{md}^a + \bar{I}_{n_bd}^a \\ \bar{B}_{k,f}^b &= \bar{I}_{ld}^b + \bar{I}_{md}^b \\ \bar{B}_{l,f}^a &= \bar{I}_{md}^a + \bar{I}_{n_bd}^a \\ \bar{B}_{l,f}^b &= \bar{I}_{md}^b \\ \bar{B}_{m,f}^a &= \bar{I}_{n_bd}^a \end{aligned} \tag{5.65}$$

The phase branch currents due to LL fault can be written in the matrix form as,

$$\left[\mathbf{B_{p,f}}\right] = \left[\mathbf{BIBC_p}\right]\left[\mathbf{I_L}\right] + \left[\mathbf{BIBC_{fp}}\right]\left[\mathbf{I_f}\right] \tag{5.66}$$

where,

$$\begin{aligned}\left[\mathbf{BIBC_{fp}}\right] &= \begin{bmatrix}1 & -1 & 0 & \cdots & 1 & -1 & 0 & \cdots & 0 & 0 & 0 & 0 & 0 & 0\end{bmatrix}^T; \\ &= \left[\mathbf{BIBC_p}(:, f_b^{q_1}) - \mathbf{BIBC_p}(:, f_b^{q_2})\right] \\ \left[\mathbf{I_f}\right] &= \left[\bar{I}_f^a\right].\end{aligned}$$

The size of $\left[\mathbf{BIBC_{fp}}\right]$ matrix for LL fault will be $(3u + 2v + w - 3) \times 1$.

Rewriting the eqs. (5.21)-(5.23) for the voltages of phase buses, neutral buses and ground buses under the fault conditions (due to LL fault) as,

$$\left[\mathbf{V_{p,f}}\right] = \left[\mathbf{V_{ss}}\right] - \left[\mathbf{BCBV_p}\right]\left[\mathbf{B_{p,f}}\right] - \left[\mathbf{BCBV_{pn}}\right]\left[\mathbf{B_n}\right] - \left[\mathbf{BCBV_{pg}}\right]\left[\mathbf{B_g}\right] \tag{5.67}$$

$$\left[\mathbf{V_{n,f}}\right] = \left[\mathbf{V_{sn}}\right] - \left[\mathbf{BCBV_{np}}\right]\left[\mathbf{B_{p,f}}\right] - \left[\mathbf{BCBV_n}\right]\left[\mathbf{B_n}\right] - \left[\mathbf{BCBV_{ng}}\right]\left[\mathbf{B_g}\right] \tag{5.68}$$

$$\left[\mathbf{V_{g,f}}\right] = \left[\mathbf{V_{sg}}\right] - \left[\mathbf{BCBV_{gp}}\right]\left[\mathbf{B_{p,f}}\right] - \left[\mathbf{BCBV_{gn}}\right]\left[\mathbf{B_n}\right] - \left[\mathbf{BCBV_g}\right]\left[\mathbf{B_g}\right] \tag{5.69}$$

Substituting the values of $\left[\mathbf{B_n}\right]$, $\left[\mathbf{B_g}\right]$ and $\left[\mathbf{B_{p,f}}\right]$ from eqs. (5.19), (5.20) and (5.66) into eqs. (5.67)-(5.69) and rewriting the expressions for the voltages of phase buses, neutral buses and ground buses under the fault conditions, we obtain,

$$\left[\mathbf{V_{p,f}}\right] = \left[\mathbf{V_{ss}}\right] - \left[\mathbf{DLF_1}\right]\left[\mathbf{I_L}\right] - \left[\mathbf{DLF_2}\right]\left[\mathbf{I_{ng}}\right] - \left[\mathbf{DFF'_1}\right]\left[\mathbf{I_f}\right] \tag{5.70}$$

$$\left[\mathbf{V_{n,f}}\right] = \left[\mathbf{V_{sn}}\right] - \left[\mathbf{DLF_3}\right]\left[\mathbf{I_L}\right] - \left[\mathbf{DLF_4}\right]\left[\mathbf{I_{ng}}\right] - \left[\mathbf{DFF'_2}\right]\left[\mathbf{I_f}\right] \tag{5.71}$$

$$\left[\mathbf{V_{g,f}}\right] = \left[\mathbf{V_{sg}}\right] - \left[\mathbf{DLF_5}\right]\left[\mathbf{I_L}\right] - \left[\mathbf{DLF_6}\right]\left[\mathbf{I_{ng}}\right] - \left[\mathbf{DFF'_3}\right]\left[\mathbf{I_f}\right] \tag{5.72}$$

where,

$$\begin{aligned}\left[\mathbf{DFF'_1}\right] &= \left[\mathbf{BCBV_p}\right]\left[\mathbf{BIBC_{fp}}\right] \\ \left[\mathbf{DFF'_2}\right] &= \left[\mathbf{BCBV_{np}}\right]\left[\mathbf{BIBC_{fp}}\right] \\ \left[\mathbf{DFF'_3}\right] &= \left[\mathbf{BCBV_{gp}}\right]\left[\mathbf{BIBC_{fp}}\right]\end{aligned}$$

Now, the neutral to ground currents are calculated with the help of neutral and ground bus voltages under the fault conditions using eqs. (5.28), (5.71) and (5.72) as,

$$\begin{aligned}\left[\mathbf{Z_{ngr}}\right]\left[\mathbf{I_{ng}}\right] &= \left\{\left[\mathbf{V_{sn}}\right]-\left[\mathbf{DLF_3}\right]\left[\mathbf{I_L}\right]-\left[\mathbf{DLF_4}\right]\left[\mathbf{I_{ng}}\right]-\left[\mathbf{DFF_2^{'}}\right]\left[\mathbf{I_f}\right]\right\} \\ &- \left\{\left[\mathbf{V_{sg}}\right]-\left[\mathbf{DLF_5}\right]\left[\mathbf{I_L}\right]-\left[\mathbf{DLF_6}\right]\left[\mathbf{I_{ng}}\right]-\left[\mathbf{DFF_3^{'}}\right]\left[\mathbf{I_f}\right]\right\}\end{aligned}$$

$$\begin{aligned}\left[\mathbf{I_{ng}}\right] &= \left[\mathbf{Z_{FNG}}\right]^{-1}\left\{\left[\mathbf{V_{sn}}\right]-\left[\mathbf{V_{sg}}\right]+\left[\left[\mathbf{DLF_5}\right]-\left[\mathbf{DLF_3}\right]\right]\left[\mathbf{I_L}\right]\right. \\ &+ \left.\left[\left[\mathbf{DFF_3^{'}}\right]-\left[\mathbf{DFF_2^{'}}\right]\right]\left[\mathbf{I_f}\right]\right\} \qquad (5.73)\end{aligned}$$

Now, substituting the value of $\left[\mathbf{I_{ng}}\right]$ from eq. (5.73) to the eqs. (5.70)-(5.72) for recalculating the voltages of phase buses, neutral buses and ground buses under fault conditions, we obtain,

$$\left[\mathbf{V_{p,f}}\right]=\left[\mathbf{V_{ss}}\right]-\left[\mathbf{F_{1ng}}\right]\left\{\left[\mathbf{V_{sn}}\right]-\left[\mathbf{V_{sg}}\right]\right\}-\left[\mathbf{F_{1PLD}}\right]\left[\mathbf{I_L}\right]-\left[\mathbf{DFF_{1n}^{'}}\right]\left[\mathbf{I_f}\right] \qquad (5.74)$$

$$\left[\mathbf{V_{n,f}}\right]=\left[\mathbf{F_{2nn}}\right]\left[\mathbf{V_{sn}}\right]-\left[\mathbf{F_{2gg}}\right]\left[\mathbf{V_{sg}}\right]-\left[\mathbf{F_{2PLD}}\right]\left[\mathbf{I_L}\right]-\left[\mathbf{DFF_{2n}^{'}}\right]\left[\mathbf{I_f}\right] \qquad (5.75)$$

$$\left[\mathbf{V_{g,f}}\right]=\left[\mathbf{F_{3gg}}\right]\left[\mathbf{V_{sg}}\right]-\left[\mathbf{F_{3nn}}\right]\left[\mathbf{V_{sn}}\right]-\left[\mathbf{F_{3PLD}}\right]\left[\mathbf{I_L}\right]-\left[\mathbf{DFF_{3n}^{'}}\right]\left[\mathbf{I_f}\right] \qquad (5.76)$$

where,

$$\left[\mathbf{DFF_{1n}^{'}}\right]=\left[\mathbf{DFF_1^{'}}\right]+\left[\mathbf{DLF_2}\right]\left[\mathbf{Z_{FNG}}\right]^{-1}\left\{\left[\mathbf{DFF_3^{'}}\right]-\left[\mathbf{DFF_2^{'}}\right]\right\}$$

$$\left[\mathbf{DFF_{2n}^{'}}\right]=\left[\mathbf{DFF_2^{'}}\right]+\left[\mathbf{DLF_4}\right]\left[\mathbf{Z_{FNG}}\right]^{-1}\left\{\left[\mathbf{DFF_3^{'}}\right]-\left[\mathbf{DFF_2^{'}}\right]\right\}$$

$$\left[\mathbf{DFF_{3n}^{'}}\right]=\left[\mathbf{DFF_3^{'}}\right]+\left[\mathbf{DLF_6}\right]\left[\mathbf{Z_{FNG}}\right]^{-1}\left\{\left[\mathbf{DFF_3^{'}}\right]-\left[\mathbf{DFF_2^{'}}\right]\right\}$$

For an LL fault at phases a and b of j^{th} bus through a fault impedance $\bar{z}_f$, as shown in Fig. 5.2(d), the voltage equation at fault bus can be written as,

$$\bar{z}_f\bar{I}_f^a = \bar{V}_{j,f}^a-\bar{V}_{j,f}^b \qquad (5.77)$$

where, $\bar{V}_{j,f}^a$ and $\bar{V}_{j,f}^b$ are the voltages of phase a and b at fault bus j under the fault conditions, respectively. Substituting the values of $\bar{V}_{j,f}^a$ and $\bar{V}_{j,f}^b$ from eq. (5.74) into eq. (5.77), with an

assumption that the neutral and ground buses at the substation end are perfectly grounded (i.e. at zero potential; $\bar{V}_s^n = 0$, $\bar{V}_s^g = 0$), and writing the resultant equation in the matrix form, we obtain,

$$\begin{aligned}\left[\mathbf{Z_f}\right]\left[\mathbf{I_f}\right] &= \bar{V}_s^a - \left[\mathbf{F_{1PLD}}(f_b^{q_1},:)\right]\left[\mathbf{I_L}\right] - \left[\mathbf{DFF'_{1n}}(f_b^{q_1},1)\right]\left[\mathbf{I_f}\right] - \bar{V}_s^b \\ &+ \left[\mathbf{F_{1PLD}}(f_b^{q_2},:)\right]\left[\mathbf{I_L}\right] + \left[\mathbf{DFF'_{1n}}(f_b^{q_2},1)\right]\left[\mathbf{I_f}\right] \end{aligned} \tag{5.78}$$

where, for LL fault (at phase a and b of j^{th} bus), $\left[\mathbf{Z_f}\right] = \bar{z}_f$; $\left[\mathbf{F_{1PLD}}(f_b^{q_1},:)\right]$ and $\left[\mathbf{F_{1PLD}}(f_b^{q_2},:)\right]$ are the row vectors of matrix $\left[\mathbf{F_{1PLD}}\right]$ corresponding to the faulty phases q_1 and q_2 (here, $q_1 = a$, $q_2 = b$) of faulted bus f_b (here, $f_b = j$), respectively; $\left[\mathbf{DFF'_{1n}}(f_b^{q_1},1)\right]$ and $\left[\mathbf{DFF'_{1n}}(f_b^{q_2},1)\right]$ are the row vectors of matrix $\left[\mathbf{DFF'_{1n}}\right]$ corresponding to the faulty phases q_1 and q_2 of faulted bus f_b, respectively. Hence, the fault current $\left[\mathbf{I_f}\right]$ is obtained from eq. (5.78) as,

$$\left[\mathbf{I_f}\right] = \left[\mathbf{Z_{F1}}\right]^{-1}(\bar{V}_s^a - \bar{V}_s^b) - \left[\mathbf{F_{11PLD}^{flt}}\right]\left[\mathbf{I_L}\right] \tag{5.79}$$

where,

$$\begin{aligned}\left[\mathbf{Z_{F1}}\right] &= \left[\mathbf{Z_f}\right] + \left[\mathbf{DFF'_{1n}}(f_b^{q_1},1)\right] - \left[\mathbf{DFF'_{1n}}(f_b^{q_2},1)\right] \\ \left[\mathbf{F_{11PLD}^{flt}}\right] &= \left[\mathbf{Z_{F1}}\right]^{-1}\left\{\left[\mathbf{F_{1PLD}}(f_b^{q_1},:)\right] - \left[\mathbf{F_{1PLD}}(f_b^{q_2},:)\right]\right\}\end{aligned}$$

Steps of algorithm for $\left[\mathrm{BIBC}\right]$ ***matrix based short-circuit analysis method for an unbalanced three phase four wire multigrounded radial distribution system***

1. Run the base case power flow of three phase four wire multigrounded system using the proposed load flow method as discussed in Section 5.2 of this chapter.

2. Convert all PQ-loads into constant impedance loads using the obtained load flow solution.

3. If a ground fault (SLG, LLG, LLLG) occurs in the system, then formulate $\left[\mathbf{BIBC_{fp}}\right]$, $\left[\mathbf{BIBC_{fg}}\right]$ and $\left[\mathbf{Z_f}\right]$ matrices corresponding to the type of fault occurring in the system. If the fault is a line to line (LL) fault, then formulate only $\left[\mathbf{BIBC_{fp}}\right]$ and $\left[\mathbf{Z_f}\right]$ matrices.

4. Set iteration counter $k = 0$. Also, set the values of voltages of phase buses, neutral buses and ground buses, and equivalent bus injection currents equal to the values obtained from pre-fault load flow solution.

5. Calculate the fault current $\left[\mathbf{I_f}\right]^k$ using eq. (5.50) for SLG fault, eq. (5.57) for LLG fault, eq. (5.64) for LLLG fault and eq. (5.79) for LL fault.

6. $k = k + 1$.

7. Calculate the voltages of phase buses, neutral buses and ground buses $\left([\mathbf{V_{p,f}}]^k, [\mathbf{V_{n,f}}]^k \text{ and } [\mathbf{V_{g,f}}]^k\right)$ of the system under the fault conditions, using eqs. (5.45)-(5.47) for ground faults (SLG, LLG, LLLG) and using eqs. (5.74)-(5.76) for LL fault, respectively.

8. Calculate the error (ϵ),

$$\epsilon = max\left(\left|[\mathbf{V_{p,f}}]^k - [\mathbf{V_{p,f}}]^{k-1}\right|, \left|[\mathbf{V_{n,f}}]^k - [\mathbf{V_{n,f}}]^{k-1}\right|, \left|[\mathbf{V_{g,f}}]^k - [\mathbf{V_{g,f}}]^{k-1}\right|\right)$$

9. If $\epsilon \geq$ tolerance(1.0×10^{-12}), go to the next step, else go to step 11.

10. Calculate the values of equivalent bus injection currents at all the phase buses of the system. The equivalent bus injection current at any phase p of i^{th} bus at k^{th} iteration under the fault condition $(\bar{I}_{id,f}^{p^k})$ is calculated as,

$$\bar{I}_{id,f}^{p^k} = \left(\frac{\bar{V}_{i,f}^{p^k} - \bar{V}_{i,f}^{n^k}}{\bar{z}_{id}^{p}}\right); (p = a \; or \; b \; or \; c)$$

where, $\bar{V}_{i,f}^{p}$ and $\bar{V}_{i,f}^{n}$ are the voltages at phase p and neutral n_i of i^{th} bus under fault conditions, respectively. $\bar{z}_{id}^{p}$ is an equivalent load impedance at phase p of i^{th} bus. Now, go to step 5.

11. The obtained values of $[\mathbf{V_{p,f}}]$, $[\mathbf{V_{n,f}}]$, $[\mathbf{V_{g,f}}]$ and $[\mathbf{I_f}]$ are the final values of voltages under the fault conditions and fault current, respectively.

The overall flow-chart of the proposed $[\mathbf{BIBC}]$ matrix based short-circuit analysis method is shown in Fig. 5.3.

5.3.2 Method 2: $\left[\mathbf{Y_{bus}}\right]$ matrix based short-circuit analysis method

In this method, first the loads at all the phase buses of the three phase four wire multigrounded distribution system are converted into equivalent load impedances (as given in eq. (5.33)) with the help of proposed DSLF solution. Next, to form the bus admittance matrix $\left[\mathbf{Y_{bus}}\right]$ of the system,

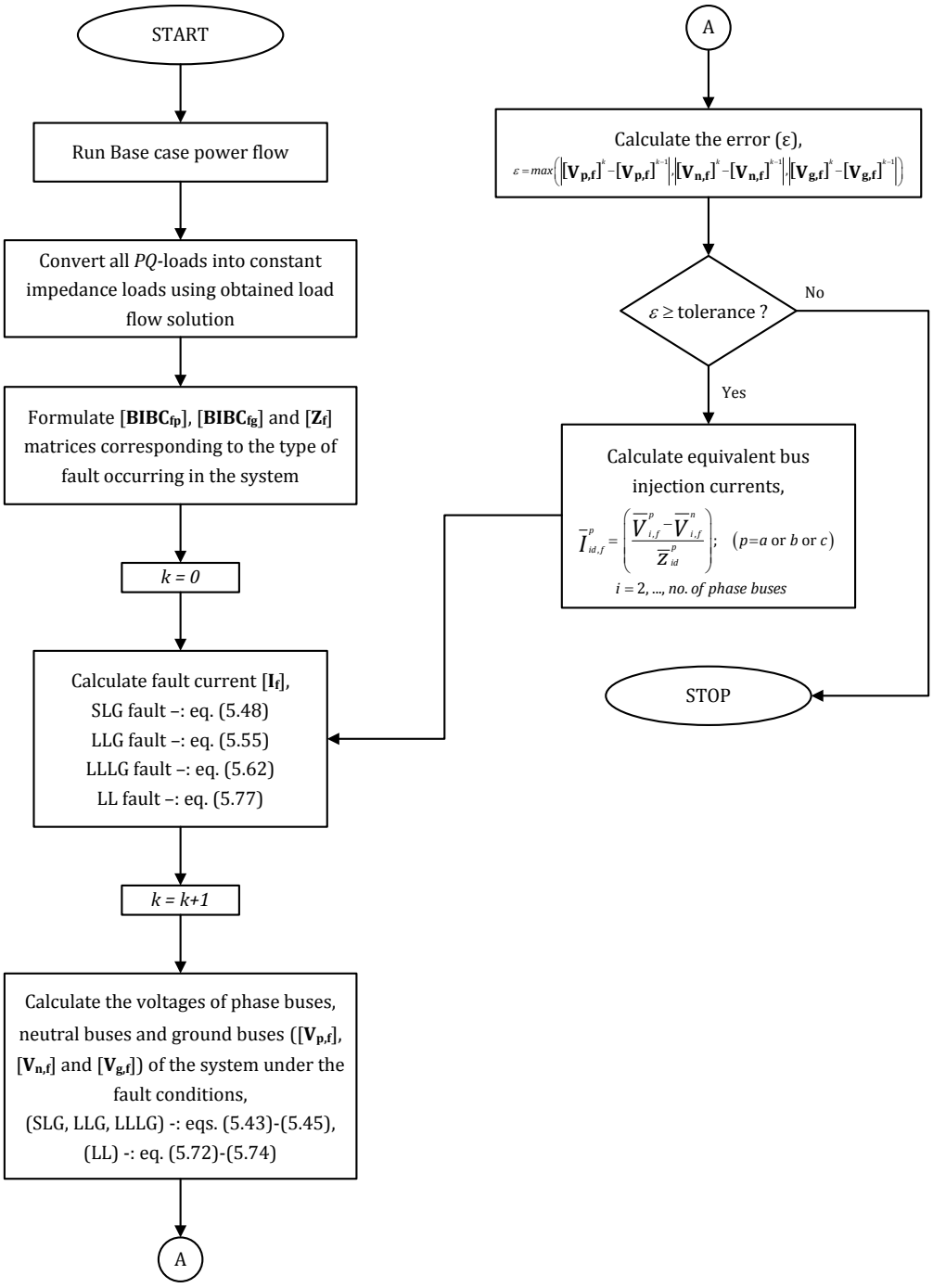

Figure 5.3: Flow-chart of the proposed [**BIBC**] matrix based short-circuit analysis method

the equivalent load admittances are then calculated at all the buses. For example, equivalent load

admittance at any phase p of bus i is calculated as,

$$\bar{y}_{id}^{p} = \frac{1}{\bar{z}_{id}^{p}} = \frac{\bar{I}_{id}^{p}}{(\bar{V}_{i}^{p} - \bar{V}_{i}^{n})}; (p = a, b, c) \tag{5.80}$$

where, $\bar{z}_{id}^{p}$ is an equivalent load impedance of p^{th} phase of i^{th} bus, $\bar{V}_{i}^{p}$ and $\bar{V}_{i}^{n}$ are the p^{th} phase and neutral bus voltage at i^{th} bus location, $\bar{I}_{id}^{p}$ is the equivalent injection current at p^{th} phase of i^{th} bus, obtained from the DSLF solution. Now, the line admittance matrix of the line section between buses i and j is calculated as,

$$\bar{\mathbf{y}}_{\mathbf{ij}}^{\mathbf{abcng}} = \left[\bar{\mathbf{z}}_{\mathbf{ij}}^{\mathbf{abcng}}\right]^{-1} = \begin{bmatrix} \bar{y}_{ij}^{aa} & \bar{y}_{ij}^{ab} & \bar{y}_{ij}^{ac} & \bar{y}_{ij}^{an} & \bar{y}_{ij}^{ag} \\ \bar{y}_{ij}^{ba} & \bar{y}_{ij}^{bb} & \bar{y}_{ij}^{bc} & \bar{y}_{ij}^{bn} & \bar{y}_{ij}^{bg} \\ \bar{y}_{ij}^{ca} & \bar{y}_{ij}^{cb} & \bar{y}_{ij}^{cc} & \bar{y}_{ij}^{cn} & \bar{y}_{ij}^{cg} \\ \bar{y}_{ij}^{na} & \bar{y}_{ij}^{nb} & \bar{y}_{ij}^{nc} & \bar{y}_{ij}^{nn} & \bar{y}_{ij}^{ng} \\ \bar{y}_{ij}^{ga} & \bar{y}_{ij}^{gb} & \bar{y}_{ij}^{gc} & \bar{y}_{ij}^{gn} & \bar{y}_{ij}^{gg} \end{bmatrix} \tag{5.81}$$

where, $\bar{y}_{ij}^{pq} = \bar{y}_{ij}^{qp};\ p, q = a, b, c, n, g;\ p \neq q$.

To obtain the $\left[\mathbf{Y_{bus}}\right]$ matrix of the unbalanced three phase four wire multigrounded distribution system, as shown in Fig. 5.1, Kirchhoff's Current Law (KCL) equations are required at all the phase, neutral and ground buses of the system. Let us consider the KCL equation at phase a of bus 2 of the system shown in Fig. 5.1, with an assumption that $\bar{V}_{s}^{n} = 0$ and $\bar{V}_{s}^{g} = 0$ as,

$$\begin{aligned} &\bar{y}_{12}^{aa}(\bar{V}_{2}^{a} - \bar{V}_{s}^{a}) + \bar{y}_{12}^{ab}(\bar{V}_{2}^{b} - \bar{V}_{s}^{b}) + \bar{y}_{12}^{ac}(\bar{V}_{2}^{c} - \bar{V}_{s}^{c}) + \bar{y}_{12}^{an}\bar{V}_{2}^{n} + \bar{y}_{12}^{ag}\bar{V}_{2}^{g} + \bar{y}_{2d}^{a}(\bar{V}_{2}^{a} - \bar{V}_{2}^{n}) \\ &+\bar{y}_{23}^{aa}(\bar{V}_{2}^{a} - \bar{V}_{3}^{a}) + \bar{y}_{23}^{ab}(\bar{V}_{2}^{b} - \bar{V}_{3}^{b}) + \bar{y}_{23}^{ac}(\bar{V}_{2}^{c} - \bar{V}_{3}^{c}) + \bar{y}_{23}^{an}(\bar{V}_{2}^{n} - \bar{V}_{3}^{n}) + \bar{y}_{23}^{ag}(\bar{V}_{2}^{g} - \bar{V}_{3}^{g}) \\ &= 0 \\ &(\bar{y}_{12}^{aa} + \bar{y}_{23}^{aa} + \bar{y}_{2d}^{a})\bar{V}_{2}^{a} + (\bar{y}_{12}^{ab} + \bar{y}_{23}^{ab})\bar{V}_{2}^{b} + (\bar{y}_{12}^{ac} + \bar{y}_{23}^{ac})\bar{V}_{2}^{c} + (\bar{y}_{12}^{an} + \bar{y}_{23}^{an} - \bar{y}_{2d}^{a})\bar{V}_{2}^{n} + (\bar{y}_{12}^{ag} \\ &+\bar{y}_{23}^{ag})\bar{V}_{2}^{g} - \bar{y}_{23}^{aa}\bar{V}_{3}^{a} - \bar{y}_{23}^{ab}\bar{V}_{3}^{b} - \bar{y}_{23}^{ac}\bar{V}_{3}^{c} - \bar{y}_{23}^{an}\bar{V}_{3}^{n} - \bar{y}_{23}^{ag}\bar{V}_{3}^{g} = \bar{y}_{12}^{aa}\bar{V}_{s}^{a} + \bar{y}_{12}^{ab}\bar{V}_{s}^{b} + \bar{y}_{12}^{ac}\bar{V}_{s}^{c} \end{aligned} \tag{5.82}$$

Similarly, the KCL equations at phases b and c of 2^{nd} bus are given in eqs. (5.83) and (5.84), respectively as,

$$\begin{aligned} &(\bar{y}_{12}^{ba} + \bar{y}_{23}^{ba})\bar{V}_{2}^{a} + (\bar{y}_{12}^{bb} + \bar{y}_{23}^{bb} + \bar{y}_{2}^{bn})\bar{V}_{2}^{b} + (\bar{y}_{12}^{bc} + \bar{y}_{23}^{bc})\bar{V}_{2}^{c} + (\bar{y}_{12}^{bn} + \bar{y}_{23}^{bn} - \bar{y}_{2}^{bn})\bar{V}_{2}^{n} + (\bar{y}_{12}^{bg} \\ &+\bar{y}_{23}^{bg})\bar{V}_{2}^{g} - \bar{y}_{23}^{ba}\bar{V}_{3}^{a} - \bar{y}_{23}^{bb}\bar{V}_{3}^{b} - \bar{y}_{23}^{bc}\bar{V}_{3}^{c} - \bar{y}_{23}^{bn}\bar{V}_{3}^{n} - \bar{y}_{23}^{bg}\bar{V}_{3}^{g} = \bar{y}_{12}^{ba}\bar{V}_{s}^{a} + \bar{y}_{12}^{bb}\bar{V}_{s}^{b} + \bar{y}_{12}^{bc}\bar{V}_{s}^{c} \end{aligned} \tag{5.83}$$

$$(\bar{y}_{12}^{ca}+\bar{y}_{23}^{ca})\bar{V}_2^a+(\bar{y}_{12}^{cb}+\bar{y}_{23}^{cb})\bar{V}_2^b+(\bar{y}_{12}^{cc}+\bar{y}_{23}^{cc}+\bar{y}_2^{cn})\bar{V}_2^c+(\bar{y}_{12}^{cn}+\bar{y}_{23}^{cn}-\bar{y}_2^{cn})\bar{V}_2^n+(\bar{y}_{12}^{cg}$$
$$+\bar{y}_{23}^{cg})\bar{V}_2^g-\bar{y}_{23}^{ca}\bar{V}_3^a-\bar{y}_{23}^{cb}\bar{V}_3^b-\bar{y}_{23}^{cc}\bar{V}_3^c-\bar{y}_{23}^{cn}\bar{V}_3^n-\bar{y}_{23}^{cg}\bar{V}_3^g=\bar{y}_{12}^{ca}\bar{V}_s^a+\bar{y}_{12}^{cb}\bar{V}_s^b+\bar{y}_{12}^{cc}\bar{V}_s^c \quad (5.84)$$

Also, the KCL equations at neutral n_2 and ground g_2 at the location of 2^{nd} bus are expressed in eqs. (5.85) and (5.86), respectively as,

$$(\bar{y}_{12}^{na}+\bar{y}_{23}^{na}-\bar{y}_{2d}^{a})\bar{V}_2^a+(\bar{y}_{12}^{nb}+\bar{y}_{23}^{nb}-\bar{y}_{2d}^{b})\bar{V}_2^b+(\bar{y}_{12}^{nc}+\bar{y}_{23}^{nc}-\bar{y}_{2d}^{c})\bar{V}_2^c+(\bar{y}_{12}^{nn}+\bar{y}_{23}^{nn}+\bar{y}_{2d}^{a}+\bar{y}_{2d}^{b}$$
$$+\bar{y}_{2d}^{c}+\bar{y}_2^{ngr})\bar{V}_2^n+(\bar{y}_{12}^{ng}+\bar{y}_{23}^{ng}-\bar{y}_2^{ngr})\bar{V}_2^g-\bar{y}_{23}^{na}\bar{V}_3^a-\bar{y}_{23}^{nb}\bar{V}_3^b-\bar{y}_{23}^{nc}\bar{V}_3^c-\bar{y}_{23}^{nn}\bar{V}_3^n-\bar{y}_{23}^{ng}\bar{V}_3^g \;=$$
$$\bar{y}_{12}^{na}\bar{V}_s^a+\bar{y}_{12}^{nb}\bar{V}_s^b+\bar{y}_{12}^{nc}\bar{V}_s^c \quad (5.85)$$

$$(\bar{y}_{12}^{ga}+\bar{y}_{23}^{ga})\bar{V}_2^a+(\bar{y}_{12}^{gb}+\bar{y}_{23}^{gb})\bar{V}_2^b+(\bar{y}_{12}^{gc}+\bar{y}_{23}^{gc})\bar{V}_2^c+(\bar{y}_{12}^{gn}+\bar{y}_{23}^{gn}-\bar{y}_2^{ngr})\bar{V}_2^n+(\bar{y}_{12}^{gg}+\bar{y}_{23}^{gg}$$
$$+\bar{y}_2^{ngr})\bar{V}_2^g-\bar{y}_{23}^{ga}\bar{V}_3^a-\bar{y}_{23}^{gb}\bar{V}_3^b-\bar{y}_{23}^{gc}\bar{V}_3^c-\bar{y}_{23}^{gn}\bar{V}_3^n-\bar{y}_{23}^{gg}\bar{V}_3^g \;=\; \bar{y}_{12}^{ga}\bar{V}_s^a+\bar{y}_{12}^{gb}\bar{V}_s^b+\bar{y}_{12}^{gc}\bar{V}_s^c \quad (5.86)$$

where, $\bar{y}_2^{ngr}=\frac{1}{\bar{Z}_2^{ngr}}$, $\bar{Z}_2^{ngr}$ is the neutral to ground impedance between neutral n_2 and ground g_2 at the location of 2^{nd} bus of the system shown in Fig. 5.1. Therefore, the KCL equations at bus 2 can be expressed in the matrix form using eqs. (5.82)-(5.86) as,

$$\mathbf{Y_{22}^{abcng}V_2^{abcng}}+\mathbf{Y_{23}^{abcng}V_3^{abcng}}=\mathbf{Y_s^{abcng}V_s^{abc}} \quad (5.87)$$

where,

$$\mathbf{Y_{22}^{abcng}}=$$
$$\begin{bmatrix}
(\bar{y}_{12}^{aa}+\bar{y}_{23}^{aa}+\bar{y}_{2d}^{a}) & (\bar{y}_{12}^{ab}+\bar{y}_{23}^{ab}) & (\bar{y}_{12}^{ac}+\bar{y}_{23}^{ac}) & (\bar{y}_{12}^{an}+\bar{y}_{23}^{an}-\bar{y}_{2d}^{a}) & (\bar{y}_{12}^{ag}+\bar{y}_{23}^{ag}) \\
(\bar{y}_{12}^{ba}+\bar{y}_{23}^{ba}) & (\bar{y}_{12}^{bb}+\bar{y}_{23}^{bb}+\bar{y}_{2d}^{b}) & (\bar{y}_{12}^{bc}+\bar{y}_{23}^{bc}) & (\bar{y}_{12}^{bn}+\bar{y}_{23}^{bn}-\bar{y}_{2d}^{b}) & (\bar{y}_{12}^{bg}+\bar{y}_{23}^{bg}) \\
(\bar{y}_{12}^{ca}+\bar{y}_{23}^{ca}) & (\bar{y}_{12}^{cb}+\bar{y}_{23}^{cb}) & (\bar{y}_{12}^{cc}+\bar{y}_{23}^{cc}+\bar{y}_{2d}^{c}) & (\bar{y}_{12}^{cn}+\bar{y}_{23}^{cn}-\bar{y}_{2d}^{c}) & (\bar{y}_{12}^{cg}+\bar{y}_{23}^{cg}) \\
(\bar{y}_{12}^{na}+\bar{y}_{23}^{na}-\bar{y}_{2d}^{a}) & (\bar{y}_{12}^{nb}+\bar{y}_{23}^{nb}-\bar{y}_{2d}^{b}) & (\bar{y}_{12}^{nc}+\bar{y}_{23}^{nc}-\bar{y}_{2d}^{c}) & (\bar{y}_{12}^{nn}+\bar{y}_{23}^{nn}+\bar{y}_{2d}^{a} & (\bar{y}_{12}^{ng}+\bar{y}_{23}^{ng} \\
 & & & +\bar{y}_{2d}^{b}+\bar{y}_{2d}^{c}+\bar{y}_2^{ngr}) & -\bar{y}_2^{ngr}) \\
(\bar{y}_{12}^{ga}+\bar{y}_{23}^{ga}) & (\bar{y}_{12}^{gb}+\bar{y}_{23}^{gb}) & (\bar{y}_{12}^{gc}+\bar{y}_{23}^{gc}) & (\bar{y}_{12}^{gn}+\bar{y}_{23}^{gn}-\bar{y}_2^{ngr}) & (\bar{y}_{12}^{gg}+\bar{y}_{23}^{gg} \\
 & & & & +\bar{y}_2^{ngr})
\end{bmatrix}$$

$$\mathbf{Y_{23}^{abcng}}=-\bar{\mathbf{y}}_{\mathbf{23}}^{\mathbf{abcng}};\mathbf{Y_s^{abcng}}=\begin{bmatrix}\bar{y}_{12}^{aa} & \bar{y}_{12}^{ba} & \bar{y}_{12}^{ca} & \bar{y}_{12}^{na} & \bar{y}_{12}^{ga}\\ \bar{y}_{12}^{ab} & \bar{y}_{12}^{bb} & \bar{y}_{12}^{cb} & \bar{y}_{12}^{nb} & \bar{y}_{12}^{gb}\\ \bar{y}_{12}^{ac} & \bar{y}_{12}^{bc} & \bar{y}_{12}^{cc} & \bar{y}_{12}^{nc} & \bar{y}_{12}^{gc}\end{bmatrix}^T;\mathbf{V_s^{abc}}=\begin{bmatrix}\bar{V}_s^a & \bar{V}_s^b & \bar{V}_s^c\end{bmatrix}^T$$

$$\mathbf{V_2^{abcng}} = \begin{bmatrix} \bar{V}_2^a & \bar{V}_2^b & \bar{V}_2^c & \bar{V}_2^n & \bar{V}_2^g \end{bmatrix}^T ; \mathbf{V_3^{abcng}} = \begin{bmatrix} \bar{V}_3^a & \bar{V}_3^b & \bar{V}_3^c & \bar{V}_3^n & \bar{V}_3^g \end{bmatrix}^T$$

Similarly, the KCL equations at three-phase bus j, two-phase bus m and single-phase bus n_b are given in eqs. (5.88), (5.89) and (5.90), respectively, as,

$$\mathbf{Y_{ji}^{abcng} V_i^{abcng} + Y_{jj}^{abcng} V_j^{abcng} = 0} \tag{5.88}$$

$$\mathbf{Y_{ml}^{abng} V_l^{abcng} + Y_{mm}^{abng} V_m^{abng} + Y_{mn_b}^{ang} V_{n_b}^{ang} = 0} \tag{5.89}$$

$$\mathbf{Y_{n_b m}^{ang} V_m^{abng} + Y_{n_b n_b}^{ang} V_{n_b}^{ang} = 0} \tag{5.90}$$

where, $\mathbf{Y_{ji}^{abcng} = -\bar{y}_{ji}^{abcng}}$;

$$\mathbf{Y_{jj}^{abcng}} = \begin{bmatrix} (\bar{y}_{ji}^{aa} + \bar{y}_{jd}^{a}) & \bar{y}_{ji}^{ab} & \bar{y}_{ji}^{ac} & (\bar{y}_{ji}^{an} - \bar{y}_{jd}^{a}) & \bar{y}_{ji}^{ag} \\ \bar{y}_{ji}^{ba} & (\bar{y}_{ji}^{bb} + \bar{y}_{jd}^{b}) & \bar{y}_{ji}^{bc} & (\bar{y}_{ji}^{bn} - \bar{y}_{jd}^{b}) & \bar{y}_{ji}^{bg} \\ \bar{y}_{ji}^{ca} & \bar{y}_{ji}^{cb} & (\bar{y}_{ji}^{cc} + \bar{y}_{jd}^{c}) & (\bar{y}_{ji}^{cn} - \bar{y}_{jd}^{c}) & \bar{y}_{ji}^{cg} \\ (\bar{y}_{ji}^{na} - \bar{y}_{jd}^{a}) & (\bar{y}_{ji}^{nb} - \bar{y}_{jd}^{b}) & (\bar{y}_{ji}^{nc} - \bar{y}_{jd}^{c}) & (\bar{y}_{ji}^{nn} + \bar{y}_{jd}^{a} + \bar{y}_{jd}^{b} + \bar{y}_{jd}^{c} + \bar{y}_{j}^{ngr}) & (\bar{y}_{ji}^{ng} - \bar{y}_{j}^{ngr}) \\ \bar{y}_{ji}^{ga} & \bar{y}_{ji}^{gb} & \bar{y}_{ji}^{gc} & (\bar{y}_{ji}^{gn} - \bar{y}_{j}^{ngr}) & (\bar{y}_{ji}^{gg} + \bar{y}_{j}^{ngr}) \end{bmatrix}$$

$$\mathbf{Y_{mm}^{abng}} = \begin{bmatrix} (\bar{y}_{ml}^{aa} + \bar{y}_{mn_b}^{aa} + \bar{y}_{md}^{a}) & \bar{y}_{ml}^{ab} & (\bar{y}_{ml}^{an} + \bar{y}_{mn_b}^{an} - \bar{y}_{md}^{a}) & (\bar{y}_{ml}^{ag} + \bar{y}_{mn_b}^{ag}) \\ \bar{y}_{ml}^{ba} & (\bar{y}_{ml}^{bb} + \bar{y}_{md}^{b}) & (\bar{y}_{ml}^{bn} - \bar{y}_{md}^{b}) & \bar{y}_{ml}^{bg} \\ (\bar{y}_{ml}^{na} + \bar{y}_{mn_b}^{na} - \bar{y}_{md}^{a}) & (\bar{y}_{ml}^{nb} - \bar{y}_{md}^{b}) & (\bar{y}_{ml}^{nn} + \bar{y}_{mn_b}^{nn} + \bar{y}_{md}^{a} & (\bar{y}_{ml}^{ng} + \bar{y}_{mn_b}^{ng} - \bar{y}_{m}^{ngr}) \\ & & +\bar{y}_{md}^{b} + \bar{y}_{md}^{c} + \bar{y}_{m}^{ngr}) & \\ (\bar{y}_{ml}^{ga} + \bar{y}_{mn_b}^{ga}) & \bar{y}_{ml}^{gb} & (\bar{y}_{ml}^{gn} + \bar{y}_{mn_b}^{gn} - \bar{y}_{m}^{ngr}) & (\bar{y}_{ml}^{gg} + \bar{y}_{mn_b}^{gg} + \bar{y}_{m}^{ngr}) \end{bmatrix}$$

$$\mathbf{Y_{n_b n_b}^{ang}} = \begin{bmatrix} (\bar{y}_{n_b m}^{aa} + \bar{y}_{n_b d}^{a}) & (\bar{y}_{n_b m}^{an} - \bar{y}_{n_b d}^{a}) & \bar{y}_{n_b m}^{ag} \\ (\bar{y}_{n_b m}^{na} - \bar{y}_{n_b d}^{a}) & (\bar{y}_{n_b m}^{nn} + \bar{y}_{n_b d}^{a} + \bar{y}_{n_b}^{ngr}) & (\bar{y}_{n_b m}^{ng} - \bar{y}_{n_b}^{ngr}) \\ \bar{y}_{n_b m}^{ga} & (\bar{y}_{n_b m}^{gn} - \bar{y}_{n_b}^{ngr}) & (\bar{y}_{n_b m}^{gg} + \bar{y}_{n_b}^{ngr}) \end{bmatrix}$$

$$\mathbf{Y_{ml}^{abng}} = -\begin{bmatrix} \bar{y}_{ml}^{aa} & \bar{y}_{ml}^{ab} & \bar{y}_{ml}^{an} & \bar{y}_{ml}^{ag} & 0 \\ \bar{y}_{ml}^{ba} & \bar{y}_{ml}^{bb} & \bar{y}_{ml}^{bn} & \bar{y}_{ml}^{bg} & 0 \\ \bar{y}_{ml}^{na} & \bar{y}_{ml}^{nb} & \bar{y}_{ml}^{nn} & \bar{y}_{ml}^{ng} & 0 \\ \bar{y}_{ml}^{ga} & \bar{y}_{ml}^{gb} & \bar{y}_{ml}^{gn} & \bar{y}_{ml}^{gg} & 0 \end{bmatrix} ; \mathbf{Y_{mn_b}^{ang}} = -\begin{bmatrix} \bar{y}_{mn_b}^{aa} & \bar{y}_{mn_b}^{an} & \bar{y}_{mn_b}^{ag} \\ \bar{y}_{mn_b}^{na} & \bar{y}_{mn_b}^{nn} & \bar{y}_{mn_b}^{ng} \\ \bar{y}_{mn_b}^{ga} & \bar{y}_{mn_b}^{gn} & \bar{y}_{mn_b}^{gg} \\ 0 & 0 & 0 \end{bmatrix} = \begin{bmatrix} \mathbf{Y_{n_b m}^{ang}} \end{bmatrix}^{\mathbf{T}}$$

$$\mathbf{V_i^{abcng}} = \begin{bmatrix} \bar{V}_i^a & \bar{V}_i^b & \bar{V}_i^c & \bar{V}_i^n & \bar{V}_i^g \end{bmatrix}^T ; \mathbf{V_j^{abcng}} = \begin{bmatrix} \bar{V}_j^a & \bar{V}_j^b & \bar{V}_j^c & \bar{V}_j^n & \bar{V}_j^g \end{bmatrix}^T$$

$$\mathbf{V_l^{abcng}} = \begin{bmatrix} \bar{V}_l^a & \bar{V}_l^b & \bar{V}_l^c & \bar{V}_l^n & \bar{V}_l^g \end{bmatrix}^T ; \mathbf{V_m^{abng}} = \begin{bmatrix} \bar{V}_m^a & \bar{V}_m^b & \bar{V}_m^n & \bar{V}_m^g \end{bmatrix}^T ; \mathbf{V_{n_b}^{ang}} = \begin{bmatrix} \bar{V}_{n_b}^a & \bar{V}_{n_b}^n & \bar{V}_{n_b}^g \end{bmatrix}^T$$

Hence, the generalized KCL equations for the unbalanced three phase four wire multigrounded distribution system, having u three-phase, v two-phase, w single-phase, $(u+v+w)$ neutral and $(u+v+w)$ ground buses, can be expressed in the matrix form as,

$$\Big[\mathbf{Y_{bus}}\Big] \cdot \Big[\mathbf{V}\Big] = \Big[\mathbf{I}\Big] \tag{5.91}$$

where,

$$\Big[\mathbf{Y_{bus}}\Big] = \begin{bmatrix} \mathbf{Y_{22}^{abcng}} & \cdots & \mathbf{Y_{2u}^{abcng}} & \mathbf{Y_{2(u+1)}^{pqng}} & \cdots & \mathbf{Y_{2(u+v)}^{pqng}} & \mathbf{Y_{2(u+v+1)}^{png}} & \cdots & \mathbf{Y_{2(u+v+w)}^{png}} \\ \vdots & \ddots & \vdots & \vdots & \vdots & \vdots & \vdots & \vdots & \vdots \\ \mathbf{Y_{u2}^{abcng}} & \cdots & \mathbf{Y_{uu}^{abcng}} & \mathbf{Y_{u(u+1)}^{pqng}} & \cdots & \mathbf{Y_{u(u+v)}^{pqng}} & \mathbf{Y_{u(u+v+1)}^{png}} & \cdots & \mathbf{Y_{u(u+v+w)}^{png}} \\ \mathbf{Y_{(u+1)2}^{pqng}} & \cdots & \mathbf{Y_{(u+1)u}^{pqng}} & \mathbf{Y_{(u+1)(u+1)}^{pqng}} & \cdots & \mathbf{Y_{(u+1)(u+v)}^{pqng}} & \mathbf{Y_{(u+1)(u+v+1)}^{png}} & \cdots & \mathbf{Y_{(u+1)(u+v+w)}^{png}} \\ \vdots & \vdots & \vdots & \vdots & \ddots & \vdots & \vdots & \vdots & \vdots \\ \mathbf{Y_{(u+v)2}^{pqng}} & \cdots & \mathbf{Y_{(u+v)u}^{pqng}} & \mathbf{Y_{(u+v)(u+1)}^{pqng}} & \cdots & \mathbf{Y_{(u+v)(u+v)}^{pqng}} & \mathbf{Y_{(u+v)(u+v+1)}^{png}} & \cdots & \mathbf{Y_{(u+v)(u+v+w)}^{png}} \\ \mathbf{Y_{(u+v+1)2}^{png}} & \cdots & \mathbf{Y_{(u+v+1)u}^{png}} & \mathbf{Y_{(u+v+1)(u+1)}^{png}} & \cdots & \mathbf{Y_{(u+v+1)(u+v)}^{png}} & \mathbf{Y_{(u+v+1)(u+v+1)}^{png}} & \cdots & \mathbf{Y_{(u+v+1)(u+v+w)}^{png}} \\ \vdots & \vdots & \vdots & \vdots & \vdots & \vdots & \vdots & \ddots & \vdots \\ \mathbf{Y_{(u+v+l)2}^{png}} & \cdots & \mathbf{Y_{(u+v+l)u}^{png}} & \mathbf{Y_{(u+v+l)(u+1)}^{png}} & \cdots & \mathbf{Y_{(u+v+l)(u+v)}^{png}} & \mathbf{Y_{(u+v+l)(u+v+1)}^{png}} & \cdots & \mathbf{Y_{(u+v+l)(u+v+w)}^{png}} \end{bmatrix}$$

$$\begin{aligned} \Big[\mathbf{V}\Big] &= \begin{bmatrix} \mathbf{V_2^{abcng}} & \cdots & \mathbf{V_u^{abcng}} & \cdots & \mathbf{V_{(u+1)}^{pqng}} & \cdots & \mathbf{V_{(u+v)}^{pqng}} & \cdots & \mathbf{V_{(u+v+1)}^{png}} & \cdots & \mathbf{V_{(u+v+w)}^{png}} \end{bmatrix}^T \\ \Big[\mathbf{I}\Big] &= \begin{bmatrix} (\mathbf{Y_s^{abcng}}.\mathbf{V_s^{abc}}) & \mathbf{0} & \mathbf{0} & \cdots & \mathbf{0} & \cdots & \mathbf{0} & \cdots & \mathbf{0} & \cdots & \mathbf{0} \end{bmatrix}^T . \end{aligned}$$

The elements of the $\Big[\mathbf{Y_{bus}}\Big]$ matrix are calculated as,

$$\begin{aligned} \bar{Y}_{ii}^{pp} &= \bar{y}_{i1}^{pp} + \bar{y}_{i2}^{pp} + \cdots + \bar{y}_{iu}^{pp} + \bar{y}_{i(u+1)}^{pp} + \cdots + \bar{y}_{i(u+v)}^{pp} + \bar{y}_{i(u+v+1)}^{pp} + \cdots + \bar{y}_{i(u+v+w)}^{pp} + \bar{y}_{id}^{p} \\ \bar{Y}_{ii}^{nn} &= \bar{y}_{i1}^{nn} + \bar{y}_{i2}^{nn} + \cdots + \bar{y}_{iu}^{nn} + \bar{y}_{i(u+1)}^{nn} + \cdots + \bar{y}_{i(u+v)}^{nn} + \bar{y}_{i(u+v+1)}^{nn} + \cdots + \bar{y}_{i(u+v+w)}^{nn} + \bar{y}_{i}^{ngr} \\ &+ \sum_{pl} \bar{y}_{id}^{pl} \\ \bar{Y}_{ii}^{gg} &= \bar{y}_{i1}^{gg} + \bar{y}_{i2}^{gg} + \cdots + \bar{y}_{iu}^{gg} + \bar{y}_{i(u+1)}^{gg} + \cdots + \bar{y}_{i(u+v)}^{gg} + \bar{y}_{i(u+v+1)}^{gg} + \cdots + \bar{y}_{i(u+v+w)}^{gg} + \bar{y}_{i}^{ngr} \\ \bar{Y}_{ii}^{pq} &= \bar{y}_{i1}^{pq} + \bar{y}_{i2}^{pq} + \cdots + \bar{y}_{iu}^{pq} + \bar{y}_{i(u+1)}^{pq} + \cdots + \bar{y}_{i(u+v)}^{pq} \\ \bar{Y}_{ii}^{pn} &= \bar{y}_{i1}^{pn} + \bar{y}_{i2}^{pn} + \cdots + \bar{y}_{iu}^{pn} + \bar{y}_{i(u+1)}^{pn} + \cdots + \bar{y}_{i(u+v)}^{pn} + \bar{y}_{i(u+v+1)}^{pn} + \cdots + \bar{y}_{i(u+v+w)}^{pn} - \bar{y}_{id}^{p} \\ &= \bar{Y}_{ii}^{np} \\ \bar{Y}_{ii}^{pg} &= \bar{y}_{i1}^{pg} + \bar{y}_{i2}^{pg} + \cdots + \bar{y}_{iu}^{pg} + \bar{y}_{i(u+1)}^{pg} + \cdots + \bar{y}_{i(u+v)}^{pg} + \bar{y}_{i(u+v+1)}^{pg} + \cdots + \bar{y}_{i(u+v+w)}^{pg} = \bar{Y}_{ii}^{gp} \end{aligned}$$

$$
\begin{aligned}
\bar{Y}_{ii}^{ng} &= \bar{y}_{i1}^{ng} + \bar{y}_{i2}^{ng} + \cdots + \bar{y}_{iu}^{ng} + \bar{y}_{i(u+1)}^{ng} + \cdots + \bar{y}_{i(u+v)}^{ng} + \bar{y}_{i(u+v+1)}^{ng} + \cdots + \bar{y}_{i(u+v+w)}^{ng} - \bar{y}_{i}^{ngr} \\
&= \bar{Y}_{ii}^{gn} \\
\bar{Y}_{ij}^{pp} &= -\bar{y}_{ij}^{pp};\ \bar{Y}_{ij}^{nn} = -\bar{y}_{ij}^{nn};\ \bar{Y}_{ij}^{gg} = -\bar{y}_{ij}^{gg}; \\
\bar{Y}_{ij}^{pq} &= -\bar{y}_{ij}^{pq};\ \bar{Y}_{ij}^{pn} = -\bar{y}_{ij}^{pn} = \bar{Y}_{ij}^{np};\ \bar{Y}_{ij}^{pg} = -\bar{y}_{ij}^{pg} = \bar{Y}_{ij}^{gp};\ \bar{Y}_{ij}^{ng} = -\bar{y}_{ij}^{ng} = \bar{Y}_{ij}^{gn}
\end{aligned}
\tag{5.92}
$$

where i=2, ..., u; j=1, ..., u; $j \neq i$; pl and $p = a, b, c$; $q = a, b, c$; $p \neq q$ for u three phase buses,

i=(u+1), ..., ($u+v$); j=(u+1), ..., ($u+v$); $j \neq i$; pl and $p = (a, b)$ or (b, c) or (c, a); $q = (a, b)$ or (b, c) or (c, a); $p \neq q$ for v two phase buses,

i=($u+v$+1), ..., ($u+v+w$); j=($u+v$+1), ..., ($u+v+w$); $j \neq i$; pl, p and $q = a$ or b or c, for w single phase buses. n and g stand for neutral and ground.

Therefore, the size of $\left[\mathbf{Y_{bus}}\right]$ matrix for an unbalanced three phase four wire multigrounded distribution system considered, is $(5u + 4v + 3w - 5) \times (5u + 4v + 3w - 5)$. Once the $\left[\mathbf{Y_{bus}}\right]$ matrix of an unbalanced three phase four wire multigrounded distribution system is formed, various unsymmetrical short-circuit faults can be analyzed as follows :

(a) Single line-to-ground (SLG) fault

Let us consider an SLG fault between phase a and the local ground g_j at j^{th} bus location through a fault impedance $\bar{z}_f$, as shown in Fig. 5.2(a) [158]. The fault current $\bar{I}_f^a$ is flowing from phase a to the ground g_j at j^{th} bus and is calculated as,

$$
\bar{I}_f^a = \frac{(\bar{V}_{j,f}^a - \bar{V}_{j,f}^g)}{\bar{z}_f} = \bar{y}_f(\bar{V}_{j,f}^a - \bar{V}_{j,f}^g) \tag{5.93}
$$

where, $\bar{y}_f = \frac{1}{\bar{z}_f}$; $\bar{V}_{j,f}^a$ and $\bar{V}_{j,f}^g$ are the voltages of phase a and ground g_j of j^{th} bus under the fault conditions, respectively. The KCL equation at faulty phase a of faulted bus j, under the fault condition can be written as,

$$
\begin{aligned}
&\bar{Y}_{j2}^{aa}.\bar{V}_{2,f}^a + \cdots + \bar{Y}_{j2}^{ag}.\bar{V}_{2,f}^g + \cdots + \bar{Y}_{jj}^{aa}.\bar{V}_{j,f}^a + \cdots + \bar{Y}_{jj}^{ag}.\bar{V}_{j,f}^g + \cdots + \bar{Y}_{j(u+v+w)}^{aa}.\bar{V}_{(u+v+w),f}^a \\
&+ \cdots + \bar{Y}_{j(u+v+w)}^{ag}.\bar{V}_{(u+v+w),f}^g + \bar{y}_f.(\bar{V}_{j,f}^a - \bar{V}_{j,f}^g) = 0
\end{aligned}
$$

$$
\begin{aligned}
&\bar{Y}_{j2}^{aa}.\bar{V}_{2,f}^a + \cdots + \bar{Y}_{j2}^{ag}.\bar{V}_{2,f}^g + \cdots + (\bar{Y}_{jj}^{aa} + \bar{y}_f).\bar{V}_{j,f}^a + \cdots + (\bar{Y}_{jj}^{ag} - \bar{y}_f).\bar{V}_{j,f}^g + \cdots \\
&\cdots + \bar{Y}_{j(u+v+w)}^{aa}.\bar{V}_{(u+v+w),f}^a + \cdots + \bar{Y}_{j(u+v+w)}^{ag}.\bar{V}_{(u+v+w),f}^g = 0
\end{aligned}
\tag{5.94}
$$

Similarly, the KCL equation at ground g_j of faulted bus j, under the fault condition, is written as,

$$\bar{Y}^{ga}_{j2}.\bar{V}^{a}_{2,f} + \cdots + \bar{Y}^{gg}_{j2}.\bar{V}^{g}_{2,f} + \cdots + \bar{Y}^{ga}_{jj}.\bar{V}^{a}_{j,f} + \cdots + \bar{Y}^{gg}_{jj}.\bar{V}^{g}_{j,f} + \cdots + \bar{Y}^{ga}_{j(u+v+w)}.\bar{V}^{a}_{(u+v+w),f}$$
$$+ \cdots + \bar{Y}^{gg}_{j(u+v+w)}.\bar{V}^{g}_{(u+v+w),f} - \bar{y}_f.(\bar{V}^{a}_{j,f} - \bar{V}^{g}_{j,f}) = 0$$

$$\bar{Y}^{ga}_{j2}.\bar{V}^{a}_{2,f} + \cdots + \bar{Y}^{gg}_{j2}.\bar{V}^{g}_{2,f} + \cdots + (\bar{Y}^{ga}_{jj} - \bar{y}_f).\bar{V}^{a}_{j,f} + \cdots + (\bar{Y}^{gg}_{jj} + \bar{y}_f).\bar{V}^{g}_{j,f} + \cdots$$
$$\cdots + \bar{Y}^{ga}_{j(u+v+w)}.\bar{V}^{a}_{(u+v+w),f} + \cdots + \bar{Y}^{gg}_{j(u+v+w)}.\bar{V}^{g}_{(u+v+w),f} = 0 \tag{5.95}$$

Hence, the following elements of the $\left[\mathbf{Y_{bus}}\right]$ matrix will be modified due to SLG fault :

$$\begin{aligned} \bar{Y}^{aa}_{jj\_new} &= \bar{Y}^{aa}_{jj} + \bar{y}_f;\ \bar{Y}^{ag}_{jj\_new} = \bar{Y}^{ag}_{jj} - \bar{y}_f \\ \bar{Y}^{ga}_{jj\_new} &= \bar{Y}^{ga}_{jj} - \bar{y}_f;\ \bar{Y}^{gg}_{jj\_new} = \bar{Y}^{gg}_{jj} + \bar{y}_f \end{aligned} \tag{5.96}$$

The bus voltages are then calculated, under the fault condition, using eq. (5.91) with the help of modified bus admittance matrix. Also, the branch current of any three-phase line section between buses i and j under fault conditions is calculated as,

$$\left[\mathbf{B^{abcng}_{ij,f}}\right] = \left[\mathbf{y^{abcng}_{ij}}\right]\left[\mathbf{V^{abcng}_{i,f}} - \mathbf{V^{abcng}_{j,f}}\right] \tag{5.97}$$

where, $\mathbf{V^{abcng}_{i,f}}$ and $\mathbf{V^{abcng}_{j,f}}$ are the voltage vectors of the buses i and j under the fault conditions, respectively.

(b) Double line-to-ground (LLG) fault

Let us assume that an LLG fault occurs between phases a and b, and the local ground g_j at j^{th} bus location through a fault impedance $\bar{z}_f$, as shown in Fig. 5.2(b) [158]. The fault currents $\bar{I}^a_f$ and $\bar{I}^b_f$ are flowing from phases a and b to the ground g_j at j^{th} bus, respectively and are calculated as,

$$\begin{aligned} \bar{I}^a_f &= \frac{(\bar{V}^{a}_{j,f} - \bar{V}^{g}_{j,f})}{\bar{z}_f} = \bar{y}_f(\bar{V}^{a}_{j,f} - \bar{V}^{g}_{j,f}) \\ \bar{I}^b_f &= \frac{(\bar{V}^{b}_{j,f} - \bar{V}^{g}_{j,f})}{\bar{z}_f} = \bar{y}_f(\bar{V}^{b}_{j,f} - \bar{V}^{g}_{j,f}) \end{aligned} \tag{5.98}$$

where, $\bar{V}^{a}_{j,f}$, $\bar{V}^{b}_{j,f}$ and $\bar{V}^{g}_{j,f}$ are the voltages of phases a and b, and ground g_j of j^{th} bus under the fault conditions, respectively. The KCL equations at phases a and b, and ground g_j of faulted bus j, under the fault condition, are given in eqs. (5.99)-(5.101), respectively, as,

$$\bar{Y}^{aa}_{j2}.\bar{V}^{a}_{2,f} + \cdots + \bar{Y}^{ag}_{j2}.\bar{V}^{g}_{2,f} + \cdots + (\bar{Y}^{aa}_{jj} + \bar{y}_f).\bar{V}^{a}_{j,f} + \cdots + (\bar{Y}^{ag}_{jj} - \bar{y}_f).\bar{V}^{g}_{j,f} + \cdots$$
$$\cdots + \bar{Y}^{aa}_{j(u+v+w)}.\bar{V}^{a}_{(u+v+w),f} + \cdots + \bar{Y}^{ag}_{j(u+v+w)}.\bar{V}^{g}_{(u+v+w),f} = 0 \tag{5.99}$$

$$\bar{Y}_{j2}^{ba}.\bar{V}_{2,f}^{a}+\cdots+\bar{Y}_{j2}^{bg}.\bar{V}_{2,f}^{g}+\cdots+(\bar{Y}_{jj}^{bb}+\bar{y}_f).\bar{V}_{j,f}^{b}+\cdots+(\bar{Y}_{jj}^{bg}-\bar{y}_f).\bar{V}_{j,f}^{g}+\cdots$$
$$\cdots+\bar{Y}_{j(u+v+w)}^{ba}.\bar{V}_{(u+v+w),f}^{a}+\cdots+\bar{Y}_{j(u+v+w)}^{bg}.\bar{V}_{(u+v+w),f}^{g}=0 \quad (5.100)$$

$$\bar{Y}_{j2}^{ga}.\bar{V}_{2,f}^{a}+\cdots+\bar{Y}_{j2}^{gg}.\bar{V}_{2,f}^{g}+\cdots+(\bar{Y}_{jj}^{ga}-\bar{y}_f).\bar{V}_{j,f}^{a}+(\bar{Y}_{jj}^{gb}-\bar{y}_f).\bar{V}_{j,f}^{b}+\cdots+(\bar{Y}_{jj}^{gg}$$
$$+2\bar{y}_f).\bar{V}_{j,f}^{g}\cdots+\bar{Y}_{j(u+v+w)}^{ga}.\bar{V}_{(u+v+w),f}^{a}+\cdots+\bar{Y}_{j(u+v+w)}^{gg}.\bar{V}_{(u+v+w),f}^{g}=0 \quad (5.101)$$

Therefore, the following elements of the $\left[\mathbf{Y_{bus}}\right]$ matrix will be modified due to LLG fault :

$$\begin{aligned}
\bar{Y}_{jj_new}^{aa} &= \bar{Y}_{jj}^{aa}+\bar{y}_f;\ \bar{Y}_{jj_new}^{bb}=\bar{Y}_{jj}^{bb}+\bar{y}_f \\
\bar{Y}_{jj_new}^{ag} &= \bar{Y}_{jj}^{ag}-\bar{y}_f;\ \bar{Y}_{jj_new}^{bg}=\bar{Y}_{jj}^{bg}-\bar{y}_f \\
\bar{Y}_{jj_new}^{ga} &= \bar{Y}_{jj}^{ga}-\bar{y}_f;\ \bar{Y}_{jj_new}^{gb}=\bar{Y}_{jj}^{gb}-\bar{y}_f \\
\bar{Y}_{jj_new}^{gg} &= \bar{Y}_{jj}^{gg}+2\bar{y}_f
\end{aligned} \quad (5.102)$$

(c) Triple line-to-ground (LLLG) fault

Let us consider an LLLG fault between all the phases a, b and c, and the local ground g_j at j^{th} bus location through a fault impedance $\bar{z}_f$, as shown in Fig. 5.2(c) [158]. The fault currents $\bar{I}_f^a$, $\bar{I}_f^b$ and $\bar{I}_f^c$ are flowing from phases a, b and c to the ground g_j at j^{th} bus, respectively and are calculated as,

$$\begin{aligned}
\bar{I}_f^a &= \frac{(\bar{V}_{j,f}^{a}-\bar{V}_{j,f}^{g})}{\bar{z}_f}=\bar{y}_f(\bar{V}_{j,f}^{a}-\bar{V}_{j,f}^{g}) \\
\bar{I}_f^b &= \frac{(\bar{V}_{j,f}^{b}-\bar{V}_{j,f}^{g})}{\bar{z}_f}=\bar{y}_f(\bar{V}_{j,f}^{b}-\bar{V}_{j,f}^{g}) \\
\bar{I}_f^c &= \frac{(\bar{V}_{j,f}^{c}-\bar{V}_{j,f}^{g})}{\bar{z}_f}=\bar{y}_f(\bar{V}_{j,f}^{c}-\bar{V}_{j,f}^{g})
\end{aligned} \quad (5.103)$$

where, $\bar{V}_{j,f}^{a}$, $\bar{V}_{j,f}^{b}$, $\bar{V}_{j,f}^{c}$ and $\bar{V}_{j,f}^{g}$ are the voltages of phases a, b and c, and ground g_j of j^{th} bus under the fault conditions, respectively. The KCL equations at phases a, b and c, and ground g_j of faulted bus j, under the fault condition, are given in eqs. (5.104)-(5.107), respectively, as,

$$\bar{Y}_{j2}^{aa}.\bar{V}_{2,f}^{a}+\cdots+\bar{Y}_{j2}^{ag}.\bar{V}_{2,f}^{g}+\cdots+(\bar{Y}_{jj}^{aa}+\bar{y}_f).\bar{V}_{j,f}^{a}+\cdots+(\bar{Y}_{jj}^{ag}-\bar{y}_f).\bar{V}_{j,f}^{g}+\cdots$$
$$\cdots+\bar{Y}_{j(u+v+w)}^{aa}.\bar{V}_{(u+v+w),f}^{a}+\cdots+\bar{Y}_{j(u+v+w)}^{ag}.\bar{V}_{(u+v+w),f}^{g}=0 \quad (5.104)$$

$$\bar{Y}_{j2}^{ba}.\bar{V}_{2,f}^{a}+\cdots+\bar{Y}_{j2}^{bg}.\bar{V}_{2,f}^{g}+\cdots+(\bar{Y}_{jj}^{bb}+\bar{y}_f).\bar{V}_{j,f}^{b}+\cdots+(\bar{Y}_{jj}^{bg}-\bar{y}_f).\bar{V}_{j,f}^{g}+\cdots$$
$$\cdots+\bar{Y}_{j(u+v+w)}^{ba}.\bar{V}_{(u+v+w),f}^{a}+\cdots+\bar{Y}_{j(u+v+w)}^{bg}.\bar{V}_{(u+v+w),f}^{g}=0 \quad (5.105)$$

$$\bar{Y}^{ca}_{j2}.\bar{V}^{a}_{2,f} + \cdots + \bar{Y}^{cg}_{j2}.\bar{V}^{g}_{2,f} + \cdots + (\bar{Y}^{cc}_{jj} + \bar{y}_f).\bar{V}^{c}_{j,f} + \cdots + (\bar{Y}^{cg}_{jj} - \bar{y}_f).\bar{V}^{g}_{j,f} + \cdots$$
$$\cdots + \bar{Y}^{ca}_{j(u+v+w)}.\bar{V}^{a}_{(u+v+w),f} + \cdots + \bar{Y}^{cg}_{j(u+v+w)}.\bar{V}^{g}_{(u+v+w),f} = 0 \quad (5.106)$$

$$\bar{Y}^{ga}_{j2}.\bar{V}^{a}_{2,f} + \cdots + \bar{Y}^{gg}_{j2}.\bar{V}^{g}_{2,f} + \cdots + (\bar{Y}^{ga}_{jj} - \bar{y}_f).\bar{V}^{a}_{j,f} + (\bar{Y}^{gb}_{jj} - \bar{y}_f).\bar{V}^{b}_{j,f} + (\bar{Y}^{gc}_{jj}$$
$$-\bar{y}_f).\bar{V}^{c}_{j,f} + \cdots + (\bar{Y}^{gg}_{jj} + 3\bar{y}_f).\bar{V}^{g}_{j,f} \cdots + \bar{Y}^{ga}_{j(u+v+w)}.\bar{V}^{a}_{(u+v+w),f} + \cdots\cdots$$
$$+\bar{Y}^{gg}_{j(u+v+w)}\bar{V}^{g}_{(u+v+w),f} = 0 \quad (5.107)$$

Therefore, the following elements of the $\left[\mathbf{Y_{bus}}\right]$ matrix will be modified due to LLLG fault :

$$\begin{aligned}
\bar{Y}^{aa}_{jj_new} &= \bar{Y}^{aa}_{jj} + \bar{y}_f;\ \bar{Y}^{bb}_{jj_new} = \bar{Y}^{bb}_{jj} + \bar{y}_f;\ \bar{Y}^{cc}_{jj_new} = \bar{Y}^{cc}_{jj} + \bar{y}_f \\
\bar{Y}^{ag}_{jj_new} &= \bar{Y}^{ag}_{jj} - \bar{y}_f;\ \bar{Y}^{bg}_{jj_new} = \bar{Y}^{bg}_{jj} - \bar{y}_f;\ \bar{Y}^{cg}_{jj_new} = \bar{Y}^{cg}_{jj} - \bar{y}_f \\
\bar{Y}^{ga}_{jj_new} &= \bar{Y}^{ga}_{jj} - \bar{y}_f;\ \bar{Y}^{gb}_{jj_new} = \bar{Y}^{gb}_{jj} - \bar{y}_f;\ \bar{Y}^{gc}_{jj_new} = \bar{Y}^{gc}_{jj} - \bar{y}_f \\
\bar{Y}^{gg}_{jj_new} &= \bar{Y}^{gg}_{jj} + 3\bar{y}_f \quad (5.108)
\end{aligned}$$

(d) Line-to-line (LL) fault

Let us assume that an LL fault occurs between phases a and b of j^{th} bus through a fault impedance $\bar{z}_f$, as shown in Fig. 5.2(d) [158]. The fault current $\bar{I}^a_f$ is flowing from phase a to b at j^{th} bus and are calculated as,

$$\bar{I}^a_f = \frac{(\bar{V}^a_{j,f} - \bar{V}^b_{j,f})}{\bar{z}_f} = \bar{y}_f(\bar{V}^a_{j,f} - \bar{V}^b_{j,f}) \quad (5.109)$$

where, $\bar{V}^a_{j,f}$ and $\bar{V}^b_{j,f}$ are the voltages of phases a and b of j^{th} bus under the fault conditions, respectively. The KCL equations at phases a and b of faulted bus j, under the fault condition, are given in eqs. (5.110), and (5.111), respectively, as,

$$\bar{Y}^{aa}_{j2}.\bar{V}^{a}_{2,f} + \cdots + \bar{Y}^{ag}_{j2}.\bar{V}^{g}_{2,f} + \cdots + (\bar{Y}^{aa}_{jj} + \bar{y}_f).\bar{V}^{a}_{j,f} + (\bar{Y}^{ab}_{jj} - \bar{y}_f).\bar{V}^{b}_{j,f} + \cdots + \bar{Y}^{ag}_{jj}.\bar{V}^{g}_{j,f}$$
$$+ \cdots\cdots + \bar{Y}^{aa}_{j(u+v+w)}.\bar{V}^{a}_{(u+v+w),f} + \cdots + \bar{Y}^{ag}_{j(u+v+w)}.\bar{V}^{g}_{(u+v+w),f} = 0 \quad (5.110)$$

$$\bar{Y}^{ba}_{j2}.\bar{V}^{a}_{2,f} + \cdots + \bar{Y}^{bg}_{j2}.\bar{V}^{g}_{2,f} + \cdots + (\bar{Y}^{ba}_{jj} - \bar{y}_f).\bar{V}^{a}_{j,f} + (\bar{Y}^{bb}_{jj} + \bar{y}_f).\bar{V}^{b}_{j,f} + \cdots + \bar{Y}^{bg}_{jj}.\bar{V}^{g}_{j,f}$$
$$+ \cdots\cdots + \bar{Y}^{ba}_{j(u+v+w)}.\bar{V}^{a}_{(u+v+w),f} + \cdots + \bar{Y}^{bg}_{j(u+v+w)}.\bar{V}^{g}_{(u+v+w),f} = 0 \quad (5.111)$$

Therefore, the following elements of the $\left[\mathbf{Y_{bus}}\right]$ matrix will be modified due to LL fault :

$$\begin{aligned}
\bar{Y}^{aa}_{jj_new} &= \bar{Y}^{aa}_{jj} + \bar{y}_f;\ \bar{Y}^{ab}_{jj_new} = \bar{Y}^{ab}_{jj} - \bar{y}_f \\
\bar{Y}^{ba}_{jj_new} &= \bar{Y}^{ba}_{jj} - \bar{y}_f;\ \bar{Y}^{bb}_{jj_new} = \bar{Y}^{bb}_{jj} + \bar{y}_f \quad (5.112)
\end{aligned}$$

First, the bus voltages for an LL fault are calculated using eq. (5.91) with the above modification in $\left[\mathbf{Y_{bus}}\right]$ matrix. Next, the branch currents under the fault conditions and fault current are then calculated using eqs. (5.97) and (5.109), respectively.

Steps of algorithm for $\left[\mathbf{Y_{bus}}\right]$ ***matrix based short-circuit analysis method for an unbalanced three phase four wire multigrounded radial distribution system***

1. Run the base case power flow of an unbalanced three phase four wire multigrounded distribution system using the proposed load flow method as discussed in Section 5.2 of this chapter.

2. Convert all PQ-loads into constant impedance loads using the obtained pre-fault load flow solution.

3. Formulate the $\left[\mathbf{Y_{bus}}\right]$ matrix of the distribution system using the above discussed formulation.

4. Modify $\left[\mathbf{Y_{bus}}\right]$ matrix corresponding to the type of fault occurring in the system, using eq. (5.96) for SLG fault, eq. (5.102) for LLG fault, eq. (5.108) for LLLG fault and eq. (5.112) for LL fault.

5. Calculate the bus voltages of the distribution system under the fault condition using eq. (5.91) with the modified $\left[\mathbf{Y_{bus}}\right]$ matrix.

6. Calculate fault currents using eq. (5.93) for SLG, eq. (5.98) for LLG, eq. (5.103) for LLLG and eq. (5.109) for LL fault. Also calculate post fault branch currents using the eq. (5.97).

5.4 Test results and discussions

To investigate the accuracy of the proposed load flow and short-circuit analysis methods, two different three phase four wire multigrounded test systems have been used in this study. The first system is IEEE 34-bus node test feeder located in Arizona and the second one is IEEE 123-bus node test feeder. Details of these test feeders are given in [159]. To calculate the primitive self and mutual line impedances of these test systems, Carson's formula [160] has been used in this study.

The primitive self impedances of the three phase four wire multigrounded system are calculated as,

$$\bar{z}_{aa} = (r_a + r_d) + jwk\ ln\frac{D_e}{D_{sa}}\ \Omega/mile \tag{5.113}$$

$$\bar{z}_{bb} = (r_b + r_d) + jwk\ ln\frac{D_e}{D_{sb}}\ \Omega/mile \tag{5.114}$$

$$\bar{z}_{cc} = (r_c + r_d) + jwk\ ln\frac{D_e}{D_{sc}}\ \Omega/mile \tag{5.115}$$

$$\bar{z}_{nn} = (r_n + r_d) + jwk\ ln\frac{D_e}{D_{sn}}\ \Omega/mile \tag{5.116}$$

where, r_a, r_b, r_c and r_n are the resistances in $\Omega/mile$ of the phase conductors a, b, c and neutral conductor n, respectively. r_d is the earth resistance and is calculated as $r_d = 1.588 \times 10^{-3} f$ $\Omega/mile$ [160], where f is the frequency in Hz. According to the Carson's line model, the quantity D_e is calculated as, $D_e = 2160 \times \sqrt{\rho/f}$ ft, where ρ is the ground resistivity. ωk is the inductance multiplying constant and its value for 60 Hz frequency system is $0.12134\ mile$ [160]. D_{sa}, D_{sb}, D_{sc} and D_{sn} are the Geometric Mean Radii (GMR) of the phase conductors a, b, c and neutral conductor n, in feet, respectively. Similarly, the primitive line to line mutual impedances of the three phase four wire multigrounded system are calculated as,

$$\bar{z}_{ab} = r_d + jwk\ ln\frac{D_e}{D_{ab}}\ \Omega/mile \tag{5.117}$$

$$\bar{z}_{bc} = r_d + jwk\ ln\frac{D_e}{D_{bc}}\ \Omega/mile \tag{5.118}$$

$$\bar{z}_{ac} = r_d + jwk\ ln\frac{D_e}{D_{ac}}\ \Omega/mile \tag{5.119}$$

$$\bar{z}_{pn} = r_d + jwk\ ln\frac{D_e}{D_{pn}}\ \Omega/mile, \quad (p = a, b, c) \tag{5.120}$$

where, D_{ab}, D_{bc} and D_{ac} are the distances between the centers of the conductors a and b, b and c and a and c, in feet, respectively. D_{pn} is the distance between the center of phase conductor p ($p = a, b, c$) and neutral conductor n, also in feet. Now, the primitive self and mutual ground impedances are calculated as [128],

$$\bar{z}_{gg} = (\pi^2 \times 10^{-4} f) - j(0.0386 \times 8\pi \times 10^{-4} f) + j\left(4\pi \times 10^{-4} f \times\ ln\frac{2}{5.6198 \times 10^{-3}}\right)\ \Omega/km \tag{5.121}$$

$$\bar{z}_{pg} = j\left(2\pi \times 10^{-4} f \times ln\frac{D_{pg}}{\sqrt{\frac{\rho}{f}}}\right)\ \Omega/km, \ \ (p = a, b, c) \tag{5.122}$$

$$\bar{z}_{ng} = j\left(2\pi \times 10^{-4} f \times ln\frac{D_{ng}}{\sqrt{\frac{\rho}{f}}}\right) \Omega/km \tag{5.123}$$

where, $\bar{z}_{gg}$ is the self ground impedance. $\bar{z}_{pg}$ is the mutual phase to ground impedance between phase conductor p $(p = a, b, c)$ and ground g; $\bar{z}_{ng}$ is the mutual neutral to ground impedance between neutral conductor n and ground g. D_{pg} is the distances between the centers of the phase conductor p $(p = a, b, c)$ and ground g; D_{ng} is the distances between the centers of neutral conductor n and ground g. The shunt capacitances, voltage regulators and transformers in both test systems have not been considered in this study. The proposed load flow and short-circuit analysis methods have been implemented in MATLAB environment with a tolerance limit (ϵ) of 1.0×10^{-12}.

5.4.1 Results of modified three phase four wire multigrounded IEEE 34-bus test system

5.4.1.1 Results of load flow studies

The bus numbers of the original IEEE 34-bus test system have been renumbered for this work and the details of renumbering are given in Appendix A. The neutral to ground impedance in this test system is assumed as $0.2\ \Omega$ [128]. The line impedances of the test system are calculated using the Carson's formula [160]. For example, consider a line section-3 of length 32230 feet between buses 3 and 4. According to the line-data information given in [159], the phase and neutral conductors used for the line section-3 are of type "ACSR, $1/0$ with spacing ID-500". Hence, for this line configuration [161],

$r_a = r_b = r_c = r_n = 1.12\Omega/mile$; $D_{sa} = D_{sb} = D_{sc} = D_{sn} = 0.00446\ ft$

$f = 60Hz, \rho = 100\ \Omega\text{-}m, r_d = 0.09528\ \Omega/mile, D_e = 2788.55\ ft$

$D_{ab} = 2.50\ ft, D_{bc} = 4.50\ ft, D_{ac} = 7.0\ ft$

$D_{an} = 5.66\ ft, D_{bn} = 4.27\ ft, D_{cn} = 5.0\ ft$

$D_{ag} = D_{bg} = D_{cg} = 28.0\ ft, D_{ng} = 24.0\ ft$

Therefore, the calculated line impedance matrix of line section-3 is given as

$$\mathbf{z_{34}^{abcng}} = \begin{bmatrix} 7.42 + j9.89 & 0.58 + j5.20 & 0.58 + j4.43 & 0.58 + j4.59 & 0.00 + j0.70 \\ 0.58 + j5.20 & 7.42 + j9.89 & 0.58 + j4.76 & 0.58 + j4.80 & 0.00 + j0.70 \\ 0.58 + j4.43 & 0.58 + j4.76 & 7.42 + 9.89 & 0.58 + 4.68 & 0.00 + j0.70 \\ 0.58 + j4.59 & 0.58 + j4.80 & 0.58 + 4.68 & 7.42 + j9.88 & 0.00 + j0.64 \\ 0.00 + j0.70 & 0.00 + j0.70 & 0.00 + j0.70 & 0.00 + j0.64 & 0.58 + j4.35 \end{bmatrix} \Omega \tag{5.124}$$

Similarly, the line impedance matrices of all other line sections of the modified IEEE 34-bus test system have been obtained by using Carson's formula. The base voltage and base volt-amperes of the modified IEEE 34-bus test system are assumed as 24.9 kV and 2500 MVA, respectively.

In this study, the load flow analysis of the test system has been performed by using the proposed method and the results have been compared with those obtained by $\left[\mathbf{Y_{bus}}\right]$ matrix based method [135] and the time domain simulation studies carried out using PSCAD/EMTDC software. In $\left[\mathbf{Y_{bus}}\right]$ matrix based method [135], the bus admittance matrix for the three-phase four wire distribution system with ground return has been developed in the same manner as that of the three-phase three wire system. In each iteration of this method, the load admittances at all the buses will be recalculated by using the updated values of bus voltages.

The bar graph for the bus voltage of phase a, of modified IEEE 34-bus test system, has been obtained by the proposed method and plotted along with the bus voltage values obtained by the $\left[\mathbf{Y_{bus}}\right]$ matrix based method and PSCAD/EMTDC simulation studies, as shown in Fig. 5.4. The figure shows that the results obtained by the proposed method are very close to the results of the $\left[\mathbf{Y_{bus}}\right]$ matrix method and PSCAD/EMTDC studies, which establishes the accuracy of the proposed method. Similarly, the bar graphs of the neutral bus and ground bus voltages obtained by the proposed method, $\left[\mathbf{Y_{bus}}\right]$ matrix method and PSCAD/EMTDC simulation are also shown in Figs. 5.5 and 5.6, respectively. A good match between the results obtained by these three methods demonstrates the correctness of the proposed approach.

The current in phase a, neutral wire and ground for the modified IEEE 34-bus test system calculated by the proposed load flow method are plotted in Figs. 5.7-5.9, respectively. The values of these three currents have also been obtained by the $\left[\mathbf{Y_{bus}}\right]$ matrix based method and PSCAD/EMTDC simulation studies, and are plotted along with the results of proposed method in Figs. 5.7-5.9. A close matching of the current values as observed in these figures validates the accuracy of the proposed method. Also, from Figs. 5.8 and 5.9, it is observed that the neutral and ground sections of branches 9 and 10 carry highest values of neutral and ground currents, respectively. This can be explained with the help of Fig. 5.10. The bus nos. 10, 11 and 12 of the IEEE 34-bus test system are single phase buses (having phase a only) and are heavily loaded. Due to this, the load bus currents $\bar{I}^a_{10d}$, $\bar{I}^a_{11d}$ and $\bar{I}^a_{12d}$ injected into the neutral buses n_{10}, n_{11} and n_{12} have high values. As a result, the neutral currents ($\bar{B}^n_9$, $\bar{B}^n_{10}$, $\bar{B}^n_{11}$), neutral to ground currents ($\bar{I}^{ng}_{10}$, $\bar{I}^{ng}_{11}$,

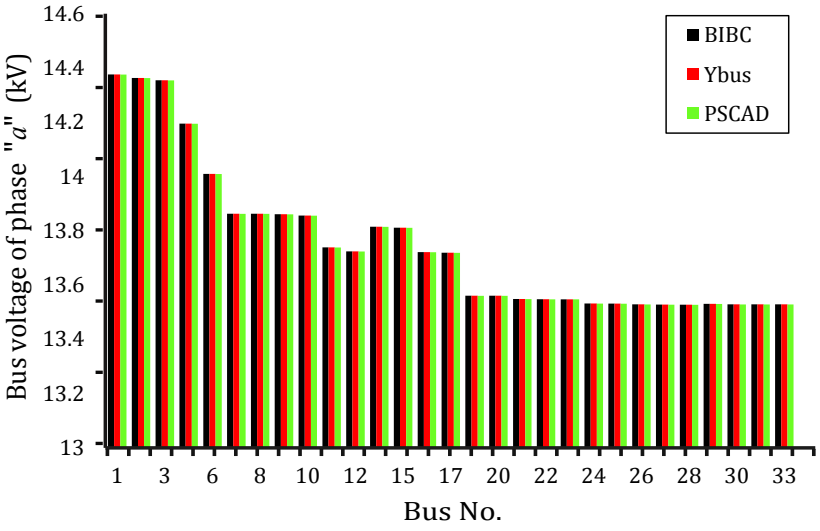

Figure 5.4: Voltage profile of phase a of modified IEEE 34-bus test system using proposed $\left[\mathbf{BIBC}\right]$ technique, $\left[\mathbf{Y_{bus}}\right]$ technique and PSCAD/EMTDC simulation under the normal operating conditions

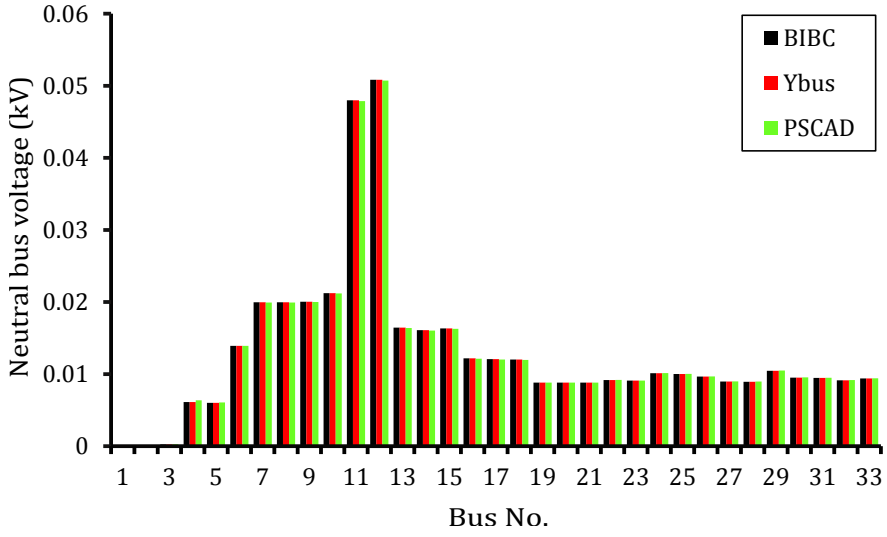

Figure 5.5: Voltage profile of neutral bus of modified IEEE 34-bus test system using proposed $\left[\mathbf{BIBC}\right]$ technique, $\left[\mathbf{Y_{bus}}\right]$ technique and PSCAD/EMTDC simulation under normal operating conditions

$\bar{I}_{12}^{ng}$) and ground currents ($\bar{B}_{9}^{g}$, $\bar{B}_{10}^{g}$, $\bar{B}_{11}^{g}$) are also carrying high values, as shown in Fig. 5.10. As a result, the voltages of neutral buses (n_{11} and n_{12}) and ground buses (g_{11} and g_{12}) of the system are also very high, as shown in Figs. 5.5 and 5.6.

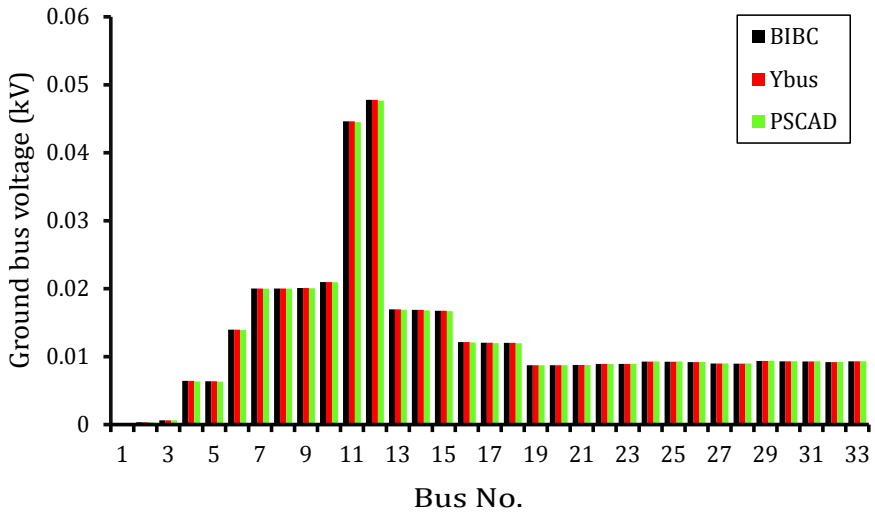

Figure 5.6: Voltage profile of ground bus of modified IEEE 34-bus test system using proposed $[\mathbf{BIBC}]$ technique, $[\mathbf{Y_{bus}}]$ technique and PSCAD/EMTDC simulation under normal operating conditions

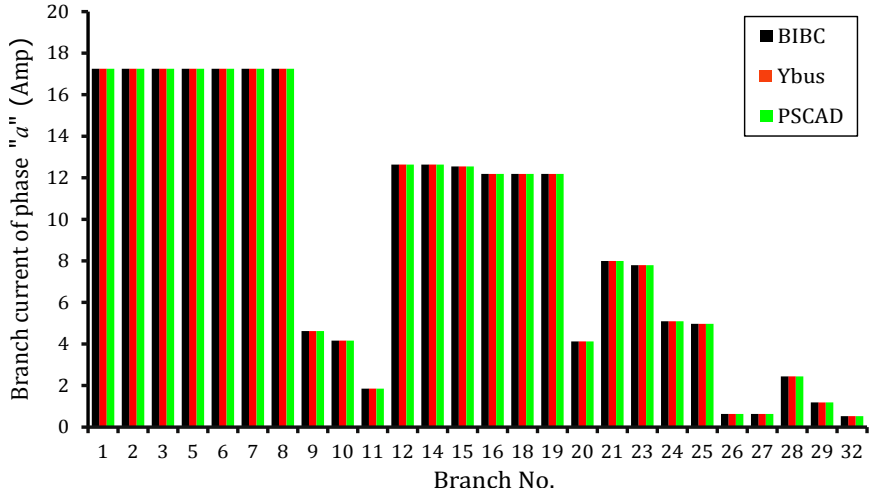

Figure 5.7: Branch current of phase a of modified IEEE 34-bus test system using proposed $[\mathbf{BIBC}]$ technique, $[\mathbf{Y_{bus}}]$ technique and PSCAD/EMTDC simulation under normal operating conditions

A case of isolated neutral has also been simulated on modified three phase four wire multi-grounded IEEE 34-bus test system using the proposed method. In this case, there is no physical connection between the neutral buses and the ground buses in the system, that is, the neutral to ground impedance at all the buses is very high (ideally infinite). Also, the fifth row and fifth

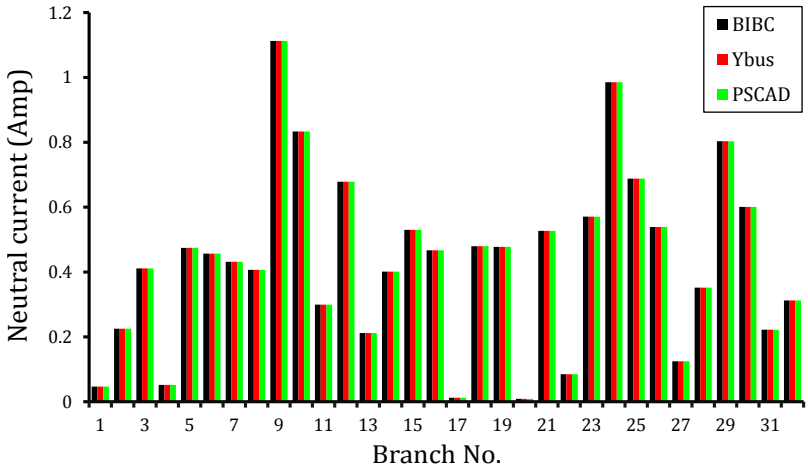

Figure 5.8: Neutral current of modified IEEE 34-bus test system using proposed $[\mathbf{BIBC}]$ technique, $[\mathbf{Y_{bus}}]$ technique and PSCAD/EMTDC simulation under normal operating conditions

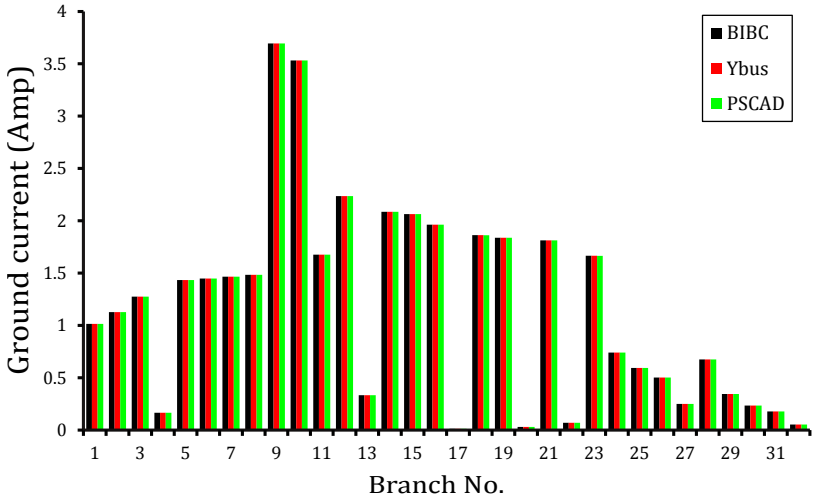

Figure 5.9: Ground current of modified IEEE 34-bus test system using proposed $[\mathbf{BIBC}]$ technique, $[\mathbf{Y_{bus}}]$ technique and PSCAD/EMTDC simulation under normal operating conditions

column of three-phase line impedance matrix, fourth row and fourth column of two-phase line impedance matrix and third row and third column of single phase line impedance matrix contain all zero elements. The neutral bus voltage profiles of the test system for ”isolated neutral” (without ground return) and ”grounded neutral” (with ground return) cases are shown in Fig. 5.11(a). The figure shows that the values of neutral voltages at all the buses in ”isolated neutral” case are higher

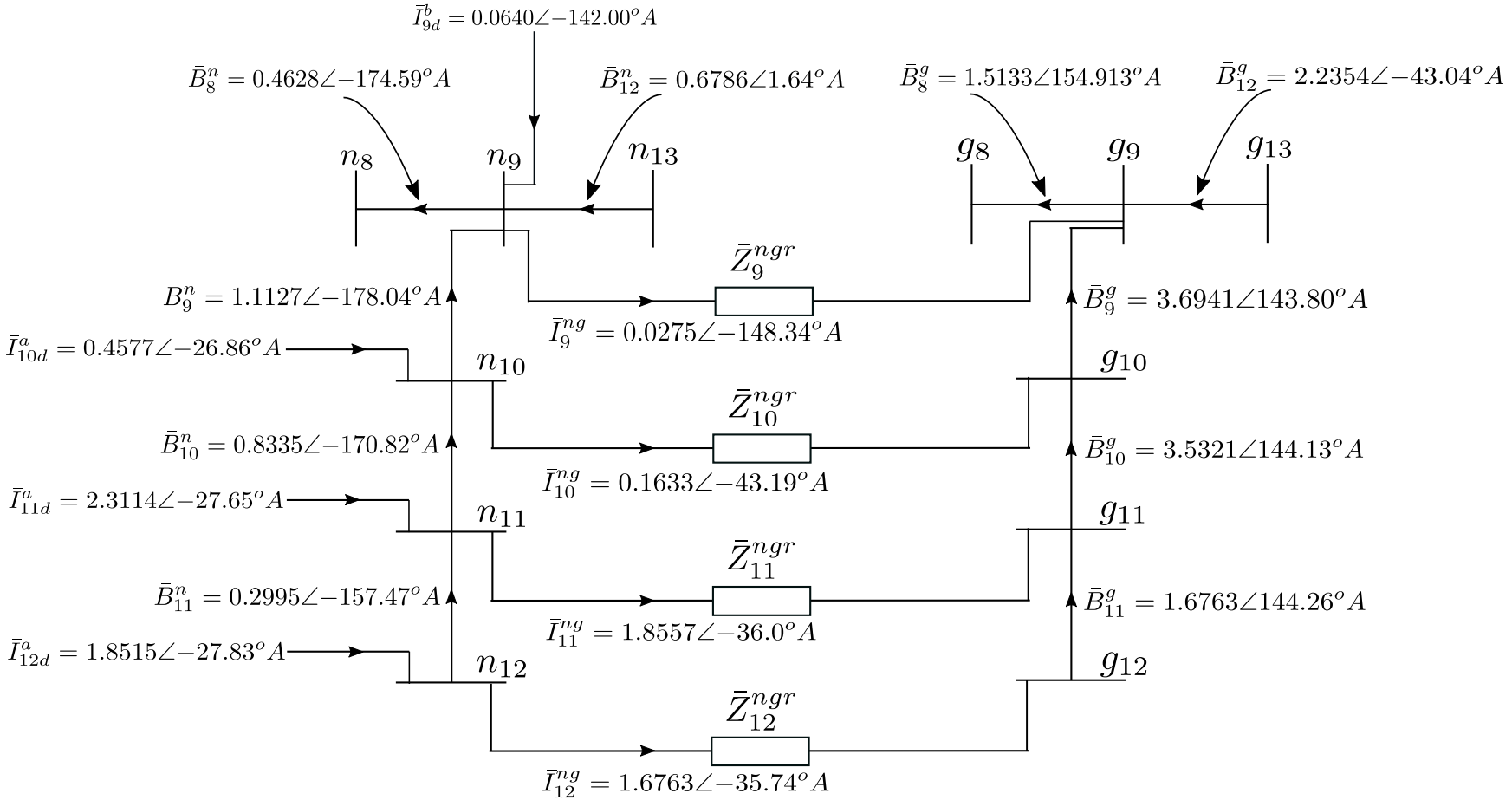

Figure 5.10: Currents distribution between neutral and ground wires of branch nos. 8, 9, 10, 11 and 12 of modified IEEE 34-bus test system under normal operating conditions

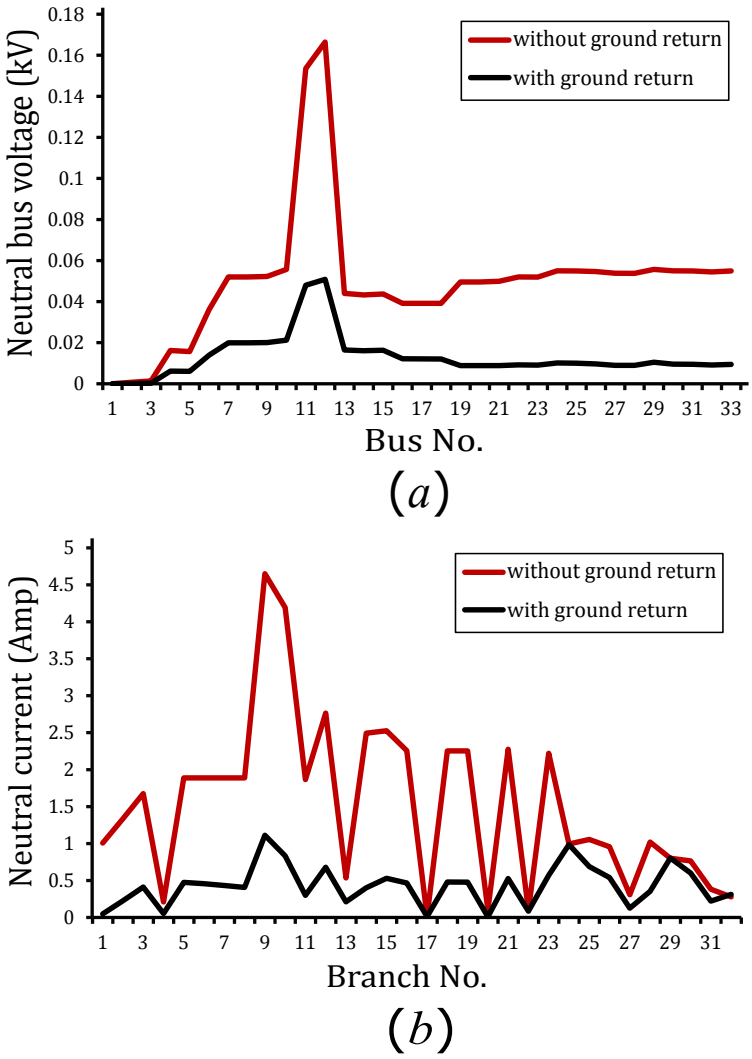

Figure 5.11: (*a*) Neutral bus voltage profile, (*b*) Neutral current of modified IEEE 34-bus test system in ”isolated neutral” and ”grounded neutral” cases under normal operating conditions

than the ”grounded neutral” case. This is due to the fact that, the return path for load currents in ”isolated neutral case” is only through the neutral wire, whereas in ”grounded neutral” case the injected load currents are divided in two paths, one part flowing through the neutral wire and the other through the ground wire. Therefore, the values of neutral currents in ”isolated neutral” case are higher than in ”grounded neutral” case, as shown in Fig. 5.11(b), and hence, the values of neutral bus voltages in ”isolated neutral” case are higher.

The value of maximum ground bus voltage and maximum ground current in modified IEEE

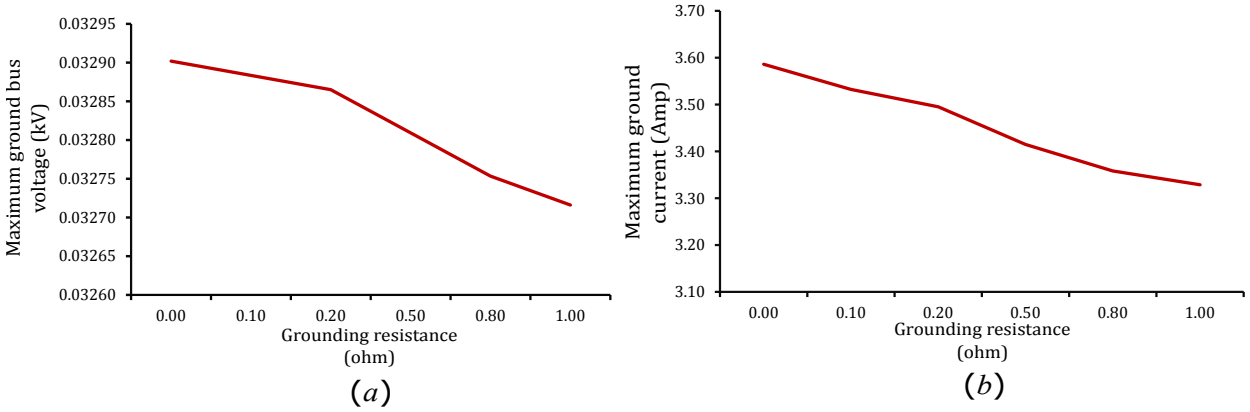

Figure 5.12: (a) Maximum ground bus voltage, (b) Maximum ground current, in modified IEEE 34-bus test system for various grounding resistance under normal operating condition

34-bus test system under normal operating condition, for various grounding resistance are plotted in Fig. 5.12(a) and (b). The figure shows that, with the increase in grounding resistance, the value of maximum ground bus voltage as well as maximum ground current in the system decreases (as shown in Fig. 5.12(a)). This is due to the fact that, with the increase in grounding resistance, the value of neutral to ground current in the system decreases and as a result the value of ground wire currents and hence the ground bus voltages of the system decreases (as shown in Fig. 5.12(b)).

5.4.1.2 Results of short-circuit studies

For investigating the efficacy of the proposed short-circuit analysis methods ($[\mathbf{BIBC}]$ matrix based method and $[\mathbf{Y_{bus}}]$ matrix based method), following short-circuit faults have been simulated on modified three phase four wire multigrounded IEEE 34-bus test system.

Case 1. A single line-to-ground fault in phase a of bus 28 with a fault impedance $\bar{z}_f$ = 0.001+0.000i p.u.

Case 2. A double line-to-ground fault between phases a and b of bus 28 with a fault impedance $\bar{z}_f$ = 0.001+0.000i p.u.

Case 3. A three line-to-ground fault at bus 28 with a fault impedance $\bar{z}_f$ = 0.001+0.000i p.u.

Case 4. A line-to-line fault between phases a and b of bus 28 with a fault impedance $\bar{z}_f$ = 0.001+0.000i p.u.

Detailed results of these fault studies, by using the proposed methods and time domain simula-

Table 5.2: Error Analysis of proposed $[\mathbf{BIBC}]$ matrix based technique and $[\mathbf{Y_{bus}}]$ matrix based technique with respect to PSCAD/EMTDC simulation study for modified three phase four wire multigrounded IEEE 34-bus radial test system

case	Fault type	phase	Fault current at fault point (I_f)			% Error in (I_f)		Current drawn from the supply (I_s)			% Error in (I_s)	
			PSCAD simulation (Amp)	[BIBC] Technique (Amp)	$[Y_{bus}]$ Technique (Amp)	[BIBC] Technique (%)	$[Y_{bus}]$ Technique (%)	PSCAD simulation (Amp)	[BIBC] Technique (Amp)	$[Y_{bus}]$ Technique (Amp)	[BIBC] Technique (%)	$[Y_{bus}]$ Technique (%)
1	SLG (a-g)	a	151.382	151.392	151.392	0.00698	0.00698	154.425	154.434	154.434	0.00611	0.00611
2	LLG (ab-g)	a	196.795	196.790	196.790	0.00237	0.00237	200.059	200.053	200.053	0.00250	0.00250
		b	247.393	247.411	247.411	**0.00730**	**0.00730**	249.824	249.851	249.851	**0.00888**	**0.00888**
3	LLLG (abc-g)	a	235.769	235.779	235.779	0.00439	0.00439	239.174	239.184	239.184	0.00434	0.00434
		b	255.303	255.320	255.320	0.00651	0.00651	257.922	257.939	257.939	0.00645	0.00645
		c	247.310	247.325	247.325	0.00583	0.00583	249.089	249.103	249.103	0.00582	0.00582
4	L-L (a-b)	a	217.701	217.702	217.702	0.00037	0.00037	220.540	220.542	220.542	0.00024	0.00024
		b	217.701	217.702	217.702	0.00037	0.00037	220.333	220.359	220.359	0.00712	0.00712

tion studies carried out using the PSCAD/EMTDC software, are given in Table 5.2. The calculated values of fault currents (I_f) and source currents (I_s) for all types of faults obtained by the proposed $[\mathbf{BIBC}]$ matrix based method and $[\mathbf{Y_{bus}}]$ matrix based method are identical, validating the correctness of the proposed methods. The maximum $\%$ errors in the calculated values of (I_f) and (I_s), obtained from the proposed short-circuit analysis methods, with respect to the PSCAD/EMTDC simulation results are 0.00730% and 0.00888%, respectively, as shown in Table 5.2. These extremely small values of errors establish that the proposed methods are sufficiently accurate.

The phase a bus voltage, neutral bus voltage and ground bus voltage, for an SLG fault at phase a of bus 28 with fault impedance of $\bar{z}_f$ = 0.001+0.000i p.u., obtained by the proposed short-circuit analysis methods $\big([\mathbf{BIBC}]$ matrix based and $[\mathbf{Y_{bus}}]$ matrix based methods $\big)$, are shown in the bar graphs of Figs. 5.13-5.15, respectively. The values of these voltages are also obtained by the time domain simulation studies carried out using the PSCAD/EMTDC software and are plotted along with the results of proposed methods, as shown in Figs. 5.13-5.15, respectively. A comparison of these plots shows that the values of bus voltages obtained by the proposed methods are very close to the values obtained by the PSCAD/EMTDC simulation studies, which again validates the accuracy of the proposed short-circuit analysis methods.

In Fig. 5.16(a), the ground bus voltage profile is plotted for various ground faults (SLG, LLG and LLLG) at bus 28 with a fault impedance of $\bar{z}_f$ = 0.001+0.000i p.u.. The plot shows that the

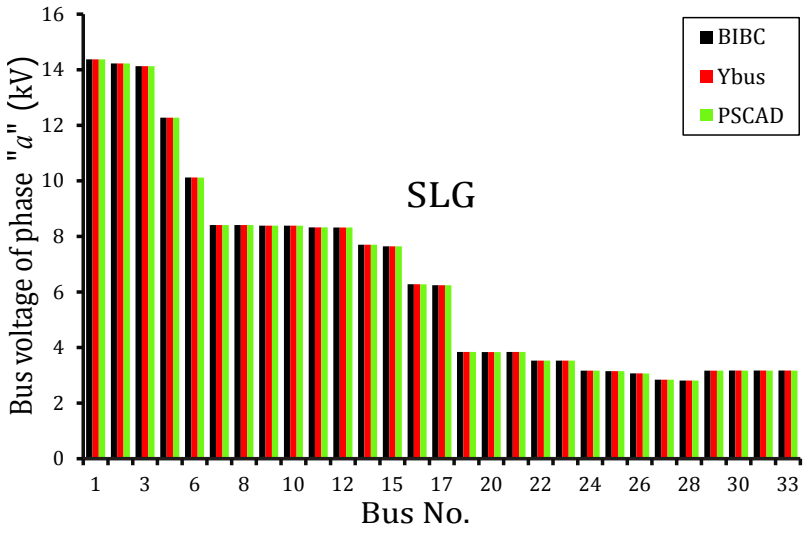

Figure 5.13: Voltage profile of phase a, for an SLG fault (a-g) at bus 28, of modified IEEE 34-bus test system using proposed $\left[\mathbf{BIBC}\right]$ technique, $\left[\mathbf{Y_{bus}}\right]$ technique and PSCAD/EMTDC simulation

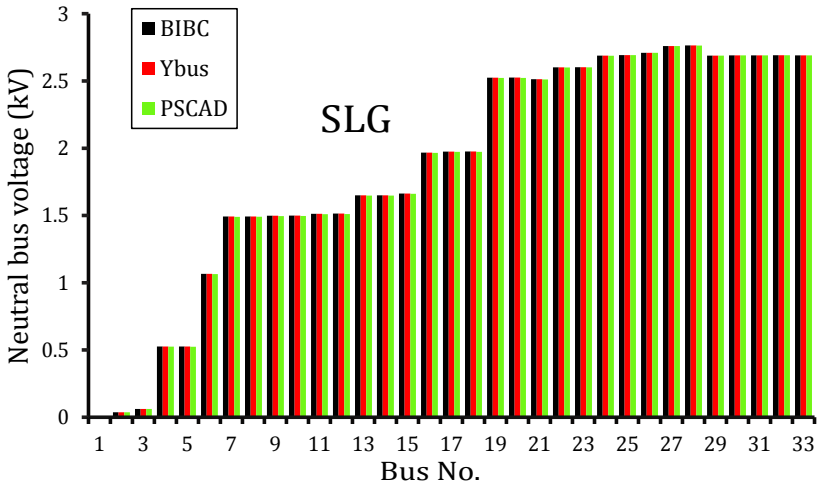

Figure 5.14: Voltage profile of neutral bus, for an SLG fault (a-g) at bus 28, of modified IEEE 34-bus test system using proposed $\left[\mathbf{BIBC}\right]$ technique, $\left[\mathbf{Y_{bus}}\right]$ technique and PSCAD/EMTDC simulation

highest ground bus voltages occur for SLG fault followed by LLG fault while the lowest values are observed for LLLG fault. This is due to the fact that the fault current injected into the fault point at ground bus is the phasor sum of the three phase fault current and its value ($\bar{I}_f^a + \bar{I}_f^b + \bar{I}_f^c = -0.34 + j5.83$ Amp $= 5.839\underline{/93.31^o}$ Amp) is smallest for LLLG fault, followed by the injected

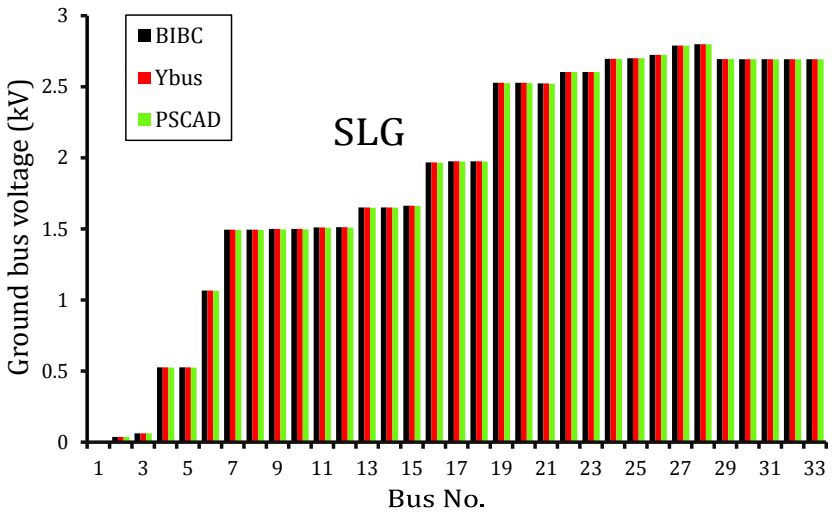

Figure 5.15: Voltage profile of ground bus, for an SLG fault (a-g) at bus 28, of modified IEEE 34-bus test system using proposed $\left[\mathbf{BIBC}\right]$ technique, $\left[\mathbf{Y_{bus}}\right]$ technique and PSCAD/EMTDC simulation

fault current corresponding to LLG fault ($\bar{I}_f^a + \bar{I}_f^b = -50.20 - j92.94$ Amp $= 105.634\underline{/-118.37^o}$ Amp) with SLG fault injecting highest current ($\bar{I}_f^a = 98.21 - j115.21$ Amp $= 151.392\underline{/-49.55^o}$ Amp) into the ground at the fault bus location. Therefore, the currents flowing through ground from fault point to the substation ground are highest for SLG fault followed by LLG fault and smallest for LLLG fault, as shown in 5.16(b). As a result, the ground bus voltages are highest for SLG fault with LLLG fault resulting in lowest ground bus voltages. From Fig. 5.16(b), it is also observed that the value of ground current at certain branches of the test system (such as branch nos. $4, 9-11, 13, 17, 20, 22, 28-32$) are nearly equal to zero. It is due to the fact that these branches are not present in the path of fault current returning through ground from fault point to the substation ground, as shown in Fig. 5.17.

Under fault conditions (for SLG, LLG and LLLG fault), as the neutral to ground resistance increases, the ground current as well as the ground bus voltage at the fault point increases, as can be observed in Figs. 5.18(a)-(f). This is due to the fact that as neutral to ground resistance is increased, fault current flowing through the ground wire increases and the current in the neutral wire decreases.

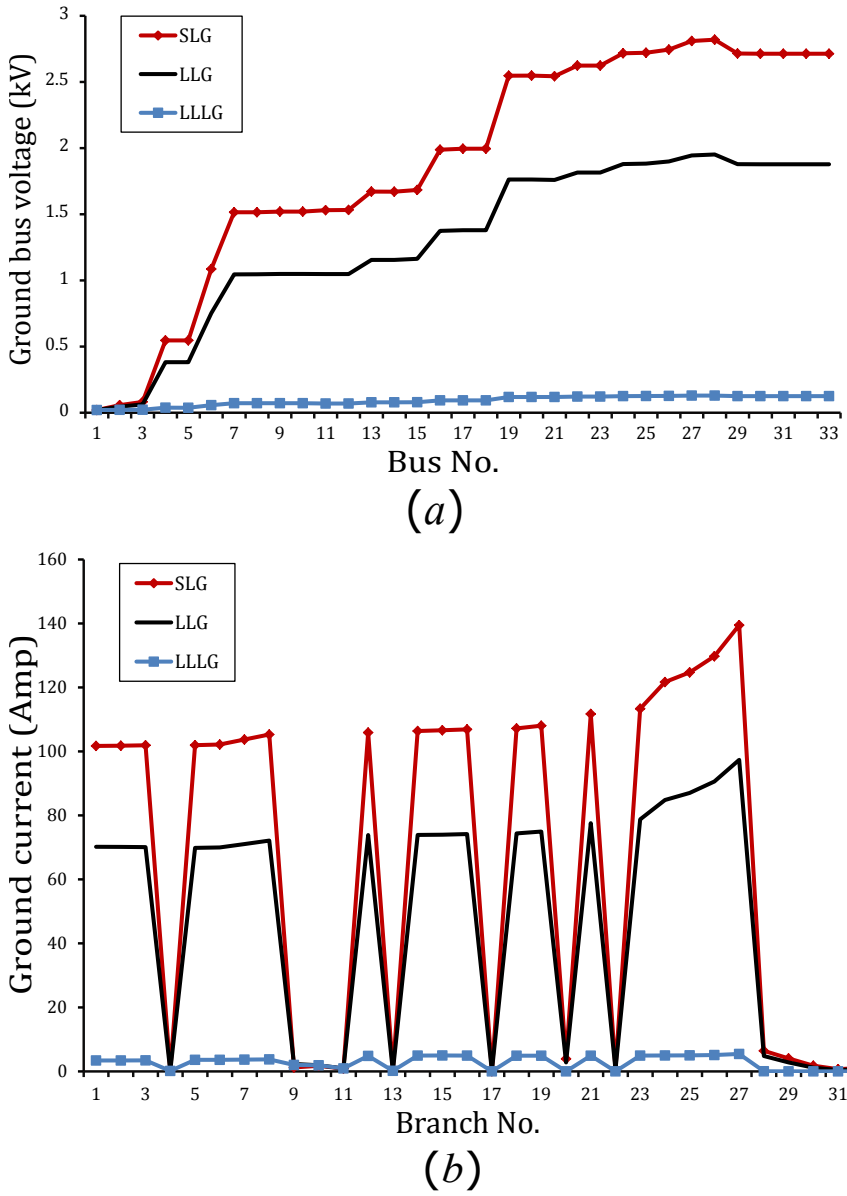

Figure 5.16: (*a*) Voltage profile of ground bus, (*b*) Ground current, for various ground faults at bus 28, of modified IEEE 34-bus test system

5.4.2 Results of modified three phase four wire multigrounded IEEE 123-bus test system

5.4.2.1 Results of load flow studies

The bus numbers of IEEE 123-bus system have also been renumbered in this study and the details of the modified test system are given in Appendix B. The value of ground resistivity (ρ) and grounding resistance in this study has been considered as $100\ \Omega$-m and $0.2\ \Omega$ [128], respectively.

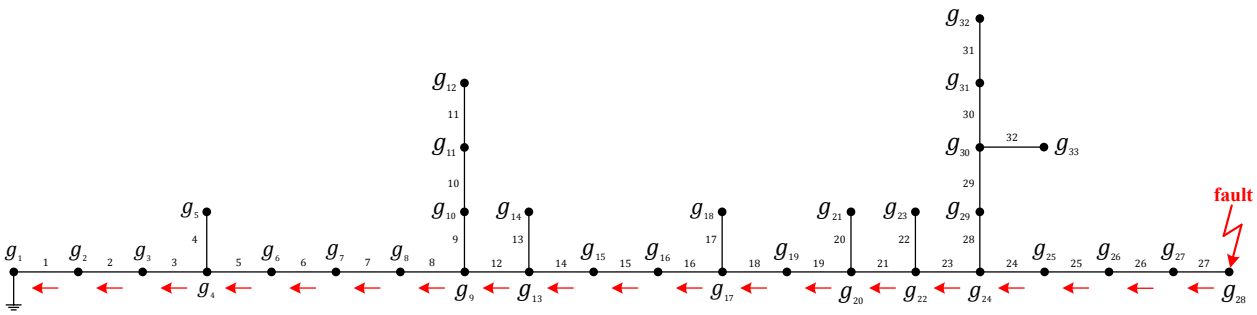

Figure 5.17: Path of the fault current for an SLG fault ($a-g$) at bus 28 in IEEE 34-bus test system

The base voltage and base volt-amperes of this test system are assumed as 4.16 kV and 5.0 MVA, respectively. The line impedance matrices of this system have also been calculated using the Carson's formula [160]. For example, the line impedance matrix of the line section-7 (phase conductor is of type "ACSR, 336.4, $26/7$" and neutral conductor is of type "ACSR, $4/0$, $6/1$" with spacing ID-500) between buses 2 and 8 of modified IEEE 123-bus test system is given as,

$$\mathbf{z_{27}^{abcng}} = \begin{bmatrix} 0.023+j0.080 & 0.005+j0.049 & 0.005+j0.041 & 0.005+j0.043 & 0.000+j0.007 \\ 0.005+j0.049 & 0.023+j0.080 & 0.005+j0.044 & 0.005+j0.045 & 0.000+j0.007 \\ 0.005+j0.041 & 0.005+j0.044 & 0.023+j0.080 & 0.005+j0.044 & 0.000+j0.007 \\ 0.005+j0.043 & 0.005+j0.045 & 0.005+j0.044 & 0.040+j0.088 & 0.000+j0.006 \\ 0.000+j0.007 & 0.000+j0.007 & 0.000+j0.007 & 0.000+j0.006 & 0.005+j0.041 \end{bmatrix} \Omega \tag{5.125}$$

The load flow analysis of this test system has been performed by using the proposed method and the results have been compared with those obtained by $\left[\mathbf{Y_{bus}}\right]$ matrix based method. The time domain simulation study of this system could not be performed with the available version of PSCAD/EMTDC software due to the node limitations.

The voltage profile of phase a of modified IEEE 123-bus test system has been obtained by the proposed method and is plotted along with the voltage profile obtained by the $\left[\mathbf{Y_{bus}}\right]$ matrix based method, as shown in Fig. 5.19. The voltage profiles of neutral bus and ground bus of the test system have also been obtained by the proposed load flow method and are plotted along with the profiles obtained by the $\left[\mathbf{Y_{bus}}\right]$ matrix based method, as shown in Figs. 5.20-5.21, respectively. These figures show that the results obtained by the proposed method are very close to the results of the $\left[\mathbf{Y_{bus}}\right]$ matrix method and this demonstrates the correctness of the proposed method.

The values of phase branch, neutral and ground currents of the modified IEEE 123-bus test system

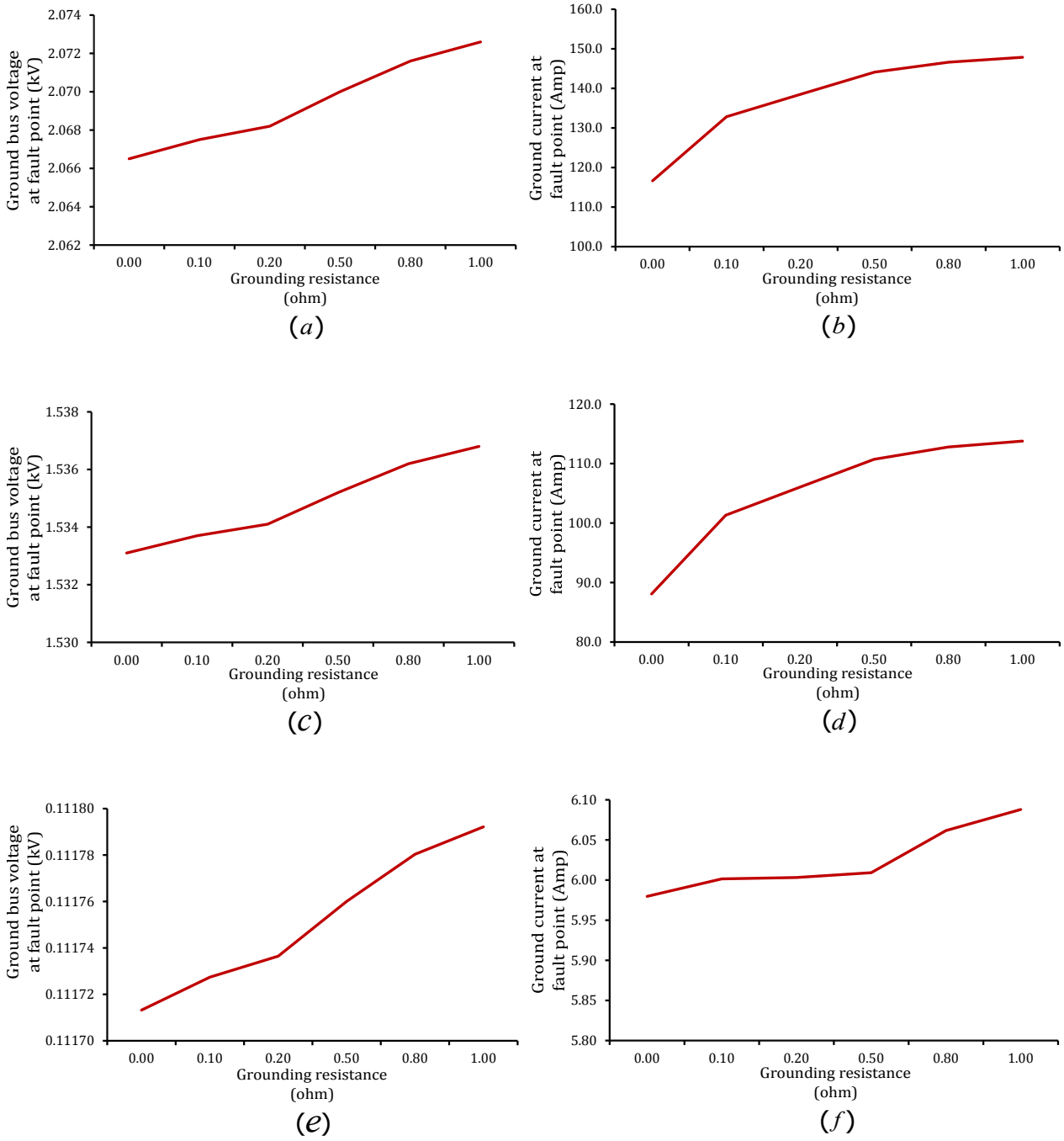

Figure 5.18: Maximum ground bus voltage and Maximum ground current in modified IEEE 34-bus test system for various grounding resistance under SLG fault ((*a*) and (*b*)), LLG fault ((*c*) and (*d*)) and LLLG fault ((*e*) and (*f*))

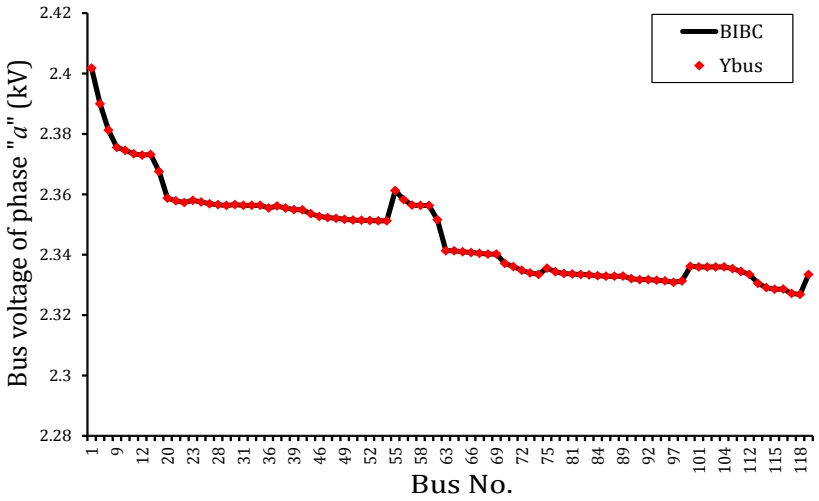

Figure 5.19: Voltage profile of phase a of modified IEEE 123-bus test system using proposed $\left[\mathbf{BIBC}\right]$ technique and $\left[\mathbf{Y_{bus}}\right]$ technique under normal operating conditions

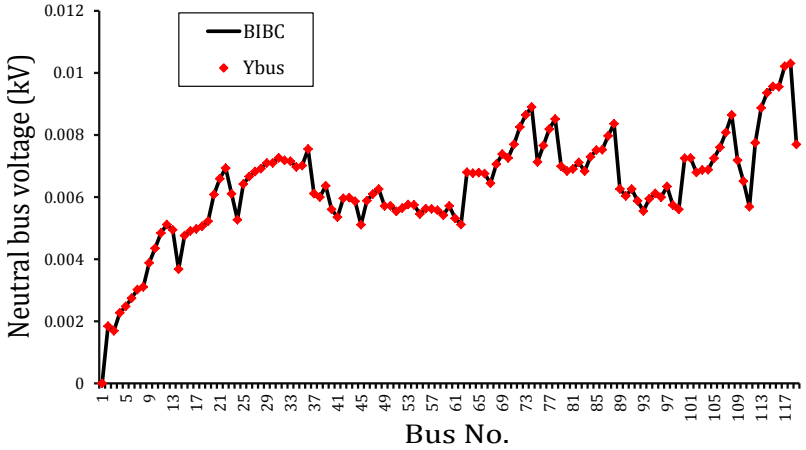

Figure 5.20: Voltage profile of neutral bus of modified IEEE 123-bus test system using proposed $\left[\mathbf{BIBC}\right]$ technique and $\left[\mathbf{Y_{bus}}\right]$ technique under normal operating conditions

calculated by the proposed load flow method are plotted along with the values calculated by the $\left[\mathbf{Y_{bus}}\right]$ matrix method, as shown in Figs. 5.22-5.24, respectively. The values of currents as obtained by the two methods exactly match which further validate the accuracy of the proposed methods.

The case of isolated neutral in modified three phase four wire IEEE 123-bus test system has also been simulated using the proposed load flow method. The neutral voltage profiles of the test system for "isolated

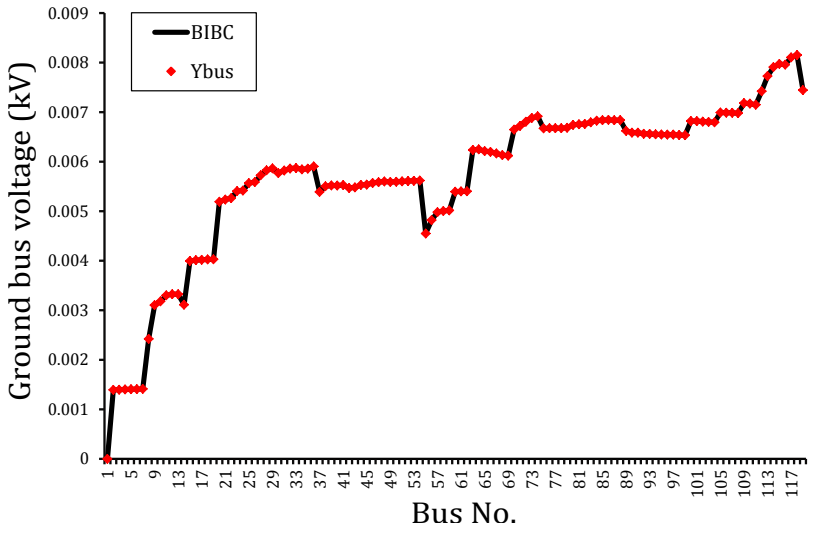

Figure 5.21: Voltage profile of ground bus of modified IEEE 123-bus test system using proposed $\left[\mathbf{BIBC}\right]$ technique and $\left[\mathbf{Y_{bus}}\right]$ technique under normal operating conditions

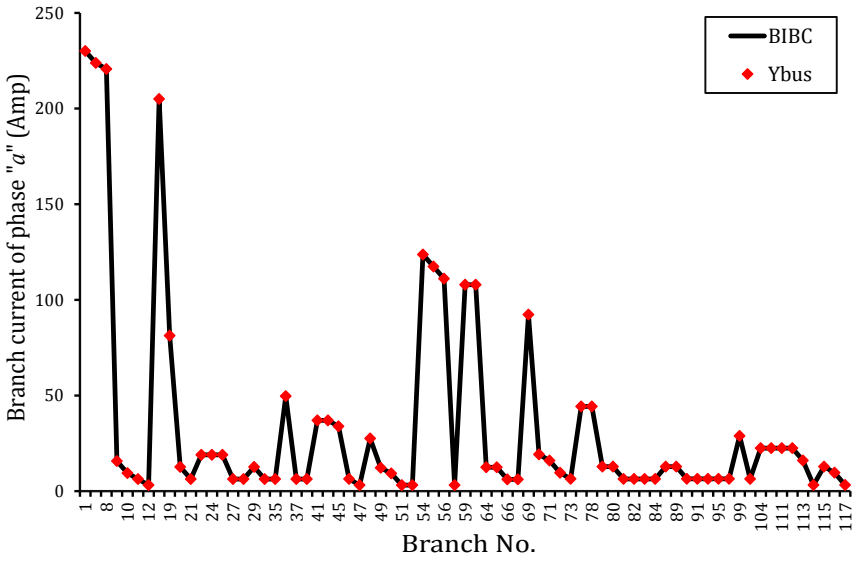

Figure 5.22: Branch current of phase a of modified IEEE 123-bus test system using proposed $\left[\mathbf{BIBC}\right]$ technique and $\left[\mathbf{Y_{bus}}\right]$ technique under normal operating conditions

neutral" (without ground return) and "grounded neutral" (with ground return) case are shown in Fig. 5.25(a). The values of neutral voltages at all the buses in "isolated neutral" case are higher than the "grounded neutral" case, as shown in Fig. 5.25(a) for the same reasons as explained for IEEE 34-bus system earlier.

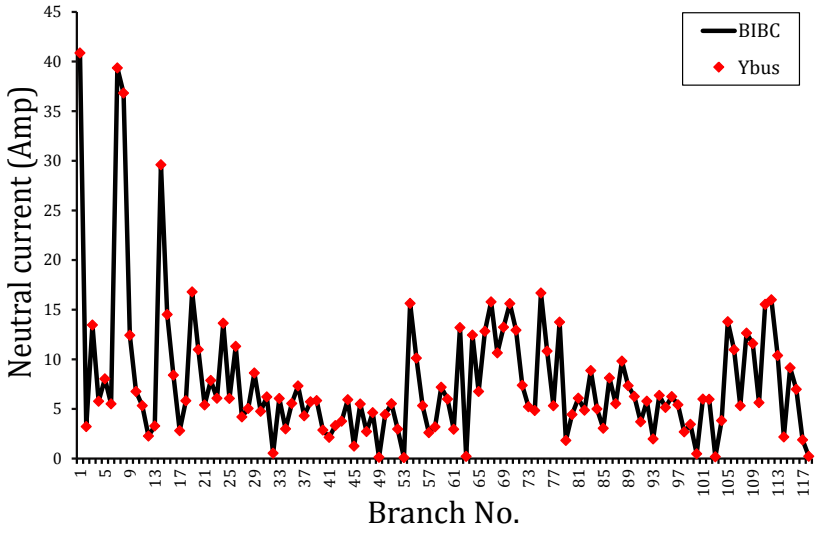

Figure 5.23: Neutral current of modified IEEE 123-bus test system using proposed $[\mathbf{BIBC}]$ technique and $[\mathbf{Y_{bus}}]$ technique under normal operating conditions

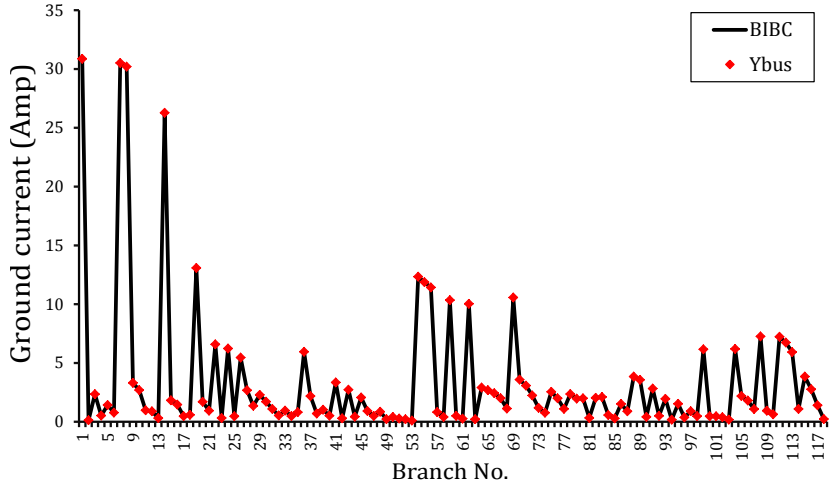

Figure 5.24: Ground current of modified IEEE 123 bus-test system using proposed $[\mathbf{BIBC}]$ technique and $[\mathbf{Y_{bus}}]$ technique under normal operating conditions

5.4.2.2 Results of short-circuit studies

To demonstrate the effectiveness of the proposed short-circuit analysis methods $\big([\mathbf{BIBC}]$ matrix based method and $[\mathbf{Y_{bus}}]$ matrix based method$\big)$, various short-circuit faults have been simulated on this test system, as given below

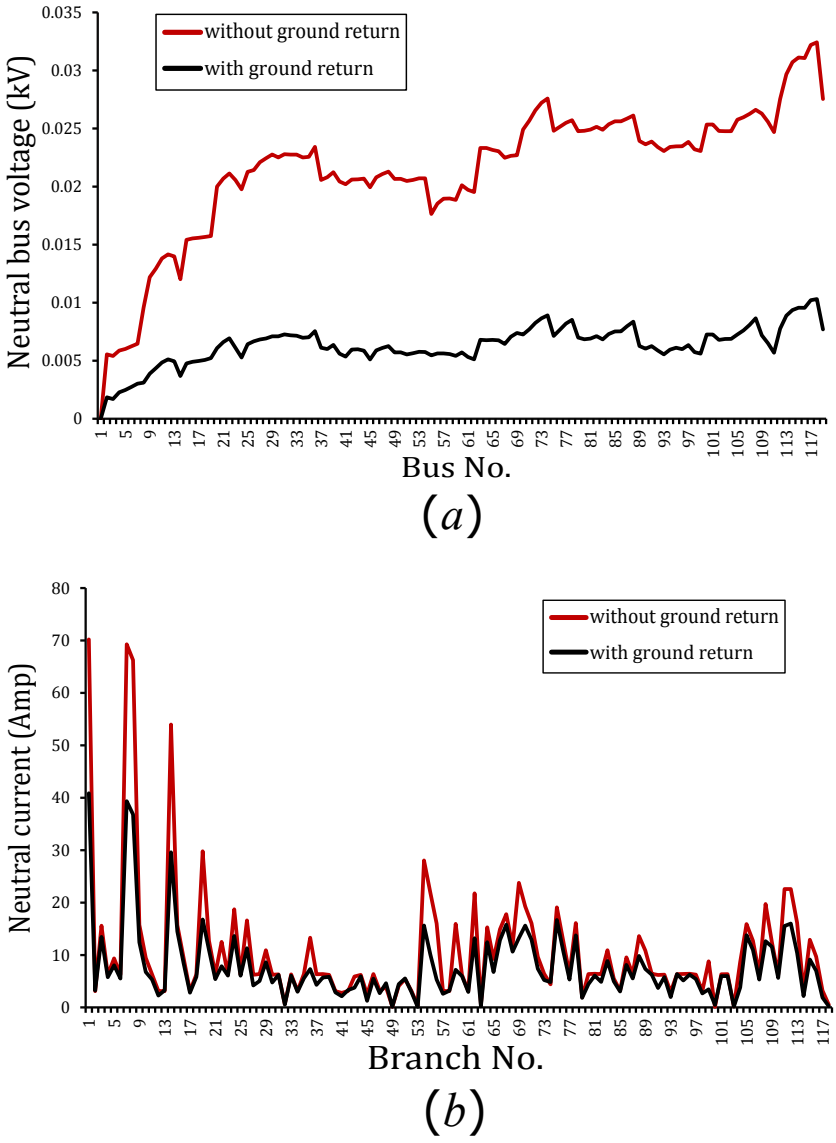

Figure 5.25: (a) Neutral bus voltage profile, (b) Neutral current of modified IEEE 123-bus test system in "isolated neutral" and "grounded neutral" cases under the normal operating conditions

Case 1. A single line-to-ground fault in phase a of bus 105 with a fault impedance $\bar{z}_f$ = 0.001+0.000i p.u.

Case 2. A double line-to-ground fault between phases a and b of bus 105 with a fault impedance $\bar{z}_f$ = 0.001+0.000i p.u.

Case 3. A three line-to-ground fault at bus 105 with a fault impedance $\bar{z}_f$ = 0.001+0.000i p.u.

Case 4. A line-to-line fault between phases a and b of bus 105 with a fault impedance $\bar{z}_f$ = 0.001+0.000i p.u.

Table 5.3: Results of the proposed short-circuit analysis methods for modified three phase four wire multigrounded IEEE 123-bus radial test system

case	Fault type	phase	Fault current at fault point (I_f)		Current drawn from the supply (I_s)	
			$[\mathbf{BIBC}]$ Technique (kA)	$[\mathbf{Y_{bus}}]$ Technique (kA)	$[\mathbf{BIBC}]$ Technique (kA)	$[\mathbf{Y_{bus}}]$ Technique (kA)
1	SLG (a-g)	a	2.43464	2.43464	2.51994	2.51994
2	LLG (ab-g)	a	4.34788	4.34788	4.44839	4.44839
		b	4.56175	4.56175	4.59517	4.59517
3	LLLG (abc-g)	a	4.48914	4.48914	4.57605	4.57605
		b	5.16022	5.16022	5.20549	5.20549
		c	4.44568	4.44568	4.50437	4.50437
4	L-L (a-b)	a	4.39293	4.39293	4.52483	4.52483
		b	4.39293	4.39293	4.39725	4.39725

The results for the above given fault cases obtained by the proposed short-circuit methods are given in Table 5.3. The calculated values of fault currents (I_f) and source currents (I_s) for all type of faults obtained by the proposed $[\mathbf{BIBC}]$ method are exactly equal to the values obtained by $[\mathbf{Y_{bus}}]$ method, as shown in Table 5.3, which establishes the accuracy of the proposed methods.

The voltage profiles of phase a bus voltage, neutral bus voltage and ground bus voltage of this test system, for an SLG fault at phase a of bus 105 with fault impedance of $\bar{z}_f$ = 0.001+0.000i p.u., obtained by the proposed short-circuit analysis methods, are shown in Figs. 5.26-5.28, respectively. These figures again demonstrate the correctness of the proposed short-circuit methods.

In Fig. 5.29(a), the ground bus voltage profile is plotted for various ground faults (SLG, LLG and LLLG) at bus-105 with a fault impedance of $\bar{z}_f$ = 0.001+0.000i p.u.. The plot shows that the highest ground bus voltages occur for SLG fault followed by LLG fault whereas, the lowest values are observed for LLLG fault. This is due to the fact that the fault current injected into the fault point at ground bus is the phasor sum of the three phase fault current and its value ($\bar{I}_f^a + \bar{I}_f^b + \bar{I}_f^c = -0.04 + j0.13$ kA $= 0.138\underline{/77.28^o}$ Amp) is smallest for LLLG fault, followed by the injected fault current of LLG fault ($\bar{I}_f^a + \bar{I}_f^b = -1.05 - j1.33$ kA $= 1.694\underline{/-128.26^o}$ kA) with SLG fault injecting highest current ($\bar{I}_f^a = 1.01 - j2.21$ kA $= 2.435\underline{/-65.40^o}$ kA) into the ground at the fault bus location. Therefore, the currents flowing through ground from fault point to the substation ground are highest for SLG fault followed by LLG fault and smallest for LLLG fault, as shown in 5.29(b). As a result, the ground bus voltages are highest for SLG fault with LLLG fault resulting

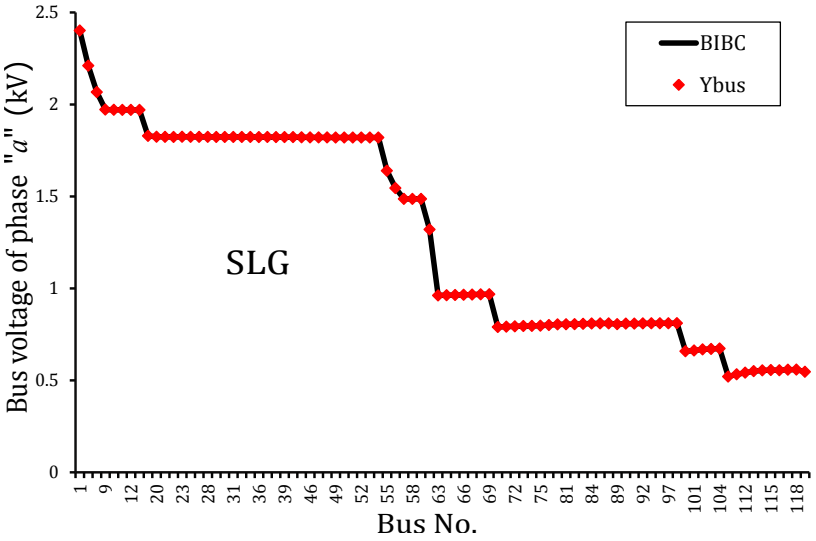

Figure 5.26: Voltage profile of phase a, for an SLG fault (a-g) at bus 105, of modified IEEE 123-bus test system using proposed $\left[\mathbf{BIBC}\right]$ technique and $\left[\mathbf{Y_{bus}}\right]$ technique

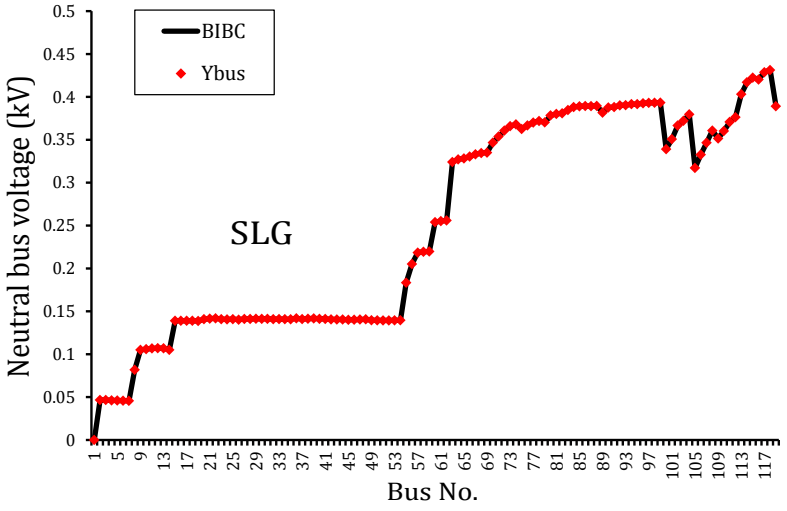

Figure 5.27: Voltage profile of neutral bus, for an SLG fault (a-g) at bus 105, of modified IEEE 123-bus test system using proposed $\left[\mathbf{BIBC}\right]$ technique and $\left[\mathbf{Y_{bus}}\right]$ technique

in lowest ground bus voltages. From Fig. 5.29(b), it is also observed that the value of ground current at certain branches (such as branch nos. $2-5, 9-13, 17-53, 81-97$ and $106-118$) of the test system are nearly equal to zero. It is due to the fact that these branches are not present in the path of fault current

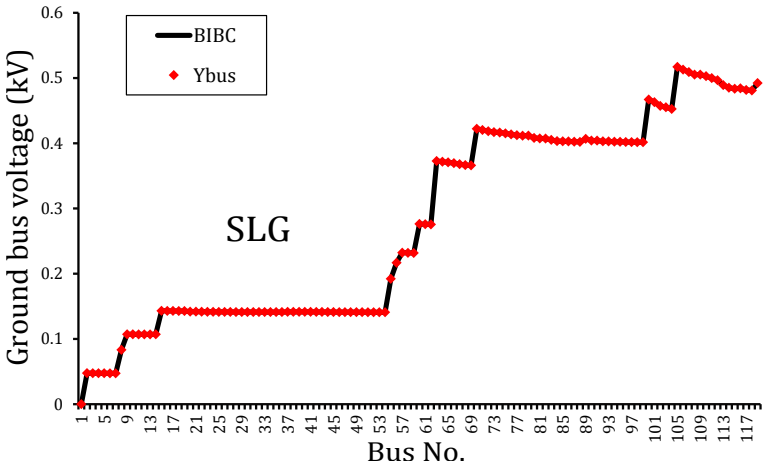

Figure 5.28: Voltage profile of ground bus, for an SLG fault (a-g) at bus 105, of modified IEEE 123-bus test system using proposed $\left[\mathbf{BIBC}\right]$ technique and $\left[\mathbf{Y_{bus}}\right]$ technique

returning through ground from fault point to the substation ground.

5.5 Conclusion

In this chapter, initially, a method for carrying out load flow analysis of an unbalanced three phase four wire multigrounded radial distribution system has been developed. The proposed load flow method is based on $\left[\mathbf{BIBC}\right]$ and $\left[\mathbf{BCBV}\right]$ matrices of the system. Separate $\left[\mathbf{BIBC}\right]$ matrix has been developed for phase branch, neutral and ground currents while, individual $\left[\mathbf{BCBV}\right]$ matrix has been developed for the voltages of phase buses, neutral buses and ground buses of the system. The results of the proposed load flow method have been compared with those obtained by $\left[\mathbf{Y_{bus}}\right]$ matrix based method and time domain simulation studies carried out using PSCAD/EMTDC software for a modified three phase four wire multigrounded IEEE 34-bus test system. A close match of the results of the three methods establishes the accuracy of the developed methods. However, the results of large system (modified three phase four wire multigrounded IEEE 123-bus test system) obtained by the proposed load flow method have only been compared with the results of $\left[\mathbf{Y_{bus}}\right]$ matrix based method, due to the node limitations in PSCAD/EMTDC software.

Subsequently, short-circuit analysis methods of unbalanced three phase four wire multigrounded radial distribution system have also been developed. Two different short-circuit methods have been developed, one is based on $\left[\mathbf{BIBC}\right]$ and $\left[\mathbf{BCBV}\right]$ matrices of the system, while the other one is based on $\left[\mathbf{Y_{bus}}\right]$ matrix of the system. The results of short-circuit analysis of modified three phase four wire multigrounded IEEE 34-bus test system obtained by using the proposed methods ($\left[\mathbf{BIBC}\right]$ matrix based and $\left[\mathbf{Y_{bus}}\right]$ matrix

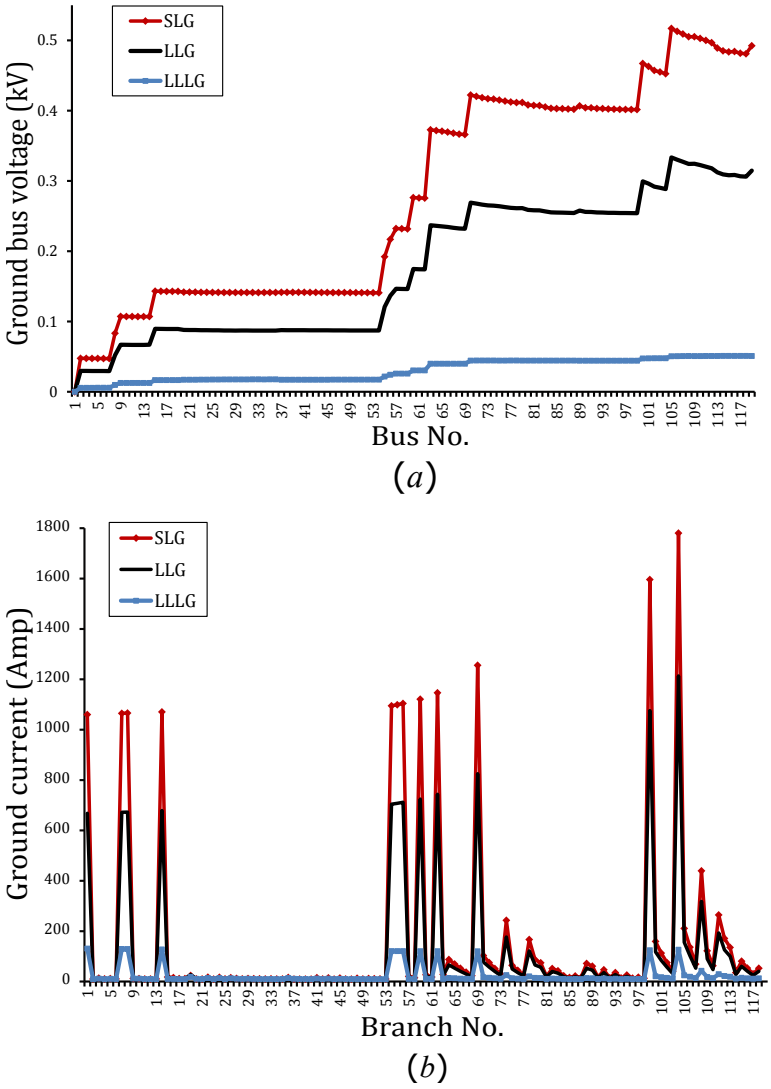

Figure 5.29: (*a*) Voltage profile of ground bus, (*b*) Ground current, for various ground faults at bus 105, of modified IEEE 123-bus test system

based) have also been compared with the results obtained by the PSCAD/EMTDC software. Again, for the large test system, the results of proposed $[\mathbf{BIBC}]$ matrix based short-circuit analysis method have been only compared with the results of $[\mathbf{Y_{bus}}]$ matrix based method due to the limited capability of the available PSCAD/EMTDC software. A good match between the obtained results demonstrate the effectiveness and accuracy of the proposed methods.

In the next chapter, algorithms for the load flow and short-circuit analysis methods for the unbalanced three phase four wire multigrounded distribution system incorporating IBDGs and various IBDG transformers have been developed.

Chapter 6

Load flow and short-circuit analysis of unbalanced three phase four wire multigrounded radial distribution system incorporating IBDG and transformer models

Abstract

In this chapter, load flow and short-circuit analysis methods have been developed for the unbalanced three phase four wire multigrounded distribution system for two different cases as. These cases are: (i) with IBDG and Δ-Y_g IBDG transformer, and (ii) with IBDG and Y_g-Y_g IBDG transformer. The load flow analysis method in both the cases is based on $[\mathbf{BIBC}]/[\mathbf{BCBV}]$ *matrices of the system. The short-circuit analysis methods for the two cases are based on* $[\mathbf{BIBC}]/[\mathbf{BCBV}]$ *matrices and* $[\mathbf{Y_{bus}}]$ *matrix of the system. The proposed load flow and short-circuit analysis methods have been implemented on two test systems, namely, modified IEEE 34-bus test system and modified IEEE 123-bus test system. The results of the modified IEEE 34-bus test system obtained by the proposed methods have been compared with the results of PSCAD/EMTDC software to validate the accuracy of the developed methods. For the larger test system (modified IEEE 123-bus system), the results obtained by the proposed* $[\mathbf{BIBC}]/[\mathbf{BCBV}]$ *matrices based method have only been compared with the results obtained by* $[\mathbf{Y_{bus}}]$ *matrix based method, due to limited capability of the available PSCAD/EMTDC software.*

6.1 Introduction

INTEGRATION of distributed generation (DG) to grid improves the system efficiency and reliability [146]. The most commonly used DGs are inverter based distributed generations (IBDGs) in distribution system. It has been observed from the literature that, mostly the analysis of distribution network in the presence of IBDGs is on three phase system [37, 58–65, 68]. But nowadays, three phase four wire multigrounded distribution networks are commonly used in the power distribution system [128]. Therefore,

it becomes necessary to analyze the three phase four wire multigrounded distribution networks with IBDGs present in the network. In this chapter, the direct approach of the load flow analysis of three phase four wire system, as discussed in Chapter 5, has been extended for the analysis of three phase four wire multigrounded distribution networks with IBDGs and IBDG transformers (used to connect the IBDG to the grid). Further, in this chapter, two different short-circuit analysis methods have been developed for three phase four wire multigrounded distribution networks in the presence of IBDGs and IBDG transformers. Two different vector group of IBDG transformers have been considered in the proposed load flow and short-circuit analysis methods, namely : $i)$ Δ-Y_g IBDG transformer, $ii)$ Yg-Y_g IBDG transformer.

This chapter is organized as follows. Section 6.2 describes the formulations of proposed load flow and short-circuit analysis methods for three phase four wire multigrounded distribution system in the presence of IBDG and Δ-Y_g IBDG transformer. Section 6.3 describes the formulations of proposed load flow and short-circuit analysis methods for three phase four wire multigrounded distribution system in the presence of IBDG and Y_g-Y_g IBDG transformer. The main results of this chapter are presented in Section 6.4 and finally Section 6.5 highlights the main conclusions of this chapter.

6.2 Three phase four wire multigrounded radial distribution system in the presence of IBDG and Δ-Y_g IBDG transformer

Let us consider an unbalanced three phase four wire multigrounded distribution system with IBDG, as shown in Fig. 6.1. The IBDG is connected at j^{th} bus through a step-down Δ-Y_g IBDG transformer. It is assumed that the primary side (high voltage side) winding of the transformer is delta connected, while the secondary side winding is star connected with ground return [150, 151]. It is assumed that the star point of the transformer secondary is solidly grounded. Therefore, the secondary currents of the transformer are circulating between the IBDG and the transformer secondary windings. The phase component based nodal admittance matrix model (p.u.) of the transformer is used in this work and is given as

$$\begin{bmatrix} \mathbf{I}^{\mathbf{abc}}_{\mathbf{T,p}} \\ \mathbf{I}^{\mathbf{abc}}_{\mathbf{T,s}} \end{bmatrix} = \begin{bmatrix} \mathbf{Y}^{\mathbf{abc}}_{\mathbf{pp,T}} & \mathbf{Y}^{\mathbf{abc}}_{\mathbf{ps,T}} \\ \mathbf{Y}^{\mathbf{abc}}_{\mathbf{sp,T}} & \mathbf{Y}^{\mathbf{abc}}_{\mathbf{ss,T}} \end{bmatrix} . \begin{bmatrix} \mathbf{V}^{\mathbf{abc}}_{\mathbf{T,p}} \\ \mathbf{V}^{\mathbf{abc}}_{\mathbf{T,s}} \end{bmatrix} = \begin{bmatrix} \mathbf{Y}^{\mathbf{abc}}_{\mathbf{T}} \end{bmatrix} \begin{bmatrix} \mathbf{V}^{\mathbf{abc}}_{\mathbf{T,p}} \\ \mathbf{V}^{\mathbf{abc}}_{\mathbf{T,s}} \end{bmatrix} = \begin{bmatrix} \mathbf{Y}^{\mathbf{abc}}_{\mathbf{T}} \end{bmatrix} \begin{bmatrix} \mathbf{V}^{\mathbf{abc}}_{\mathbf{j}} \\ \mathbf{V}^{\mathbf{abc}}_{\mathbf{inv}} \end{bmatrix} \tag{6.1}$$

where $\mathbf{Y}^{\mathbf{abc}}_{\mathbf{pp,T}}$, $\mathbf{Y}^{\mathbf{abc}}_{\mathbf{ps,T}}$, $\mathbf{Y}^{\mathbf{abc}}_{\mathbf{sp,T}}$ and $\mathbf{Y}^{\mathbf{abc}}_{\mathbf{ss,T}}$ are the sub-matrices, of size (3×3) each, of the transformer nodal admittance matrix $\mathbf{Y}^{\mathbf{abc}}_{\mathbf{T}}$. $\mathbf{V}^{\mathbf{abc}}_{\mathbf{T,p}}$ and $\mathbf{V}^{\mathbf{abc}}_{\mathbf{T,s}}$ are the three phase voltage vectors of the primary and secondary sides of the transformers, respectively. $\mathbf{V}^{\mathbf{abc}}_{\mathbf{j}}$ and $\mathbf{V}^{\mathbf{abc}}_{\mathbf{inv}}$ are the three phase voltage vectors at j^{th} bus and inverter bus (inv), respectively. $\mathbf{I}^{\mathbf{abc}}_{\mathbf{T,p}}$ and $\mathbf{I}^{\mathbf{abc}}_{\mathbf{T,s}}$ are the three phase injection current vectors at the primary and secondary sides of the transformer, respectively.

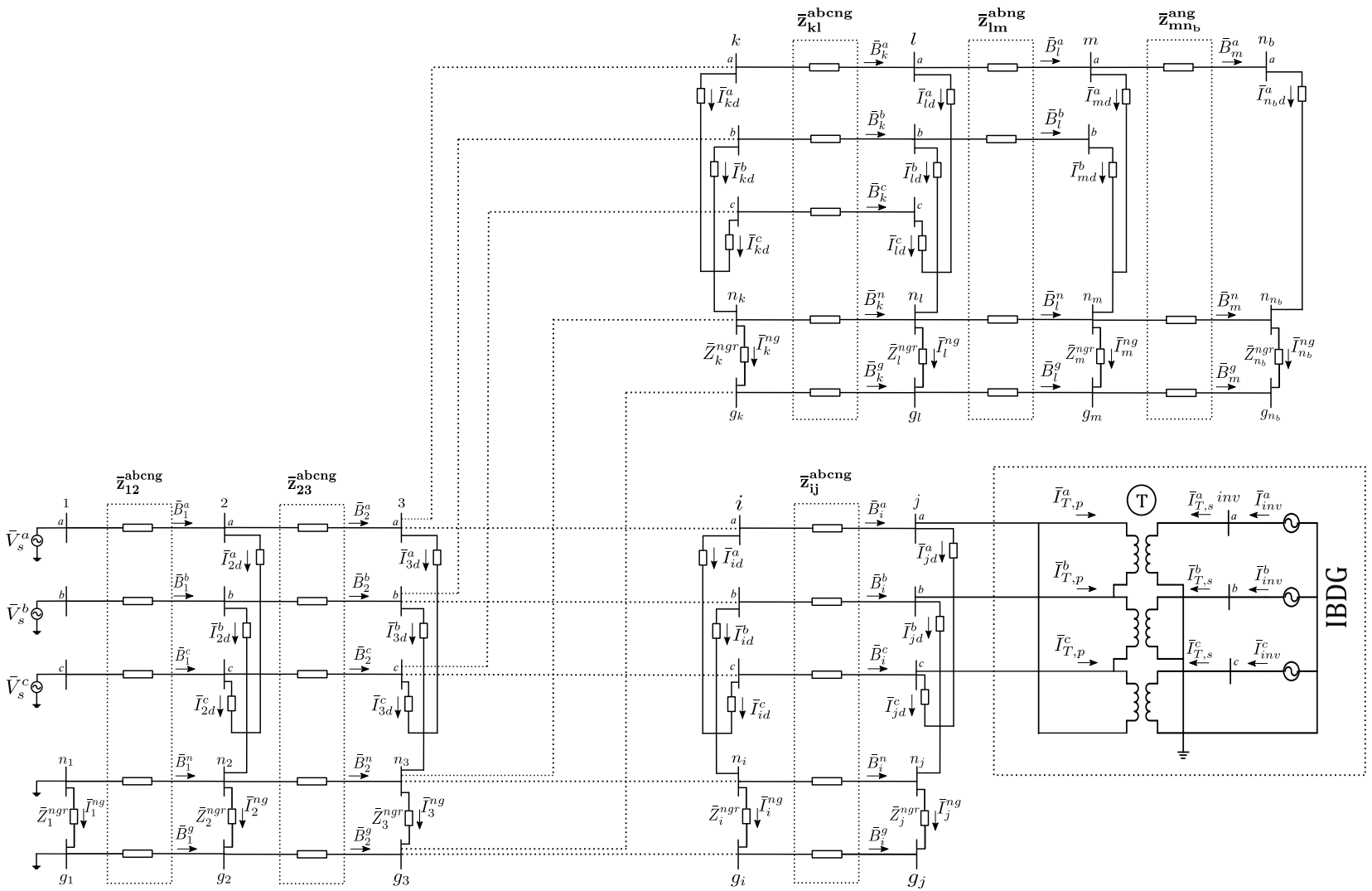

Figure 6.1: An unbalanced three phase four wire multigrounded radial distribution system with IBDG and Δ-Y_g IBDG transformer

6.2.1 Load flow analysis with Delta/Star-grounded (Δ-Y_g) IBDG transformer for the connection of IBDG

The proposed load flow analysis method of unbalanced three phase four wire multigrounded radial distribution system with IBDG is based on $\left[\mathbf{BIBC}\right]$ and $\left[\mathbf{BCBV}\right]$ matrices of the system. In this method, it is assumed that the IBDG is operating in "Constant active power mode" (by operating at unity power factor) under steady state conditions. The IBDG is connected to the grid through a step-down transformer (namely "IBDG transformer"). In this section, Delta/Star-grounded (Δ-Y_g) configuration of IBDG transformer has been considered. The formulation of $\left[\mathbf{BIBC}\right]$ and $\left[\mathbf{BCBV}\right]$ matrices for the proposed load flow method is given in the following subsections.

6.2.1.1 Formulation of [BIBC] matrix

By applying KCL equation at each phase bus (excluding substation bus and inverter bus) of the distribution system shown in Fig. 6.1, the currents in the phase branches of the distribution system can be obtained in terms of equivalent bus injection currents. The branch currents of phases a, b and c of all line sections in Fig. 6.1 can be expressed in terms of equivalent bus injection currents as,

$$
\begin{aligned}
\bar{B}_1^a &= \bar{I}_{2d}^a + \bar{I}_{3d}^a + \cdots + \bar{I}_{id}^a + \bar{I}_{jd}^a + \bar{I}_{T,p}^a + \cdots + \bar{I}_{kd}^a + \bar{I}_{ld}^a + \bar{I}_{md}^a + \bar{I}_{n_b d}^a \\
\bar{B}_1^b &= \bar{I}_{2d}^b + \bar{I}_{3d}^b + \cdots + \bar{I}_{id}^b + \bar{I}_{jd}^b + \bar{I}_{T,p}^b + \cdots + \bar{I}_{kd}^b + \bar{I}_{ld}^b + \bar{I}_{md}^b \\
\bar{B}_1^c &= \bar{I}_{2d}^c + \bar{I}_{3d}^c + \cdots + \bar{I}_{id}^c + \bar{I}_{jd}^c + \bar{I}_{T,p}^c + \cdots + \bar{I}_{kd}^c + \bar{I}_{ld}^c \\
\bar{B}_2^a &= \bar{I}_{3d}^a + \cdots + \bar{I}_{id}^a + \bar{I}_{jd}^a + \bar{I}_{T,p}^a + \cdots + \bar{I}_{kd}^a + \bar{I}_{ld}^a + \bar{I}_{md}^a + \bar{I}_{n_b d}^a \\
\bar{B}_2^b &= \bar{I}_{3d}^b + \cdots + \bar{I}_{id}^b + \bar{I}_{jd}^b + \bar{I}_{T,p}^b + \cdots + \bar{I}_{kd}^b + \bar{I}_{ld}^b + \bar{I}_{md}^b \\
\bar{B}_2^c &= \bar{I}_{3d}^c + \cdots + \bar{I}_{id}^c + \bar{I}_{jd}^c + \bar{I}_{T,p}^c + \cdots + \bar{I}_{kd}^c + \bar{I}_{ld}^c \\
\bar{B}_i^a &= \bar{I}_{jd}^a + \bar{I}_{T,p}^a \\
\bar{B}_i^b &= \bar{I}_{jd}^b + \bar{I}_{T,p}^b \\
\bar{B}_i^c &= \bar{I}_{jd}^c + \bar{I}_{T,p}^c \\
\bar{B}_k^a &= \bar{I}_{ld}^a + \bar{I}_{md}^a + \bar{I}_{n_b d}^a \\
\bar{B}_k^b &= \bar{I}_{ld}^b + \bar{I}_{md}^b \\
\bar{B}_k^c &= \bar{I}_{ld}^c \\
\bar{B}_l^a &= \bar{I}_{md}^a + \bar{I}_{n_b d}^a \\
\bar{B}_l^b &= \bar{I}_{md}^b; \quad \bar{B}_m^a = \bar{I}_{n_b d}^a
\end{aligned}
\tag{6.2}
$$

Therefore, the currents of the phase branches can be expressed in the matrix form as,

$$\left[\mathbf{B_p}\right] = \left[\mathbf{BIBC_p}\right]\left[\mathbf{I_L}\right] + \left[\mathbf{TIBC_{Tm}}\right]\left[\mathbf{I_{T,p}}\right] \tag{6.3}$$

where, details of $\left[\mathbf{BIBC_p}\right]$ matrix have already been discussed in eq. (5.5) of Subsection 5.2.1.1 of Chapter 5 and

$$\begin{aligned}
\left[\mathbf{TIBC_{Tm}}\right] &= \begin{bmatrix}\mathbf{BIBC_p}(:,T_b a)\\ \mathbf{BIBC_p}(:,T_b b)\\ \mathbf{BIBC_p}(:,T_b c)\end{bmatrix}^T = \begin{bmatrix}1&0&0&\cdots&1&0&0&\cdots&0&0&0&0&0&0\\ 0&1&0&\cdots&0&1&0&\cdots&0&0&0&0&0&0\\ 0&0&1&\cdots&0&0&1&\cdots&0&0&0&0&0&0\end{bmatrix}^T; \\
\left[\mathbf{I_{T,p}}\right] &= \begin{bmatrix}\bar{I}^a_{T,p} & \bar{I}^b_{T,p} & \bar{I}^c_{T,p}\end{bmatrix}^T.
\end{aligned}$$

The $\left[\mathbf{TIBC_{Tm}}\right]$ matrix contains column vectors of $\left[\mathbf{BIBC_p}\right]$ matrix corresponding to the phases a, b and c of the transformer bus T_b (where the three phase primary windings of the transformer are connected and in Fig. 6.1 $T_b = j$). Further, it is assumed that the system considered has u three-phase, v two-phase, w single-phase, $(u+v+w)$ neutral and $(u+v+w)$ ground buses with nt number of IBDG transformers. This generalized system will be considered throughout this chapter. The size of $\left[\mathbf{TIBC_{Tm}}\right]$ matrix for this system will therefore be $(3u+2v+w-3)\times 3nt$.

Now, there is no physical connection between the neutral as well as ground buses of the system and IBDG transformer and the inverter current is confined only to the secondary winding of IBDG transformer. Therefore, the neutral and ground currents for the distribution system shown in Fig. 6.1 (with IBDG and Δ-Y_g IBDG transformer) are exactly same as the neutral and ground currents of system shown in Fig. 5.1 (without IBDG and IBDG transformer) and are given as (from eqs. (5.8) and (5.10) of Chapter 5, respectively),

$$\left[\mathbf{B_n}\right] = -\left[\mathbf{BIBC_{pn}}\right]\left[\mathbf{I_L}\right] + \left[\mathbf{BIBC_g}\right]\left[\mathbf{I_{ng}}\right] \tag{6.4}$$

$$\left[\mathbf{B_g}\right] = -\left[\mathbf{BIBC_g}\right]\left[\mathbf{I_{ng}}\right] \tag{6.5}$$

The matrices $\left[\mathbf{BIBC_{pn}}\right]$ and $\left[\mathbf{BIBC_g}\right]$ have already been defined in eq. (5.8) of Subsection 5.2.1.2 of Chapter 5.

6.2.1.2 Formulation of [BCBV] matrix

The voltages of the phase buses (except inverter bus), neutral buses and ground buses of the distribution system shown in Fig. 6.1 can be calculated using eqs. (5.21)-(5.23) of Chapter 5, respectively, as,

$$\left[\mathbf{V_p}\right] = \left[\mathbf{V_{ss}}\right] - \left[\mathbf{BCBV_p}\right]\left[\mathbf{B_p}\right] - \left[\mathbf{BCBV_{pn}}\right]\left[\mathbf{B_n}\right] - \left[\mathbf{BCBV_{pg}}\right]\left[\mathbf{B_g}\right] \quad (6.6)$$

$$\left[\mathbf{V_n}\right] = \left[\mathbf{V_{sn}}\right] - \left[\mathbf{BCBV_{np}}\right]\left[\mathbf{B_p}\right] - \left[\mathbf{BCBV_n}\right]\left[\mathbf{B_n}\right] - \left[\mathbf{BCBV_{ng}}\right]\left[\mathbf{B_g}\right] \quad (6.7)$$

$$\left[\mathbf{V_g}\right] = \left[\mathbf{V_{sg}}\right] - \left[\mathbf{BCBV_{gp}}\right]\left[\mathbf{B_p}\right] - \left[\mathbf{BCBV_{gn}}\right]\left[\mathbf{B_n}\right] - \left[\mathbf{BCBV_g}\right]\left[\mathbf{B_g}\right] \quad (6.8)$$

The details of $\left[\mathbf{BCBV_p}\right]$, $\left[\mathbf{BCBV_{pn}}\right]$, $\left[\mathbf{BCBV_{pg}}\right]$, $\left[\mathbf{BCBV_{np}}\right]$, $\left[\mathbf{BCBV_n}\right]$, $\left[\mathbf{BCBV_{ng}}\right]$, $\left[\mathbf{BCBV_{gp}}\right]$, $\left[\mathbf{BCBV_{gn}}\right]$ and $\left[\mathbf{BCBV_g}\right]$ matrices have already been described in eqs. (5.12)-(5.17) of subsections 5.2.2.1-5.2.2.3 of Chapter 5. Also, the inverter bus voltage of the system considered, is calculated using eq. (6.1) as,

$$\mathbf{V_{inv}^{abc}} = \mathbf{Y_{ss,T}^{abc}}^{-1}(\mathbf{I_{T,s}^{abc}} - \mathbf{Y_{sp,T}^{abc}}\mathbf{V_j^{abc}}) \quad (6.9)$$

From Fig. 6.1, $\mathbf{I_{T,s}^{abc}} = \mathbf{I_{inv}^{abc}}$, where $\mathbf{I_{inv}^{abc}}$ is the three-phase inverter current vector.

The voltages of the phase buses of the distribution system can be recalculated using eqs. (6.3)-(6.6) as,

$$\begin{aligned}\left[\mathbf{V_p}\right] &= \left[\mathbf{V_{ss}}\right] - \left[\mathbf{BCBV_p}\right]\left\{\left[\mathbf{BIBC_p}\right]\left[\mathbf{I_L}\right] + \left[\mathbf{TIBC_{Tm}}\right]\left[\mathbf{I_{T,p}}\right]\right\} - \left[\mathbf{BCBV_{pn}}\right]\left\{\right. \\ &- \left[\mathbf{BIBC_{pn}}\right]\left[\mathbf{I_L}\right] + \left[\mathbf{BIBC_g}\right]\left[\mathbf{I_{ng}}\right]\left.\right\} - \left[\mathbf{BCBV_{pg}}\right]\left\{ - \left[\mathbf{BIBC_g}\right]\left[\mathbf{I_{ng}}\right]\right\}\end{aligned}$$

$$\left[\mathbf{V_p}\right] = \left[\mathbf{V_{ss}}\right] - \left[\mathbf{DLF_1}\right]\left[\mathbf{I_L}\right] - \left[\mathbf{DLF_2}\right]\left[\mathbf{I_{ng}}\right] - \left[\mathbf{DLF_{Tm_p}}\right]\left[\mathbf{I_{T,p}}\right] \quad (6.10)$$

where, $\left[\mathbf{DLF_1}\right]$ and $\left[\mathbf{DLF_2}\right]$ matrices have already been described in eq. (5.24) of Chapter 5 and

$$\left[\mathbf{DLF_{Tm_p}}\right] = \left[\mathbf{BCBV_p}\right]\left[\mathbf{TIBC_{Tm}}\right]$$

Similarly, the neutral bus voltages can be recalculated using eqs. (6.3)-(6.5) and (6.7) as,

$$\begin{aligned}\left[\mathbf{V_n}\right] &= \left[\mathbf{V_{sn}}\right] - \left[\mathbf{BCBV_{np}}\right]\left\{\left[\mathbf{BIBC_p}\right]\left[\mathbf{I_L}\right] + \left[\mathbf{TIBC_{Tm}}\right]\left[\mathbf{I_{T,p}}\right]\right\} - \left[\mathbf{BCBV_n}\right]\left\{\right. \\ &- \left[\mathbf{BIBC_{pn}}\right]\left[\mathbf{I_L}\right] + \left[\mathbf{BIBC_g}\right]\left[\mathbf{I_{ng}}\right]\left.\right\} - \left[\mathbf{BCBV_{ng}}\right]\left\{ - \left[\mathbf{BIBC_g}\right]\left[\mathbf{I_{ng}}\right]\right\}\end{aligned}$$

$$\left[\mathbf{V_n}\right] = \left[\mathbf{V_{sn}}\right] - \left[\mathbf{DLF_3}\right]\left[\mathbf{I_L}\right] - \left[\mathbf{DLF_4}\right]\left[\mathbf{I_{ng}}\right] - \left[\mathbf{DLF_{Tm_n}}\right]\left[\mathbf{I_{T,p}}\right] \quad (6.11)$$

where, $\left[\mathbf{DLF_3}\right]$ and $\left[\mathbf{DLF_4}\right]$ matrices have already been defined in (eq. 5.25) of Chapter 5 and

$$\left[\mathbf{DLF_{Tm_n}}\right] = \left[\mathbf{BCBV_{np}}\right]\left[\mathbf{TIBC_{Tm}}\right]$$

Also, the ground bus voltages of the system considered, can be recalculated using eqs. (6.3)-(6.5) and (6.8) as,

$$\begin{aligned}\left[\mathbf{V_g}\right] &= \left[\mathbf{V_{sg}}\right] - \left[\mathbf{BCBV_{gp}}\right]\left\{\left[\mathbf{BIBC_p}\right]\left[\mathbf{I_L}\right] + \left[\mathbf{TIBC_{Tm}}\right]\left[\mathbf{I_{T,p}}\right]\right\} - \left[\mathbf{BCBV_{gn}}\right]\left\{\right. \\ &- \left[\mathbf{BIBC_{pn}}\right]\left[\mathbf{I_L}\right] + \left[\mathbf{BIBC_g}\right]\left[\mathbf{I_{ng}}\right]\left.\right\} - \left[\mathbf{BCBV_g}\right]\left\{ - \left[\mathbf{BIBC_g}\right]\left[\mathbf{I_{ng}}\right]\right\}\end{aligned}$$

$$\left[\mathbf{V_g}\right] = \left[\mathbf{V_{sg}}\right] - \left[\mathbf{DLF_5}\right]\left[\mathbf{I_L}\right] - \left[\mathbf{DLF_6}\right]\left[\mathbf{I_{ng}}\right] - \left[\mathbf{DLF_{Tm_g}}\right]\left[\mathbf{I_{T,p}}\right] \tag{6.12}$$

where, $\left[\mathbf{DLF_5}\right]$ and $\left[\mathbf{DLF_6}\right]$ matrices have already defined in eq. (5.26) of Chapter 5 and

$$\left[\mathbf{DLF_{Tm_g}}\right] = \left[\mathbf{BCBV_{gp}}\right]\left[\mathbf{TIBC_{Tm}}\right]$$

Now, the voltage drops between neutral buses and ground buses are calculated using eq. (5.28) of Chapter 5 as,

$$\left[\mathbf{Z_{ngr}}\right]\left[\mathbf{I_{ng}}\right] = \left[\mathbf{V_n}\right] - \left[\mathbf{V_g}\right] \tag{6.13}$$

Now, from eqs. (6.10), (6.11) and (6.13), the neutral to ground current $\left[\mathbf{I_{ng}}\right]$ is calculated as,

$$\left[\mathbf{I_{ng}}\right] = \left[\mathbf{Z_{FNG}}\right]^{-1}\left\{\left[\mathbf{V_{sn}}\right] - \left[\mathbf{V_{sg}}\right] + \left[\left[\mathbf{DLF_5}\right] - \left[\mathbf{DLF_3}\right]\right]\left[\mathbf{I_L}\right] + \left[\mathbf{DLF_{Tm_{gn}}}\right]\left[\mathbf{I_{T,p}}\right]\right\} \tag{6.14}$$

where, $\left[\mathbf{Z_{FNG}}\right]$ matrix has already been defined in eq. (5.29) of Chapter 5 and

$$\left[\mathbf{DLF_{Tm_{gn}}}\right] = \left[\mathbf{DLF_{Tm_g}}\right] - \left[\mathbf{DLF_{Tm_n}}\right]$$

Therefore, the voltages of the phase buses (except inverter bus), neutral buses and ground buses can be obtained using eqs. (6.10)-(6.12) and (6.14) as,

$$\left[\mathbf{V_p}\right] = \left[\mathbf{V_{ss}}\right] - \left[\mathbf{F_{1ng}}\right]\left\{\left[\mathbf{V_{sn}}\right] - \left[\mathbf{V_{sg}}\right]\right\} - \left[\mathbf{F_{1PLD}}\right]\left[\mathbf{I_L}\right] - \left[\mathbf{F_{1Tm}}\right]\left[\mathbf{I_{T,p}}\right] \tag{6.15}$$

$$\left[\mathbf{V_n}\right] = \left[\mathbf{F_{2nn}}\right]\left[\mathbf{V_{sn}}\right] - \left[\mathbf{F_{2gg}}\right]\left[\mathbf{V_{sg}}\right] - \left[\mathbf{F_{2PLD}}\right]\left[\mathbf{I_L}\right] - \left[\mathbf{F_{2Tm}}\right]\left[\mathbf{I_{T,p}}\right] \tag{6.16}$$

$$\left[\mathbf{V_g}\right] = \left[\mathbf{F_{3gg}}\right]\left[\mathbf{V_{sg}}\right] - \left[\mathbf{F_{3nn}}\right]\left[\mathbf{V_{sn}}\right] - \left[\mathbf{F_{3PLD}}\right]\left[\mathbf{I_L}\right] - \left[\mathbf{F_{3Tm}}\right]\left[\mathbf{I_{T,p}}\right] \tag{6.17}$$

where,

$$\left[\mathbf{F_{1Tm}}\right] = \left[\mathbf{DLF_2}\right]\left[\mathbf{Z_{FNG}}\right]^{-1}\left[\mathbf{DLF_{Tm_{gn}}}\right] + \left[\mathbf{DLF_{Tm_p}}\right]$$

$$\left[\mathbf{F_{2Tm}}\right] = \left[\mathbf{DLF_4}\right]\left[\mathbf{Z_{FNG}}\right]^{-1}\left[\mathbf{DLF_{Tm_{gn}}}\right] + \left[\mathbf{DLF_{Tm_n}}\right]$$

$$\left[\mathbf{F_{3Tm}}\right] = \left[\mathbf{DLF_6}\right]\left[\mathbf{Z_{FNG}}\right]^{-1}\left[\mathbf{DLF_{Tm_{gn}}}\right] + \left[\mathbf{DLF_{Tm_g}}\right]$$

Steps of algorithm for the load flow analysis of unbalanced three phase four wire multigrounded radial distribution system in the presence of IBDG and Δ-Y_g IBDG transformer

1. Initialize and then generate the $\left[\mathbf{BIBC}\right]$ matrices for the phase, neutral and ground currents, and $\left[\mathbf{BCBV}\right]$ matrices for the voltages of phase buses, neutral buses and ground buses.

2. Set the iteration counter $k = 0$. Also, set the values of all phase a bus voltages at $(1.0 + j0.0)$ p.u., phase b bus voltages at $(-0.500 - j0.866)$ p.u., phase c bus voltages at $(-0.500 + j0.866)$ p.u. and all neutral and ground bus voltages at $(0.0 + j0.0)$ p.u. throughout the system.

3. Calculate the equivalent bus injection currents $\left[\mathbf{I_L}\right]^k$ at all the phase buses of the system using eq. (5.3) of Chapter 5. Also, calculate the inverter current of the IBDG as,

$$\bar{I}^p_{inv} = \bar{I}^p_{T,s} = \left(\frac{\bar{S}^p_{dg}}{\bar{V}^p_{inv}}\right)^* = \left(\frac{P^p_{dg} + jQ^p_{dg}}{\bar{V}^p_{inv}}\right)^*; \quad (p = a, b, c)$$

   where, $\bar{S}^p_{dg}$ is the complex power injected by the IBDG at phase p of inverter bus; P^p_{dg} and Q^p_{dg} are the active and reactive power generated by the IBDG at phase p of inverter bus, respectively; $\bar{V}^p_{inv}$ is the p^{th} phase voltage of inverter bus.

4. Calculate the primary winding currents $\left[\mathbf{I^{abc}_{T,p}}\right]^k$ of the IBDG transformer by using eq. (6.1).

5. $k = k + 1$.

6. Calculate the voltages of phase buses, neutral buses and ground buses $\left([\mathbf{V_p}]^k, [\mathbf{V_n}]^k \text{ and } [\mathbf{V_g}]^k\right)$ of the system using eqs. (6.15)-(6.17). Also, calculate the inverter bus voltage $\left[\mathbf{V^{abc}_{inv}}\right]^k$ of the IBDG by using eq. (6.9).

7. Calculate the error (ϵ),

$$\epsilon = max\left(\left|[\mathbf{V_p}]^k - [\mathbf{V_p}]^{k-1}\right|, \left|[\mathbf{V_n}]^k - [\mathbf{V_n}]^{k-1}\right|, \left|[\mathbf{V_g}]^k - [\mathbf{V_g}]^{k-1}\right|\right)$$

8. If $\epsilon \geq$ tolerance(1.0×10^{-12}), then go to step 3, else go to the next step.

9. The obtained values of the voltages $[\mathbf{V_p}]$, $[\mathbf{V_n}]$ and $[\mathbf{V_g}]$ are the final values of load flow solution and stop the simulation.

6.2.2 Short-circuit analysis of unbalanced three phase four wire multigrounded radial distribution system in the presence of IBDG and Δ-Y_g IBDG transformer

In this chapter, two different short-circuit analysis methods have been proposed. One of the proposed method is based on $\left[\mathbf{BIBC}\right]$ and $\left[\mathbf{BCBV}\right]$ matrices, while the other one is a $\left[\mathbf{Y_{bus}}\right]$ matrix based approach. Both these methods are discussed in details in the following sub-sections.

6.2.2.1 Method 1: $\left[\mathrm{BIBC}\right]$ matrix based method

From the load flow analysis of the distribution system (using the proposed load flow method), the equivalent load impedances are calculated at all phase buses (except inverter bus) of the system using eq. (5.33) of Chapter 5. Now, different short-circuit faults are discussed as follows,

(a) Single line-to-ground (SLG) fault

Let us assume that an SLG fault occurs between the phase a and the local ground g_l at l^{th} bus location through a fault impedance $\bar{z}_f$, as shown in Fig. 6.2(a), and the fault current $\bar{I}_f^a$ is flowing from phase a to the ground g_l at l^{th} bus. Therefore, only the phase and the ground currents of the system will get modified due to the SLG fault. The modified phase branch currents (only of phase a) due to SLG fault, can be written as,

$$\begin{aligned}
\bar{B}^a_{1,f} &= \bar{I}^a_{2d} + \bar{I}^a_{3d} + \cdots + \bar{I}^a_{id} + \bar{I}^a_{jd} + \bar{I}^a_{T,p} + \cdots + \bar{I}^a_{kd} + \bar{I}^a_{ld} + \bar{I}^a_{md} + \bar{I}^a_{n_bd} + \bar{I}^a_f \\
\bar{B}^a_{2,f} &= \bar{I}^a_{3d} + \cdots + \bar{I}^a_{id} + \bar{I}^a_{jd} + \bar{I}^a_{T,p} + \cdots + \bar{I}^a_{kd} + \bar{I}^a_{ld} + \bar{I}^a_{md} + \bar{I}^a_{n_bd} + \bar{I}^a_f \\
\bar{B}^a_{i,f} &= \bar{I}^a_{jd} + \bar{I}^a_{T,p} \\
\bar{B}^a_{k,f} &= \bar{I}^a_{ld} + \bar{I}^a_{md} + \bar{I}^a_{n_bd} + \bar{I}^a_f \\
\bar{B}^a_{l,f} &= \bar{I}^a_{md} + \bar{I}^a_{n_bd} \\
\bar{B}^a_{m,f} &= \bar{I}^a_{n_bd}
\end{aligned} \tag{6.18}$$

Hence, the modified phase branch currents due to SLG fault can be expressed in the matrix form as,

$$\left[\mathbf{B_{p,f}}\right] = \left[\mathbf{BIBC_p}\right]\left[\mathbf{I_L}\right] + \left[\mathbf{TIBC_{Tm}}\right]\left[\mathbf{I_{T,p}}\right] + \left[\mathbf{BIBC_{fp}}\right]\left[\mathbf{I_f}\right] \tag{6.19}$$

where,

$$\left[\mathbf{BIBC_{fp}}\right] = \left[\mathbf{BIBC_p}(:, f_b^q)\right] = \begin{bmatrix} 1 & 0 & 0 & \cdots & 0 & 0 & 0 & \cdots & 1 & 0 & 0 & 0 & 0 & 0 \end{bmatrix}^T ; \left[\mathbf{I_f}\right] = \bar{I}^a_f$$

Definition of $\left[\mathbf{BIBC_{fp}}\right]$ matrix for an SLG fault (faulted bus $f_b = l$, and faulted phase $q = a$) is given in eq. (5.35) of Chapter 5.

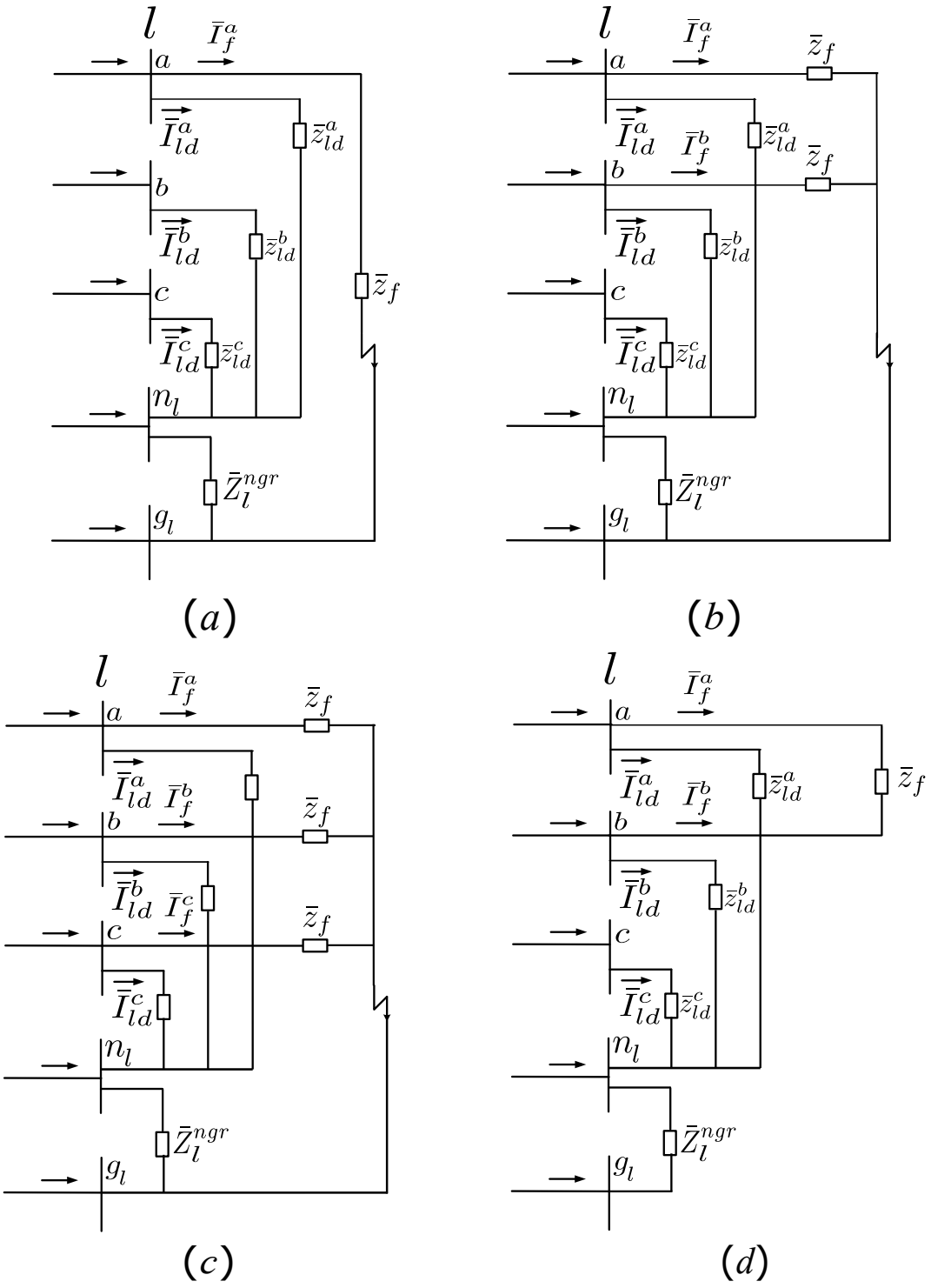

Figure 6.2: Unsymmetrical short-circuit faults, (a) SLG fault, (b) LLG fault, (c) LLLG fault, (d) LL fault

Similarly, the modified ground currents due to SLG fault can be written as,

$$\begin{aligned}
\bar{B}^g_{1,f} &= -\bar{I}^{ng}_2 - \bar{I}^{ng}_3 - \cdots - \bar{I}^{ng}_i - \bar{I}^{ng}_j - \cdots - \bar{I}^{ng}_k - \bar{I}^{ng}_l - \bar{I}^{ng}_m - \bar{I}^{ng}_{n_b} - \bar{I}^a_f \\
\bar{B}^g_{2,f} &= -\bar{I}^{ng}_3 - \cdots - \bar{I}^{ng}_i - \bar{I}^{ng}_j - \cdots - \bar{I}^{ng}_k - \bar{I}^{ng}_l - \bar{I}^{ng}_m - \bar{I}^{ng}_{n_b} - \bar{I}^a_f \\
\bar{B}^g_{i,f} &= -\bar{I}^{ng}_j \\
\bar{B}^g_{k,f} &= -\bar{I}^{ng}_l - \bar{I}^{ng}_m - \bar{I}^{ng}_{n_b} - \bar{I}^a_f \\
\bar{B}^g_{l,f} &= -\bar{I}^{ng}_m - \bar{I}^{ng}_{n_b} \\
\bar{B}^g_{m,f} &= -\bar{I}^{ng}_{n_b}
\end{aligned} \tag{6.20}$$

Hence, the modified ground currents due to SLG fault can be expressed in the matrix form as,

$$\left[\mathbf{B_{g,f}}\right] = -\left[\mathbf{BIBC_g}\right]\left[\mathbf{I_{ng}}\right] - \left[\mathbf{BIBC_{fg}}\right]\left[\mathbf{I_f}\right] \tag{6.21}$$

where,

$$\left[\mathbf{BIBC_{fg}}\right] = \left[\mathbf{BIBC_g}(:, g_{f_b})\right] = \begin{bmatrix} 1 & 1 & \cdots & 0 & \cdots & 1 & 0 & 0 \end{bmatrix}^T$$

$\left[\mathbf{BIBC_{fg}}\right]$ matrix for an SLG fault has already been defined in eq. (5.37) of Chapter 5.

Therefore, the voltages of phase buses under the fault conditions are calculated using the modified phase branch and ground currents (using eq. (6.6)) as,

$$\left[\mathbf{V_{p,f}}\right] = \left[\mathbf{V_{ss}}\right] - \left[\mathbf{BCBV_p}\right]\left[\mathbf{B_{p,f}}\right] - \left[\mathbf{BCBV_{pn}}\right]\left[\mathbf{B_n}\right] - \left[\mathbf{BCBV_{pg}}\right]\left[\mathbf{B_{g,f}}\right] \tag{6.22}$$

The phase bus voltages under the fault conditions are recalculated using eqs. (6.4), (6.19), (6.21) and (6.22) as,

$$\begin{aligned}
\left[\mathbf{V_{p,f}}\right] &= \left[\mathbf{V_{ss}}\right] - \left[\mathbf{BCBV_p}\right]\left\{\left[\mathbf{BIBC_p}\right]\left[\mathbf{I_L}\right] + \left[\mathbf{TIBC_{Tm}}\right]\left[\mathbf{I_{T,p}}\right] + \left[\mathbf{BIBC_{fp}}\right]\left[\mathbf{I_f}\right]\right\} \\
&- \left[\mathbf{BCBV_{pn}}\right]\left\{-\left[\mathbf{BIBC_{pn}}\right]\left[\mathbf{I_L}\right] + \left[\mathbf{BIBC_g}\right]\left[\mathbf{I_{ng}}\right]\right\} - \left[\mathbf{BCBV_{pg}}\right]\left\{\right. \\
&- \left.\left[\mathbf{BIBC_g}\right]\left[\mathbf{I_{ng}}\right] - \left[\mathbf{BIBC_{fg}}\right]\left[\mathbf{I_f}\right]\right\}
\end{aligned}$$

$$\left[\mathbf{V_{p,f}}\right] = \left[\mathbf{V_{ss}}\right] - \left[\mathbf{DLF_1}\right]\left[\mathbf{I_L}\right] - \left[\mathbf{DLF_2}\right]\left[\mathbf{I_{ng}}\right] - \left[\mathbf{DLF_{Tm_p}}\right]\left[\mathbf{I_{T,p}}\right] - \left[\mathbf{DFF_1}\right]\left[\mathbf{I_f}\right] \tag{6.23}$$

where,

$$\left[\mathbf{DFF_1}\right] = \left[\mathbf{BCBV_p}\right]\left[\mathbf{BIBC_{fp}}\right] - \left[\mathbf{BCBV_{pg}}\right]\left[\mathbf{BIBC_{fg}}\right]$$

Similarly, the neutral bus and ground bus voltages under the fault conditions are calculated using eqs. (6.4), (6.7), (6.8), (6.19) and (6.21) as,

$$\left[\mathbf{V_{n,f}}\right] = \left[\mathbf{V_{sn}}\right] - \left[\mathbf{DLF_3}\right]\left[\mathbf{I_L}\right] - \left[\mathbf{DLF_4}\right]\left[\mathbf{I_{ng}}\right] - \left[\mathbf{DLF_{Tm_n}}\right]\left[\mathbf{I_{T,p}}\right] - \left[\mathbf{DFF_2}\right]\left[\mathbf{I_f}\right] \tag{6.24}$$

$$\left[\mathbf{V_{g,f}}\right] = \left[\mathbf{V_{sg}}\right] - \left[\mathbf{DLF_5}\right]\left[\mathbf{I_L}\right] - \left[\mathbf{DLF_6}\right]\left[\mathbf{I_{ng}}\right] - \left[\mathbf{DLF_{Tm_g}}\right]\left[\mathbf{I_{T,p}}\right] - \left[\mathbf{DFF_3}\right]\left[\mathbf{I_f}\right] \quad (6.25)$$

where,

$$\left[\mathbf{DFF_2}\right] = \left[\mathbf{BCBV_{np}}\right]\left[\mathbf{BIBC_{fp}}\right] - \left[\mathbf{BCBV_{ng}}\right]\left[\mathbf{BIBC_{fg}}\right]$$
$$\left[\mathbf{DFF_3}\right] = \left[\mathbf{BCBV_{gp}}\right]\left[\mathbf{BIBC_{fp}}\right] - \left[\mathbf{BCBV_{g}}\right]\left[\mathbf{BIBC_{fg}}\right]$$

Now, the neutral to ground currents under the fault conditions are calculated using the voltages of neutral buses and ground buses (using eqs. (6.13), (6.24) and (6.25)) as,

$$\begin{aligned}\left[\mathbf{I_{ng}}\right] &= \left[\mathbf{Z_{FNG}}\right]^{-1}\left\{\left[\mathbf{V_{sn}}\right] - \left[\mathbf{V_{sg}}\right] + \left[\left[\mathbf{DLF_5}\right] - \left[\mathbf{DLF_3}\right]\right]\left[\mathbf{I_L}\right] + \left[\mathbf{DLF_{Tm_{gn}}}\right]\left[\mathbf{I_{T,p}}\right]\right. \\ &+ \left.\left[\left[\mathbf{DFF_3}\right] - \left[\mathbf{DFF_2}\right]\right]\left[\mathbf{I_f}\right]\right\} \end{aligned} \quad (6.26)$$

Therefore, the voltages of phase buses, neutral buses and ground buses under the fault conditions are obtained using eqs. (6.23)-(6.26) as,

$$\left[\mathbf{V_{p,f}}\right] = \left[\mathbf{V_{ss}}\right] - \left[\mathbf{F_{1ng}}\right]\left\{\left[\mathbf{V_{sn}}\right] - \left[\mathbf{V_{sg}}\right]\right\} - \left[\mathbf{F_{1PLD}}\right]\left[\mathbf{I_L}\right] - \left[\mathbf{F_{1Tm}}\right]\left[\mathbf{I_{T,p}}\right] - \left[\mathbf{DFF_{1n}}\right]\left[\mathbf{I_f}\right] \quad (6.27)$$

$$\left[\mathbf{V_{n,f}}\right] = \left[\mathbf{F_{2nn}}\right]\left[\mathbf{V_{sn}}\right] - \left[\mathbf{F_{2gg}}\right]\left[\mathbf{V_{sg}}\right] - \left[\mathbf{F_{2PLD}}\right]\left[\mathbf{I_L}\right] - \left[\mathbf{F_{2Tm}}\right]\left[\mathbf{I_{T,p}}\right] - \left[\mathbf{DFF_{2n}}\right]\left[\mathbf{I_f}\right] \quad (6.28)$$

$$\left[\mathbf{V_{g,f}}\right] = \left[\mathbf{F_{3gg}}\right]\left[\mathbf{V_{sg}}\right] - \left[\mathbf{F_{3nn}}\right]\left[\mathbf{V_{sn}}\right] - \left[\mathbf{F_{3PLD}}\right]\left[\mathbf{I_L}\right] - \left[\mathbf{F_{3Tm}}\right]\left[\mathbf{I_{T,p}}\right] - \left[\mathbf{DFF_{3n}}\right]\left[\mathbf{I_f}\right] \quad (6.29)$$

where,

$$\left[\mathbf{DFF_{1n}}\right] = \left[\mathbf{DFF_1}\right] + \left[\mathbf{DLF_2}\right]\left[\mathbf{Z_{FNG}}\right]^{-1}\left\{\left[\mathbf{DFF_3}\right] - \left[\mathbf{DFF_2}\right]\right\}$$
$$\left[\mathbf{DFF_{2n}}\right] = \left[\mathbf{DFF_2}\right] + \left[\mathbf{DLF_4}\right]\left[\mathbf{Z_{FNG}}\right]^{-1}\left\{\left[\mathbf{DFF_3}\right] - \left[\mathbf{DFF_2}\right]\right\}$$
$$\left[\mathbf{DFF_{3n}}\right] = \left[\mathbf{DFF_3}\right] + \left[\mathbf{DLF_6}\right]\left[\mathbf{Z_{FNG}}\right]^{-1}\left\{\left[\mathbf{DFF_3}\right] - \left[\mathbf{DFF_2}\right]\right\}$$

Now, the voltage equation at fault bus is written as,

$$\bar{z}_f \bar{I}_f^a = \bar{V}_{l,f}^a - \bar{V}_{l,f}^g \quad (6.30)$$

where, $\bar{V}_{l,f}^a$ and $\bar{V}_{l,f}^g$ are the voltages of phase a and ground g at fault bus l, respectively. Substitute the values of $\bar{V}_{l,f}^a$ and $\bar{V}_{l,f}^g$ from eqs. (6.27) and (6.29) into eq. (6.30), with an assumption that the neutral and ground buses at the substation end are perfectly grounded (i.e. at zero potential; $\bar{V}_s^n = 0$, $\bar{V}_s^g = 0$), and express it in the matrix form as,

$$\begin{aligned}\left[\mathbf{Z_f}\right]\left[\mathbf{I_f}\right] &= \bar{V}_s^a - \left[\mathbf{F_{1PLD}}(f_b^q,:)\right]\left[\mathbf{I_L}\right] - \left[\mathbf{F_{1Tm}}(f_b^q,:)\right]\left[\mathbf{I_{T,p}}\right] - \left[\mathbf{DFF_{1n}}(f_b^q,1)\right]\left[\mathbf{I_f}\right] \\ &+ \left[\mathbf{F_{3PLD}}(g_{f_b},:)\right]\left[\mathbf{I_L}\right] + \left[\mathbf{F_{3Tm}}(g_{f_b},:)\right]\left[\mathbf{I_{T,p}}\right] + \left[\mathbf{DFF_{3n}}(g_{f_b},1)\right]\left[\mathbf{I_f}\right] \end{aligned} \quad (6.31)$$

where, for SLG fault (at phase a of l^{th} bus), $\left[\mathbf{Z_f}\right] = \bar{z}_f$; $\left[\mathbf{F_{1PLD}}(f_b^q,:)\right]$ represents the row vector of matrix $\left[\mathbf{F_{1PLD}}\right]$ corresponding to the faulty phase p (here, $q = a$) of faulted bus f_b (here, $f_b = l$); $\left[\mathbf{F_{1Tm}}(f_b^q,:)\right]$ represents the row vector of matrix $\left[\mathbf{F_{1Tm}}\right]$ corresponding to the faulty phase q (here, $q = a$) of faulted bus f_b; $\left[\mathbf{DFF_{1n}}(f_b^q,1)\right]$ represents the row vector of matrix $\left[\mathbf{DFF_{1n}}\right]$ corresponding to the faulty phase p of faulted bus f_b; $\left[\mathbf{F_{3PLD}}(g_{f_b},:)\right]$ represents the row vector of matrix $\left[\mathbf{F_{3PLD}}\right]$ corresponding to the ground g_{f_b} at the location of faulted bus f_b; $\left[\mathbf{F_{3Tm}}(g_{f_b},:)\right]$ represents the row vector of matrix $\left[\mathbf{F_{3Tm}}\right]$ corresponding to the ground g_{f_b} at the location of faulted bus f_b; $\left[\mathbf{DFF_{3n}}(g_{f_b},1)\right]$ represents the row vector of matrix $\left[\mathbf{DFF_{3n}}\right]$ corresponding to the ground g_{f_b} at the location of faulted bus f_b.
Hence, the fault current $\left[\mathbf{I_f}\right]$ is obtained from eq. (6.31) as,

$$\left[\mathbf{I_f}\right] = \left[\mathbf{Z_{F1}}\right]^{-1} \bar{V}_s^a - \left[\mathbf{F}_{\mathbf{13PLD}}^{flt}\right]\left[\mathbf{I_L}\right] - \left[\mathbf{F}_{\mathbf{13Tm}}^{flt}\right]\left[\mathbf{I_{T,p}}\right] \tag{6.32}$$

where,

$$\begin{aligned}
\left[\mathbf{Z_{F1}}\right] &= \left[\mathbf{Z_f}\right] + \left[\mathbf{DFF_{1n}}(f_b^q,1)\right] - \left[\mathbf{DFF_{3n}}(g_{f_b},1)\right] \\
\left[\mathbf{F}_{\mathbf{13PLD}}^{flt}\right] &= \left[\mathbf{Z_{F1}}\right]^{-1}\left\{\left[\mathbf{F_{1PLD}}(f_b^q,:)\right] - \left[\mathbf{F_{3PLD}}(g_{f_b},:)\right]\right\} \\
\left[\mathbf{F}_{\mathbf{13Tm}}^{flt}\right] &= \left[\mathbf{Z_{F1}}\right]^{-1}\left\{\left[\mathbf{F_{1Tm}}(f_b^q,:)\right] - \left[\mathbf{F_{3Tm}}(g_{f_b},:)\right]\right\}
\end{aligned}$$

Once the value of fault current $\left[\mathbf{I_f}\right]$ is obtained, the initial estimates of voltages of phase buses (except inverter bus), neutral buses and ground buses under the fault condition are obtained using eqs. (6.27)-(6.29). Also, the initial estimate of inverter current for an SLG fault (at phase a of l^{th} bus in the system) is obtained with the help of calculated bus voltages and eq. (6.1) as,

$$\mathbf{I}_{\mathbf{inv,f,est}}^{\mathbf{abc}} = \mathbf{Y}_{\mathbf{sp,T}}^{\mathbf{abc}}\mathbf{V}_{\mathbf{j,f}}^{\mathbf{abc}} + \mathbf{Y}_{\mathbf{ss,T}}^{\mathbf{abc}}\mathbf{V}_{\mathbf{inv,st}}^{\mathbf{abc}} \tag{6.33}$$

where, $\mathbf{V}_{\mathbf{j,f}}^{\mathbf{abc}}$ is the estimated three-phase voltage vector of j^{th} bus (where an IBDG is connected through a step-down Δ-Y_g IBDG transformer) under the fault conditions; $\mathbf{V}_{\mathbf{inv,st}}^{\mathbf{abc}}$ is the three-phase inverter bus voltage vector obtained from the steady state load flow solution.

Now, depending upon the magnitude of $\mathbf{I}_{\mathbf{inv,f,est}}^{\mathbf{abc}}$, there can be two possible cases of inverter operation during fault as discussed in Subsection 3.2.2 of Chapter 3,

Case 1: If $|\bar{I}_{inv,f,est}^{p}| \leq I_{sc}^{inv}$ (short-circuit current capacity of the inverter); $(p = a, b, c)$

If the magnitude of inverter current $|\bar{I}_{inv,f,est}^{p}|$ for each phase, calculated using eq. (6.33), is less than the short-circuit capacity of the inverter (I_{sc}^{inv}), then the voltages of phase buses, neutral buses and ground buses calculated using eqs. (6.27)-(6.29) are the final values of the voltages of the system under the fault conditions.

Case 2: If $|\bar{I}^{p}_{inv,f,est}| > I^{inv}_{sc}$; ($p = a$, or b, or c)

In this case, the magnitude of the inverter current is restricted to its short-circuit capacity (I^{inv}_{sc}), by operating the inverter in constant current control mode (as discussed in Subsection 3.2.2 of Chapter 3). Hence the inverter current under the fault conditions is given as,

$$\bar{I}^{p}_{inv,f} = |\bar{I}^{p}_{inv,f}|\angle\Psi^{p}_{inv,f} = I^{inv}_{sc}\angle\Psi^{p}_{inv,f}; \quad (p = a, b, c) \tag{6.34}$$

where $\Psi^{p}_{inv,f}$ is the unknown inverter current angle corresponding to phase p under the fault conditions. To solve for these unknown angles, it is assumed that, $\mathbf{\Psi^{abc}_{inv,f}} = \frac{\pi}{2} + \theta^{\mathbf{abc}}_{\mathbf{inv,f}}$ (as discussed in Subsection 3.2.2 of Chapter 3), where $\theta^{\mathbf{abc}}_{\mathbf{inv,f}}$ is the three phase voltage angle vector of the inverter bus under the fault conditions, $\mathbf{\Psi^{abc}_{inv,f}} = \begin{bmatrix}\Psi^{a}_{inv,f} & \Psi^{b}_{inv,f} & \Psi^{c}_{inv,f}\end{bmatrix}^{\mathbf{T}}$, $\theta^{\mathbf{abc}}_{\mathbf{inv,f}} = \begin{bmatrix}\theta^{a}_{inv,f} & \theta^{b}_{inv,f} & \theta^{c}_{inv,f}\end{bmatrix}^{T}$. This is done so as to ensure that the inverter injects reactive power only during fault conditions.

Hence with this inverter control strategy, the inverter bus voltage along with the unknown current angles under the fault conditions can be calculated by solving eq. (6.33). Rewriting eq. (6.33) for phase a as,

$$\begin{aligned}
&I^{inv}_{sc}\angle\Psi^{a}_{inv,f} = I^{inv}_{sc}\underline{/(\tfrac{\pi}{2} + \theta^{a}_{inv,f})} = \bar{Y}^{aa}_{sp,T}\bar{V}^{a}_{j,f} + \bar{Y}^{ab}_{sp,T}\bar{V}^{b}_{j,f} + \bar{Y}^{ac}_{sp,T}\bar{V}^{c}_{j,f} + \bar{Y}^{aa}_{ss,T}\bar{V}^{a}_{inv,f} + \bar{Y}^{ab}_{ss,T}\bar{V}^{b}_{inv,f} \\
&\qquad + \bar{Y}^{ac}_{ss,T}\bar{V}^{c}_{inv,f} \\
&|\bar{Y}^{aa}_{sp,T}||\bar{V}^{a}_{j,f}|\underline{/(\theta^{aa}_{sp,T} + \theta^{a}_{j,f})} + |\bar{Y}^{ab}_{sp,T}||\bar{V}^{b}_{j,f}|\underline{/(\theta^{ab}_{sp,T} + \theta^{b}_{j,f})} + |\bar{Y}^{ac}_{sp,T}||\bar{V}^{c}_{j,f}|\underline{/(\theta^{ac}_{sp,T} + \theta^{c}_{j,f})} + \\
&|\bar{Y}^{aa}_{ss,T}||\bar{V}^{a}_{inv,f}|\underline{/(\theta^{aa}_{ss,T} + \theta^{a}_{inv,f})} + |\bar{Y}^{ab}_{ss,T}||\bar{V}^{b}_{inv,f}|\underline{/(\theta^{ab}_{ss,T} + \theta^{b}_{inv,f})} + |\bar{Y}^{ac}_{ss,T}||\bar{V}^{c}_{inv,f}|\underline{/(\theta^{ac}_{ss,T} + \theta^{c}_{inv,f})} \\
&-I^{inv}_{sc}\underline{/(\tfrac{\pi}{2} + \theta^{a}_{inv,f})} = 0
\end{aligned} \tag{6.35}$$

The real and imaginary part of eq. (6.35) for phase a can be written as,

Real Part

$$\begin{aligned}
&|\bar{Y}^{aa}_{sp,T}||\bar{V}^{a}_{j,f}|cos(\theta^{aa}_{sp,T} + \theta^{a}_{j,f}) + |\bar{Y}^{ab}_{sp,T}||\bar{V}^{b}_{j,f}|cos(\theta^{ab}_{sp,T} + \theta^{b}_{j,f}) + |\bar{Y}^{ac}_{sp,T}||\bar{V}^{c}_{j,f}|cos(\theta^{ac}_{sp,T} + \theta^{c}_{j,f}) + \\
&|\bar{Y}^{aa}_{ss,T}||\bar{V}^{a}_{inv,f}|cos(\theta^{aa}_{ss,T} + \theta^{a}_{inv,f}) + |\bar{Y}^{ab}_{ss,T}||\bar{V}^{b}_{inv,f}|cos(\theta^{ab}_{ss,T} + \theta^{b}_{inv,f}) + \\
&|\bar{Y}^{ac}_{ss,T}||\bar{V}^{c}_{inv,f}|cos(\theta^{ac}_{ss,T} + \theta^{c}_{inv,f}) - I^{inv}_{sc}cos\left(\frac{\pi}{2} + \theta^{a}_{inv,f}\right) = 0 \\
&= f^{a}_{re}(|\bar{V}^{a}_{inv,f}|, |\bar{V}^{b}_{inv,f}|, |\bar{V}^{c}_{inv,f}|, \theta^{a}_{inv,f}, \theta^{b}_{inv,f}, \theta^{c}_{inv,f})
\end{aligned} \tag{6.36}$$

Imaginary Part

$$\begin{aligned}
&|\bar{Y}^{aa}_{sp,T}||\bar{V}^{a}_{j,f}|sin(\theta^{aa}_{sp,T} + \theta^{a}_{j,f}) + |\bar{Y}^{ab}_{sp,T}||\bar{V}^{b}_{j,f}|sin(\theta^{ab}_{sp,T} + \theta^{b}_{j,f}) + |\bar{Y}^{ac}_{sp,T}||\bar{V}^{c}_{j,f}|sin(\theta^{ac}_{sp,T} + \theta^{c}_{j,f}) + \\
&|\bar{Y}^{aa}_{ss,T}||\bar{V}^{a}_{inv,f}|sin(\theta^{aa}_{ss,T} + \theta^{a}_{inv,f}) + |\bar{Y}^{ab}_{ss,T}||\bar{V}^{b}_{inv,f}|sin(\theta^{ab}_{ss,T} + \theta^{b}_{inv,f}) + \\
&|\bar{Y}^{ac}_{ss,T}||\bar{V}^{c}_{inv,f}|sin(\theta^{ac}_{ss,T} + \theta^{c}_{inv,f}) - I^{inv}_{sc}sin\left(\frac{\pi}{2} + \theta^{a}_{inv,f}\right) = 0 \\
&= f^{a}_{im}(|\bar{V}^{a}_{inv,f}|, |\bar{V}^{b}_{inv,f}|, |\bar{V}^{c}_{inv,f}|, \theta^{a}_{inv,f}, \theta^{b}_{inv,f}, \theta^{c}_{inv,f})
\end{aligned} \tag{6.37}$$

Similarly, the real and imaginary parts of eq. (6.35) for phase b are given as,

Real Part

$$
\begin{aligned}
&|\bar{Y}^{ba}_{sp,T}||\bar{V}^{a}_{j,f}|cos(\theta^{ba}_{sp,T}+\theta^{a}_{j,f})+|\bar{Y}^{bb}_{sp,T}||\bar{V}^{b}_{j,f}|cos(\theta^{bb}_{sp,T}+\theta^{b}_{j,f})+|\bar{Y}^{bc}_{sp,T}||\bar{V}^{c}_{j,f}|cos(\theta^{bc}_{sp,T}+\theta^{c}_{j,f})+\\
&|\bar{Y}^{ba}_{ss,T}||\bar{V}^{a}_{inv,f}|cos(\theta^{ba}_{ss,T}+\theta^{a}_{inv,f})+|\bar{Y}^{bb}_{ss,T}||\bar{V}^{b}_{inv,f}|cos(\theta^{bb}_{ss,T}+\theta^{b}_{inv,f})+\\
&|\bar{Y}^{bc}_{ss,T}||\bar{V}^{c}_{inv,f}|cos(\theta^{bc}_{ss,T}+\theta^{c}_{inv,f})-I^{inv}_{sc}cos\left(\frac{\pi}{2}+\theta^{b}_{inv,f}\right)=0\\
&=f^{b}_{re}(|\bar{V}^{a}_{inv,f}|,|\bar{V}^{b}_{inv,f}|,|\bar{V}^{c}_{inv,f}|,\theta^{a}_{inv,f},\theta^{b}_{inv,f},\theta^{c}_{inv,f})
\end{aligned}
\tag{6.38}
$$

Imaginary Part

$$
\begin{aligned}
&|\bar{Y}^{ba}_{sp,T}||\bar{V}^{a}_{j,f}|sin(\theta^{ba}_{sp,T}+\theta^{a}_{j,f})+|\bar{Y}^{bb}_{sp,T}||\bar{V}^{b}_{j,f}|sin(\theta^{bb}_{sp,T}+\theta^{b}_{j,f})+|\bar{Y}^{bc}_{sp,T}||\bar{V}^{c}_{j,f}|sin(\theta^{bc}_{sp,T}+\theta^{c}_{j,f})+\\
&|\bar{Y}^{ba}_{ss,T}||\bar{V}^{a}_{inv,f}|sin(\theta^{ba}_{ss,T}+\theta^{a}_{inv,f})+|\bar{Y}^{bb}_{ss,T}||\bar{V}^{b}_{inv,f}|sin(\theta^{bb}_{ss,T}+\theta^{b}_{inv,f})+\\
&|\bar{Y}^{bc}_{ss,T}||\bar{V}^{c}_{inv,f}|sin(\theta^{bc}_{ss,T}+\theta^{c}_{inv,f})-I^{inv}_{sc}sin\left(\frac{\pi}{2}+\theta^{b}_{inv,f}\right)=0\\
&=f^{b}_{im}(|\bar{V}^{a}_{inv,f}|,|\bar{V}^{b}_{inv,f}|,|\bar{V}^{c}_{inv,f}|,\theta^{a}_{inv,f},\theta^{b}_{inv,f},\theta^{c}_{inv,f})
\end{aligned}
\tag{6.39}
$$

Also, the real and imaginary part of eq. (6.35) for phase c are given as,

Real Part

$$
\begin{aligned}
&|\bar{Y}^{ca}_{sp,T}||\bar{V}^{a}_{j,f}|cos(\theta^{ca}_{sp,T}+\theta^{a}_{j,f})+|\bar{Y}^{cb}_{sp,T}||\bar{V}^{b}_{j,f}|cos(\theta^{cb}_{sp,T}+\theta^{b}_{j,f})+|\bar{Y}^{cc}_{sp,T}||\bar{V}^{c}_{j,f}|cos(\theta^{cc}_{sp,T}+\theta^{c}_{j,f})+\\
&|\bar{Y}^{ca}_{ss,T}||\bar{V}^{a}_{inv,f}|cos(\theta^{ca}_{ss,T}+\theta^{a}_{inv,f})+|\bar{Y}^{cb}_{ss,T}||\bar{V}^{b}_{inv,f}|cos(\theta^{cb}_{ss,T}+\theta^{b}_{inv,f})+\\
&|\bar{Y}^{cc}_{ss,T}||\bar{V}^{c}_{inv,f}|cos(\theta^{cc}_{ss,T}+\theta^{c}_{inv,f})-I^{inv}_{sc}cos\left(\frac{\pi}{2}+\theta^{c}_{inv,f}\right)=0\\
&=f^{c}_{re}(|\bar{V}^{a}_{inv,f}|,|\bar{V}^{b}_{inv,f}|,|\bar{V}^{c}_{inv,f}|,\theta^{a}_{inv,f},\theta^{b}_{inv,f},\theta^{c}_{inv,f})
\end{aligned}
\tag{6.40}
$$

Imaginary Part

$$
\begin{aligned}
&|\bar{Y}^{ca}_{sp,T}||\bar{V}^{a}_{j,f}|sin(\theta^{ca}_{sp,T}+\theta^{a}_{j,f})+|\bar{Y}^{cb}_{sp,T}||\bar{V}^{b}_{j,f}|sin(\theta^{cb}_{sp,T}+\theta^{b}_{j,f})+|\bar{Y}^{cc}_{sp,T}||\bar{V}^{c}_{j,f}|sin(\theta^{cc}_{sp,T}+\theta^{c}_{j,f})+\\
&|\bar{Y}^{ca}_{ss,T}||\bar{V}^{a}_{inv,f}|sin(\theta^{ca}_{ss,T}+\theta^{a}_{inv,f})+|\bar{Y}^{cb}_{ss,T}||\bar{V}^{b}_{inv,f}|sin(\theta^{cb}_{ss,T}+\theta^{b}_{inv,f})+\\
&|\bar{Y}^{cc}_{ss,T}||\bar{V}^{c}_{inv,f}|sin(\theta^{cc}_{ss,T}+\theta^{c}_{inv,f})-I^{inv}_{sc}sin\left(\frac{\pi}{2}+\theta^{c}_{inv,f}\right)=0\\
&=f^{c}_{im}(|\bar{V}^{a}_{inv,f}|,|\bar{V}^{b}_{inv,f}|,|\bar{V}^{c}_{inv,f}|,\theta^{a}_{inv,f},\theta^{b}_{inv,f},\theta^{c}_{inv,f})
\end{aligned}
\tag{6.41}
$$

Hence, for the unbalanced three-phase four wire multigrounded radial distribution system having nt number of Δ-Y_g IBDG transformers, there is a total of $6nt$ non-linear equations. To solve these non-linear equations, Newton-Raphson method has been used in this work. The set of non-linear equations for the

system shown in Fig. 6.1 with one Δ-Y_g IBDG transformer is given as,

$$
\begin{aligned}
f_{re}^{a}(|\bar{V}_{inv,f}^{a}|, |\bar{V}_{inv,f}^{b}|, |\bar{V}_{inv,f}^{c}|, \theta_{inv,f}^{a}, \theta_{inv,f}^{b}, \theta_{inv,f}^{c}) = 0 \\
f_{im}^{a}(|\bar{V}_{inv,f}^{a}|, |\bar{V}_{inv,f}^{b}|, |\bar{V}_{inv,f}^{c}|, \theta_{inv,f}^{a}, \theta_{inv,f}^{b}, \theta_{inv,f}^{c}) = 0 \\
f_{re}^{b}(|\bar{V}_{inv,f}^{a}|, |\bar{V}_{inv,f}^{b}|, |\bar{V}_{inv,f}^{c}|, \theta_{inv,f}^{a}, \theta_{inv,f}^{b}, \theta_{inv,f}^{c}) = 0 \\
f_{im}^{b}(|\bar{V}_{inv,f}^{a}|, |\bar{V}_{inv,f}^{b}|, |\bar{V}_{inv,f}^{c}|, \theta_{inv,f}^{a}, \theta_{inv,f}^{b}, \theta_{inv,f}^{c}) = 0 \\
f_{re}^{c}(|\bar{V}_{inv,f}^{a}|, |\bar{V}_{inv,f}^{b}|, |\bar{V}_{inv,f}^{c}|, \theta_{inv,f}^{a}, \theta_{inv,f}^{b}, \theta_{inv,f}^{c}) = 0 \\
f_{im}^{c}(|\bar{V}_{inv,f}^{a}|, |\bar{V}_{inv,f}^{b}|, |\bar{V}_{inv,f}^{c}|, \theta_{inv,f}^{a}, \theta_{inv,f}^{b}, \theta_{inv,f}^{c}) = 0
\end{aligned} \tag{6.42}
$$

The above set of non-linear equations, for calculating the unknown inverter bus voltage magnitudes and their respective phase angles, are solved using Newton-Raphson method as,

$$
\begin{bmatrix} \mathbf{\Delta V_{inv,f}} \\ \mathbf{\Delta \theta_{inv,f}} \end{bmatrix} = \begin{bmatrix} \mathbf{J_1} & \mathbf{J_2} \\ \mathbf{J_3} & \mathbf{J_4} \end{bmatrix}^{-1} . \begin{bmatrix} \mathbf{\Delta f_{real}} \\ \mathbf{\Delta f_{imag}} \end{bmatrix} \tag{6.43}
$$

where $\mathbf{\Delta V_{inv,f}}$ and $\mathbf{\Delta \theta_{inv,f}}$ are the correction vectors calculated at t^{th} iteration. Hence,
$\mathbf{\Delta V_{inv,f}} = \left[\Delta V_{inv,f}^{a(t)}, \Delta V_{inv,f}^{b(t)}, \Delta V_{inv,f}^{c(t)}\right]^{\mathbf{T}}$;
$\mathbf{\Delta \theta_{inv,f}} = \left[\Delta \theta_{inv,f}^{a(t)}, \Delta \theta_{inv,f}^{b(t)}, \Delta \theta_{inv,f}^{c(t)}\right]^{\mathbf{T}}$.
$\mathbf{\Delta f_{real}}$ and $\mathbf{\Delta f_{imag}}$ are the mismatch vectors calculated at t^{th} iteration and are given as
$\mathbf{\Delta f_{real}} = \left[-f_{re}^{a(t)}, -f_{re}^{b(t)}, -f_{re}^{c(t)}\right]^{\mathbf{T}}$;
$\mathbf{\Delta f_{imag}} = \left[-f_{im}^{a(t)}, -f_{im}^{b(t)}, -f_{im}^{c(t)}\right]^{\mathbf{T}}$.
$\mathbf{J_1}$, $\mathbf{J_2}$, $\mathbf{J_3}$ and $\mathbf{J_4}$ are the sub-matrices of the Jacobian matrix [$\mathbf{J}$], and are given as,

$$
\mathbf{J_1} = \frac{\partial \mathbf{f_{real}}}{\partial \mathbf{V_{inv,f}}} = \begin{bmatrix} \frac{\partial f_{re}^{a}}{\partial |\bar{V}_{inv,f}^{a}|} & \frac{\partial f_{re}^{a}}{\partial |\bar{V}_{inv,f}^{b}|} & \frac{\partial f_{re}^{a}}{\partial |\bar{V}_{inv,f}^{c}|} \\ \frac{\partial f_{re}^{b}}{\partial |\bar{V}_{inv,f}^{a}|} & \frac{\partial f_{re}^{b}}{\partial |\bar{V}_{inv,f}^{b}|} & \frac{\partial f_{re}^{b}}{\partial |\bar{V}_{inv,f}^{c}|} \\ \frac{\partial f_{re}^{c}}{\partial |\bar{V}_{inv,f}^{a}|} & \frac{\partial f_{re}^{c}}{\partial |\bar{V}_{inv,f}^{b}|} & \frac{\partial f_{re}^{c}}{\partial |\bar{V}_{inv,f}^{c}|} \end{bmatrix}; \quad \mathbf{J_2} = \frac{\partial \mathbf{f_{real}}}{\partial \theta_{\mathbf{inv,f}}} = \begin{bmatrix} \frac{\partial f_{re}^{a}}{\partial \theta_{inv,f}^{a}} & \frac{\partial f_{re}^{a}}{\partial \theta_{inv,f}^{b}} & \frac{\partial f_{re}^{a}}{\partial \theta_{inv,f}^{c}} \\ \frac{\partial f_{re}^{b}}{\partial \theta_{inv,f}^{a}} & \frac{\partial f_{re}^{b}}{\partial \theta_{inv,f}^{b}} & \frac{\partial f_{re}^{b}}{\partial \theta_{inv,f}^{c}} \\ \frac{\partial f_{re}^{c}}{\partial \theta_{inv,f}^{a}} & \frac{\partial f_{re}^{c}}{\partial \theta_{inv,f}^{b}} & \frac{\partial f_{re}^{c}}{\partial \theta_{inv,f}^{c}} \end{bmatrix}
$$

$$
\mathbf{J_3} = \frac{\partial \mathbf{f_{imag}}}{\partial \mathbf{V_{inv,f}}} = \begin{bmatrix} \frac{\partial f_{im}^{a}}{\partial |\bar{V}_{inv,f}^{a}|} & \frac{\partial f_{im}^{a}}{\partial |\bar{V}_{inv,f}^{b}|} & \frac{\partial f_{im}^{a}}{\partial |\bar{V}_{inv,f}^{c}|} \\ \frac{\partial f_{im}^{b}}{\partial |\bar{V}_{inv,f}^{a}|} & \frac{\partial f_{im}^{b}}{\partial |\bar{V}_{inv,f}^{b}|} & \frac{\partial f_{im}^{b}}{\partial |\bar{V}_{inv,f}^{c}|} \\ \frac{\partial f_{im}^{c}}{\partial |\bar{V}_{inv,f}^{a}|} & \frac{\partial f_{im}^{c}}{\partial |\bar{V}_{inv,f}^{b}|} & \frac{\partial f_{im}^{c}}{\partial |\bar{V}_{inv,f}^{c}|} \end{bmatrix}; \quad \mathbf{J_4} = \frac{\partial \mathbf{f_{imag}}}{\partial \theta_{\mathbf{inv,f}}} = \begin{bmatrix} \frac{\partial f_{im}^{a}}{\partial \theta_{inv,f}^{a}} & \frac{\partial f_{im}^{a}}{\partial \theta_{inv,f}^{b}} & \frac{\partial f_{im}^{a}}{\partial \theta_{inv,f}^{c}} \\ \frac{\partial f_{im}^{b}}{\partial \theta_{inv,f}^{a}} & \frac{\partial f_{im}^{b}}{\partial \theta_{inv,f}^{b}} & \frac{\partial f_{im}^{b}}{\partial \theta_{inv,f}^{c}} \\ \frac{\partial f_{im}^{c}}{\partial \theta_{inv,f}^{a}} & \frac{\partial f_{im}^{c}}{\partial \theta_{inv,f}^{b}} & \frac{\partial f_{im}^{c}}{\partial \theta_{inv,f}^{c}} \end{bmatrix}
$$

Elements of Jacobian matrix $[\mathbf{J}]$ are calculated as,

$$\begin{aligned}
\frac{\partial f^p_{re}}{\partial |\bar{V}^q_{inv,f}|} &= |\bar{Y}^{pq}_{ss,T}| cos(\theta^{pq}_{ss,T} + \theta^q_{inv,f}) \\
\left.\frac{\partial f^p_{re}}{\partial \theta^q_{inv,f}}\right|_{p\neq q} &= -|\bar{Y}^{pq}_{ss,T}||\bar{V}^q_{inv,f}| sin(\theta^{pq}_{ss,T} + \theta^q_{inv,f}) \\
\frac{\partial f^p_{re}}{\partial \theta^p_{inv,f}} &= -|\bar{Y}^{pp}_{ss,T}||\bar{V}^p_{inv,f}| sin(\theta^{pp}_{ss,T} + \theta^p_{inv,f}) + I^{inv}_{sc} sin\left(\frac{\pi}{2} + \theta^p_{inv,f}\right) \\
\frac{\partial f^p_{im}}{\partial |\bar{V}^q_{inv,f}|} &= |\bar{Y}^{pq}_{ss,T}| sin(\theta^{pq}_{ss,T} + \theta^q_{inv,f}) \\
\left.\frac{\partial f^p_{im}}{\partial \theta^q_{inv,f}}\right|_{p\neq q} &= |\bar{Y}^{pq}_{ss,T}||\bar{V}^q_{inv,f}| cos(\theta^{pq}_{ss,T} + \theta^q_{inv,f}) \\
\frac{\partial f^p_{im}}{\partial \theta^p_{inv,f}} &= |\bar{Y}^{pp}_{ss,T}||\bar{V}^p_{inv,f}| cos(\theta^{pp}_{ss,T} + \theta^p_{inv,f}) - I^{inv}_{sc} cos\left(\frac{\pi}{2} + \theta^p_{inv,f}\right)
\end{aligned}$$

where $p, q = a, b, c$. The size of Jacobian matrix $\left[\mathbf{J}\right]$ is (6×6) and its all four sub-matrices ($\mathbf{J_1}$, $\mathbf{J_2}$, $\mathbf{J_3}$ and $\mathbf{J_4}$) is (3×3) for one Δ-Y_g IBDG transformer. Hence, for nt number of IBDG transformers in the system, there is total nt number of Jacobian matrices $\left[\mathbf{J}\right]$ which will be required to calculate the values of their inverter bus voltages under the fault conditions. With the help of calculated inverter bus voltages, the primary winding currents of IBDG transformer under the fault conditions are calculated by using eq. (6.1). Therefore, the new value of fault current is calculated by eq. (6.32). Similarly, new values of voltages of phase buses, neutral buses and ground buses under the fault conditions are also calculated (with the help of obtained new values of fault current and primary winding currents of IBDG transformer) by eqs. (6.27)-(6.29).

(b) Double line-to-ground (LLG) fault

Let us consider an LLG fault between phases a and b, and the local ground g_l at l^{th} bus location through a fault impedance $\bar{z}_f$, as shown in Fig. 6.2(b). The two fault currents $\bar{I}^a_f$ and $\bar{I}^b_f$ are flowing from phases a and b to the ground g_l at l^{th} bus, respectively. The modified phase branch currents (of phases a and b) due to LLG fault in Fig. 6.2(b), can be written as,

$$\begin{aligned}
\bar{B}^a_{1,f} &= \bar{I}^a_{2d} + \bar{I}^a_{3d} + \cdots + \bar{I}^a_{id} + \bar{I}^a_{jd} + \bar{I}^a_{T,p} + \cdots + \bar{I}^a_{kd} + \bar{I}^a_{ld} + \bar{I}^a_{md} + \bar{I}^a_{n_bd} + \bar{I}^a_f \\
\bar{B}^b_{1,f} &= \bar{I}^b_{2d} + \bar{I}^b_{3d} + \cdots + \bar{I}^b_{id} + \bar{I}^b_{jd} + \bar{I}^b_{T,p} + \cdots + \bar{I}^b_{kd} + \bar{I}^b_{ld} + \bar{I}^b_{md} + \bar{I}^b_f \\
\bar{B}^a_{2,f} &= \bar{I}^a_{3d} + \cdots + \bar{I}^a_{id} + \bar{I}^a_{jd} + \bar{I}^a_{T,p} + \cdots + \bar{I}^a_{kd} + \bar{I}^a_{ld} + \bar{I}^a_{md} + \bar{I}^a_{n_bd} + \bar{I}^a_f \\
\bar{B}^b_{2,f} &= \bar{I}^b_{3d} + \cdots + \bar{I}^b_{id} + \bar{I}^b_{jd} + \bar{I}^b_{T,p} + \cdots + \bar{I}^b_{kd} + \bar{I}^b_{ld} + \bar{I}^b_{md} + \bar{I}^b_f
\end{aligned}$$

$$
\begin{aligned}
\bar{B}^a_{i,f} &= \bar{I}^a_{jd} + \bar{I}^a_{T,p} \\
\bar{B}^b_{i,f} &= \bar{I}^b_{jd} + \bar{I}^b_{T,p} \\
\bar{B}^a_{k,f} &= \bar{I}^a_{ld} + \bar{I}^a_{md} + \bar{I}^a_{n_b d} + \bar{I}^a_f \\
\bar{B}^b_{k,f} &= \bar{I}^b_{ld} + \bar{I}^b_{md} + \bar{I}^b_f \\
\bar{B}^a_{l,f} &= \bar{I}^a_{md} + \bar{I}^a_{n_b d}; \\
\bar{B}^b_{l,f} &= \bar{I}^b_{md} \\
\bar{B}^a_{m,f} &= \bar{I}^a_{n_b d}
\end{aligned} \tag{6.44}
$$

The above equations can be put in the matrix form as,

$$
\left[\mathbf{B_{p,f}}\right] = \left[\mathbf{BIBC_p}\right]\left[\mathbf{I_L}\right] + \left[\mathbf{TIBC_{Tm}}\right]\left[\mathbf{I_{T,p}}\right] + \left[\mathbf{BIBC_{fp}}\right]\left[\mathbf{I_f}\right] \tag{6.45}
$$

where,

$$
\begin{aligned}
\left[\mathbf{BIBC_{fp}}\right] &= \begin{bmatrix} \mathbf{BIBC_p}(:, f_b^{q_1}) \\ \mathbf{BIBC_p}(:, f_b^{q_2}) \end{bmatrix}^T = \begin{bmatrix} 1 & 0 & 0 & \cdots & 0 & 0 & 0 & \cdots & 1 & 0 & 0 & 0 & 0 & 0 \\ 0 & 1 & 0 & \cdots & 0 & 0 & 0 & \cdots & 0 & 1 & 0 & 0 & 0 & 0 \end{bmatrix}^T; \\
\left[\mathbf{I_f}\right] &= \begin{bmatrix} \bar{I}^a_f & \bar{I}^b_f \end{bmatrix}^T.
\end{aligned}
$$

Definition of $\left[\mathbf{BIBC_{fp}}\right]$ matrix for LLG fault (faulted bus $f_b = l$, and faulted phases $q_1 = a$ and $q_2 = b$) is given in eq. (5.52) of Chapter 5.

The modified ground currents due to LLG fault, as shown in Fig. 6.2(b), can be written as,

$$
\begin{aligned}
\bar{B}^g_{1,f} &= -\bar{I}^{ng}_2 - \bar{I}^{ng}_3 - \cdots - \bar{I}^{ng}_i - \bar{I}^{ng}_j - \cdots - \bar{I}^{ng}_k - \bar{I}^{ng}_l - \bar{I}^{ng}_m - \bar{I}^{ng}_{n_b} - \bar{I}^a_f - \bar{I}^b_f \\
\bar{B}^g_{2,f} &= -\bar{I}^{ng}_3 - \cdots - \bar{I}^{ng}_i - \bar{I}^{ng}_j - \cdots - \bar{I}^{ng}_k - \bar{I}^{ng}_l - \bar{I}^{ng}_m - \bar{I}^{ng}_{n_b} - \bar{I}^a_f - \bar{I}^b_f \\
\bar{B}^g_{i,f} &= -\bar{I}^{ng}_j - \bar{I}^a_f - \bar{I}^b_f \\
\bar{B}^g_{k,f} &= -\bar{I}^{ng}_l - \bar{I}^{ng}_m - \bar{I}^{ng}_{n_b} \\
\bar{B}^g_{l,f} &= -\bar{I}^{ng}_m - \bar{I}^{ng}_{n_b} \\
\bar{B}^g_{m,f} &= -\bar{I}^{ng}_{n_b}
\end{aligned} \tag{6.46}
$$

Hence, the modified ground currents due to LLG fault can be expressed in the matrix form as,

$$
\left[\mathbf{B_{g,f}}\right] = -\left[\mathbf{BIBC_g}\right]\left[\mathbf{I_{ng}}\right] - \left[\mathbf{BIBC_{fg}}\right]\left[\mathbf{I_f}\right] \tag{6.47}
$$

where,

$$
\left[\mathbf{BIBC_{fg}}\right] = \begin{bmatrix} \mathbf{BIBC_g}(:, g_{f_b}) \\ \mathbf{BIBC_g}(:, g_{f_b}) \end{bmatrix}^T = \begin{bmatrix} 1 & 1 & \cdots & 0 & \cdots & 1 & 0 & 0 \\ 1 & 1 & \cdots & 0 & \cdots & 1 & 0 & 0 \end{bmatrix}^T
$$

$\left[\mathbf{BIBC_{fg}}\right]$ matrix for LLG fault has already been defined in eq. (5.54) of Chapter 5. The voltage equations for the phase buses, neutral buses and ground buses for LLG fault will remain same as given in case of SLG fault (eqs. (6.27)-(6.29)) .

For an LLG fault at phases a and b of l^{th} bus through a fault impedance $\bar{z}_f$, as shown in Fig. 6.2(b), the voltage equations at faulted bus can be written as,

$$\begin{aligned} \bar{z}_f \bar{I}_f^a &= \bar{V}_{l,f}^a - \bar{V}_{l,f}^g \\ \bar{z}_f \bar{I}_f^b &= \bar{V}_{l,f}^b - \bar{V}_{l,f}^g \end{aligned} \tag{6.48}$$

where, $\bar{V}_{l,f}^a$ and $\bar{V}_{l,f}^b$ are the voltages of phases a and b of fault bus l under the fault conditions, respectively; $\bar{V}_{j,f}^g$ is the ground bus voltage under the fault conditions at fault location. Substitute the values of $\bar{V}_{j,f}^a$, $\bar{V}_{j,f}^b$ and $\bar{V}_{j,f}^g$ from eqs. (6.27) and (6.29) into eq. (6.48), with an assumption that the neutral and ground buses at the substation end are perfectly grounded (i.e. at zero potential; $\bar{V}_s^n = 0$, $\bar{V}_s^g = 0$), and expressing it in the matrix form as,

$$\begin{aligned} \left[\mathbf{Z_f}\right]\left[\mathbf{I_f}\right] &= \begin{bmatrix} \bar{V}_s^a \\ \bar{V}_s^b \end{bmatrix} - \begin{bmatrix} \mathbf{F_{1PLD}}(f_b^{q_1},:) \\ \mathbf{F_{1PLD}}(f_b^{q_2},:) \end{bmatrix}\left[\mathbf{I_L}\right] - \begin{bmatrix} \mathbf{F_{1Tm}}(f_b^{q_1},:) \\ \mathbf{F_{1Tm}}(f_b^{q_2},:) \end{bmatrix}\left[\mathbf{I_{T,p}}\right] - \begin{bmatrix} \mathbf{DFF_{1n}}(f_b^{q_1},:) \\ \mathbf{DFF_{1n}}(f_b^{q_2},:) \end{bmatrix}\left[\mathbf{I_f}\right] \\ &+ \begin{bmatrix} \mathbf{F_{3PLD}}(g_{f_b},:) \\ \mathbf{F_{3PLD}}(g_{f_b},:) \end{bmatrix}\left[\mathbf{I_L}\right] + \begin{bmatrix} \mathbf{F_{3Tm}}(g_{f_b},:) \\ \mathbf{F_{3Tm}}(g_{f_b},:) \end{bmatrix}\left[\mathbf{I_{T,p}}\right] + \begin{bmatrix} \mathbf{DFF_{3n}}(g_{f_b},:) \\ \mathbf{DFF_{3n}}(g_{f_b},:) \end{bmatrix}\left[\mathbf{I_f}\right] \end{aligned} \tag{6.49}$$

where, for an LLG fault (at phases a and b of l^{th} bus), $\left[\mathbf{Z_f}\right] = \begin{bmatrix} \bar{z}_f & 0 \\ 0 & \bar{z}_f \end{bmatrix}$; $\left[\mathbf{F_{1Tm}}(f_b^{q_1},:)\right]$ and $\left[\mathbf{F_{1Tm}}(f_b^{q_2},:)\right]$ are the row vectors of matrix $\left[\mathbf{F_{1Tm}}\right]$ corresponding to the faulty phases q_1 and q_2 (here, $q_1 = a$, $q_2 = b$) of faulted bus f_b (here, $f_b = l$), respectively; $\left[\mathbf{F_{3Tm}}(g_{f_b},:)\right]$ represents the row vector of matrix $\left[\mathbf{F_{3Tm}}\right]$ corresponding to the ground g_{f_b} at the location of faulted bus f_b. The matrices $\left[\mathbf{F_{1PLD}}(f_b^{q_1},:)\right]$, $\left[\mathbf{F_{1PLD}}(f_b^{q_1},:)\right]$, $\left[\mathbf{DFF_{1n}}(f_b^{q_1},:)\right]$, $\left[\mathbf{DFF_{1n}}(f_b^{q_2},:)\right]$, $\left[\mathbf{F_{3PLD}}(g_{f_b},:)\right]$, $\left[\mathbf{F_{3PLD}}(g_{f_b},:)\right]$, $\left[\mathbf{DFF_{3n}}(g_{f_b},:)\right]$, $\left[\mathbf{DFF_{3n}}(g_{f_b},:)\right]$ for LLG fault have already been defined in eq. (5.56) of Chapter 5. Hence, the fault current $\left[\mathbf{I_f}\right]$ for an LLG fault is obtained from eq. (6.49) as,

$$\left[\mathbf{I_f}\right] = \left[\mathbf{Z_{F1}}\right]^{-1}\begin{bmatrix} \bar{V}_s^a \\ \bar{V}_s^b \end{bmatrix} - \left[\mathbf{F_{13PLD}^{flt}}\right]\left[\mathbf{I_L}\right] - \left[\mathbf{F_{13Tm}^{flt}}\right]\left[\mathbf{I_{T,p}}\right] \tag{6.50}$$

where, $\left[\mathbf{Z_{F1}}\right]$ and $\left[\mathbf{F_{13PLD}^{flt}}\right]$ matrices for LLG fault have already been defined in eq. (5.57) of Chapter 5 and

$$\left[\mathbf{F_{13Tm}^{flt}}\right] = \left[\mathbf{Z_{F1}}\right]^{-1}\left\{\begin{bmatrix} \mathbf{F_{1Tm}}(f_b^{q_1},:) \\ \mathbf{F_{1Tm}}(f_b^{q_2},:) \end{bmatrix} - \begin{bmatrix} \mathbf{F_{3Tm}}(g_{f_b},:) \\ \mathbf{F_{3Tm}}(g_{f_b},:) \end{bmatrix}\right\}$$

The initial estimate of fault currents for LLG fault is obtained from the eq. (6.50) (with the help of pre-fault load flow solution). Once, the value of fault current is obtained, the initial estimate of voltages of phase bus, neutral bus and ground bus of the system under the fault conditions would be obtained by eqs. (6.27)-(6.29). The initial estimate of inverter current under the fault conditions is then obtained by eq. (6.33). Depending upon the magnitude of estimated inverter current, appropriate inverter control strategy will be applied to obtain the final solution under the fault conditions, as discussed previously for the SLG fault.

(c) Triple line-to-ground (LLLG) fault

Let us consider an LLLG fault between all the phases a, b and c, and the local ground g_l at l^{th} bus location through a fault impedance $\bar{z}_f$, as shown in Fig. 6.2(c). The fault currents $\bar{I}_f^a$, $\bar{I}_f^b$ and $\bar{I}_f^c$ are flowing from phases a, b and c to the ground g_l at l^{th} bus, respectively. The modified phase branch currents (of phases a, b and c) due to LLLG fault in Fig. 6.2(c), can be written as,

$$\begin{aligned}
\bar{B}^a_{1,f} &= \bar{I}^a_{2d} + \bar{I}^a_{3d} + \cdots + \bar{I}^a_{id} + \bar{I}^a_{jd} + \bar{I}^a_{T,p} + \cdots + \bar{I}^a_{kd} + \bar{I}^a_{ld} + \bar{I}^a_{md} + \bar{I}^a_{n_bd} + \bar{I}^a_f \\
\bar{B}^b_{1,f} &= \bar{I}^b_{2d} + \bar{I}^b_{3d} + \cdots + \bar{I}^b_{id} + \bar{I}^b_{jd} + \bar{I}^b_{T,p} + \cdots + \bar{I}^b_{kd} + \bar{I}^b_{ld} + \bar{I}^b_{md} + \bar{I}^b_f \\
\bar{B}^c_{1,f} &= \bar{I}^c_{2d} + \bar{I}^c_{3d} + \cdots + \bar{I}^c_{id} + \bar{I}^c_{jd} + \bar{I}^c_{T,p} + \cdots + \bar{I}^c_{kd} + \bar{I}^c_{ld} + \bar{I}^c_f \\
\bar{B}^a_{2,f} &= \bar{I}^a_{3d} + \cdots + \bar{I}^a_{id} + \bar{I}^a_{jd} + \bar{I}^a_{T,p} + \cdots + \bar{I}^a_{kd} + \bar{I}^a_{ld} + \bar{I}^a_{md} + \bar{I}^a_{n_bd} + \bar{I}^a_f \\
\bar{B}^b_{2,f} &= \bar{I}^b_{3d} + \cdots + \bar{I}^b_{id} + \bar{I}^b_{jd} + \bar{I}^b_{T,p} + \cdots + \bar{I}^b_{kd} + \bar{I}^b_{ld} + \bar{I}^b_{md} + \bar{I}^b_f \\
\bar{B}^c_{2,f} &= \bar{I}^c_{3d} + \cdots + \bar{I}^c_{id} + \bar{I}^c_{jd} + \bar{I}^c_{T,p} + \cdots + \bar{I}^c_{kd} + \bar{I}^c_{ld} + \bar{I}^c_f \\
\bar{B}^a_{i,f} &= \bar{I}^a_{jd} + \bar{I}^a_{T,p} \\
\bar{B}^b_{i,f} &= \bar{I}^b_{jd} + \bar{I}^b_{T,p} \\
\bar{B}^c_{i,f} &= \bar{I}^c_{jd} + \bar{I}^c_{T,p} \\
\bar{B}^a_{k,f} &= \bar{I}^a_{ld} + \bar{I}^a_{md} + \bar{I}^a_{n_bd} + \bar{I}^a_f \\
\bar{B}^b_{k,f} &= \bar{I}^b_{ld} + \bar{I}^b_{md} + \bar{I}^b_f \\
\bar{B}^c_{k,f} &= \bar{I}^c_{ld} + \bar{I}^c_f \\
\bar{B}^a_{l,f} &= \bar{I}^a_{md} + \bar{I}^a_{n_bd} \\
\bar{B}^b_{l,f} &= \bar{I}^b_{md} \\
\bar{B}^a_{m,f} &= \bar{I}^a_{n_bd}
\end{aligned} \tag{6.51}$$

The above mentioned equations can be put in the matrix form as,

$$\left[\mathbf{B_{p,f}}\right] = \left[\mathbf{BIBC_p}\right]\left[\mathbf{I_L}\right] + \left[\mathbf{TIBC_{Tm}}\right]\left[\mathbf{I_{T,p}}\right] + \left[\mathbf{BIBC_{fp}}\right]\left[\mathbf{I_f}\right] \tag{6.52}$$

where,

$$\left[\mathbf{BIBC_{fp}}\right] = \begin{bmatrix}\mathbf{BIBC_p}(:, f_b^{q_1})\\ \mathbf{BIBC_p}(:, f_b^{q_2})\\ \mathbf{BIBC_p}(:, f_b^{q_3})\end{bmatrix}^T = \begin{bmatrix}1&0&0&\cdots&0&0&0&\cdots&1&0&0&0&0&0\\ 0&1&0&\cdots&0&0&0&\cdots&0&1&0&0&0&0\\ 0&0&1&\cdots&0&0&0&\cdots&0&0&1&0&0&0\end{bmatrix}^T ;$$

$$\left[\mathbf{I_f}\right] = \begin{bmatrix}\bar{I}_f^a & \bar{I}_f^b & \bar{I}_f^c\end{bmatrix}^T .$$

The $\left[\mathbf{BIBC_{fp}}\right]$ matrix for a LLLG fault has already been described in eq. (5.59) of Chapter 5.

The modified ground currents due to LLLG fault, as shown in Fig. 6.2(c), can be written as,

$$\begin{aligned}
\bar{B}_{1,f}^g &= -\bar{I}_2^{ng} - \bar{I}_3^{ng} - \cdots - \bar{I}_i^{ng} - \bar{I}_j^{ng} - \cdots - \bar{I}_k^{ng} - \bar{I}_l^{ng} - \bar{I}_m^{ng} - \bar{I}_{n_b}^{ng} - \bar{I}_f^a - \bar{I}_f^b - \bar{I}_f^c\\
\bar{B}_{2,f}^g &= -\bar{I}_3^{ng} - \cdots - \bar{I}_i^{ng} - \bar{I}_j^{ng} - \cdots - \bar{I}_k^{ng} - \bar{I}_l^{ng} - \bar{I}_m^{ng} - \bar{I}_{n_b}^{ng} - \bar{I}_f^a - \bar{I}_f^b - \bar{I}_f^c\\
\bar{B}_{i,f}^g &= -\bar{I}_j^{ng} - \bar{I}_f^a - \bar{I}_f^b - \bar{I}_f^c\\
\bar{B}_{k,f}^g &= -\bar{I}_l^{ng} - \bar{I}_m^{ng} - \bar{I}_{n_b}^{ng}\\
\bar{B}_{l,f}^g &= -\bar{I}_m^{ng} - \bar{I}_{n_b}^{ng}\\
\bar{B}_{m,f}^g &= -\bar{I}_{n_b}^{ng}
\end{aligned} \tag{6.53}$$

Hence, the modified ground currents due to LLLG fault can be expressed in the matrix form as,

$$\left[\mathbf{B_{g,f}}\right] = -\left[\mathbf{BIBC_g}\right]\left[\mathbf{I_{ng}}\right] - \left[\mathbf{BIBC_{fg}}\right]\left[\mathbf{I_f}\right] \tag{6.54}$$

where,

$$\left[\mathbf{BIBC_{fg}}\right] = \begin{bmatrix}\mathbf{BIBC_g}(:, g_{f_b})\\ \mathbf{BIBC_g}(:, g_{f_b})\\ \mathbf{BIBC_g}(:, g_{f_b})\end{bmatrix}^T = \begin{bmatrix}1&1&\cdots&0&\cdots&1&0&0\\ 1&1&\cdots&0&\cdots&1&0&0\\ 1&1&\cdots&0&\cdots&1&0&0\end{bmatrix}^T$$

Definition of $\left[\mathbf{BIBC_{fg}}\right]$ matrix for LLLG fault has already been given in eq. (5.61) of Chapter 5. The voltage equations for the phase buses, neutral buses and ground buses for LLLG fault will be same as given in case of SLG fault (eqs. (6.27-(6.29)) .

The voltage equations at fault bus can be written as,

$$\begin{aligned}
\bar{z}_f \bar{I}_f^a &= \bar{V}_{l,f}^a - \bar{V}_{l,f}^g\\
\bar{z}_f \bar{I}_f^b &= \bar{V}_{l,f}^b - \bar{V}_{l,f}^g\\
\bar{z}_f \bar{I}_f^c &= \bar{V}_{l,f}^c - \bar{V}_{l,f}^g
\end{aligned} \tag{6.55}$$

where, $\bar{V}_{l,f}^a$, $\bar{V}_{l,f}^b$ and $\bar{V}_{l,f}^c$ are the voltages of phases a, b and c of fault bus l under the fault conditions, respectively. $\bar{V}_{l,f}^g$ is the ground bus voltage at the fault location under the fault conditions. Substituting

the values of $\bar{V}_{l,f}^{a}$, $\bar{V}_{l,f}^{b}$, $\bar{V}_{l,f}^{c}$ and $\bar{V}_{l,f}^{g}$ from eqs. (6.27) and (6.29) into eq. (6.55), with an assumption that the neutral and ground buses at the substation end are perfectly grounded (i.e. at zero potential; $\bar{V}_{s}^{n} = 0$, $\bar{V}_{s}^{g} = 0$), and writing it in the matrix form, we obtain,

$$\begin{aligned}\left[\mathbf{Z_f}\right]\left[\mathbf{I_f}\right] &= \begin{bmatrix}\bar{V}_s^a\\ \bar{V}_s^b\\ \bar{V}_s^c\end{bmatrix} - \begin{bmatrix}\mathbf{F_{1PLD}}(f_b^{q_1},:)\\ \mathbf{F_{1PLD}}(f_b^{q_2},:)\\ \mathbf{F_{1PLD}}(f_b^{q_3},:)\end{bmatrix}\left[\mathbf{I_L}\right] - \begin{bmatrix}\mathbf{F_{1Tm}}(f_b^{q_1},:)\\ \mathbf{F_{1Tm}}(f_b^{q_2},:)\\ \mathbf{F_{1Tm}}(f_b^{q_3},:)\end{bmatrix}\left[\mathbf{I_{T,p}}\right] - \begin{bmatrix}\mathbf{DFF_{1n}}(f_b^{q_1},:)\\ \mathbf{DFF_{1n}}(f_b^{q_2},:)\\ \mathbf{DFF_{1n}}(f_b^{q_3},:)\end{bmatrix}\left[\mathbf{I_f}\right]\\ &+ \begin{bmatrix}\mathbf{F_{3PLD}}(g_{f_b},:)\\ \mathbf{F_{3PLD}}(g_{f_b},:)\\ \mathbf{F_{3PLD}}(g_{f_b},:)\end{bmatrix}\left[\mathbf{I_L}\right] + \begin{bmatrix}\mathbf{F_{3Tm}}(g_{f_b},:)\\ \mathbf{F_{3Tm}}(g_{f_b},:)\\ \mathbf{F_{3Tm}}(g_{f_b},:)\end{bmatrix}\left[\mathbf{I_{T,p}}\right] + \begin{bmatrix}\mathbf{DFF_{3n}}(g_{f_b},:)\\ \mathbf{DFF_{3n}}(g_{f_b},:)\\ \mathbf{DFF_{3n}}(g_{f_b},:)\end{bmatrix}\left[\mathbf{I_f}\right] \end{aligned} \tag{6.56}$$

where, for an LLLG fault (at j^{th} bus), $\left[\mathbf{Z_f}\right] = \begin{bmatrix}\bar{z}_f & 0 & 0\\ 0 & \bar{z}_f & 0\\ 0 & 0 & \bar{z}_f\end{bmatrix}$; $\left[\mathbf{F_{1Tm}}(f_b^{q_1},:)\right]$, $\left[\mathbf{F_{1Tm}}(f_b^{q_2},:)\right]$ and $\left[\mathbf{F_{1Tm}}(f_b^{q_3},:)\right]$ are the row vectors of matrix $\left[\mathbf{F_{1Tm}}\right]$ corresponding to the faulty phases q_1, q_2 and q_3 (here, $q_1 = a$, $q_2 = b$, $q_3 = c$) of faulted bus f_b (here, $f_b = l$), respectively; $\left[\mathbf{F_{3Tm}}(g_{f_b},:)\right]$ is the row vector of matrix $\left[\mathbf{F_{3Tm}}\right]$ corresponding to the ground g_{f_b} at the location of faulted bus f_b; The matrices $\left[\mathbf{F_{1PLD}}(f_b^{q_1},:)\right]$, $\left[\mathbf{F_{1PLD}}(f_b^{q_2},:)\right]$, $\left[\mathbf{F_{1PLD}}(f_b^{q_3},:)\right]$, $\left[\mathbf{DFF_{1n}}(f_b^{q_1},:)\right]$, $\left[\mathbf{DFF_{1n}}(f_b^{q_2},:)\right]$, $\left[\mathbf{DFF_{1n}}(f_b^{q_3},:)\right]$, $\left[\mathbf{F_{3PLD}}(g_{f_b},:)\right]$ and $\left[\mathbf{DFF_{3n}}(g_{f_b},:)\right]$ for LLLG fault have already been described in eq. (5.63) of Chapter 5.

Hence, the fault current $\left[\mathbf{I_f}\right]$ for LLLG fault is obtained from eq. (6.56) as,

$$\left[\mathbf{I_f}\right] = \left[\mathbf{Z_{F1}}\right]^{-1}\begin{bmatrix}\bar{V}_s^a\\ \bar{V}_s^b\\ \bar{V}_s^c\end{bmatrix} - \left[\mathbf{F_{13PLD}^{flt}}\right]\left[\mathbf{I_L}\right] - \left[\mathbf{F_{13Tm}^{flt}}\right]\left[\mathbf{I_{T,p}}\right] \tag{6.57}$$

where, $\left[\mathbf{Z_{F1}}\right]$ and $\left[\mathbf{F_{13PLD}^{flt}}\right]$ matrices for LLLG fault have already been defined in eq. (5.64) of Chapter 5 and

$$\left[\mathbf{F_{13Tm}^{flt}}\right] = \left[\mathbf{Z_{F1}}\right]^{-1}\left\{\begin{bmatrix}\mathbf{F_{1Tm}}(f_b^{q_1},:)\\ \mathbf{F_{1Tm}}(f_b^{q_2},:)\\ \mathbf{F_{1Tm}}(f_b^{q_3},:)\end{bmatrix} - \begin{bmatrix}\mathbf{F_{3Tm}}(g_{f_b},:)\\ \mathbf{F_{3Tm}}(g_{f_b},:)\\ \mathbf{F_{3Tm}}(g_{f_b},:)\end{bmatrix}\right\}$$

The initial estimate of fault currents for LLLG fault is then obtained from the eq. (6.57) (with the help of pre-fault load flow solution). Once, the value of fault current is obtained, the initial estimate of voltages under the fault conditions are calculated by eqs. (6.27)-(6.29). The initial estimate of inverter current under

the fault conditions is calculated next using eq. (6.33). The appropriate inverter control strategy is then applied, depending upon the magnitude of estimated inverter current, to obtain the final solution under the fault conditions (as discussed in SLG fault).

(d) Line-to-line (LL) fault

Let us consider an LL fault between phases a and b of l^{th} bus through a fault impedance $\bar{z}_f$, as shown in Fig. 6.2(d). The fault current $\bar{I}_f^a$ is flowing from phase a to b at l^{th} bus. Hence, only the phase branch currents will be modified due to LL fault. The modified phase branch currents (of phase a and b) due to LL fault in Fig. 6.2(d), can be written as,

$$\begin{aligned}
\bar{B}^a_{1,f} &= \bar{I}^a_{2d} + \bar{I}^a_{3d} + \cdots + \bar{I}^a_{id} + \bar{I}^a_{jd} + \bar{I}^a_{T,p} + \cdots + \bar{I}^a_{kd} + \bar{I}^a_{ld} + \bar{I}^a_{md} + \bar{I}^a_{n_bd} + \bar{I}^a_f \\
\bar{B}^b_{1,f} &= \bar{I}^b_{2d} + \bar{I}^b_{3d} + \cdots + \bar{I}^b_{id} + \bar{I}^b_{jd} + \bar{I}^b_{T,p} + \cdots + \bar{I}^b_{kd} + \bar{I}^b_{ld} + \bar{I}^b_{md} - \bar{I}^a_f \\
\bar{B}^a_{2,f} &= \bar{I}^a_{3d} + \cdots + \bar{I}^a_{id} + \bar{I}^a_{jd} + \bar{I}^a_{T,p} + \cdots + \bar{I}^a_{kd} + \bar{I}^a_{ld} + \bar{I}^a_{md} + \bar{I}^a_{n_bd} + \bar{I}^a_f \\
\bar{B}^b_{2,f} &= \bar{I}^b_{3d} + \cdots + \bar{I}^b_{id} + \bar{I}^b_{jd} + \bar{I}^b_{T,p} + \cdots + \bar{I}^b_{kd} + \bar{I}^b_{ld} + \bar{I}^b_{md} - \bar{I}^a_f \\
\bar{B}^a_{i,f} &= \bar{I}^a_{jd} + \bar{I}^a_{T,p} \\
\bar{B}^b_{i,f} &= \bar{I}^b_{jd} + \bar{I}^b_{T,p} \\
\bar{B}^a_{k,f} &= \bar{I}^a_{ld} + \bar{I}^a_{md} + \bar{I}^a_{n_bd} + \bar{I}^a_f \\
\bar{B}^b_{k,f} &= \bar{I}^b_{ld} + \bar{I}^b_{md} - \bar{I}^a_f \\
\bar{B}^a_{l,f} &= \bar{I}^a_{md} + \bar{I}^a_{n_bd} \\
\bar{B}^b_{l,f} &= \bar{I}^b_{md} \\
\bar{B}^a_{m,f} &= \bar{I}^a_{n_bd}
\end{aligned} \tag{6.58}$$

The above mentioned equations can be put in the matrix form as,

$$\left[\mathbf{B_{p,f}}\right] = \left[\mathbf{BIBC_p}\right]\left[\mathbf{I_L}\right] + \left[\mathbf{TIBC_{Tm}}\right]\left[\mathbf{I_{T,p}}\right] + \left[\mathbf{BIBC_{fp}}\right]\left[\mathbf{I_f}\right] \tag{6.59}$$

where,

$$\begin{aligned}
\left[\mathbf{BIBC_{fp}}\right] &= \begin{bmatrix} 1 & -1 & 0 & \cdots & 0 & 0 & 0 & \cdots & 1 & -1 & 0 & 0 & 0 & 0 \end{bmatrix}^T; \\
&= \left[\mathbf{BIBC_p}(:, f_b^{q_1}) - \mathbf{BIBC_p}(:, f_b^{q_2})\right] \\
\left[\mathbf{I_f}\right] &= \left[\bar{I}^a_f\right].
\end{aligned}$$

The $\left[\mathbf{BIBC_{fp}}\right]$ matrix for an LL fault has already been defined in eq. (5.66) of Chapter 5.

Now, the voltages of phase bus, neutral bus and ground bus under the fault conditions (using eqs. (6.6)-(6.8)) are calculated using the modified phase branch currents as obtained in eq. (6.59) as,

$$\left[\mathbf{V_{p,f}}\right] = \left[\mathbf{V_{ss}}\right] - \left[\mathbf{DLF_1}\right]\left[\mathbf{I_L}\right] - \left[\mathbf{DLF_2}\right]\left[\mathbf{I_{ng}}\right] - \left[\mathbf{DLF_{Tm_p}}\right]\left[\mathbf{I_{T,p}}\right] - \left[\mathbf{DFF'_1}\right]\left[\mathbf{I_f}\right] \quad (6.60)$$

$$\left[\mathbf{V_{n,f}}\right] = \left[\mathbf{V_{sn}}\right] - \left[\mathbf{DLF_3}\right]\left[\mathbf{I_L}\right] - \left[\mathbf{DLF_4}\right]\left[\mathbf{I_{ng}}\right] - \left[\mathbf{DLF_{Tm_n}}\right]\left[\mathbf{I_{T,p}}\right] - \left[\mathbf{DFF'_2}\right]\left[\mathbf{I_f}\right] \quad (6.61)$$

$$\left[\mathbf{V_{g,f}}\right] = \left[\mathbf{V_{sg}}\right] - \left[\mathbf{DLF_5}\right]\left[\mathbf{I_L}\right] - \left[\mathbf{DLF_6}\right]\left[\mathbf{I_{ng}}\right] - \left[\mathbf{DLF_{Tm_g}}\right]\left[\mathbf{I_{T,p}}\right] - \left[\mathbf{DFF'_3}\right]\left[\mathbf{I_f}\right] \quad (6.62)$$

where,

$$\begin{aligned}\left[\mathbf{DFF'_1}\right] &= \left[\mathbf{BCBV_p}\right]\left[\mathbf{BIBC_{fp}}\right]\\ \left[\mathbf{DFF'_2}\right] &= \left[\mathbf{BCBV_{np}}\right]\left[\mathbf{BIBC_{fp}}\right]\\ \left[\mathbf{DFF'_3}\right] &= \left[\mathbf{BCBV_{gp}}\right]\left[\mathbf{BIBC_{fp}}\right]\end{aligned}$$

Now, the neutral to ground currents under the fault conditions are calculated with the help of neutral and ground bus voltages under the fault conditions using eqs. (6.13), (6.61) and (6.62) as,

$$\begin{aligned}\left[\mathbf{Z_{ngr}}\right]\left[\mathbf{I_{ng}}\right] &= \left\{\left[\mathbf{V_{sn}}\right] - \left[\mathbf{DLF_3}\right]\left[\mathbf{I_L}\right] - \left[\mathbf{DLF_4}\right]\left[\mathbf{I_{ng}}\right] - \left[\mathbf{DLF_{Tm_n}}\right]\left[\mathbf{I_{T,p}}\right] - \left[\mathbf{DFF'_2}\right]\left[\mathbf{I_f}\right]\right\}\\ &- \left\{\left[\mathbf{V_{sg}}\right] - \left[\mathbf{DLF_5}\right]\left[\mathbf{I_L}\right] - \left[\mathbf{DLF_6}\right]\left[\mathbf{I_{ng}}\right] - \left[\mathbf{DLF_{Tm_g}}\right]\left[\mathbf{I_{T,p}}\right] - \left[\mathbf{DFF'_3}\right]\left[\mathbf{I_f}\right]\right\}\end{aligned}$$

$$\begin{aligned}\left[\mathbf{I_{ng}}\right] &= \left[\mathbf{Z_{FNG}}\right]^{-1}\left\{\left[\mathbf{V_{sn}}\right] - \left[\mathbf{V_{sg}}\right] + \left[\left[\mathbf{DLF_5}\right] - \left[\mathbf{DLF_3}\right]\right]\left[\mathbf{I_L}\right] + \left[\mathbf{DLF_{Tm_{gn}}}\right]\left[\mathbf{I_{T,p}}\right]\right.\\ &+ \left.\left[\left[\mathbf{DFF'_3}\right] - \left[\mathbf{DFF'_2}\right]\right]\left[\mathbf{I_f}\right]\right\} \quad (6.63)\end{aligned}$$

Now, substituting the value of $\left[\mathbf{I_{ng}}\right]$ from eq. (6.63) to eqs. (6.60)- (6.62) to recalculate the voltages of phase, neutral and ground buses under the fault conditions as,

$$\left[\mathbf{V_{p,f}}\right] = \left[\mathbf{V_{ss}}\right] - \left[\mathbf{F_{1ng}}\right]\left\{\left[\mathbf{V_{sn}}\right] - \left[\mathbf{V_{sg}}\right]\right\} - \left[\mathbf{F_{1PLD}}\right]\left[\mathbf{I_L}\right] - \left[\mathbf{F_{1Tm}}\right]\left[\mathbf{I_{T,p}}\right] - \left[\mathbf{DFF'_{1n}}\right]\left[\mathbf{I_f}\right] \quad (6.64)$$

$$\left[\mathbf{V_{n,f}}\right] = \left[\mathbf{F_{2nn}}\right]\left[\mathbf{V_{sn}}\right] - \left[\mathbf{F_{2gg}}\right]\left[\mathbf{V_{sg}}\right] - \left[\mathbf{F_{2PLD}}\right]\left[\mathbf{I_L}\right] - \left[\mathbf{F_{2Tm}}\right]\left[\mathbf{I_{T,p}}\right] - \left[\mathbf{DFF'_{2n}}\right]\left[\mathbf{I_f}\right] \quad (6.65)$$

$$\left[\mathbf{V_{g,f}}\right] = \left[\mathbf{F_{3gg}}\right]\left[\mathbf{V_{sg}}\right] - \left[\mathbf{F_{3nn}}\right]\left[\mathbf{V_{sn}}\right] - \left[\mathbf{F_{3PLD}}\right]\left[\mathbf{I_L}\right] - \left[\mathbf{F_{3Tm}}\right]\left[\mathbf{I_{T,p}}\right] - \left[\mathbf{DFF'_{3n}}\right]\left[\mathbf{I_f}\right] \quad (6.66)$$

where,

$$\left[\mathbf{DFF'_{1n}}\right] = \left[\mathbf{DFF'_1}\right] + \left[\mathbf{DLF_2}\right]\left[\mathbf{Z_{FNG}}\right]^{-1}\left\{\left[\mathbf{DFF'_3}\right] - \left[\mathbf{DFF'_2}\right]\right\}$$

$$\left[\mathbf{DFF'_{2n}}\right] = \left[\mathbf{DFF'_2}\right] + \left[\mathbf{DLF_4}\right]\left[\mathbf{Z_{FNG}}\right]^{-1}\left\{\left[\mathbf{DFF'_3}\right] - \left[\mathbf{DFF'_2}\right]\right\}$$

$$\left[\mathbf{DFF'_{3n}}\right] = \left[\mathbf{DFF'_{3}}\right] + \left[\mathbf{DLF_{6}}\right]\left[\mathbf{Z_{FNG}}\right]^{-1}\left\{\left[\mathbf{DFF'_{3}}\right] - \left[\mathbf{DFF'_{2}}\right]\right\}$$

The voltage equation at fault bus is written as,

$$\bar{z}_f \bar{I}_f^a = \bar{V}_{l,f}^a - \bar{V}_{l,f}^b \tag{6.67}$$

where, $\bar{V}_{l,f}^a$ and $\bar{V}_{l,f}^b$ are the voltages of phase a and b at fault bus l, respectively. Substituting the values of $\bar{V}_{l,f}^a$ and $\bar{V}_{l,f}^b$ from eq. (6.64) into eq. (6.67), with an assumption that the neutral and ground buses at the substation end are perfectly grounded (i.e. $\bar{V}_s^n = 0$, $\bar{V}_s^g = 0$), and write it in the matrix form as,

$$\begin{aligned}\left[\mathbf{Z_f}\right]\left[\mathbf{I_f}\right] &= \bar{V}_s^a - \left[\mathbf{F_{1PLD}}(f_b^{q_1},:)\right]\left[\mathbf{I_L}\right] - \left[\mathbf{F_{1Tm}}(f_b^{q_1},:)\right]\left[\mathbf{I_{T,p}}\right] - \left[\mathbf{DFF'_{1n}}(f_b^{q_1},1)\right]\left[\mathbf{I_f}\right] \\ &- \bar{V}_s^b + \left[\mathbf{F_{1PLD}}(f_b^{q_2},:)\right]\left[\mathbf{I_L}\right] + \left[\mathbf{F_{1Tm}}(f_b^{q_2},:)\right]\left[\mathbf{I_{T,p}}\right] + \left[\mathbf{DFF'_{1n}}(f_b^{q_2},1)\right]\left[\mathbf{I_f}\right]\end{aligned} \tag{6.68}$$

where, for LL fault (at phase a and b of l^{th} bus), $\left[\mathbf{Z_f}\right] = \bar{z}_f$; $\left[\mathbf{F_{1PLD}}(f_b^{q_1},:)\right]$ and $\left[\mathbf{F_{1PLD}}(f_b^{q_2},:)\right]$ are the row vectors of matrix $\left[\mathbf{F_{1PLD}}\right]$ corresponding to the faulty phases q_1 and q_2 (here, $q_1 = a$, $q_2 = b$) of faulted bus f_b (here, $f_b = j$), respectively; $\left[\mathbf{F_{1Tm}}(f_b^{q_1},:)\right]$ and $\left[\mathbf{F_{1Tm}}(f_b^{q_2},:)\right]$ are the row vectors of matrix $\left[\mathbf{F_{1Tm}}\right]$ corresponding to the faulty phases q_1 and q_2 of faulted bus f_b, respectively; $\left[\mathbf{DFF'_{1n}}(f_b^{q_1},1)\right]$ and $\left[\mathbf{DFF'_{1n}}(f_b^{q_2},1)\right]$ are the row vectors of matrix $\left[\mathbf{DFF'_{1n}}\right]$ corresponding to the faulty phases q_1 and q_2 of faulted bus f_b, respectively. Hence, the fault current $\left[\mathbf{I_f}\right]$ is obtained from eq. (6.68) as,

$$\left[\mathbf{I_f}\right] = \left[\mathbf{Z_{F1}}\right]^{-1}(\bar{V}_s^a - \bar{V}_s^b) - \left[\mathbf{F_{11PLD}^{flt}}\right]\left[\mathbf{I_L}\right] - \left[\mathbf{F_{11Tm}^{flt}}\right]\left[\mathbf{I_{T,p}}\right] \tag{6.69}$$

where,

$$\begin{aligned}\left[\mathbf{Z_{F1}}\right] &= \left[\mathbf{Z_f}\right] + \left[\mathbf{DFF'_{1n}}(f_b^{q_1},1)\right] - \left[\mathbf{DFF'_{1n}}(f_b^{q_2},1)\right] \\ \left[\mathbf{F_{11PLD}^{flt}}\right] &= \left[\mathbf{Z_{F1}}\right]^{-1}\left\{\left[\mathbf{F_{1PLD}}(f_b^{q_1},:)\right] - \left[\mathbf{F_{1PLD}}(f_b^{q_2},:)\right]\right\} \\ \left[\mathbf{F_{11Tm}^{flt}}\right] &= \left[\mathbf{Z_{F1}}\right]^{-1}\left\{\left[\mathbf{F_{1Tm}}(f_b^{q_1},:)\right] - \left[\mathbf{F_{1Tm}}(f_b^{q_2},:)\right]\right\}\end{aligned}$$

Once, the initial estimate of fault current is made by using eq. (6.69) (with the help of pre-fault load flow solution), the bus voltages and inverter current under the fault conditions are then estimated by using eqs. (6.64)-(6.66) and (6.33), respectively. Again, depending upon the magnitude of estimated inverter current, appropriate control strategy of inverter will be applied to obtain the final solution for an LL fault (as discussed in SLG fault).

Steps of algorithm for $\left[\mathbf{BIBC}\right]$ ***matrix based short-circuit analysis method for an unbalanced three phase four wire multigrounded radial distribution system in the presence of IBDG and*** Δ***-***Y_g ***IBDG transformer***

1. Run the base case power flow of three phase four wire multigrounded system in the presence of IBDG and Δ-Y_g IBDG transformer using the proposed load flow method as discussed in Section 6.2.1 of this chapter.

2. Convert all PQ-loads into constant impedance loads using the obtained load flow solution.

3. If a ground fault (SLG, LLG, LLLG) occurs in the system, then formulate $\left[\mathbf{BIBC_{fp}}\right]$, $\left[\mathbf{BIBC_{fg}}\right]$ and $\left[\mathbf{Z_f}\right]$ matrices corresponding to the type of fault occurring in the system using the proposed $\left[\mathbf{BIBC}\right]$ matrix based short-circuit analysis method. If a line to line (LL) fault occurs, then formulate only $\left[\mathbf{BIBC_{fp}}\right]$ and $\left[\mathbf{Z_f}\right]$ matrices.

4. Set iteration counter $k = 0$. Also, set the values of voltages of phase bus, neutral bus and ground bus, equivalent injection currents $\left[\mathbf{I_L}\right]^k$ and transformer primary winding currents $\left[\mathbf{I_{T,p}}\right]^k$ equal to the values obtained from the pre-fault load flow solutions.

5. Calculate the fault current $\left[\mathbf{I_f}\right]^k$ using eq. (6.32) for SLG fault, eq. (6.50) for LLG fault, eq. (6.57) for LLLG fault and eq. (6.69) for LL fault.

6. Increment the iteration counter by one, $k = k + 1$. Calculate the voltages of phase buses, neutral buses and ground buses $\left([\mathbf{V_{p,f}}]^k, [\mathbf{V_{n,f}}]^k \text{ and } [\mathbf{V_{g,f}}]^k\right)$ of the system under the fault conditions, using eqs. (6.27)-(6.29), for ground faults and using eqs. (6.64)-(6.66), for LL fault, respectively.

7. Calculate the inverter current $\mathbf{I^{abc}_{inv,f,est}}$ of the IBDG under fault conditions using the transformer nodal admittance matrix based current equation as given in eq. (6.1) (with the new values of voltages under the fault conditions as obtained in previous step).

8. Check the condition, whether $|\bar{I}^p_{inv,f,est}| \leq I^{inv}_{sc}$; $(p = a, b, c)$ for all IBDGs in the system. The three possible cases are:

   Case (A): If $|\bar{I}^p_{inv,f,est}| \leq I^{inv}_{sc}$, $(p = a, b, c)$ for all nd - no. of IBDGs, then go to step 12, else

   Case (B): If $|\bar{I}^p_{inv,f,est}|$, $(p = a, b, c)$ of all nd - no. of IBDGs are greater than their corresponding short-circuit current capacities, then operate the inverter of all the IBDGs in constant current mode with, $\bar{I}^p_{inv,f} = I^{inv}_{sc} \angle \frac{\pi}{2} + \theta^p_{inv,f}$, $(p = a, b, c)$ and calculate the inverter bus voltages under the fault

conditions ($\mathbf{V^{abc}_{inv,f}}$) using the Newton-Raphson method as discussed in Subsection 6.2.2.1(a) and go to step 9, else

Case (C): If out of nd - no. of IBDGs, for kd - no. of IBDGs $|\bar{I}^p_{inv,f,est}| \leq I^{inv}_{sc}$, $(p = a, b, c)$ and for the remaining $(nd - kd)$ - no. of IBDGs $|\bar{I}^p_{inv,f,est}| > I^{inv}_{sc}$, $(p = a, b, c)$, then set $\bar{I}^{abc}_{inv,f} = I^{inv}_{sc}\angle(\frac{\pi}{2} + \theta^p_{inv,f})$, $(p = a, b, c)$ for $(nd - kd)$ - no. of IBDGs, while for kd - no. of IBDGs set $\mathbf{I^{abc}_{inv,f}} = \mathbf{I^{abc}_{inv,f,est}}$ and calculate the inverter bus voltages under the fault conditions ($\mathbf{V^{abc}_{inv,f}}$), for $(nd - kd)$ - no. of IBDGs, using the Newton-Raphson method as discussed in Subsection 6.2.2.1(a) and go to step 9.

9. Calculate the transformer primary winding currents and equivalent injection currents at all the phase buses under the fault conditions as,

$$\mathbf{I^{abc}_{T,p,f}} = \mathbf{Y^{abc}_{pp,T}V^{abc}_{T,p,f}} + \mathbf{Y^{abc}_{ps,T}V^{abc}_{inv,f}}$$

$$\bar{I}^p_{id} = \left(\frac{\bar{V}^p_{i,f} - \bar{V}^n_{i,f}}{\bar{z}^p_{id}}\right); \quad (p = a,\ or\ b,\ or\ c); \quad (i = 2, \cdots, n_b)$$

where, $\bar{V}^p_{i,f}$ and $\bar{V}^n_{i,f}$ are the voltages at phase p and neutral n of i^{th} bus under fault conditions, respectively. $\bar{z}^p_{id}$ is an equivalent load impedance at phase p of i^{th} bus.

10. Calculate the error (ϵ),

$$\epsilon = max\left(\left|\left[\mathbf{V_{p,f}}\right]^k - \left[\mathbf{V_{p,f}}\right]^{k-1}\right|, \left|\left[\mathbf{V_{n,f}}\right]^k - \left[\mathbf{V_{n,f}}\right]^{k-1}\right|, \left|\left[\mathbf{V_{g,f}}\right]^k - \left[\mathbf{V_{g,f}}\right]^{k-1}\right|\right)$$

11. If $\epsilon <$ tolerance(1.0×10^{-12}), then go to the next step, else go to step 5.

12. The obtained values of voltages $[\mathbf{V_{p,f}}]$, $[\mathbf{V_{n,f}}]$ and $[\mathbf{V_{g,f}}]$ are the final post-fault values of the voltages and stop the simulation..

The overall flow-chart of the proposed $\left[\mathbf{BIBC}\right]$ matrix based short-circuit analysis method with IBDG and Δ-Y_g IBDG transformer is shown in Fig 6.3.

6.2.2.2 Method 2: $\left[\mathbf{Y_{bus}}\right]$ matrix based method

The proposed short-circuit analysis method is based on the $\left[\mathbf{Y_{bus}}\right]$ matrix of the distribution system. To obtain the $\left[\mathbf{Y_{bus}}\right]$ matrix of the system, KCL equations are required at all the phase (except inverter bus), neutral and ground buses of the system. The details of KCL equations at all the buses (except at inverter bus) of the unbalanced three phase four wire multigrounded distribution system have already been described in eqs. (5.82)-(5.92) of Subsection 5.3.2 of Chapter 5. With the addition of IBDG at j^{th} bus of the system,

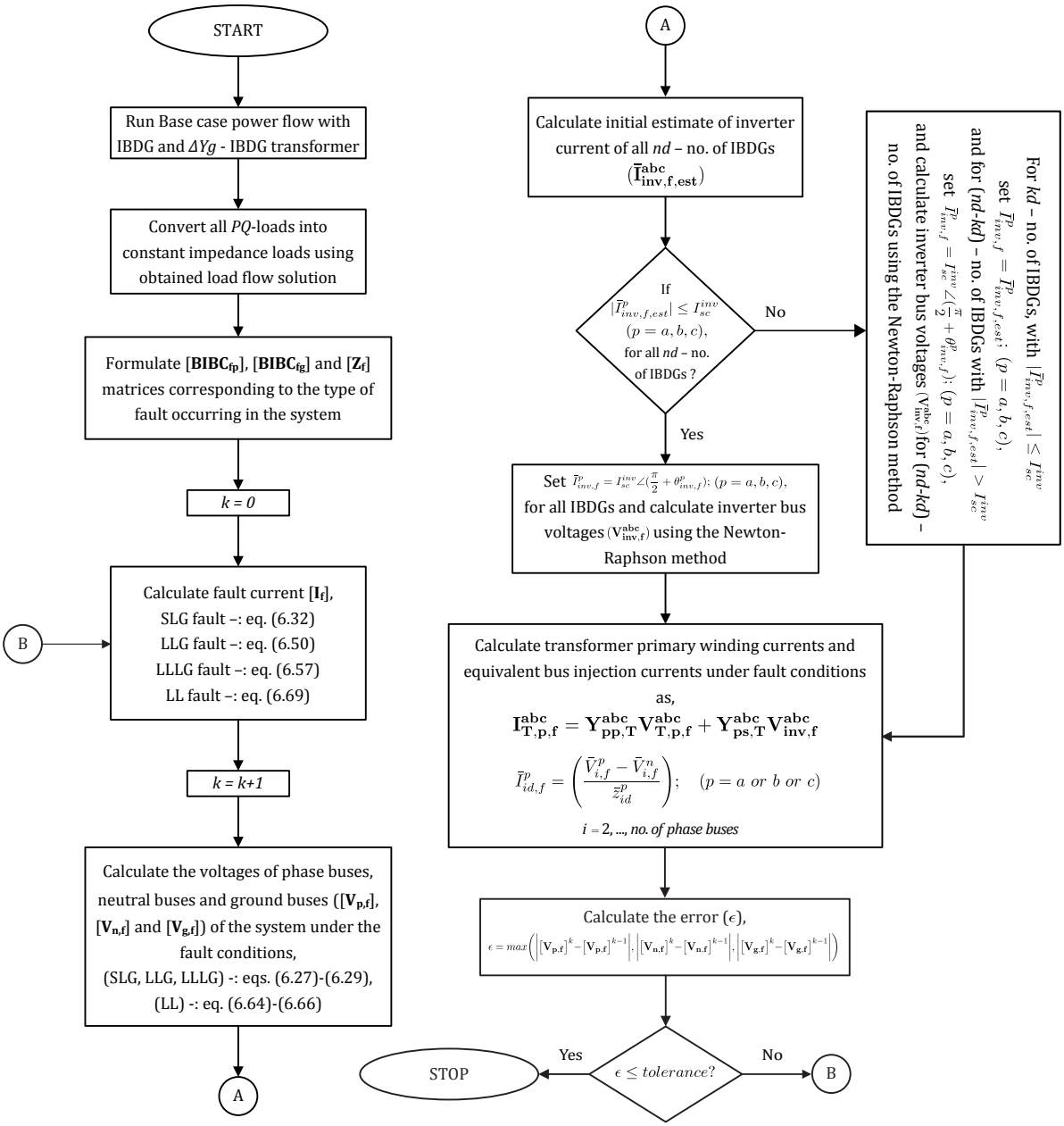

Figure 6.3: Flow-chart of the proposed $\left[\mathbf{BIBC}\right]$ matrix based short-circuit analysis method in the presence of IBDG and Δ-Y_g IBDG transformer

through a Δ-Y_g IBDG transformer, the KCL equation at j^{th} bus of the system shown in Fig. 6.1 will be modified as,

$$\mathbf{Y}_{\mathbf{ji}}^{\mathbf{abcng}}\mathbf{V}_{\mathbf{i}}^{\mathbf{abcng}} + \mathbf{Y}_{\mathbf{jj\_new}}^{\mathbf{abcng}}\mathbf{V}_{\mathbf{j}}^{\mathbf{abcng}} = -\mathbf{Y}_{\mathbf{ps,T_{(\Delta-Y_g)}}}^{\mathbf{abcng}}\mathbf{V}_{\mathbf{inv,st}}^{\mathbf{abcng}} \tag{6.70}$$

where, $\mathbf{Y}_{\mathbf{jj\_new}}^{\mathbf{abcng}} = \mathbf{Y}_{\mathbf{jj}}^{\mathbf{abcng}} + \mathbf{Y}_{\mathbf{pp,T_{(\Delta-Y_g)}}}^{\mathbf{abcng}}$,

$$\mathbf{Y}^{\mathbf{abcng}}_{\mathbf{pp,T_{(\Delta-Y_g)}}} = \begin{bmatrix} \bar{Y}^{aa}_{pp,T} & \bar{Y}^{ab}_{pp,T} & \bar{Y}^{ac}_{pp,T} & 0 & 0 \\ \bar{Y}^{ba}_{pp,T} & \bar{Y}^{bb}_{pp,T} & \bar{Y}^{bc}_{pp,T} & 0 & 0 \\ \bar{Y}^{ca}_{pp,T} & \bar{Y}^{cb}_{pp,T} & \bar{Y}^{cc}_{pp,T} & 0 & 0 \\ 0 & 0 & 0 & 0 & 0 \\ 0 & 0 & 0 & 0 & 0 \end{bmatrix}; \quad \mathbf{Y}^{\mathbf{abcng}}_{\mathbf{ps,T_{(\Delta-Y_g)}}} = \begin{bmatrix} \bar{Y}^{aa}_{ps,T} & \bar{Y}^{ab}_{ps,T} & \bar{Y}^{ac}_{ps,T} & 0 & 0 \\ \bar{Y}^{ba}_{ps,T} & \bar{Y}^{bb}_{ps,T} & \bar{Y}^{bc}_{ps,T} & 0 & 0 \\ \bar{Y}^{ca}_{ps,T} & \bar{Y}^{cb}_{ps,T} & \bar{Y}^{cc}_{ps,T} & 0 & 0 \\ 0 & 0 & 0 & 0 & 0 \\ 0 & 0 & 0 & 0 & 0 \end{bmatrix};$$

$\mathbf{V}^{\mathbf{abcng}}_{\mathbf{inv,st}} = \begin{bmatrix} \bar{V}^{a}_{inv,st} & \bar{V}^{b}_{inv,st} & \bar{V}^{c}_{inv,st} & 0 & 0 \end{bmatrix}^T$ is the inverter bus voltage vector, obtained from pre-fault steady state load flow solution. As mutual coupling has been considered only between primary and secondary phases of IBDG transformer, the rows and columns of matrices $\mathbf{Y}^{\mathbf{abcng}}_{\mathbf{pp,T_{(\Delta-Y_g)}}}$ and $\mathbf{Y}^{\mathbf{abcng}}_{\mathbf{ps,T_{(\Delta-Y_g)}}}$, corresponding to neutral and ground buses, are zero. Also, the neutral point of the IBDG is solidly grounded (as shown in Fig. 6.1), therefore, the elements of the inverter bus voltage vector $\mathbf{V}^{\mathbf{abcng}}_{\mathbf{inv,st}}$, corresponding to the neutral and ground buses, are zero. The KCL equations of the system (except at the inverter bus) shown in Fig. 6.1 can then be written in the matrix form as,

$$\left[\mathbf{Y_{bus\_Tm}}\right] \cdot \left[\mathbf{V}\right] = \left[\mathbf{I}\right] \tag{6.71}$$

The size of $\left[\mathbf{Y_{bus\_Tm}}\right]$ matrix for the unbalanced three-phase four wire multigrounded distribution system with IBDG is exactly same as for the system without IBDG. Once, the $\left[\mathbf{Y_{bus\_Tm}}\right]$ matrix of the system is formed, the elements of this matrix will be modified corresponding to the type of fault occurring in the system. The procedure of modifying the elements of $\left[\mathbf{Y_{bus\_Tm}}\right]$ matrix, for different type of unsymmetrical faults is similar to the procedure given in the Subsections 5.3.2(a)-(d) of Chapter 5. Therefore, the initial value of bus voltages under the fault conditions are then calculated by using eq. (6.71) with the modified bus admittance matrix. The initial estimate of inverter current under the fault conditions is then made as,

$$\mathbf{I}^{\mathbf{abc}}_{\mathbf{inv,f,est}} = \mathbf{Y}^{\mathbf{abc}}_{\mathbf{sp,T}}\mathbf{V}^{\mathbf{abc}}_{\mathbf{j,f}} + \mathbf{Y}^{\mathbf{abc}}_{\mathbf{ss,T}}\mathbf{V}^{\mathbf{abc}}_{\mathbf{inv,st}} \tag{6.72}$$

Now, depending upon the magnitude of $\mathbf{I}^{\mathbf{abc}}_{\mathbf{inv,f,est}}$, there can be two possible cases of inverter operation during fault as discussed in Subsection 3.2.2 of Chapter 3,

Case 1: If $|\bar{I}^{p}_{inv,f,est}| \leq I^{inv}_{sc}$ (short-circuit current capacity of the inverter); (p = a,b,c)

If the magnitude of estimated inverter current $|\bar{I}^{p}_{inv,f,est}|$ for each phase ($p = a, b, c$), calculated using eq. (6.72), is less than the short-circuit capacity of the inverter (I^{inv}_{sc}), then the estimated voltages of phase buses, neutral buses and ground buses are the final values of the voltages of the system under the fault conditions.

Case 2: If $|\bar{I}^{p}_{inv,f,est}| > I^{inv}_{sc}$; ($p$=$a$, or b, or c)

In this case, the estimated inverter current magnitude of the inverter is restricted to its short-circuit capacity (I^{inv}_{sc}), by operating the inverter in constant current control mode (as discussed in Subsection 3.2.2 of Chapter 3). Hence the post fault inverter current is given as,

$$\bar{I}^{p}_{inv,f} = |I^{p}_{inv,f}|\angle\Psi^{p}_{inv,f} = I^{inv}_{sc}\angle\Psi^{p}_{inv,f}; \quad (p = a, b, c) \tag{6.73}$$

where $\Psi^{p}_{inv,f}$ is the unknown inverter current angle corresponding to phase 'p' under the fault conditions. To solve these unknown angles, it is assumed that, $\mathbf{\Psi^{abc}_{inv,f}} = \frac{\pi}{2} + \theta^{\mathbf{abc}}_{\mathbf{inv,f}}$, where $\theta^{\mathbf{abc}}_{\mathbf{inv,f}}$ is the three phase voltage angle vector of the inverter bus under the fault conditions. With the unknown inverter current angles ($\mathbf{\Psi^{abc}_{inv,f}}$), the set of KCL equations of the distribution system (eq. (6.71)) become non-linear equations. To solve these set of non-linear equations to obtain the values of bus voltages under the fault conditions, numerical method (Newton Raphson method) is been used in this work. The details of the Newton-Raphson method for the unbalanced three-phase distribution system with IBDG is given in Subsection 3.2.2 of Chapter 3. This method can also be applicable to the unbalanced three-phase four wire multigrounded distribution system with IBDG. Hence, the voltages of phase buses, neutral buses and ground buses of the unbalanced distribution system under the fault conditions, with the above given inverter control strategy, have been obtained by the method proposed in Subsection 3.2.2 of Chapter 3.

Steps of algorithm for $\mathbf{[Y_{bus}]}$ ***matrix based short-circuit analysis method for the unbalanced three phase four wire multigrounded radial distribution system in the presence of IBDG and*** Δ***-***Y_g ***IBDG transformer***

1. Run the base case power flow of the unbalanced three phase four wire multigrounded distribution system with IBDG and Δ-Y_g IBDG transformer, using the proposed load flow method as discussed in Section 6.2.1 of this chapter.

2. Convert all PQ-loads into constant impedance loads using the obtained pre-fault load flow solution.

3. Formulate the $\mathbf{[Y_{bus\_Tm}]}$ matrix of the unbalanced three phase four wire multigrounded system with IBDG and Δ-Y_g IBDG transformer, using the formulation discussed in Subsection 6.2.2.2.

4. Modify $\mathbf{[Y_{bus\_Tm}]}$ matrix corresponding to the type of fault occurring in the system, using eq. (5.96) for SLG fault, eq. (5.102) for LLG fault, eq. (5.108) for LLLG fault and eq. (5.112) for LL fault given in Chapter 5.

5. Calculate the values of bus voltages under the fault conditions using eq. (6.71) with the modified $\mathbf{[Y_{bus\_Tm}]}$ matrix.

6. Calculate the inverter current $\mathbf{I^{abc}_{inv,f,est}}$ of the IBDG under fault conditions using eq. (6.72).

7. Check the condition, whether $|\bar{I}^{p}_{inv,f,est}| \leq I^{inv}_{sc}$; $(p = a, b, c)$, for all IBDGs. The three possible cases are:

   Case (A): If $|\bar{I}^{p}_{inv,f,est}| \leq \bar{I}^{inv}_{sc}$, $(p = a, b, c)$ for all nd - no. of IBDGs, then go to step 6, else

   Case (B): If $|\bar{I}^{p}_{inv,f,est}|$, $(p = a, b, c)$ of all nd - no. of IBDGs are greater than their corresponding short-circuit current capacities, then operate the inverter in constant current mode with $\bar{I}^{p}_{inv,f} = I^{inv}_{sc} \underline{\angle(\frac{\pi}{2} + \theta^{p}_{inv,f})}$, $(p = a, b, c)$ for all IBDGs and recalculate the bus voltages of the system under the fault conditions using the Newton-Raphson method given in Subsection 3.2.2 of Chapter 3 and go to step 8, else

   Case (C): If out of nd - no. of IBDGs, for kd - no. of IBDGs $|\bar{I}^{p}_{inv,f,est}| \leq I^{inv}_{sc}$, $(p = a, b, c)$ and for the remaining $(nd - kd)$ - no. of IBDGs $|\bar{I}^{p}_{inv,f,est}| > I^{inv}_{sc}$, $(p = a, b, c)$, then set $\bar{I}^{p}_{inv,f} = I^{inv}_{sc}\angle(\frac{\pi}{2} + \theta^{p}_{inv,f})$, $(p = a, b, c)$ for $(nd - kd)$ - no. of IBDGs, while for kd - no. of IBDGs set $\mathbf{\bar{I}^{abc}_{inv,f}} = \mathbf{\bar{I}^{abc}_{inv,f,est}}$ and recalculate the bus voltages of the system under the fault conditions using the Newton-Raphson method given in subsection 3.2.2 of Chapter 3 and go to step 8

8. Calculate fault currents using eq. (5.93) for SLG, eq. (5.98) for LLG, eq. (5.103) for LLLG and eq. (5.109) for LL fault of Chapter 5. Also calculate branch currents under the fault conditions using eq. (5.97) of Chapter 5.

6.3 Three phase four wire multigrounded radial distribution system with IBDG and Y_g-Y_g IBDG transformer

The unbalanced three-phase four wire multigrounded distribution system with IBDG and Y_g-Y_g IBDG transformer is shown in Fig. 6.4. In this system, an IBDG is connected at j^{th} bus of the system through a step-down Yg-Yg IBDG transformer. The primary as well as secondary windings of IBDG transformer are star connected with ground return (through local ground) [151]. The neutral point on the primary side of the IBDG transformer is connected to the local ground g_j at j^{th} bus (where primary windings of the the IBDG transformer are connected) through an impedance $\bar{Z}_{gtp}$ (grounding impedance on primary side of the IBDG transformer). Again, it is assumed that the star point of the IBDG is solidly grounded, the inverter current of the IBDG is confined only to the secondary winding of the IBDG transformer. The grounding impedance on the secondary side of the IBDG transformer is $\bar{Z}_{gts}$ (connected between the neutral and ground on the secondary side of the IBDG transformer, as shown in Fig. 6.4). Hence, the neutral to ground currents on the

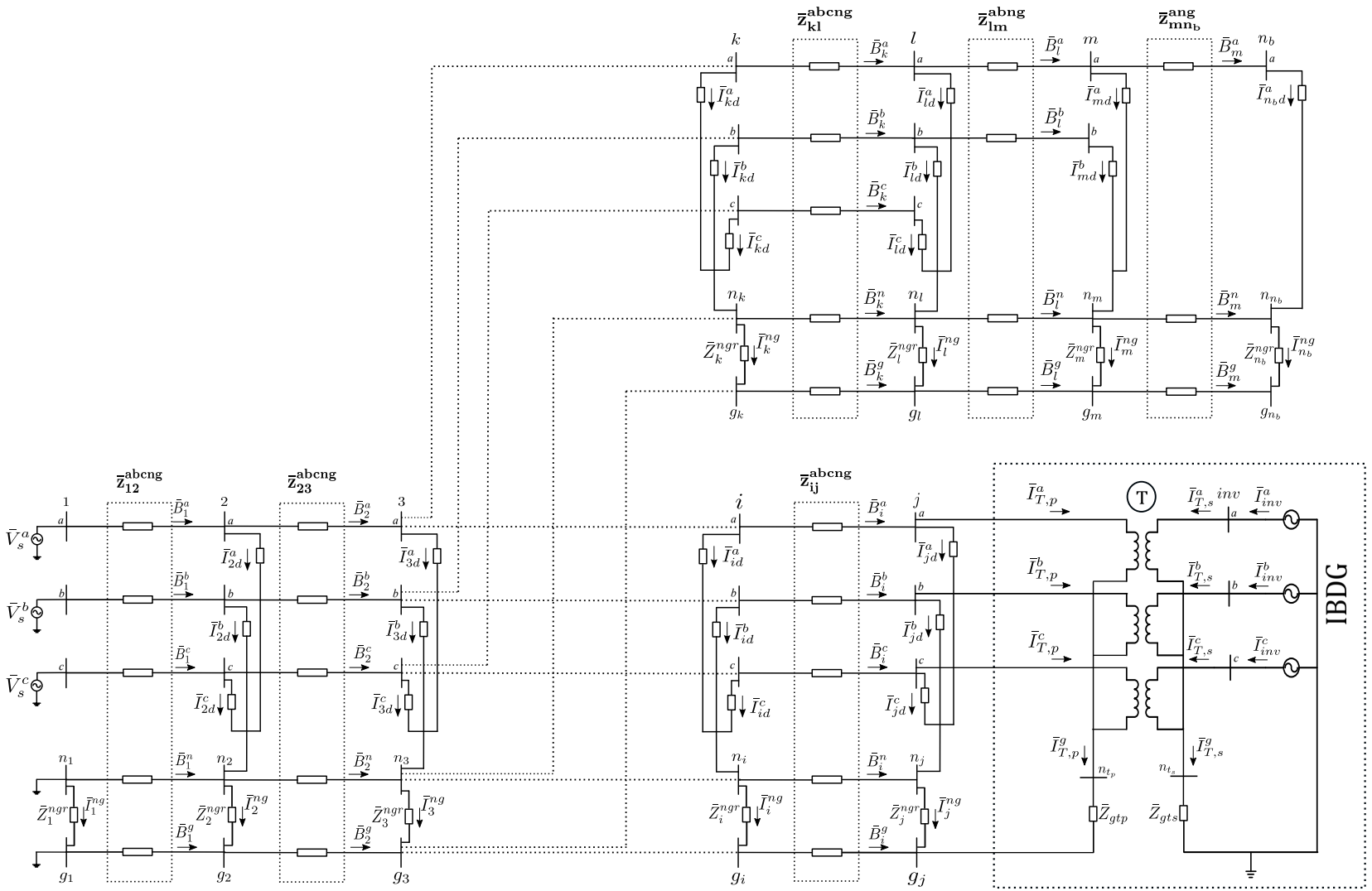

Figure 6.4: An unbalanced three phase four wire multigrounded radial distribution system with IBDG and Y_g-Y_g IBDG transformer

primary and secondary side of the IBDG transformer are given as,

$$\begin{aligned}\bar{I}^{g}_{T,p} &= \bar{I}^{a}_{T,p} + \bar{I}^{b}_{T,p} + \bar{I}^{c}_{T,p} \\ \bar{I}^{g}_{T,s} &= \bar{I}^{a}_{T,s} + \bar{I}^{b}_{T,s} + \bar{I}^{c}_{T,s} = \bar{I}^{a}_{inv} + \bar{I}^{b}_{inv} + \bar{I}^{c}_{inv}\end{aligned} \tag{6.74}$$

The nodal admittance matrix based model of the transformer, given in eq. (6.1), is only applicable to the case where the neutral point on the primary and secondary side of the transformer is perfectly grounded, and is at zero potential. But in this case, the voltage at the neutral point on primary as well as secondary side of the transformer is calculated as,

$$\begin{aligned}\bar{V}^{n}_{T,p} &= \bar{Z}_{gtp}\bar{I}^{g}_{T,p} + \bar{V}^{g}_{j} = \bar{Z}_{gtp}(\bar{I}^{a}_{T,p} + \bar{I}^{b}_{T,p} + \bar{I}^{c}_{T,p}) + \bar{V}^{g}_{j} \\ \bar{V}^{n}_{T,s} &= \bar{Z}_{gts}\bar{I}^{g}_{T,s} = \bar{Z}_{gts}(\bar{I}^{a}_{inv} + \bar{I}^{b}_{inv} + \bar{I}^{c}_{inv})\end{aligned} \tag{6.75}$$

Therefore, the nodal admittance matrix of Y_g-Y_g transformer, connected to an unbalanced three-phase four wire multigrounded distribution system, will be modified as discussed next.

Let us consider the Y_g-Y_g-0 configuration of the IBDG transformer, as shown in Fig. 6.4. The currents in the primary and secondary windings of the Y_g-Y_g-0 transformer can be written as,

Primary winding currents

$$\begin{aligned}\bar{I}^{a}_{T,p} &= y_t[(\bar{V}^{a}_{T,p} - \bar{V}^{n}_{T,p}) - (\bar{V}^{a}_{T,s} - \bar{V}^{n}_{T,s})] \\ \bar{I}^{b}_{T,p} &= y_t[(\bar{V}^{b}_{T,p} - \bar{V}^{n}_{T,p}) - (\bar{V}^{b}_{T,s} - \bar{V}^{n}_{T,s})] \\ \bar{I}^{c}_{T,p} &= y_t[(\bar{V}^{c}_{T,p} - \bar{V}^{n}_{T,p}) - (\bar{V}^{c}_{T,s} - \bar{V}^{n}_{T,s})]\end{aligned} \tag{6.76}$$

Secondary winding currents

$$\begin{aligned}\bar{I}^{a}_{T,s} &= -\bar{I}^{a}_{T,p} = -y_t[(\bar{V}^{a}_{T,p} - \bar{V}^{n}_{T,p}) - (\bar{V}^{a}_{T,s} - \bar{V}^{n}_{T,s})] \\ \bar{I}^{b}_{T,s} &= -\bar{I}^{b}_{T,p} = -y_t[(\bar{V}^{b}_{T,p} - \bar{V}^{n}_{T,p}) - (\bar{V}^{b}_{T,s} - \bar{V}^{n}_{T,s})] \\ \bar{I}^{c}_{T,s} &= -\bar{I}^{c}_{T,p} = -y_t[(\bar{V}^{c}_{T,p} - \bar{V}^{n}_{T,p}) - (\bar{V}^{c}_{T,s} - \bar{V}^{n}_{T,s})]\end{aligned} \tag{6.77}$$

The eqs. (6.76) and (6.77) combined can be put in the matrix form as,

$$\begin{bmatrix}\bar{I}^{a}_{T,p}\\ \bar{I}^{b}_{T,p}\\ \bar{I}^{c}_{T,p}\\ \bar{I}^{a}_{T,s}\\ \bar{I}^{b}_{T,s}\\ \bar{I}^{c}_{T,s}\end{bmatrix} = y_t \left[\begin{array}{ccc|ccc} 1 & 0 & 0 & -1 & 0 & 0 \\ 0 & 1 & 0 & 0 & -1 & 0 \\ 0 & 0 & 1 & 0 & 0 & -1 \\ \hline -1 & 0 & 0 & 1 & 0 & 0 \\ 0 & -1 & 0 & 0 & 1 & 0 \\ 0 & 0 & -1 & 0 & 0 & 1 \end{array}\right] \begin{bmatrix}\bar{V}^{a}_{T,p}\\ \bar{V}^{b}_{T,p}\\ \bar{V}^{c}_{T,p}\\ \bar{V}^{a}_{T,s}\\ \bar{V}^{b}_{T,s}\\ \bar{V}^{c}_{T,s}\end{bmatrix} + y_t \left[\begin{array}{cc} -1 & 1 \\ -1 & 1 \\ -1 & 1 \\ \hline 1 & -1 \\ 1 & -1 \\ 1 & -1 \end{array}\right] \begin{bmatrix}\bar{V}^{n}_{T,p}\\ \bar{V}^{n}_{T,s}\end{bmatrix} \tag{6.78}$$

$$\begin{bmatrix} \mathbf{I^{abc}_{T,p}} \\ \mathbf{I^{abc}_{T,s}} \end{bmatrix} = \begin{bmatrix} \mathbf{Y^{abc}_{pp,T}} & \mathbf{Y^{abc}_{ps,T}} \\ \mathbf{Y^{abc}_{sp,T}} & \mathbf{Y^{abc}_{ss,T}} \end{bmatrix} \begin{bmatrix} \mathbf{V^{abc}_{T,p}} \\ \mathbf{V^{abc}_{T,s}} \end{bmatrix} + \begin{bmatrix} \mathbf{Y^{n}_{pp,T}} & \mathbf{Y^{n}_{ps,T}} \\ \mathbf{Y^{n}_{sp,T}} & \mathbf{Y^{n}_{ss,T}} \end{bmatrix} \begin{bmatrix} \mathbf{V^{n}_{T,p}} \\ \mathbf{V^{n}_{T,s}} \end{bmatrix} \tag{6.79}$$

Therefore, the modified nodal admittance matrix based current equation of Y_g-Y_g IBDG transformer, shown in Fig. 6.4, can be written as,

$$\begin{bmatrix} \mathbf{I^{abc}_{T,p}} \\ \mathbf{I^{abc}_{inv}} \end{bmatrix} = \begin{bmatrix} \mathbf{Y^{abc}_{pp,T}} & \mathbf{Y^{abc}_{ps,T}} \\ \mathbf{Y^{abc}_{sp,T}} & \mathbf{Y^{abc}_{ss,T}} \end{bmatrix} \begin{bmatrix} \mathbf{V^{abc}_{j}} \\ \mathbf{V^{abc}_{inv}} \end{bmatrix} + \begin{bmatrix} \mathbf{Y^{n}_{pp,T}} & \mathbf{Y^{n}_{ps,T}} \\ \mathbf{Y^{n}_{sp,T}} & \mathbf{Y^{n}_{ss,T}} \end{bmatrix} \begin{bmatrix} \mathbf{V^{n}_{T,p}} \\ \mathbf{V^{n}_{T,s}} \end{bmatrix} \tag{6.80}$$

6.3.1 Load flow analysis with Star-grounded/Star-grounded (Y_g-Y_g) IBDG transformer for the connection of IBDG

The proposed load flow method for the unbalanced three-phase four wire multigrounded distribution system in the presence of IBDG and Y_g-Y_g IBDG transformer is also based on $[\mathbf{BIBC}]$ and $[\mathbf{BCBV}]$ matrices of the system, as discussed in the previous section.

6.3.1.1 Formulation of $[\mathbf{BIBC}]$ matrices

The currents of the phase branches of the distribution system can be obtained in terms of equivalent injection currents, by applying KCL equation at each phase bus (excluding substation bus and inverter bus) of the distribution system shown in Fig. 6.4. The currents of the phase branches can be written as (similar to the current equations given in eq. (6.2) for the case of Δ-Y_g IBDG transformer),

$$\left[\mathbf{B_p}\right] = \left[\mathbf{BIBC_p}\right]\left[\mathbf{I_L}\right] + \left[\mathbf{TIBC_{Tm}}\right]\left[\mathbf{I_{T,p}}\right] \tag{6.81}$$

As there is no physical connection between the neutral bus of the system (at the location of j^{th} bus) and of the IBDG transformer, the neutral currents for the distribution system shown in Fig. 6.4 (with IBDG and Y_g-Y_g IBDG transformer) are exactly same as the neutral currents of system shown in Fig. 5.1 (without IBDG and IBDG transformer) and are given as (from eq. (5.8) of Chapter 5),

$$\left[\mathbf{B_n}\right] = -\left[\mathbf{BIBC_{pn}}\right]\left[\mathbf{I_L}\right] + \left[\mathbf{BIBC_g}\right]\left[\mathbf{I_{ng}}\right] \tag{6.82}$$

From Fig. 6.4, it is observed that the neutral point at the primary side of the IBDG transformer is connected to the ground bus g_j at j^{th} bus through an impedance of $\bar{Z}_{gtp}$. Therefore, the modification in ground currents

of the system are given as,

$$\begin{aligned}
\bar{B}_1^g &= -\bar{I}_2^{ng} - \bar{I}_3^{ng} - \cdots - \bar{I}_i^{ng} - \bar{I}_j^{ng} - \cdots - \bar{I}_k^{ng} - \bar{I}_l^{ng} - \bar{I}_m^{ng} - \bar{I}_{n_b}^{ng} - \bar{I}_{T,p}^g \\
\bar{B}_2^g &= -\bar{I}_3^{ng} - \cdots - \bar{I}_i^{ng} - \bar{I}_j^{ng} - \cdots - \bar{I}_k^{ng} - \bar{I}_l^{ng} - \bar{I}_m^{ng} - \bar{I}_{n_b}^{ng} - \bar{I}_{T,p}^g \\
\bar{B}_i^g &= -\bar{I}_j^{ng} - \bar{I}_{T,p}^g \\
\bar{B}_k^g &= -\bar{I}_l^{ng} - \bar{I}_m^{ng} - \bar{I}_{n_b}^{ng} \\
\bar{B}_l^g &= -\bar{I}_m^{ng} - \bar{I}_{n_b}^{ng} \\
\bar{B}_m^g &= -\bar{I}_{n_b}^{ng}
\end{aligned} \tag{6.83}$$

$$\left[\mathbf{B_g}\right] = -\left[\mathbf{BIBC_g}\right]\left[\mathbf{I_{ng}}\right] - \left[\mathbf{BIBC_{gT}}\right]\left[\mathbf{I_{gT}}\right] \tag{6.84}$$

where, $\left[\mathbf{BIBC_g}\right]$ matrix has already been described in eq. (5.8) of Subsections 5.2.1.3 of Chapter 5 and

$$\begin{aligned}
\left[\mathbf{BIBC_{gT}}\right] &= \left[\mathbf{BIBC_g}(:, T_b g)\right] = \begin{bmatrix} 1 & 1 & \cdots & 1 & \cdots & 0 & 0 & 0 \end{bmatrix}^T \\
\left[\mathbf{I_{gT}}\right] &= \bar{I}_{T,p}^g = \bar{I}_{T,p}^a + \bar{I}_{T,p}^b + \bar{I}_{T,p}^c
\end{aligned}$$

The $\left[\mathbf{BIBC_{gT}}\right]$ matrix contains column vector of $\left[\mathbf{BIBC_g}\right]$ matrix corresponding to the ground g at the location of transformer bus T_b (in Fig. 6.4, T_b = j). The size of $\left[\mathbf{BIBC_{gT}}\right]$ matrix for an unbalanced three phase four wire multigrounded distribution system, having u three-phase, v two-phase, w single-phase, $(u+v+w)$ neutral and $(u+v+w)$ ground buses with nt number of IBDG transformers, will be $(u+v+w-1) \times nt$.

Now, the voltage equations of the phase buses, neutral buses and ground buses are similar to the case of Δ-Y_g IBDG transformer is used in the distribution system, as given in Subsection 6.2.1.2 (eqs. (6.6)-(6.8)). Therefore, the voltages of phase buses, neutral buses and ground buses are calculated with the help of eqs. (6.6)-(6.8), (6.81), (6.82) and (6.84) as,

$$\left[\mathbf{V_p}\right] = \left[\mathbf{V_{ss}}\right] - \left[\mathbf{DLF_1}\right]\left[\mathbf{I_L}\right] - \left[\mathbf{DLF_2}\right]\left[\mathbf{I_{ng}}\right] - \left[\mathbf{DLF_{Tm_p}}\right]\left[\mathbf{I_{T,p}}\right] - \left[\mathbf{DLF_{GT_p}}\right]\left[\mathbf{I_{gT}}\right] \tag{6.85}$$

$$\left[\mathbf{V_n}\right] = \left[\mathbf{V_{sn}}\right] - \left[\mathbf{DLF_3}\right]\left[\mathbf{I_L}\right] - \left[\mathbf{DLF_4}\right]\left[\mathbf{I_{ng}}\right] - \left[\mathbf{DLF_{Tm_n}}\right]\left[\mathbf{I_{T,p}}\right] - \left[\mathbf{DLF_{GT_n}}\right]\left[\mathbf{I_{gT}}\right] \tag{6.86}$$

$$\left[\mathbf{V_g}\right] = \left[\mathbf{V_{sg}}\right] - \left[\mathbf{DLF_5}\right]\left[\mathbf{I_L}\right] - \left[\mathbf{DLF_6}\right]\left[\mathbf{I_{ng}}\right] - \left[\mathbf{DLF_{Tm_g}}\right]\left[\mathbf{I_{T,p}}\right] - \left[\mathbf{DLF_{GT_g}}\right]\left[\mathbf{I_{gT}}\right] \tag{6.87}$$

where,

$$\left[\mathbf{DLF_{GT_p}}\right] = -\left[\mathbf{BCBV_{pg}}\right]\left[\mathbf{BIBC_{gT}}\right]$$

$$\left[\mathbf{DLF_{GT_n}}\right] = -\left[\mathbf{BCBV_{pn}}\right]\left[\mathbf{BIBC_{gT}}\right]$$

$$\left[\mathbf{DLF_{GT_g}}\right] = -\left[\mathbf{BCBV_g}\right]\left[\mathbf{BIBC_{gT}}\right]$$

The neutral to ground current $\left[\mathbf{I_{ng}}\right]$ is then calculated using eqs. (6.13), (6.86) and (6.87)

$$\begin{aligned}\left[\mathbf{I_{ng}}\right] &= \left[\mathbf{Z_{FNG}}\right]^{-1}\left\{\left[\mathbf{V_{sn}}\right]-\left[\mathbf{V_{sg}}\right]+\left[\left[\mathbf{DLF_5}\right]-\left[\mathbf{DLF_3}\right]\right]\left[\mathbf{I_L}\right]+\left[\mathbf{DLF_{Tm_{gn}}}\right]\left[\mathbf{I_{T,p}}\right]\right. \\ &+ \left.\left[\mathbf{DLF_{GT_{gn}}}\right]\left[\mathbf{I_{gT}}\right]\right\} \end{aligned} \tag{6.88}$$

where,

$$\left[\mathbf{DLF_{GT_{gn}}}\right]=\left[\mathbf{DLF_{GT_g}}\right]-\left[\mathbf{DLF_{GT_n}}\right]$$

Therefore, the voltages of the phase buses (except inverter bus), neutral buses and ground buses can be obtained using eqs. (6.85)-(6.88) as,

$$\left[\mathbf{V_p}\right]=\left[\mathbf{V_{ss}}\right]-\left[\mathbf{F_{1ng}}\right]\left\{\left[\mathbf{V_{sn}}\right]-\left[\mathbf{V_{sg}}\right]\right\}-\left[\mathbf{F_{1PLD}}\right]\left[\mathbf{I_L}\right]-\left[\mathbf{F_{1Tm}}\right]\left[\mathbf{I_{T,p}}\right]-\left[\mathbf{F_{1GT}}\right]\left[\mathbf{I_{gT}}\right] \tag{6.89}$$

$$\left[\mathbf{V_n}\right]=\left[\mathbf{F_{2nn}}\right]\left[\mathbf{V_{sn}}\right]-\left[\mathbf{F_{2gg}}\right]\left[\mathbf{V_{sg}}\right]-\left[\mathbf{F_{2PLD}}\right]\left[\mathbf{I_L}\right]-\left[\mathbf{F_{2Tm}}\right]\left[\mathbf{I_{T,p}}\right]-\left[\mathbf{F_{2GT}}\right]\left[\mathbf{I_{gT}}\right] \tag{6.90}$$

$$\left[\mathbf{V_g}\right]=\left[\mathbf{F_{3gg}}\right]\left[\mathbf{V_{sg}}\right]-\left[\mathbf{F_{3nn}}\right]\left[\mathbf{V_{sn}}\right]-\left[\mathbf{F_{3PLD}}\right]\left[\mathbf{I_L}\right]-\left[\mathbf{F_{3Tm}}\right]\left[\mathbf{I_{T,p}}\right]-\left[\mathbf{F_{3GT}}\right]\left[\mathbf{I_{gT}}\right] \tag{6.91}$$

where,

$$\left[\mathbf{F_{1GT}}\right]=\left[\mathbf{DLF_2}\right]\left[\mathbf{Z_{FNG}}\right]^{-1}\left[\mathbf{DLF_{GT_{gn}}}\right]+\left[\mathbf{DLF_{GT_p}}\right]$$

$$\left[\mathbf{F_{2GT}}\right]=\left[\mathbf{DLF_4}\right]\left[\mathbf{Z_{FNG}}\right]^{-1}\left[\mathbf{DLF_{GT_{gn}}}\right]+\left[\mathbf{DLF_{GT_n}}\right]$$

$$\left[\mathbf{F_{3GT}}\right]=\left[\mathbf{DLF_6}\right]\left[\mathbf{Z_{FNG}}\right]^{-1}\left[\mathbf{DLF_{GT_{gn}}}\right]+\left[\mathbf{DLF_{GT_g}}\right]$$

The inverter bus voltage of the system shown in Fig. 6.4 is calculated using eq. (6.80) as,

$$\mathbf{V_{inv}^{abc}}=\mathbf{Y_{ss,T}^{abc}}^{-1}\left(\mathbf{I_{inv}^{abc}}-\mathbf{Y_{sp,T}^{abc}V_j^{abc}}-\mathbf{Y_{sp,T}^{n}V_{T,p}^{n}}-\mathbf{Y_{ss,T}^{n}V_{T,s}^{n}}\right) \tag{6.92}$$

Steps of algorithm for the load flow analysis of unbalanced three phase four wire multigrounded radial distribution system in the presence of IBDG and Y_g-Y_g IBDG transformer

1. Initialize and then generate the $\left[\mathbf{BIBC}\right]$ matrices for the phase branch, neutral and ground currents, and $\left[\mathbf{BCBV}\right]$ matrices for the voltages of phase buses, neutral buses and ground buses of the unbalanced three-phase four wire multigrounded distribution system with IBDG and Y_g-Y_g IBDG transformer.

2. Set the iteration counter $k=0$. Also, set the values of all phase a bus voltages at $(1.0+j0.0)$ p.u., phase b bus voltages at $(-0.500-j0.866)$ p.u., phase c bus voltages at $(-0.500+j0.866)$ p.u. and all neutral and ground bus voltages at $(0.0+j0.0)$ p.u. throughout the system.

3. Calculate the equivalent bus injection currents $\left[\mathbf{I_L}\right]^k$ at all the phase buses of the system using eq. (5.3) of Chapter 5. Also, calculate the inverter current of the IBDG as,

$$\bar{I}^p_{inv} = \bar{I}^p_{T,s} = \left(\frac{\bar{S}^p_{dg}}{\bar{V}^p_{inv} - \bar{V}^n_{T,s}}\right)^* = \left(\frac{P^p_{dg} + jQ^p_{dg}}{\bar{V}^p_{inv} - \bar{V}^n_{T,s}}\right)^*; \quad (p = a, b, c)$$

where, $\bar{S}^p_{dg}$ is the complex power injected by the IBDG at phase p of inverter bus; P^p_{dg} and Q^p_{dg} are the active and reactive power generated by the IBDG at phase p of inverter bus, respectively; $\bar{V}^p_{inv}$ is the p^{th} phase voltage of inverter bus; $\bar{V}^n_{T,s}$ is the neutral bus voltage on the secondary side of the IBDG transformer.

4. Calculate the primary winding currents $\left[\mathbf{I^{abc}_{T,p}}\right]^k$ of the Y_g-Y_g IBDG transformer by using eq. (6.80).

5. $k = k + 1$.

6. Calculate the voltages of phase buses, neutral buses and ground buses $\left([\mathbf{V_p}]^k,\ [\mathbf{V_n}]^k \text{ and } [\mathbf{V_g}]^k\right)$ of the system using eqs. (6.89)-(6.91). Also, calculate the neutral bus voltages on the primary and secondary side of the transformer ($\bar{V}^n_{T,p}$ and $\bar{V}^n_{T,s}$) using eq. (6.75). The inverter bus voltage $\left[\mathbf{V^{abc}_{inv}}\right]^k$ of the IBDG is then calculated by using eq. (6.92).

7. Calculate the error (ϵ),

$$\epsilon = max\left(\left|\left[\mathbf{V_p}\right]^k - \left[\mathbf{V_p}\right]^{k-1}\right|, \left|\left[\mathbf{V_n}\right]^k - \left[\mathbf{V_n}\right]^{k-1}\right|, \left|\left[\mathbf{V_g}\right]^k - \left[\mathbf{V_g}\right]^{k-1}\right|\right)$$

8. If $\epsilon \geq$ tolerance(1.0×10^{-12}), then go to step 3, else go to the next step.

9. The obtained values of the voltages $\left[\mathbf{V_p}\right]$, $\left[\mathbf{V_n}\right]$ and $\left[\mathbf{V_g}\right]$ are the final values of the load flow solution.

6.3.2 Short-circuit analysis of unbalanced three phase four wire multigrounded radial distribution system with IBDG and Y_g-Y_g IBDG transformer

Two different short-circuit analysis methods have been proposed for the unbalanced three phase four wire multigrounded distribution system with IBDG and Y_g-Y_g IBDG transformer. One of the proposed method is based on $\left[\mathbf{BIBC}\right]$ and $\left[\mathbf{BCBV}\right]$ matrices of the system, while the other one is based on $\left[\mathbf{Y_{bus}}\right]$ matrix of the system. Both the methods are discussed in details in the following sub-sections.

6.3.2.1 Method 1: $\left[\mathrm{BIBC}\right]$ matrix based method

Different short-circuit faults are discussed in the following subsections.

(a) Single line-to-ground (SLG) fault

Let us assume that an SLG fault occurs between the phase a and the local ground g_l at l^{th} bus location through a fault impedance $\bar{z}_f$, as shown in Fig. 6.2(a) [158], and the fault current $\bar{I}_f^a$ is flowing from phase a to the ground g_l at l^{th} bus. Therefore, the phase branch current due to SLG fault can be calculated as (similar to the case discussed in Subsection 6.2.2.1(a) for Δ-Y_g IBDG transformer)

$$\left[\mathbf{B_{p,f}}\right] = \left[\mathbf{BIBC_p}\right]\left[\mathbf{I_L}\right] + \left[\mathbf{TIBC_{Tm}}\right]\left[\mathbf{I_{T,p}}\right] + \left[\mathbf{BIBC_{fp}}\right]\left[\mathbf{I_f}\right] \tag{6.93}$$

where, definition of $\left[\mathbf{BIBC_{fp}}\right]$ matrix for an SLG fault has already been given in eq. (6.19) of Subsection 6.2.2.1(a). Now, the modified ground currents due to SLG fault at phase a of the l^{th} bus of the system, as shown in Fig. 6.4, can be written as,

$$\begin{aligned}
\bar{B}^g_{1,f} &= -\bar{I}^{ng}_2 - \bar{I}^{ng}_3 - \cdots - \bar{I}^{ng}_i - \bar{I}^{ng}_j - \cdots - \bar{I}^{ng}_k - \bar{I}^{ng}_l - \bar{I}^{ng}_m - \bar{I}^{ng}_{n_b} - \bar{I}^g_{T,p} - \bar{I}^a_f \\
\bar{B}^g_{2,f} &= -\bar{I}^{ng}_3 - \cdots - \bar{I}^{ng}_i - \bar{I}^{ng}_j - \cdots - \bar{I}^{ng}_k - \bar{I}^{ng}_l - \bar{I}^{ng}_m - \bar{I}^{ng}_{n_b} - \bar{I}^g_{T,p} - \bar{I}^a_f \\
\bar{B}^g_{i,f} &= -\bar{I}^{ng}_j - \bar{I}^g_{T,p} \\
\bar{B}^g_{k,f} &= -\bar{I}^{ng}_l - \bar{I}^{ng}_m - \bar{I}^{ng}_{n_b} - \bar{I}^a_f \\
\bar{B}^g_{l,f} &= -\bar{I}^{ng}_m - \bar{I}^{ng}_{n_b} \\
\bar{B}^g_{m,f} &= -\bar{I}^{ng}_{n_b}
\end{aligned} \tag{6.94}$$

Hence, the modified ground currents due to SLG fault can be expressed in the matrix form as,

$$\left[\mathbf{B_{g,f}}\right] = -\left[\mathbf{BIBC_g}\right]\left[\mathbf{I_{ng}}\right] - \left[\mathbf{BIBC_{gT}}\right]\left[\mathbf{I_{gT}}\right] - \left[\mathbf{BIBC_{fg}}\right]\left[\mathbf{I_f}\right] \tag{6.95}$$

where, definition of $\left[\mathbf{BIBC_{fg}}\right]$ matrix for an SLG fault has already been given in eq. (6.21) of Subsection 6.2.2.1(a).

Therefore, the voltages of phase buses, neutral buses and ground buses under the fault conditions are calculated using the modified phase and ground currents (using eqs. (6.4),(6.6)-(6.8), (6.93) and (6.95)) as,

$$\begin{aligned}
\left[\mathbf{V_{p,f}}\right] &= \left[\mathbf{V_{ss}}\right] - \left[\mathbf{DLF_1}\right]\left[\mathbf{I_L}\right] - \left[\mathbf{DLF_2}\right]\left[\mathbf{I_{ng}}\right] - \left[\mathbf{DLF_{Tm_p}}\right]\left[\mathbf{I_{T,p}}\right] - \left[\mathbf{DLF_{GT_p}}\right]\left[\mathbf{I_{gT}}\right] \\
&- \left[\mathbf{DFF_1}\right]\left[\mathbf{I_f}\right]
\end{aligned} \tag{6.96}$$

$$\begin{aligned}
\left[\mathbf{V_{n,f}}\right] &= \left[\mathbf{V_{sn}}\right] - \left[\mathbf{DLF_3}\right]\left[\mathbf{I_L}\right] - \left[\mathbf{DLF_4}\right]\left[\mathbf{I_{ng}}\right] - \left[\mathbf{DLF_{Tm_n}}\right]\left[\mathbf{I_{T,p}}\right] - \left[\mathbf{DLF_{GT_n}}\right]\left[\mathbf{I_{gT}}\right] \\
&- \left[\mathbf{DFF_2}\right]\left[\mathbf{I_f}\right]
\end{aligned} \tag{6.97}$$

$$\begin{aligned}\left[\mathbf{V_{g,f}}\right] &= \left[\mathbf{V_{sg}}\right] - \left[\mathbf{DLF_5}\right]\left[\mathbf{I_L}\right] - \left[\mathbf{DLF_6}\right]\left[\mathbf{I_{ng}}\right] - \left[\mathbf{DLF_{Tm_g}}\right]\left[\mathbf{I_{T,p}}\right] - \left[\mathbf{DLF_{GT_g}}\right]\left[\mathbf{I_{gT}}\right] \\ &- \left[\mathbf{DFF_3}\right]\left[\mathbf{I_f}\right] \end{aligned} \tag{6.98}$$

where, $\left[\mathbf{DFF_1}\right]$, $\left[\mathbf{DFF_2}\right]$ and $\left[\mathbf{DFF_3}\right]$ matrices for an SLG fault have already been defined in eqs. (6.23)-(6.25).

Now, the neutral to ground currents are calculated using the voltages of neutral buses and ground buses under the fault condition (using eqs. (6.13), (6.97) and (6.98)) as,

$$\begin{aligned}\left[\mathbf{I_{ng}}\right] &= \left[\mathbf{Z_{FNG}}\right]^{-1}\left\{\left[\mathbf{V_{sn}}\right] - \left[\mathbf{V_{sg}}\right] + \left[\left[\mathbf{DLF_5}\right] - \left[\mathbf{DLF_3}\right]\right]\left[\mathbf{I_L}\right] + \left[\mathbf{DLF_{Tm_{gn}}}\right]\left[\mathbf{I_{T,p}}\right]\right. \\ &+ \left.\left[\mathbf{DLF_{GT_{gn}}}\right]\left[\mathbf{I_{gT}}\right] + \left[\left[\mathbf{DFF_3}\right] - \left[\mathbf{DFF_2}\right]\right]\left[\mathbf{I_f}\right]\right\} \end{aligned} \tag{6.99}$$

Therefore, the voltages of phase buses, neutral buses and ground buses under the fault conditions are obtained using eqs. (6.96)-(6.99) as,

$$\begin{aligned}\left[\mathbf{V_{p,f}}\right] &= \left[\mathbf{V_{ss}}\right] - \left[\mathbf{F_{1ng}}\right]\left\{\left[\mathbf{V_{sn}}\right] - \left[\mathbf{V_{sg}}\right]\right\} - \left[\mathbf{F_{1PLD}}\right]\left[\mathbf{I_L}\right] - \left[\mathbf{F_{1Tm}}\right]\left[\mathbf{I_{T,p}}\right] - \left[\mathbf{F_{1GT}}\right]\left[\mathbf{I_{gT}}\right] \\ &- \left[\mathbf{DFF_{1n}}\right]\left[\mathbf{I_f}\right] \end{aligned} \tag{6.100}$$

$$\begin{aligned}\left[\mathbf{V_{n,f}}\right] &= \left[\mathbf{F_{2nn}}\right]\left[\mathbf{V_{sn}}\right] - \left[\mathbf{F_{2gg}}\right]\left[\mathbf{V_{sg}}\right] - \left[\mathbf{F_{2PLD}}\right]\left[\mathbf{I_L}\right] - \left[\mathbf{F_{2Tm}}\right]\left[\mathbf{I_{T,p}}\right] - \left[\mathbf{F_{2GT}}\right]\left[\mathbf{I_{gT}}\right] \\ &- \left[\mathbf{DFF_{2n}}\right]\left[\mathbf{I_f}\right] \end{aligned} \tag{6.101}$$

$$\begin{aligned}\left[\mathbf{V_{g,f}}\right] &= \left[\mathbf{F_{3gg}}\right]\left[\mathbf{V_{sg}}\right] - \left[\mathbf{F_{3nn}}\right]\left[\mathbf{V_{sn}}\right] - \left[\mathbf{F_{3PLD}}\right]\left[\mathbf{I_L}\right] - \left[\mathbf{F_{3Tm}}\right]\left[\mathbf{I_{T,p}}\right] - \left[\mathbf{F_{3GT}}\right]\left[\mathbf{I_{gT}}\right] \\ &- \left[\mathbf{DFF_{3n}}\right]\left[\mathbf{I_f}\right] \end{aligned} \tag{6.102}$$

where, matrices $\left[\mathbf{DFF_{1n}}\right]$, $\left[\mathbf{DFF_{2n}}\right]$ and $\left[\mathbf{DFF_{3n}}\right]$ for an SLG fault have already been defined in eqs. (6.27)-(6.29).

Now, the voltage equation at fault bus is written as,

$$\bar{z}_f \bar{I}_f^a = \bar{V}_{l,f}^a - \bar{V}_{l,f}^g \tag{6.103}$$

where, $\bar{V}_{l,f}^a$ and $\bar{V}_{l,f}^g$ are the voltages of phase a and ground g at fault bus l, respectively. Substituting the values of $\bar{V}_{l,f}^a$ and $\bar{V}_{l,f}^g$ from eqs. (6.100) and (6.102) into eq. (6.103), with an assumption that the neutral and ground buses at the substation end are perfectly grounded (i.e. at zero potential; $\bar{V}_s^n = 0$, $\bar{V}_s^g = 0$), and writing it in the matrix form as,

$$\begin{aligned}\left[\mathbf{Z_f}\right]\left[\mathbf{I_f}\right] &= \bar{V}_s^a - \left[\mathbf{F_{1PLD}}(f_b^q,:)\right]\left[\mathbf{I_L}\right] - \left[\mathbf{F_{1Tm}}(f_b^q,:)\right]\left[\mathbf{I_{T,p}}\right] - \left[\mathbf{F_{1GT}}(f_b^q,:)\right]\left[\mathbf{I_{gT}}\right] \\ &- \left[\mathbf{DFF_{1n}}(f_b^q,1)\right]\left[\mathbf{I_f}\right] + \left[\mathbf{F_{3PLD}}(g_{f_b},:)\right]\left[\mathbf{I_L}\right] + \left[\mathbf{F_{3Tm}}(g_{f_b},:)\right]\left[\mathbf{I_{T,p}}\right] \\ &+ \left[\mathbf{F_{3GT}}(g_{f_b},:)\right]\left[\mathbf{I_{gT}}\right] + \left[\mathbf{DFF_{3n}}(g_{f_b},1)\right]\left[\mathbf{I_f}\right] \end{aligned} \tag{6.104}$$

where, for SLG fault (at phase a of l^{th} bus), $\left[\mathbf{F_{1GT}}(f_b^q,:)\right]$ represents the row vector of matrix $\left[\mathbf{F_{1GT}}\right]$ corresponding to the faulty phase q (here, $q=a$) of faulted bus f_b (here, $f_b=l$); $\left[\mathbf{F_{3GT}}(g_{f_b},:)\right]$ represents the row vector of matrix $\left[\mathbf{F_{3GT}}\right]$ corresponding to the ground g_{f_b} at the location of faulted bus f_b; rest of the matrices for an SLG fault have already been defined in Subsection 6.2.2.1(a).

Hence, the fault current $\left[\mathbf{I_f}\right]$ is obtained from eq. (6.104) as,

$$\left[\mathbf{I_f}\right] = \left[\mathbf{Z_{F1}}\right]^{-1} \bar{V}_s^a - \left[\mathbf{F_{13PLD}^{flt}}\right]\left[\mathbf{I_L}\right] - \left[\mathbf{F_{13Tm}^{flt}}\right]\left[\mathbf{I_{T,p}}\right] - \left[\mathbf{F_{13GT}^{flt}}\right]\left[\mathbf{I_{gT}}\right] \tag{6.105}$$

where, $\left[\mathbf{Z_{F1}}\right]$, $\left[\mathbf{F_{13PLD}^{flt}}\right]$ and $\left[\mathbf{F_{13Tm}^{flt}}\right]$ matrices for an SLG fault have already been described in eq. (6.32) of subsection 6.2.2.1(a) and

$$\left[\mathbf{F_{13GT}^{flt}}\right] = \left[\mathbf{Z_{F1}}\right]^{-1}\left\{\left[\mathbf{F_{1GT}}(f_b^q,:)\right] - \left[\mathbf{F_{3GT}}(g_{f_b},:)\right]\right\}$$

Once the value of fault current $\left[\mathbf{I_f}\right]$ is estimated from eq. (6.105) (with the help of pre-fault load flow solution), the initial values of voltages of phase buses (except inverter bus), neutral buses and ground buses under the fault conditions are calculated using eqs. (6.100)-(6.102). Also, the initial estimate of inverter current for an SLG fault (at phase a of l^{th} bus in the system shown in Fig. 6.4) is obtained with the help of calculated bus voltages and eq. (6.80) as,

$$\mathbf{I_{inv,f,est}^{abc}} = \mathbf{Y_{sp,T}^{abc}V_{j,f}^{abc}} + \mathbf{Y_{ss,T}^{abc}V_{inv,st}^{abc}} + \mathbf{Y_{sp,T}^{n}V_{T,p,f}^{n}} + \mathbf{Y_{ss,T}^{n}V_{T,s,st}^{n}} \tag{6.106}$$

where, $\mathbf{V_{j,f}^{abc}}$ is the estimated three phase voltage vector of j^{th} bus (where an IBDG is connected through a step-down Y_g-Y_g IBDG transformer) under the fault conditions; $\mathbf{V_{T,p,f}^{n}}$ is the estimated voltage vector of neutral bus at the primary side of IBDG transformer under the fault conditions; $\mathbf{V_{inv,st}^{abc}}$ is the inverter bus voltage vector obtained from the steady state load flow solution; $\mathbf{V_{T,s,st}^{n}}$ is the neutral bus voltage vector on the secondary side of IBDG transformer obtained from the steady state load flow solution.

Now, depending upon the magnitude of $\mathbf{I_{inv,f,est}^{abc}}$, there can be two possible cases of inverter operation during fault as discussed in Subsection 6.2.2.1(a),

Case 1: If $|\bar{I}_{inv,f,est}^{p}| \leq I_{sc}^{inv}$; ($p$ = a,b,c)

If the magnitude of estimated inverter current $|\bar{I}_{inv,f,est}^{p}|$ for each phase, calculated using eq. (6.106), is less than the short-circuit capacity of the inverter (I_{sc}^{inv}), then the voltages of phase buses, neutral buses and ground buses calculated using eqs. (6.100)-(6.102) are the final values of the voltages of the system under the fault conditions.

Case 2: If $|\bar{I}_{inv,f,est}^{p}| > I_{sc}^{inv}$; ($p$=$a$, or b, or c)

In this case, the magnitude of inverter current is restricted to its short-circuit capacity (I_{sc}^{inv}), by operating the inverter in constant current control mode (similar to the case discussed in Subsection 6.2.2.1(a)). Hence the inverter current under the fault conditions is given as,

$$\bar{I}_{inv,f}^{p} = |\bar{I}_{inv,f}^{p}| \angle \Psi_{inv,f}^{p} = I_{sc}^{inv} \angle \Psi_{inv,f}^{p}; \quad (p = a, b, c) \tag{6.107}$$

where $\Psi_{inv,f}^{p}$ is the unknown inverter current angle corresponding to phase 'p' under the fault conditions. To solve for these unknown angles, it is assumed that, $\mathbf{\Psi_{inv,f}^{abc}} = \frac{\pi}{2} + \theta_{\mathbf{inv,f}}^{\mathbf{abc}}$, where $\theta_{\mathbf{inv,f}}^{\mathbf{abc}}$ is the three phase voltage angle vector of the inverter bus under the fault conditions. Therefore,

$$\bar{I}_{inv,f}^{p} = I_{sc}^{inv} \underline{\angle \frac{\pi}{2} + \theta_{inv,f}^{p}}; \quad (p = a, b, c) \tag{6.108}$$

Hence with this inverter control strategy (eq. (6.108)), the inverter bus voltage along with the unknown current angles under the fault conditions can be calculated by solving the eq. (6.106). To solve the non-linear equation (eq. (6.106)), Newton Raphson method, as discussed in Subsection 6.2.2.1(a), has also been used here. Once, the inverter bus voltages under the fault conditions are obtained, the primary winding currents of the IBDG transformer under the fault conditions would be calculated using eq. (6.80). Also, the neutral to ground currents on primary and secondary side of the IBDG transformer would be calculated using eq. (6.74). Therefore, the final solution of bus voltages under the fault conditions are then calculated using the eqs. (6.100)-(6.102).

(b) Double line-to-ground (LLG) fault

Let us assume that an LLG fault occurs between phases a and b, and the local ground g_l at the location of l^{th} bus through a fault impedance $\bar{z}_f$, as shown in Fig. 6.2(b) [158]. The fault currents $\bar{I}_f^a$ and $\bar{I}_f^b$ are flowing from phases a and b to the ground g_l at l^{th} bus, respectively. Therefore, the modified phase branch currents and ground currents of the system due to LLG fault are given as,

$$\left[\mathbf{B_{p,f}}\right] = \left[\mathbf{BIBC_p}\right]\left[\mathbf{I_L}\right] + \left[\mathbf{TIBC_{Tm}}\right]\left[\mathbf{I_{T,p}}\right] + \left[\mathbf{BIBC_{fp}}\right]\left[\mathbf{I_f}\right] \tag{6.109}$$

$$\left[\mathbf{B_{g,f}}\right] = -\left[\mathbf{BIBC_g}\right]\left[\mathbf{I_{ng}}\right] - \left[\mathbf{BIBC_{gT}}\right]\left[\mathbf{I_{gT}}\right] - \left[\mathbf{BIBC_{fg}}\right]\left[\mathbf{I_f}\right] \tag{6.110}$$

where, definitions of $\left[\mathbf{BIBC_{fp}}\right]$ and $\left[\mathbf{BIBC_{fg}}\right]$ matrices for an LLG fault have already been given in eqs. (6.45) and (6.47) of Subsection 6.2.2.1(b), respectively. The bus voltages for LLG fault are then estimated by eqs. (6.100)-(6.102). Now, the voltage equations for an LLG fault at fault bus can be written as,

$$\begin{aligned} \bar{z}_f \bar{I}_f^a &= \bar{V}_{l,f}^a - \bar{V}_{l,f}^g \\ \bar{z}_f \bar{I}_f^b &= \bar{V}_{l,f}^b - \bar{V}_{l,f}^g \end{aligned} \tag{6.111}$$

Hence, the fault current $\left[\mathbf{I_f}\right]$ for an LLG fault can be obtained from eqs. (6.100), (6.102) and (6.111) as,

$$\left[\mathbf{I_f}\right] = \left[\mathbf{Z_{F1}}\right]^{-1} \begin{bmatrix} \bar{V}_s^a \\ \bar{V}_s^b \end{bmatrix} - \left[\mathbf{F}_{\mathbf{13PLD}}^{flt}\right]\left[\mathbf{I_L}\right] - \left[\mathbf{F}_{\mathbf{13Tm}}^{flt}\right]\left[\mathbf{I_{T,p}}\right] - \left[\mathbf{F}_{\mathbf{13GT}}^{flt}\right]\left[\mathbf{I_{gT}}\right] \tag{6.112}$$

where, $\left[\mathbf{Z_{F1}}\right]$, $\left[\mathbf{F}_{\mathbf{13PLD}}^{flt}\right]$ and $\left[\mathbf{F}_{\mathbf{13Tm}}^{flt}\right]$ matrices for LLG fault have already been defined in eq. (6.50) of Subsection 6.2.2.1(b) and

$$\left[\mathbf{F}_{\mathbf{13GT}}^{flt}\right] = \left[\mathbf{Z_{F1}}\right]^{-1} \left\{ \begin{bmatrix} \mathbf{F_{1GT}}(f_b^{q_1},:) \\ \mathbf{F_{1GT}}(f_b^{q_2},:) \end{bmatrix} - \begin{bmatrix} \mathbf{F_{3GT}}(g_{f_b},:) \\ \mathbf{F_{3GT}}(g_{f_b},:) \end{bmatrix} \right\}$$

Hence, the initial estimate of fault currents for an LLG fault is obtained from the eq. (6.112) (with the help of pre-fault load flow solution) and rest of the procedure to obtain the final solution for an LLG fault is similar to the procedure described in Subsection 6.3.2.1(a) for SLG fault.

(c) Triple line-to-ground (LLLG) fault

Let us consider an LLLG fault between all the a, b and c phases, and the local ground g_l at l^{th} bus through a fault impedance $\bar{z}_f$, as shown in Fig. 6.2(c) [158]. The fault currents $\bar{I}_f^a$, $\bar{I}_f^b$ and $\bar{I}_f^c$ are flowing from phases a, b and c to the ground g_l at l^{th} bus, respectively. Therefore, the modified phase branch currents and ground currents of the system due to LLLG fault can be written as,

$$\left[\mathbf{B_{p,f}}\right] = \left[\mathbf{BIBC_p}\right]\left[\mathbf{I_L}\right] + \left[\mathbf{TIBC_{Tm}}\right]\left[\mathbf{I_{T,p}}\right] + \left[\mathbf{BIBC_{fp}}\right]\left[\mathbf{I_f}\right] \tag{6.113}$$

$$\left[\mathbf{B_{g,f}}\right] = -\left[\mathbf{BIBC_g}\right]\left[\mathbf{I_{ng}}\right] - \left[\mathbf{BIBC_{gT}}\right]\left[\mathbf{I_{gT}}\right] - \left[\mathbf{BIBC_{fg}}\right]\left[\mathbf{I_f}\right] \tag{6.114}$$

where, definitions of $\left[\mathbf{BIBC_{fp}}\right]$ and $\left[\mathbf{BIBC_{fg}}\right]$ matrices for an LLLG fault have already been given in eqs. (6.52) and (6.54) of Subsection 6.2.2.1(c), respectively. The bus voltages for LLLG fault are then estimated by eqs. (6.100)-(6.102). The voltage equations for an LLLG fault at fault bus can be written as,

$$\begin{aligned} \bar{z}_f \bar{I}_f^a &= \bar{V}_{l,f}^a - \bar{V}_{l,f}^g \\ \bar{z}_f \bar{I}_f^b &= \bar{V}_{l,f}^b - \bar{V}_{l,f}^g \\ \bar{z}_f \bar{I}_f^c &= \bar{V}_{l,f}^c - \bar{V}_{l,f}^g \end{aligned} \tag{6.115}$$

Hence, the fault current $\left[\mathbf{I_f}\right]$ for an LLLG fault is obtained from eqs. (6.100), (6.102) and (6.115) as,

$$\left[\mathbf{I_f}\right] = \left[\mathbf{Z_{F1}}\right]^{-1} \begin{bmatrix} \bar{V}_s^a \\ \bar{V}_s^b \\ \bar{V}_s^c \end{bmatrix} - \left[\mathbf{F}_{\mathbf{13PLD}}^{flt}\right]\left[\mathbf{I_L}\right] - \left[\mathbf{F}_{\mathbf{13Tm}}^{flt}\right]\left[\mathbf{I_{T,p}}\right] - \left[\mathbf{F}_{\mathbf{13GT}}^{flt}\right]\left[\mathbf{I_{gT}}\right] \tag{6.116}$$

where, $\left[\mathbf{Z_{F1}}\right]$, $\left[\mathbf{F}_{\mathbf{13PLD}}^{flt}\right]$ and $\left[\mathbf{F}_{\mathbf{13Tm}}^{flt}\right]$ matrices for LLLG fault have already been defined in eq. (6.57) of Subsection 6.2.2.1(c) and

$$\left[\mathbf{F}_{\mathbf{13GT}}^{flt}\right] = \left[\mathbf{Z_{F1}}\right]^{-1} \left\{ \begin{bmatrix} \mathbf{F_{1GT}}(f_b^{q_1},:) \\ \mathbf{F_{1GT}}(f_b^{q_2},:) \\ \mathbf{F_{1GT}}(f_b^{q_3},:) \end{bmatrix} - \begin{bmatrix} \mathbf{F_{3GT}}(g_{f_b},:) \\ \mathbf{F_{3GT}}(g_{f_b},:) \\ \mathbf{F_{3GT}}(g_{f_b},:) \end{bmatrix} \right\}$$

Hence, the initial estimate of fault currents for LLLG fault is obtained from the eq. (6.116) (with the help of pre-fault load flow solution) and rest of the procedure to obtain the final solution for LLLG fault is same as described in Subsection 6.3.2.1(a) for SLG fault.

(d) Line-to-line (LL) fault

Let us consider an LL fault occurs between phases a and b of l^{th} bus through a fault impedance $\bar{z}_f$, as shown in Fig. 6.2(d) [158]. The fault current $\bar{I}_f^a$ is flowing from phase a to b at l^{th} bus. Hence, only the phase branch currents will modify due to LL fault and can be written as,

$$\left[\mathbf{B_{p,f}}\right] = \left[\mathbf{BIBC_p}\right]\left[\mathbf{I_L}\right] + \left[\mathbf{TIBC_{Tm}}\right]\left[\mathbf{I_{T,p}}\right] + \left[\mathbf{BIBC_{fp}}\right]\left[\mathbf{I_f}\right] \tag{6.117}$$

where, definition of $\left[\mathbf{BIBC_{fp}}\right]$ matrix for an LL fault has already been given in eq. (6.59) of Subsection 6.2.2.1(d), respectively.

The voltages of phase bus, neutral bus and ground bus under the fault conditions are calculated using the modified phase branch currents as obtained in eq. (6.117) as,

$$\begin{aligned} \left[\mathbf{V_{p,f}}\right] &= \left[\mathbf{V_{ss}}\right] - \left[\mathbf{DLF_1}\right]\left[\mathbf{I_L}\right] - \left[\mathbf{DLF_2}\right]\left[\mathbf{I_{ng}}\right] - \left[\mathbf{DLF_{Tm_p}}\right]\left[\mathbf{I_{T,p}}\right] - \left[\mathbf{DLF_{GT_p}}\right]\left[\mathbf{I_{gT}}\right] \\ &- \left[\mathbf{DFF_1'}\right]\left[\mathbf{I_f}\right] \end{aligned} \tag{6.118}$$

$$\begin{aligned} \left[\mathbf{V_{n,f}}\right] &= \left[\mathbf{V_{sn}}\right] - \left[\mathbf{DLF_3}\right]\left[\mathbf{I_L}\right] - \left[\mathbf{DLF_4}\right]\left[\mathbf{I_{ng}}\right] - \left[\mathbf{DLF_{Tm_n}}\right]\left[\mathbf{I_{T,p}}\right] - \left[\mathbf{DLF_{GT_n}}\right]\left[\mathbf{I_{gT}}\right] \\ &- \left[\mathbf{DFF_2'}\right]\left[\mathbf{I_f}\right] \end{aligned} \tag{6.119}$$

$$\begin{aligned} \left[\mathbf{V_{g,f}}\right] &= \left[\mathbf{V_{sg}}\right] - \left[\mathbf{DLF_5}\right]\left[\mathbf{I_L}\right] - \left[\mathbf{DLF_6}\right]\left[\mathbf{I_{ng}}\right] - \left[\mathbf{DLF_{Tm_g}}\right]\left[\mathbf{I_{T,p}}\right] - \left[\mathbf{DLF_{GT_g}}\right]\left[\mathbf{I_{gT}}\right] \\ &- \left[\mathbf{DFF_3'}\right]\left[\mathbf{I_f}\right] \end{aligned} \tag{6.120}$$

where, $\left[\mathbf{DFF_1'}\right]$, $\left[\mathbf{DFF_2'}\right]$ and $\left[\mathbf{DFF_3'}\right]$ matrices for an LL fault have already been defined in eqs. (6.60)-(6.62).

The neutral to ground current under the fault conditions is then calculated by using eqs. (6.13), (6.119) and (6.120) as,

$$\begin{aligned}\left[\mathbf{I_{ng}}\right] &= \left[\mathbf{Z_{FNG}}\right]^{-1}\left\{\left[\mathbf{V_{sn}}\right]-\left[\mathbf{V_{sg}}\right]+\left[\left[\mathbf{DLF_5}\right]-\left[\mathbf{DLF_3}\right]\right]\left[\mathbf{I_L}\right]+\left[\mathbf{DLF_{Tm_{gn}}}\right]\left[\mathbf{I_{T,p}}\right]\right. \\ &+ \left.\left[\mathbf{DLF_{GT_{gn}}}\right]\left[\mathbf{I_{gT}}\right]+\left[\left[\mathbf{DFF_3^{'}}\right]-\left[\mathbf{DFF_2^{'}}\right]\right]\left[\mathbf{I_f}\right]\right\} \end{aligned} \tag{6.121}$$

Therefore, the voltages of phase, neutral and ground buses under the fault conditions are then recalculated using eqs. (6.118)-(6.121) as,

$$\begin{aligned}\left[\mathbf{V_{p,f}}\right] &= \left[\mathbf{V_{ss}}\right]-\left[\mathbf{F_{1ng}}\right]\left\{\left[\mathbf{V_{sn}}\right]-\left[\mathbf{V_{sg}}\right]\right\}-\left[\mathbf{F_{1PLD}}\right]\left[\mathbf{I_L}\right]-\left[\mathbf{F_{1Tm}}\right]\left[\mathbf{I_{T,p}}\right] \\ &- \left[\mathbf{F_{1GT}}\right]\left[\mathbf{I_{gT}}\right]-\left[\mathbf{DFF_{1n}^{'}}\right]\left[\mathbf{I_f}\right] \end{aligned} \tag{6.122}$$

$$\begin{aligned}\left[\mathbf{V_{n,f}}\right] &= \left[\mathbf{F_{2nn}}\right]\left[\mathbf{V_{sn}}\right]-\left[\mathbf{F_{2gg}}\right]\left[\mathbf{V_{sg}}\right]-\left[\mathbf{F_{2PLD}}\right]\left[\mathbf{I_L}\right]-\left[\mathbf{F_{2Tm}}\right]\left[\mathbf{I_{T,p}}\right] \\ &- \left[\mathbf{F_{2GT}}\right]\left[\mathbf{I_{gT}}\right]-\left[\mathbf{DFF_{2n}^{'}}\right]\left[\mathbf{I_f}\right] \end{aligned} \tag{6.123}$$

$$\begin{aligned}\left[\mathbf{V_{g,f}}\right] &= \left[\mathbf{F_{3gg}}\right]\left[\mathbf{V_{sg}}\right]-\left[\mathbf{F_{3nn}}\right]\left[\mathbf{V_{sn}}\right]-\left[\mathbf{F_{3PLD}}\right]\left[\mathbf{I_L}\right]-\left[\mathbf{F_{3Tm}}\right]\left[\mathbf{I_{T,p}}\right] \\ &- \left[\mathbf{F_{3GT}}\right]\left[\mathbf{I_{gT}}\right]-\left[\mathbf{DFF_{3n}^{'}}\right]\left[\mathbf{I_f}\right] \end{aligned} \tag{6.124}$$

where, $\left[\mathbf{DFF_{1n}^{'}}\right]$, $\left[\mathbf{DFF_{2n}^{'}}\right]$ and $\left[\mathbf{DFF_{3n}^{'}}\right]$ matrices for an LL fault have already been defined in eqs. (6.64)-(6.66).

The voltage equation for an LL fault at fault bus can be written as,

$$\bar{z}_f\bar{I}_f^a = \bar{V}_{l,f}^a-\bar{V}_{l,f}^b \tag{6.125}$$

Therefore, the fault current $\left[\mathbf{I_f}\right]$ for an LL fault is calculated using eqs. (6.122) and (6.125) as,

$$\left[\mathbf{I_f}\right]=\left[\mathbf{Z_{F1}}\right]^{-1}(\bar{V}_s^a-\bar{V}_s^b)-\left[\mathbf{F_{11PLD}^{flt}}\right]\left[\mathbf{I_L}\right]-\left[\mathbf{F_{11Tm}^{flt}}\right]\left[\mathbf{I_{T,p}}\right]-\left[\mathbf{F_{11GT}^{flt}}\right]\left[\mathbf{I_{T,p}}\right] \tag{6.126}$$

where, $\left[\mathbf{Z_{F1}}\right]$, $\left[\mathbf{F_{11PLD}^{flt}}\right]$ and $\left[\mathbf{F_{11Tm}^{flt}}\right]$ matrices for an LL fault have already been defined in eq. (6.69) and

$$\left[\mathbf{F_{11GT}^{flt}}\right] = \left[\mathbf{Z_{F1}}\right]^{-1}\left\{\left[\mathbf{F_{1GT}}(f_b^{q_1},:)\right]-\left[\mathbf{F_{1GT}}(f_b^{q_2},:)\right]\right\}$$

The matrices $\left[\mathbf{F_{1GT}}(f_b^{q_1},:)\right]$ and $\left[\mathbf{F_{1GT}}(f_b^{q_2},:)\right]$ are the row vectors of matrix $\left[\mathbf{F_{1GT}}\right]$ corresponding to the faulty phases q_1 and p_2 of faulted bus f_b (here, f_b = l, q_1 = a, q_2 = b), respectively. Therefore, the initial

estimate of fault current is calculated by using eq. (6.126) (with the help of pre-fault load flow solution) and rest of the procedure, to obtain the final solution under the LL fault, is similar to the procedure discussed in Subsection 6.3.2.1(a) for SLG fault.

Steps of algorithm for $\left[\mathbf{BIBC}\right]$ ***matrix based short-circuit analysis method for the unbalanced three phase four wire multigrounded radial distribution system in the presence of IBDG and*** Y_g***-***Y_g ***IBDG transformer***

1. Run the base case power flow of three phase four wire multigrounded system in the presence of IBDG and Y_g-Y_g IBDG transformer using the proposed load flow method as discussed in Subsection 6.3.1 of this chapter.

2. Convert all PQ-loads into constant impedance loads using the obtained load flow solution.

3. If a ground fault (SLG, LLG, LLLG) occurs in the system, then formulate $\left[\mathbf{BIBC_{fp}}\right]$, $\left[\mathbf{BIBC_{fg}}\right]$ and $\left[\mathbf{Z_f}\right]$ matrices corresponding to the type of fault occurring in the system using the proposed $\left[\mathbf{BIBC}\right]$ and $\left[\mathbf{BCBV}\right]$ matrices based short-circuit analysis method. If a line to line (LL) fault occurs, then formulate only $\left[\mathbf{BIBC_{fp}}\right]$ and $\left[\mathbf{Z_f}\right]$ matrices.

4. Set iteration counter $k = 0$. Also, set the values of voltages of phase bus, neutral bus and ground bus, equivalent injection currents $\left[\mathbf{I_L}\right]^k$ and transformer primary winding currents $\left[\mathbf{I_{T,p}}\right]^k$ equal to the values obtained from the pre-fault load flow solutions.

5. Calculate the fault current $\left[\mathbf{I_f}\right]^k$ using eq. (6.105) for SLG fault, eq. (6.112) for LLG fault, eq. (6.116) for LLLG fault and eq. (6.126) for LL fault.

6. Increment the iteration counter by one, $k = k+1$. Calculate the voltages of phase buses, neutral buses and ground buses $\left(\left[\mathbf{V_{p,f}}\right]^k, \left[\mathbf{V_{n,f}}\right]^k \text{ and } \left[\mathbf{V_{g,f}}\right]^k\right)$ of the system under the fault conditions, using eqs. (6.100)-(6.102), for ground faults and using eqs. (6.122)-(6.124), for LL fault, respectively.

7. Calculate the inverter current $\mathbf{I^{abc}_{inv,f}}$ of the IBDG under fault conditions using the transformer nodal admittance matrix based current equation as given in eq. (6.80) (with the new values of bus voltages under the fault conditions as obtained in previous step).

8. Check the condition, whether $|\bar{I}^p_{inv,f,est}| \leq I^{inv}_{sc}$; $(p = a, b, c)$ for all IBDGs in the system. The three possible cases are:

   Case (A): If $|\bar{I}^p_{inv,f,est}| \leq I^{inv}_{sc}$, $(p = a, b, c)$ for all nd - no. of IBDGs, then go to step 12, else

Case (B): If $|\bar{I}^p_{inv,f,est}|$, $(p = a, b, c)$ of all nd - no. of IBDGs are greater than their corresponding short-circuit current capacities, then operate the inverter of all the IBDGs in constant current mode with, $\bar{I}^p_{inv,f} = I^{inv}_{sc} \angle \underline{\frac{\pi}{2} + \theta^p_{inv,f}}$, $(p = a, b, c)$ and calculate the inverter bus voltages under the fault conditions ($\mathbf{V^{abc}_{inv,f}}$) using the Newton-Raphson method as discussed in Subsection 6.2.2.1(a). Also, calculate the neutral bus voltages ($\bar{V}^n_{T,p}$ and $\bar{V}^n_{T,s}$) on primary as well as secondary side of the IBDG transformers using eq. (6.75) and go to step 9, else

Case (C): If out of nd - no. of IBDGs, for kd - no. of IBDGs $|\bar{I}^p_{inv,f,est}| \leq I^{inv}_{sc}$, $(p = a, b, c)$ and for the remaining $(nd - kd)$ - no. of IBDGs $|\bar{I}^p_{inv,f,est}| > I^{inv}_{sc}$, $(p = a, b, c)$, then set $\bar{I}^p_{inv,f} = I^{inv}_{sc} \angle (\frac{\pi}{2} + \theta^p_{inv,f})$, $(p = a, b, c)$ for $(nd - kd)$ - no. of IBDGs, while for kd - no. of IBDGs set $\mathbf{I^{abc}_{inv,f}} = \mathbf{I^{abc}_{inv,f,est}}$ and calculate the inverter bus voltages under the fault conditions ($\mathbf{V^{abc}_{inv,f}}$), for $(nd - kd)$ - no. of IBDGs, using the Newton-Raphson method as discussed in Subsection 6.2.2.1(a). Also, calculate the neutral bus voltages ($\bar{V}^n_{T,p}$ and $\bar{V}^n_{T,s}$) on primary as well as secondary side of the IBDG transformers using eq. (6.75) and go to step 9.

9. Calculate the transformer primary winding currents and equivalent bus injection currents at all the phase buses under the fault conditions as,

$$\mathbf{I^{abc}_{T,p,f}} = \mathbf{Y^{abc}_{pp,T}V^{abc}_{T,p,f}} + \mathbf{Y^{abc}_{ps,T}V^{abc}_{inv,f}} + \mathbf{Y^{n}_{pp,T}V^{n}_{T,p}} + \mathbf{Y^{n}_{ps,T}V^{n}_{T,s}}$$

$$\bar{I}^p_{id} = \left(\frac{\bar{V}^p_{i,f} - \bar{V}^n_{i,f}}{\bar{z}^p_{id}} \right); \quad (p = a,\ or\ b,\ or\ c); \quad (i = 2, \cdots, n_b)$$

where, $\bar{V}^p_{i,f}$ and $\bar{V}^n_{i,f}$ are the voltages at phase p and neutral n of i^{th} bus under fault conditions, respectively. $\bar{z}^p_{id}$ is an equivalent load impedance at phase p of i^{th} bus.

10. Calculate the error (ϵ),

$$\epsilon = max\left(\left| \left[\mathbf{V_{p,f}}\right]^k - \left[\mathbf{V_{p,f}}\right]^{k-1} \right|, \left| \left[\mathbf{V_{n,f}}\right]^k - \left[\mathbf{V_{n,f}}\right]^{k-1} \right|, \left| \left[\mathbf{V_{g,f}}\right]^k - \left[\mathbf{V_{g,f}}\right]^{k-1} \right| \right)$$

11. If $\epsilon <$ tolerance(1.0×10^{-12}), then go to the next step, else go to step 5.

12. The obtained values of voltages $\left[\mathbf{V_{p,f}}\right]$, $\left[\mathbf{V_{n,f}}\right]$ and $\left[\mathbf{V_{g,f}}\right]$ are the final values of the voltages under the fault condition and stop the simulation..

The overall flow-chart of the proposed $\left[\mathbf{BIBC}\right]$ matrix based short-circuit analysis method with IBDG and Y_g-Y_g IBDG transformer is shown in Fig 6.5.

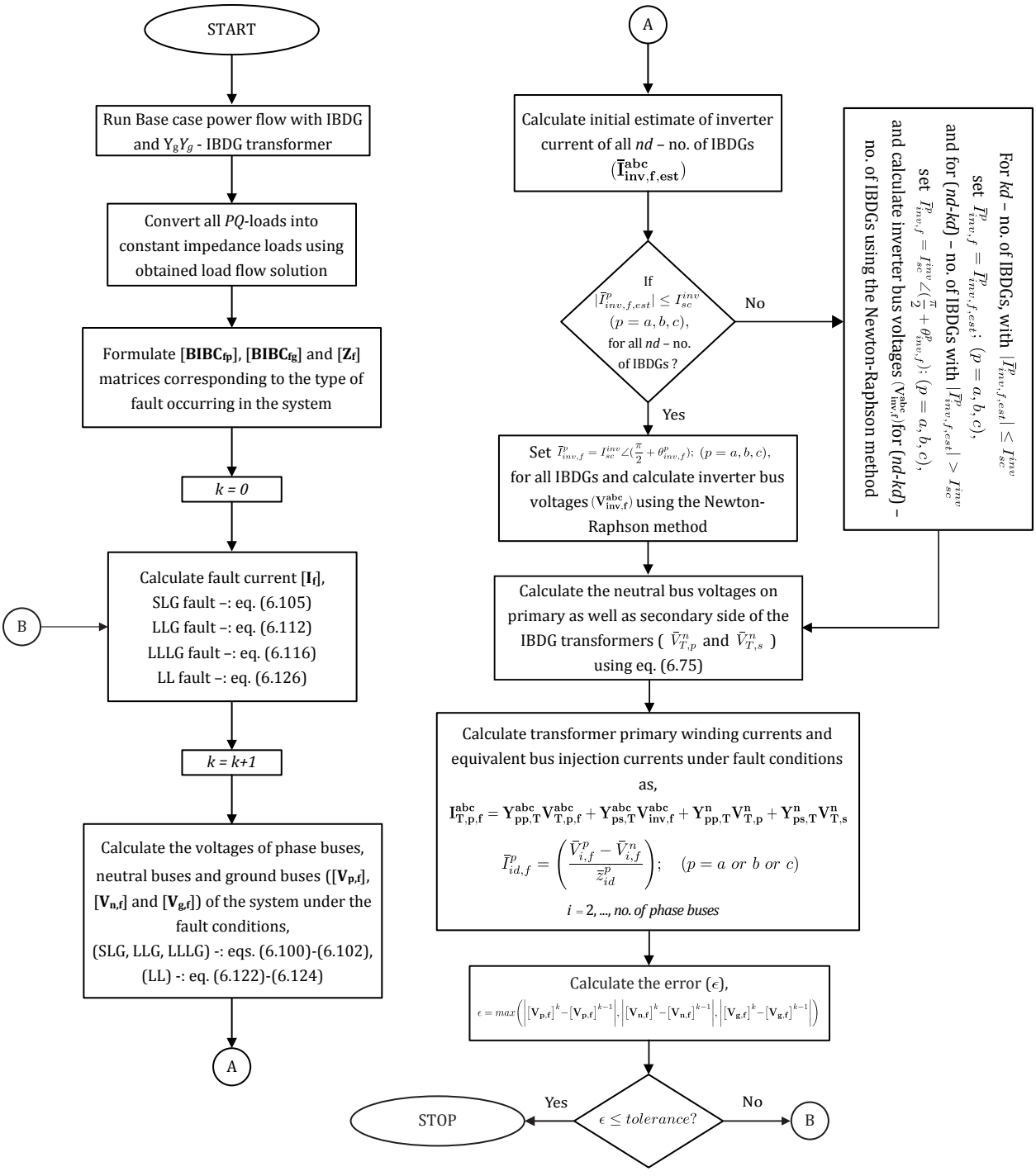

Figure 6.5: Flow-chart of the proposed $\left[\mathbf{BIBC}\right]$ matrix based short-circuit analysis method with IBDG and Y_g-Y_g IBDG transformer

6.3.2.2 Method 2: $\left[\mathbf{Y_{bus}}\right]$ matrix based method

The details of KCL equations at all the buses (except at inverter bus) of unbalanced three-phase four wire multigrounded distribution system have already been described in eqs. (5.82)-(5.92) of Subsection 5.3.2 of

Chapter 5. With the addition of IBDG at j^{th} bus of the system, through a Y_g-Y_g IBDG transformer, the KCL equation at j^{th} bus of the system shown in Fig. 6.4 will be modified as,

$$\mathbf{Y}_{\mathbf{ji}}^{\mathbf{abcng}}\mathbf{V}_{\mathbf{i}}^{\mathbf{abcng}} + \mathbf{Y}_{\mathbf{jj\_new}}^{\mathbf{abcng}}\mathbf{V}_{\mathbf{j}}^{\mathbf{abcng}} + \mathbf{Y}_{\mathbf{pp,T_{md}}}^{\mathbf{n}}\mathbf{V}_{\mathbf{T,p}}^{\mathbf{n}} = -\mathbf{Y}_{\mathbf{ps,T_{(Y_g-Y_g)}}}^{\mathbf{abcng}}\mathbf{V}_{\mathbf{inv,st}}^{\mathbf{abcng}} - \mathbf{Y}_{\mathbf{ps,T_{md}}}^{\mathbf{n}}\mathbf{V}_{\mathbf{T,s,st}}^{\mathbf{n}} \tag{6.127}$$

where, $\mathbf{Y}_{\mathbf{jj\_new}}^{\mathbf{abcng}} = \mathbf{Y}_{\mathbf{jj}}^{\mathbf{abcng}} + \mathbf{Y}_{\mathbf{pp,T_{(Y_g-Y_g)}}}^{\mathbf{abcng}}$,

$$\mathbf{Y}_{\mathbf{pp,T_{(Y_g-Y_g)}}}^{\mathbf{abcng}} = \begin{bmatrix} \bar{Y}_{pp,T}^{aa} & \bar{Y}_{pp,T}^{ab} & \bar{Y}_{pp,T}^{ac} & 0 & 0 \\ \bar{Y}_{pp,T}^{ba} & \bar{Y}_{pp,T}^{bb} & \bar{Y}_{pp,T}^{bc} & 0 & 0 \\ \bar{Y}_{pp,T}^{ca} & \bar{Y}_{pp,T}^{cb} & \bar{Y}_{pp,T}^{cc} & 0 & 0 \\ 0 & 0 & 0 & 0 & 0 \\ 0 & 0 & 0 & 0 & \bar{Y}_{gtp} \end{bmatrix}; \quad \mathbf{Y}_{\mathbf{ps,T_{(Y_g-Y_g)}}}^{\mathbf{abcng}} = \begin{bmatrix} \bar{Y}_{ps,T}^{aa} & \bar{Y}_{ps,T}^{ab} & \bar{Y}_{ps,T}^{ac} & 0 & 0 \\ \bar{Y}_{ps,T}^{ba} & \bar{Y}_{ps,T}^{bb} & \bar{Y}_{ps,T}^{bc} & 0 & 0 \\ \bar{Y}_{ps,T}^{ca} & \bar{Y}_{ps,T}^{cb} & \bar{Y}_{ps,T}^{cc} & 0 & 0 \\ 0 & 0 & 0 & 0 & 0 \\ 0 & 0 & 0 & 0 & 0 \end{bmatrix};$$

$$\mathbf{Y}_{\mathbf{pp,T_{md}}}^{\mathbf{n}} = \begin{bmatrix} -y_t & -y_t & -y_t & 0 & -\bar{Y}_{gtp} \end{bmatrix}^T; \quad \mathbf{Y}_{\mathbf{ps,T_{md}}}^{\mathbf{n}} = \begin{bmatrix} y_t & y_t & y_t & 0 & \bar{Y}_{gts} \end{bmatrix}^T$$

$\bar{Y}_{gtp} = \frac{1}{\bar{Z}_{gtp}}$; $\bar{Y}_{gts} = \frac{1}{\bar{Z}_{gts}}$; $\mathbf{V}_{\mathbf{inv,st}}^{\mathbf{abcng}} = \begin{bmatrix} \bar{V}_{inv,st}^{a} & \bar{V}_{inv,st}^{b} & \bar{V}_{inv,st}^{c} & 0 & 0 \end{bmatrix}^T$ is an inverter bus voltage vector and $\mathbf{V}_{\mathbf{T,s,st}}^{\mathbf{n}} = \bar{V}_{T,s,st}^{n}$ is neutral bus voltage on the secondary side of the transformer, obtained from pre-fault steady state load flow solution. As mutual coupling has been considered only between primary and secondary phases of IBDG transformer, the entries of mutual admittances between phases and neutral, and between phases and ground in matrices $\mathbf{Y}_{\mathbf{pp,T_{(Y_g-Y_g)}}}^{\mathbf{abcng}}$ and $\mathbf{Y}_{\mathbf{ps,T_{(Y_g-Y_g)}}}^{\mathbf{abcng}}$, are zero. Also, the neutral point of the IBDG is solidly grounded (as shown in Fig. 6.4), therefore, the elements of the inverter bus voltage vector $\mathbf{V}_{\mathbf{inv,st}}^{\mathbf{abcng}}$, corresponding to the neutral and ground buses, are zero. A new neutral bus on primary side of the IBDG transformer has also been introduced in the system (due to connection of neutral bus on primary side of (Y_g-Y_g) IBDG transformer to the ground bus at the location of j^{th} system bus), the KCL equation is also applied on this bus as,

$$\bar{Y}_{gtp}(\bar{V}_{T,p}^{n} - \bar{V}_{j}^{g}) = \bar{I}_{T,p}^{g} = \bar{I}_{T,p}^{a} + \bar{I}_{T,p}^{b} + \bar{I}_{T,p}^{c} \tag{6.128}$$

Now, the eq. (6.128) can be rewritten using eq. (6.77) as,

$$\bar{Y}_{gtp}(\bar{V}_{T,p}^{n} - \bar{V}_{j}^{g}) = y_t\bar{V}_{j}^{a} + y_t\bar{V}_{j}^{b} + y_t\bar{V}_{j}^{c} - y_t\bar{V}_{inv}^{a} - y_t\bar{V}_{inv}^{b} - y_t\bar{V}_{invj}^{c} - 3y_t\bar{V}_{T,p}^{n} + 3y_t\bar{V}_{T,s}^{n}$$

$$- y_t\bar{V}_{j}^{a} - y_t\bar{V}_{j}^{b} - y_t\bar{V}_{j}^{c} - \bar{Y}_{gtp}\bar{V}_{j}^{g} + (\bar{Y}_{gtp} + 3y_t)\bar{V}_{T,p}^{n} = -y_t\bar{V}_{inv}^{a} - y_t\bar{V}_{inv}^{b} - y_t\bar{V}_{invj}^{c} + 3y_t\bar{V}_{T,s}^{n} \tag{6.129}$$

Therefore, the KCL equations (combined eqs. (5.82)-(5.92), (6.127) and (6.129)) of the system (except at the inverter bus) can then be written in the matrix form as,

$$\begin{bmatrix} \mathbf{Y}_{\mathbf{bus\_Tm}} \end{bmatrix} \cdot \begin{bmatrix} \mathbf{V} \end{bmatrix} = \begin{bmatrix} \mathbf{I} \end{bmatrix} \tag{6.130}$$

The size of $\left[\mathbf{Y_{bus\_Tm}}\right]$ matrix for the unbalanced distribution system considered is $(5u+4v+3w+nt-5)\times(5u+4v+3w+nt-5)$. Once, the $\left[\mathbf{Y_{bus\_Tm}}\right]$ matrix of the system has been formed, rest of the formulation for various short-circuit faults is exactly similar to the formulation given in Subsection 6.2.2.2 for the case with Δ-Y_g IBDG transformer.

6.4 Test results and discussions

To investigate the accuracy of the proposed load flow and short-circuit analysis method, two different three phase four wire multigrounded test systems, with IBDGs and IBDG transformers have been used in this study. The first test system is modified IEEE 34-bus test feeder and the second one is modified IEEE 123-bus test feeder. Details of these systems are given in Section 5.4 of Chapter 5. The proposed load flow and short-circuit analysis methods have been implemented in MATLAB environment with a tolerance limit (ϵ) of 1.0×10^{-12}.

6.4.1 Results of test systems with IBDGs and Δ-Y_g IBDG transformers

In this subsection, Δ-Y_g type of IBDG transformer has been used for the connection of IBDG to the grid. The ΔY_g-1 IBDG transformer is used in this work and its nodal admittance matrix model (p.u.) is given as [80],

$$\mathbf{Y_{T(\Delta Y_g-1)}} = y_t \begin{bmatrix} \frac{2}{3} & -\frac{1}{3} & -\frac{1}{3} & -\frac{1}{\sqrt{3}} & \frac{1}{\sqrt{3}} & 0 \\ -\frac{1}{3} & \frac{2}{3} & -\frac{1}{3} & 0 & -\frac{1}{\sqrt{3}} & \frac{1}{\sqrt{3}} \\ -\frac{1}{3} & -\frac{1}{3} & \frac{2}{3} & \frac{1}{\sqrt{3}} & 0 & -\frac{1}{\sqrt{3}} \\ -\frac{1}{\sqrt{3}} & 0 & \frac{1}{\sqrt{3}} & 1 & 0 & 0 \\ \frac{1}{\sqrt{3}} & -\frac{1}{\sqrt{3}} & 0 & 0 & 1 & 0 \\ 0 & \frac{1}{\sqrt{3}} & -\frac{1}{\sqrt{3}} & 0 & 0 & 1 \end{bmatrix} \tag{6.131}$$

where, y_t is an equivalent transformer leakage admittance in p.u. and its value is assumed as $(0.000-16.92i)$ p.u. [146]. It is a step down transformer with its turns ratio assumed as $24.9/0.480$ kV for the modified IEEE 34-bus test system and as $4.16/0.480$ kV for the modified IEEE 123-bus test system..

6.4.1.1 Results of modified three phase four wire multigrounded IEEE 34-bus test system in the presence of IBDGs and Δ-Y_g IBDG transformers

(a). Results of load flow studies

Three different sized IBDGs have been considered in this system and their detailed informations are given in Table 6.1. These IBDGs are connected at different buses of the system, as shown in column 2 of Table 6.1. The total installed capacity of IBDGs is considered as 20% of total active power load [146] in

Table 6.1: Details of the IBDGs installed in the modified IEEE 34-bus test system

IBDG No.	**IBDG location (Bus No.)**	**IBDG installed capacity**, P_{dg} **(per phase) (kW)**	**Short-circuit current capacity**, I_{sc}^{inv} **(per phase) (Amp)**
1.	16	53	95.26
2.	25	53	95.26
3.	30	71	127.02

the system and is given in column 3 of Table 6.1. The short-circuit current capacity (I_{sc}^{inv}) of each IBDG is assumed as 150% of the rated inverter current [146]. The value of I_{sc}^{inv} for various IBDGs is given in column 4 of Table 6.1. It is also assumed that all IBDGs are operating at unity power factor under normal operating condition. The load flow analysis of the test system has been performed by using the proposed method (as discussed in subsection 6.2.1 for Δ-Y_g IBDG transformer). The results obtained by the proposed method have been compared with those obtained by the $[\mathbf{Y_{bus}}]$ matrix based method [135], which also incorporates the nodal admittance matrix of the transformer in system admittance matrix, and the time domain simulation studies carried out using PSCAD/EMTDC software.

The bar graph for the bus voltage of phase a of the test system with IBDGs, has been obtained by the proposed method and plotted along with the bus voltage values obtained by the $\left[\mathbf{Y_{bus}}\right]$ matrix based method and PSCAD/EMTDC simulation studies, as shown in Fig. 6.6. The figure shows that the results obtained by the proposed method are very close to the results of the $\left[\mathbf{Y_{bus}}\right]$ matrix method and PSCAD/EMTDC studies, which establishes the accuracy of the proposed method. Similarly, the bar graphs of the neutral bus and ground bus voltages obtained by the proposed method, $\left[\mathbf{Y_{bus}}\right]$ matrix method and PSCAD/EMTDC simulation are also shown in Figs. 6.7 and 6.8, respectively. A good match between the results obtained by these three methods demonstrates the correctness of the proposed approach.

The current in the phase a, neutral wire and ground for the given test system calculated by the proposed load flow method are plotted in Figs. 6.9-6.11, respectively. The values of these three currents have also been obtained by the $\left[\mathbf{Y_{bus}}\right]$ matrix based method and PSCAD/EMTDC simulation studies, and are plotted along with the results of proposed method in Figs. 6.9-6.11. A close matching of the current values, as observed in these figures, again validates the accuracy of the proposed method. It can also be observed form Figs. 6.10 and 6.11, that the neutral and ground sections of branches 9 and 10 carry highest value of neutral

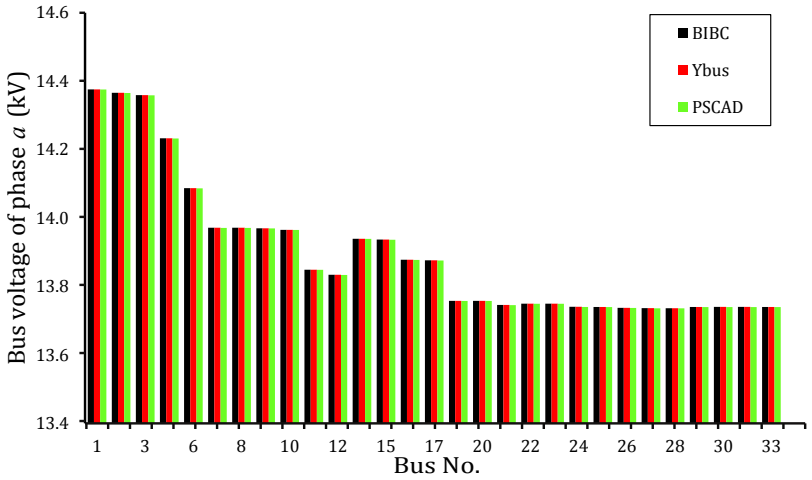

Figure 6.6: Voltage profile of phase a of modified IEEE 34-bus test system in the presence of IBDG and Δ-Y_g IBDG transformer using proposed $\left[\mathbf{BIBC}\right]$ technique, $\left[\mathbf{Y_{bus}}\right]$ technique and PSCAD/EMTDC simulation under normal operating conditions

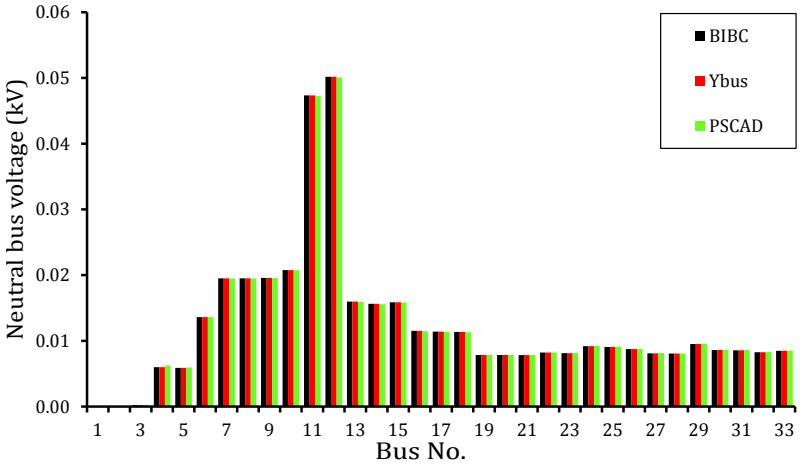

Figure 6.7: Voltage profile of neutral bus of modified IEEE 34-bus test system in the presence of IBDG and Δ-Y_g IBDG transformer using proposed $\left[\mathbf{BIBC}\right]$ technique, $\left[\mathbf{Y_{bus}}\right]$ technique and PSCAD/EMTDC simulation under normal operating conditions

and ground currents, respectively. The reason for this has already been explained in Subsection 5.4.1 of Chapter 5.

The inverter currents ($\mathbf{I_{inv}^{abc}}$) and the inverter bus voltages ($\mathbf{V_{inv}^{abc}}$) calculated by the proposed $[\mathbf{BIBC}]$

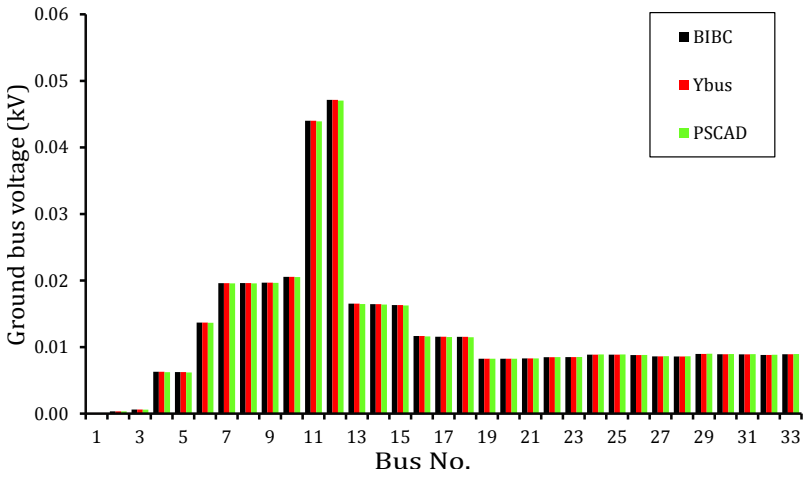

Figure 6.8: Voltage profile of ground bus of modified IEEE 34-bus test system in the presence of IBDG and Δ-Y_g IBDG transformer using proposed $\left[\mathbf{BIBC}\right]$ technique, $\left[\mathbf{Y_{bus}}\right]$ technique and PSCAD/EMTDC simulation under normal operating conditions

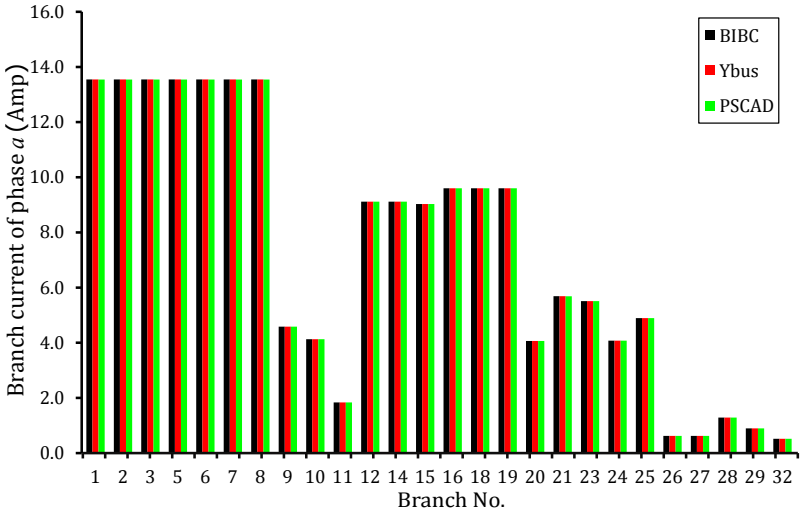

Figure 6.9: Branch current of phase a of modified IEEE 34-bus test system in the presence of IBDG and Δ-Y_g IBDG transformer using proposed $\left[\mathbf{BIBC}\right]$ technique, $\left[\mathbf{Y_{bus}}\right]$ technique and PSCAD/EMTDC simulation under normal operating conditions

matrix based method and the $\left[\mathbf{Y_{bus}}\right]$ matrix based method are shown in Tables 6.2 and 6.3, respectively. The values of ($\mathbf{I_{inv}^{abc}}$) and ($\mathbf{V_{inv}^{abc}}$) of all IBDGs obtained by the proposed method are exactly equal to the values

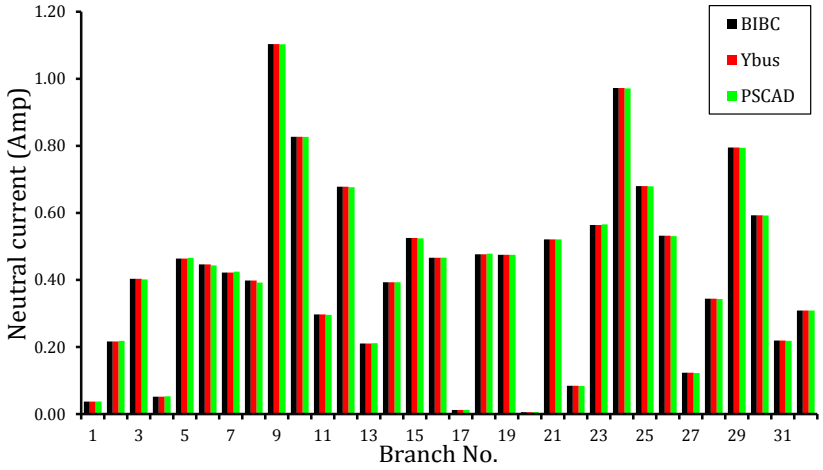

Figure 6.10: Neutral current of modified IEEE 34-bus test system in the presence of IBDG and Δ-Y_g IBDG transformer using proposed $\left[\mathbf{BIBC}\right]$ technique, $\left[\mathbf{Y_{bus}}\right]$ technique and PSCAD/EMTDC simulation under normal operating conditions

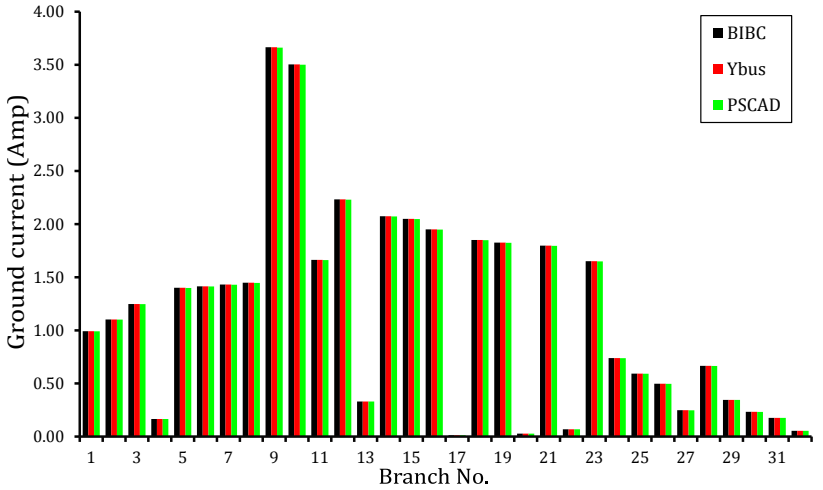

Figure 6.11: Ground current of modified IEEE 34-bus test system in the presence of IBDG and Δ-Y_g IBDG transformer using proposed $\left[\mathbf{BIBC}\right]$ technique, $\left[\mathbf{Y_{bus}}\right]$ technique and PSCAD/EMTDC simulation under normal operating conditions

obtained by the $\left[\mathbf{Y_{bus}}\right]$ matrix based method, which again establish the accuracy of the proposed method. Since, all IBDGs are operating at unity power factor under the normal operating conditions, the phase angles of inverter currents and the inverter bus voltages are same, as shown in Tables 6.2 and 6.3.

Table 6.2: Inverter currents of modified IEEE 34-bus test system in the presence of IBDGs and Δ-Y_g IBDG transformers under normal operating conditions

IBDG location (Bus No.)	**Inverter current, $\mathbf{I_{inv}^{abc}}$ (Amp)**					
	[BIBC] Technique			**[$\mathbf{Y_{bus}$] Technique**		
	Phase a	**Phase b**	**Phase c**	**Phase a**	**Phase b**	**Phase c**
16	65.71∠-29.73^o	65.57∠-149.58^o	65.48∠90.23^o	65.71∠-29.73^o	65.57∠-149.58^o	65.48∠90.23^o
25	66.54∠-29.51^o	66.31∠-149.41^o	66.32∠90.37^o	66.54∠-29.51^o	66.31∠-149.41^o	66.32∠90.37^o
30	88.72∠-29.47^o	88.41∠-149.37^o	88.43∠90.40^o	88.72∠-29.47^o	88.41∠-149.37^o	88.43∠90.40^o

Table 6.3: Inverter bus voltages of modified IEEE 34-bus test system in the presence of IBDGs and Δ-Y_g IBDG transformers under normal operating conditions

IBDG location (Bus No.)	**Inverter bus voltage, $\mathbf{V_{inv}^{abc}}$ (kV)**					
	[BIBC] Technique			**[$\mathbf{Y_{bus}$] Technique**		
	Phase a	**Phase b**	**Phase c**	**Phase a**	**Phase b**	**Phase c**
16	0.2678∠-29.73^o	0.2684∠-149.58^o	0.2688∠90.23^o	0.2678∠-29.73^o	0.2684∠-149.58^o	0.2688∠90.23^o
25	0.2645∠-29.51^o	0.2654∠-149.41^o	0.2654∠90.37^o	0.2645∠-29.51^o	0.2654∠-149.41^o	0.2654∠90.37^o
30	0.2645∠-29.47^o	0.2654∠-149.37^o	0.2654∠90.40^o	0.2645∠-29.47^o	0.2654∠-149.37^o	0.2654∠90.40^o

A case of isolated neutral has also been simulated on the given test system with IBDGs using the proposed method. The neutral bus voltage profiles of the test system for "isolated neutral" and "grounded neutral" cases are shown in Fig. 6.12(a). The values of neutral voltages at all the buses in "isolated neutral" case are higher than the "grounded neutral" case. This is due to the fact that, the return path for load currents in "isolated neutral case" is only through the neutral wire, whereas in "grounded neutral" case the injected load currents are divided in two paths, one through the neutral wire and the other through the ground wire. Therefore, the values of neutral currents in "isolated neutral" case are higher than in "grounded neutral" case, as shown in Fig. 6.12(b), and hence, the values of neutral bus voltages in "isolated neutral" case are higher.

The value of maximum ground bus voltage and maximum ground current in the test system under normal operating condition, for various grounding resistance are plotted in Fig. 6.13(a) and (b). The figure shows that, with the increase in grounding resistance, the value of maximum ground bus voltage as well as maximum ground current in the system decreases (as shown in Fig. 6.13(a)). This is due to the fact that, with the increase in grounding resistance, the value of neutral to ground current in the system decreases and

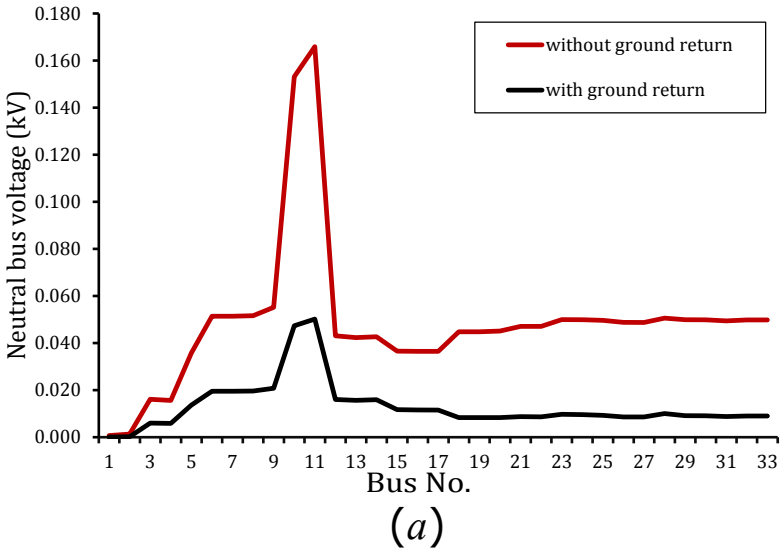

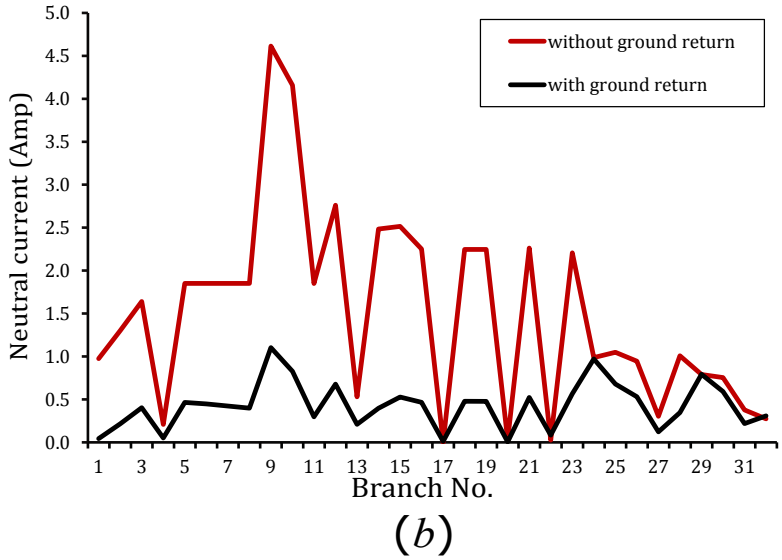

Figure 6.12: (*a*) Neutral bus voltage profile, (*b*) Neutral current of modified IEEE 34-bus test system in the presence of IBDG and Δ-Y_g IBDG transformer in "isolated neutral" and "grounded neutral" cases under normal operating conditions

as a result the value of ground wire currents and hence the ground bus voltages of the system decreases (as shown in Fig. 6.13(b)).

(b). Results of short-circuit studies

For investigating the efficacy of the proposed short-circuit analysis methods ($[\mathbf{BIBC}]$ and $[\mathbf{BCBV}]$ matrices based method and $[\mathbf{Y_{bus}}]$ matrix based method) for the case with Δ-Y_g IBDG transformer, an SLG

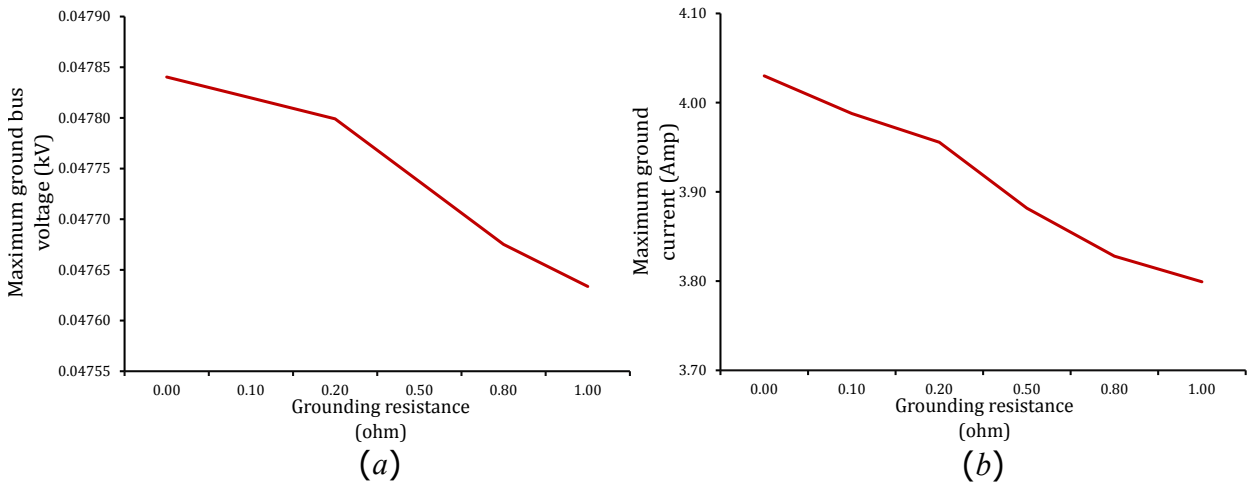

Figure 6.13: (a) Maximum ground bus voltage, (b) Maximum ground current, in modified IEEE 34-bus test system in the presence of IBDG and Δ-Y_g IBDG transformer for various grounding resistance under normal operating condition

fault in phase a of bus 28, with a fault impedance $\bar{z}_f$ = $0.001 + 0.000i$ p.u. has been simulated. In the first step, the inverter currents ($\mathbf{I^{abc}_{inv,f,est}}$) of all the three IBDGs have been calculated by assuming that the inverter bus voltages of all IBDGs under the fault conditions are maintained at their pre-fault values i.e., $\mathbf{V^{abc}_{inv,f}}$ = $\mathbf{V^{abc}_{inv,f,st}}$. The calculated values of the inverter currents obtained by both proposed methods are given in columns 2-4 of Tables 6.4 and 6.5, respectively. These tables show that the magnitude of inverter currents of all IBDGs are greater than their short-circuit current capacities (I^{inv}_{sc}). Hence, according to the proposed methods, the magnitudes of inverter currents of all the phases are to be maintained at their short-circuit current capacities $\left(|I^{p}_{inv,f}|= I^{inv}_{sc}, p = a, b, c\ \right)$ and their angles are maintained in such a way that all IBDGs will deliver reactive power to the system during the short-circuit condition i.e., $\Psi^{p}_{inv,f} = \frac{\pi}{2} + \theta^{p}_{inv,f}$, $p = a, b, c$. With this strategy, the fault current, the bus voltages and the inverter currents of all IBDGs under the fault conditions are recalculated using the proposed short-circuit analysis methods. The final values of inverter currents and injected powers (capacitive reactive power) by all IBDGs, obtained by the two proposed methods, are shown in columns 5-10 of Tables 6.4 and 6.5, respectively. It is also observed from these tables that the final values of inverter currents and injected powers by the IBDGs obtained by the two proposed methods are identical, which again validates the accuracy of the proposed methods. The fault current (I_f) and source current (I_s) in phase a for this case using the proposed methods and PSCAD/EMTDC simulation studies are given in Table 6.6. The % error in the calculated values of I_f and I_s with respect to the values obtained by PSCAD/EMTDC simulation study are 0.00693% and 0.00580%, respectively, as shown in Table

Table 6.4: Results for SLG(a-g) fault at bus 28 in modified three phase four wire multigrounded IEEE 34-bus radial test system in the presence of IBDGs and Δ-Y_g IBDG transformers using proposed $[\mathbf{BIBC}]$ method

IBDG location (bus No.)	**Initial estimate of inverter current, $\mathbf{I}^{\mathbf{abc}}_{\mathbf{inv,f,est}}$, (kA) when $\mathbf{V}^{\mathbf{abc}}_{\mathbf{inv,f}} = \mathbf{V}^{\mathbf{abc}}_{\mathbf{inv,st}}$**			**final value of inverter current, (kA) $\mathbf{I}^{\mathbf{abc}}_{\mathbf{inv,f}} = I^{inv}_{sc}\angle(\frac{\pi}{2} + \theta^{\mathbf{abc}}_{\mathbf{inv,f}})$**			**final value of injected IBDG power (kVAR)**		
	Phase-a	**Phase-b**	**Phase-c**	**Phase-a**	**Phase-b**	**Phase-c**	**Phase-a**	**Phase-b**	**Phase-c**
16	11.363∠-107.36^o	10.789∠68.57^o	0.974∠124.51^o	0.0953∠-125.76^o	0.0953∠130.62^o	0.0953∠-1.82^o	59.205	66.553	77.932
25	16.365∠-109.74^o	15.651∠66.35^o	1.303∠125.06^o	0.0953∠-128.23^o	0.0953∠137.28^o	0.0953∠-2.37^o	50.230	62.837	77.267
30	16.340∠-109.65^o	15.604∠66.40^o	1.319∠124.52^o	0.1270∠-128.23^o	0.1270∠137.22^o	0.1270∠-2.38^o	67.102	83.855	103.079

Table 6.5: Results for SLG(a-g) fault at bus 28 in modified three phase four wire multigrounded IEEE 34-bus radial test system in the presence of IBDGs and Δ-Y_g IBDG transformers using proposed $[\mathbf{Y_{bus}}]$ method

IBDG location (bus No.)	**Initial estimate of inverter current, $\mathbf{I}^{\mathbf{abc}}_{\mathbf{inv,f,est}}$, (kA) when $\mathbf{V}^{\mathbf{abc}}_{\mathbf{inv,f}} = \mathbf{V}^{\mathbf{abc}}_{\mathbf{inv,st}}$**			**final value of inverter current, (kA) $\mathbf{I}^{\mathbf{abc}}_{\mathbf{inv,f}} = I^{inv}_{sc}\angle(\frac{\pi}{2} + \theta^{\mathbf{abc}}_{\mathbf{inv,f}})$**			**final value of injected IBDG power (kVAR)**		
	Phase-a	**Phase-b**	**Phase-c**	**Phase-a**	**Phase-b**	**Phase-c**	**Phase-a**	**Phase-b**	**Phase-c**
16	1.308∠-42.46^o	1.254∠139.18^o	0.0648∠103.76^o	0.0953∠-125.76^o	0.0953∠130.62^o	0.0953∠-1.82^o	59.205	66.553	77.932
25	2.931∠-71.68^o	2.818∠107.19^o	0.1260∠134.24^o	0.0953∠-128.23^o	0.0953∠137.28^o	0.0953∠-2.37^o	50.230	62.837	77.267
30	2.775∠-65.52^o	2.661∠113.74^o	0.1189∠130.80^o	0.1270∠-128.23^o	0.1270∠137.22^o	0.1270∠-2.38^o	67.102	83.855	103.079

6.6. The above results show that the values of I_f and I_s calculated by both the proposed methods are very close to the values obtained by the PSCAD/EMTDC software, thereby validating the proposed methods.

Different fault cases namely, LLG (ab-g), LLLG (abc-g), and LL (a-b) fault with $\bar{z}_f$ = 0.001+0.000i p.u., have also been simulated at bus 28 in the same system using the proposed methods and PSCAD/EMTDC software. The calculated values of fault currents (I_f) and source currents (I_s) for all type of faults obtained by the proposed methods and PSCAD/EMTDC simulation study are given in Table 6.6. The maximum $\%$ errors in the calculated values of (I_f) and (I_s), obtained from the proposed short-circuit analysis methods, with respect to the PSCAD/EMTDC simulation results are 0.00737% and 0.00716%, respectively. These extremely small values of errors establish that the proposed methods are sufficiently accurate.

The phase a bus voltage, neutral bus voltage and ground bus voltage of the test system with IBDGs and Δ-Y_g IBDG transformers, for an SLG fault at phase a of bus 28 with fault impedance of $\bar{z}_f$ = 0.001+0.000i p.u., obtained by using the proposed short-circuit analysis methods $\big([\mathbf{BIBC}]$ matrix based and $[\mathbf{Y_{bus}}]$ matrix based methods $\big)$, are shown in the bar graphs of Figs. 6.14-6.16, respectively. The values of these voltages are also obtained by the time domain simulation studies carried out using the PSCAD/EMTDC software and are plotted along with the results of proposed methods, as shown in Figs. 6.14-6.16, respec-

Table 6.6: Error Analysis of proposed $[\mathbf{BIBC}]$ matrix based technique and $[\mathbf{Y_{bus}}]$ matrix based technique with respect to PSCAD/EMTDC simulation study for modified three phase four wire multigrounded IEEE 34-bus radial test system in the presence of IBDGs and Δ-Y_g IBDG transformers

case	Fault type	phase	Fault current at fault point (I_f)			% Error in (I_f)		Current drawn from the supply (I_s)			% Error in (I_s)	
			PSCAD simulation (Amp)	[BIBC] Technique (Amp)	$[Y_{bus}]$ Technique (Amp)	[BIBC] Technique (%)	$[Y_{bus}]$ Technique (%)	PSCAD simulation (Amp)	[BIBC] Technique (Amp)	$[Y_{bus}]$ Technique (Amp)	[BIBC] Technique (%)	$[Y_{bus}]$ Technique (%)
1	SLG (a-g)	a	152.924	152.935	152.935	0.00693	0.00693	151.643	151.652	151.652	0.00580	0.00580
2	LLG (ab-g)	a	197.496	197.491	197.491	0.00258	0.00258	200.957	200.952	200.952	0.00241	0.00241
		b	249.527	249.545	249.545	**0.00737**	**0.00737**	247.833	247.841	247.841	0.00327	0.00327
3	LLLG (abc-g)	a	237.856	237.866	237.866	0.00423	0.00423	238.910	238.921	238.921	0.00438	0.00438
		b	257.485	257.501	257.501	0.00634	0.00634	257.661	257.678	257.678	0.00647	0.00647
		c	249.728	249.743	249.743	0.00578	0.00578	248.803	248.818	248.818	0.00577	0.00577
4	L-L (a-b)	a	219.068	219.069	219.069	0.00038	0.00038	223.237	223.238	223.238	0.00062	0.00062
		b	219.068	219.069	219.069	0.00038	0.00038	217.150	217.165	217.165	**0.00716**	**0.00716**

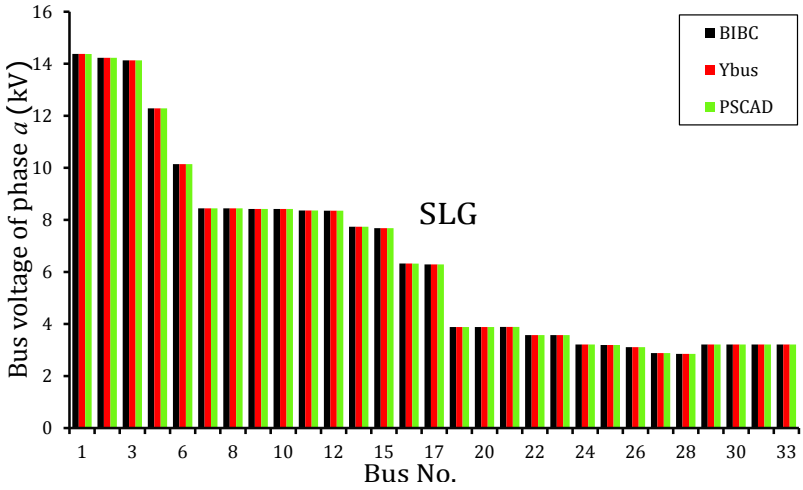

Figure 6.14: Voltage profile of phase a, for an SLG fault (a-g) at bus 28, of modified IEEE 34-bus test system in the presence of IBDG and Δ-Y_g IBDG transformer using proposed $[\mathbf{BIBC}]$ technique, $[\mathbf{Y_{bus}}]$ technique and PSCAD/EMTDC simulation

tively. A comparison of these plots shows that the values of bus voltages obtained by proposed methods are very close to the values obtained by the PSCAD/EMTDC simulation studies, which again validates the accuracy of the proposed short-circuit analysis methods.

In Fig. 6.17(a), the ground bus voltage profile is plotted for various ground faults (SLG, LLG and

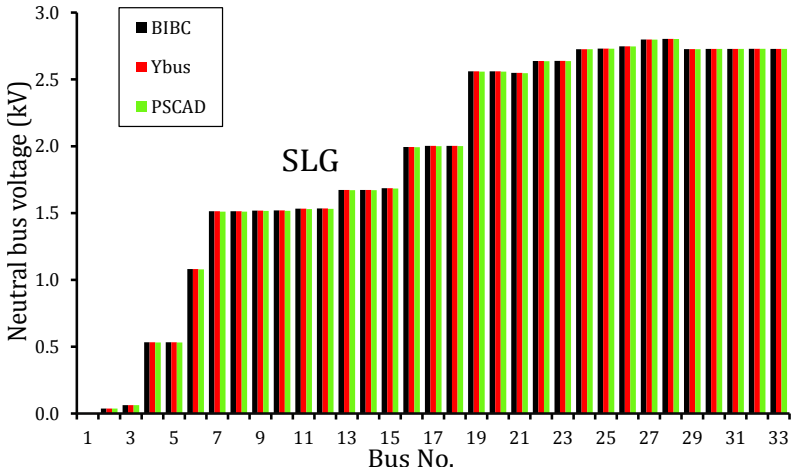

Figure 6.15: Voltage profile of neutral bus, for an SLG fault (a-g) at bus 28, of modified IEEE 34-bus test system in the presence of IBDG and Δ-Y_g IBDG transformer using proposed $\left[\mathbf{BIBC}\right]$ technique, $\left[\mathbf{Y_{bus}}\right]$ technique and PSCAD/EMTDC simulation

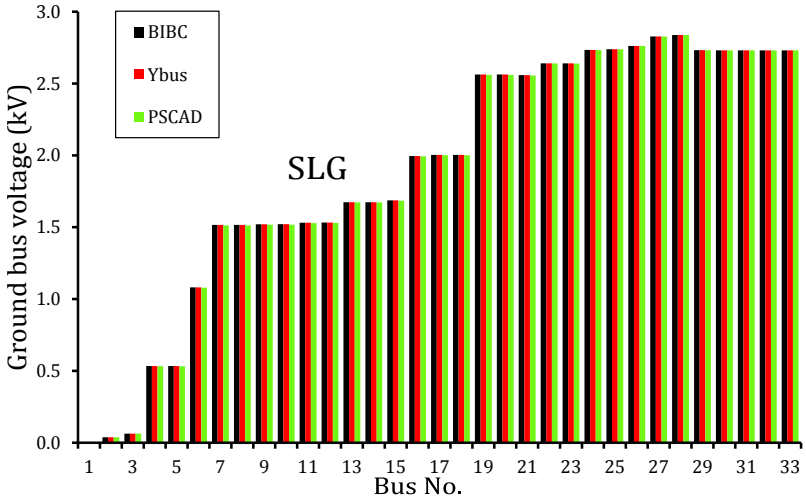

Figure 6.16: Voltage profile of ground bus, for an SLG fault (a-g) at bus 28, of modified IEEE 34-bus test system in the presence of IBDG and Δ-Y_g IBDG transformer using proposed $\left[\mathbf{BIBC}\right]$ technique, $\left[\mathbf{Y_{bus}}\right]$ technique and PSCAD/EMTDC simulation

LLLG) at bus 28 with a fault impedance of $\bar{z}_f$ = 0.001+0.000i p.u.. The plot shows that the highest ground bus voltages occur for SLG fault followed by LLG fault while the lowest values are observed for LLLG fault. This is due to the fact that the fault current injected into the fault point at ground bus is the phasor sum

Table 6.7: Details of the IBDGs installed in the modified IEEE 123-bus distribution system

IBDG No.	**IBDG location (Bus No.)**	**IBDG installed capacity,** P_{dg} **(per phase) (kW)**	**Short-circuit capacity,** I_{sc}^{inv} **(per phase) (Amp)**
1.	20	140	251.87
2.	25	105	188.90
3.	75	140	251.87
4.	98	175	314.84
5.	104	140	251.87

of the three phase fault currents and its value ($\bar{I}_f^a + \bar{I}_f^b + \bar{I}_f^c = -0.32 + j5.82$ Amp $= 5.831\underline{/93.19^o}$ Amp) is smallest for LLLG fault, followed by the injected fault current of LLG fault ($\bar{I}_f^a + \bar{I}_f^b = -52.99 - j93.10$ Amp $= 107.126\underline{/-119.64^o}$ Amp) with SLG fault injecting highest current ($\bar{I}_f^a = 97.08 - j118.17$ Amp $= 152.935\underline{/-50.59^o}$ Amp) into the ground at the fault bus location. Therefore, the currents flowing through ground from fault point to the substation ground are highest for SLG fault followed by LLG fault and smallest for LLLG fault, as shown in 6.17(b). As a result, the ground bus voltages are highest for SLG fault with LLLG fault resulting in lowest ground bus voltages. From Fig. 6.17(b), it is also observed that the value of ground current at certain branches of the test system (like branch nos. $4, 9-11, 13, 17, 20, 22, 28-32$) are nearly equal to zero. It is due the fact, that these branches are not present in the path of fault current returning through ground from fault point to the substation ground.

Under fault conditions (for SLG, LLG and LLLG fault), as the neutral to ground resistance increases, the ground current as well as the ground bus voltage at the fault point increases, as can be observed in Figs. 6.18(a)-(f). This is due to the fact that as neutral to ground resistance is increased, fault current flowing through the ground wire increases and the current in the neutral wire decreases.

6.4.1.2 Results of modified three phase four wire multigrounded IEEE 123-bus test system in the presence of IBDGs and Δ-Y_g IBDG transformers

(a). Results of load flow studies

Five different sized IBDGs have been considered in this test system and their detailed informations are given in Table 6.7. These IBDGs are connected at different buses of the system, as shown in column 2 of Table 6.7. The total installed capacity and the short-circuit current capacity (I_{sc}^{inv}) of IBDGs are shown in column 3-4 of Table 6.7, respectively.

The load flow analysis of the given test system with IBDGs has been performed by using the proposed

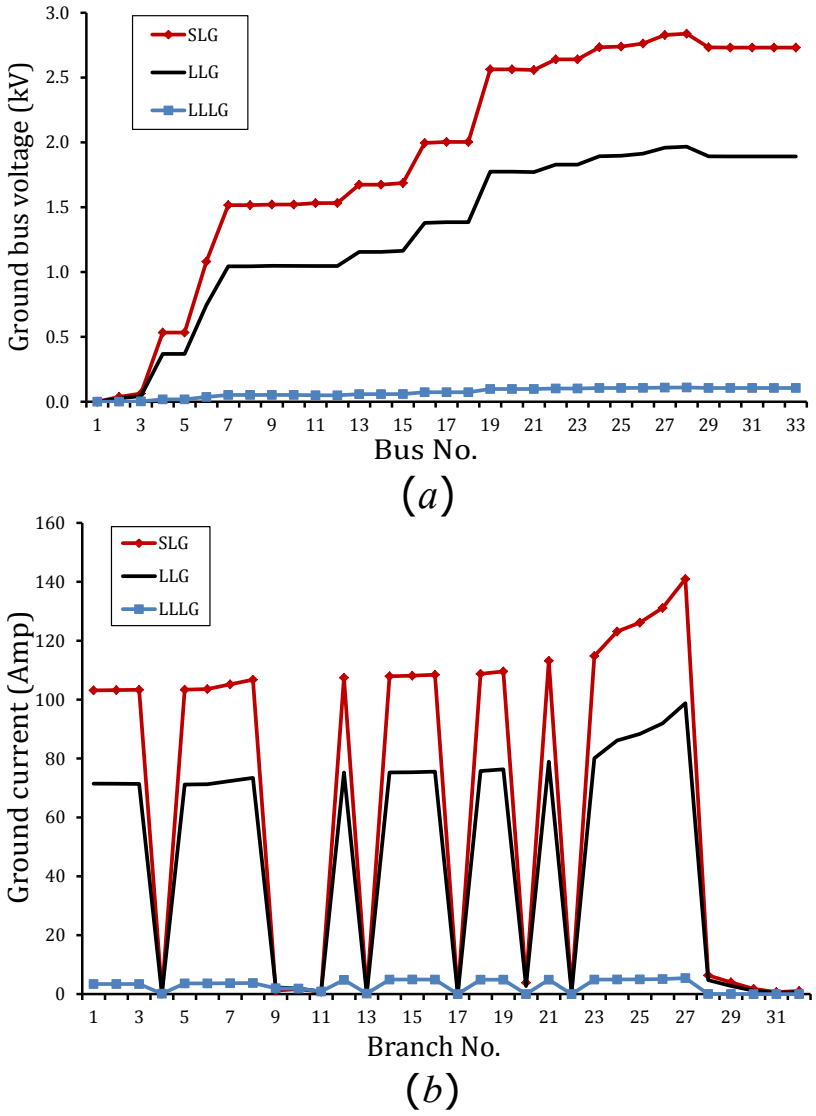

Figure 6.17: (a) Voltage profile of ground bus, (b) Ground current, for various ground faults at bus 28, of modified IEEE 34-bus test system in the presence of IBDG and Δ-Y_g IBDG transformer

method. The results obtained by the proposed load flow analysis method have been compared with those obtained by the $[\mathbf{Y_{bus}}]$ matrix based method.

The voltage profile of phase a, neutral bus and ground bus of the test system obtained by the proposed load flow method and $[\mathbf{Y_{bus}}]$ matrix based method are shown in Figs. 6.19-6.21, respectively. A good match between the results obtained by these two methods again demonstrates the perfectness of the proposed approach.

The current in the phase a, neutral wire and ground for the given test system calculated by the proposed

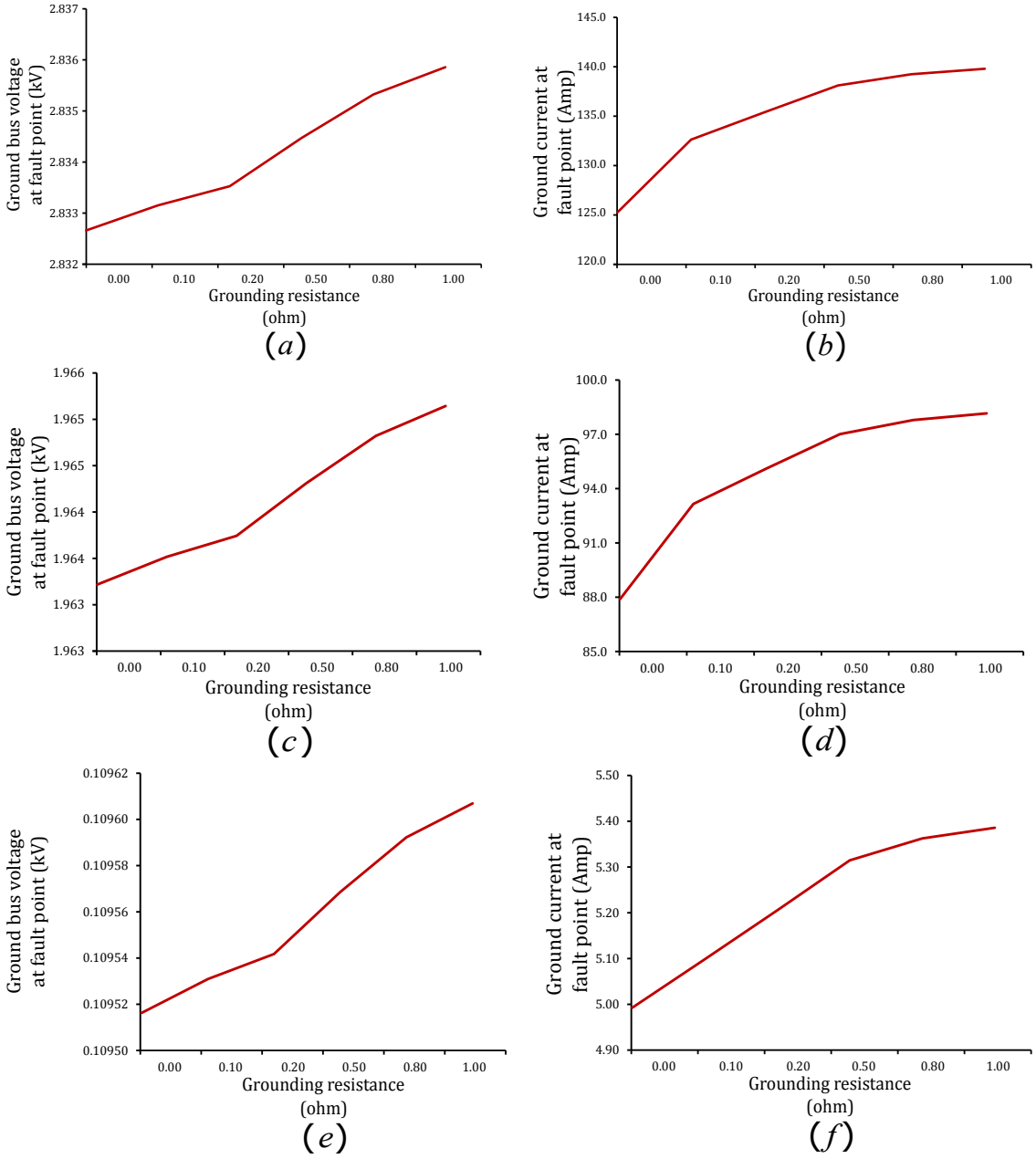

Figure 6.18: Ground bus voltage and ground current at fault point in modified IEEE 34-bus test system in the presence of IBDG and Δ-Y_g IBDG transformer for various grounding resistance under SLG fault (a) and (b), LLG fault (c) and (d) and LLLG fault (e) and (f)

load flow method and $\left[\mathbf{Y_{bus}}\right]$ matrix based method are plotted in Figs. 6.22-6.24, respectively. A close matching of the current values, obtained by the two methods, as observed in these figures again validates the accuracy of the proposed method.

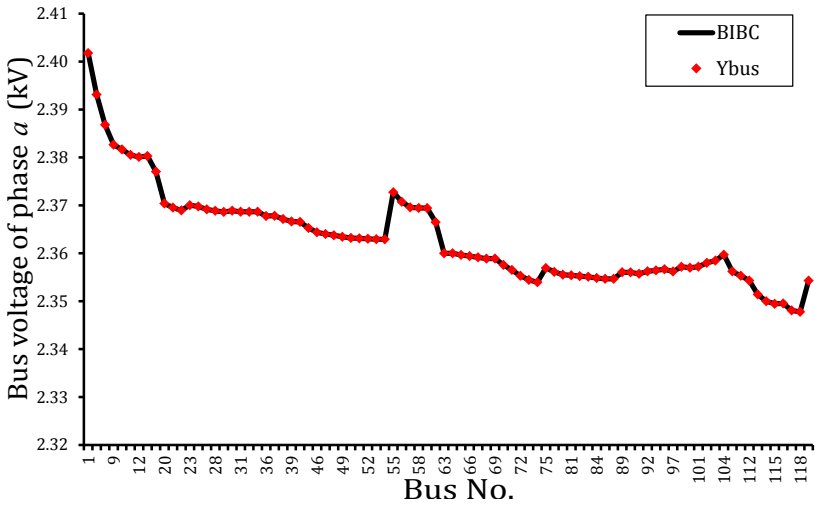

Figure 6.19: Voltage profile of phase a of modified IEEE 123-bus test system in the presence of IBDG and Δ-Y_g IBDG transformer using proposed $\left[\mathbf{BIBC}\right]$ technique and $\left[\mathbf{Y_{bus}}\right]$ technique under normal operating conditions

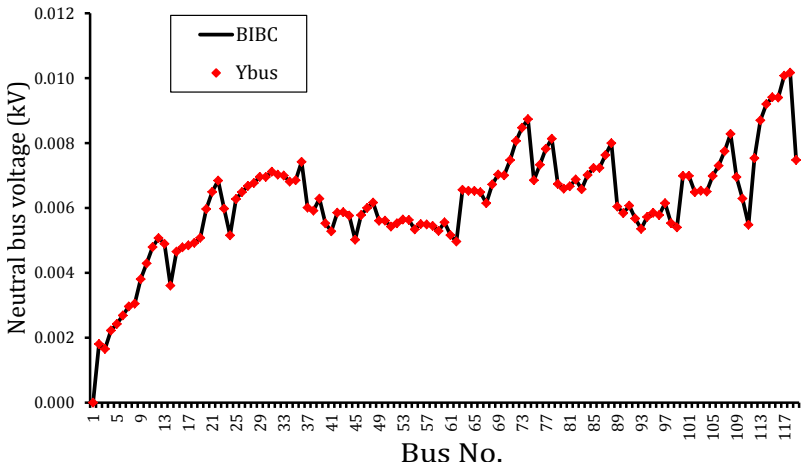

Figure 6.20: Voltage profile of neutral bus of modified IEEE 123-bus test system in the presence of IBDG and Δ-Y_g IBDG transformer using proposed $\left[\mathbf{BIBC}\right]$ technique and $\left[\mathbf{Y_{bus}}\right]$ technique under normal operating conditions

The inverter currents ($\mathbf{I_{inv}^{abc}}$) and the inverter bus voltages ($\mathbf{V_{inv}^{abc}}$) calculated by the proposed $[\mathbf{BIBC}]$ matrix based method and the $[\mathbf{Y_{bus}}]$ matrix based method are shown in Tables 6.8 and 6.9, respectively. The values of ($\mathbf{I_{inv}^{abc}}$) and ($\mathbf{V_{inv}^{abc}}$) of all IBDGs obtained by the proposed method are exactly equal to the values obtained by the $[\mathbf{Y_{bus}}]$ matrix based method, which again establish the accuracy of the proposed method. The phase angles of inverter currents and the inverter bus voltages are same (as shown in Tables 6.8 and

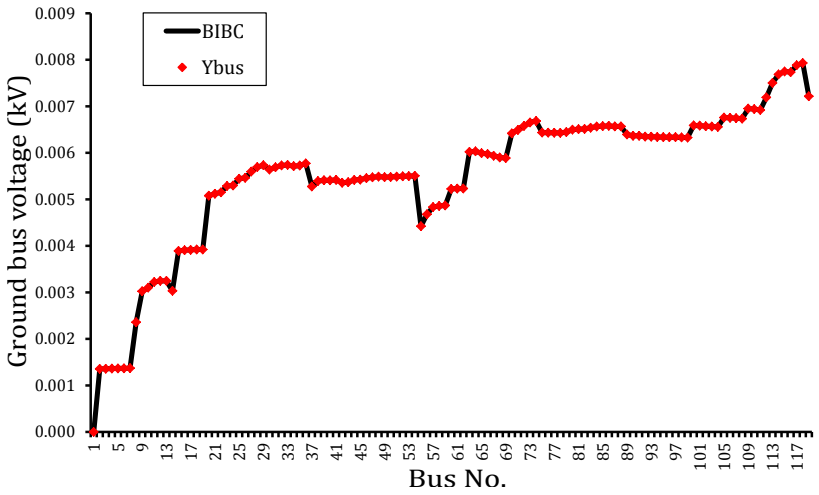

Figure 6.21: Voltage profile of ground bus of modified IEEE 123-bus test system in the presence of IBDG and Δ-Y_g IBDG transformer using proposed $\left[\mathbf{BIBC}\right]$ technique and $\left[\mathbf{Y_{bus}}\right]$ technique under normal operating conditions

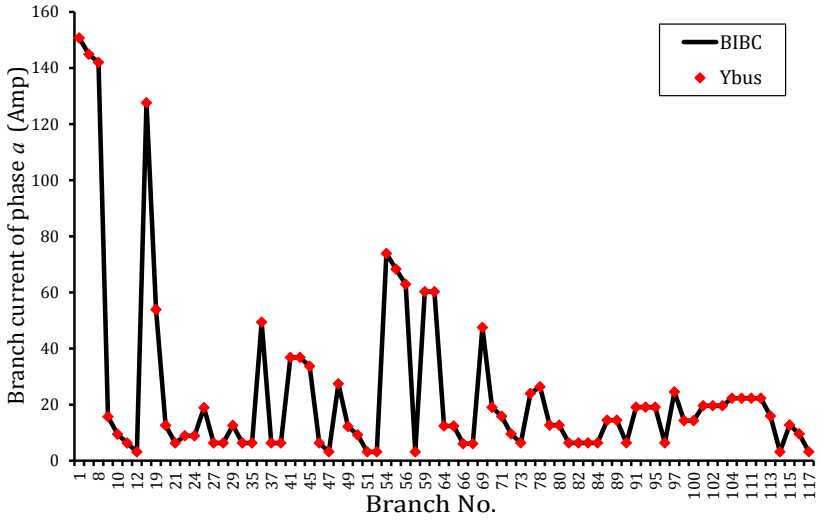

Figure 6.22: Branch current of phase a of modified IEEE 123-bus test system in the presence of IBDG and Δ-Y_g IBDG transformer using proposed $\left[\mathbf{BIBC}\right]$ technique and $\left[\mathbf{Y_{bus}}\right]$ technique under normal operating conditions

6.9) it is due to the fact that all the IBDGs are operating at unity power factor under the normal operating conditions.

A case of isolated neutral has also been simulated on the considered test system using the proposed load flow method. The neutral bus voltage profiles and the neutral wire currents of the test system for

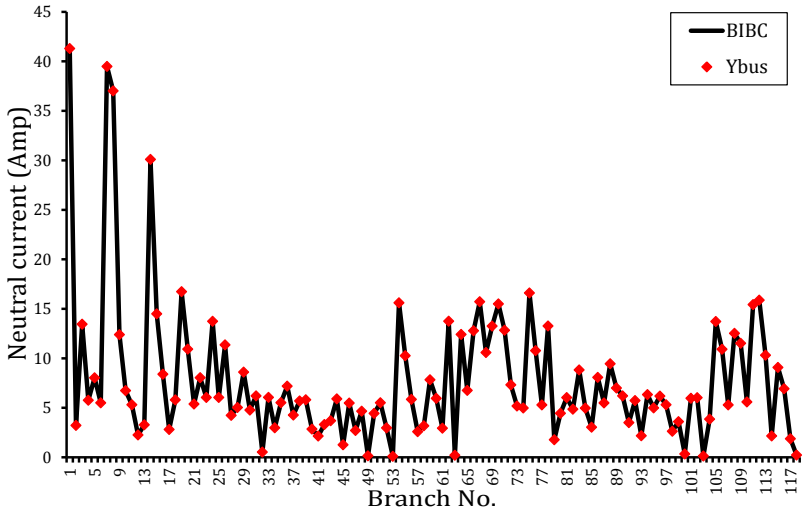

Figure 6.23: Neutral current of modified IEEE 123-bus test system in the presence of IBDG and Δ-Y_g IBDG transformer using proposed $\left[\mathbf{BIBC}\right]$ technique and $\left[\mathbf{Y_{bus}}\right]$ technique under normal operating conditions

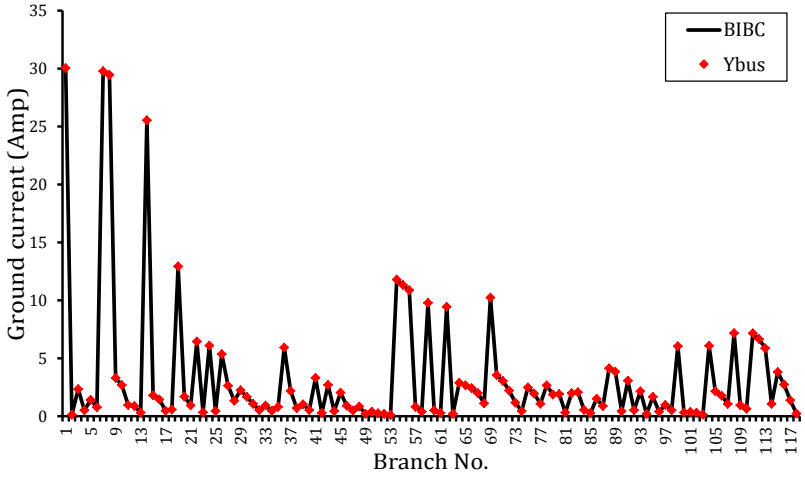

Figure 6.24: Ground current of modified IEEE 123 bus-test system in the presence of IBDG and Δ-Y_g IBDG transformer using proposed $\left[\mathbf{BIBC}\right]$ technique and $\left[\mathbf{Y_{bus}}\right]$ technique under normal operating conditions

"isolated neutral" and "grounded neutral" cases are shown in Figs. 6.25(a) and (b), respectively. The values of voltages at all the neutral buses in "isolated neutral" case are higher than the "grounded neutral" case (as shown in Fig. 6.25(a)) for the same reasons as explained for modified IEEE 34-bus test system earlier.

(b). Results of short-circuit studies

To further investigate the effectiveness of the two proposed short-circuit analysis methods $\left(\left[\mathbf{BIBC}\right]\right.$

Table 6.8: Inverter currents of modified IEEE 123-bus test system in the presence of IBDGs and Δ-Y_g IBDG transformers under normal operating conditions

IBDG location (Bus No.)	**Inverter current, $\mathbf{I_{inv}^{abc}}$ (Amp)**					
	[BIBC] Technique			**[$\mathbf{Y_{bus}$]} Technique**		
	Phase a	**Phase b**	**Phase c**	**Phase a**	**Phase b**	**Phase c**
20	169.54∠-30.09^o	169.48∠-149.85^o	168.90∠90.01^o	169.54∠-30.09^o	169.48∠-149.85^o	168.90∠90.01^o
25	127.19∠-30.11^o	127.12∠-149.86^o	126.67∠89.99^o	127.19∠-30.11^o	127.12∠-149.86^o	126.67∠89.99^o
75	170.52∠-30.07^o	170.23∠-149.77^o	169.61∠89.99^o	170.52∠-30.07^o	170.23∠-149.77^o	169.61∠89.99^o
98	213.04∠-29.92^o	212.75∠-149.66^o	212.07∠90.14^o	213.04∠-29.92^o	212.75∠-149.66^o	212.07∠90.14^o
104	170.36∠-29.97^o	170.06∠-149.69^o	169.49∠90.08^o	170.36∠-29.97^o	170.06∠-149.69^o	169.49∠90.08^o

Table 6.9: Inverter bus voltages of modified IEEE 123-bus test system in the presence of IBDGs and Δ-Y_g IBDG transformers under normal operating conditions

IBDG location (Bus No.)	**Inverter bus voltage, $\mathbf{V_{inv}^{abc}}$ (kV)**					
	[BIBC] Technique			**[$\mathbf{Y_{bus}$]} Technique**		
	Phase a	**Phase b**	**Phase c**	**Phase a**	**Phase b**	**Phase c**
20	0.2745∠-30.09^o	0.2746∠-149.85^o	0.2755∠90.01^o	0.2745∠-30.09^o	0.2746∠-149.85^o	0.2755∠90.01^o
25	0.2744∠-30.11^o	0.2745∠-149.86^o	0.2755∠89.99^o	0.2744∠-30.11^o	0.2745∠-149.86^o	0.2755∠89.99^o
75	0.2729∠-30.07^o	0.2734∠-149.77^o	0.2744∠89.99^o	0.2729∠-30.07^o	0.2734∠-149.77^o	0.2744∠89.99^o
98	0.2730∠-29.92^o	0.2734∠-149.66^o	0.2743∠90.14^o	0.2730∠-29.92^o	0.2734∠-149.66^o	0.2743∠90.14^o
104	0.2731∠-29.97^o	0.2736∠-149.69^o	0.2745∠90.08^o	0.2731∠-29.97^o	0.2736∠-149.69^o	0.2745∠90.08^o

matrix based method and $[\mathbf{Y_{bus}}]$ matrix based method$\big)$, an SLG fault in phase a of bus 105, with a fault impedance $\bar{z}_f = 0.001 + 0.000i$ p.u. has been simulated. In the initial step, the inverter currents ($\mathbf{I_{inv,f,est}^{abc}}$) of all the five IBDGs have been calculated by assuming that the inverter bus voltages of all IBDGs under the fault conditions are maintained at their pre-fault values i.e., $\mathbf{V_{inv,f}^{abc}} = \mathbf{V_{inv,f,st}^{abc}}$. The calculated values of the inverter currents obtained by both proposed methods are given in columns 2-4 of Tables 6.10 and 6.11, respectively. These values show that the magnitude of inverter currents of all IBDGs are greater than their short-circuit current capacities (I_{sc}^{inv}). Therefore, the fault current, the bus voltages and the inverter currents of all IBDGs under the fault conditions are recalculated with the appropriate inverter current control strategy as discussed in the proposed short-circuit analysis methods. The final values of inverter currents and injected powers (capacitive reactive power) by all IBDGs, obtained by the two proposed methods, are

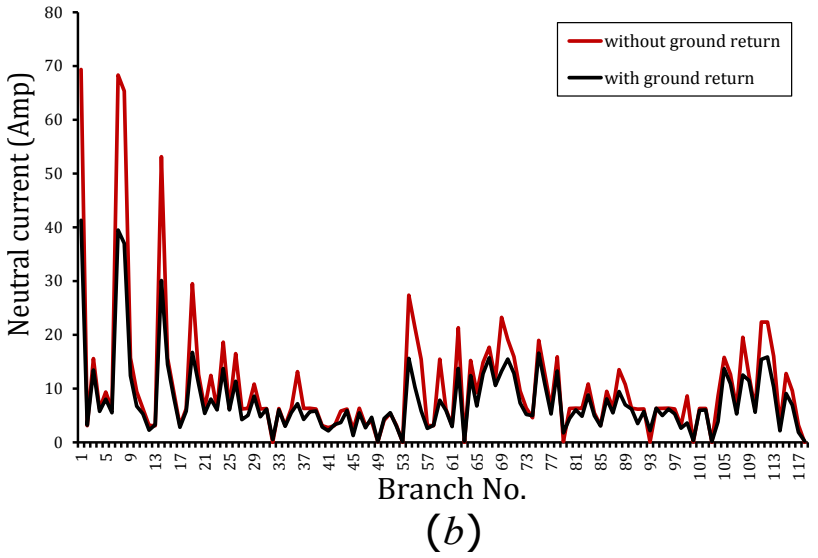

Figure 6.25: (a) Neutral bus voltage profile, (b) Neutral current of modified IEEE 123-bus test system in the presence of IBDG and Δ-Y_g IBDG transformer in "isolated neutral" and "grounded neutral" cases under normal operating conditions

shown in columns 5-10 of Tables 6.10 and 6.11, respectively. It can also be observed from these tables that the final values of inverter currents and injected powers by the IBDGs obtained by both the methods are identical, which again validates the accuracy of the proposed methods. The fault current (I_f) and source current (I_s) in phase a for this case using the proposed methods are given in Table 6.12. The above results show that the values of I_f and I_s calculated by both the proposed methods are identical, thereby validating the proposed short-circuit analysis methods.

Table 6.10: Results for SLG(a-g) fault at bus 105 in modified three phase four wire multigrounded IEEE 123-bus radial test system in the presence of IBDGs and Δ-Y_g IBDG transformers using proposed $[\mathbf{BIBC}]$ method

IBDG location (bus No.)	**Initial estimate of inverter current, $\mathbf{I}^{\mathbf{abc}}_{\mathbf{inv,f,est}}$, (kA) when $\mathbf{V}^{\mathbf{abc}}_{\mathbf{inv,f}} = \mathbf{V}^{\mathbf{abc}}_{\mathbf{inv,st}}$**			**final value of inverter current, (kA) $\mathbf{I}^{\mathbf{abc}}_{\mathbf{inv,f}} = I^{inv}_{sc}\angle(\frac{\pi}{2} + \theta^{\mathbf{abc}}_{\mathbf{inv,f}})$**			**final value of injected IBDG power (kVAR)**		
	Phase-a	**Phase-b**	**Phase-c**	**Phase-a**	**Phase-b**	**Phase-c**	**Phase-a**	**Phase-b**	**Phase-c**
20	10.075∠-89.01^o	8.524∠87.27^o	1.661∠110.37^o	0.2519∠-124.12^o	0.2519∠122.37^o	0.2519∠-1.56^o	191.492	194.504	211.608
25	10.053∠-89.22^o	8.548∠87.03^o	1.621∠110.89^o	0.1889∠-124.17^o	0.1889∠122.34^o	0.1889∠-1.59^o	143.554	145.819	158.686
75	28.172∠-89.55^o	24.126∠86.65^o	4.397∠111.73^o	0.2519∠-132.60^o	0.2519∠128.51^o	0.2519∠-3.58^o	161.352	168.936	214.695
98	28.200∠-89.47^o	24.118∠86.74^o	4.427∠111.55^o	0.3148∠-132.78^o	0.3148∠128.28^o	0.3148∠-3.71^o	202.830	211.821	269.323
104	30.249∠-89.57^o	25.913∠86.62^o	4.714∠111.77^o	0.2519∠-133.78^o	0.2519∠129.31^o	0.2519∠-3.80^o	158.618	166.493	215.550

Table 6.11: Results for SLG(a-g) fault at bus 105 in modified three phase four wire multigrounded IEEE 123-bus radial test system in the presence of IBDGs and Δ-Y_g IBDG transformers using proposed $[\mathbf{Y_{bus}}]$ method

IBDG location (bus No.)	**Initial estimate of inverter current, $\mathbf{I}^{\mathbf{abc}}_{\mathbf{inv,f,est}}$, (kA) when $\mathbf{V}^{\mathbf{abc}}_{\mathbf{inv,f}} = \mathbf{V}^{\mathbf{abc}}_{\mathbf{inv,st}}$**			**final value of inverter current, (kA) $\mathbf{I}^{\mathbf{abc}}_{\mathbf{inv,f}} = I^{inv}_{sc}\angle(\frac{\pi}{2} + \theta^{\mathbf{abc}}_{\mathbf{inv,f}})$**			**final value of injected IBDG power (kVAR)**		
	Phase-a	**Phase-b**	**Phase-c**	**Phase-a**	**Phase-b**	**Phase-c**	**Phase-a**	**Phase-b**	**Phase-c**
20	1.105∠-59.28^o	0.934∠125.42^o	0.190∠97.10^o	0.2519∠-124.12^o	0.2519∠122.37^o	0.2519∠-1.56^o	191.492	194.504	211.608
25	0.828∠-53.54^o	0.726∠131.88^o	0.125∠93.31^o	0.1889∠-124.17^o	0.1889∠122.34^o	0.1889∠-1.59^o	143.554	145.819	158.686
75	6.391∠-72.75^o	5.742∠105.77^o	0.665∠120.02^o	0.2519∠-132.60^o	0.2519∠128.51^o	0.2519∠-3.58^o	161.352	168.936	214.695
98	2.635∠-56.46^o	2.465∠125.59^o	0.191∠95.99^o	0.3148∠-132.78^o	0.3148∠128.28^o	0.3148∠-3.71^o	202.830	211.821	269.323
104	4.539∠-65.04^o	4.191∠114.55^o	0.348∠119.70^o	0.2519∠-133.78^o	0.2519∠129.31^o	0.2519∠-3.80^o	158.618	166.493	215.550

Different fault cases namely, LLG (ab-g), LLLG (abc-g), and LL (a-b) fault with $\bar{z}_f$ = 0.001+0.000i p.u., have also been simulated at bus 105 of the same system using the proposed methods. The calculated values of fault currents (I_f) and source currents (I_s) for all types of faults obtained by the proposed methods are given in Table 6.12. It can be observed from the table that the values obtained by the proposed $[\mathbf{BIBC}]$ method are exactly equal to the values obtained by the $[\mathbf{Y_{bus}}]$ method, which again establishes the accuracy of the proposed methods.

The voltage profiles of phase a bus voltage, neutral bus voltage and ground bus voltage of the modified IEEE 123-bus test system, for an SLG fault at phase a of bus 105 with fault impedance of $\bar{z}_f$ = 0.001+0.000i p.u., obtained by using the proposed short-circuit analysis methods, are shown in Figs. 6.26-6.28, respectively. It can be observed, from these figures, that the results obtained from these two methods are identical and this again demonstrates the correctness of the proposed short-circuit methods.

In Fig. 6.29(a), the ground bus voltage profile is plotted for various ground faults (SLG, LLG and

Table 6.12: Results of the proposed short-circuit analysis methods for modified three phase four wire multigrounded IEEE 123-bus radial test system in the presence of IBDGs and Δ-Y_g IBDG transformers

case	Fault type	phase	Fault current at fault point (I_f)		Current drawn from the supply (I_s)	
			$[\mathbf{BIBC}]$ Technique (kA)	$[\mathbf{Y_{bus}}]$ Technique (kA)	$[\mathbf{BIBC}]$ Technique (kA)	$[\mathbf{Y_{bus}}]$ Technique (kA)
1	SLG (a-g)	a	2.47555	2.47555	2.44377	2.44377
2	LLG (ab-g)	a	4.40065	4.40065	4.43822	4.43822
		b	4.62304	4.62304	4.52799	4.52799
3	LLLG (abc-g)	a	4.56943	4.56943	4.53893	4.53893
		b	5.24708	5.24708	5.16524	5.16524
		c	4.53549	4.53549	4.46304	4.46304
4	L-L (a-b)	a	4.44763	4.44763	4.53721	4.53721
		b	4.44763	4.44763	4.32394	4.32394

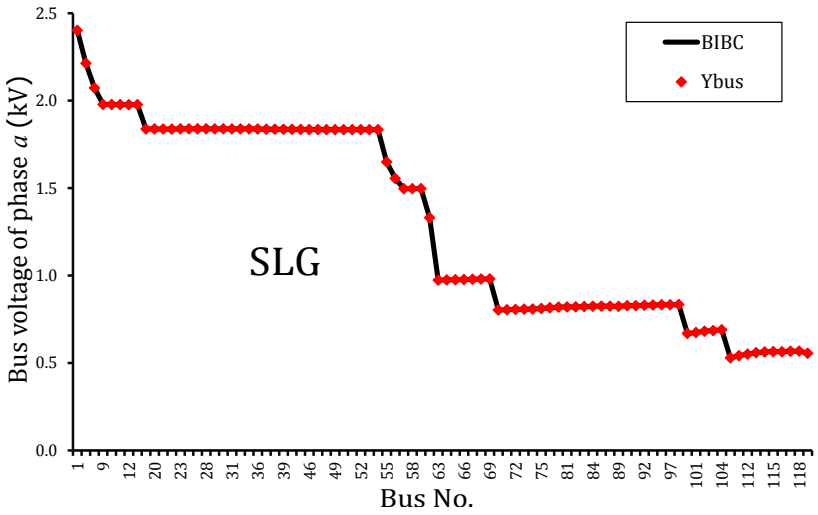

Figure 6.26: Voltage profile of phase a, for an SLG fault (a-g) at bus 105, of modified IEEE 123-bus test system in the presence of IBDG and Δ-Y_g IBDG transformer using proposed $[\mathbf{BIBC}]$ technique and $[\mathbf{Y_{bus}}]$ technique

LLLG) at bus 105 with a fault impedance of $\bar{z}_f$ = 0.001+0.000i p.u.. The plot shows that the highest ground bus voltages occur for SLG fault followed by LLG fault while the lowest values are observed for LLLG fault. This is due to the fact that the fault current injected into the fault point at ground bus is the phasor

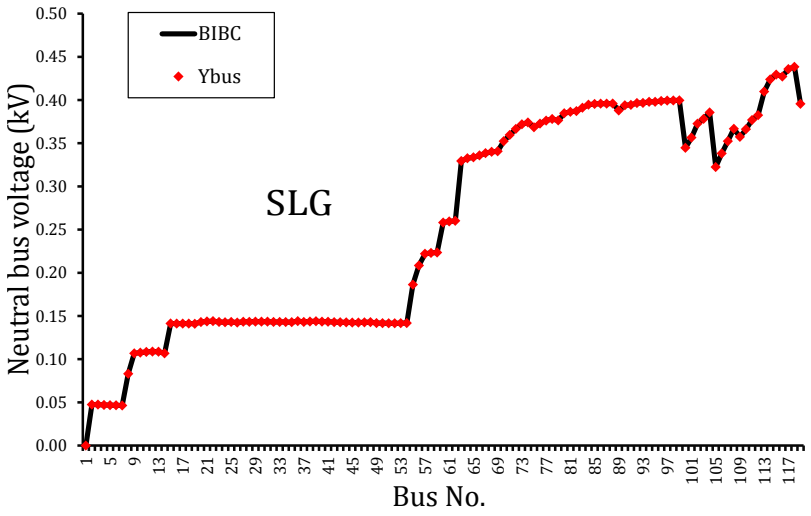

Figure 6.27: Voltage profile of neutral bus, for an SLG fault (a-g) at bus 105, of modified IEEE 123-bus test system in the presence of IBDG and Δ-Y_g IBDG transformer using proposed $\left[\mathbf{BIBC}\right]$ technique and $\left[\mathbf{Y_{bus}}\right]$ technique

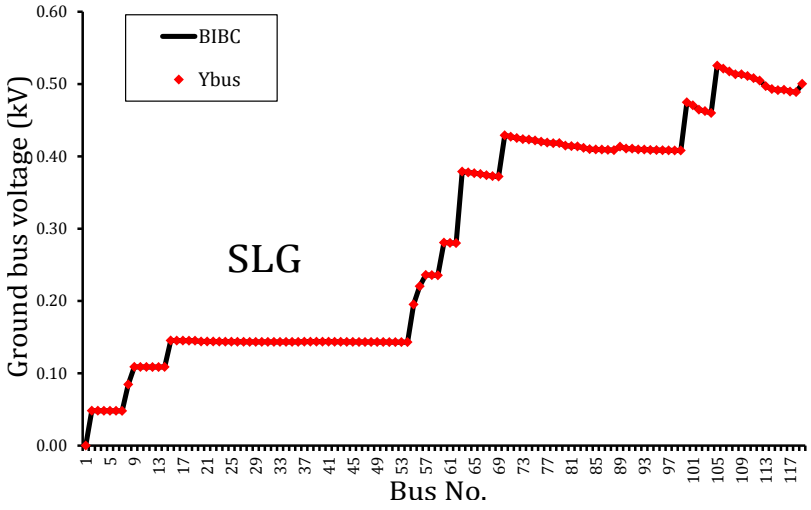

Figure 6.28: Voltage profile of ground bus, for an SLG fault (a-g) at bus 105, of modified IEEE 123-bus test system in the presence of IBDG and Δ-Y_g IBDG transformer using proposed $\left[\mathbf{BIBC}\right]$ technique and $\left[\mathbf{Y_{bus}}\right]$ technique

sum of the three phase fault currents and its value ($\bar{I}_f^a + \bar{I}_f^b + \bar{I}_f^c = 0.03 + j0.14$ kA $= 0.138\underline{/77.17^o}$ kA) is smallest for LLLG fault, followed by the injected fault current of LLG fault ($\bar{I}_f^a + \bar{I}_f^b = -1.09 - j1.35$ kA $= 1.736\underline{/-128.87^o}$ kA) with SLG fault injecting highest current ($\bar{I}_f^a = 1.00 - j2.26$ kA $= 2.476\underline{/-66.08^o}$ kA) into the ground at the fault bus location. Therefore, the currents flowing through ground from fault point

to the substation ground are highest for SLG fault followed by LLG fault and smallest for LLLG fault, as shown in 6.29(b). As a result, the ground bus voltages are highest for SLG fault with LLLG fault resulting in lowest ground bus voltages. From Fig. 6.29(b), it is also observed that the value of ground current at certain branches of the test system (like branch nos. $2-5, 9-13, 17-53, 81-97$ and $106-118$) are nearly equal to zero. It is due to the fact, that these branches are not present in the path of fault current returning through ground from fault point to the substation ground.

6.4.2 Results of test systems with IBDGs and Y_g-Y_g IBDG transformers

In this subsection, Y_gY_g-0 type of IBDG transformer is used for the connection of IBDG to the grid and its nodal admittance matrix model (p.u.) is given as [80],

$$\mathbf{Y_{T}}_{(Y_gY_g0)} = y_t \begin{bmatrix} 1 & 0 & 0 & -1 & 0 & 0 \\ 0 & 1 & 0 & 0 & -1 & 0 \\ 0 & 0 & 1 & 0 & 0 & -1 \\ -1 & 0 & 0 & 1 & 0 & 0 \\ 0 & -1 & 0 & 0 & 1 & 0 \\ 0 & 0 & -1 & 0 & 0 & 1 \end{bmatrix} \tag{6.132}$$

where, the value of y_t is assumed as $(0.000 - 16.92i)$ p.u. It is a step down transformer with its turns ratio assumed as $24.9/0.480$ kV for the modified IEEE 34-bus test system and as $4.16/0.480$ kV for the modified IEEE 123-bus test system. The value of grounding impedances on primary and secondary side of the IBDG transformer ($\bar{Z}_{gtp}$ and $\bar{Z}_{gts}$) is assumed as $0.2\ \Omega$, equal to the value of neutral to ground impedance of the test system .

6.4.2.1 Results of modified three phase four wire multigrounded IEEE 34-bus test system in the presence of IBDGs and Y_g-Y_g IBDGs transformers

(a). Results of load flow studies

Three different sized IBDGs have also been considered in this test system and their detailed informations are given in Table 6.1. It is assumed that all IBDGs are operating at unity power factor under normal operating condition. The load flow analysis of this test system has been performed by using the proposed method (as discussed in Subsection 6.3.1 for Y_g-Y_g IBDG transformer). The results obtained by the proposed method have been compared with those obtained by the $[\mathbf{Y_{bus}}]$ matrix based method and the time domain simulation studies carried out using PSCAD/EMTDC software.

The bar graph for the phase a bus voltages, neutral bus voltages and ground bus voltages of the test system with IBDGs, have been obtained by the proposed method, $\left[\mathbf{Y_{bus}}\right]$ matrix method and PSCAD/EMTDC

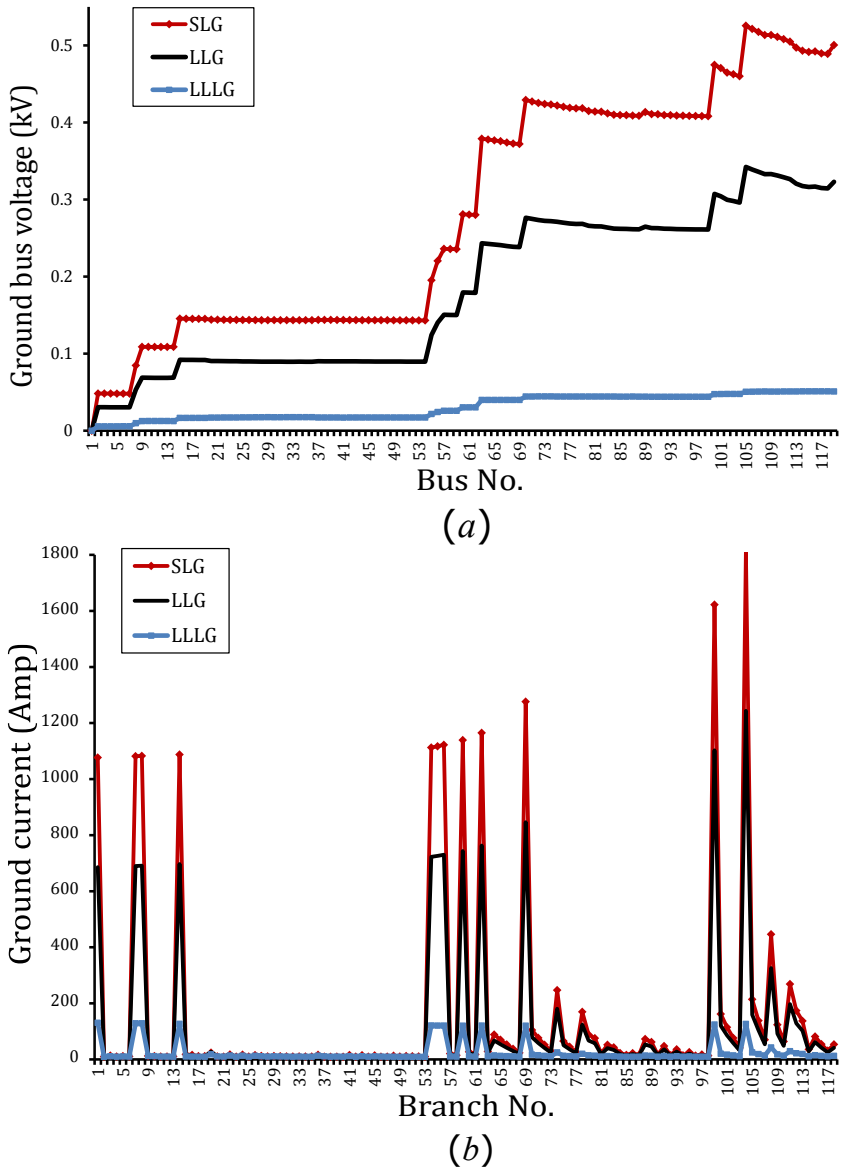

Figure 6.29: (a) Voltage profile of ground bus, (b) Ground current, for various ground faults at bus 105, of modified IEEE 123-bus test system in the presence of IBDG and Δ-Y_g IBDG transformer

simulation studies, and are shown in Figs. 6.30-6.32. These figures show that the results obtained by the proposed method are very close to the results of the $\left[\mathbf{Y_{bus}}\right]$ matrix method and PSCAD/EMTDC simulation studies, which demonstrates the correctness of the proposed approach.

The currents in the phase a, neutral wire and ground for the considered test system calculated by the proposed load flow method are plotted in Figs. 6.33-6.35, respectively. The values of these three currents have also been obtained by the $\left[\mathbf{Y_{bus}}\right]$ matrix based method and PSCAD/EMTDC simulation studies, and

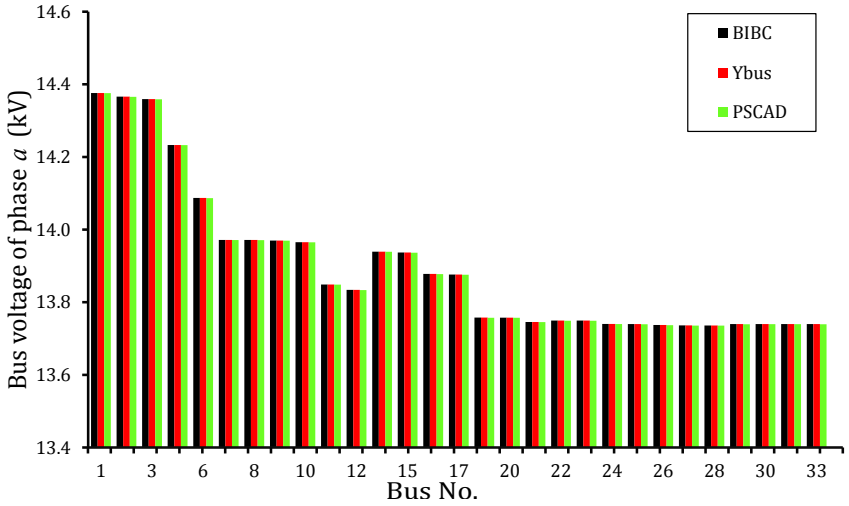

Figure 6.30: Voltage profile of phase a of modified IEEE 34-bus test system in the presence of IBDG and Y_g-Y_g IBDG transformer using proposed $\left[\mathbf{BIBC}\right]$ technique, $\left[\mathbf{Y_{bus}}\right]$ technique and PSCAD/EMTDC simulation under normal operating conditions

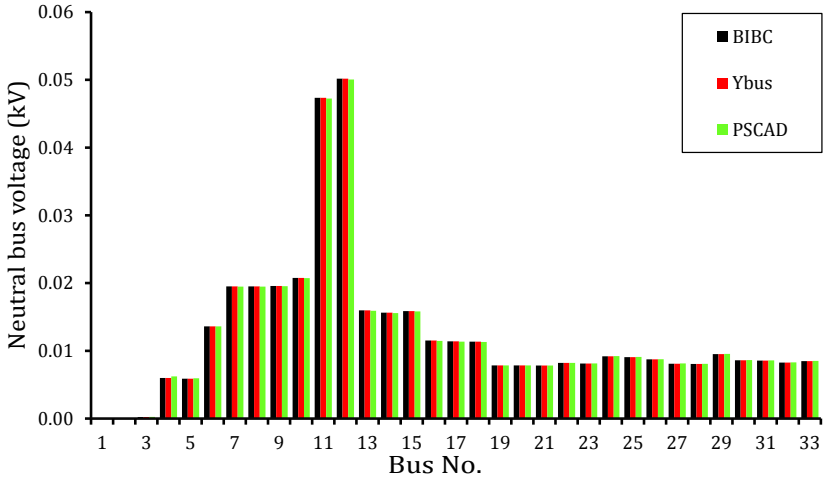

Figure 6.31: Voltage profile of neutral bus of modified IEEE 34-bus test system in the presence of IBDG and Y_g-Y_g IBDG transformer using proposed $\left[\mathbf{BIBC}\right]$ technique, $\left[\mathbf{Y_{bus}}\right]$ technique and PSCAD/EMTDC simulation under normal operating conditions

are plotted along with the results of proposed method in Figs. 6.33-6.35. A close matching of the current values, obtained by the three methods, as observed in these figures again validates the accuracy of the proposed method.

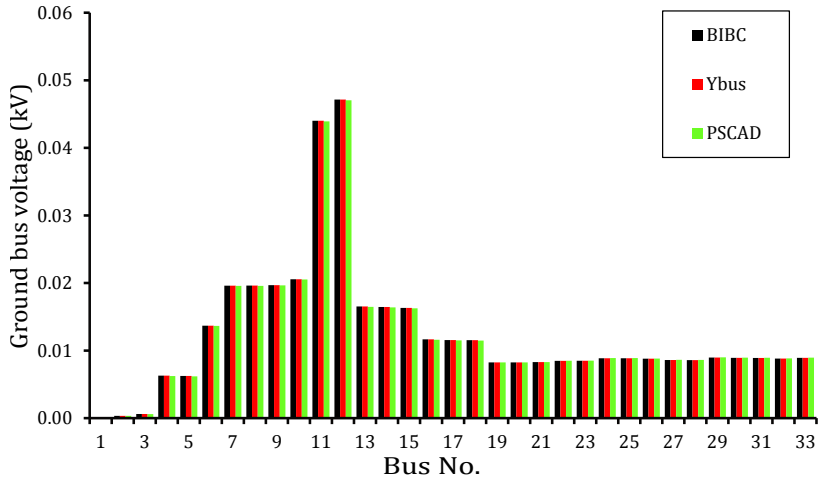

Figure 6.32: Voltage profile of ground bus of modified IEEE 34-bus test system in the presence of IBDG and Y_g-Y_g IBDG transformer using proposed $\left[\mathbf{BIBC}\right]$ technique, $\left[\mathbf{Y_{bus}}\right]$ technique and PSCAD/EMTDC simulation under normal operating conditions

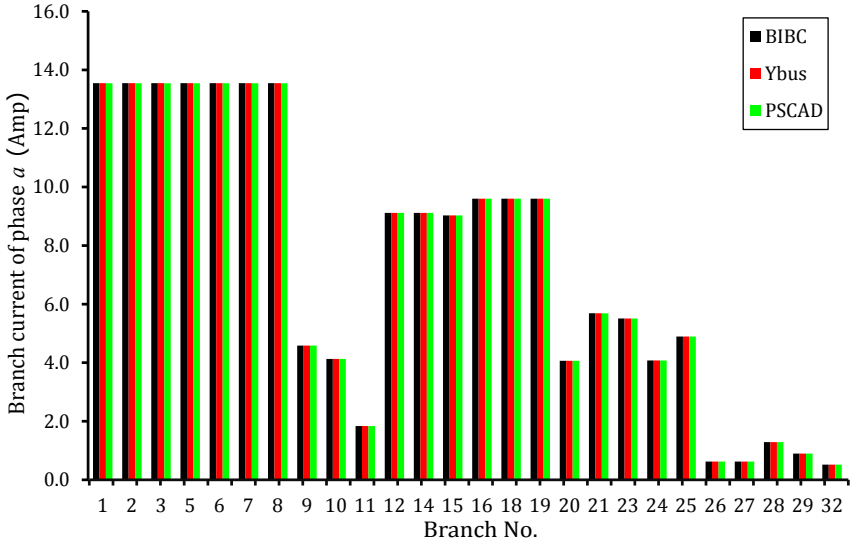

Figure 6.33: Branch current of phase a of modified IEEE 34-bus test system in the presence of IBDG and Y_g-Y_g IBDG transformer using proposed $\left[\mathbf{BIBC}\right]$ technique, $\left[\mathbf{Y_{bus}}\right]$ technique and PSCAD/EMTDC simulation under normal operating conditions

The inverter currents ($\mathbf{I_{inv}^{abc}}$) and the inverter bus voltages ($\mathbf{V_{inv}^{abc}}$) calculated by the proposed $[\mathbf{BIBC}]$ matrix based method and the $\left[\mathbf{Y_{bus}}\right]$ matrix based method are shown in Tables 6.13 and 6.14, respectively.

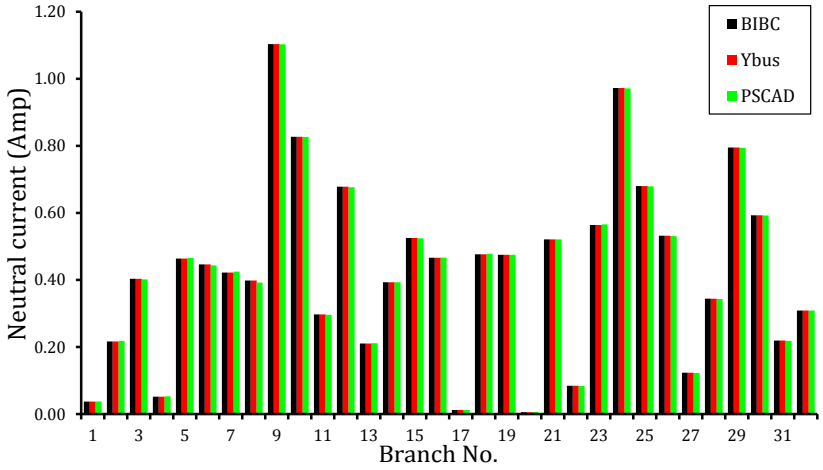

Figure 6.34: Neutral current of modified IEEE 34-bus test system in the presence of IBDG and Y_g-Y_g IBDG transformer using proposed $\left[\mathbf{BIBC}\right]$ technique, $\left[\mathbf{Y_{bus}}\right]$ technique and PSCAD/EMTDC simulation under normal operating conditions

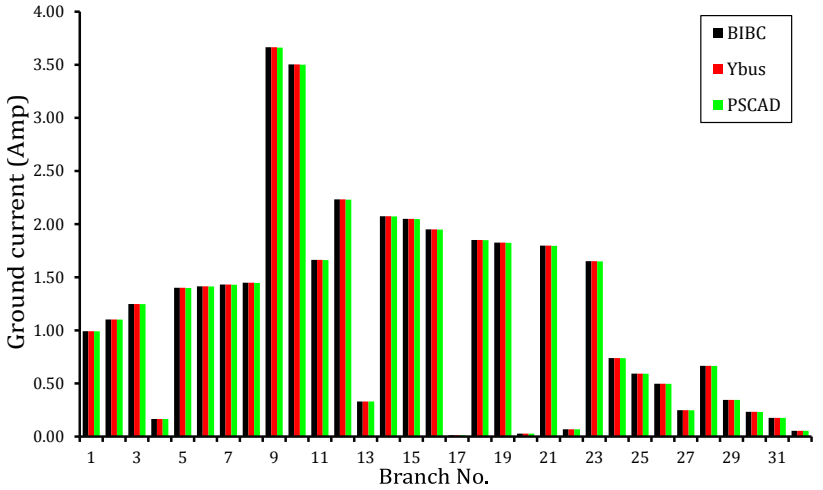

Figure 6.35: Ground current of modified IEEE 34-bus test system in the presence of IBDG and Y_g-Y_g IBDG transformer using proposed $\left[\mathbf{BIBC}\right]$ technique, $\left[\mathbf{Y_{bus}}\right]$ technique and PSCAD/EMTDC simulation under normal operating conditions

The values of ($\mathbf{I_{inv}^{abc}}$) and ($\mathbf{V_{inv}^{abc}}$) of all IBDGs obtained by the proposed method are exactly equal to the values obtained by the $\left[\mathbf{Y_{bus}}\right]$ matrix based method, which again establishes the accuracy of the proposed method. Also, the phase angles of inverter currents and the inverter bus voltages are same, since all IBDGs

Table 6.13: Inverter currents of modified IEEE 34-bus test system in the presence of IBDG and Y_g-Y_g IBDG transformers under normal operating conditions

IBDG location (Bus No.)	**Inverter current, $\mathbf{I_{inv}^{abc}}$ (Amp)**					
	[BIBC] Technique			**[$\mathbf{Y_{bus}$]} Technique**		
	Phase a	**Phase b**	**Phase c**	**Phase a**	**Phase b**	**Phase c**
16	65.81∠0.2765^o	65.30∠-119.69^o	65.65∠120.33^o	65.81∠0.2765^o	65.30∠-119.69^o	65.65∠120.33^o
25	66.42∠0.5403^o	66.20∠-119.46^o	66.55∠120.38^o	66.42∠0.5403^o	66.20∠-119.46^o	66.55∠120.38^o
30	88.55∠0.5740^o	88.28∠ -119.43^o	88.74∠120.41^o	88.55∠0.5740^o	88.28∠-119.43^o	88.74∠120.41^o

Table 6.14: Inverter bus voltages of modified IEEE 34-bus test system in the presence of IBDG and Y_g-Y_g IBDG transformers under normal operating conditions

IBDG location (Bus No.)	**Inverter bus voltage, $\mathbf{V_{inv}^{abc}}$ (Amp)**					
	[BIBC] Technique			**[$\mathbf{Y_{bus}$]} Technique**		
	Phase a	**Phase b**	**Phase c**	**Phase a**	**Phase b**	**Phase c**
16	0.2674∠0.2765^o	0.2695∠-119.69^o	0.2681∠120.33^o	0.2674∠0.2765^o	0.2695∠-119.69^o	0.2681∠120.33^o
25	0.2650∠0.5403^o	0.2659∠-119.46^o	0.2645∠120.38^o	0.2650∠0.5403^o	0.2659∠-119.46^o	0.2645∠120.38^o
30	0.2650∠0.5740^o	0.2658∠-119.43^o	0.2645∠120.41^o	0.2650∠0.5740^o	0.2658∠-119.43^o	0.2645∠120.41^o

are operating at unity power factor under the normal operating conditions.

A case of isolated neutral has also been simulated on the considered test system with IBDGs and Y_g-Y_g IBDG transformers, using the proposed method. The neutral bus voltage profiles and neutral currents of the test system for "isolated neutral" and "grounded neutral" cases are shown in Figs. 6.36(a) and (b), respectively. The values of neutral voltages at all the buses in "isolated neutral" case are higher than the "grounded neutral" case for the same reasons as explained for modified IEEE 34-bus test system with Δ-Y_g IBDG transformer case earlier.

The value of maximum ground bus voltage and maximum ground current in the test system under normal operating condition, for various grounding resistance are plotted in Fig. 6.37(a) and (b). The figure shows that, with the increase in grounding resistance, the value of maximum ground bus voltage as well as maximum ground current in the system decreases (as shown in Fig. 6.37(a)). This is due to the fact that, with the increase in grounding resistance, the value of neutral to ground current in the system decreases and as a result the value of ground wire currents and hence the ground bus voltages of the system decreases (as shown in Fig. 6.37(b)).

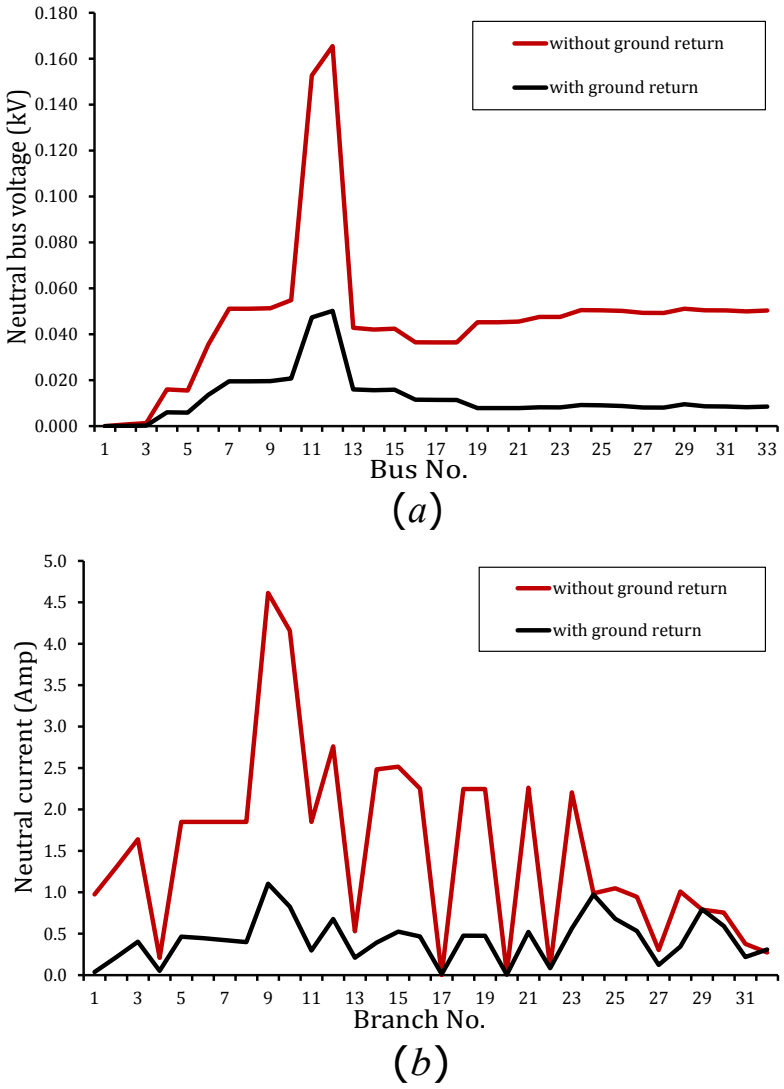

Figure 6.36: (a) Neutral bus voltage profile, (b) Neutral current of modified IEEE 34-bus test system in the presence of IBDG and Y_g-Y_g IBDG transformer in "isolated neutral" and "grounded neutral" cases under normal operating conditions

(b). Results of short-circuit studies

For investigating the efficacy of the proposed short-circuit analysis methods ($\left[\mathbf{BIBC}\right]$ matrix based method and $[\mathbf{Y_{bus}}]$ matrix based method) for the case with Y_g-Y_g IBDG transformer, an SLG fault in phase a of bus 28, with a fault impedance $\bar{z}_f = 0.001 + 0.000i$ p.u. has been simulated. The initial values of the inverter currents ($\mathbf{I^{abc}_{inv,f,est}}$) of all the IBDGs, under the fault conditions, have been calculated by assuming that the inverter bus voltages of all IBDGs are maintained at their pre-fault values i.e., $\mathbf{V^{abc}_{inv,f}} = \mathbf{V^{abc}_{inv,f,st}}$.

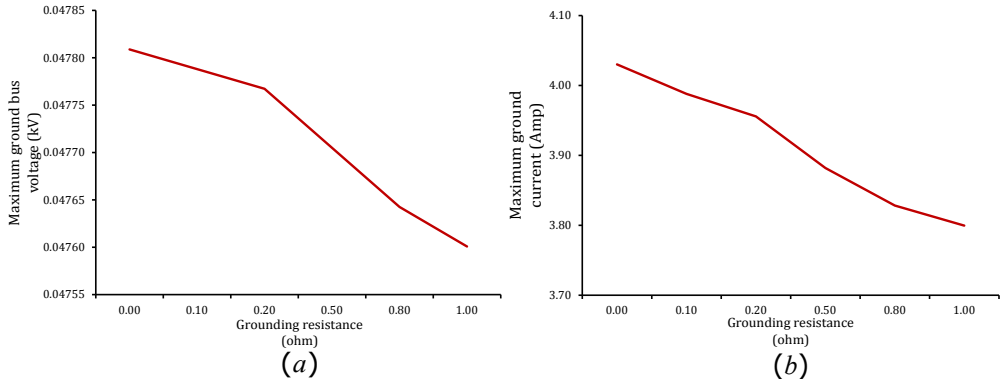

Figure 6.37: (a) Maximum ground bus voltage, (b) Maximum ground current, in modified IEEE 34-bus test system in the presence of IBDG and Y_g-Y_g IBDG transformer for various grounding resistance under normal operating condition

The calculated values of the inverter currents obtained by two proposed methods are given in columns 2-4 of Tables 6.15 and 6.16, respectively. These tables show that the magnitude of inverter currents of all IBDGs are greater than their short-circuit current capacities. Hence, according to the proposed methods, the magnitudes of inverter currents of all the phases are to be maintained at their short-circuit current capacities $\left(|I^p_{inv,f}| = I^{inv}_{sc}, p = a, b, c\ \right)$ and their angles are maintained in such a way that all IBDGs will deliver reactive power to the system during the short-circuit condition i.e., $\Psi^p_{inv,f} = \frac{\pi}{2} + \theta^p_{inv,f}$, $p = a, b, c$. With this strategy, the fault current, the bus voltages and the inverter currents of all IBDGs under the fault conditions are recalculated using the proposed short-circuit analysis methods.

The final values of inverter currents and injected powers by all IBDGs, obtained by both the proposed methods, are shown in columns 5-10 of Tables 6.15 and 6.16, respectively. From both the tables, it can be observed that the final values of inverter currents and injected powers by the IBDGs obtained by both the methods are identical, which again validates the accuracy of the proposed methods. The fault current (I_f) and source current (I_s) in phase a for this case using the proposed methods and PSCAD/EMTDC simulation studies are given in Table 6.17. The % error in the calculated values of I_f and I_s with respect to the values obtained by PSCAD/EMTDC simulation studies are 0.00665% and 0.00817%, respectively, as shown in Table 6.17. The above results show that the values of I_f and I_s calculated by both the proposed methods are very close to the values obtained by the PSCAD/EMTDC software, thereby validating the proposed methods.

Different fault cases namely, LLG (ab-g), LLLG (abc-g), and LL (a-b) fault with $\bar{z}_f$ = 0.001+0.000i p.u., have also been simulated at bus 28 in the same system using the proposed methods and PSCAD/EMTDC

Table 6.15: Results for SLG(a-g) fault at bus 28 in modified three phase four wire multigrounded IEEE 34-bus radial test system in the presence of IBDGs and Y_g-Y_g IBDG transformers using proposed $[\mathbf{BIBC}]$ method

IBDG location (bus No.)	**Initial estimate of inverter current, $\mathbf{I}^{\mathbf{abc}}_{\mathbf{inv,f,est}}$, (kA) when $\mathbf{V}^{\mathbf{abc}}_{\mathbf{inv,f}} = \mathbf{V}^{\mathbf{abc}}_{\mathbf{inv,st}}$**			**final value of inverter current, (kA) $\mathbf{I}^{\mathbf{abc}}_{\mathbf{inv,f}} = I^{inv}_{sc}\angle(\frac{\pi}{2} + \theta^{\mathbf{abc}}_{\mathbf{inv,f}})$**			**final value of injected IBDG power (kVAR)**		
	Phase-a	**Phase-b**	**Phase-c**	**Phase-a**	**Phase-b**	**Phase-c**	**Phase-a**	**Phase-b**	**Phase-c**
16	26.912∠-92.81^o	10.966∠-59.87^o	9.285∠-60.67^o	0.0953∠-94.69^o	0.0953∠140.45^o	0.0953∠45.64^o	24.64	99.15	83.16
25	37.833∠-95.14^o	14.867∠-59.80^o	12.620∠-60.67^o	0.0953∠-95.25^o	0.0953∠138.08^o	0.0953∠50.99^o	2.85	106.69	85.69
30	37.767∠-95.10^o	14.856∠-59.87^o	12.579∠-60.67^o	0.1270∠-95.01^o	0.1270∠138.08^o	0.1270∠50.93^o	4.05	142.20	114.29

Table 6.16: Results for SLG(a-g) fault at bus 28 in modified three phase four wire multigrounded IEEE 34-bus radial test system in the presence of IBDGs and Y_g-Y_g IBDG transformers using proposed $[\mathbf{Y_{bus}}]$ method

IBDG location (bus No.)	**Initial estimate of inverter current, $\mathbf{I}^{\mathbf{abc}}_{\mathbf{inv,f,est}}$, (kA) when $\mathbf{V}^{\mathbf{abc}}_{\mathbf{inv,f}} = \mathbf{V}^{\mathbf{abc}}_{\mathbf{inv,st}}$**			**final value of inverter current, (kA) $\mathbf{I}^{\mathbf{abc}}_{\mathbf{inv,f}} = I^{inv}_{sc}\angle(\frac{\pi}{2} + \theta^{\mathbf{abc}}_{\mathbf{inv,f}})$**			**final value of injected IBDG power (kVAR)**		
	Phase-a	**Phase-b**	**Phase-c**	**Phase-a**	**Phase-b**	**Phase-c**	**Phase-a**	**Phase-b**	**Phase-c**
16	11.089∠-55.39^o	2.459∠169.31^o	2.241∠170.07^o	0.0953∠-94.69^o	0.0953∠140.45^o	0.0953∠45.64^o	24.64	99.15	83.16
25	29.901∠-81.41^o	1.918∠-141.61^o	2.052∠-150.52^o	0.0953∠-95.25^o	0.0953∠138.08^o	0.0953∠50.99^o	2.85	106.69	85.69
30	26.567∠-76.12^o	2.083∠173.53^o	2.263∠173.97^o	0.1270∠-95.01^o	0.1270∠138.08^o	0.1270∠50.93^o	4.05	142.20	114.29

software. The calculated values of fault currents (I_f) and source currents (I_s) for all type of faults obtained by the proposed methods and PSCAD/EMTDC simulation studies are given in Table 6.17. The maximum $\%$ errors in the calculated values of (I_f) and (I_s), obtained from the proposed short-circuit analysis methods, with respect to the PSCAD/EMTDC simulation results are 0.00741% and 0.00817%, respectively. These extremely small values of errors establish that the proposed methods are sufficiently accurate.

The phase a bus voltage, neutral bus voltage and ground bus voltage of the considered test system, for an SLG fault at phase a of bus 28 with fault impedance of $\bar{z}_f$ = 0.001+0.000i p.u., obtained by using the proposed short-circuit analysis methods $\big([\mathbf{BIBC}]$ matrix based and $[\mathbf{Y_{bus}}]$ matrix based methods$\big)$, are shown in the bar graphs of Figs. 6.38-6.40, respectively. The values of these voltages are also obtained by the time domain simulation studies carried out using the PSCAD/EMTDC software and are plotted along with the results of proposed methods, as shown in Figs. 6.38-6.40, respectively. A comparison of these plots shows that the values of bus voltages obtained by proposed methods are very close to the values obtained by the PSCAD/EMTDC simulation studies, which again validates the accuracy of the proposed short-circuit analysis methods.

In Fig. 6.41(a), the ground bus voltage profile is plotted for various ground faults (SLG, LLG and

Table 6.17: Error Analysis of proposed $[\mathbf{BIBC}]$ matrix based technique and $[\mathbf{Y_{bus}}]$ matrix based technique with respect to PSCAD/EMTDC simulation study for modified three phase four wire multigrounded IEEE 34-bus radial test system in the presence of IBDGs and Y_g-Y_g IBDG transformers

case	Fault type	phase	Fault current at fault point (I_f)			% Error in (I_f)		Current drawn from the supply (I_s)			% Error in (I_s)	
			PSCAD simulation (Amp)	[BIBC] Technique (Amp)	$[Y_{bus}]$ Technique (Amp)	[BIBC] Technique (%)	$[Y_{bus}]$ Technique (%)	PSCAD simulation (Amp)	[BIBC] Technique (Amp)	$[Y_{bus}]$ Technique (Amp)	[BIBC] Technique (%)	$[Y_{bus}]$ Technique (%)
1	SLG (a-g)	a	151.627	151.637	151.637	0.00665	0.00665	150.284	150.296	150.296	**0.00817**	**0.00817**
2	LLG (ab-g)	a	198.477	198.466	198.466	0.00537	0.00537	200.698	200.695	200.695	0.00136	0.00136
		b	249.579	249.598	249.598	**0.00741**	**0.00741**	248.082	248.101	248.101	0.00702	0.00702
3	LLLG (abc-g)	a	237.883	237.891	237.891	0.00333	0.00333	238.906	238.918	238.918	0.00519	0.00519
		b	257.463	257.481	257.481	0.00663	0.00663	257.664	257.680	257.680	0.00623	0.00623
		c	249.725	249.738	249.738	0.00545	0.00545	248.802	248.817	248.817	0.00593	0.00593
4	L-L (a-b)	a	218.132	218.133	218.133	0.00010	0.00010	225.227	225.231	225.231	0.00157	0.00157
		b	218.132	218.133	218.133	0.00010	0.00010	215.224	215.239	215.239	0.00666	0.00666

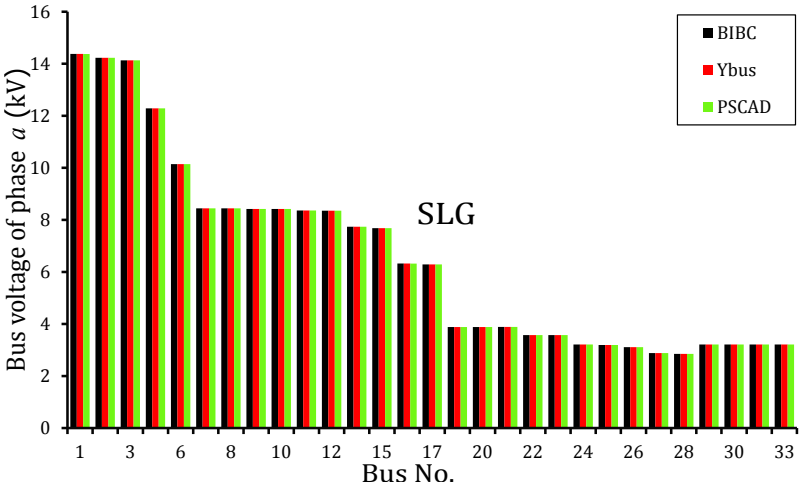

Figure 6.38: Voltage profile of phase a, for an SLG fault (a-g) at bus 28, of modified IEEE 34-bus test system in the presence of IBDG and Y_g-Y_g IBDG transformer using proposed $[\mathbf{BIBC}]$ technique, $[\mathbf{Y_{bus}}]$ technique and PSCAD/EMTDC simulation

LLLG) at bus 28 with a fault impedance of $\bar{z}_f$ = 0.001+0.000i p.u.. From this plot, again it can be observed that the highest ground bus voltages occurs for SLG fault followed by LLG fault while the lowest values are observed for LLLG fault. This is due to the fact that the fault current injected into the fault point at ground bus is the phasor sum of the three phase fault currents and its value ($\bar{I}_f^a + \bar{I}_f^b + \bar{I}_f^c = -0.27 + j5.79$

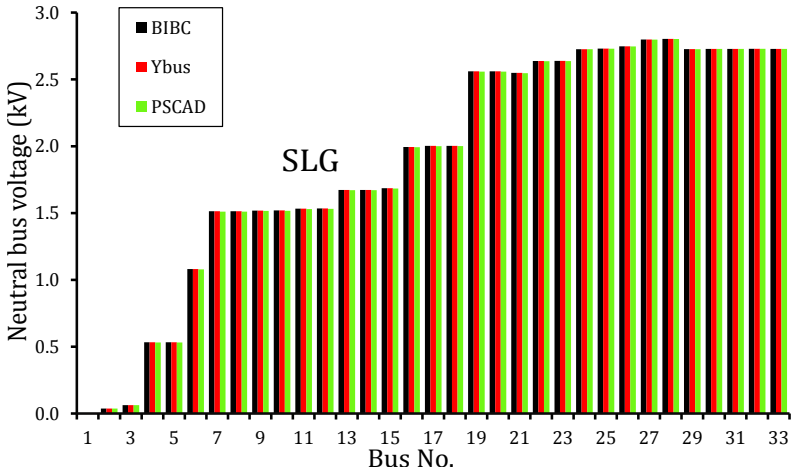

Figure 6.39: Voltage profile of neutral bus, for an SLG fault (a-g) at bus 28, of modified IEEE 34-bus test system in the presence of IBDG and Y_g-Y_g IBDG transformer using proposed $\left[\mathbf{BIBC}\right]$ technique, $\left[\mathbf{Y_{bus}}\right]$ technique and PSCAD/EMTDC simulation

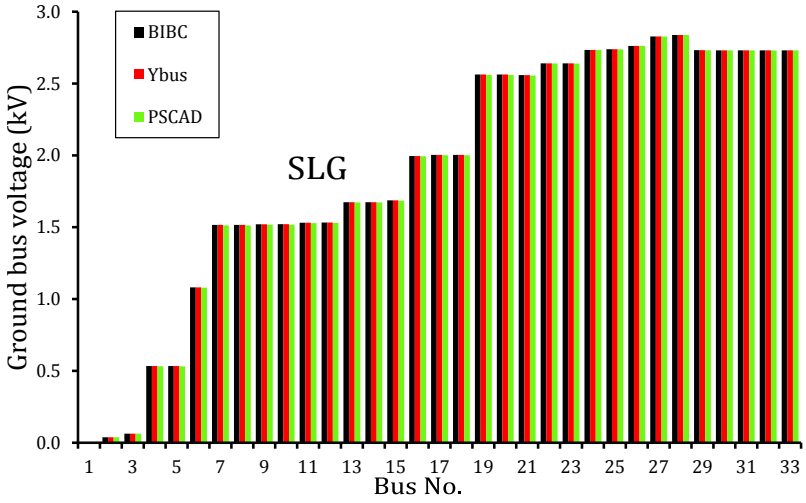

Figure 6.40: Voltage profile of ground bus, for an SLG fault (a-g) at bus 28, of modified IEEE 34-bus test system in the presence of IBDG and Y_g-Y_g IBDG transformer using proposed $\left[\mathbf{BIBC}\right]$ technique, $\left[\mathbf{Y_{bus}}\right]$ technique and PSCAD/EMTDC simulation

Amp $= 5.794\underline{/92.66^o}$ Amp) is smallest for LLLG fault, followed by the injected fault current of LLG fault ($\bar{I}_f^a + \bar{I}_f^b = -52.58 - j92.17$ Amp $= 106.108\underline{/-119.70^o}$ Amp) with SLG fault injecting highest current ($\bar{I}_f^a = 95.66 - j117.66$ Amp $= 151.637\underline{/-50.89^o}$ Amp) into the ground at the fault bus location. Therefore,

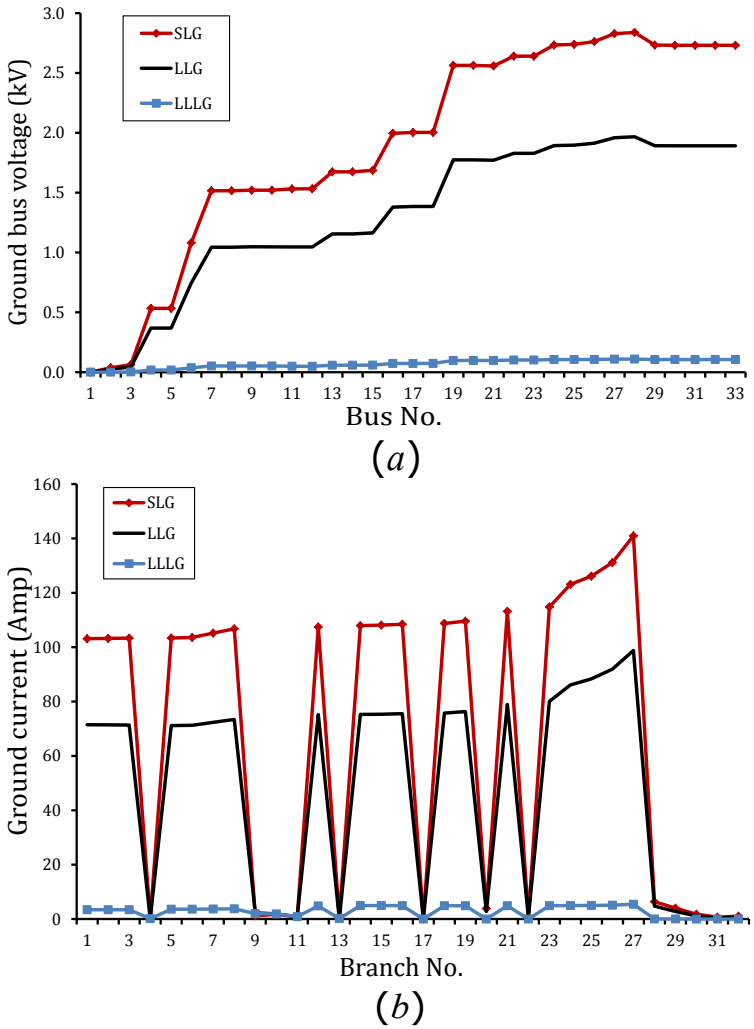

Figure 6.41: (a) Voltage profile of ground bus, (b) Ground current, for various ground faults at bus 28, of modified IEEE 34-bus test system in the presence of IBDG and Y_g-Y_g IBDG transformer

the currents flowing through ground from fault point to the substation ground are highest for SLG fault followed by LLG fault and smallest for LLLG fault, as shown in 6.41(b). As a result, the ground bus voltages are highest for SLG fault with LLLG fault resulting in lowest ground bus voltages.

6.4.2.2 Results of modified three phase four wire multigrounded IEEE 123-bus test system in the presence of IBDGs and Y_g-Y_g IBDG transformers

(a). Results of load flow studies

Five different sized IBDGs have also been considered in this test system with IBDGs and Y_g-Y_g IBDG transformers and their detailed informations are given in Table 6.7.

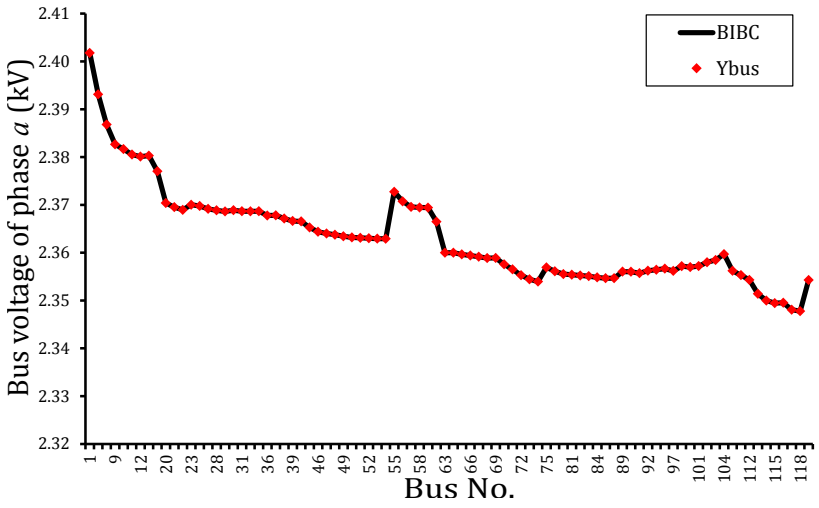

Figure 6.42: Voltage profile of phase a of modified IEEE 123-bus test system in the presence of IBDG and Y_g-Y_g IBDG transformer using proposed $\left[\mathbf{BIBC}\right]$ technique and $\left[\mathbf{Y_{bus}}\right]$ technique under normal operating conditions

The load flow analysis of the given test system has been performed by using the proposed method. The results obtained by the proposed load flow analysis method have been compared with those obtained by the $[\mathbf{Y_{bus}}]$ matrix based method.

The voltage profile of phase a, neutral bus and ground bus of the test system with IBDGs and Y_g-Y_g IBDG transformers obtained by the proposed load flow method and $\left[\mathbf{Y_{bus}}\right]$ matrix method are shown in Figs. 6.42-6.44, respectively. A good match between the results obtained by these two methods again demonstrates the accuracy of the proposed approach.

Also, the current in the phase a, neutral and ground branches of the test system with Y_g-Y_g IBDG transformers, calculated by the proposed load flow method and $\left[\mathbf{Y_{bus}}\right]$ matrix based method are plotted in Figs. 6.45-6.47, respectively. A close match of the current values, obtained from the two methods, as observed in these figures again validates the accuracy of the proposed method.

The inverter currents ($\mathbf{I_{inv}^{abc}}$) and the inverter bus voltages ($\mathbf{V_{inv}^{abc}}$) calculated by the proposed $[\mathbf{BIBC}]$ matrix based method and the $[\mathbf{Y_{bus}}]$ matrix based method are shown in Tables 6.18 and 6.19, respectively. The values of ($\mathbf{I_{inv}^{abc}}$) and ($\mathbf{V_{inv}^{abc}}$) of all IBDGs obtained by the proposed method are exactly equal to the values obtained by the $[\mathbf{Y_{bus}}]$ matrix based method, which again establishes the accuracy of the proposed method. The phase angles of inverter currents and the inverter bus voltages are same (as shown in Tables 6.18 and 6.19) due to the fact that all the IBDGs are operating at unity power factor under the normal operating conditions.

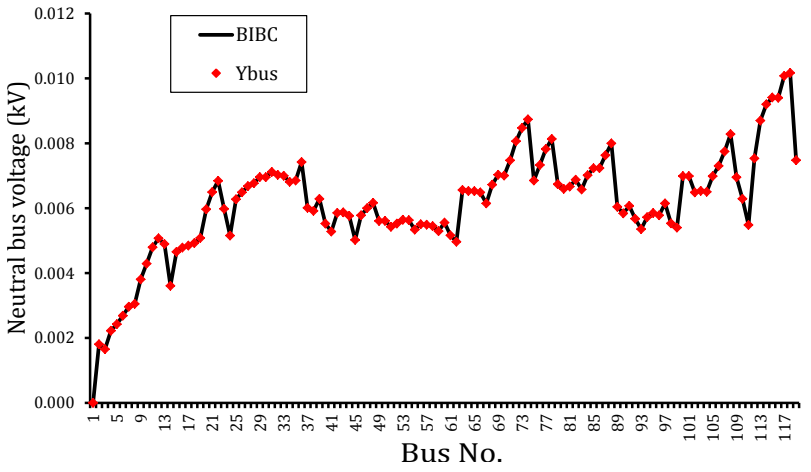

Figure 6.43: Voltage profile of neutral bus of modified IEEE 123-bus test system in the presence of IBDG and Y_g-Y_g IBDG transformer using proposed $\left[\mathbf{BIBC}\right]$ technique and $\left[\mathbf{Y_{bus}}\right]$ technique under normal operating conditions

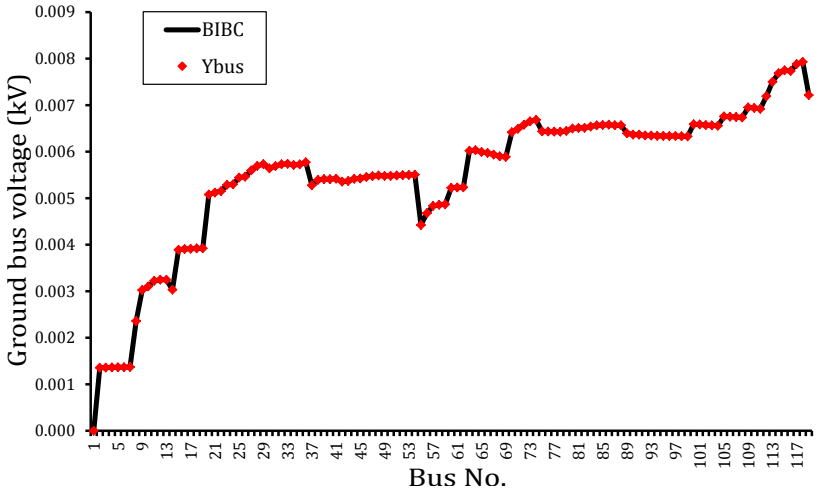

Figure 6.44: Voltage profile of ground bus of modified IEEE 123-bus test system in the presence of IBDG and Y_g-Y_g IBDG transformer using proposed $\left[\mathbf{BIBC}\right]$ technique and $\left[\mathbf{Y_{bus}}\right]$ technique under normal operating conditions

A case of isolated neutral has also been simulated on the given test system using the proposed load flow method. The neutral bus voltage profiles and the neutral wire currents of the test system for "isolated neutral" and "grounded neutral" cases are shown in Figs. 6.48(a) and (b), respectively. The values of voltages at all the neutral buses in "isolated neutral" case are higher than the "grounded neutral" case (as shown in Fig. 6.48(a)) for the same reasons as explained for modified IEEE 34-bus test system earlier.

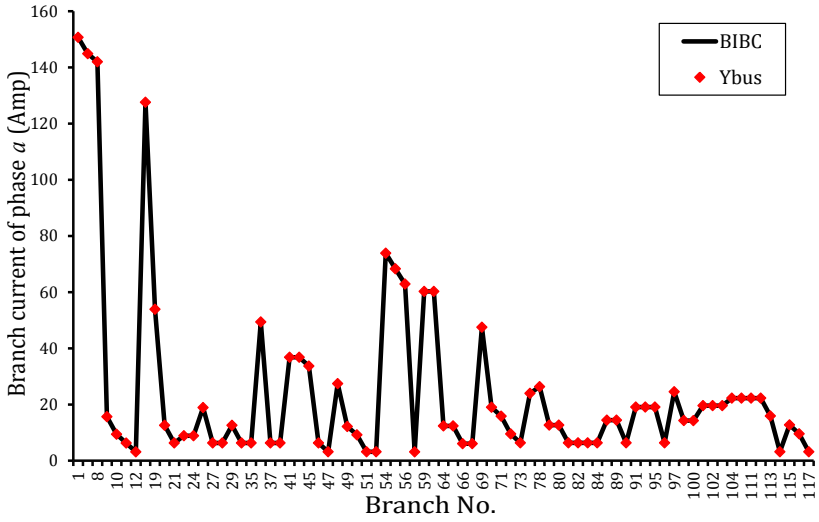

Figure 6.45: Branch current of phase a of modified IEEE 123-bus test system in the presence of IBDG and Y_g-Y_g IBDG transformer using proposed $\left[\mathbf{BIBC}\right]$ technique and $\left[\mathbf{Y_{bus}}\right]$ technique under normal operating conditions

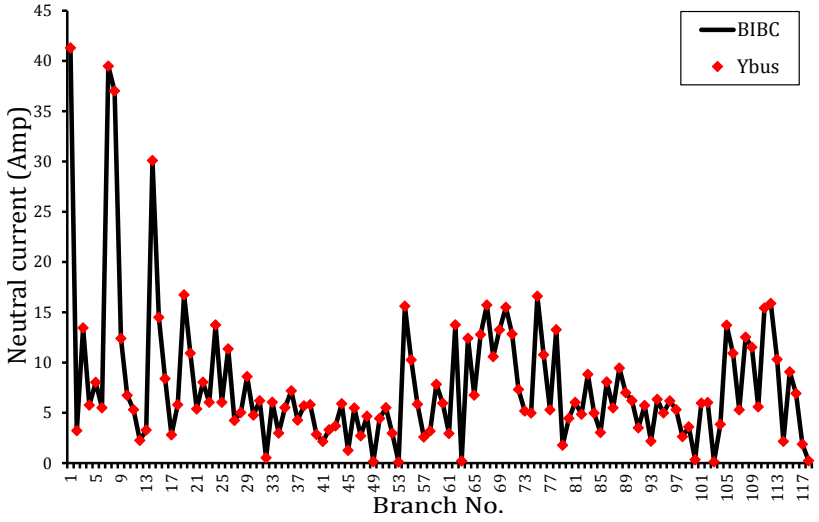

Figure 6.46: Neutral current of modified IEEE 123-bus test system in the presence of IBDG and Y_g-Y_g IBDG transformer using proposed $\left[\mathbf{BIBC}\right]$ technique and $\left[\mathbf{Y_{bus}}\right]$ technique under normal operating conditions

(b). Results of short-circuit studies

To carry out investigation to verify the effectiveness of the proposed short-circuit analysis methods $\left(\left[\mathbf{BIBC}\right]\right.$ and $\left[\mathbf{BCBV}\right]$ matrices based method and $\left.\left[\mathbf{Y_{bus}}\right]\right.$ matrix based method$\left.\right)$, an SLG fault in phase a of bus 105, with a fault impedance $\bar{z}_f$ = $0.001 + 0.000i$ p.u. has been simulated. In the initial step,

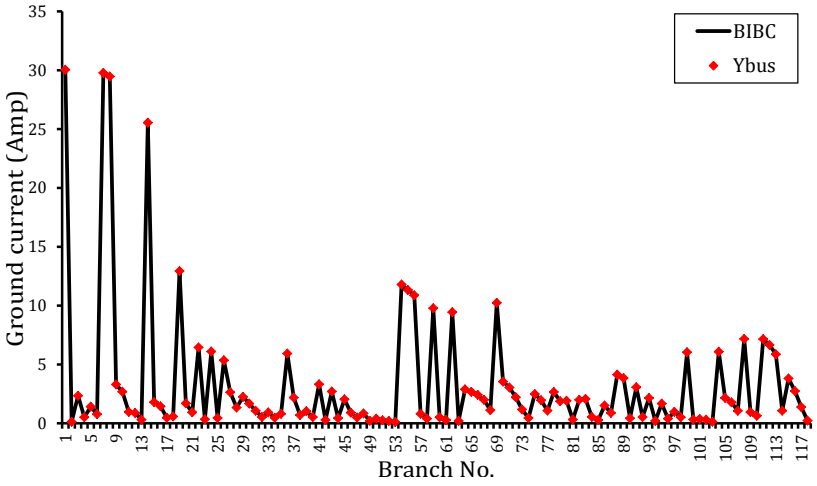

Figure 6.47: Ground current of modified IEEE 123 bus-test system in the presence of IBDG and Y_g-Y_g IBDG transformer using proposed $\left[\mathbf{BIBC}\right]$ technique and $\left[\mathbf{Y_{bus}}\right]$ technique under normal operating conditions

Table 6.18: Inverter currents of modified IEEE 123-bus test system in the presence of IBDGs and Y_g-Y_g IBDG transformers under normal operating conditions

IBDG location (Bus No.)	**Inverter current, $\mathbf{I_{inv}^{abc}}$ (Amp)**					
	[BIBC] Technique			**[$\mathbf{Y_{bus}}$] Technique**		
	Phase a	**Phase b**	**Phase c**	**Phase a**	**Phase b**	**Phase c**
20	170.30∠-0.26^o	168.05∠-119.90^o	169.60∠120.22^o	170.30∠-0.26^o	168.05∠-119.90^o	169.60∠120.22^o
25	127.76∠-0.30^o	125.98∠-119.89^o	127.27∠120.21^o	127.76∠-0.30^o	125.98∠-119.89^o	127.27∠120.21^o
75	171.29∠-0.26^o	168.46∠-119.85^o	170.65∠120.25^o	171.29∠-0.26^o	168.46∠-119.85^o	170.65∠120.25^o
98	214.14∠-0.08^o	210.72∠-119.79^o	213.05∠120.43^o	214.14∠-0.08^o	210.72∠-119.79^o	213.05∠120.43^o
104	171.09∠-0.18^o	168.32∠-119.76^o	170.54∠120.35^o	171.09∠-0.18^o	168.32∠-119.76^o	170.54∠120.35^o

the inverter currents ($\mathbf{I_{inv,f,est}^{abc}}$) of all the five IBDGs have been calculated by assuming that the inverter bus voltages of all IBDGs under the fault conditions are maintained at their pre-fault values i.e., $\mathbf{V_{inv,f}^{abc}}$ = $\mathbf{V_{inv,f,st}^{abc}}$. The calculated values of the inverter currents obtained by two proposed methods are given in columns 2-4 of Tables 6.20 and 6.21, respectively. These values show that the magnitude of inverter currents of all IBDGs are greater than their short-circuit current capacities (I_{sc}^{inv}). Therefore, the fault current, the bus voltages and the inverter currents of all IBDGs under the fault conditions are recalculated with the appropriate inverter current control strategy, as discussed in the proposed short-circuit analysis methods.

Table 6.19: Inverter bus voltages of modified IEEE 123-bus test system in the presence of IBDGs and Y_g-Y_g IBDG transformers under normal operating conditions

IBDG location (Bus No.)	**Inverter bus voltage, $\mathbf{V_{inv}^{abc}}$ (kV)**					
	[BIBC] Technique			**[$\mathbf{Y_{bus}$]} Technique**		
	Phase a	**Phase b**	**Phase c**	**Phase a**	**Phase b**	**Phase c**
20	0.2732∠-0.26^o	0.2769∠-119.90^o	0.2744∠120.22^o	0.2732∠-0.26^o	0.2769∠-119.90^o	0.2744∠120.22^o
25	0.2732∠-0.30^o	0.2770∠-119.89^o	0.2742∠120.21^o	0.2732∠-0.30^o	0.2770∠-119.89^o	0.2742∠120.21^o
75	0.2717∠-0.26^o	0.2762∠-119.85^o	0.2727∠120.25^o	0.2717∠-0.26^o	0.2762∠-119.85^o	0.2727∠120.25^o
98	0.2716∠-0.08^o	0.2760∠-119.79^o	0.2730∠120.43^o	0.2716∠-0.08^o	0.2760∠-119.79^o	0.2730∠120.43^o
104	0.2720∠-0.18^o	0.2765∠-119.76^o	0.2729∠120.35^o	0.2720∠-0.18^o	0.2765∠-119.76^o	0.2729∠120.35^o

Table 6.20: Results for SLG(a-g) fault at bus 105 in modified three phase four wire multigrounded IEEE 123-bus radial test system in the presence of IBDGs and Y_g-Y_g IBDG transformers using proposed [$\mathbf{BIBC}$] method

IBDG location (bus No.)	**Initial estimate of inverter current, $\mathbf{I_{inv,f,est}^{abc}}$, (kA) when $\mathbf{V_{inv,f}^{abc} = V_{inv,st}^{abc}}$**			**final value of inverter current, (kA) $\mathbf{I_{inv,f}^{abc} = I_{sc}^{inv}\angle(\frac{\pi}{2} + \theta_{inv,f}^{abc})}$**			**final value of injected IBDG power (kVAR)**		
	Phase-a	**Phase-b**	**Phase-c**	**Phase-a**	**Phase-b**	**Phase-c**	**Phase-a**	**Phase-b**	**Phase-c**
20	23.307∠-90.44^o	8.568∠-86.52^o	5.875∠-94.72^o	0.2519∠-89.83^o	0.2519∠142.49^o	0.2519∠34.47^o	148.13	226.26	225.00
25	23.299∠-90.54^o	8.525∠-86.34^o	5.902∠-94.47^o	0.1889∠-90.00^o	0.1889∠142.56^o	0.1889∠34.44^o	111.06	169.68	168.63
75	66.133∠-90.66^o	24.460∠-86.08^o	17.366∠-93.80^o	0.2519∠-82.08^o	0.2519∠131.77^o	0.2519∠42.05^o	34.49	264.96	257.98
98	65.608∠-90.67^o	23.941∠-86.18^o	16.800∠-94.19^o	0.3148∠-80.42^o	0.3148∠131.64^o	0.3148∠41.28^o	47.12	328.86	322.64
104	71.254∠-90.70^o	26.491∠-86.19^o	18.893∠-93.86^o	0.2519∠-72.61^o	0.2519∠130.47^o	0.2519∠42.77^o	20.50	271.14	263.72

The final values of inverter currents and injected powers by all IBDGs, obtained by both the proposed methods, are shown in columns 5-10 of Tables 6.20 and 6.21, respectively. From both the tables, again it can be observed that the final values of inverter currents and injected powers by the IBDGs obtained by both the methods are identical, which again validates the accuracy of the proposed methods. The fault current (I_f) and source current (I_s) in phase a for this case using the proposed methods are given in Table 6.22. The above results show that the values of I_f and I_s calculated by both the proposed methods are identical, thereby validating the proposed short-circuit analysis methods.

Different fault cases namely, LLG (ab-g), LLLG (abc-g), and LL (a-b) fault with $\bar{z}_f$ = 0.001+0.000i p.u., have also been simulated at bus 105 in the same system using the proposed methods. The calculated values of fault currents (I_f) and source currents (I_s) for all type of faults obtained by the proposed methods are given in Table 6.22. It can be observed from the table that the values obtained by the proposed [$\mathbf{BIBC}$]

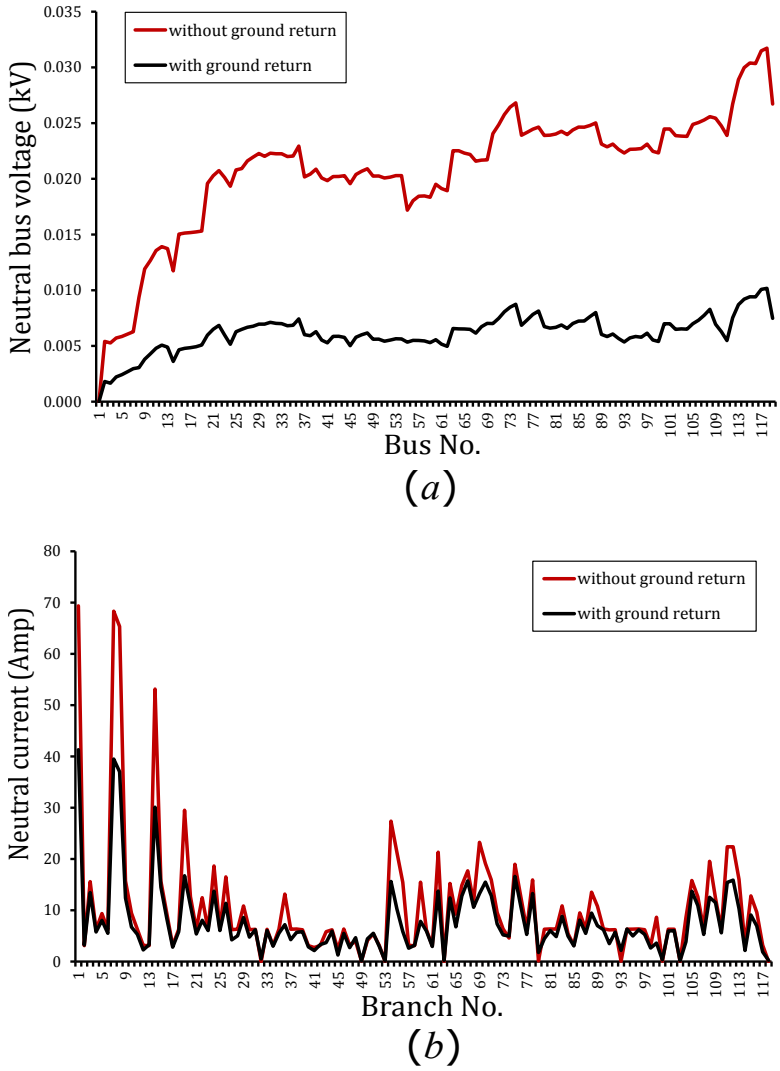

Figure 6.48: (a) Neutral bus voltage profile, (b) Neutral current of modified IEEE 123-bus test system in the presence of IBDG and Y_g-Y_g IBDG transformer in "isolated neutral" and "grounded neutral" cases under normal operating conditions

method are exactly equal to the values obtained by the $[\mathbf{Y_{bus}}]$ method, which again establishes the accuracy of the proposed methods.

The voltage profiles of phase a bus voltage, neutral bus voltage and ground bus voltage of the considered test system with IBDGs and Y_g-Y_g IBDG transformers, for an SLG fault at phase a of bus 105 with fault impedance of $\bar{z}_f$ = 0.001+0.000i p.u., obtained by using the proposed short-circuit analysis methods $\big([\mathbf{BIBC}]$ matrix based and $[\mathbf{Y_{bus}}]$ matrix based methods $\big)$, are shown in Figs. 6.49-6.51, respectively. These figures again demonstrate the correctness of the proposed short-circuit methods.

Table 6.21: Results for SLG(a-g) fault at bus 105 in modified three phase four wire multigrounded IEEE 123-bus radial test system in the presence of IBDGs and Y_g-Y_g IBDG transformers using proposed $[\mathbf{Y_{bus}}]$ method

IBDG location (bus No.)	**Initial estimate of inverter current, $\mathbf{I^{abc}_{inv,f,est}}$, (kA) when $\mathbf{V^{abc}_{inv,f}} = \mathbf{V^{abc}_{inv,st}}$**			**final value of inverter current, (kA) $\mathbf{I^{abc}_{inv,f}} = I^{inv}_{sc}\angle(\frac{\pi}{2} + \theta^{abc}_{inv,f})$**			**final value of injected IBDG power (kVAR)**		
	Phase-a	**Phase-b**	**Phase-c**	**Phase-a**	**Phase-b**	**Phase-c**	**Phase-a**	**Phase-b**	**Phase-c**
20	17.329∠-81.24^o	15.450∠-84.69^o	15.131∠-84.77^o	0.2519∠-89.83^o	0.2519∠142.49^o	0.2519∠34.47^o	148.13	226.26	225.00
25	16.910∠-80.61^o	15.540∠-83.80^o	15.347∠-83.78^o	0.1889∠-90.00^o	0.1889∠142.56^o	0.1889∠34.44^o	111.06	169.68	168.63
75	54.652∠-84.82^o	42.011∠-88.55^o	40.898∠-89.50^o	0.2519∠-82.08^o	0.2519∠131.77^o	0.2519∠42.05^o	34.49	264.96	257.98
98	44.492∠-84.78^o	39.810∠-88.90^o	39.569∠-88.86^o	0.3148∠-80.42^o	0.3148∠131.64^o	0.3148∠41.28^o	47.12	328.86	322.64
104	52.772∠-85.08^o	44.010∠-89.53^o	43.537∠-89.91^o	0.2519∠-72.61^o	0.2519∠130.47^o	0.2519∠42.77^o	20.50	271.14	263.72

Table 6.22: Results of proposed short-circuit analysis methods for modified three phase four wire multigrounded IEEE 123-bus radial test system in the presence of IBDGs and Y_g-Y_g IBDG transformers

case	**Fault type**	**phase**	**Fault current at fault point (I_f)**		**Current drawn from the supply (I_s)**	
			$[\mathbf{BIBC}]$ **Technique (kA)**	$[\mathbf{Y_{bus}}]$ **Technique (kA)**	$[\mathbf{BIBC}]$ **Technique (kA)**	$[\mathbf{Y_{bus}}]$ **Technique (kA)**
1	SLG (a-g)	a	2.47361	2.47361	2.42218	2.42218
2	LLG (ab-g)	a	4.40322	4.40322	4.43376	4.43376
		b	4.63930	4.63930	4.52809	4.52809
3	LLLG (abc-g)	a	4.56958	4.56958	4.53906	4.53906
		b	5.24557	5.24557	5.16540	5.16540
		c	4.53662	4.53662	4.46277	4.46277
4	L-L (a-b)	a	4.41444	4.41444	4.57222	4.57222
		b	4.41444	4.41444	4.29969	4.29969

The ground bus voltage profile for various ground faults (SLG, LLG and LLLG) at bus 105 with a fault impedance of $\bar{z}_f$ = 0.001+0.000i p.u. is plotted in Fig. 6.52(a). It shows that the highest ground bus voltages occurs for SLG fault followed by LLG fault while the lowest values are observed for LLLG fault. This is due to the fact that the fault current injected into the fault point at ground bus is the phasor sum of the three phase fault currents and its value ($\bar{I}^a_f + \bar{I}^b_f + \bar{I}^c_f = 0.03 + j0.14$ kA $= 0.142\underline{/77.28^o}$ kA) is smallest for LLLG fault, followed by the injected fault current of LLG fault ($\bar{I}^a_f + \bar{I}^b_f = -1.11 - j1.36$ kA $= 1.757\underline{/-129.30^o}$ kA) with SLG fault injecting highest current ($\bar{I}^a_f = 1.02 - j2.25$ kA $= 2.474\underline{/-65.48^o}$ kA) into the ground

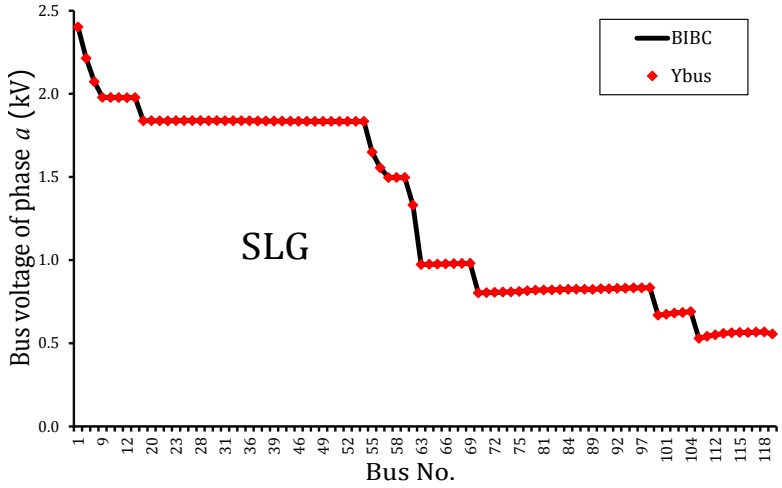

Figure 6.49: Voltage profile of phase a, for an SLG fault (a-g) at bus 105, of modified IEEE 123-bus test system in the presence of IBDG and Y_g-Y_g IBDG transformer using proposed $\left[\mathbf{BIBC}\right]$ technique and $\left[\mathbf{Y_{bus}}\right]$ technique

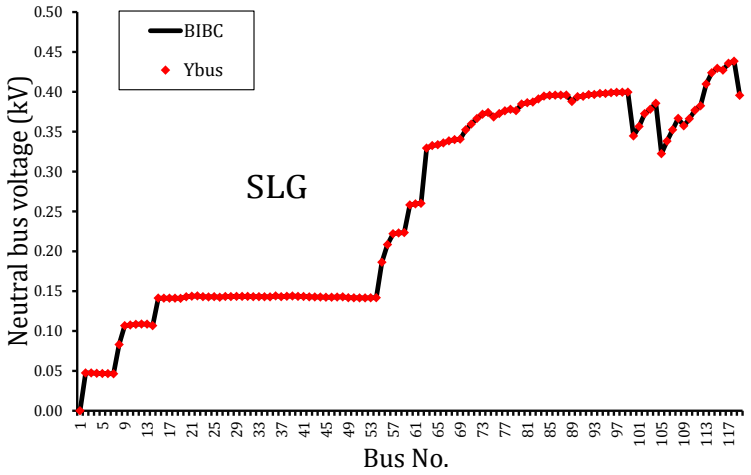

Figure 6.50: Voltage profile of neutral bus, for an SLG fault (a-g) at bus 105, of modified IEEE 123-bus test system in the presence of IBDG and Y_g-Y_g IBDG transformer using proposed $\left[\mathbf{BIBC}\right]$ technique and $\left[\mathbf{Y_{bus}}\right]$ technique

at the fault bus location. Therefore, the currents flowing through ground from fault point to the substation ground are highest for SLG fault followed by LLG fault and smallest for LLLG fault, as shown in 6.52(b). As a result, the ground bus voltages are highest for SLG fault with LLLG fault resulting in lowest ground bus voltages. From Fig. 6.52(b), it is also observed that the value of ground current at certain branches of the test system (such as branch nos. $2-5, 9-13, 17-53, 81-97$ and $106-118$) are nearly equal to zero.

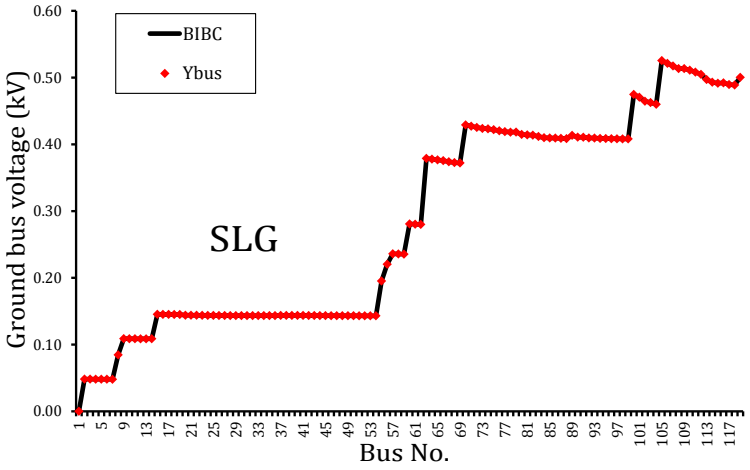

Figure 6.51: Voltage profile of ground bus, for an SLG fault (a-g) at bus 105, of modified IEEE 123-bus test system in the presence of IBDG and Y_g-Y_g IBDG transformer using proposed $[\mathbf{BIBC}]$ technique and $[\mathbf{Y_{bus}}]$ technique

It is due to the fact, that these branches are not present in the path of fault current returning through ground from fault point to the substation ground.

6.5 Conclusion

In this chapter, the efficient and accurate load flow and short-circuit analysis methods for an unbalanced three phase four wire multigrounded radial distribution system with IBDGs and IBDG transformers have been developed. Two different vector groups of the transformer models have been considered in this work, namely, Delta/star-grounded (Δ-Y_g) and star-grounded/star-grounded (Y_g-Y_g) transformer. The nodal admittance matrix based model of both the transformers has been considered in this work [80]. The proposed load flow method is based on $[\mathbf{BIBC}]$ and $[\mathbf{BCBV}]$ matrices of the system. The results of the proposed load flow analysis method have been compared with the $[\mathbf{Y_{bus}}]$ matrix based method and time domain simulation studies carried out using PSCAD/EMTDC software for a modified three phase four wire multigrounded IEEE 34-bus test system with IBDGs and IBDG transformers. The results of these three methods show the accuracy of the developed method. The proposed load flow method has also been implemented on large system (modified three phase four wire multigrounded IEEE 123-bus test system) with IBDGs and IBDG transformers and the results have only been compared with the results of $[\mathbf{Y_{bus}}]$ matrix based method, due to the node limitations in available PSCAD/EMTDC software.

Two different short-circuit analysis methods for an unbalanced three phase four wire multigrounded radial distribution system with IBDGs and IBDG transformers (one is $[\mathbf{BIBC}]$ matrix based method and

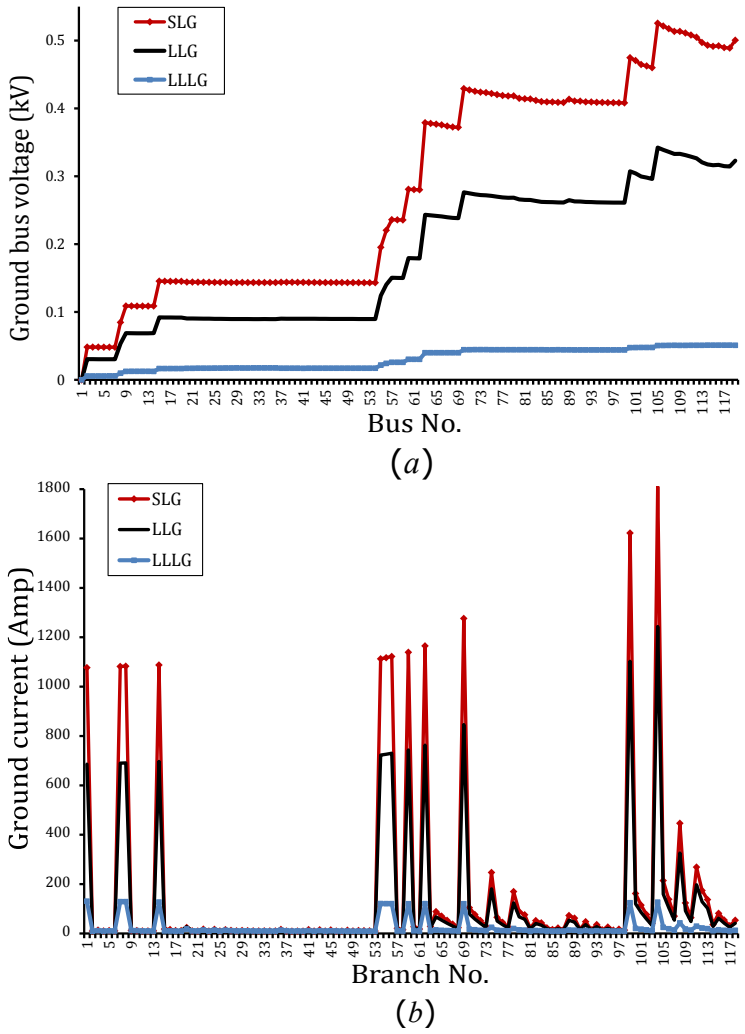

Figure 6.52: (a) Voltage profile of ground bus, (b) Ground current, for various ground faults at bus 105, of modified IEEE 123-bus test system in the presence of IBDG and Y_g-Y_g IBDG transformer

next one is $[\mathbf{Y_{bus}}]$ matrix based method) with appropriate inverter control strategy of the IBDGs have also been developed in this chapter. The results of short-circuit analysis of modified IEEE 34-bus test system obtained by using proposed methods have been compared with the results obtained by the PSCAD/EMTDC software. However, for the large system, the results of proposed $[\mathbf{BIBC}]$ matrix based method have only been compared with the results of proposed $[\mathbf{Y_{bus}}]$ matrix based method. A very close matching of the obtained results establishes the accuracy of the proposed methods.

In the next chapter, the main conclusions of the thesis and suggestions for extending this work are presented.

Chapter 7

Conclusions and scope of further works

This chapter summarizes the major findings of the work presented in this thesis and suggests directions for further investigations in the short-circuit analysis of the three-phase three wire and three-phase four wire unbalanced distribution systems.

7.1 Conclusions

Based on the work reported in this thesis, the following conclusions are drawn:

- The algorithm developed for the short-circuit analysis of unbalanced radial as well weakly meshed distribution system considering loads is based on admittance matrix of the network. The obtained results show that the method is quite accurate and effective. It is also applicable for the analysis of multiple faults in the network.

- The method proposed for the short-circuit analysis of distribution system with IBDGs is considered the current controlled mode of operation of IBDGs during the short-circuit calculations. The method is based on Newton-Raphson based technique to solve the non-linear KCL equations of the system. It is also capable of including voltage dependent control modes of IBDGs under the short-circuit conditions. This method is also capable of incorporating the voltage dependent load models (ZIP-loads) in the fault calculations.

- The efficient and accurate load flow analysis method is developed in this work for the unbalanced distribution system which incorporates three-phase transformer models (of any vector group) and IBDGs simultaneously. Two modes of operation have been considered for the IBDGs, namely, *i).* Constant active power mode, *ii).* Power and Voltage control (PV) mode. Singularity problem for particular type of transformer configurations has also been addressed in the proposed method.

- The short-circuit analysis method for the unbalanced distribution system with three-phase transformer models and IBDGs is also developed in this thesis. The results obtained by the proposed method have been compared with the results of time domain simulation studies carried out using PSCAD/EMTDC simulink software. These results establish the accuracy of the proposed method.

- The load flow analysis method, based on $[\mathbf{BIBC}]$ and $[\mathbf{BCBV}]$ matrices of the system, has been developed for the three-phase four wire unbalanced radial distribution system with ground return. Separate $[\mathbf{BCBV}]$ and $[\mathbf{BIBC}]$ matrices have been developed for the phase, neutral and ground bus voltages and currents. Two different short-circuit analysis methods, one is based on $[\mathbf{BIBC}]$ and $[\mathbf{BCBV}]$ matrices of the system and the other one is based on $[\mathbf{Y_{bus}}]$ matrix of the system, have also been developed for the three-phase four wire distribution system with ground return. The results obtained by these methods demonstrate their accuracy and effectiveness.

- The load flow (based on $[\mathbf{BIBC}]$ and $[\mathbf{BCBV}]$ matrices of the system) and short-circuit analysis methods (one is based on $[\mathbf{BIBC}]$ and $[\mathbf{BCBV}]$ matrices of the system and the other one is based on $[\mathbf{Y_{bus}}]$ matrix of the system) for the three-phase four wire distribution system with ground return with IBDGs and three-phase transformer models have been developed in this work. Two different configurations of the transformer models have been considered in this work, one is Delta/star-grounded (Δ-Y_g) and next one is star-grounded/star-grounded (Y_g-Y_g) transformer model. Separate load flow and short-circuit analysis methods have been developed for both the transformer models. The proposed methods have been tested on two different test systems, first is modified IEEE 34-bus three-phase four wire distribution system with ground return, and second one is modified IEEE 123-bus three-phase four wire distribution system with ground return. The obtained results establish the effectiveness and correctness of the proposed methods.

7.2 Scope of further Works

- The proposed load flow and short-circuit analysis methods for the three-phase four wire distribution system with ground return have been developed only for the radial systems. The proposed methodologies can also be modified for the weakly meshed distribution networks.

- The load flow and short-circuit methodologies have been developed only for the three-phase four wire radial distribution system with ground return with IBDGs and IBDG transformers. It can also be extended for a three-phase four wire weakly meshed distribution network.

- The three-phase transformer models have only been used with the IBDGs in the proposed methodologies of the three-phase four wire radial distribution system with ground return, i.e. the transformer models used in the system have only been connected at the end nodes of the network. The proposed methodologies can be modified for the transformers connected anywhere in the network.

- The short-circuit algorithms for three-phase four wire systems considers constant power load models

only. These methodologies can also be extended to include non-linear load models like, ZIP loads (voltage dependent load models).

Publications from the research work

1. A. Mathur, V. Pant, B. Das, ”Unsymmetrical short-circuit analysis for distribution system considering loads,” International Journal of Electrical Power & Energy Systems, vol.70, pp.27-38, September 2015.

2. A. Mathur, B. Das, V. Pant, ”Fault analysis of unbalanced radial and meshed distribution system with Inverter based Distributed generation (IBDG),” International Journal of Electrical Power & Energy Systems, vol.85, pp.164-177, February 2017.

Bibliography

[1] J. J. G. Stevenson Jr. WD., *Power System Analysis*. McGraw-Hill, 1994.

[2] "IEEE Standard definitions for power switchgear," *IEEE std C37 100-1992*, 1992.

[3] S. P. Valsan and K. S. Swarup, "High-speed fault classification in power lines: Theory and FPGA-based implementation," *IEEE Transactions on Industrial Electronics*, vol. 56, no. 5, pp. 1793–1800, May 2009.

[4] W. Sinsukthavorn, E. Ortjohann, A. Mohd, N. Hamsic, and D. Morton, "Control strategy for three/four-wire-inverter-based distributed generation," *IEEE Transactions on Industrial Electronics*, vol. 59, no. 10, pp. 3890–3899, October 2012.

[5] P. S. Georgilakis and N. D. Hatziargyriou, "Optimal distributed generation placement in power distribution networks: Models, methods, and future research," *IEEE Transactions on Power Systems*, vol. 28, no. 3, pp. 3420–3428, August 2013.

[6] E. Pouresmaeil, C. Miguel-Espinar, M. Massot-Campos, D. Montesinos-Miracle, and O. Gomis-Bellmunt, "A control technique for integration of DG units to the electrical networks," *IEEE Transactions on Industrial Electronics*, vol. 60, no. 7, pp. 2881–2893, July 2013.

[7] J. Barr and R. Majumder, "Integration of distributed generation in the Volt/VAR management system for active distribution networks," *IEEE Transactions on Smart Grid*, vol. 6, no. 2, pp. 576–586, March 2015.

[8] L. Zhang, W. Tang, Y. Liu, and T. Lv, "Multiobjective optimization and decision-making for DG planning considering benefits between distribution company and DGs owner," *International Journal of Electrical Power & Energy Systems*, vol. 73, no. Supplement C, pp. 465 – 474, December 2015.

[9] K. K. Vanukuru, J. V. Rao, S. R. Davu, and A. Ramisetti, "Fuzzy control based APF with DG integration for power quality improvement in disribution system," in *2016 International Conference on Signal Processing, Communication, Power and Embedded System (SCOPES)*, October 2016, pp. 1410–1417.

[10] J. Xiao, Z. Zhang, L. Bai, and H. Liang, "Determination of the optimal installation site and capacity of battery energy storage system in distribution network integrated with distributed generation," *IET Generation, Transmission & Distribution*, vol. 10, no. 3, pp. 601–607, March 2016.

[11] H. Xing, H. Cheng, Y. Zhang, and P. Zeng, "Active distribution network expansion planning integrating dispersed energy storage systems," *IET Generation, Transmission & Distribution*, vol. 10, no. 3, pp. 638–644, March 2016.

[12] H. Zhan, C. Wang, Y. Wang, X. Yang, X. Zhang, C. Wu, and Y. Chen, "Relay protection coordination integrated optimal placement and sizing of distributed generation sources in distribution networks," *IEEE Transactions on Smart Grid*, vol. 7, no. 1, pp. 55–65, January 2016.

[13] T. Adefarati and R. C. Bansal, "Integration of renewable distributed generators into the distribution system: a review," *IET Renewable Power Generation*, vol. 10, no. 7, pp. 873–884, July 2016.

[14] W. Pan, S. C. Dhulipala, and A. S. Bretas, "A distributed approach for DG integration and power quality management in railway power systems," in *2017 IEEE International Conference on Environment and Electrical Engineering and 2017 IEEE Industrial and Commercial Power Systems Europe (EEEIC / I CPS Europe)*, June 2017, pp. 1–6.

[15] C. Lin, W. Wu, B. Zhang, B. Wang, W. Zheng, and Z. Li, "Decentralized reactive power optimization method for transmission and distribution networks accommodating large-scale DG integration," *IEEE Transactions on Sustainable Energy*, vol. 8, no. 1, pp. 363–373, January 2017.

[16] N. K. Meena, A. Swarnkar, N. Gupta, and K. R. Niazi, "Multi-objective Taguchi approach for optimal DG integration in distribution systems," *IET Generation, Transmission & Distribution*, vol. 11, no. 9, pp. 2418–2428, July 2017.

[17] N. C. Koutsoukis, D. O. Siagkas, P. S. Georgilakis, and N. D. Hatziargyriou, "Online reconfiguration of active distribution networks for maximum integration of distributed generation," *IEEE Transactions on Automation Science and Engineering*, vol. 14, no. 2, pp. 437–448, April 2017.

[18] M. Ali, R. J. Millar, and M. Lehtonen, "A framework to split the benefits of DR between wind integration and network management," *IEEE Transactions on Power Systems*, vol. PP, no. 99, pp. 1–1, June 2017.

[19] S. Lei, Y. Hou, F. Qiu, and J. Yan, "Identification of critical switches for integrating renewable distributed generation by dynamic network reconfiguration," *IEEE Transactions on Sustainable Energy*, vol. 9, no. 1, pp. 420–432, January 2018.

[20] C. Wang, K. Yuan, P. Li, B. Jiao, and G. Song, "A projective integration method for transient stability assessment of power systems with a high penetration of distributed generation," *IEEE Transactions on Smart Grid*, vol. 9, no. 1, pp. 386–395, January 2018.

[21] W. El-Khattam and M. Salama, "Distributed generation technologies, definitions and benefits," *Electric Power Systems Research*, vol. 71, no. 2, pp. 119 – 128, October 2004.

[22] S. Kotamarty, S. Khushalani, and N. Schulz, "Impact of distributed generation on distribution contingency analysis," *Electric Power Systems Research*, vol. 78, no. 9, pp. 1537 – 1545, September 2008.

[23] T. N. Shukla, S. P. Singh, V. Srinivasarao, and K. B. Naik, "Optimal sizing of distributed generation placed on radial distribution systems," *Electric Power Components and Systems*, vol. 38, no. 3, pp. 260–274, January 2010.

[24] N. Jain, S. Singh, and S. Srivastava, "Pso based placement of multiple wind dgs and capacitors utilizing probabilistic load flow model," *Swarm and Evolutionary Computation*, vol. 19, pp. 15 – 24, December 2014.

[25] N. Jain, S. N. Singh, and S. C. Srivastava, "A generalized approach for DG planning and viability analysis under market scenario," *IEEE Transactions on Industrial Electronics*, vol. 60, no. 11, pp. 5075–5085, November 2013.

[26] B. Singh and S. N. Singh, "Reactive capability limitations of doubly-fed induction generators," *Electric Power Components and Systems*, vol. 37, no. 4, pp. 427–440, March 2009.

[27] B. Singh, E. Kyriakides, and S. N. Singh, "Intelligent control of grid connected unified doubly-fed induction generator," in *IEEE PES General Meeting*, July 2010, pp. 1–7.

[28] T. Gzel and M. H. Hocaoglu, "An analytical method for the sizing and siting of distributed generators in radial systems," *Electric Power Systems Research*, vol. 79, no. 6, pp. 912 – 918, June 2009.

[29] A. K. Srivastava, A. A. Kumar, and N. N. Schulz, "Impact of distributed generations with energy storage devices on the electric grid," *IEEE Systems Journal*, vol. 6, no. 1, pp. 110–117, March 2012.

[30] B. Singh and S. Singh, "Development of grid connection requirements for wind power generators in india," *Renewable and Sustainable Energy Reviews*, vol. 15, no. 3, pp. 1669 – 1674, April 2011.

[31] R. Ciric, H. Nouri, and V. Terzija, "Impact of distributed generators on arcing faults in distribution networks," *IET Generation, Transmission & Distribution*, vol. 5, no. 5, pp. 596–601, May 2011.

[32] A. Keane, L. F. Ochoa, C. L. T. Borges, G. W. Ault, A. D. Alarcon-Rodriguez, R. A. F. Currie, F. Pilo, C. Dent, and G. P. Harrison, "State-of-the-art techniques and challenges ahead for distributed generation planning and optimization," *IEEE Transactions on Power Systems*, vol. 28, no. 2, pp. 1493–1502, May 2013.

[33] N. K. Roy and H. R. Pota, "Current status and issues of concern for the integration of distributed generation into electricity networks," *IEEE Systems Journal*, vol. 9, no. 3, pp. 933–944, September 2015.

[34] N. K. Roy, H. R. Pota, and M. A. Mahmud, "DG integration issues in unbalanced multi-phase distribution networks," in *2016 Australasian Universities Power Engineering Conference (AUPEC)*, September 2016, pp. 1–5.

[35] P. Mohammadi and S. Mehraeen, "Challenges of PV integration in low-voltage secondary networks," *IEEE Transactions on Power Delivery*, vol. 32, no. 1, pp. 525–535, February 2017.

[36] Z. Liu, C. Su, H. K. Hidalen, and Z. Chen, "A multiagent system-based protection and control scheme for distribution system with distributed-generation integration," *IEEE Transactions on Power Delivery*, vol. 32, no. 1, pp. 536–545, February 2017.

[37] A. Naiem, Y. Hegazy, A. Abdelaziz, and M. Elsharkawy, "A classification technique for recloser-fuse coordination in distribution systems with distributed generation," *IEEE Transactions on Power Delivery*, vol. 27, no. 1, pp. 176–185, January 2012.

[38] S. M. Halpin and L. L. Grigsby, "A comparison of fault calculation procedures for industrial power distribution systems: the past, the present, and the future," in *Proceedings of the IEEE International Conference on Industrial Technology, 1994*, December 1994, pp. 842–846.

[39] M. Abdel-Akher and K. Nor, "Fault analysis of multiphase distribution systems using symmetrical components," *IEEE Transactions on Power Delivery*, vol. 25, no. 4, pp. 2931–2939, October 2010.

[40] K. Gampa, S. Vemprala, and S. Brahma, "Errors in fault analysis of power distribution systems using sequence components approach," in *2010 IEEE PES Transmission and Distribution Conference and Exposition*, April 2010, pp. 1–6.

[41] R. A. Jabr and I. Dafi, "A fortescue approach for real-time short circuit computation in multiphase distribution networks," *IEEE Transactions on Power Systems*, vol. 30, no. 6, pp. 3276–3285, November 2015.

[42] T. Chen, M.-S. Chen, W.-J. Lee, P. Kotas, and P. Van Olinda, "Distribution system short circuit analysis-a rigid approach," in *Conference Proceedings Power Industry Computer Application Conference, 1991.*, May 1991, pp. 22–28.

[43] S. Halpin, L. Grigsby, C. Gross, and R. Nelms, "An improved fault analysis algorithm for unbalanced multi-phase power distribution systems," *IEEE Transactions on Power Delivery,*, vol. 9, no. 3, pp. 1332–1338, July 1994.

[44] X. Zhang, F. Soudi, D. Shirmohammadi, and C. Cheng, "A distribution short circuit analysis approach using hybrid compensation method," *IEEE Transactions on Power Systems*, vol. 10, no. 4, pp. 2053–2059, November 1995.

[45] Y. Mao and K. Miu, "Radial distribution system short circuit analysis with lateral and load equivalencing: solution algorithms and numerical results," in *IEEE Power Engineering Society Summer Meeting, 2000*, vol. 1, 2000, pp. 449–453.

[46] R. Ciric, L. Ochoa, A. Padilla-Feltrin, and H. Nouri, "Fault analysis in four-wire distribution networks," *IEE Proceedings-Generation, Transmission and Distribution*, vol. 152, no. 6, pp. 977–982, November 2005.

[47] J. H. Teng, "Fast short circuit analysis method for unbalanced distribution systems," in *IEEE Power Engineering Society General Meeting, 2003*, vol. 1, July 2003, pp. 240–245.

[48] ——, "Unsymmetrical short-circuit fault analysis for weakly meshed distribution systems," *IEEE Transactions on Power Systems*, vol. 25, no. 1, pp. 96–105, February 2010.

[49] ——, "Systematic short-circuit-analysis method for unbalanced distribution systems," *IEE Proceedings-Generation, Transmission and Distribution,*, vol. 152, no. 4, pp. 549–555, July 2005.

[50] T. H. Chen, M. S. Chen, T. Inoue, P. Kotas, and E. A. Chebli, "Three-phase cogenerator and transformer models for distribution system analysis," *IEEE Transactions on Power Delivery*, vol. 6, no. 4, pp. 1671–1681, October 1991.

[51] M. C. R. Paz, R. G. Ferraz, A. S. Bretas, and R. C. Leborgne, "System unbalance and fault impedance effect on faulted distribution networks," *Computers & Mathematics with Applications*, vol. 60, no. 4, pp. 1105 – 1114, 2010.

[52] W. M. Lin and T. C. Ou, "Unbalanced distribution network fault analysis with hybrid compensation," *IET Generation, Transmission & Distribution*, vol. 5, no. 1, pp. 92–100, January 2011.

[53] A. D. Filomena, M. Resener, R. H. Salim, and A. S. Bretas, "Distribution systems fault analysis considering fault resistance estimation," *International Journal of Electrical Power & Energy Systems*, vol. 33, no. 7, pp. 1326–1335, September 2011.

[54] T. C. Ou, "A novel unsymmetrical faults analysis for microgrid distribution systems," *International Journal of Electrical Power & Energy Systems*, vol. 43, no. 1, pp. 1017–1024, December 2012.

[55] S. Saha, M. Aldeen, and C. Tan, "Unsymmetrical fault diagnosis in transmission/distribution networks," *International Journal of Electrical Power & Energy Systems*, vol. 45, no. 1, pp. 252 – 263, February 2013.

[56] J. S. Lacroix, I. Kocar, and M. Belletłte, "Accelerated computation of multiphase short circuit summary for unbalanced distribution systems using the concept of selected inversion," *IEEE Transactions on Power Systems*, vol. 28, no. 2, pp. 1515–1522, May 2013.

[57] J. Tailor and A. Osman, "Restoration of fuse-recloser coordination in distribution system with high DG penetration," in *IEEE Power and Energy Society General Meeting - Conversion and Delivery of Electrical Energy in the 21st Century, 2008*, July 2008, pp. 1–8.

[58] C. Plet, M. Graovac, T. Green, and R. Iravani, "Fault response of grid-connected inverter dominated networks," in *IEEE Power and Energy Society General Meeting, 2010*, July 2010, pp. 1–8.

[59] C. A. Plet and T. C. Green, "Fault response of inverter interfaced distributed generators in grid-connected applications," *Electric Power Systems Research*, vol. 106, no. 0, pp. 21 – 28, January 2014.

[60] P. Rodriguez, A. Timbus, R. Teodorescu, M. Liserre, and F. Blaabjerg, "Flexible active power control of distributed power generation systems during grid faults," *IEEE Transactions on Industrial Electronics*, vol. 54, no. 5, pp. 2583–2592, October 2007.

[61] A. Camacho, M. Castilla, J. Miret, J. Vasquez, and E. Alarcon-Gallo, "Flexible voltage support control for three-phase distributed generation inverters under grid fault," *IEEE Transactions on Industrial Electronics*, vol. 60, no. 4, pp. 1429–1441, April 2013.

[62] J. Miret, M. Castilla, A. Camacho, L. Garcia de Vicuna, and J. Matas, "Control scheme for photovoltaic three-phase inverters to minimize peak currents during unbalanced grid-voltage sags," *IEEE Transactions on Power Electronics*, vol. 27, no. 10, pp. 4262–4271, October 2012.

[63] Q. Wang, N. Zhou, and L. Ye, "Fault analysis for distribution networks with current-controlled three-phase inverter-interfaced distributed generators," *IEEE Transactions on Power Delivery*, vol. 30, no. 3, pp. 1532–1542, June 2015.

[64] N. Nimpitiwan, G. Heydt, R. Ayyanar, and S. Suryanarayanan, "Fault current contribution from synchronous machine and inverter based distributed generators," *IEEE Transactions on Power Delivery*, vol. 22, no. 1, pp. 634–641, January 2007.

[65] E. Ebrahimi, M. J. Sanjari, and G. B. Gharehpetian, "Control of three-phase inverter-based (DG) system during fault condition without changing protection coordination," *International Journal of Electrical Power & Energy Systems*, vol. 63, no. 0, pp. 814 – 823, December 2014.

[66] MATLAB, Mathworks inc., Massachusetts, USA, Version R2012a.

[67] A. Darwish, A. Abdel-Khalik, A. Elserougi, S. Ahmed, and A. Massoud, "Fault current contribution scenarios for grid-connected voltage source inverter-based distributed generation with an (LCL) filter," *Electric Power Systems Research*, vol. 104, no. 0, pp. 93 – 103, November 2013.

[68] M. Baran and I. El-Markaby, "Fault analysis on distribution feeders with distributed generators," *IEEE Transactions on Power Systems*, vol. 20, no. 4, pp. 1757–1764, November 2005.

[69] T. C. Ou, "Ground fault current analysis with a direct building algorithm for microgrid distribution," *International Journal of Electrical Power & Energy Systems*, vol. 53, no. 0, pp. 867–875, December 2013.

[70] J.-H. Teng, "A direct approach for distribution system load flow solutions," *IEEE Transactions on Power Delivery*, vol. 18, no. 3, pp. 882–887, July 2003.

[71] A. P. Moura, J. P. Lopes, A. A. de Moura, J. Sumaili, and C. Moreira, "(IMICV) fault analysis method with multiple (PV) grid-connected inverters for distribution systems," *Electric Power Systems Research*, vol. 119, no. 0, pp. 119 – 125, February 2015.

[72] L. Strezoski, M. Prica, and K. A. Loparo, "Generalized delta-circuit concept for integration of distributed generators in online short-circuit calculations," *IEEE Transactions on Power Systems*, vol. 32, no. 4, pp. 3237–3245, July 2017.

[73] M. J. E. Alam, K. M. Muttaqi, and D. Sutanto, "A three-phase power flow approach for integrated 3-wire MV and 4-wire multigrounded LV networks with rooftop solar PV," *IEEE Transactions on Power Systems*, vol. 28, no. 2, pp. 1728–1737, May 2013.

[74] M. Coppo, F. Bignucolo, and R. Turri, "Generalised transformer modelling for power flow calculation in multi-phase unbalanced networks," *IET Generation, Transmission & Distribution*, vol. 11, no. 15, pp. 3843–3852, November 2017.

[75] M. E. Baran and E. A. Staton, "Distribution transformer models for branch current based feeder analysis," *IEEE Transactions on Power Systems*, vol. 12, no. 2, pp. 698–703, May 1997.

[76] W. H. Kersting, W. H. Phillips, and W. Carr, "A new approach to modeling three-phase transformer connections," in *1998 Rural Electric Power Conference Presented at 42nd Annual Conference*, April 1998, pp. b21–1–8.

[77] Z. Wang, F. Chen, and J. Li, "Implementing transformer nodal admittance matrices into backward/forward sweep-based power flow analysis for unbalanced radial distribution systems," *IEEE Transactions on Power Systems*, vol. 19, no. 4, pp. 1831–1836, November 2004.

[78] P. Xiao, D. C. Yu, and W. Yan, "A unified three-phase transformer model for distribution load flow calculations," *IEEE Transactions on Power Systems*, vol. 21, no. 1, pp. 153–159, February 2006.

[79] I. Kocar and J. S. Lacroix, "Implementation of a modified augmented nodal analysis based transformer model into the backward forward sweep solver," *IEEE Transactions on Power Systems*, vol. 27, no. 2, pp. 663–670, May 2012.

[80] G. J. Wakileh, *Power Systems Harmonics, fundamentals, analysis and filter design*. Springer, 2001.

[81] J. M. Cano, M. R. R. Mojumdar, J. G. Norniella, and G. A. Orcajo, "Phase shifting transformer model for direct approach power flow studies," *International Journal of Electrical Power & Energy Systems*, vol. 91, pp. 71 – 79, October 2017.

[82] A. Tan, W. H. Liu, and D. Shirmohammadi, "Transformer and load modeling in short circuit analysis for distribution systems," *IEEE Transactions on Power Systems*, vol. 12, no. 3, pp. 1315–1322, August 1997.

[83] M. Todorovski and D. Rajicic, "Handling three-winding transformers and loads in short circuit analysis by the admittance summation method," *IEEE Transactions on Power Systems*, vol. 18, no. 3, pp. 993–1000, August 2003.

[84] D. Das, D. Kothari, and A. Kalam, "Simple and efficient method for load flow solution of radial distribution networks," *International Journal of Electrical Power & Energy Systems*, vol. 17, no. 5, pp. 335 – 346, October 1995.

[85] R. Broadwater, A. Chandrasekaran, C. Huddleston, and A. Khan, "Power flow analysis of unbalanced multiphase radial distribution systems," *Electric Power Systems Research*, vol. 14, no. 1, pp. 23 – 33, February 1988.

[86] T. H. Chen, M. S. Chen, K. J. Hwang, P. Kotas, and E. A. Chebli, "Distribution system power flow analysis-a rigid approach," *IEEE Transactions on Power Delivery*, vol. 6, no. 3, pp. 1146–1152, July 1991.

[87] S. Ghosh and D. Das, "Method for load-flow solution of radial distribution networks," *IEE Proceedings - Generation, Transmission and Distribution*, vol. 146, no. 6, pp. 641–648, November 1999.

[88] G. X. Luo and A. Semlyen, "Efficient load flow for large weakly meshed networks," *IEEE Transactions on Power Systems*, vol. 5, no. 4, pp. 1309–1316, November 1990.

[89] Y. Zhu and K. Tomsovic, "Adaptive power flow method for distribution systems with dispersed generation," *IEEE Transactions on Power Delivery*, vol. 17, no. 3, pp. 822–827, July 2002.

[90] C. S. Cheng and D. Shirmohammadi, "A three-phase power flow method for real-time distribution system analysis," *IEEE Transactions on Power Systems*, vol. 10, no. 2, pp. 671–679, May 1995.

[91] A. G. Expsito and E. R. Ramos, "Reliable load flow technique for radial distribution networks," *IEEE Transactions on Power Systems*, vol. 14, no. 3, pp. 1063–1069, August 1999.

[92] E. Bompard, E. Carpaneto, G. Chicco, and R. Napoli, "Convergence of the backward/forward sweep method for the load-flow analysis of radial distribution systems," *International Journal of Electrical Power & Energy Systems*, vol. 22, no. 7, pp. 521 – 530, October 2000.

[93] U. Eminoglu and M. H. Hocaoglu, "A new power flow method for radial distribution systems including voltage dependent load models," *Electric Power Systems Research*, vol. 76, no. 1, pp. 106 – 114, September 2005.

[94] G. W. Chang, S. Y. Chu, and H. L. Wang, "An improved backward/forward sweep load flow algorithm for radial distribution systems," *IEEE Transactions on Power Systems*, vol. 22, no. 2, pp. 882–884, May 2007.

[95] A. Augugliaro, L. Dusonchet, S. Favuzza, M. Ippolito, and E. R. Sanseverino, "A backward sweep method for power flow solution in distribution networks," *International Journal of Electrical Power & Energy Systems*, vol. 32, no. 4, pp. 271 – 280, May 2010.

[96] A. Mahmoudi and S. H. Hosseinian, "Direct solution of distribution system load flow using forward/backward sweep," in *2011 19th Iranian Conference on Electrical Engineering*, May 2011, pp. 1–6.

[97] W.-M. Lin, Y.-S. Su, H.-C. Chin, and J.-H. Teng, "Three-phase unbalanced distribution power flow solutions with minimum data preparation," *IEEE Transactions on Power Systems*, vol. 14, no. 3, pp. 1178–1183, August 1999.

[98] X. Yang, S. P. Carullo, K. Miu, and C. O. Nwankpa, "Reconfigurable distribution automation and control laboratory: Multiphase, radial power flow experiment," *IEEE Transactions on Power Systems*, vol. 20, no. 3, pp. 1207–1214, August 2005.

[99] S. Khushalani, J. M. Solanki, and N. N. Schulz, "Development of three-phase unbalanced power flow using PV and PQ models for distributed generation and study of the impact of DG models," *IEEE Transactions on Power Systems*, vol. 22, no. 3, pp. 1019–1025, August 2007.

[100] J. C. M. Vieira, W. Freitas, and A. Morelato, "Phase-decoupled method for three-phase power-flow analysis of unbalanced distribution systems," *IEE Proceedings - Generation, Transmission and Distribution*, vol. 151, no. 5, pp. 568–574, September 2004.

[101] M. Z. Kamh and R. Iravani, "Unbalanced model and power-flow analysis of microgrids and active distribution systems," *IEEE Transactions on Power Delivery*, vol. 25, no. 4, pp. 2851–2858, October 2010.

[102] B. M. Kalesar and A. R. Seifi, "Fuzzy load flow in balanced and unbalanced radial distribution systems incorporating composite load model," *International Journal of Electrical Power & Energy Systems*, vol. 32, no. 1, pp. 17 – 23, January 2010.

[103] J. H. Teng, "Modelling distributed generations in three-phase distribution load flow," *IET Generation, Transmission & Distribution*, vol. 2, no. 3, pp. 330–340, May 2008.

[104] H. D. Chiang, T. Q. Zhao, J. J. Deng, and K. Koyanagi, "Homotopy-enhanced power flow methods for general distribution networks with distributed generators," *IEEE Transactions on Power Systems*, vol. 29, no. 1, pp. 93–100, January 2014.

[105] P. Arboleya, C. Gonzlez-Morn, and M. Coto, "Unbalanced power flow in distribution systems with embedded transformers using the complex theory in $\alpha\beta 0$; stationary reference frame," *IEEE Transactions on Power Systems*, vol. 29, no. 3, pp. 1012–1022, May 2014.

[106] M. Z. Kamh and R. Iravani, "A unified three-phase power-flow analysis model for electronically coupled distributed energy resources," *IEEE Transactions on Power Delivery*, vol. 26, no. 2, pp. 899–909, April 2011.

[107] Y. Ju, W. Wu, B. Zhang, and H. Sun, "An extension of FBS three-phase power flow for handling PV nodes in active distribution networks," *IEEE Transactions on Smart Grid*, vol. 5, no. 4, pp. 1547–1555, July 2014.

[108] A. J. G. Mena and J. A. M. Garcia, "An approximate power flow for distribution systems," *IEEE Latin America Transactions*, vol. 12, no. 8, pp. 1432–1440, December 2014.

[109] A. Garces, "A linear three-phase load flow for power distribution systems," *IEEE Transactions on Power Systems*, vol. 31, no. 1, pp. 827–828, January 2016.

[110] I. Dafi, H. T. Neisius, M. Gilles, S. Henselmeyer, and V. Landerberger, "Three-phase power flow in distribution networks using fortescue transformation," *IEEE Transactions on Power Systems*, vol. 28, no. 2, pp. 1027–1034, May 2013.

[111] H. Sun, D. Nikovski, T. Ohno, T. Takano, and Y. Kojima, "A fast and robust load flow method for distribution systems with distributed generations," *Energy Procedia*, vol. 12, no. Supplement C, pp. 236 – 244, September 2011, the Proceedings of International Conference on Smart Grid and Clean Energy Technologies (ICSGCE) 2011.

[112] I. Kocar, J. Mahseredjian, U. Karaagac, G. Soykan, and O. Saad, "Multiphase load-flow solution for large-scale distribution systems using MANA," *IEEE Transactions on Power Delivery*, vol. 29, no. 2, pp. 908–915, April 2014.

[113] H. Hooshyar and L. Vanfretti, "Power flow solution for multiphase unbalanced distribution networks with high penetration of photovoltaics," in *2013 8th International Conference on Electrical and Electronics Engineering (ELECO)*, November 2013, pp. 167–171.

[114] H. Li, Y. Jin, A. Zhang, X. Shen, C. Li, and B. Kong, "An improved hybrid load flow calculation algorithm for weakly-meshed power distribution system," *International Journal of Electrical Power & Energy Systems*, vol. 74, no. Supplement C, pp. 437 – 445, January 2016.

[115] M. Shakarami, H. Beiranvand, A. Beiranvand, and E. Sharifipour, "A recursive power flow method for radial distribution networks: Analysis, solvability and convergence," *International Journal of Electrical Power & Energy Systems*, vol. 86, no. Supplement C, pp. 71 – 80, March 2017.

[116] U. Ghatak and V. Mukherjee, "An improved load flow technique based on load current injection for modern distribution system," *International Journal of Electrical Power & Energy Systems*, vol. 84, no. Supplement C, pp. 168 – 181, January 2017.

[117] H. Ahmadi, J. R. Mart, and A. von Meier, "A linear power flow formulation for three-phase distribution systems," *IEEE Transactions on Power Systems*, vol. 31, no. 6, pp. 5012–5021, November 2016.

[118] K. Mahmoud and N. Yorino, "Robust quadratic-based BFS power flow method for multi-phase distribution systems," *IET Generation, Transmission & Distribution*, vol. 10, no. 9, pp. 2240–2250, June 2016.

[119] M. Afsari, S. P. Singh, G. S. Raju, and G. K. Rao, "A fast power flow solution of radial distribution networks," *Electric Power Components and Systems*, vol. 30, no. 10, pp. 1065–1074, November 2002.

[120] S. Khushalani and N. Schulz, "Unbalanced distribution power flow with distributed generation," in *2005/2006 IEEE/PES Transmission and Distribution Conference and Exhibition*, May 2006, pp. 301–306.

[121] R. K. Gajbhiye, B. Gopi, P. Kulkarni, and S. A. Soman, "Computationally efficient methodology for analysis of faulted power systems with series-compensated transmission lines: A phase coordinate approach," *IEEE Transactions on Power Delivery*, vol. 23, no. 2, pp. 873–880, April 2008.

[122] M. P. Selvan and K. S. Swarup, "Unbalanced distribution system short circuit analysis 2014 an object-oriented approach," in *TENCON 2008 - 2008 IEEE Region 10 Conference*, November 2008, pp. 1–6.

[123] E. Makram, M. Bou-Rabee, and A. Girgis, "Three-phase modeling of unbalanced distribution systems during open conductors and/or shunt fault conditions using the bus impedance matrix," *Electric Power Systems Research*, vol. 13, no. 3, pp. 173 – 183, December 1987.

[124] E. B. Makram and A. A. Girgis, "A fault-induced transient analysis of unbalanced distribution systems with harmonic distortion," *Electric Power Systems Research*, vol. 17, no. 2, pp. 89 – 99, September 1989.

[125] N. Rajaei, M. H. Ahmed, M. M. A. Salama, and R. K. Varma, "Analysis of fault current contribution from inverter based distributed generation," in *2014 IEEE PES General Meeting — Conference Exposition*, July 2014, pp. 1–5.

[126] N. Rajaei, M. Ahmed, M. Salama, and R. Varma, "Fault current management using inverter-based distributed generators in smart grids," in *2015 IEEE Power Energy Society General Meeting*, July 2015, pp. 1–1.

[127] N. Rajaei and M. M. A. Salama, "Management of fault current contribution of synchronous dgs using inverter-based dgs," *IEEE Transactions on Smart Grid*, vol. 6, no. 6, pp. 3073–3081, November 2015.

[128] R. M. Ciric, A. P. Feltrin, and L. F. Ochoa, "Power flow in four-wire distribution networks-general approach," *IEEE Transactions on Power Systems*, vol. 18, no. 4, pp. 1283–1290, November 2003.

[129] D. R. R. Penido, L. R. de Araujo, S. Carneiro, J. L. R. Pereira, and P. A. N. Garcia, "Three-phase power flow based on four-conductor current injection method for unbalanced distribution networks," *IEEE Transactions on Power Systems*, vol. 23, no. 2, pp. 494–503, May 2008.

[130] M. Monfared, A. M. Daryani, and M. Abedi, "Three phase asymmetrical load flow for four-wire distribution networks," in *2006 IEEE PES Power Systems Conference and Exposition*, October 2006, pp. 1899–1903.

[131] T.-H. Chen and W.-C. Yang, "Analysis of multi-grounded four-wire distribution systems considering the neutral grounding," in *PICA 2001. Innovative Computing for Power - Electric Energy Meets the Market. 22nd IEEE Power Engineering Society. International Conference on Power Industry Computer Applications (Cat. No.01CH37195)*, May 2001, pp. 393–396.

[132] R. M. Ciric, L. F. Ochoa, and A. Padilha, "Power flow in distribution networks with earth return," *International Journal of Electrical Power & Energy Systems*, vol. 26, no. 5, pp. 373 – 380, June 2004.

[133] K. M. Sunderland and M. F. Conlon, "4-wire load flow analysis of a representative urban network incoprating SSEG," in *2012 47th International Universities Power Engineering Conference (UPEC)*, September 2012, pp. 1–6.

[134] C. D. Halevidis and E. I. Koufakis, "Power flow in PME distribution systems during an open neutral condition," *IEEE Transactions on Power Systems*, vol. 28, no. 2, pp. 1083–1092, May 2013.

[135] K. Sunderland, M. Coppo, M. Conlon, and R. Turri, "A correction current injection method for power flow analysis of unbalanced multiple-grounded 4-wire distribution networks," *Electric Power Systems Research*, vol. 132, no. Supplement C, pp. 30 – 38, March 2016.

[136] D. R. R. Penido, L. R. de Araujo, and M. de Carvalho Filho, "An enhanced tool for fault analysis in multiphase electrical systems," *International Journal of Electrical Power & Energy Systems*, vol. 75, no. Supplement C, pp. 215 – 225, February 2016.

[137] J. Klucznik, "Earth wires currents calculation by tableau analysis," *Electric Power Systems Research*, vol. 151, no. Supplement C, pp. 329 – 337, October 2017.

[138] H. Hooshyar and M. Baran, "Fault analysis on distribution feeders with high penetration of PV systems," *IEEE Transactions on Power Systems*, vol. 28, no. 3, pp. 2890–2896, August 2013.

[139] "Available online, https://hvdc.ca/pscad/, "pscad/emtdc," x4 (4.3) ed: Manitoba hvdc research center."

[140] "Available online, "http://ewh.ieee.org/soc/pes/dsacom/testfeeders/", ieee pes."

[141] W. Kersting and W. Phillips, "Distribution system short circuit analysis," in *Proceedings of the 25th Intersociety Energy Conversion Engineering Conference, 1990. IECEC-90.*, vol. 1, August 1990, pp. 310–315.

[142] ——, "Distribution feeder line models," in *1994 Papers Presented at the 38th Annual Conference Rural Electric Power Conference*, April 1994, pp. A4/1–A4/8.

[143] B. A. and W. Xu, "Analysis of faulted power systems by phase coordinates," *IEEE Transaction on Power Delivery,*, vol. 13, no. 2, pp. 587–595, April 1998.

[144] G. W. Stagg and E.-A. A. H., *Computer method in Power system Analysis*, T. (Japan), Ed. McGraw-Hill Kogakusha Ltd., 1968.

[145] R. A. Walling, R. Saint, R. C. Dugan, J. Burke, and L. A. Kojovic, "Summary of distributed resources impact on power delivery systems," *IEEE Transactions on Power Delivery*, vol. 23, no. 3, pp. 1636–1644, July 2008.

[146] A. Mathur, B. Das, and V. Pant, "Fault analysis of unbalanced radial and meshed distribution system with inverter based distributed generation (IBDG)," *International Journal of Electrical Power & Energy Systems*, vol. 85, no. Supplement C, pp. 164 – 177, February 2017.

[147] J. Marti, H. Ahmadi, and L. Bashualdo, "Linear power-flow formulation based on a voltage-dependent load model," *IEEE Transactions on Power Delivery*, vol. 28, no. 3, pp. 1682–1690, July 2013.

[148] "IEEE Standard for interconnecting distributed resources with electric power systems - amendment 1," *IEEE Std 1547a-2014 (Amendment to IEEE Std 1547-2003)*, pp. 1–16, May 2014.

[149] A. Camacho, M. Castilla, J. Miret, R. Guzman, and A. Borrell, "Reactive power control for distributed generation power plants to comply with voltage limits during grid faults," *IEEE Transactions on Power Electronics*, vol. 29, no. 11, pp. 6224–6234, November 2014.

[150] W. S. Moon, J. S. Hur, and J. C. Kim, "A protection of interconnection transformer for DG in korea distribution power system," in *2012 IEEE Power and Energy Society General Meeting*, July 2012, pp. 1–5.

[151] E. Weisgerber, P. K. Sen, and K. Malmedal, "Application guidelines for transformer connection and grounding for distributed generation: An update," in *2013 IEEE IAS Electrical Safety Workshop*, March 2013, pp. 99–104.

[152] J. C. Balda, A. R. Oliva, D. W. McNabb, and R. D. Richardson, "Measurements of neutral currents and voltages on a distribution feeder," *IEEE Transactions on Power Delivery*, vol. 12, no. 4, pp. 1799–1804, October 1997.

[153] J. C. Das and R. H. Osman, "Grounding of AC and DC low-voltage and medium-voltage drive systems," *IEEE Transactions on Industry Applications*, vol. 34, no. 1, pp. 205–216, January 1998.

[154] "IEEE Recommended practice for grounding of industrial and commercial power systems," *IEEE Std 142-1991*, pp. 1–240, June 1992.

[155] T. A. Short, J. R. Stewart, D. R. Smith, J. O'Brien, and K. Hampton, "Five-wire distribution system demonstration project," *IEEE Transactions on Power Delivery*, vol. 17, no. 2, pp. 649–654, April 2002.

[156] D. R. R. Penido, L. R. Araujo, J. L. R. Pereira, P. A. N. Garcia, and S. Carneiro, "Four wire newton-raphson power flow based on the current injection method," in *IEEE PES Power Systems Conference and Exposition, 2004*, October 2004, pp. vol. 1 239–242.

[157] L. R. de Araujo, D. R. R. Penido, S. Carneiro, and J. L. R. Pereira, "A study of neutral conductors and grounding impacts on the load-flow solutions of unbalanced distribution systems," *IEEE Transactions on Power Systems*, vol. 31, no. 5, pp. 3684–3692, September 2016.

[158] A. Mathur, V. Pant, and B. Das, "Unsymmetrical short-circuit analysis for distribution system considering loads," *International Journal of Electrical Power & Energy Systems*, vol. 70, no. Supplement C, pp. 27 – 38, September 2015.

[159] "Distribution test feeders," *https://ewh.ieee.org/soc/pes/dsacom/testfeeders/*.

[160] P. M. ANDERSON, *Analysis of Faulted Power Systems*. Wiley Interscience IEEE, 1973.

[161] W. H. Kersting, "Radial distribution test feeders," in *2001 IEEE Power Engineering Society Winter Meeting. Conference Proceedings*, vol. 2, 2001, pp. 908–912.

Appendix A

Modified IEEE 34-Bus three-phase four wire multigrounded Distribution System

Table A.1: Line Data

From Bus		To Bus		Line configuration	Length (ft)
Actual Bus No.	Modified Bus No.	Actual Bus No.	Modified Bus No.		
800	1	802	2	300	2580
802	2	806	3	300	1730
806	3	808	4	300	32230
808	4	810	5	303	5804
808	4	812	6	300	37500
812	6	814	7	300	29730
814	7	850	8	301	10
850	8	816	9	301	310
816	9	818	10	302	1710
818	10	820	11	302	48150
820	11	820	12	302	13740
816	9	824	13	301	10210
824	13	826	14	303	3030
824	13	828	15	301	840
828	15	830	16	301	20440
830	16	854	17	301	520
854	17	856	18	303	23330
854	17	852	19	301	36830
852	19	832	20	301	10
888	20	890	21	300	10560
832	20	858	22	301	4900
858	22	864	23	302	1620
858	22	834	24	301	5830
834	24	842	25	301	280
842	25	844	26	301	1350
844	26	846	27	301	3640
846	27	848	28	301	530
834	24	860	29	301	2020
860	29	836	30	301	2680
834	30	842	31	301	280
862	31	838	32	304	4860
836	30	840	33	301	860

Table A.2: Load Data

Bus No.	P_a (kW)	Q_a (kVAR)	P_b (kW)	Q_b (kVAR)	P_c (kW)	Q_c (kVAR)
1	0.0	0.0	0.0	0.0	0.0	0.0
2	0.0	0.0	15.5	7.5	12.5	7.0
3	0.0	0.0	15.5	7.5	12.5	7.0
4	0.0	0.0	8.0	4.0	0.0	0.0
5	0.0	0.0	8.0	4.0	0.0	0.0
6	0.0	0.0	0.0	0.0	0.0	0.0
7	0.0	0.0	0.0	0.0	0.0	0.0
8	0.0	0.0	0.0	0.0	0.0	0.0
9	0.0	0.0	2.5	1.0	0.0	0.0
10	17.0	8.5	0.0	0.0	0.0	0.0
11	84.5	43.5	0.0	0.0	0.0	0.0
12	67.5	35.0	0.0	0.0	0.0	0.0
13	0.0	0.0	22.5	11.0	2.0	1.0
14	0.0	0.0	20.0	10.0	0.0	0.0
15	3.5	1.5	0.0	0.0	2.0	1.0
16	13.5	6.5	12.0	6.0	25.0	10.0
17	0.0	0.0	2.0	1.0	0.0	0.0
18	0.0	0.0	0.0	0.0	0.0	0.0
19	0.0	0.0	0.0	0.0	0.0	0.0
20	3.5	1.5	1.0	0.5	3.0	1.5
21	150.0	75.0	150.0	75.0	150.0	75.0
22	6.5	3.0	8.5	4.5	9.5	5.0
23	1.0	0.5	0.0	0.0	0.0	0.0
24	10.0	5.0	17.5	9.0	61.5	31.0
25	4.5	2.5	0.0	0.0	0.0	0.0
26	139.5	107.5	147.5	111.0	145.0	110.5
27	0.0	0.0	24.0	11.5	0.0	0.0
28	20.0	16.0	31.5	21.5	20.0	16.0
29	43.0	27.5	35.0	24.0	96.0	54.5
30	24.0	12.0	16.0	8.5	21.0	11.0
31	0.0	0.0	14.0	7.0	0.0	0.0
32	0.0	0.0	14.0	7.0	0.0	0.0
33	18.0	11.5	20.0	12.5	9.0	7.0

Table A.3: Overhead Line Configurations

Configuration	Phasing	Phase Conductor (ACSR)	Neutral Conductor (ACSR)	Spacing ID
300	A B C N	1/0	1/0	500
301	A B C N	#2 6/1	#2 6/1	500
302	A N	#4 6/1	#4 6/1	510
303	B N	#4 6/1	#4 6/1	510
304	B N	#2 6/1	#2 6/1	510

Appendix B

Modified IEEE 123-Bus three-phase four wire multigrounded Distribution System

Table B.1: Line Data

From Bus		To Bus		Line configuration	Length (ft)
Actual Bus No.	Modified Bus No.	Actual Bus No.	Modified Bus No.		
149	1	1	2	1	400
1	2	2	3	10	175
1	2	3	4	11	250
3	4	4	5	11	200
3	4	5	6	11	325
5	6	6	7	11	250
1	2	7	8	1	300
7	8	8	9	1	200
8	9	9	10	9	225
9	10	14	11	9	425
14	11	11	12	9	250
14	11	10	13	9	250
8	9	12	14	10	225
8	9	13	15	1	300
13	15	34	16	11	150
34	16	15	17	11	100
15	17	17	18	11	350
15	17	16	19	11	375
13	15	18	20	2	825
18	20	19	21	9	250
19	21	20	22	9	325
18	20	21	23	2	300
21	23	22	24	10	525
21	23	23	25	2	250
23	25	24	26	11	550
23	25	25	27	2	275
25	27	26	28	7	350
26	28	27	29	7	275
25	27	28	30	2	200
28	30	29	31	2	300
29	31	30	32	2	350

From Bus		To Bus		Line configuration	Length (ft)
Actual Bus No.	Modified Bus No.	Actual Bus No.	Modified Bus No.		
30	32	250	33	2	200
26	28	31	34	11	225
31	34	32	35	11	300
27	29	33	36	9	500
135	20	35	37	4	375
35	37	36	38	8	650
36	38	37	39	9	300
36	38	38	40	10	250
38	40	39	41	10	325
35	37	40	42	1	250
40	42	41	43	11	325
40	42	42	44	1	250
42	44	43	45	10	500
42	44	44	46	1	200
44	46	45	47	9	200
45	47	46	48	9	300
44	46	47	49	1	250
47	49	48	50	4	150
47	49	49	51	4	250
49	51	50	52	4	250
50	52	51	53	4	250
51	53	151	54	4	500
152	15	52	55	1	400
52	55	53	56	1	200
53	56	54	57	1	125
54	57	55	58	1	275
55	58	56	59	1	275
54	57	57	60	3	350
57	60	58	61	10	250
58	61	59	62	10	250
57	60	60	63	3	750
60	63	61	64	5	550
60	63	62	65	12	250
62	65	63	66	12	175
63	66	64	67	12	350
64	67	65	68	12	425
65	68	66	69	12	325
160	63	67	70	6	350
67	70	68	71	9	200
68	71	69	72	9	275
69	72	70	73	9	325
70	73	71	74	9	275
67	70	72	75	3	275

From Bus		To Bus		Line configuration	Length (ft)
Actual Bus No.	Modified Bus No.	Actual Bus No.	Modified Bus No.		
72	75	73	76	11	275
73	76	74	77	11	350
74	77	75	78	11	400
72	75	76	79	3	200
76	79	77	80	6	400
77	80	78	81	6	100
78	81	79	82	6	225
78	81	80	83	6	475
80	83	81	84	6	475
81	84	82	85	6	250
82	85	83	86	6	250
81	84	84	87	11	675
84	87	85	88	11	475
76	79	86	89	3	700
86	89	87	90	6	450
87	90	88	91	9	175
87	90	89	92	6	275
89	92	90	93	10	225
89	92	91	94	6	225
91	94	92	95	11	300
91	94	93	96	6	225
93	96	94	97	9	275
93	96	95	98	6	300
95	98	96	99	10	200
67	70	97	100	3	250
97	100	98	101	3	275
98	101	99	102	3	550
99	102	100	103	3	300
100	103	450	104	3	800
197	100	101	105	3	250
101	105	102	106	11	225
102	106	103	107	11	325
103	107	104	108	11	700
101	105	105	109	3	275
105	109	106	110	10	225
106	110	107	111	10	575
105	109	108	112	3	325
108	112	109	113	9	450
109	113	110	114	9	300
110	114	111	115	9	575
110	114	112	116	9	125
112	116	113	117	9	525
113	117	114	118	9	325
108	112	300	119	3	1000

Table B.2: Load Data

Bus No.	P_a (kW)	Q_a (kVAR)	P_b (kW)	Q_b (kVAR)	P_c (kW)	Q_c (kVAR)
1	0	0	0	0	0	0
2	40	20	0	0	0	0
3	0	0	20	10	0	0
4	0	0	0	0	0	0
5	0	0	0	0	40	20
6	0	0	0	0	20	10
7	0	0	0	0	40	20
8	20	10	0	0	0	0
9	0	0	0	0	0	0
10	40	20	0	0	0	0
11	0	0	0	0	0	0
12	40	20	0	0	0	0
13	20	10	0	0	0	0
14	0	0	20	10	0	0
15	0	0	0	0	0	0
16	0	0	0	0	40	20
17	0	0	0	0	0	0
18	0	0	0	0	20	10
19	0	0	0	0	40	20
20	0	0	0	0	0	0
21	40	20	0	0	0	0
22	40	20	0	0	0	0
23	0	0	0	0	0	0
24	0	0	40	20	0	0
25	0	0	0	0	0	0
26	0	0	0	0	40	20
27	0	0	0	0	0	0
28	0	0	0	0	0	0
29	0	0	0	0	0	0
30	40	20	0	0	0	0
31	40	20	0	0	0	0
32	0	0	0	0	40	20
33	0	0	0	0	0	0
34	0	0	0	0	20	10
35	0	0	0	0	20	10
36	40	20	0	0	0	0
37	40	20	0	0	0	0
38	0	0	0	0	0	0
39	40	20	0	0	0	0
40	0	0	20	10	0	0
41	0	0	20	10	0	0
42	0	0	0	0	0	0
43	0	0	0	0	20	10
44	20	10	0	0	0	0
45	0	0	40	20	0	0

Bus No.	P_a (kW)	Q_a (kVAR)	P_b (kW)	Q_b (kVAR)	P_c (kW)	Q_c (kVAR)
46	0	0	0	0	0	0
47	20	10	0	0	0	0
48	20	10	0	0	0	0
49	35	25	35	25	35	25
50	70	50	70	50	70	50
51	35	25	70	50	35	20
52	0	0	0	0	40	20
53	20	10	0	0	0	0
54	0	0	0	0	0	0
55	40	20	0	0	0	0
56	40	20	0	0	0	0
57	0	0	0	0	0	0
58	20	10	0	0	0	0
59	0	0	20	10	0	0
60	0	0	0	0	0	0
61	0	0	20	10	0	0
62	0	0	20	10	0	0
63	20	10	0	0	0	0
64	0	0	0	0	0	0
65	0	0	0	0	40	20
66	40	20	0	0	0	0
67	0	0	75	35	0	0
68	35	25	35	25	70	50
69	0	0	0	0	75	35
70	0	0	0	0	0	0
71	20	10	0	0	0	0
72	40	20	0	0	0	0
73	20	10	0	0	0	0
74	40	20	0	0	0	0
75	0	0	0	0	0	0
76	0	0	0	0	40	20
77	0	0	0	0	40	20
78	0	0	0	0	40	20
79	105	80	70	50	70	50
80	0	0	40	20	0	0
81	0	0	0	0	0	0
82	40	20	0	0	0	0
83	0	0	40	20	0	0
84	0	0	0	0	0	0
85	40	20	0	0	0	0
86	0	0	0	0	20	10
87	0	0	0	0	20	10
88	0	0	0	0	40	20
89	0	0	20	10	0	0
90	0	0	40	20	0	0

Bus No.	P_a (kW)	Q_a (kVAR)	P_b (kW)	Q_b (kVAR)	P_c (kW)	Q_c (kVAR)
91	40	20	0	0	0	0
92	0	0	0	0	0	0
93	0	0	40	20	0	0
94	0	0	0	0	0	0
95	0	0	0	0	40	20
96	0	0	0	0	0	0
97	40	20	0	0	0	0
98	0	0	20	10	0	0
99	0	0	20	10	0	0
100	0	0	0	0	0	0
101	40	20	0	0	0	0
102	0	0	40	20	0	0
103	0	0	0	0	40	20
104	0	0	0	0	0	0
105	0	0	0	0	0	0
106	0	0	0	0	20	10
107	0	0	0	0	40	20
108	0	0	0	0	40	20
109	0	0	0	0	0	0
110	0	0	40	20	0	0
111	0	0	40	20	0	0
112	0	0	0	0	0	0
113	40	20	0	0	0	0
114	0	0	0	0	0	0
115	20	10	0	0	0	0
116	20	10	0	0	0	0
117	40	20	0	0	0	0
118	20	10	0	0	0	0
119	0	0	0	0	0	0

Table B.3: Overhead Line Configurations

Configuration	Phasing	Phase Conductor (ACSR)	Neutral Conductor (ACSR)	Spacing ID
1	A B C N	336, 400 26/7	4/0 6/1	500
2	A B C N	336, 400 26/7	4/0 6/1	500
3	A B C N	336, 400 26/7	4/0 6/1	500
4	A B C N	336, 400 26/7	4/0 6/1	500
5	A B C N	336, 400 26/7	4/0 6/1	500
6	A B C N	336, 400 26/7	4/0 6/1	500
7	A C N	336, 400 26/7	4/0 6/1	505
8	A B N	336, 400 26/7	4/0 6/1	505
9	A N	1/0	1/0	510
10	B N	1/0	1/0	510
11	C N	1/0	1/0	510